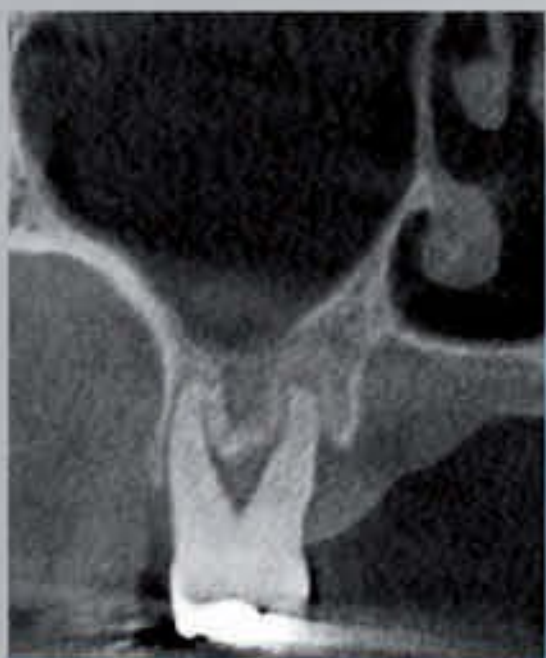


Dental Radiology

Andreas Fuhrmann



Dental Radiology

Andreas Fuhrmann, DDS
Forensic Odontologist
Department of Legal Medicine
Center for Diagnostics
University Medical Center Hamburg-Eppendorf
Hamburg, Germany

304 illustrations

Thieme
Stuttgart • New York • Delhi • Rio de Janeiro

Library of Congress Cataloging-in-Publication Data

Fuhrmann, Andreas, author.

[Zahnärztliche Radiologie. English]

Dental radiology / Andreas Fuhrmann.

p. ; cm.

Includes bibliographical references and index.

ISBN 978-3-13-200421-4 (alk. paper) –

ISBN 978-3-13-200431-3 (e-book)

I. Title.

[DNLM: 1. Diagnostic Imaging. 2. Radiography, Dental—methods. WN 230]

RK309

617.6'07572—dc23

2014047560

This book is an authorized translation of the 1st German edition published and copyrighted 2013 by Georg Thieme Verlag, Stuttgart. Title of the German edition: Zahnärztliche Radiologie

Translator: Suzyon O'Neal Wandrey, Berlin, Germany

Illustrators: Angelika Branner, Hohenpeissenberg, Germany; Joachim Hormann, Stuttgart, Germany

Eugen Roth poem translated and reproduced with kind permission of Carl Hanser Verlag, Munich, Germany
© 2015 by Georg Thieme Verlag KG

Important note: Medicine is an ever-changing science undergoing continual development. Research and clinical experience are continually expanding our knowledge, in particular our knowledge of proper treatment and drug therapy. Insofar as this book mentions any dosage or application, readers may rest assured that the authors, editors, and publishers have made every effort to ensure that such references are in accordance with the state of knowledge at the time of production of the book.

Nevertheless, this does not involve, imply, or express any guarantee or responsibility on the part of the publishers in respect to any dosage instructions and forms of applications stated in the book. Every user is requested to examine carefully the manufacturers' leaflets accompanying each drug and to check, if necessary in consultation with a physician or specialist, whether the dosage schedules mentioned therein or the contraindications stated by the manufacturers differ from the statements made in the present book. Such examination is particularly important with drugs that are either rarely used or have been newly released on the market. Every dosage schedule or every form of application used is entirely at the user's own risk and responsibility. The authors and publishers request every user to report to the publishers any discrepancies or inaccuracies noticed. If errors in this work are found after publication, errata will be posted at www.thieme.com on the product description page.

Some of the product names, patents, and registered designs referred to in this book are in fact registered trademarks or proprietary names even though specific reference to this fact is not always made in the text. Therefore, the appearance of a name without designation as proprietary is not to be construed as a representation by the publisher that it is in the public domain.

Thieme Publishers Stuttgart

Rüdigerstrasse 14, 70469 Stuttgart, Germany

+49 [0]711 8931 421, customerservice@thieme.de

Thieme Publishers New York

333 Seventh Avenue, New York, NY 10001 USA

+1 800 782 3488, customerservice@thieme.com

Thieme Publishers Delhi

A-12, Second Floor, Sector-2, Noida-201301

Uttar Pradesh, India

+91 120 45 566 00, customerservice@thieme.in

Thieme Publishers Rio, Thieme Publicações Ltda.

Argentina Building 16th floor, Ala A, 228 Praia do Botafogo

Rio de Janeiro 22250-040 Brazil

+55 21 3736-3631

Cover design: Thieme Publishing Group

Typesetting by L42 Media Solutions, Berlin, Germany

Printed in Germany by Aprinta, Wemding

5 4 3 2 1

ISBN 978-3-13200-421-4

Also available as an e-book:

eISBN 978-3-13200-431-3



This book, including all parts thereof, is legally protected by copyright. Any use, exploitation, or commercialization outside the narrow limits set by copyright legislation without the publisher's consent is illegal and liable to prosecution. This applies in particular to photostat reproduction, copying, mimeographing or duplication of any kind, translating, preparation of microfilms, and electronic data processing and storage.

To Chrissi and Kati

A master advised his devotees
To only believe in what one sees.
And yet – this we should reconceive,
Some only see what they believe.

Eugen Roth

Contents

Preface	x
Acknowledgments	xi
1 History and Development of Dental Radiography	2
2 Radiation Physics	8
2.1 Types of Radiation	8
2.2 Direct and Indirect Ionization	8
2.3 Corpuscular and Photon Radiation	8
2.3.1 Corpuscular Radiation	8
2.3.2 Photon Radiation	8
2.4 Interactions between Radiation and Matter	9
2.5 Fundamental Physical Processes Involved in the Transfer of Photon Energy to Matter	10
2.5.1 Excitation	10
2.5.2 Ionization	10
2.6 Interactions between X-rays and Matter	10
2.6.1 Absorption—Photoelectric Effect	10
2.6.2 Scattered Radiation—Compton Effect	11
2.7 Radioactivity	11
2.8 Production of X-rays	12
2.8.1 Dental X-ray Equipment	12
2.8.2 Additional Equipment Needed for Dose Limitation and Improvement of X-ray Image Quality	17
3 Dose Terms and Dose Units Used for Ionizing Radiation	22
4 The Biology of Radiation Effects	26
4.1 Fundamentals	26
4.2 Direct and Indirect Effects of Radiation	27
4.3 Effects of Ionizing Radiation on DNA	27
4.4 Repair Mechanisms for the Restoration of DNA	27
4.5 Biological Effects of Radiation Damage	27
5 Radiation Pathology	30
5.1 Natural Radiation Exposure	30
5.1.1 Cosmic Radiation	30
5.1.2 Terrestrial Radionuclides	30
5.2 Artificial Radiation Exposure	30
5.3 Stochastic and Deterministic Effects of Ionizing Radiation	31
5.3.1 Stochastic Effects	31
5.3.2 Deterministic Effects	31
6 Image Formation and Image Processing	34
6.1 Fundamentals	34
6.1.1 Summation Effect	34
6.1.2 Tangential Effect	35
6.2 Image Receptor-Independent Factors Influencing Image Formation	35
6.2.1 Object Contrast	36
6.2.2 Current Intensity and Exposure Time	36
6.2.3 Inverse Square Law	36
6.2.4 High Voltage	36
6.2.5 Scattered Radiation	37

6.3	Radiographic Film and Intensifying Screen-Dependent Factors that Influence Image Formation	37	6.3.2	Radiographic Film with Intensifying Screens	41
6.3.1	Screenless Films	37	6.4	Processing of Radiographic Films	42
7	Digital Dental Radiography	46	7.1	Sensors	47
7.1.1	Spatial Resolution	48	7.2	Storage Phosphor Imaging Plates	48
			7.3	Advantages of Digital Radiography	50
8	Radiation Protection and Quality Assurance in Dental Radiology	54	8.1	History of Radiation Protection	54
8.1.1	Structure of the International Commission on Radiological Protection	54	8.1.2	Tasks and Content of the Various Activities of the International Commission on Radiological Protection	54
8.2	Responsibility for Radiation Protection	55	8.2.1	Supervisory Duty of the Government	55
8.2.2	Administration and Management of Safety	55	8.3	Need and Justification	55
8.4	Optimization of Radiation Protection	55	8.4.1	Limitation and Monitoring of Individual Dose Limits	55
8.4.2	Prevention of Accidents and Protection against Existing or Unregulated Radiation Risks	55	8.5	Implementation of Recommendations by the International Commission on Radiological Protection	55
8.6	Quality Assurance in Dental Radiology	56	8.6.1	Standards	56
8.7	Procedures to Ensure Compliance with Basic Principles of Radiation Protection	56	9	Practical Dental Radiography	58
9.1	Intraoral Radiography	58	9.1.1	Quality Criteria for Intraoral Radiography	58
9.1.2	Principles of Projection Geometry	59	9.1.3	Paralleling Technique	61
9.1.4	Bisecting-angle Technique	67	9.1.5	Right-angle Technique	72
9.1.6	Bitewing Radiography	73	9.1.7	Radiographic Measurement Techniques	74
9.1.8	Occlusal Radiography	74	9.2	Conventional Tomography	77
9.3	Panoramic Tomography	79	9.3.1	Panoramic Radiography with a Slit Collimator	79
			9.3.2	Panoramic Radiography with an Intraoral Source	80
			9.3.3	Rotational Panoramic Radiography	80
9.4	Cone Beam Computed Tomography	109	9.4.1	Technique and Image Formation in Cone Beam Computed Tomography	109
9.4.2	Limitations of Computed Tomography and Cone Beam Computed Tomography	112	9.4.3	Volume Size	114
9.4.4	Clinical Indications for Cone Beam Computed Tomography	114	10	Anatomy and Topography of the Facial Skeleton	120
10.1	The Teeth and Tooth-supporting Structures	121	10.3	The Maxilla	124
10.2	The Mandible	123	10.4	Panoramic Radiographic Anatomy	125
			10.4.1	The Mandible	125
			10.4.2	The Maxilla and Midface	128

11	Radiographic Findings and Diagnosis	134
11.1	Systematic Image Analysis and Interpretation	134
11.1.1	Film and Monitor Viewing Conditions	134
11.1.2	Steps from Findings to Diagnosis	134
11.2	Assessment and Diagnosis of the Most Common Pathological Changes	136
11.2.1	Carious Lesions	136
11.2.2	Horizontal Bone Loss with Vertical Bone Defects	139
11.2.3	Apical Periodontitis	141
11.2.4	Cystic Lesions	143
11.2.5	Malignant Lesions	145
11.2.6	Bone Diseases of the Jaw	155
11.2.7	Sialolithiasis	157
11.2.8	Tooth Fractures	158
	References	161

Preface

Great progress has been made in dental radiology in the last 30 years. This is particularly true for technical developments, but also for education and training in dental radiology at universities.

The introduction of digital image receptors can be viewed as a milestone in the technological development of dental radiology. The introduction of cone beam computed tomography gave dentists the first fully fledged technology for three-dimensional imaging of the oromaxillofacial region.

In parallel, radiation protection legislation has been thoroughly revised. Radiation protection and image quality are two closely intertwined pillars of the X-ray ordinance. Over the years, the International Commission on Radiological Protection has introduced increasingly concrete and detailed provisions. The “as low as reasonably achievable” (ALARA) principle, which states that the patient should only be exposed to as much radiation as reasonably necessary, must also be applied in full to dental radiology.

The key to high-quality radiographic diagnosis is comprehensive training during dental school; this serves to ensure that, in later practice, individuals will only be exposed to X-rays if really necessary. Dentists also learn in dental school how to perform practical radiation protection procedures and how to obtain radiographs of good diagnostic image quality. Moreover, continuing education and training during the course of professional practice is essential. Only those professionals who have up-to-date radiological knowledge and skills can perform X-ray procedures responsibly.

This book describes the essentials of dental radiography without which it would be impossible to understand the concepts of image quality and radiation protection.

Likewise, it explains the fundamentals of X-ray physics and provides practical information and instructions for the different techniques used in dental radiography. The book is designed as a step-by-step guide to help students learn dental radiography. At the same time, it was conceived as a reference to help dentists in private practice and hospitals achieve optimal results in dental X-ray diagnostics in-office or in the university teaching setting.

A good knowledge of the techniques of intraoral radiography and dental panoramic radiography is crucial to obtaining good radiographic image quality. The technique of cone beam computed tomography is becoming more and more established. An exact knowledge of X-ray image formation and of the diverse possibilities for using the enormous amounts of data collected is necessary for optimal use of this wide-ranging technique.

At the end of the X-ray examination, the task at hand is interpretation of the findings, which plays an increasingly important role in dental radiology. Even panoramic radiographs can provide a large number of findings. Images from cone beam computed tomography yield far more diagnostic information. Therefore, many practical aids are given for the optimal interpretation of results.

In order to keep radiation exposure as low as possible, a justifying indication must be established before beginning any type of X-ray examination. A precise knowledge of the many diagnostic possibilities is also absolutely necessary, in order to respect the ALARA principle in dental radiology. Correct practical performance of the examination results in high diagnostic image quality. If all steps are performed and executed according to the latest standards of science and technology, then optimal diagnosis is assured.

Andreas Fuhrmann, DDS

Acknowledgments

First and foremost, I would like to thank Professor Dr. Friedrich Anton Pasler, who asked and encouraged me to write a textbook of dentomaxillofacial radiology. I give him great credit for this because, by doing so, he virtually designated his successor. I consider it a great honor that he chose me.

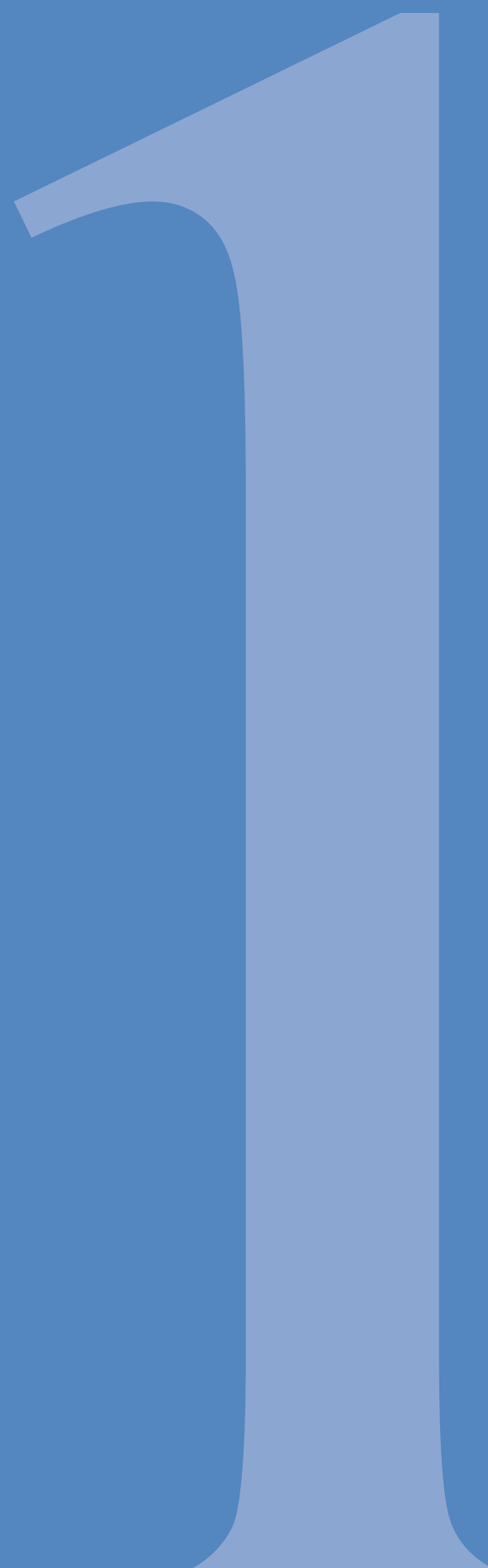
This book is the product of many years of practical and theoretical experience gained while teaching at the Department of Radiology of the Center for Dental and Oral Medicine, University Medical Center Hamburg-Eppendorf, Germany. However, it is not possible to write such a book without support. First, I would like to thank my wife Anne for her patience and understanding. Likewise, I am very much indebted to my staff for a wide range of support.

I would also like to express my gratitude to Dr. Christian Urbanowicz and Dr. Daria Wojciukiewicz from Thieme

Verlag, who supervised the original German edition with large amounts of understanding and practical assistance, and to Angelika-Marie Findgott from Thieme Publishers Stuttgart, without whom there would have been no English edition. The English version has again shown that dental radiology is a very special and challenging field of radiology that demands a high level of expertise and a deep understanding of the complex issues involved. Suzyon O'Neal Wandrey, who provided the translation of the German edition, and Dr. Martina Habeck, who managed the editorial stages of the project, did an outstanding job in creating this English version and making many valuable suggestions for improvement. Finally, I would like to extend a note of thanks to Ruth Gutberlet, who translated the poem by Eugen Roth with wit and skill.

Chapter 1

History and Development of Dental Radiography



1 History and Development of Dental Radiography

While conducting experiments in his laboratory at the Physics Institute of the University of Würzburg, Germany, on November 8, 1895, physicist Wilhelm Conrad Röntgen observed that “a paper screen washed with barium–platinocyanide lights up brilliantly and fluoresces equally well, whether the treated side or the other be turned toward the discharge tube. The fluorescence was observable two meters away from the apparatus.” (□ Fig. 1.1). These are the words that Röntgen used to describe the discovery he made while experimenting with cathode ray tubes. After repeating the experiments several times, he felt certain that he had indeed discovered “a new kind of rays.”

The first preliminary photographic evidence of this discovery probably showed his own hand, but the first “roentgenogram” on reliable record was that of his wife’s hand, taken on December 22, 1895.

Röntgen published the details of his discovery and findings in three communications:

- Preliminary communication dated December 28, 1895: *On a New Kind of Rays* (□ Fig. 1.2)
- Second communication dated March 9, 1896: *On a New Kind of Rays*
- Third communication dated March 10, 1897: *Further Observations on the Properties of X-rays*.

Röntgen himself referred to this new type of radiation as “X-rays.” At the meeting of German Physico-Medical Society on January 23, 1896, where he presented his discovery, it was decided to call them “Roentgen rays” instead. The name “X-rays” is still used in English-speaking countries today. Important dates in the history and development of dental radiography are described below.

- 1896: The first X-rays of the teeth were probably taken in late January and early February 1896. The first dental radiographs on record are those of Friedrich Otto Walkhoff, a German dentist who lay motionless on the floor for 25 minutes to achieve blur-free images during the long exposure time needed. Other dental X-rays from this early period were taken by German

physicist Walter König. In the following years, the introduction of X-ray tubes with a platinum plate anode cut the exposure time in half.

- 1896: C. Edmund Kells described the first film-holder for dental radiography, which was made of highly permeable aluminum. Kells is thus credited as being the father of the paralleling technique. However, the glass plates used as image receptors at that time were generally held in the patient’s mouth by the dentist.
- 1897: The first double-coated celluloid films were made in 1897 but were not used in routine practice until 1923.
- 1897: Edison and Gehler developed intensifying screens that were coated with calcium tungstate.
- 1904–1907: The bisecting-angle technique of intraoral radiography was described by two independent researchers, Price (1904) and Cieszynski (1907) (□ Fig. 1.3).
- 1904–1925: The first dental X-ray machine was developed in 1904. However, the angular tube required for this machine was not developed until 1919 by Garretson, and was first installed in dental X-ray equipment in 1925. These technical advances made it possible to capture different angles of incidence of the beam with much better precision.
- 1921: French inventor André Bocage, the founder of conventional tomography, applied for a patent for a functional tomographic unit.
- 1921: Owing to the lack of suitable film-holders for the paralleling technique, Collins Le Master proposed the use of “a roll of absorbent cotton cemented or otherwise secured to the film holder,” to align the plane of the film perpendicular to the axis of the teeth.
- 1925: Howard R. Raper developed the bitewing examination technique for optimal detection and diagnosis of approximal caries.

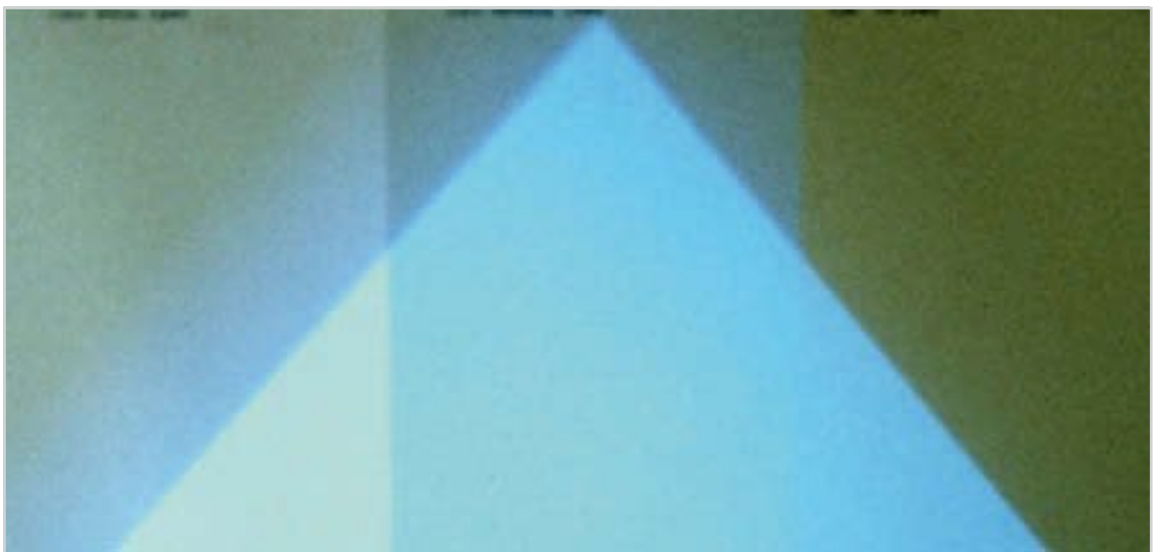


Fig. 1.1 Fluorescence of intensifying screens of three different thicknesses.



Fig. 1.2 Detail of the title page of the Proceedings of the Meeting of the Würzburg Physico-Medical Society, Germany, in 1895.

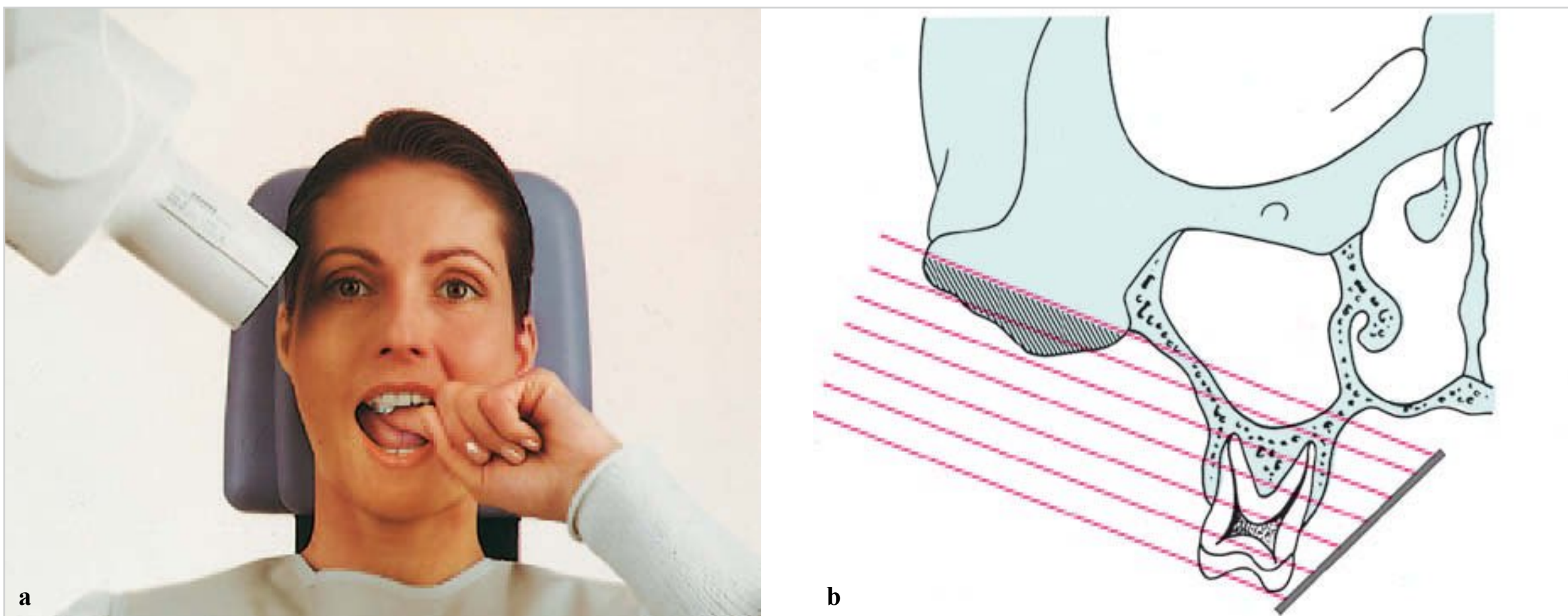


Fig. 1.3a, b Image distortion in the root region associated with use of the bisecting-angle technique. (From: Pasler FA, Visser H. Zahnmedizinische Radiologie. 2nd ed. Stuttgart: Thieme; 2000. Farbatlanten der Zahnmedizin; Band 5.)

- a** Bisecting-angle technique: Positioning of the film packet.
b Zygomatic bone projecting to the root region.



Fig. 1.4 X-ray sphere introduced by Siemens.

- 1928: The first dental X-ray units with high-voltage protection were placed on the market.
- 1931: Hofrath and Broadbent introduced cephalometric radiography into orthodontics.
- 1933: The first X-ray systems housing the X-ray tube and generator in a single unit were developed. The Siemens X-ray sphere is the most famous representative of this group of dental X-ray machines (□ Fig. 1.4). The so-called single-tank construction method was thus introduced into dental radiography (□ Fig. 1.5).
- 1933: Numata developed a panoramic radiography method capable of imaging the entire upper or lower dental arch using a slit-beam technique (□ Fig. 1.6).
- 1946–1952: Paatero independently developed a similar system in 1946. Unlike Numata, Paatero continued to develop his invention. Between 1949 and 1952, he introduced an X-ray machine for panoramic tomography or pantomography (□ Fig. 1.7).

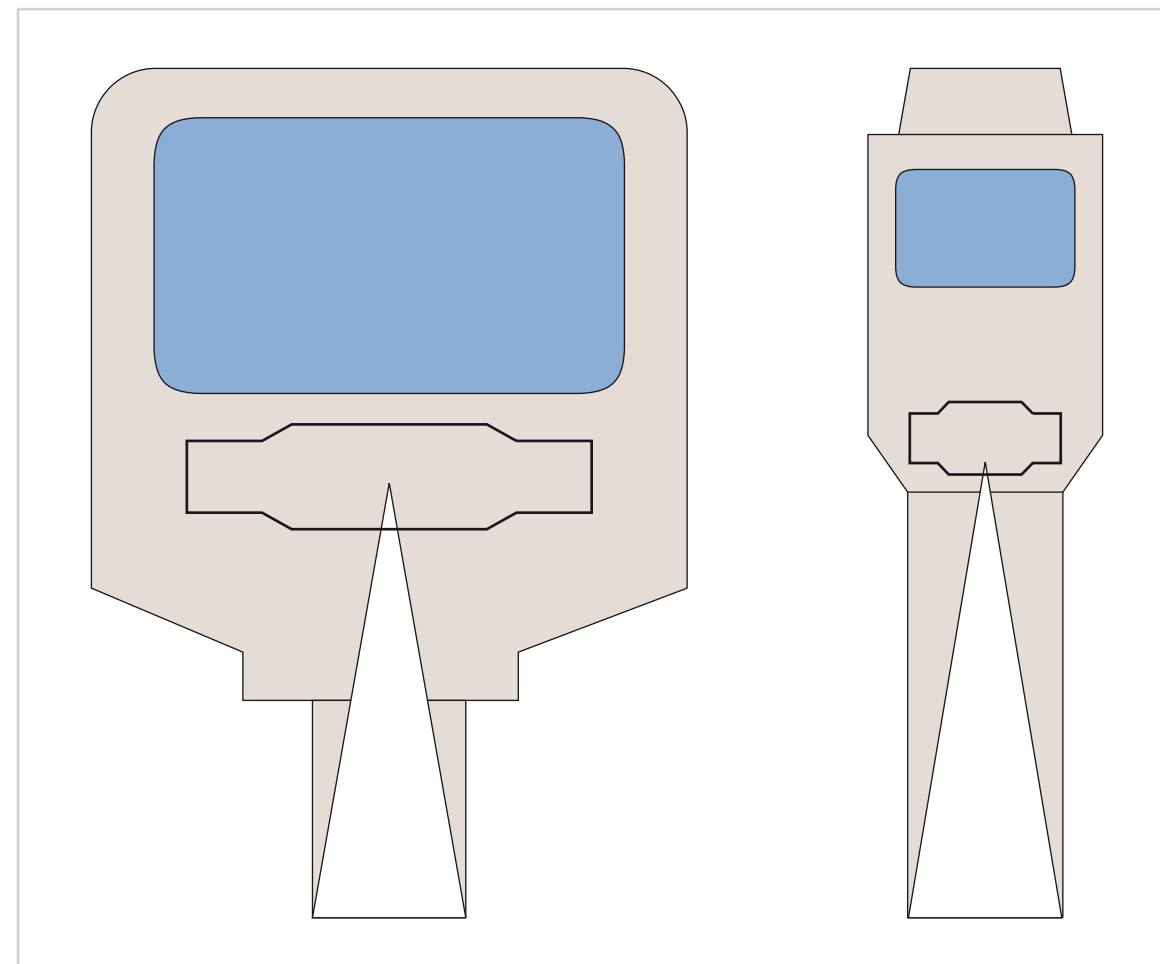


Fig. 1.5 Modern technology has greatly reduced the size of the dental X-ray head. A large older model is shown on the left, and a significantly scaled-down modern dental X-ray head (Heliodent 70) is shown on the right. The space required for the transformer is highlighted in blue.

- 1956: This year marked the introduction of the Panorex X-ray machine, the first double eccentric panoramic unit.
- 1959–1961: In this period, there was continued development proceeding from the pantomograph to the orthopantomogram.
- 1961: Magnification was introduced to panoramic radiography by Ott and Blackman (□ Fig. 1.8 and □ Fig. 1.9).
- 1974: Further development of dental panoramic tomography started in 1974.
- 1982: The Zonarc panoramic X-ray machine (□ Fig. 1.10), which had many new scanning programs for the head and neck region, was introduced (□ Fig. 1.11).

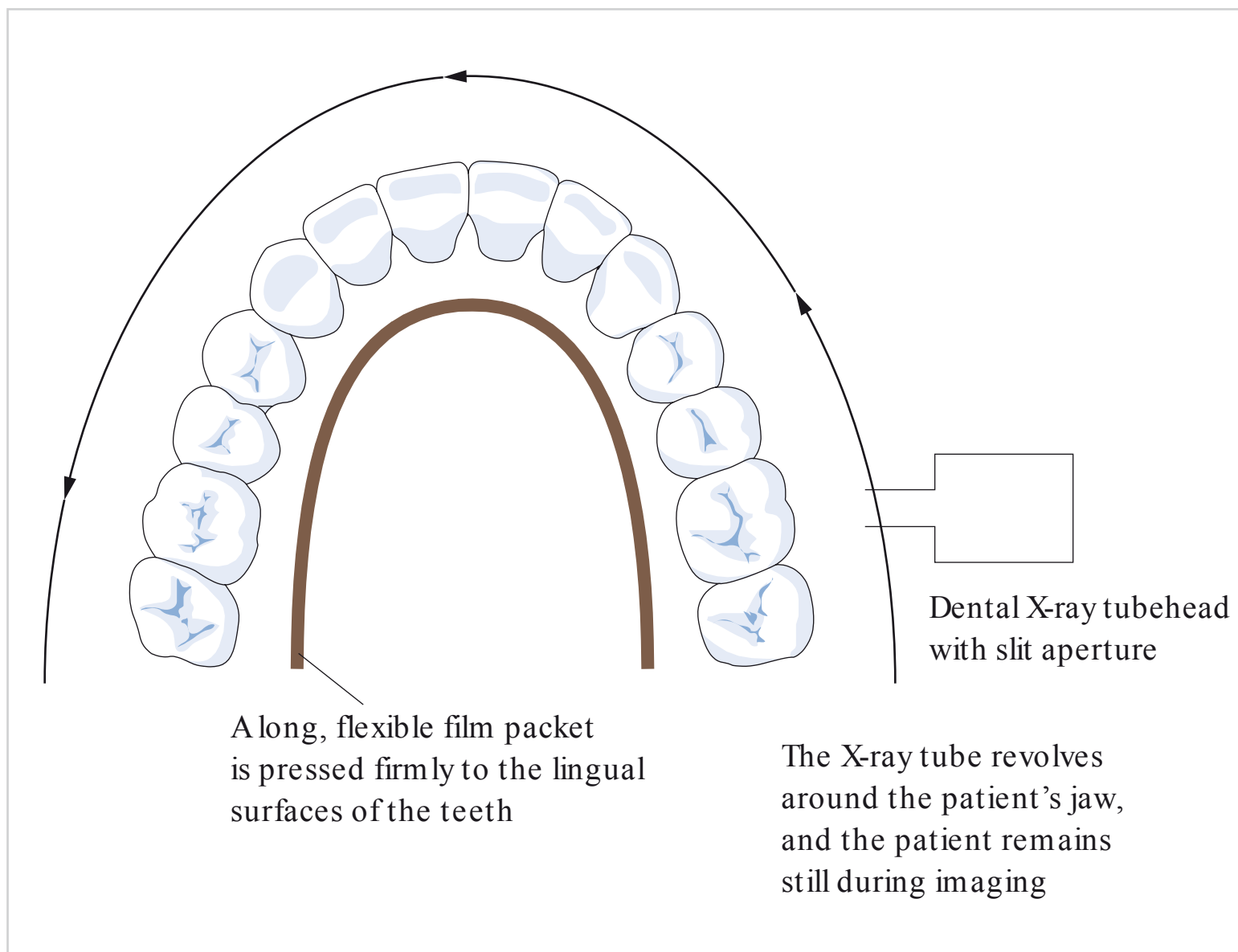


Fig. 1.6 Schematic diagram of a panoramic radiograph (based on Numata's method of slit-beam intraoral panoramic radiography).



Fig. 1.7 Panoramic radiograph of a patient by Paatero.

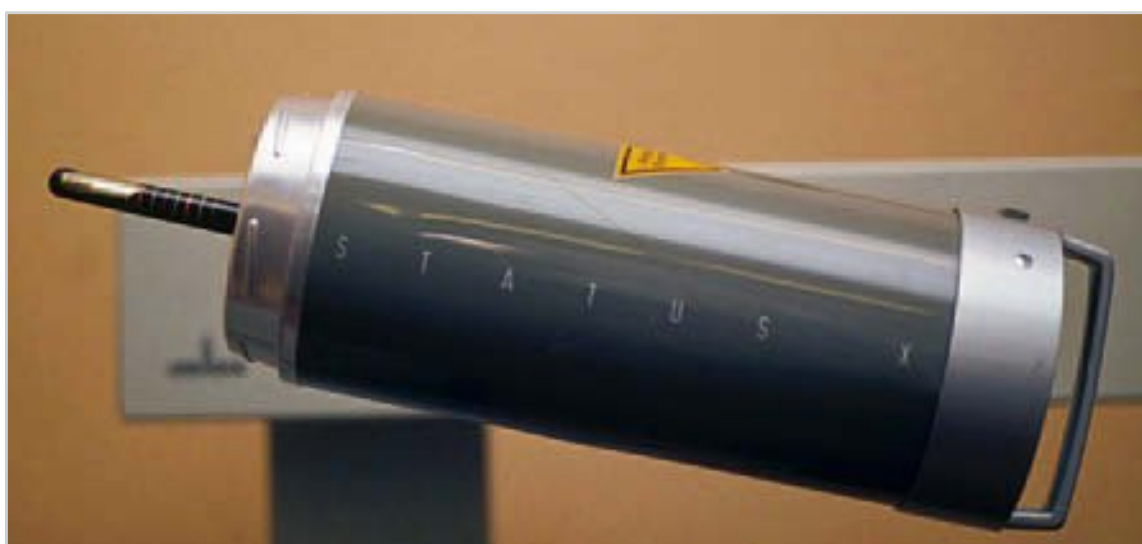


Fig. 1.8 Status-X panoramic X-ray apparatus by Siemens.



Fig. 1.9 This magnified panoramic radiograph taken with the Status-X shows a residual root in the right maxillary sinus of the upper jaw.



Fig. 1.10 Zonarc panoramic radiography device for supine patients.



Fig. 1.11 Zonarc panoramic radiography device for midfacial imaging.



Fig. 1.12 NewTom cone beam computed tomography system for supine patients.



Fig. 1.13 Galileos cone beam computed tomography system.

- 1985: The Scanora, a combined system for panoramic radiography and conventional spiral tomography, was introduced in 1985.
- 1987: This year marked the beginning of digital radiography in dental, oral, and maxillofacial surgery.
- 1995: Digital technology for panoramic radiography was introduced.
- 1995: “Transverse panoramic tomography” was the buzzword in 1995.

- 1998: Digital cone beam computed tomography (CBCT) was introduced as a tomographic method designed specifically for imaging of bony structures in the head region (□ Fig. 1.12).
- 2007: The Galileos digital CBCT system for standing and seated patients (□ Fig. 1.13) was launched on the market.
- 2010: A combined panoramic radiography and CBCT system was introduced.

Chapter 2

Radiation Physics

2.1	Types of Radiation	8
2.2	Direct and Indirect Ionization	8
2.3	Corpuscular and Photon Radiation	8
2.4	Interactions between Radiation and Matter	9
2.5	Fundamental Physical Processes Involved in the Transfer of Photon Energy to Matter	10
2.6	Interactions between X-rays and Matter	10
2.7	Radioactivity	11
2.8	Production of X-rays	12

2 Radiation Physics

2.1 Types of Radiation

All life on our planet is exposed to different types of naturally occurring radiation. This radiation generally occurs in the form of electromagnetic waves that differ only by wavelength. Some radiation can be seen or felt if it occurs at a few specific wavelengths but, in most cases, radiation cannot be detected by our sense organs. This applies in particular to rays with very short wavelengths beyond the ultraviolet end of the light spectrum.

Radiation is defined as the emission and propagation of energy.

When radiation strikes an object, the energy generated in the radiation field triggers interactions in the object. The body can withstand a good deal of radiation but biological damage starts when it is exposed to short-wavelength radiation.

Radiation in the infrared range is perceived as heat radiation that is not uncomfortable. Ultraviolet radiation, however, starts to induce damage associated with chemical reactions in the skin that can produce sunburn.

Radiation at even shorter wavelengths is able to knock electrons out of an atom. This process is called ionization and such radiation is referred to as ionizing radiation.

Note

There are two basic types of radiation: ionizing radiation and nonionizing radiation.

2.2 Direct and Indirect Ionization

Radiation is further characterized by the manner in which its ionizing effects occur.

In the case of directly ionizing radiation, the energy from electrically charged particles is transferred directly to the irradiated structures. Alpha particles, beta particles, and protons are types of directly ionizing radiation.

In indirectly ionizing radiation, interactions with the irradiated matter result in the generation of electrically charged particles which, in turn, transfer their energy to surrounding structures. X-rays and gamma rays are forms of indirectly ionizing radiation.

2.3 Corpuscular and Photon Radiation

Ionizing radiation can be divided into two types, according to its physical consistency: corpuscular radiation and photon radiation.

The fact that nuclei may be stable or unstable is one reason why these two types of radiation occur. Stable nuclei are an important part of our everyday lives and are generally harmless. Unstable nuclei, on the other hand, emit ionizing radiation and it is important to protect the body from this type of radiation as well as possible.

2.3.1 Corpuscular Radiation

Alpha and beta radiation are common types of corpuscular radiation. Corpuscular radiation is directly ionizing radiation generated by the spontaneous decay of unstable atomic nuclei. This process is known as radioactivity.

Alpha particles consist of helium nuclei, while beta particles are high-energy free electrons.

Alpha and beta rays consist of particles with rest mass; therefore, they have a relatively short range. Typically, alpha radiation has a range of only a few centimeters in air. Its range in tissue is less than 1 mm because the attenuation of radiation passing through tissue is very large. The range of beta radiation depends on the energy of the radiation and varies from a few meters in air to only a few millimeters in tissue.

2.3.2 Photon Radiation

X-rays and gamma rays are forms of electromagnetic radiation.

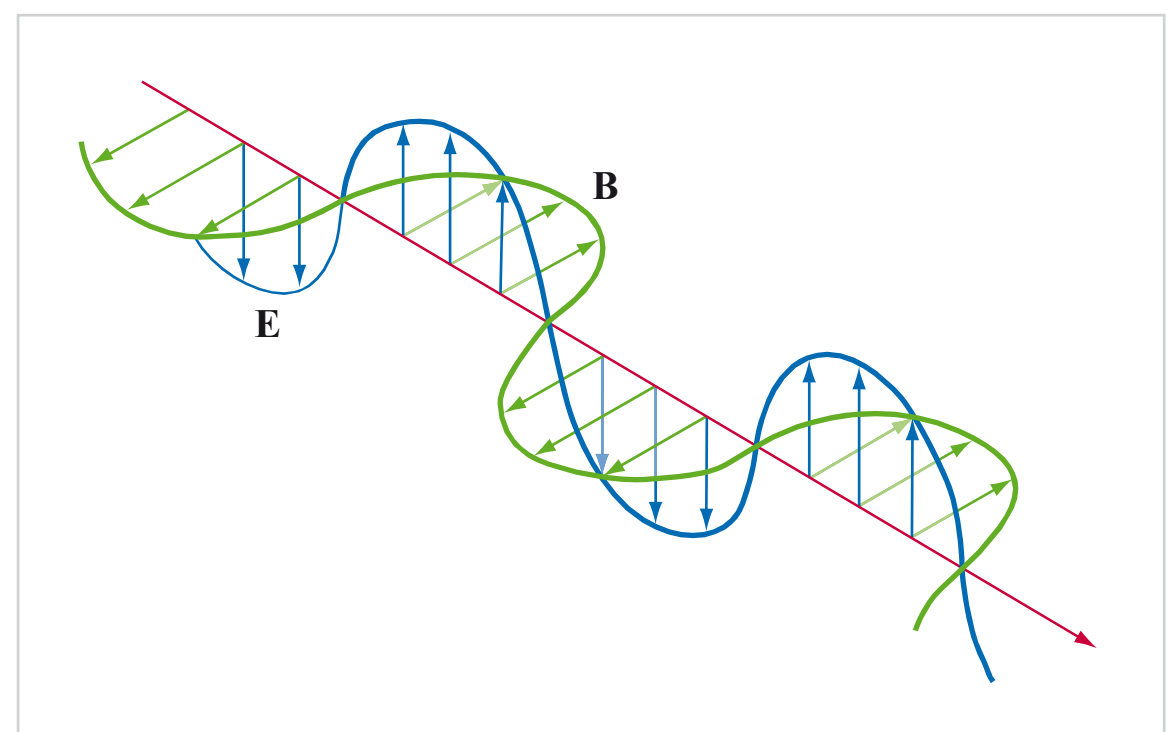


Fig. 2.1 Electromagnetic waves. **B**: magnetic flux density; **E**: electric field strength. (Adapted from: Zabel H. Kurzlehrbuch Physik. Stuttgart: Thieme; 2011.)

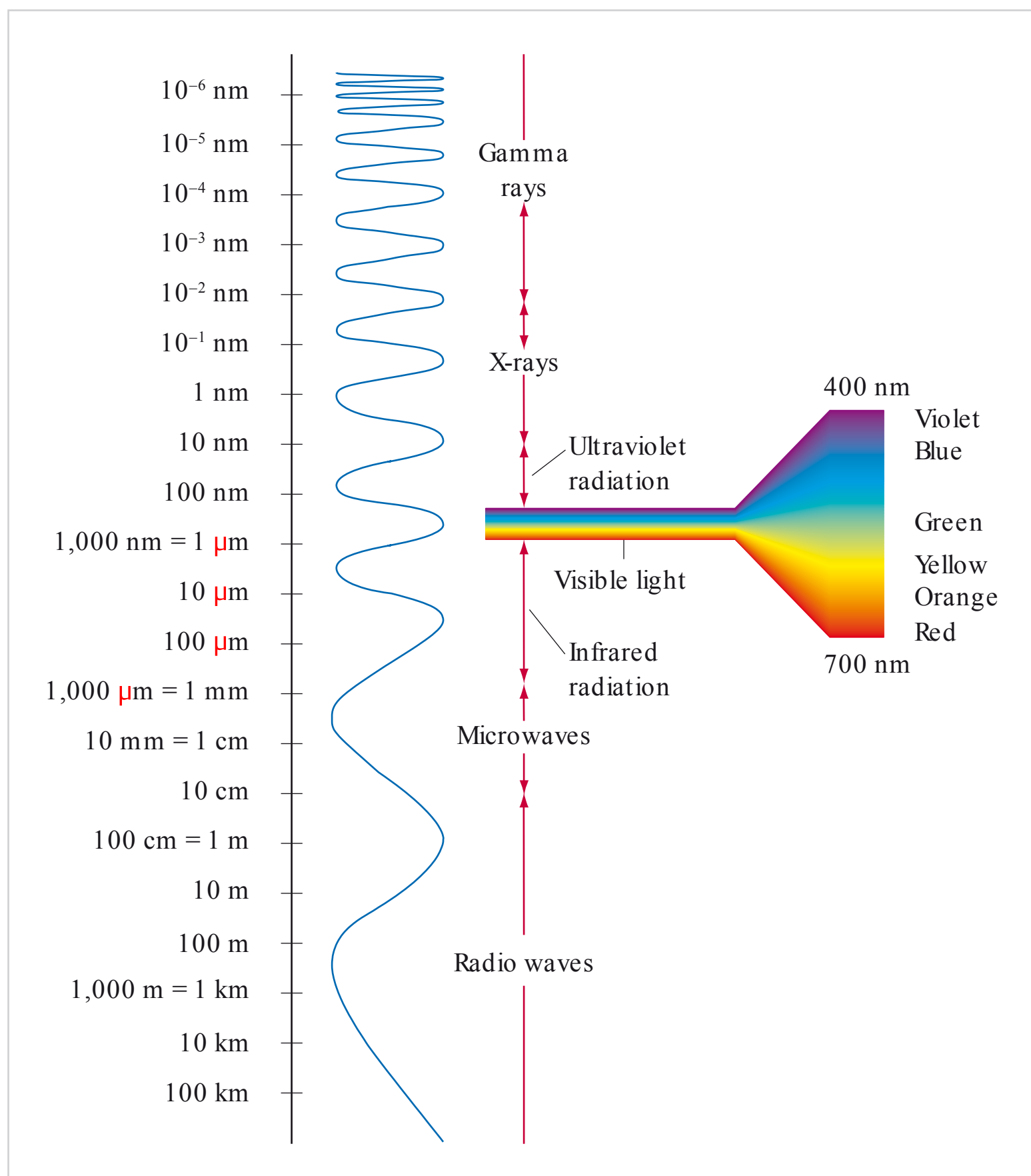


Fig. 2.2 The electromagnetic spectrum. (From: Zabel H. Kurzlehrbuch Physik. Stuttgart: Thieme; 2011.)

Electromagnetic waves are made from electric and magnetic fields. Electric fields and magnetic fields are closely related. Electromagnetic waves are transverse waves because the electric field waves are perpendicular to the magnetic flux density (□ Fig. 2.1).

Unlike corpuscular radiation, photon radiation has no rest mass. Therefore, it travels at the speed of light in air as well as in a vacuum.

The entire electromagnetic spectrum consists of photon and electromagnetic radiation wavelengths, ranging from very long-wavelength radio waves to very short-wavelength gamma rays (□ Fig. 2.2).

2.4 Interactions between Radiation and Matter

The main physical processes involved in energy transfer are the excitation and ionization of atoms exposed to radiation.

Knowledge of the structure of atoms is therefore needed to understand the processes associated with ionization.

From the work of Ernest Rutherford (1911) and Niels Bohr (1913), it is known that an atom consists of a positively charged nucleus surrounded by a shell of negatively charged electrons that travel in circular orbits around the nucleus.

The number of electrons corresponds to the atomic number or nuclear charge of the atom. The atomic number is equivalent to the number of protons in the nucleus. The characteristic position of an element on the periodic table is determined by its atomic number. Atoms normally have an equal number of electrons and protons, so they are electrically neutral.

The fact that the electrons revolve around the nucleus in different paths is important for various reactions involving photons. The orbits or shells are represented, from the nucleus outwards, by the letters K, L, M, N, O, P, and Q. Each shell can accommodate a fixed number of electrons. The shell capacity ranges from two electrons in the K shell to 18 electrons in the M shell. The number of electrons that can be accommodated in a shell increases with the atomic number of an element. The higher the atomic number of an element, the larger the number of electrons that it can accommodate. This, in turn, has an effect on the absorption behavior of the element.

Note

The more electrons an element has, the more photons it can absorb. This fact plays an important role in the recognition of different tissues and in diagnostics.

2.5 Fundamental Physical Processes Involved in the Transfer of Photon Energy to Matter

When incoming photons strike matter, two physical processes may occur: excitation or ionization.

2.5.1 Excitation

The addition of energy to an atom from an external source can cause electrons to be displaced from an inner shell of the atom to an outer shell. This very brief state is called excitation. In the process of excitation, no electron is ejected from the atom and no ionization occurs. Since the shells of an atom must always be full, the vacancies created in now incomplete inner shells must, in turn, be filled by electrons from outer shells. In the process, the electrons that fall from the outer shells to fill the vacancies in the inner shells emit energy in the form of electromagnetic photon radiation. The vacancies left in the outer shell resulting from this electron movement must, in turn, be filled by other free electrons.

If these electron shell-to-shell transitions occur in the region of the innermost shell, then enough energy is generated for the production of X-rays. Since the wavelength of these X-rays is dependent on the specific type of anode material, this kind of radiation is referred to as characteristic X-rays. Conversely, electron shell-to-shell transitions in the region of the middle shells result in the production of ultraviolet light, and those in the region of the outermost shell result in the production of low-level energy perceived as visible light.

Note

Electron shell-to-shell transitions in the region of the innermost shell of an atom result in the release of energy in the form of electromagnetic radiation at wavelengths in the range of X-rays.

2.5.2 Ionization

Ionization occurs when the energy of an incident photon is completely absorbed and transferred to an electron. The amount of energy transferred in the process is so great that it overcomes the binding energy of the electron, knocking the electron out of its shell and ejecting it from the atom. Such an atom is said to be ionized. The ejected electron can, in turn, ionize other atoms.

2.6 Interactions between X-rays and Matter

When incident X-rays collide with matter, they pass through the matter but are attenuated in the process. In physical terms, the energy of the photons is either absorbed or propagates further as scattered radiation. The amount of attenuation is determined by the thickness, density, and atomic number of the irradiated material.

Note

As X-rays pass through the body, the X-ray beam is attenuated, or weakened as a result of the absorption of photons and the production of scattered radiation.

2.6.1 Absorption—Photoelectric Effect

The absorption of radiation takes place mainly within the inner shells of an atom. Since X-ray beams consist of photons, X-ray absorption is also referred to as the photoelectric effect (□ Fig. 2.3). A fraction of the energy of the incoming X-ray photon is used to eject an electron from its inner shell, and the emitted photon receives the remaining energy as kinetic energy. Subsequently, the ejected electron induces more photoelectric effects in other atoms.

As in excitation, the vacancy left in the inner shell of an atom due to the ejection of electrons is then filled by electrons dropping down from outer shells. The energy released in the process is emitted from the atom in the form of characteristic X-radiation.

The photoelectric effect plays a crucial role in diagnostic radiography, where voltages of up to 100 kilovolts (kV) are applied. The lower the kilovoltage level, the greater the photoelectric absorption, and the higher the atomic number of the irradiated material, the greater the photoelectric effect. This is why bony structures are best visualized at lower kilovoltage levels of around 50 kV. From levels of around 60 kV, the photoelectric effect decreases sharply with increasing kilovoltage, with a proportional increase in scattered radiation. The size of the two fractions is approximately equal at 60 kV.

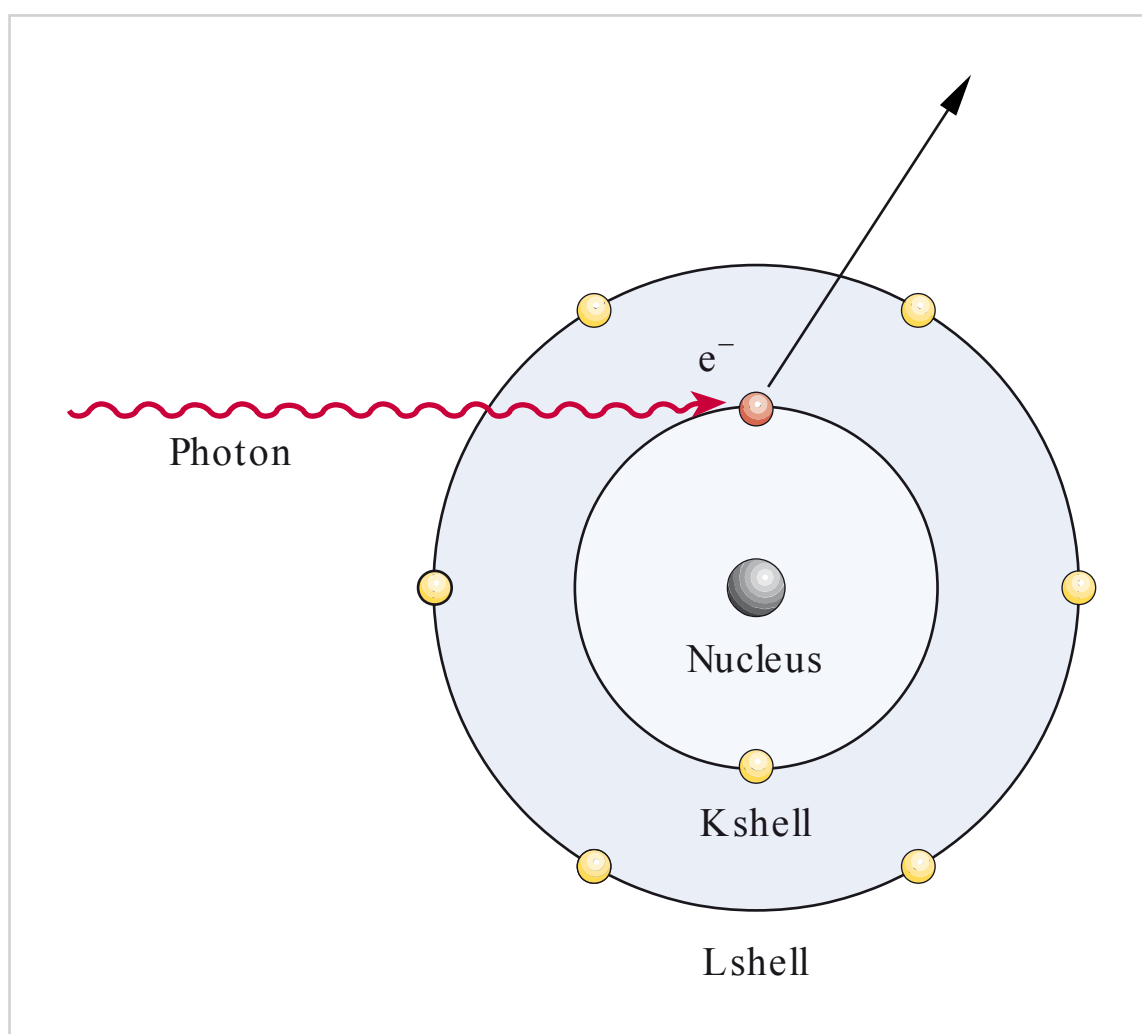


Fig. 2.3 Photoelectric effect. (From: Schwenzer N, Ehrenfeldt M, eds. Chirurgische Grundlagen. 4th ed. Stuttgart: Thieme; 2008.)

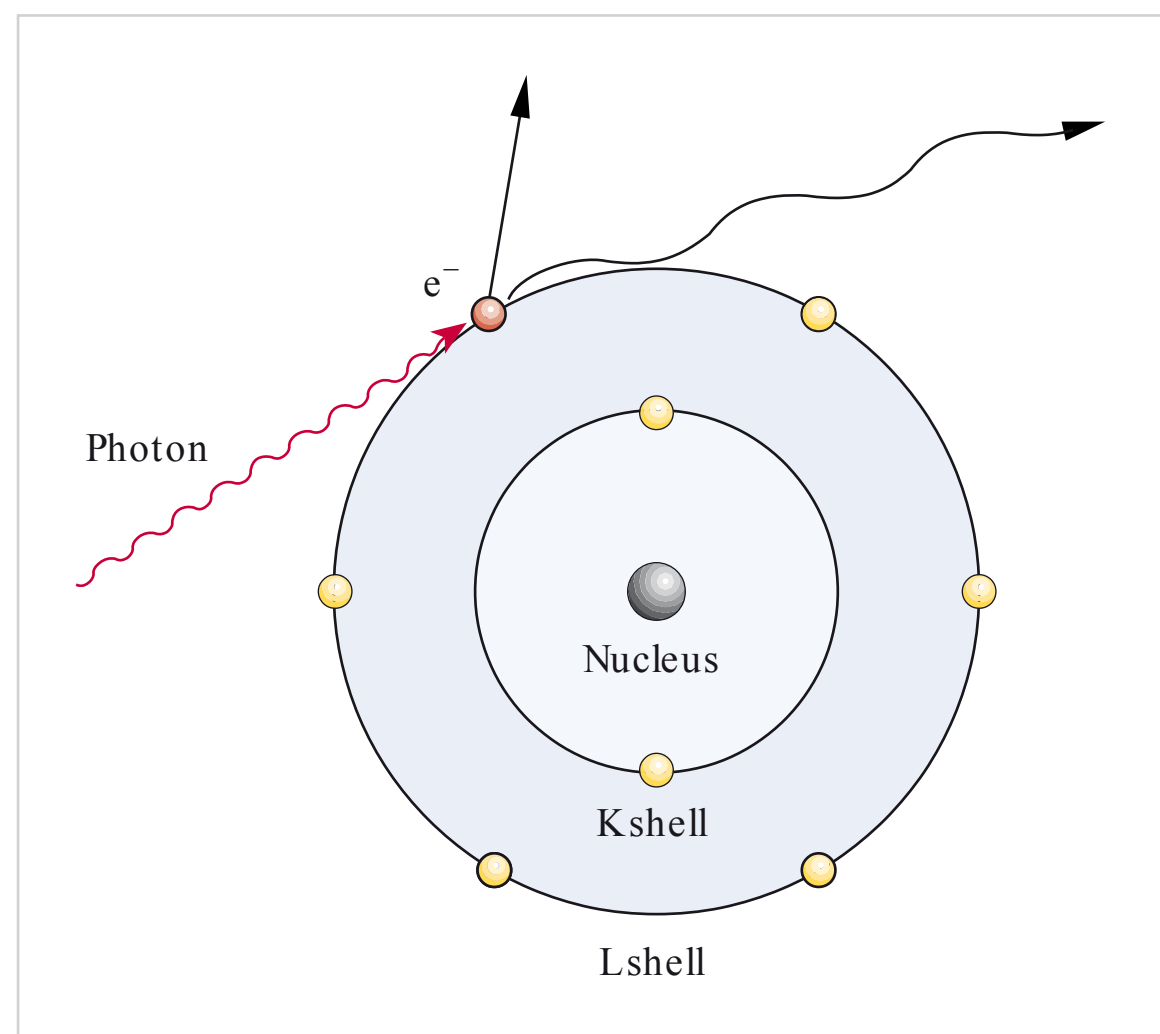


Fig. 2.4 Compton scattering. (From: Schwenzer N, Ehrenfeldt M, eds. Chirurgische Grundlagen. 4th ed. Stuttgart: Thieme; 2008.)

2.6.2 Scattered Radiation—Compton Effect

Besides the photoelectric effect, the second physical process that plays an important role in diagnostic radiology is the Compton effect, or Compton scattering. The Compton effect also involves the ejection of an electron from its atomic shell. However, unlike the photoelectric effect, outer-shell electrons are affected rather than inner-shell electrons. Because outer-shell electrons have relatively low binding energy, they can be more easily ejected from an atom. Therefore, only a fraction of the incoming photon energy is required to eject these electrons. The remaining energy is deflected from the atom, at an angle of 0 to 180 degrees, as a scattered photon. Therefore, the angle of scattering can be quite large (□ Fig. 2.4). In spite of the energy loss, the ejected electron and scattered radiation can still undergo further ionization interactions.

Since scattered X-rays can travel in all directions, they strike the image receptor (e.g., X-ray film) from arbitrary angles. Therefore, scattering results in a significant reduction of contrast.

The Compton effect is a major factor determining the energy level used in dental X-ray imaging. At 60 kV, photoelectric and Compton-effect interactions are approximately equal.

Classical scattering without energy loss and pair production does not play a role in diagnostic radiology. The reason for this is that classical scattering only occurs with very “soft” X-rays and pair production only occurs in the mega electron volt (MeV) range.

Note

The photoelectric effect has its greatest effect at low voltages of up to ~50 kV. X-ray images produced in this low-voltage range are characterized by high contrast. This high contrast is possible because the scattered radiation component is very small, resulting in very sharp visualization of bony structures. On the other hand, these so-called soft-rays are associated with a very large degree of absorption and thus disproportionately high radiation exposure.

This is why all dental X-ray machines that used to operate at 50 kV were prohibited. Today, radiation protection guidelines stipulate that the kilovoltage of dental X-ray machines must not be less than 60 kV. This operating kilovoltage achieves a good compromise between the quality of the dental X-ray image and radiation exposure.

2.7 Radioactivity

Atoms with stable nuclei have an equal number of protons and neutrons. If, however, the number of neutrons differs from the number of protons (that is, if the neutron to proton ratio is too low or too high), then the atom has an unstable nucleus. Unstable nuclei undergo radioactive decay at variable rates and are ultimately converted back into stable nuclei. Nuclei undergoing radioactive decay are termed radioactive nuclides (radioactive isotopes), or radionuclides (radioisotopes) for short. Radioactivity refers to the process of radioactive decay.

Radioactive radiation consists mainly of alpha particles (helium nuclei), beta particles (electrons), and gamma rays (very high-energy electromagnetic radiation).

It is categorized by source as terrestrial, cosmic, or artificial radiation. The different types of radiation have different mechanisms of action.

2.8 Production of X-rays

2.8.1 Dental X-ray Equipment

In dental X-ray equipment, the X-ray generator and X-ray tube are contained together in the same radiation-proof housing. This modern single-tank design allows the manufacture of small and easy-to-handle X-ray machines, which are very well suited for use in dental radiography (□ Fig. 2.5 and □ Fig. 2.6).

The X-rays are generated in a glass X-ray tube (□ Fig. 2.7). The glass X-ray tube contains all the essential technical components required for the generation of X-rays.

The X-ray tube and the generator producing the high and low voltage needed for the production of X-rays are located together in the radiation-proof housing. The radiation-proof X-ray tube housing is completely filled with oil, which acts as an insulator.

The radiation-proof housing of all X-ray machines must be inspected regularly to prevent leakage radiation. Oil leakage is a sure sign of defects in the radiation-proof housing. If oil leakage is detected, operation of the equipment must be stopped immediately.

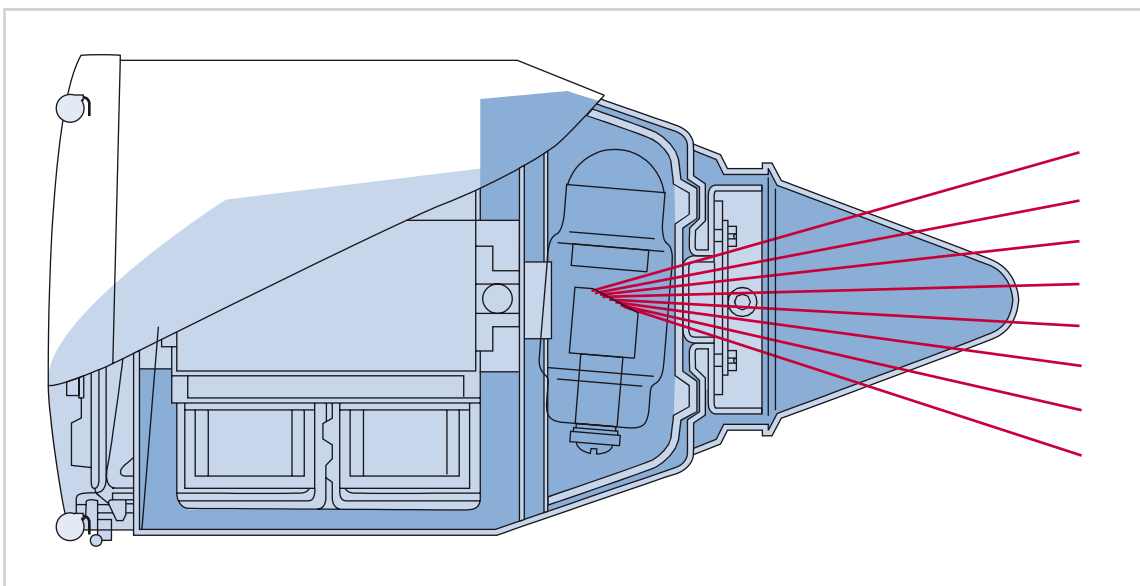


Fig. 2.5 Dental X-ray tube with a short spacer cone (may no longer be used today).

X-ray Tube Design

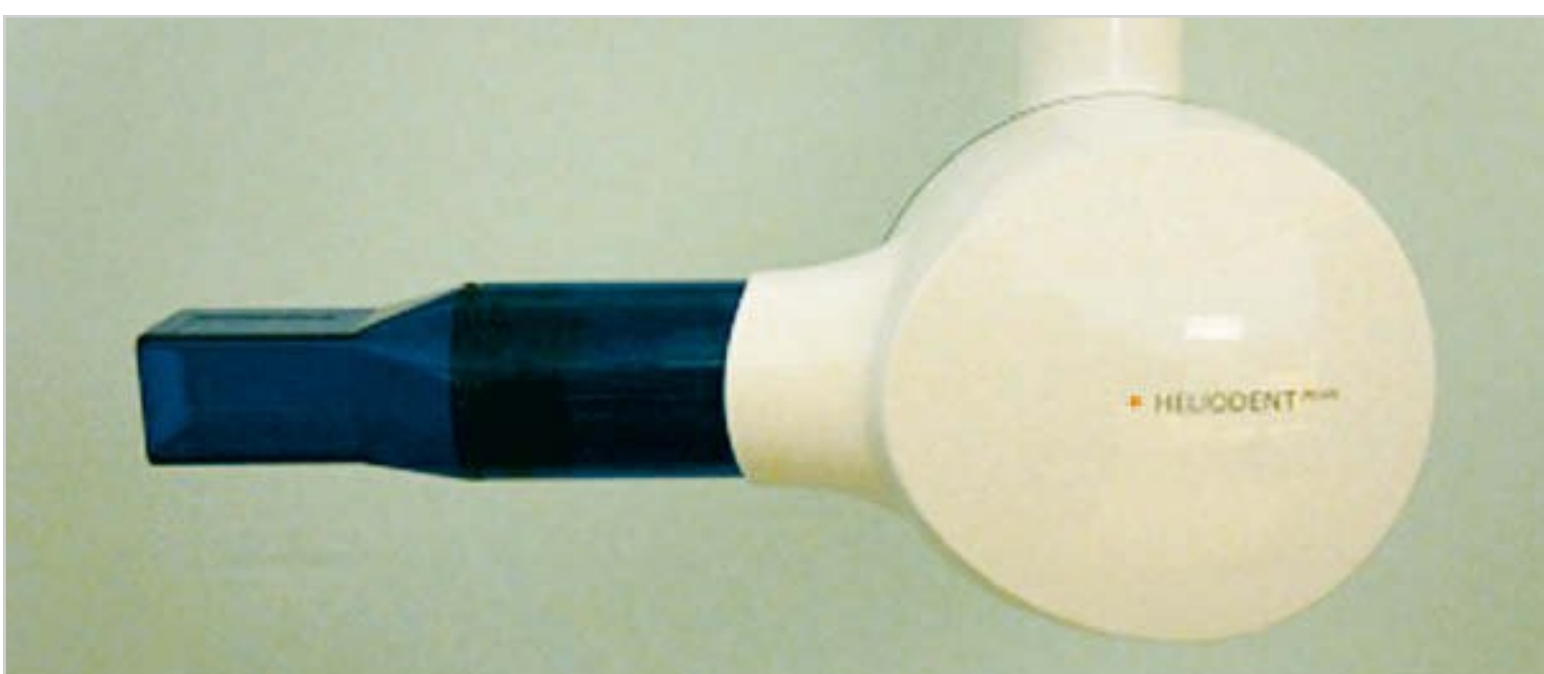
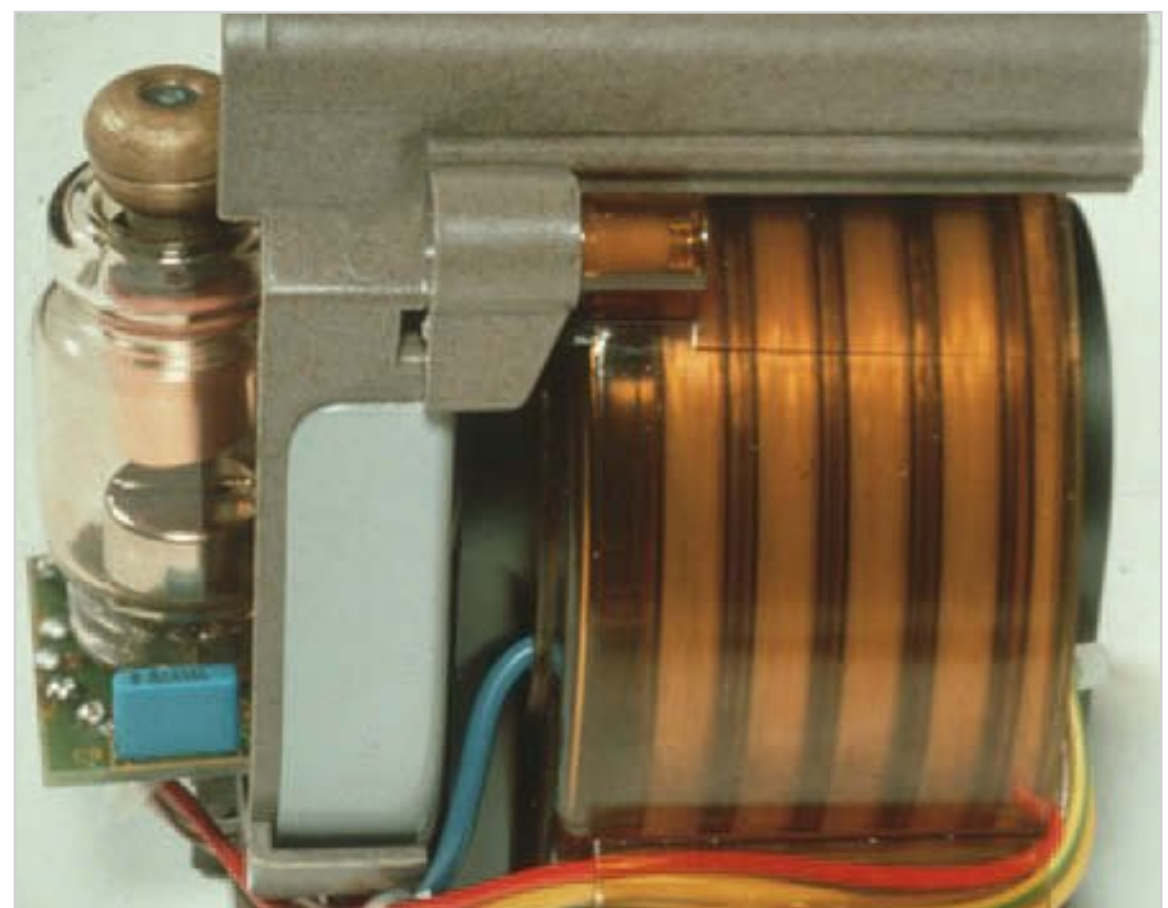
X-rays are produced when high-speed electrons coming from the cathode are suddenly decelerated or stopped by the anode (□ Fig. 2.8).

To produce X-rays, several technical requirements must be met. First, the X-ray tube must be sealed in an evacuated glass envelope. Second, it must have a cathode that serves as the source of electrons. Third, a braking mechanism must be present that is capable of withstanding the high temperatures produced by the deceleration of high-energy electrons, when temperatures as high as 2,500 °C may occur.

The material requirements for the cathode and anode are thus extremely high. Last but not least, the X-ray tube must have a good cooling system that must be able to conduct heat away efficiently.

Cathode

To ensure an adequate supply of electrons for acceleration, a filament heating circuit delivers low voltage (8–12 V) and current (3–6 A) to the cathode filament. The filament, which generally consists of a coiled tungsten wire, is thus heated to incandescence (2,000 °C). Owing to the intense heat, electrons detach from the metal surface and



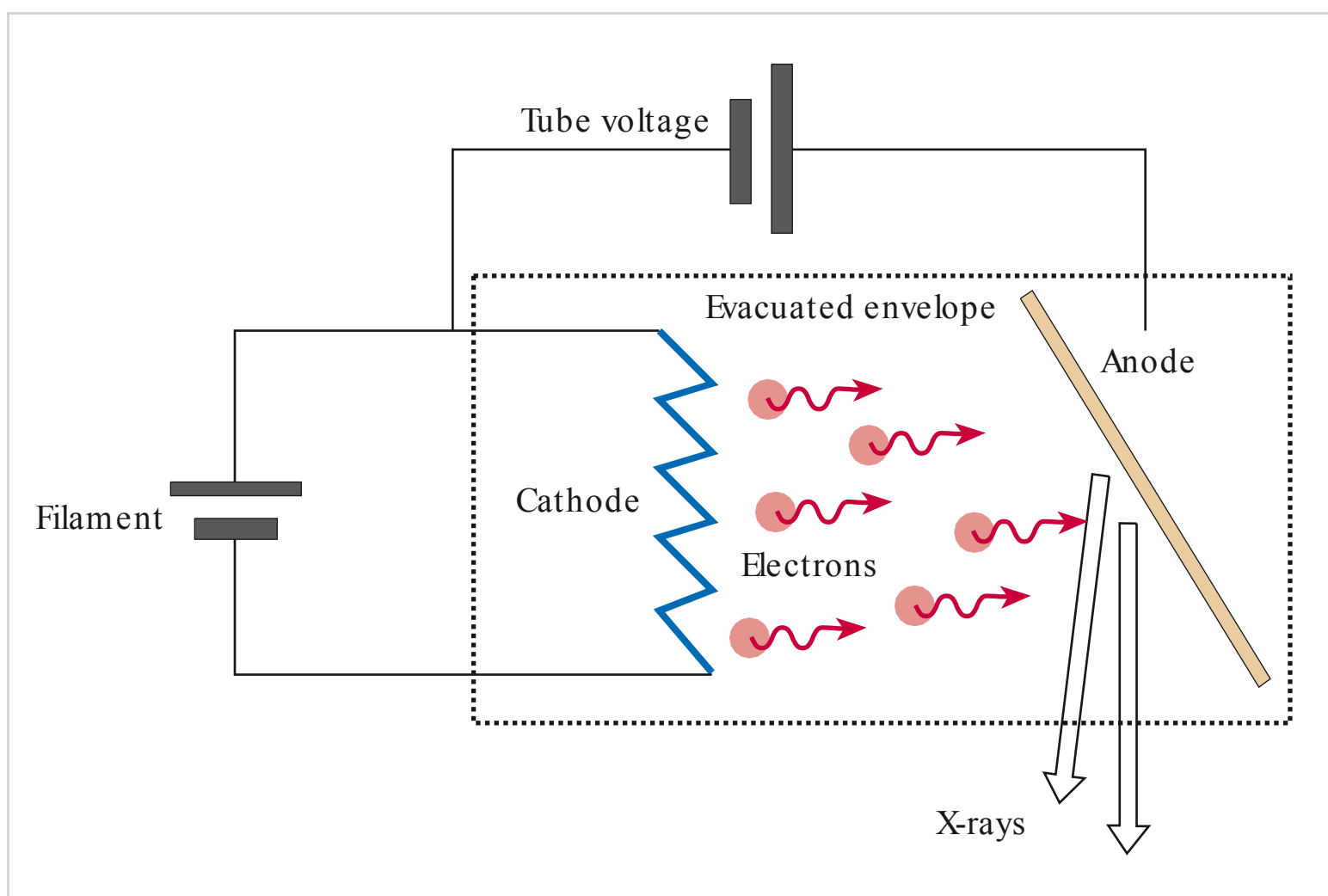
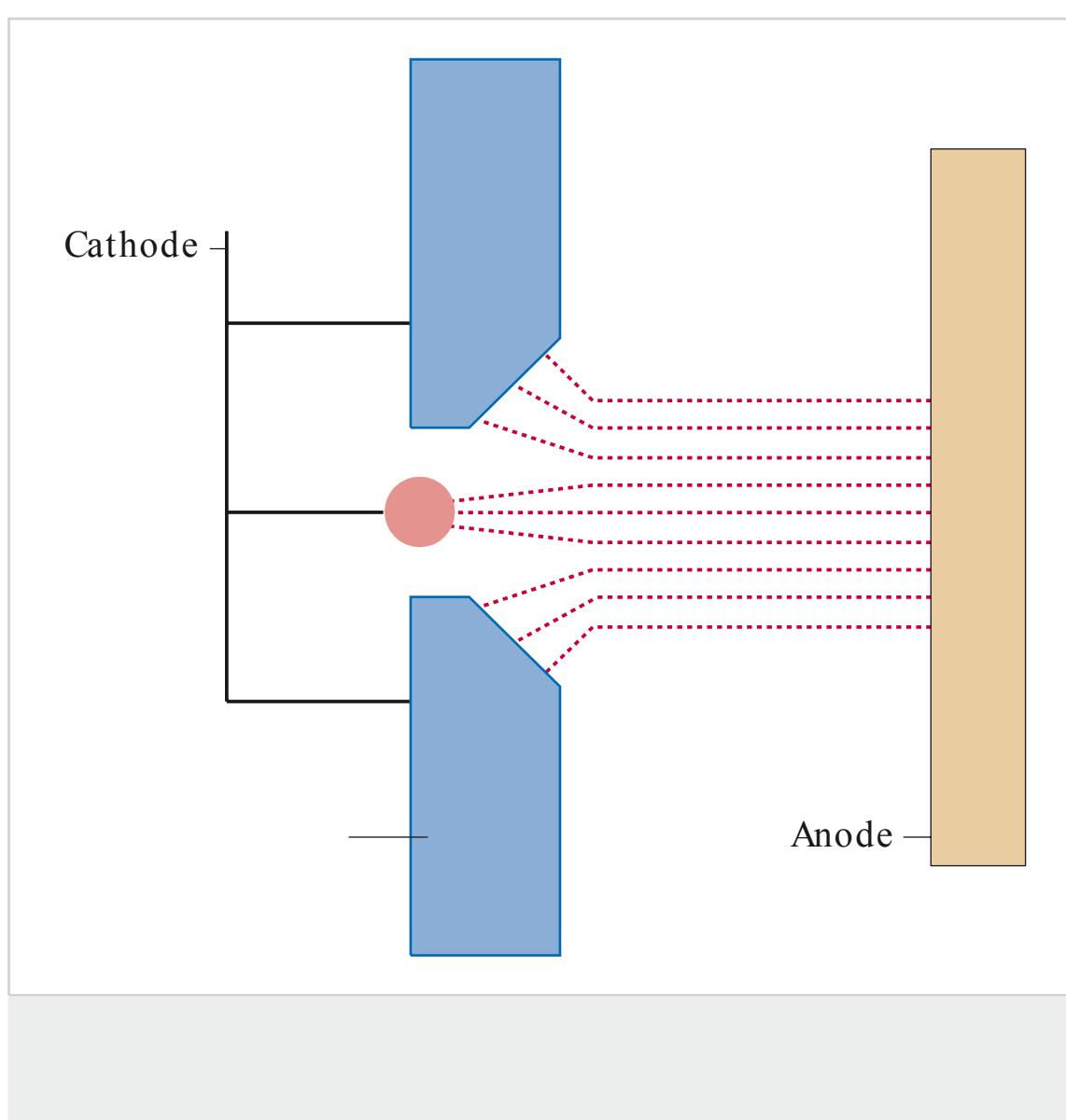


Fig. 2.8 High-speed electrons striking the anode. (From: Albes G. Facharztprüfung Radiologie. 2nd ed. Stuttgart: Thieme; 2010.)



are released as a cloud of electrons in a process known as thermionic emission.

Since the focal spot on the anode is smaller than the electron cloud emitted from the tungsten wire, the electrons must be guided toward the anode. The Wehnelt cylinder, a negatively charged electrode that surrounds the cathode, serves to focus and guide the emitted electron beam so that it converges and strikes the anode at a precisely defined point, to produce the smallest focal spot possible (□ Fig. 2.9).

Anode

A second circuit is needed to produce the high voltage required to accelerate the electrons toward the anode. Unlike the filament heating circuit, the accelerating circuit runs on very high voltage and low current.

High voltage is necessary for the generation of X-rays. In accordance with radiation protection guidelines, dental X-ray machines must not be operated at voltages of less than 60 kV. The current intensity is generally less than 1 A.

Since dental X-ray machines work on low tube current, stationary anodes can be used (□ Fig. 2.10).

Stationary anodes consist of a small tungsten–rhenium plate (anode target) embedded in a block of copper designed to dissipate heat.

Rotating anodes are used in X-ray machines with higher performance, that is, machines that produce more electrons that bombard the anode (□ Fig. 2.11). William Coolidge introduced the rotating anode in 1916. Rotating anodes have a circular rotating plate that rotates at speeds of 3,000 to 90,000 rpm. Rotating anodes distribute the heat produced in the process of X-ray generation over a larger area, which reduces the overheating and wearing of anode material. Tungsten–rhenium alloy is used as the anode material.

To reduce geometric unsharpness, the size of the focal spot should be as small as possible. However, for material reasons (owing to high-temperature heat production), the so-called focal spot can never be an actual point source. Therefore, there will always be some degree of geometric unsharpness, which will inevitably impair image quality to some extent.

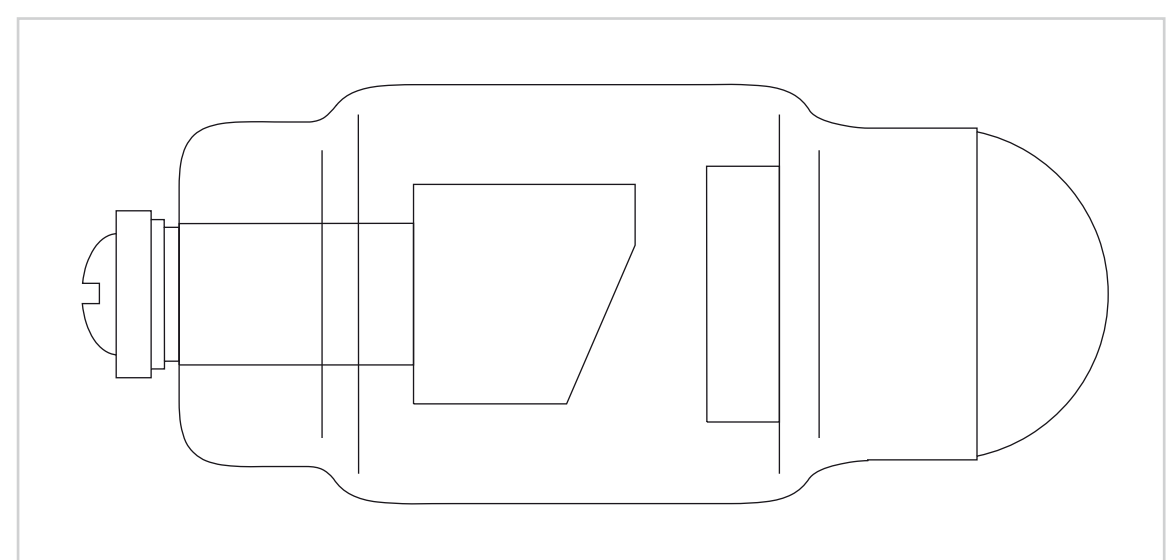


Fig. 2.10 Stationary anode.

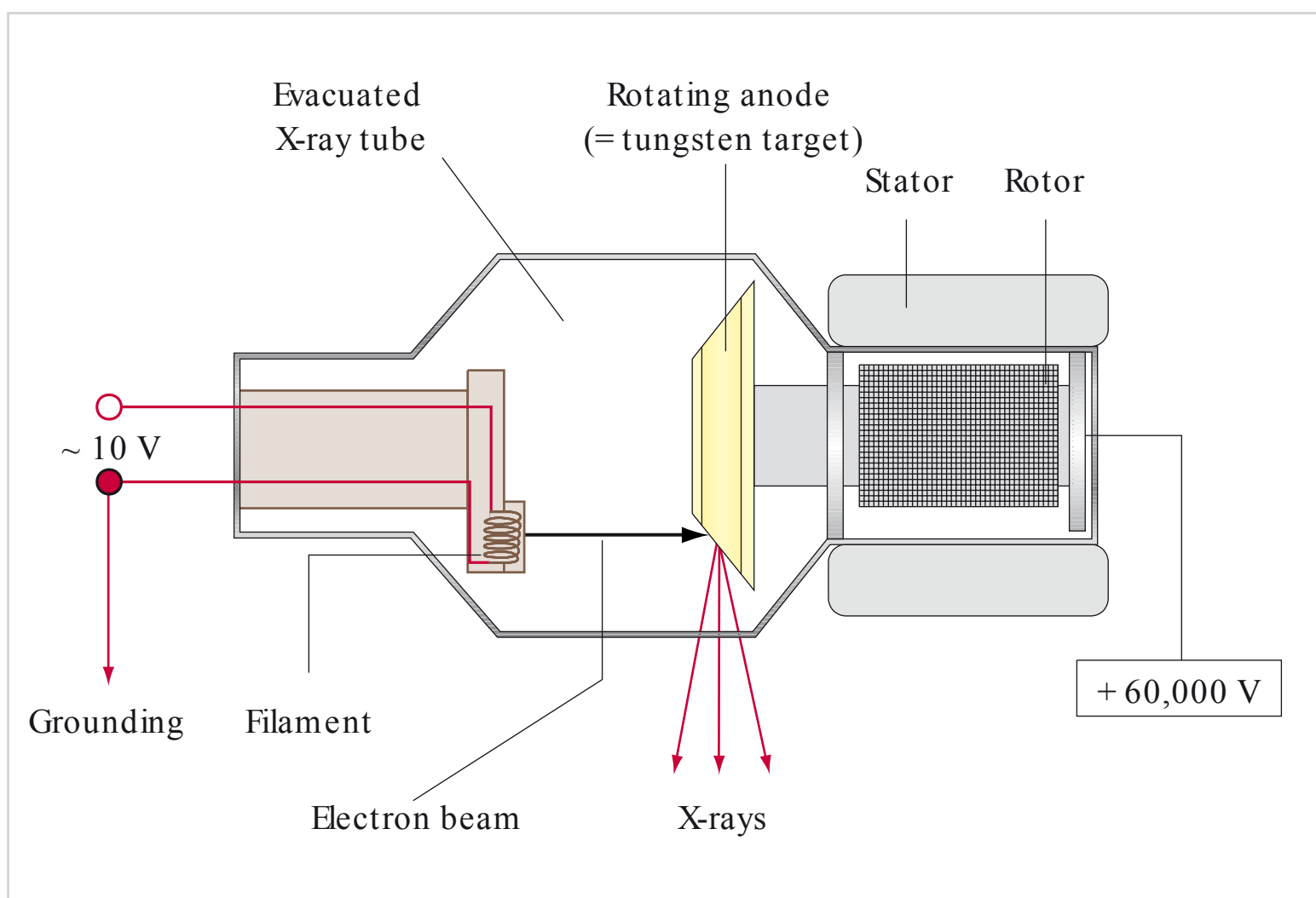


Fig. 2.11 Rotating anode. (From: Zabel H. Kurzlehrbuch Physik. Stuttgart: Thieme; 2011.)

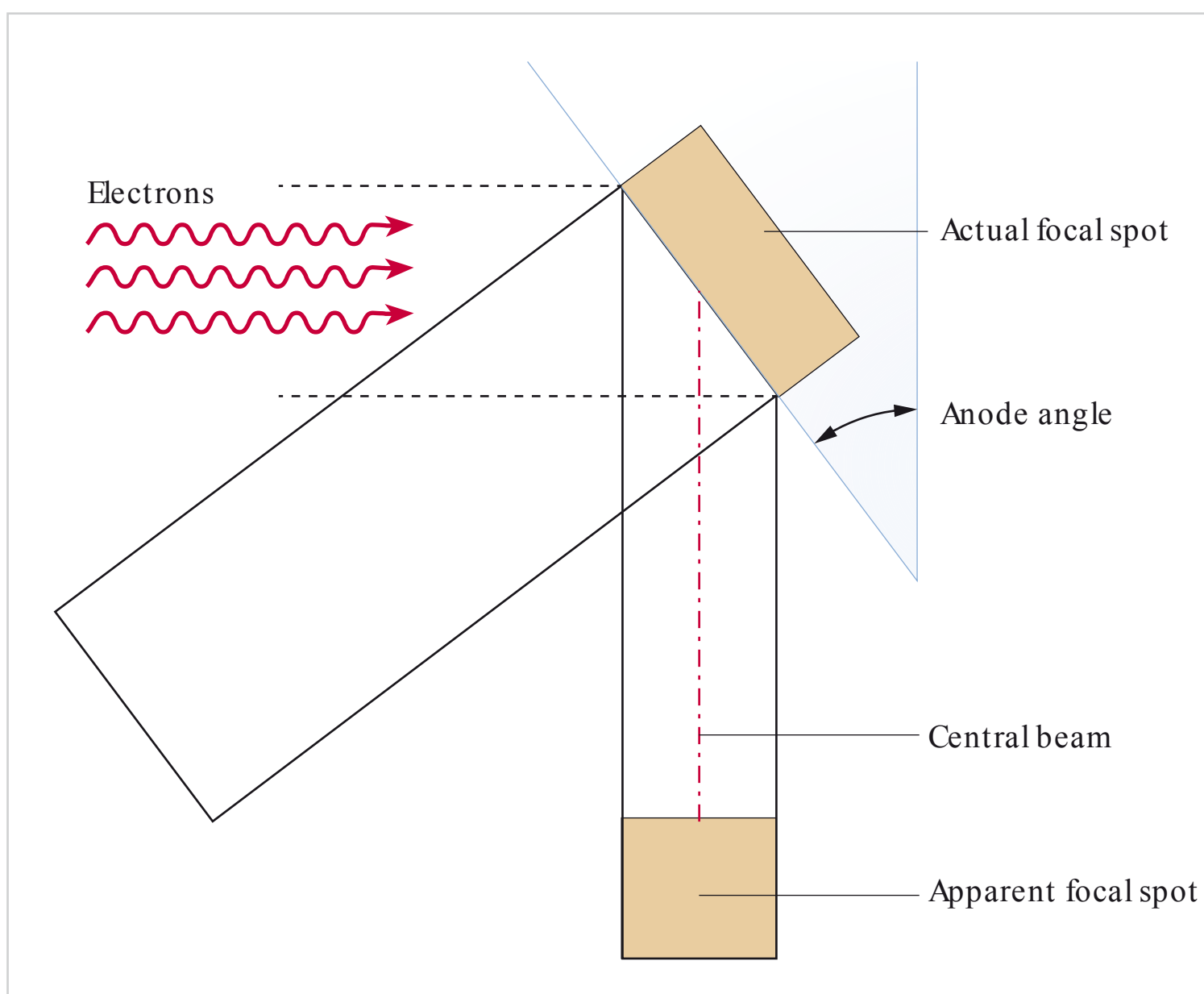


Fig. 2.12 Angulation of the anode for the production of a small apparent focal spot (schematic diagram).

To make the focal spot size as small as possible, it is artificially reduced by using an angled target and the line focus principle. Consequently, the size of the *effective* focal spot is smaller than that of the *actual* focal spot. This is accomplished by angulation of the anode relative to the beam (□ Fig. 2.12). Owing to the vertical configuration of the filament and Wehnelt cylinder, a narrow rectangular focal spot is produced on the small (~2 mm) tungsten–rhenium plate of the anode. By changing the anode angle to ~15 degrees, the shape of the apparent focal spot also changes. Instead of appearing as a line, the projected electrons from the filament are now focused as a rectangle, corresponding to the apparent (effective) focal spot. Dental X-ray machines have an effective focal spot size of ~0.6 × 0.6 mm.

Multi-pulse Generators

Multi-pulse generators have been used for many years to improve the performance of dental X-ray machines. In generators of this type, the primary mains voltage of alternating (AC) current is rectified and smoothed and then processed and transformed into higher-frequency AC voltage. This transformed voltage is subjected to further high-frequency transformation, rectification, and smoothing (□ Fig. 2.13).

Multi-pulse generators increase the efficiency of dental X-ray machines significantly and protect them from voltage fluctuations in the power grid.

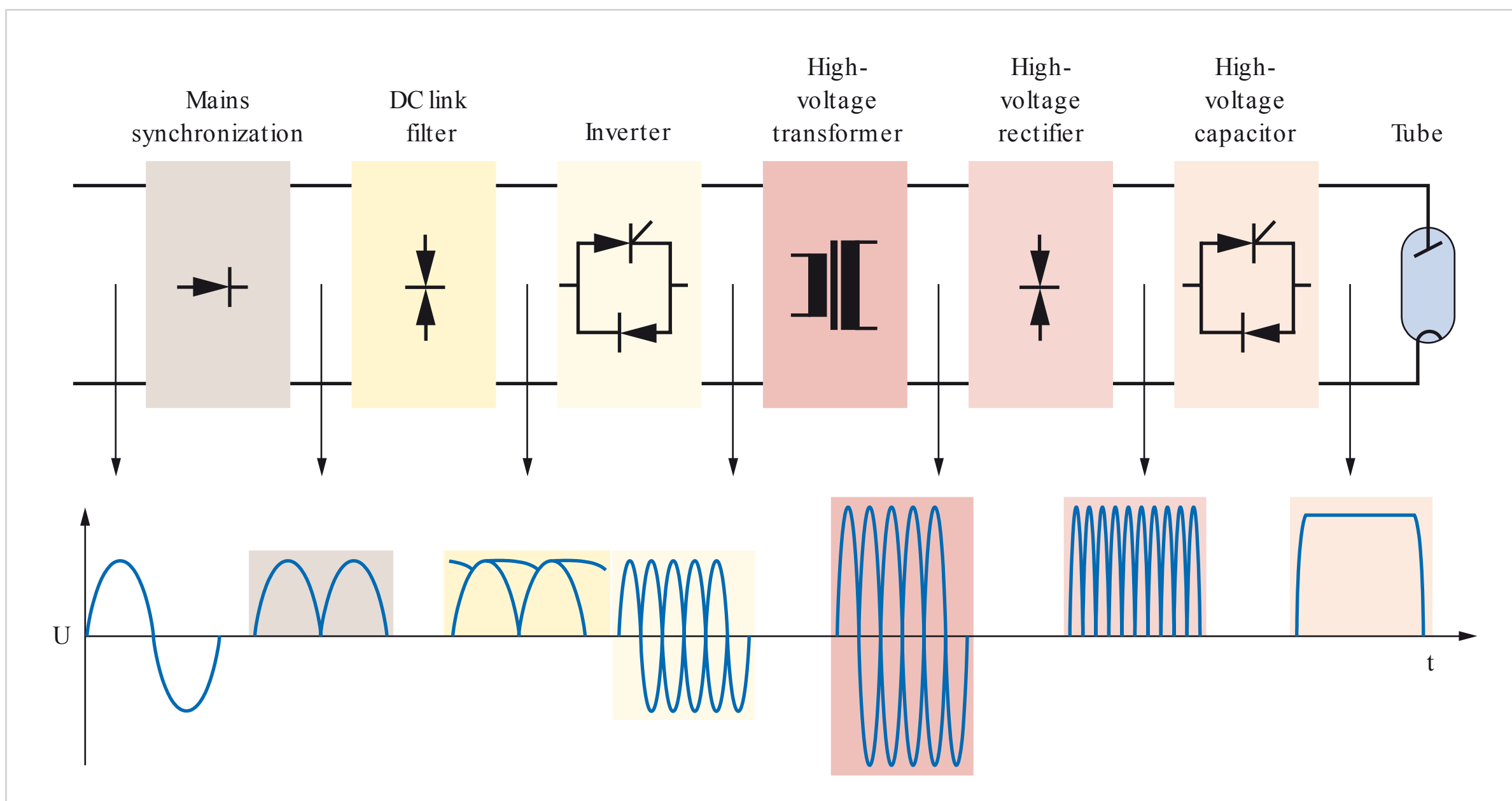


Fig. 2.13 Operating principle of a multi-pulse generator.

Note

An X-ray tube has two electrical circuits: a filament heating circuit that supplies low voltage and current to the cathode for the generation and emission of electrons, and a high-voltage circuit that supplies accelerating voltage to the anode for the acceleration of electrons produced at the filament.

An increase in filament heating voltage results in increased emission of electrons. If the filament heating voltage cannot be adjusted, then the number of electrons produced must be controlled by adjusting the exposure time. The amount of electrons affects the degree of blackening (density) of X-ray film.

An increase in voltage (kV) results in generation of X-rays with higher energy, shorter wavelengths, and greater penetrating power. The decision to use high voltage depends on the thickness and density of the imaged object. An increase in voltage affects contrast but not density (the degree of darkening of X-ray film).

Interactions of Electrons with the Anode Material

When electrons are suddenly decelerated or stopped by the anode, 99% of the energy of the electrons is converted into heat, and only 1% is converted into X-rays.

Two physical processes lead to the generation of two different types of X-rays: (1) characteristic X-rays, which are produced when electrons from the cathode strike electrons on the innermost shells of an atom, and (2)

bremsstrahlung, or “braking radiation,” which is produced from the kinetic energy lost by electrons that are decelerated by the nucleus of an atom.

Characteristic X-rays

Characteristic X-rays are produced by interactions of the electrons coming from the cathode with shell electrons in the atoms of the anode material.

According to the Bohr model of the atom, electrons can move from shell to shell around the nucleus of an atom, but cannot exist outside of the shells. The number of electrons in a given shell is exactly defined and cannot be changed without consequences for the atom. When a high-speed electron coming from the cathode enters the atom, displaces an electron from an inner shell, and ejects it from the atom, leaving a vacancy in the shell, then this vacancy must be filled by another electron. Consequently, an electron from a higher-energy outer shell must fall down to the lower-energy inner shell to fill the vacancy left by the ejected electron. The vacancy in the outer shell must, in turn, be filled by another electron. Energy is thereby released in the form of characteristic X-rays, or characteristic radiation (□ Fig. 2.14).

Bremsstrahlung

When electrons from the cathode come close to the nucleus, they are deflected in the electric field of the nucleus. The kinetic energy lost by the electrons in the process does not “vanish” but is converted into photons, or energy quanta.

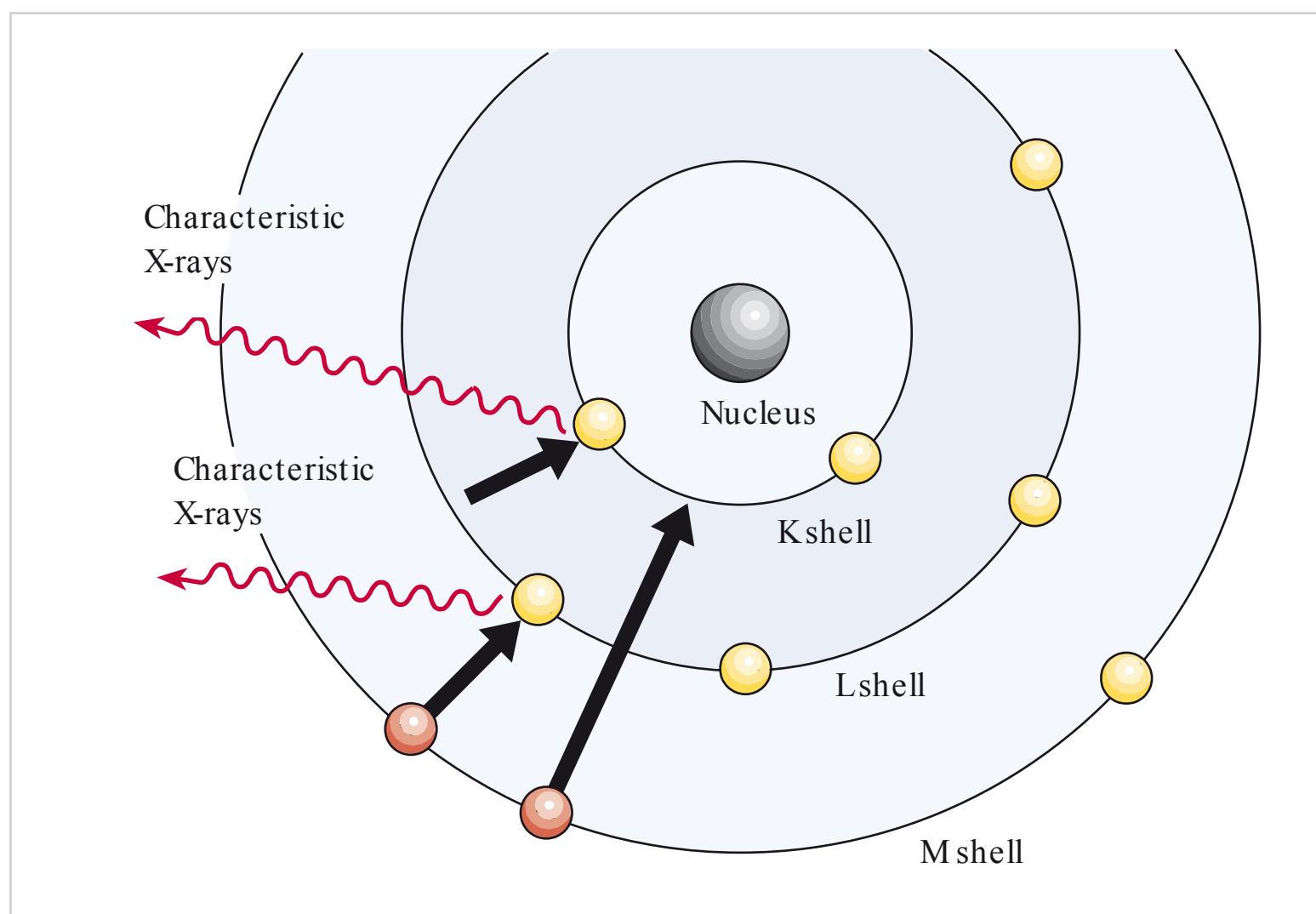


Fig. 2.14 Characteristic X-rays (schematic diagram). (From: Albes G. Facharztprüfung Radiologie. 2nd ed. Stuttgart: Thieme; 2010.)

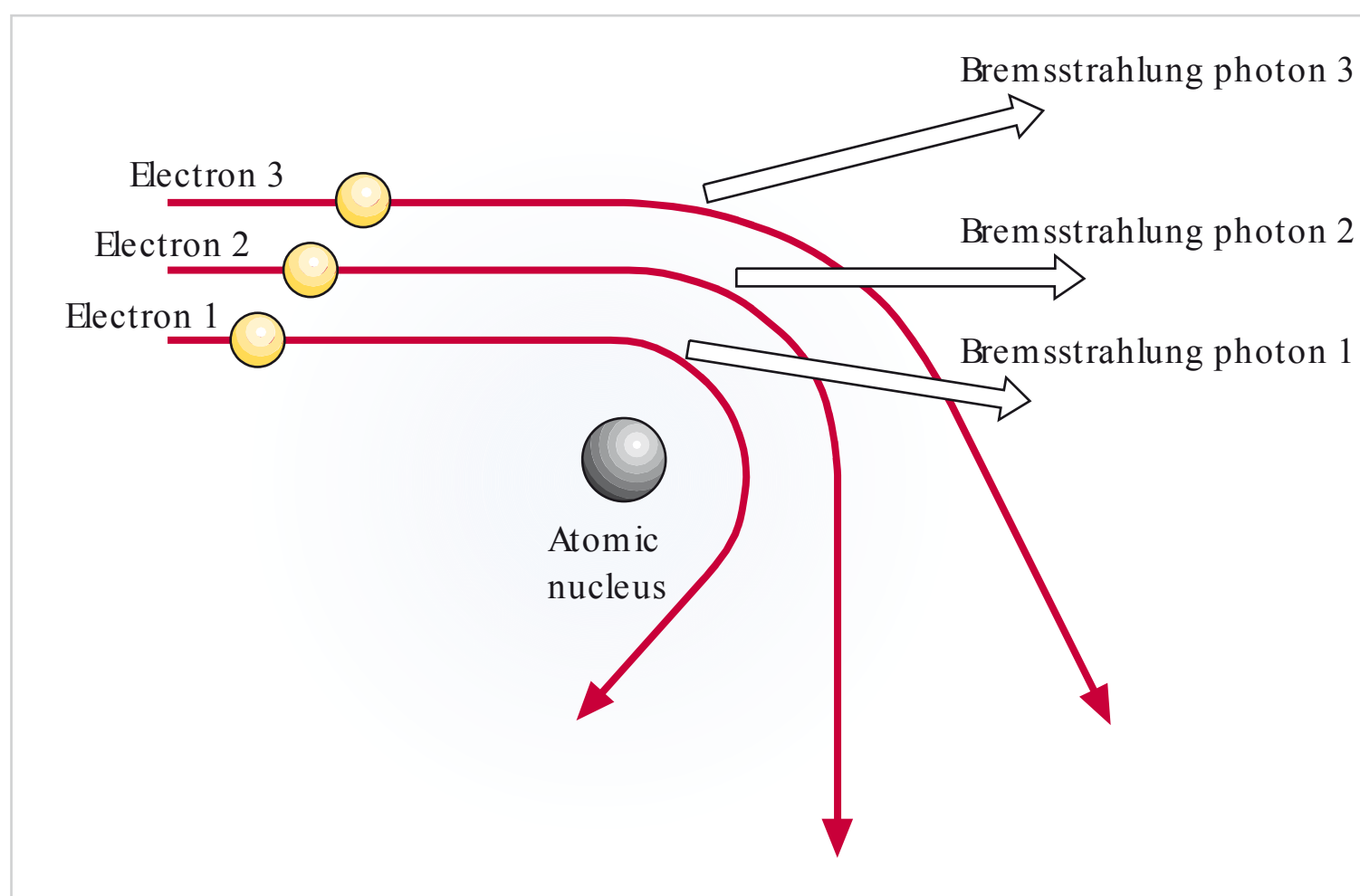


Fig. 2.15 Bremsstrahlung (schematic diagram). (From: Albes G. Facharztprüfung Radiologie. 2nd ed. Stuttgart: Thieme; 2010.)

Very tiny fractions (a few thousandths) of the electrons lose all of their kinetic energy immediately. In other words, the total energy level of these electrons is used for the production of photons. Therefore, the vast majority of the electrons emit only a variable portion of their kinetic energy in the form of heat until they are converted, so most of the photons emitted by these electrons have a lower energy level than the former type. Therefore, all energy levels are represented and this produces a continuous spectrum of bremsstrahlung (□ Fig. 2.15).

Note

Bremsstrahlung is the product of the interaction of incident electrons with the electric fields of the nuclei of the anode material. Because the individual electrons are decelerated differently, this results in the production of an X-ray spectrum with a range of different wavelengths.

Properties and Characteristics of X-rays

Owing to their ionizing effect, X-rays have very special properties and characteristics that can be utilized in various ways.

- **Attenuation:** When X-rays penetrate matter, they are attenuated (weakened) by absorption and scattering.
- **Luminescence:** X-rays stimulate certain substances to emit light. The principle of luminescence is used for X-ray image intensification and dose reduction (□ Fig. 2.16).
- **Ionization:** X-rays ionize air and gases and can thus be measured.
- **Photoelectric effect:** X-rays have a photoelectric effect and darken X-ray film (□ Fig. 2.17).
- **Semiconductor effect:** X-rays change the charge and conductivity of semiconductors (this has applications in digital radiography).



Fig. 2.16 X-ray beam generates light on an intensifying screen.

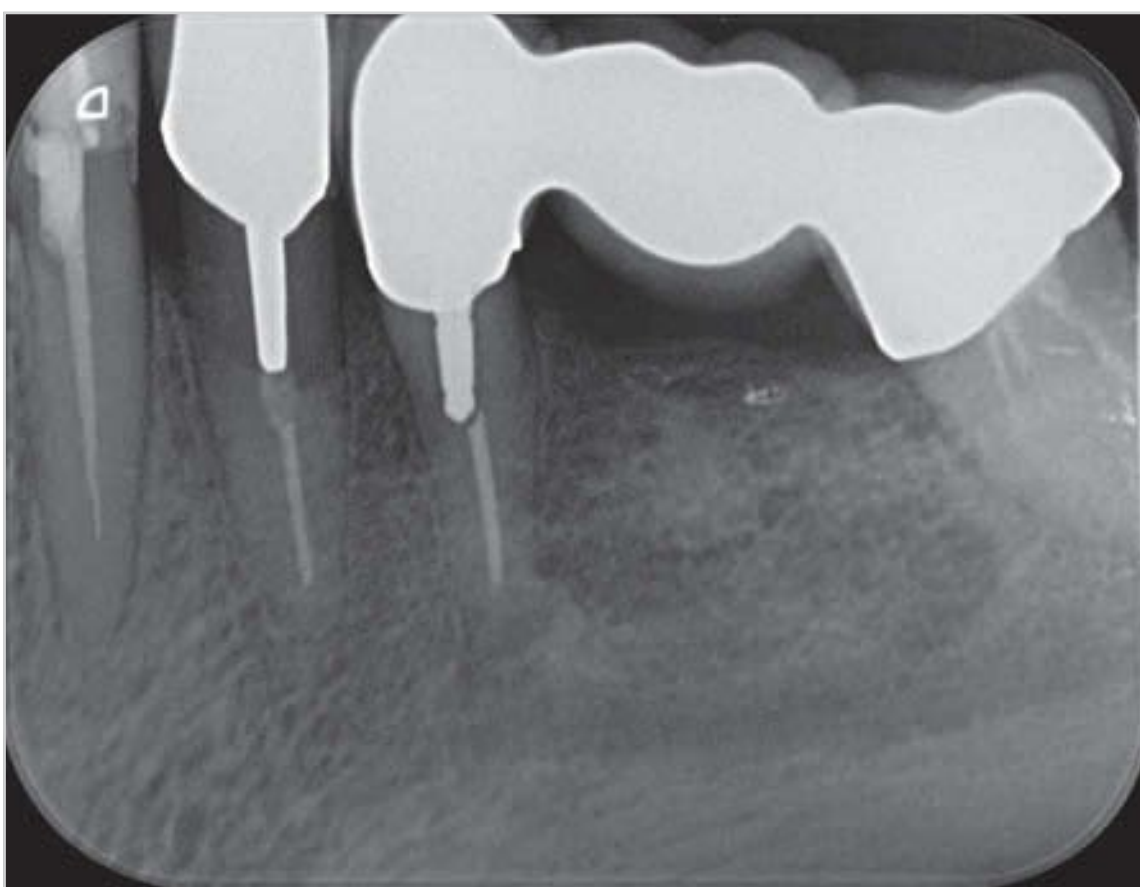


Fig. 2.17 Dental X-ray film.

2.8.2 Additional Equipment Needed for Dose Limitation and Improvement of X-ray Image Quality

Some additional equipment is needed to ensure the optimal implementation of X-ray machines, especially in dental radiography.

Full compliance with the current guidelines for radiation protection and image quality is required for every X-ray taken. This also applies to the additional equipment used in radiography.

Filtration of X-rays

Filtration of X-rays is mandatory, owing to the inhomogeneity of bremsstrahlung. Most X-rays consist of low-energy radiation that is completely absorbed in body tissues and thus does not contribute to image formation.

Although this low-energy radiation does not have any useful effects, it may, however, have injurious effects. Consequently, aluminum filters must be used to prevent individuals from being exposed to these rays.

However, the weakest X-rays in the beam are already filtered by materials present within the radiation-proof tube housing before they reach the exit window of the tube housing. The materials responsible for this inherent filtration are the glass envelope of the X-ray tube and the surrounding oil that insulates the radiation-proof X-ray tube housing. Inherent filtration has the effect of an aluminum filter with a thickness of 1 to 2.5 mm.

Total tube filtration is therefore defined as inherent filtration and additional filtration by aluminum filters.

Note

Total tube filtration is required by law. According to international standards, the total tube filtration must be equivalent to at least 1.5 mm of aluminum in dental X-ray equipment operating up to 70 kV, and equivalent to at least 2.5 mm of aluminum in equipment operating at more than 70 kV.

Collimator

Collimators are used to narrow the beam to the desired size and shape. When extraoral radiography is performed using large image receptors, the beam must be limited, in order to leave a visible unexposed margin. This serves to ensure that the beam is not larger than necessary.

Intraoral radiography is performed using small image receptors, however, so it is not advisable or necessary to leave an unexposed margin. Intraoral X-rays are subject to different principles, which require that a collimator or spacer cone is used to limit the beam and thus reduce the area of the radiation field at the end of the spacer cone to a diameter of no more than 6 cm.

To ensure that image receptors of all types and sizes are covered, the guidelines further stipulate that the diagonal of the useful radiation field at the end of the spacer cone must be no more than 1 cm larger than the diagonal of the active surface area of the largest image receptor used.

In practice, this means that a smaller secondary collimator must be used when the image receptor is smaller than 3×4 cm.

Spacer Cone

The spacer cone (□ Fig. 2.18 and □ Fig. 2.19) is of special importance in dental radiography. It has three important functions:

- Beam-indicating device (BID): In intraoral radiography, it is imperative that the X-ray beam and the target teeth of interest be properly aligned with each other.
 - When using the bisecting-angle technique without focusing adjustment, it is best to attach a pointed spacer cone to the X-ray tube housing, to ensure proper alignment of the X-ray beam and image receptor.



Fig. 2.18 Round cone with a round collimator and a radiation field of 6 cm.



Fig. 2.19 Secondary collimator with an adapted rectangular aperture designed to limit the dose to a small area of skin (field).



Fig. 2.20 Long spacer cone with a small secondary collimator.

- When the paralleling technique is used, it is best to use a long straight spacer cone with a small secondary collimator, to ensure proper alignment with the localizer ring (□ Fig. 2.20).
- Spacer:
 - Independent of shape and length, the spacer cone must be positioned as close as possible to the skin on the patient's cheek.
 - If the distance were larger, the irradiated area of skin (radiation field) would be large. This would result in patient exposure exceeding the maximum dose limits, and the X-ray image contrast would decrease because of an increase in the amount of scattered radiation reaching the image receptor.
- Collimator holder: The collimator is mounted on the spacer cone because the length of the spacer cone correlates with the size of the collimator field. Because the radiation field size must remain constant, the collimator field size must increase or decrease in accordance with changes in the length of the spacer cone.
- For example, if the spacer cone is relatively short (10 cm), then a relatively large collimator field size is needed to maintain the radiation field at a constant size of 6 cm (□ Fig. 2.21).
- Owing to beam divergence, the size of the collimator field decreases as the length of the spacer cone increases, to prevent the radiation field from exceeding the prescribed diameter size of 6 cm (□ Fig. 2.22).

Collimator Geometry and Radiographic Technique

When using the paralleling technique of intraoral radiography, the image receptor (e.g., film packet) is placed inside a film-holder. Targeting accuracy increases significantly when image receptors are used. Small, rectangular secondary collimators that are specifically designed for the image receptor may be used for this purpose. Secondary collimators can reduce the field size on the skin surface by up to 50% which is a major advantage (□ Fig. 2.23).

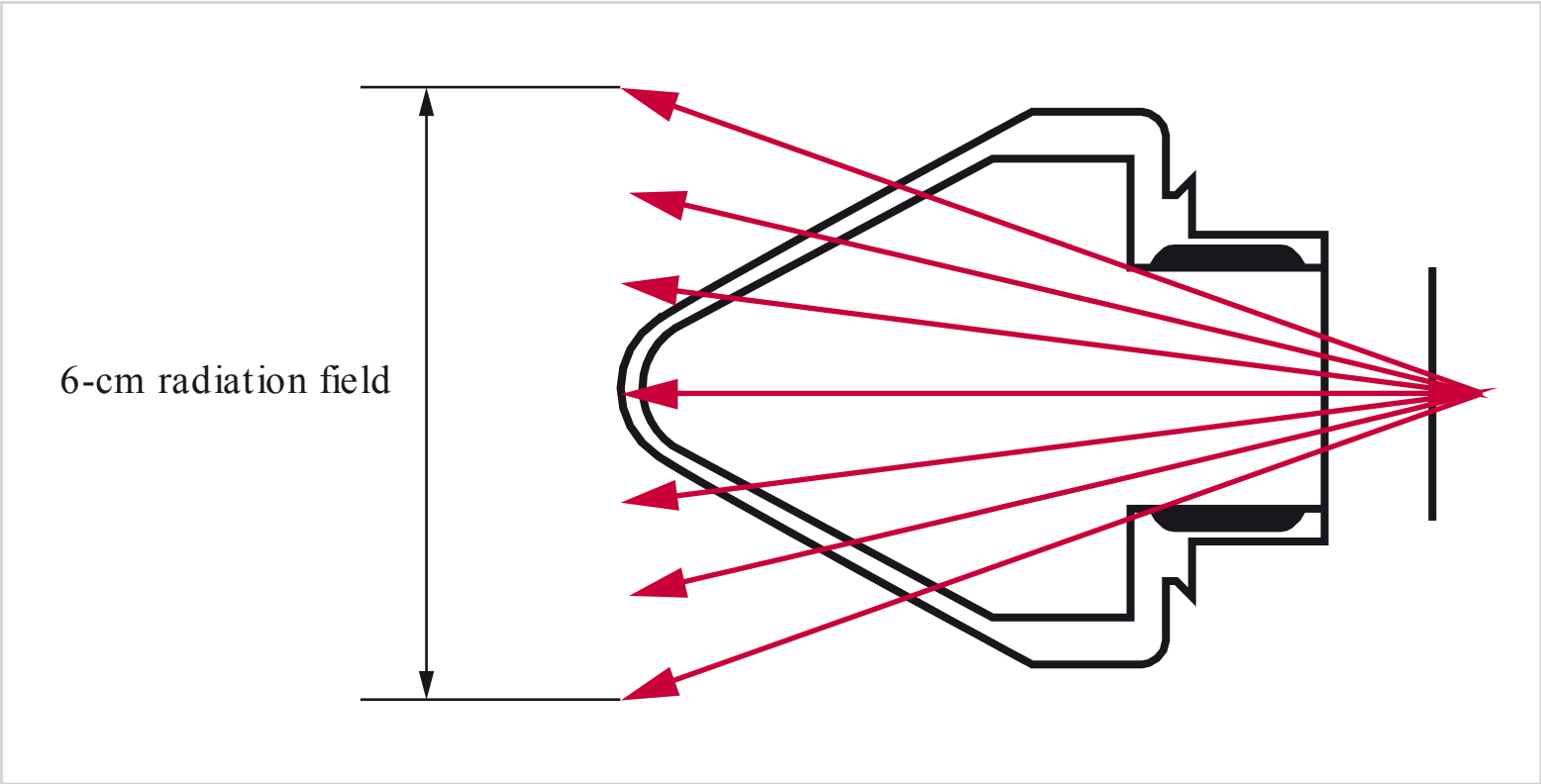


Fig. 2.21 Short spacer cone with a large collimator.

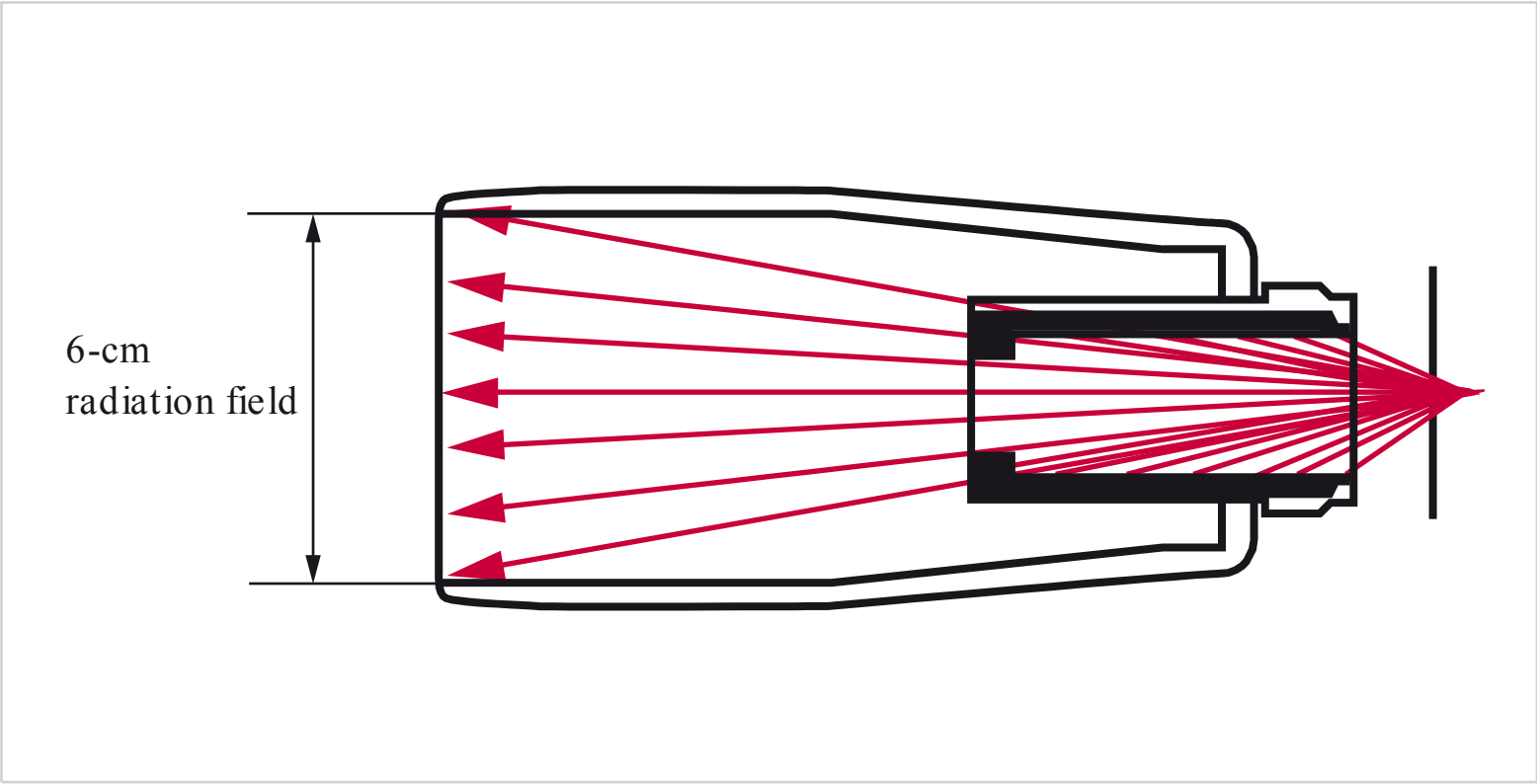


Fig. 2.22 Long spacer cone with a small collimator.

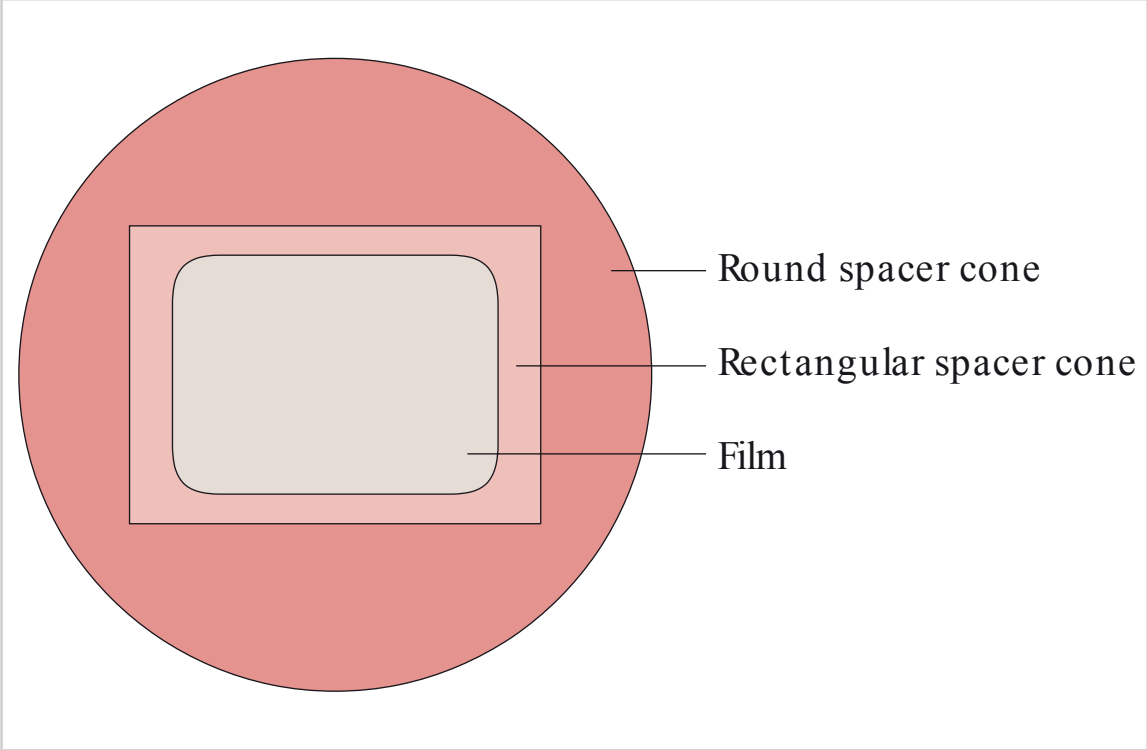


Fig. 2.23 Comparison of round versus rectangular collimation.

Chapter 3

Dose Terms and Dose Units Used for Ionizing Radiation



3 Dose Terms and Dose Units Used for Ionizing Radiation

To quantitatively describe the extent and the effects of ionizing radiation on the body, units for the measurement of ionizing radiation must be defined. Because the extent and effects of radiation depend on many factors, several different dose units are needed to describe the various interactions. The most important of these dose units are defined below.

□ Ion dose: The ion dose is a measure of the charges produced by the X-ray tube in a given volume of air. This dose unit is used in metrology. Its physical unit is the coulomb per kilogram (SI unit: C/kg). Therefore, the ion dose can also be described as the quotient of charge and mass.

□ Radiation absorbed dose: The radiation absorbed dose is a measure of the amount of radiation absorbed by the body, referring to the effect of radiation on the different types of body tissues. Because the effects of the radiation vary by tissue type, the absorption of radiation is also dependent on the type of tissue involved. The radiation absorbed dose is thus a measure of absorbed energy. It is defined as the quotient of the absorbed energy imparted by ionizing radiation on a given volume element of a specific material and the mass of this volume element. The radiation absorbed dose cannot be measured directly but can only be calculated from the ion dose and the absorption coefficient. Its physical unit is the gray (SI unit: Gy), where one gray equals one joule per kilogram ($1 \text{ Gy} = 1 \text{ J/kg}$).

□ Equivalent dose: The equivalent dose takes into account the different biological effect of radiation of different ionization density in tissue. The equivalent dose is thus the unit used in radiation protection. Its physical unit is the sievert (SI unit: Sv), which is used to distinguish the equivalent dose from the radiation absorbed dose.

- Radiation weighting factor (W_R): Different radiations have different ionization densities. Therefore, some forms of radiation have high biological effectiveness, while others have low biological effectiveness. X-rays, beta rays, gamma rays, and electron beams are assigned a radiation weighting factor (W_R) of 1. The W_R of neutron beams is 10 to 20, and that of alpha particles is 20.
- Linear energy transfer (LET): The intensity and spatial distribution of ionization produced by radiation is greatly dependent on the type of radiation. The LET is a measure of the so-called radiation quality. This unit indicates the order of magnitude of interaction between a certain type of radiation and irradiated matter. The number of ionizations that radiation produces per unit distance as it travels through tissue is a measurable parameter of linear energy transfer. Alpha particles are very densely ionizing radiation. Neutrons and protons are only half as densely ionizing, and X-radiation is sparsely ionizing radiation with a low ionization density (□ Fig. 3.1).

Therefore, the equivalent dose corresponds to the radiation absorbed dose multiplied by the radiation weight-

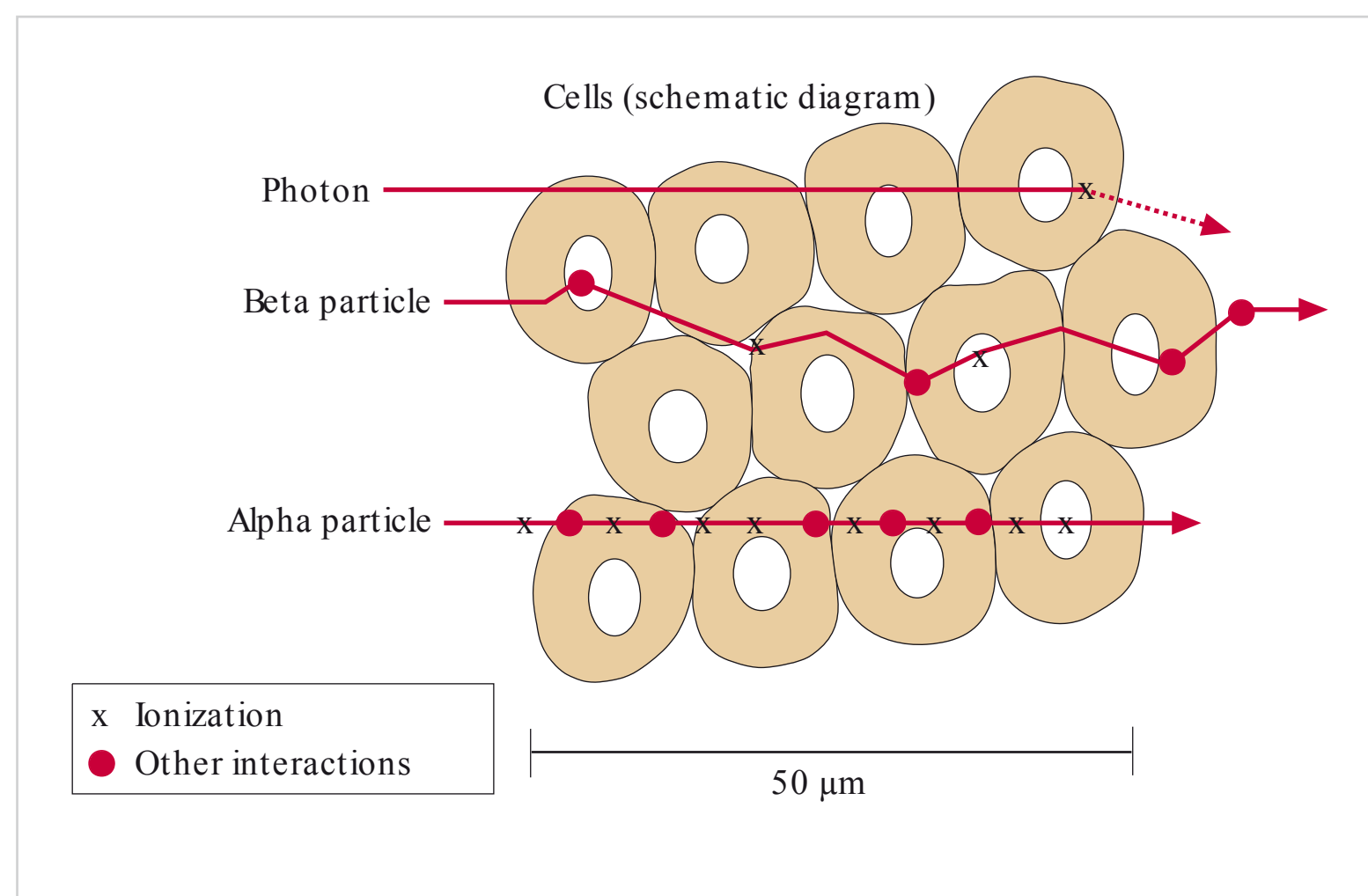


Fig. 3.1 Linear energy transfer (LET). (From: Pasler FA, Visser H. Zahnmedizinische Radiologie. 2nd ed. Stuttgart: Thieme; 2000. Farbatlant der Zahnmedizin; Band 5.)

ing factor, W_R . Since X-rays have a W_R of 1, the equivalent dose is numerically equivalent to the radiation absorbed dose in dental radiography.

□ **Effective dose:** The **effective** dose equivalent, or **effective** dose, was introduced as a parameter for estimating the risk of cancer associated with radiation exposure, in a **differentiated** manner. The rationale behind this is that some organs of the body are more sensitive to radiation than others.

The radiosensitivity estimates for the various tissue types are accurate, because they are based on data from a large number of cases, including survivors of the atomic bombings in Hiroshima and Nagasaki. By taking the number of deaths as the basis of calculation, it is possible to calculate an organ or tissue weighting factor for each part of the body, based on its radiosensitivity.

The International Commission on Radiological Protection (ICRP) recalculated its tissue weighting factors in 2007. Because of this, the values for many organs have changed since the last ICRP recommendations were published in 1979 (□ Table 3.1).

The **effective** dose is the sum of the equivalent doses for each organ or tissue irradiated, multiplied by their respective tissue weighting factors. It thus represents the **effective** dose for the whole body. The SI unit of **effective** dose is the sievert (Sv).

In addition to these basic dose terms and units used in dosimetry, other important dose terms play an important role in the everyday use of X-rays.

Table 3.1 Tissue weighting factors (W_T)		
Tissue or organ	W_T 1991	W_T 2007
Gonads	0.20	0.05
Red bone marrow	0.12	0.12
Colon	0.12	0.12
Lung	0.12	0.12
Stomach	0.12	0.12
Breast	0.05	0.12
Liver	0.05	0.05
Esophagus	0.05	0.05
Thyroid	0.05	0.05
Skin	0.01	0.01
Bone surface	0.01	0.01
Brain		0.01
Kidney		0.01
Salivary glands		0.01
Remainder	0.05	0.10

□ **Dose–area product:** The dose–area product is the incident radiation dose multiplied by the irradiated surface area. All new X-ray machines, including those used in dentistry, must calculate and display values of dose–area product. A record of the DAP meter reading is made after each examination (□ Fig. 3.2).

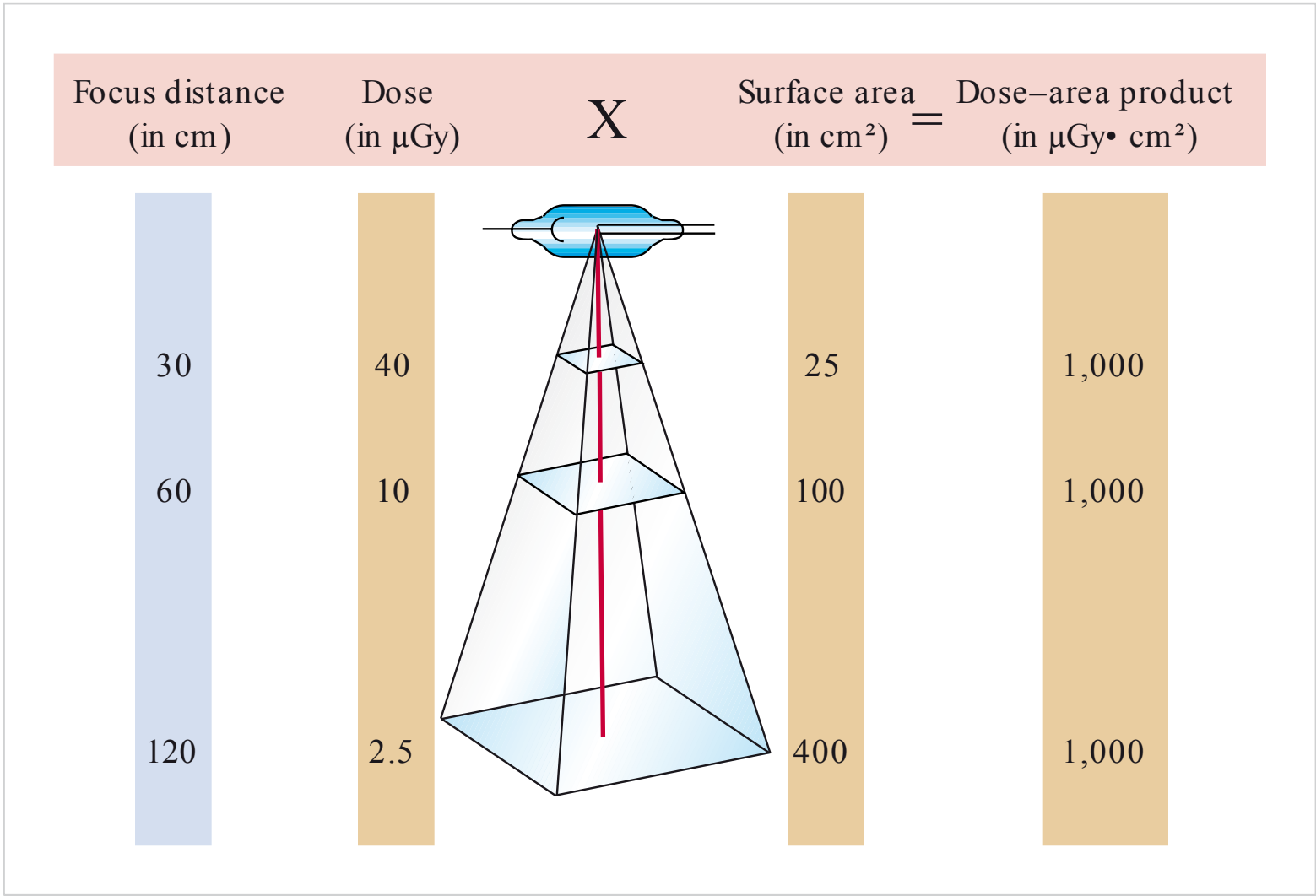


Fig. 3.2 Dose–area product. (From: Pasler FA, Visser H. Zahnmedizinische Radiologie. 2nd ed. Stuttgart: Thieme; 2000. Farbatlanten der Zahnmedizin; Band 5.)

Chapter 4
The Biology of
Radiation Effects

4.1	Fundamentals	26
4.2	Direct and Indirect Effects of Radiation	27
4.3	Effects of Ionizing Radiation on DNA	27
4.4	Repair Mechanisms for the Restoration of DNA	27
4.5	Biological Effects of Radiation Damage	27



4 The Biology of Radiation Effects

4.1 Fundamentals

The processes that ultimately lead to the biological effects of radiation in tissues start with the physical process of absorption. The energy input from radiation induces considerable structural changes in the tissues. Compared with other agents with toxic effects on cells, ionizing radiation has the highest biological efficiency and the highest damage potential. The biological effect of radiation develops in a series of processes, starting with physical changes (physical phase) that lead to chemical changes (chemical phase) and, ultimately, biological changes in the DNA (biological phase).

When radiation passes through matter, it is attenuated by absorption and scattering processes. The resultant transfer of energy to the irradiated material leads to the

release of electrons. These charged particles, in turn, continuously induce further ionization processes with constantly decreasing energy.

The electrons released in photoelectric and Compton interactions have sufficient energy to induce further ionization or stimulate the emission of further radiation on their own. This results in the production of photons with less energy. However, even these lower-energy photons from these various processes still have enough energy for further stimulation of atoms and molecules. Overall, considerable heat is generated by the primary and secondary processes involved in the interaction of radiation with matter. These physical processes lead to chemical changes in the irradiated area, which can ultimately lead to biological changes.

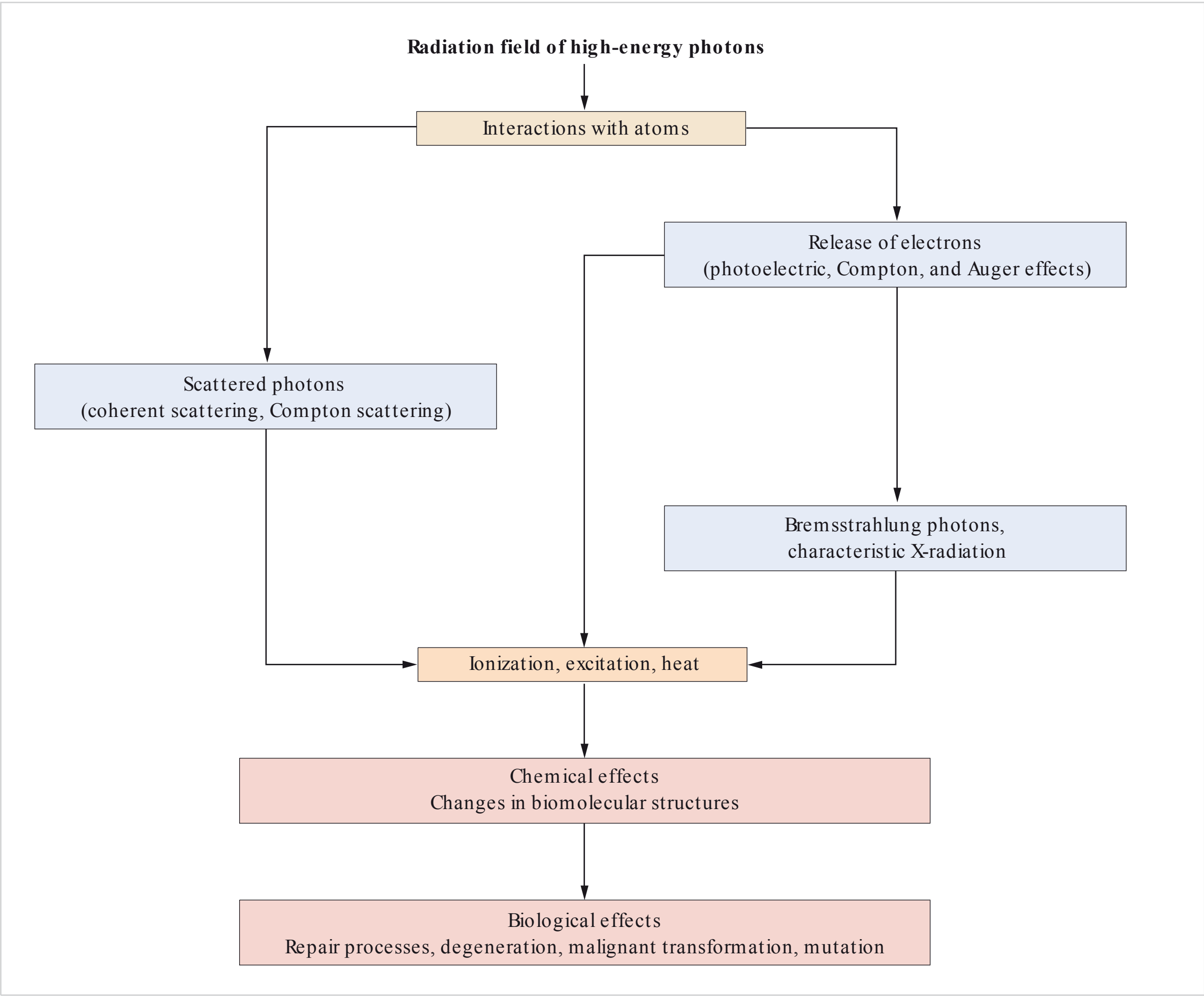


Fig. 4.1 Schematic diagram of the effects of radiation in tissue. (From: Pasler FA, Visser H. Zahnmedizinische Radiologie. 2nd ed. Stuttgart: Thieme; 2000. Farbatlant der Zahnmedizin; Band 5.)

Note

Only the fraction of ionizing radiation that undergoes interaction with the tissue can cause biological effects. All the biological effects of ionizing radiation are the result of the transfer of energy to the tissue (□ Fig. 4.1).

4.2 Direct and Indirect Effects of Radiation

Ionizing radiation can have direct or indirect effects. Structural changes within the cells, and macromolecular changes, are direct effects, and changes due to the production of free radicals in the water of the cell are indirect effects. Free radicals are highly reactive fragments of molecules. They trigger a variety of biochemical reactions, such as hydroxylation, decarboxylation, reduction, and oxidation. These processes can induce biochemical alterations in normal biomolecular structures and bonds.

Living cells are ~90 % water. The radiolysis of water results in the production of OH^\bullet radicals as an oxidant species, and in the production of hydrogen radicals, free electrons, OH^- ions and H^+ ions as reducing species. The formation of peroxide can also occur due to interaction with oxygen.

Exposure to X-rays and other types of low linear energy transfer ionizing radiation predominantly causes indirect effects, which are responsible for up to 70 % of the overall effect.

4.3 Effects of Ionizing Radiation on DNA

DNA is by far the most critical target for radiation damage in a cell. It is, however, the main point of attack of ionizing radiation.

DNA is the carrier of genetic information. It serves to preserve and repair the body through its ability to produce identical replicas in cell division and the capacity to pass on genetic information through the generations. Damage to DNA seriously interferes with the biological balance of the living organism.

Ionizing radiation can result in several types of damage to DNA. The most common types are changes in bases such as thymine, cytosine, adenine, and guanine. DNA single-strand breaks and changes in sugars are the second most common type. DNA double-strand breaks are not so common (□ Fig. 4.2).

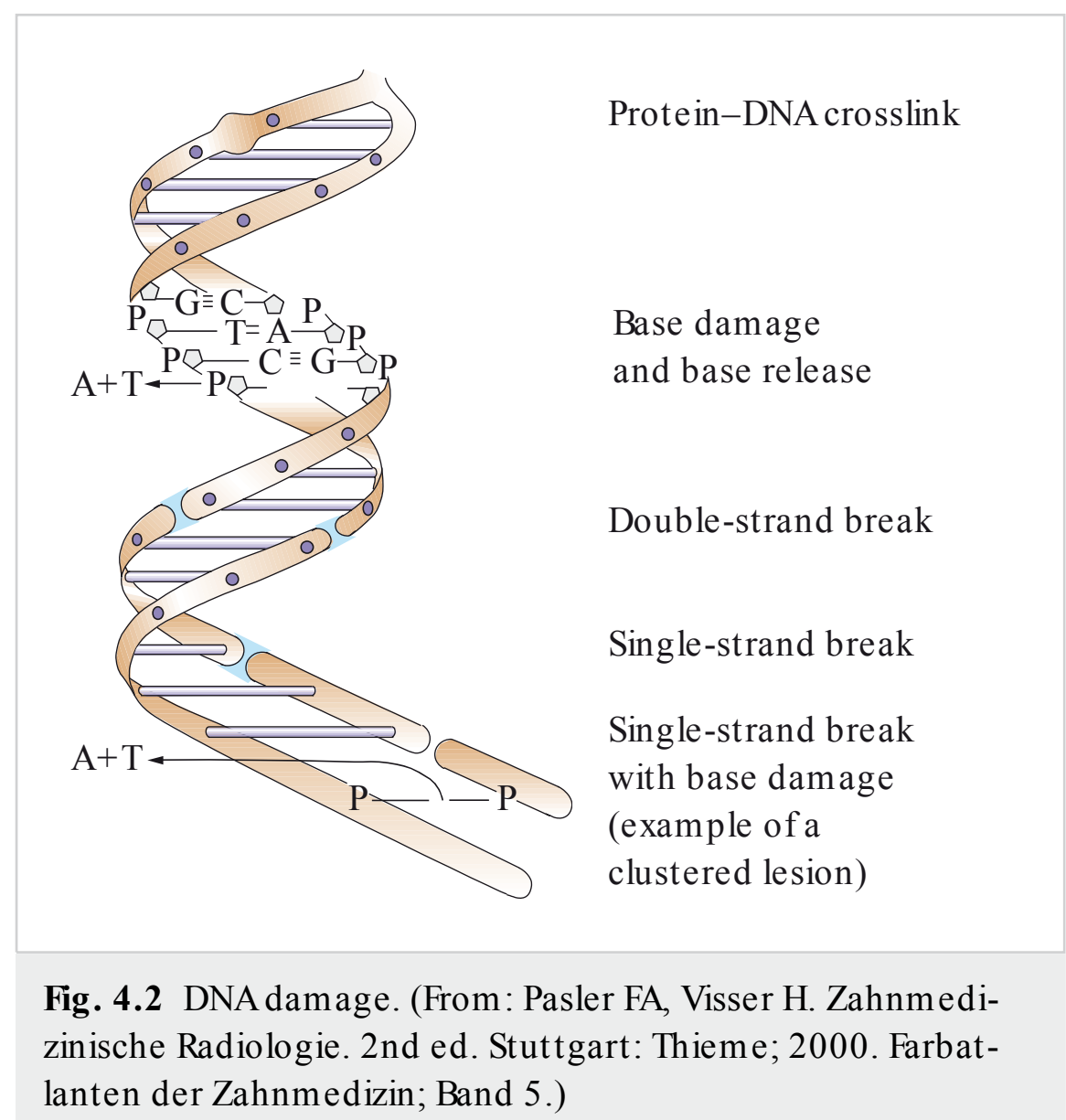


Fig. 4.2 DNA damage. (From: Pasler FA, Visser H. Zahnmedizinische Radiologie. 2nd ed. Stuttgart: Thieme; 2000. Farbatlant der Zahnmedizin; Band 5.)

4.4 Repair Mechanisms for the Restoration of DNA

Cells have effective mechanisms for the flawless repair of the major portion (up to 97 %) of radiation-induced damage to their DNA within a few hours. These repair mechanisms serve to restore the DNA, suppress cancer development, and prevent mutations.

The repair processes occur quickly—some repairs are completed in only a few minutes. Most of the damage is repaired within several hours. The remaining residual damage accounts for less than 5 % of the total damage.

In DNA single-strand breaks, the complementary strand of the DNA double helix that is still present is used as a template for the restoration, via the respective enzymes. Even DNA double-strand breaks can be repaired; this occurs in a process referred to as nonhomologous end-joining.

4.5 Biological Effects of Radiation Damage

Radiation-induced damage to the DNA may cause different types of effects, depending on the severity and location of damage.

- Impairment of cell function generally leads to programmed cell death, depending on the severity of impairment.
- Programmed cell death (apoptosis) is a normal physiological process that occurs in all living organisms. It serves to ensure that cells that are not functioning properly are identified as such and destroyed before the

start of cell division. Apoptosis may, however, result in deterministic radiation damage if the radiation causes the cell death rate to rise above a certain level. Deterministic radiation effects occur above a threshold dose.

- Mutations result in changes in the genetic characteristics of subsequent generations of cells. Mutations may cause or contribute to the malignant transformation of somatic cells.

Chapter 5
Radiation Pathology

5.1	Natural Radiation Exposure	30
5.2	Artificial Radiation Exposure	30
5.3	Stochastic and Deterministic Effects of Ionizing Radiation	31



5 Radiation Pathology

5.1 Natural Radiation

Exposure

Exposure to natural background radiation is inevitable because it is a natural part of the environment. Major sources of natural radiation include cosmic radiation and the decay of radionuclides that occur naturally in the human environment and in the human body.

5.1.1 Cosmic Radiation

It is known that cosmic rays consist of radionuclides from galactic and solar sources, but their origin is still not completely understood. Primary cosmic radiation consists mainly of protons, photons, and electrons that interact with atoms in the atmosphere, resulting in the production of secondary cosmic rays. The amount of natural exposure to cosmic radiation depends on the altitude of the location of measurement. In central Europe, the annual effective dose of cosmic radiation is ~ 0.3 mSv at sea level, and ~ 1 mSv at an altitude of 2,500 m.

Exposure to cosmic radiation is of special significance to flight personnel. Therefore, guidelines recommending that the exposure of air crew to cosmic radiation should be taken into account in occupational exposure estimates are already in place.

While the intensity of cosmic radiation remains relatively constant, the intensity of solar radiation varies depending on the solar cycle and solar activity (flares).

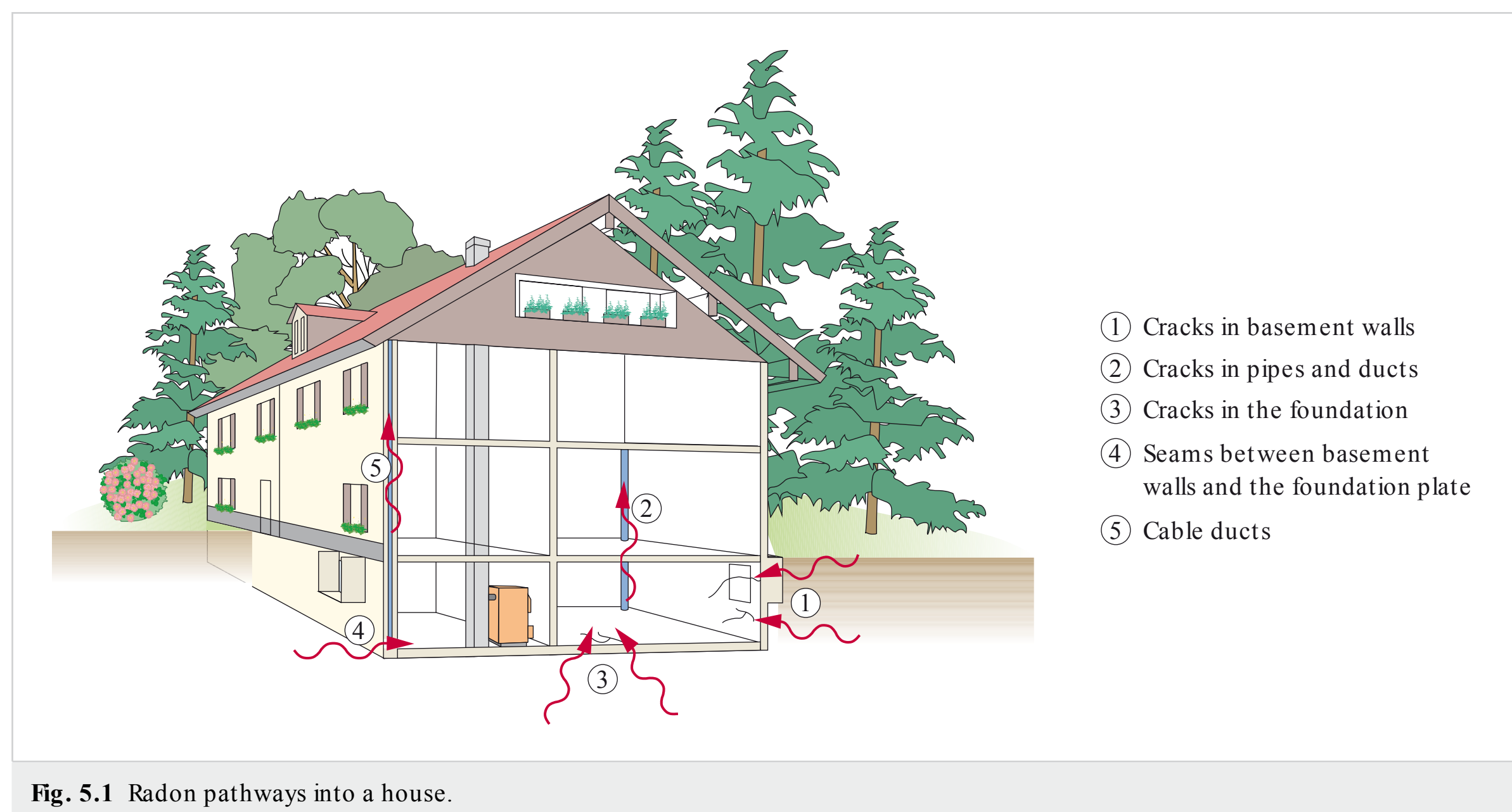
5.1.2 Terrestrial Radionuclides

Terrestrial radiation is natural radiation originating from the decay of the radionuclides in the Earth's surface. Radionuclides are taken up in the human body with food, air, and drinking water. The three main radionuclides in the Earth's crust are uranium, thorium, and potassium. Other radionuclides are members of the natural decay series of uranium and thorium. Radon exposure (1.4 mSv) makes up the largest fraction of the total radiation dose due to terrestrial radionuclides. Radon is inhaled as a gas in enclosed spaces. Radon gas is a product of the radioactive decay of uranium and thorium. It escapes by diffusion from the soil into the air and then seeps into houses and buildings (□ Fig. 5.1).

5.2 Artificial Radiation Exposure

The ionizing radiation and radioactive materials used in medicine are the largest source of artificial radiation exposure associated with civilization. Diagnostic radiation makes up the largest fraction of these exposures. Radiotherapy and nuclear medicine contribute only 10 % to the total annual dose of 1.5 mSv from medical radiation.

All other sources such as the Chernobyl nuclear power plant accident, atomic bomb fallout, nuclear power plants, and radiation used in research and nuclear technology produce less than 0.02 mSv per year (□ Fig. 5.2).



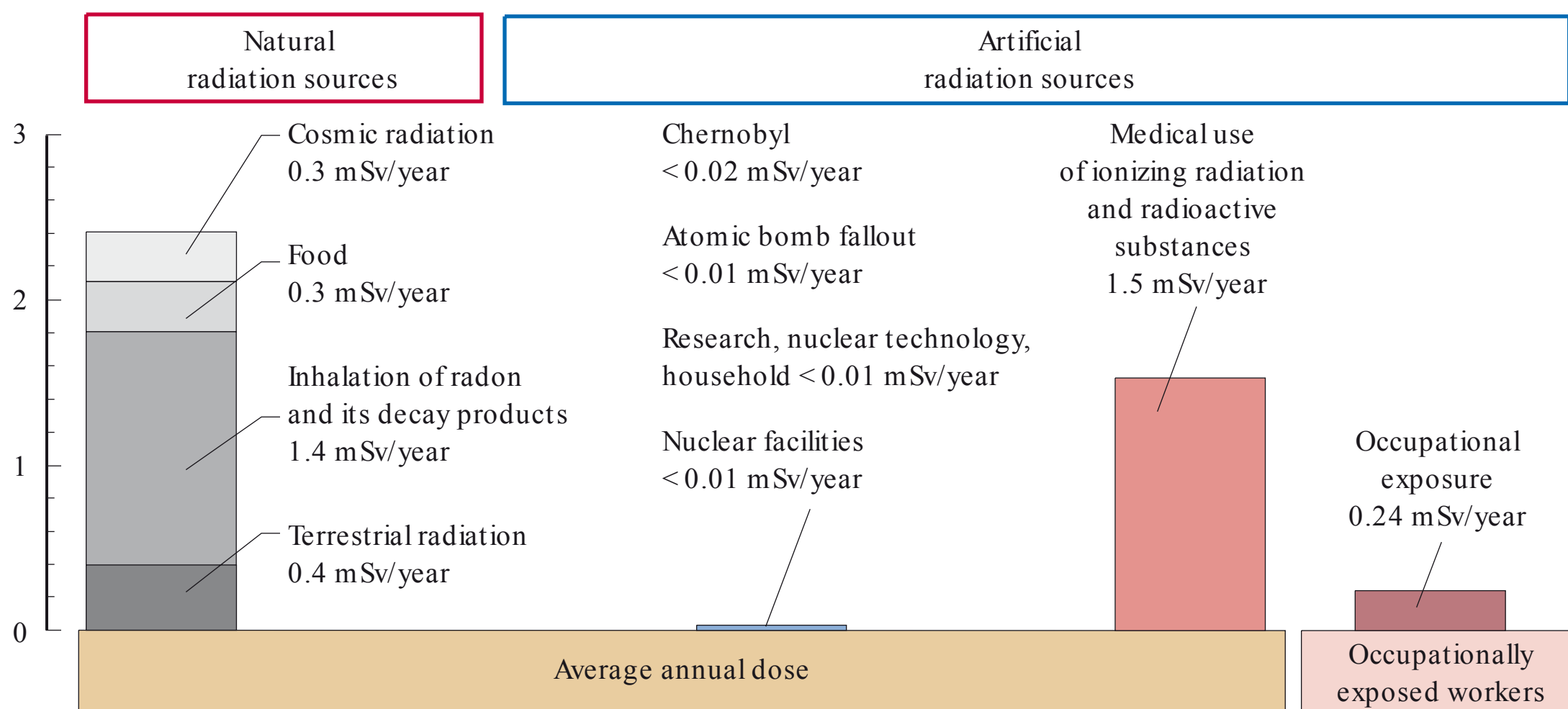


Fig. 5.2 Radiation exposure (dose per person per year). (Adapted from: Pasler FA, Visser H. Zahnmedizinische Radiologie. 2nd ed. Stuttgart: Thieme; 2000. Farbatlant der Zahnmedizin; Band 5.)

5.3 Stochastic and Deterministic Effects of Ionizing Radiation

5.3.1 Stochastic Effects

The stochastic effects of ionizing radiation occur by chance, that is, are determined by a random distribution of probabilities (□ Fig. 5.3). Therefore, one can only predict the statistical probability of biological effects occurring in a given population of individuals with identical radiation exposure. Stochastic effects may not occur until after a latent period of several years. It is impossible to predict whether stochastic effects will occur in a given individual.

There is no threshold dose for the occurrence of stochastic effects.

Unicellular processes are involved in the occurrence of stochastic radiation effects. Malignant transformation of a somatic cell, or a mutagenic effect on germ cells, is a random occurrence determined by chance damage to the respective DNA. Theoretically, a single high-energy photon can release secondary electrons that, on their orbit in the cell nucleus, may induce DNA damage resulting in stochastic effects. The probability of occurrence of stochastic effects increases with dose. However, the severity of the resulting effect is not dose dependent.

The stochastic effects of radiation include:

- Genetic defects
- Cancer.

5.3.2 Deterministic Effects

A biological effect of radiation is characterized as deterministic if the effect occurs as a direct result of exposure to a specific dose of radiation. Unlike stochastic effects, deterministic effects occur only after exposure to radiation exceeding a certain threshold dose. The threshold dose is the dose where the number of cells killed by radiation increases to such a degree that it rises above the normal level. The severity of damage to the affected tissue increases with increasing dose. The latent period between exposure and the onset of the deterministic effect varies, depending on the type of tissue involved and the radiation dose level. The acute effects of radiation appear after a latent period of a few hours to days, while the chronic late effects may take years to manifest themselves.

The deterministic effects of radiation (□ Fig. 5.4) always arise from multicellular mechanisms. The induction of damage exceeding the cellular repair capacity leads to an increase in cell death or degenerative processes. The effects only become clinically manifest after a large number of cells have been damaged.

It is imperative that the radiation doses used in diagnostic imaging do not cause deterministic damage.

The most common forms of early radiation-induced damage due to deterministic effects include:

- Erythema
- Ulcers
- Acute radiation sickness.

Late effects include a variety of:

- Tissue changes
- Vascular changes.

- There is no threshold dose
- Severity is not dose dependent
- The probability of occurrence increases with dose
- Even the smallest doses have the potential to induce damage
- Effects become statistically significant only after a certain frequency of occurrence
- Cancer, leukemia, and mutations may be induced by radiation

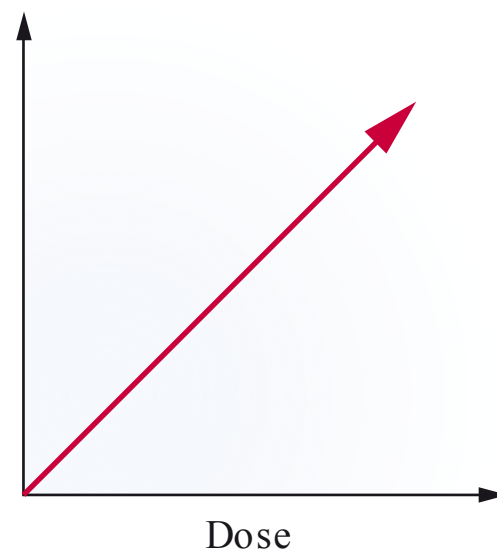


Fig. 5.3 Stochastic effects of radiation (effects that occur by chance).

5

- There is a threshold dose
- The severity of damage increases with dose

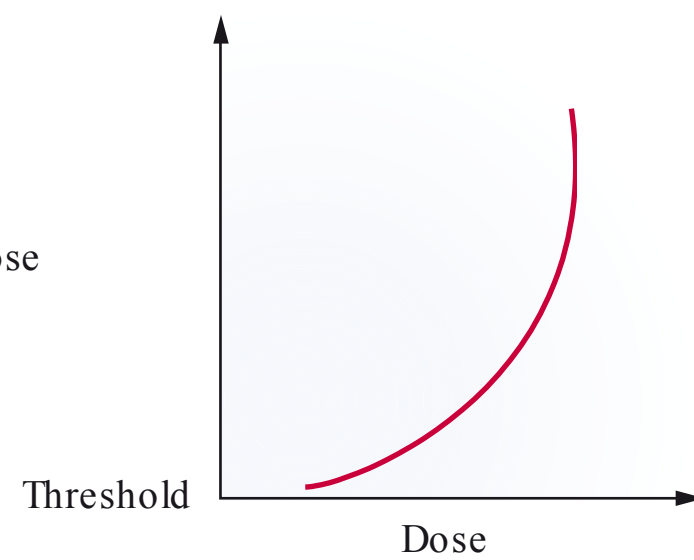


Fig. 5.4 Deterministic effects of radiation.

Image Formation and Image Processing

6.1	Fundamentals	34
6.2	Image Receptor-Independent Factors Influencing Image Formation	35
6.3	Radiographic Film and Intensifying Screen-Dependent Factors that Influence Image Formation	37
6.4	Processing of Radiographic Films	42

6 Image Formation and Image Processing

6.1 Fundamentals

Image formation with X-rays is significantly different from the formation of images by visible light that we are familiar with.

Unlike visible light, X-rays pass through the body and form images of the different structures they encounter, according to the laws of central projection.

Central projection means that X-rays diverge as they travel in a straight line from a point source focus to the anode. As X-rays pass through tissues, different structures of different densities absorb and scatter different fractions of the radiation, resulting in attenuation of the beam. The degree of X-ray attenuation varies depending on the composition (density) of the irradiated objects. The variable pattern of blackening resulting from this reflects these differences in optical density of the objects.

The degree of absorption of X-rays is determined by the number of electrons per atom of a given element. Structures made of elements with a large number of electrons, as reflected by a high atomic number, absorb more X-rays than those made of elements with a low atomic number. Osseous structures contain calcium, which has a relatively high atomic number. Therefore, bone appears white and particularly prominent on radiographs. The reason for this is that X-rays that strike bone are almost entirely absorbed and do not reach the image receiver. Tissues that are not as dense as bone absorb much less X-radiation and therefore appear as variably dark to black shadows. Between these two extremes—white or black—are many shades of gray. The corresponding image generated by the image receptor is made visible by developing the film, or by digital image processing. The number of gray levels or contrast displayed varies from system to system.

Unlike photography, X-radiation does not produce a “picture.” An X-ray image is merely the result of the variable attenuation of X-rays by the irradiated objects. The resulting light and dark areas must be interpreted and correlated to their respective anatomical structures. A precise understanding of the principles of X-ray image formation, and a detailed knowledge of the anatomy of the region of the body being examined, are thus necessary for the interpretation of radiographic images.

However, observer experience is just as important: comparison with known radiographic images is the only way to improve the reliability and accuracy of interpretation of the radiographic appearances of anatomical structures of variable density. The fact that we compare things we observe with similar and familiar things stored in our memory is a natural mental process. The larger the number of similar and familiar things stored in the memory (for example, radiographic images), the greater the experience of the observer. Greater experience allows the observer to identify structures on radiographs more quickly and accurately.

6.1.1 Summation Effect

The fact that an X-ray image is the summation of different consecutive structures in three-dimensional space into a two-dimensional imaging plane makes radiographic interpretation even more challenging. Individual details on an X-ray image may be indistinguishable, owing to this summation effect (□ Fig. 6.1). It may be necessary to take an X-ray from a different projection angle, to visualize such “hidden” structures.

The main problem of X-ray imaging is that it depicts three-dimensional objects in a two-dimensional plane. It is difficult for the inexperienced radiographer to mentally translate a three-dimensional object into a two-dimensional radiograph. Likewise, it is hard to gain an impression of three-dimensionality from a two-dimensional image.

Considering this knowledge of the physical principles of X-ray image formation, the first step is to learn to perceive the different gray levels as different degrees of attenuation caused by tissues of different densities.

The next step is to learn to translate the gray-scale information into vivid three-dimensional impressions of the irradiated organs. The last step is to learn to distinguish normal from abnormal. In other words, the observer must learn to distinguish the radiographic appearances of normal anatomical structures and variants from abnormal anatomical structures and pathological changes.

Thus, radiographic interpretation is complicated by the two-dimensionality of X-ray images and by the summation (superimposition) of shadows from consecutive structures. Another X-ray optical phenomenon that influences the identification and interpretation of radiographic appearances must also be considered: the tangential effect.

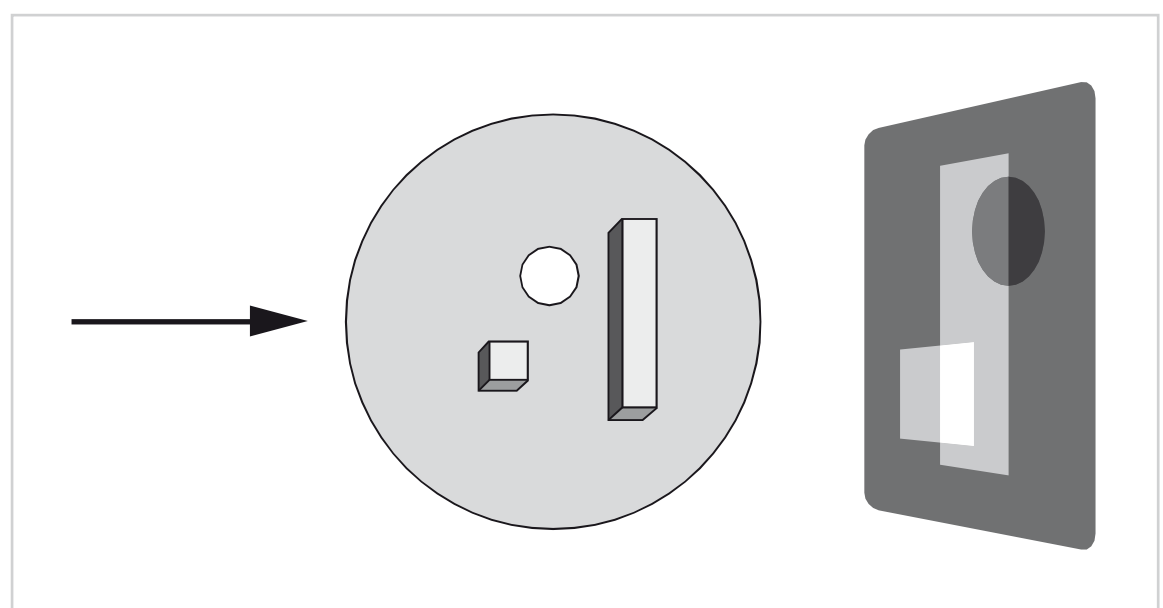


Fig. 6.1 Summation of shadows in an X-ray image (schematic representation). (From: Pasler FA. Zahnärztliche Radiologie. 5th ed. Stuttgart: Thieme; 2008.)

6.1.2 Tangential Effect

Objects that are very dense or thick are readily seen on radiographic images. Conversely, structures that are very small absorb very little radiation; therefore, they may be very hard to visualize if the X-ray image was taken from the wrong projection angle. The only way to clearly display small, curved, and thin structures is to align the beam parallel to these objects. This applies, in particular, to structures in the alveolar region and to the thin bone walls in the maxillary sinus area. The image formed is then the summation of bone wall structures aligned parallel to the central ray. Hard-tissue structures aligned perpendicular or oblique to the central ray at the moment of exposure are either not visible or only slightly visible on radiographs, even if they are very dense and thick.

Take, for example, the hard palate, which can be visualized in only a few beam projections. If the thin hard palate is aligned perpendicular to the central ray, the area of the hard palate will not be visible, owing to its lack of thickness. Only the marginal areas are visible as shadow lines, owing to their curvature (□ Fig. 6.2).

Despite these difficulties, the goal of radiography must be to depict anatomical structures as accurately and realistically as possible. To facilitate radiographic interpretation and prevent errors, it is essential to ensure that the gray-level information used to produce the X-ray images is processed exactly in accordance with prescribed rules. This is done by using standard radiographic projections.



Fig. 6.2 Tangential effect in the maxillary region.

Radiologist Guido Holzkecht (1931) said, “From the total number of possible radiographic projections, the ones best suited to display the largest number of changes known to occur by experience with the smallest number of projections must be selected.”

Note

The use of standard radiographic procedures is an important element of dental radiography. Standardized imaging procedures contribute to quality assurance and reduce radiation exposure.

By acquiring standard radiographic projections according to recognized rules, target structures can be imaged with the greatest accuracy possible.

The visualization of organs using well-known standard projections has distinct benefits for radiographic diagnostics. It is the only way to obtain a true-to-scale reproduction of specific structures in a known form. Moreover, radiographs should always provide an exact indication of the density of anatomical structures, so that changes can be clearly identified.

In dental radiography, we know that certain laws of projection must be known and applied, especially when taking intraoral radiographs. For better understanding, the factors that influence X-ray image formation can be divided into two main categories:

- Factors that are independent of the image receptor
- Factors that are determined by the image receptor system.

6.2 Image Receptor-Independent Factors Influencing Image Formation

The degree of penetration of X-rays is dependent on the X-ray wavelength, which, in turn, is dependent on the high voltage applied to the X-ray tube. As the thickness or density of an irradiated object increases, the degree of penetration of X-rays must also be increased by increasing the voltage.

The variable absorption of X-rays by the different tissues of the body produces variable shadow patterns of the irradiated structures and organs, which are seen as projection images on the radiograph. Dense structures such as bones strongly absorb X-rays and produce variable degrees of shadowing. Loose structures such as soft-tissues, cavities, and air absorb little or no X-rays and thus appear radiolucent (white), owing to their low density.

The superimposition of structures from different levels of an object is referred to as addition. The opposite effect, caused by spaces containing air, is called subtraction. These addition and subtraction effects may complicate

radiographic diagnostics, especially when they occur in the craniofacial region, where a very large number of angular bony structures of different thicknesses are closely positioned together in close proximity to soft-tissues and air-filled cavities.

The age of the patient is another important factor, particularly in dental radiography, because of age-related changes in the calcium content of bone. Last but not least, pathological changes result in altered absorption deviating from the characteristic X-ray absorption of healthy tissues.

6.2.1 Object Contrast

Very low and very high degrees of absorption produce very dark, dense, and bright low-density areas on the radiograph. The large differences between these extreme densities result in high contrast. The degrees of absorption between these extremes form the gray-scale range of radiography. The difference between the maximum and minimum optical density with which a structure is displayed is referred to as object contrast. The only factors that influence object contrast are the object type and beam quality. Other factors such as current intensity, source-to-film distance, exposure time, and film characteristics have no effect on object contrast. Digital image processing is the only way to change the primary object contrast of a radiographic image.

6.2.2 Current Intensity and Exposure Time

The amount of X-rays generated in a given exposure time, in seconds (s), depends on the amount of current, in milliamperes (mA), applied to the filament of the cathode. Accordingly, the product of current and exposure time determines the image density without affecting the contrast. If technically possible, the same effect can be achieved by changing the exposure time, or, if this is not possible, by varying the current. The milliamperage-second product (the product of milliamperage and exposure time in seconds) remains the same in either case.

6.2.3 Inverse Square Law

The distance from the radiation source to the irradiated object is another factor to consider. As the distance from the source increases, the intensity of X-radiation decreases, owing to attenuation, and the density per unit area decreases, owing to the divergence and cone-shaped spatial distribution of the beam. Therefore, distance has a major influence on the degree of film darkening, or radiographic density.

X-rays, as well as light rays, follow the inverse square law (□ Fig. 6.3), which states that the intensity of radia-

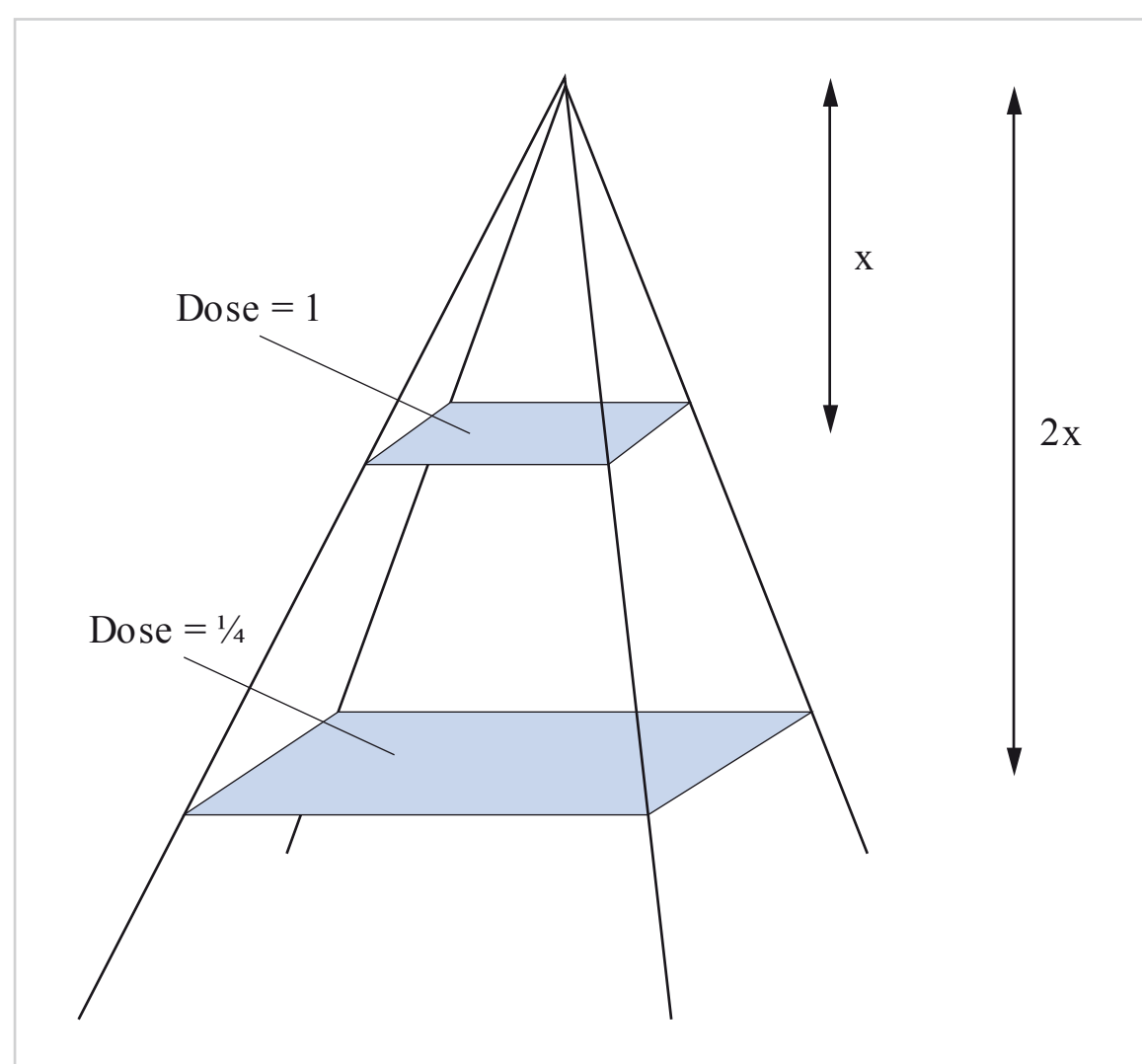


Fig. 6.3 Inverse square law (schematic representation). (From: Pasler FA. Zahnärztliche Radiologie. 5th ed. Stuttgart: Thieme; 2008.)

tion decreases in inverse proportion to the square of the distance from the radiation source. This has important implications for radiation protection. Distance is the best protection against radiation.

Theoretically, if the distance from the X-ray source to the object increases by a factor of two, the radiation intensity must be increased by a factor of four to obtain the same degree of blackening. However, when the source-to-target distance is increased, a smaller collimator size is used to keep the field size constant (6 cm) without higher radiation exposure.

6.2.4 High Voltage

Any change in voltage results in a change in the penetrating power of X-rays. The higher the penetrating power, the smaller the fraction of X-rays absorbed and the larger the number of X-rays reaching the image receptor. The end result is a reduction of contrast, which occurs because the absorption differences in tissue become smaller and fewer contrast levels are displayed. At the same time, the proportion of scattered radiation increases with increasing voltage. From a voltage of ~60 kV and higher, the percentage of scattered radiation exceeds the percentage of absorbed radiation.

Higher voltage does have an influence on film darkening, but the price for this is a loss of contrast. The reduction of contrast due to scattered radiation can be decreased to a certain extent. In dental radiography, this can be accomplished by reducing the size of the radiation field, and through appropriate filtering.

In general radiology, anti-scatter grids are used to reduce scattering. Anti-scatter grids consist of parallel strips

of lead, which serve to absorb scattered radiation that strikes the grid at an angle. Anti-scatter grids are positioned between the patient and the film. They do not attenuate the primary beam, which is important for image formation.

6.2.5 Scattered Radiation

When X-rays pass through an object, they are either absorbed or scattered in all directions. Because this so-called secondary radiation scattered from the object has different angles of incidence, it leads to a reduction of contrast.

A practical way to reduce the scattered radiation component is to use the smallest collimator possible. When taking skull radiographs with larger formats, anti-scatter grids are placed between the patient and the image receptor, to intercept scattered radiation (□ Fig. 6.4).

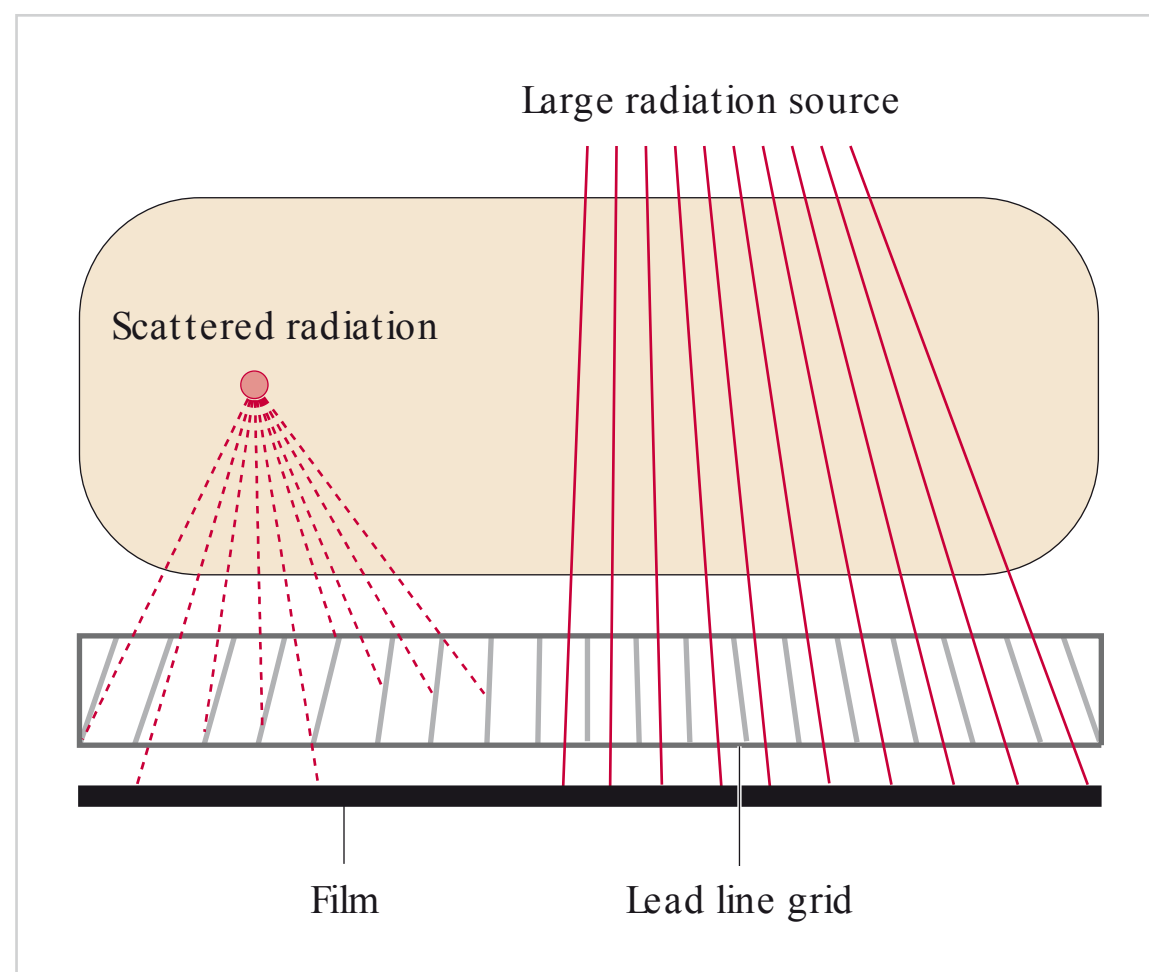


Fig. 6.4 Scattered radiation and anti-scatter grid. (From: Zabel H. Kurzlehrbuch Physik. Stuttgart: Thieme; 2011.)



Fig. 6.5 Dental X-ray film.

6.3 Radiographic Film and Intensifying Screen-Dependent Factors that Influence Image Formation

6.3.1 Screenless Films

Dental radiology is unique, in that the films used to acquire dental radiographs come both with and without intensifying screens.

Intraoral radiography is the only branch of radiography where screenless films are used. Intraoral radiographs are expected to provide high contrast and very high resolution (sharpness) on the one hand, and high film speed and sensitivity on the other (□ Fig. 6.5).

Note

The main characteristics used to describe the quality of radiographic films are:

- Contrast
- Sharpness (resolution)
- Film speed (sensitivity).

□ Contrast: As a general rule, dental radiographic film must have high contrast to be able to accurately differentiate between fine structures located close together in the dental region. Factors related to scattered radiation and film development influence film contrast. Film contrast increases with higher film-development temperature. Re-use of developer results in a decrease in film contrast.



Fig. 6.6 Lead line grid.

□ Sharpness (resolution): Because intraoral radiography is intended for the visualization and differentiation of very fine structures, it requires the use of films with a high degree of sharpness. Generally speaking, film sharpness is measured in terms of resolution, or resolving power. In practice, resolution is measured using high-contrast lead line grids in units of line pairs (lp) per millimeter (□ Fig. 6.6).

□ Film speed (sensitivity): Film speed is affected both by the number and by the shape and size of the silver bromide (AgBr) crystals present in the film emulsion. The more crystals there are, the faster the film will be. However, there are limits to the number of silver bromide crystals that is technically feasible. The shape and structure of the silver bromide crystals has been improved through the development of new crystalline forms.

Conventional silver bromide crystals were very small and characterized by high resolution. However, because their sensitivity was low, they required significantly longer exposure times than modern crystals. Further research led to the development of tabular crystals (T-grains), which lie along the surface of the emulsion layer such that the flat side of the crystal is struck by the incident X-ray beam (□ Fig. 6.7 and □ Fig. 6.8). Owing to this configuration, tabular crystals have significantly higher absorption characteristics than the older spherical crystals. In accordance with ISO 3665 standards for the classification of intraoral radiographic film, three different classes of film speed are distinguished and are characterized by the letters D, E, and F.

The use of E-speed film results in ~50% dose reduction compared with D-speed film, but the difference between E-speed and F-speed film is not as high.

The only reason why F-speed film is faster is because of its higher developing temperature. According to the ISO 3665 standards, intraoral film developed in automatic processors using a roller transport system and at higher temperature (28 °C) is classified as F-speed film. However, if it is developed manually or on another type of automatic processor at 20 °C, then it is classified as E-speed film.

Note

Only the faster E-speed and F-speed films should be used in intraoral radiography because they provide the same diagnostic imaging quality as D-speed film but can reduce the radiation dose by up to 50 %

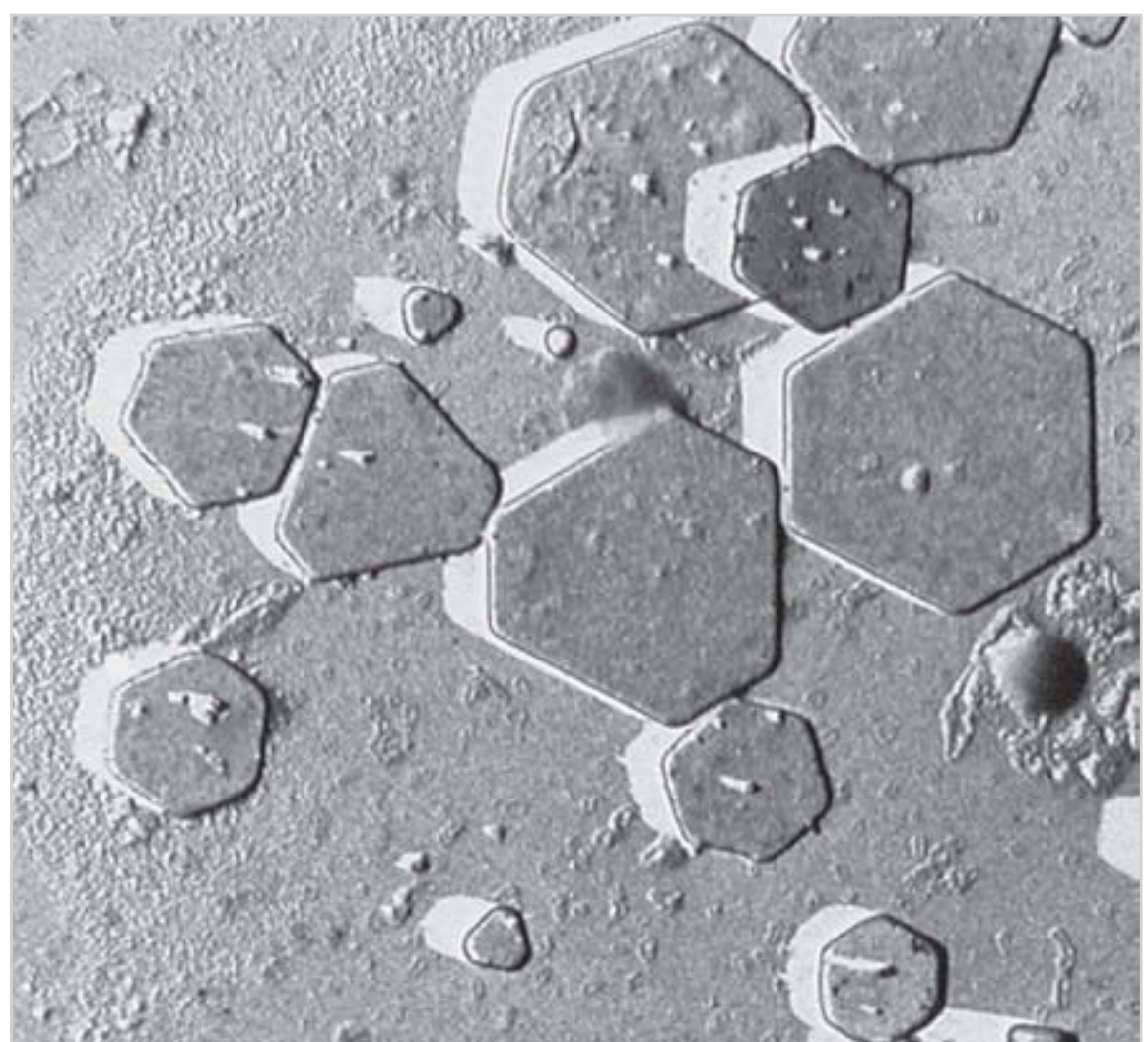


Fig. 6.8 T-grain crystals under an electron microscope.

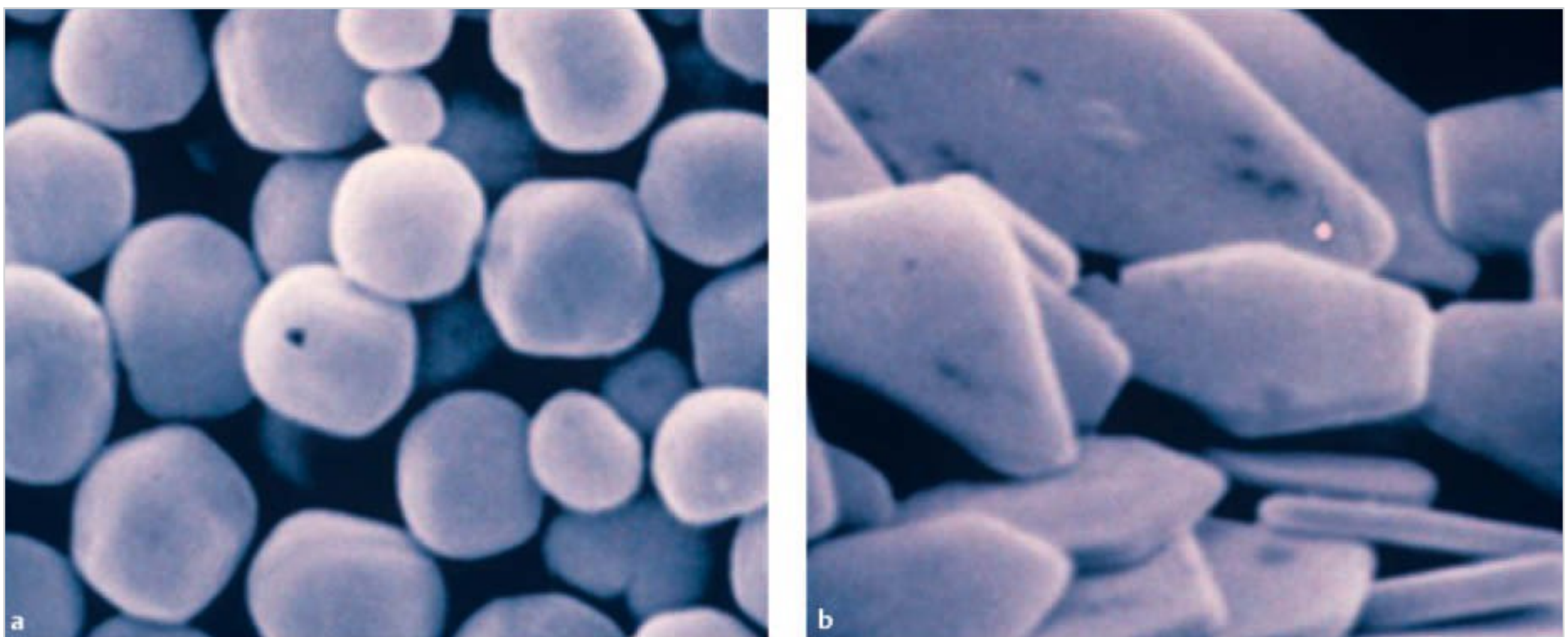


Fig. 6.7a, b Comparison of different film crystals.
a Conventional crystals.
b T-grain crystals.

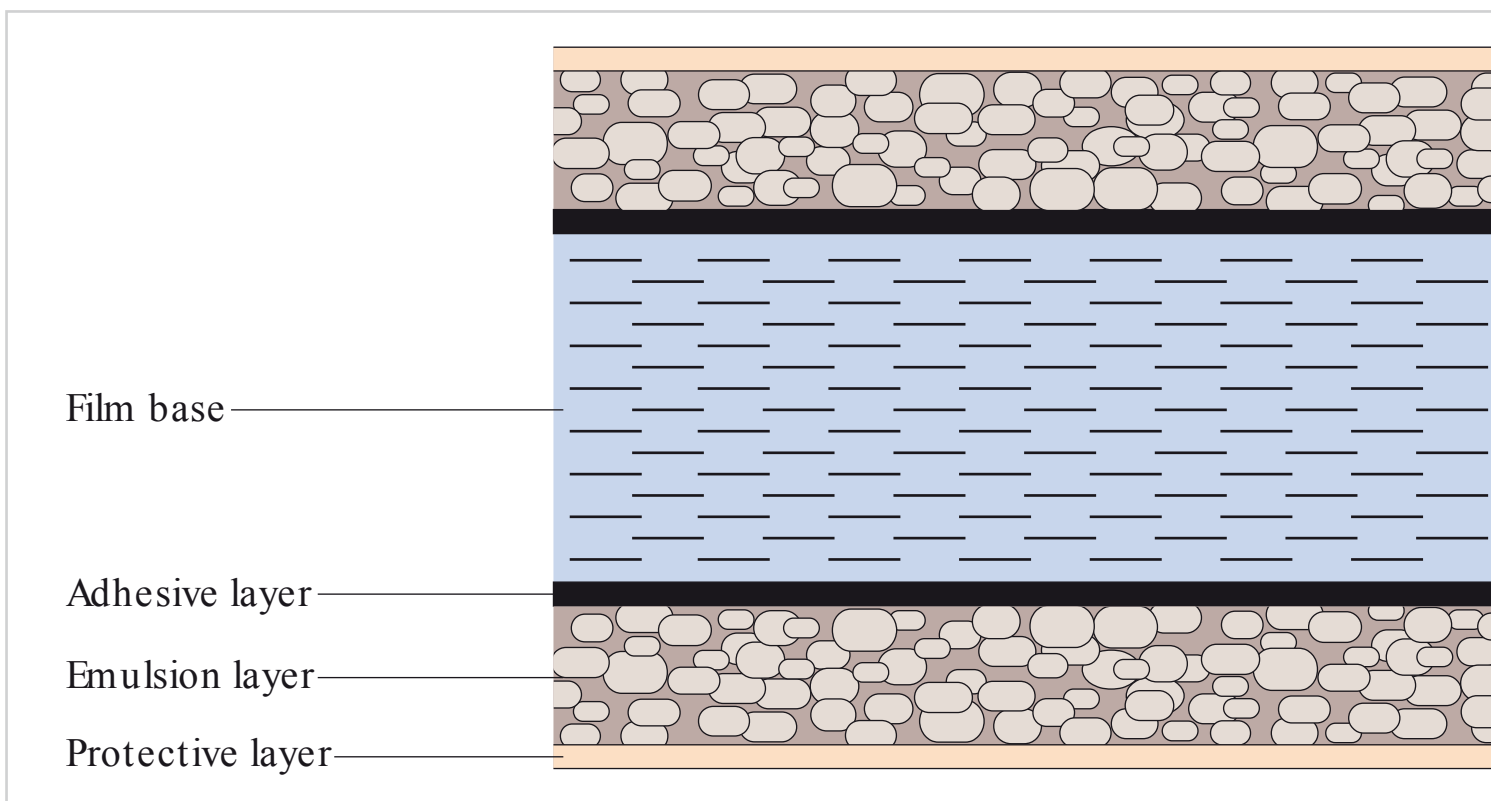


Fig. 6.9 Cross-sectional structure of radiographic film.



Fig. 6.10 Dental X-ray film packaging and components (from left to right): plastic cover, front and back, film, black cardboard, and lead foil.

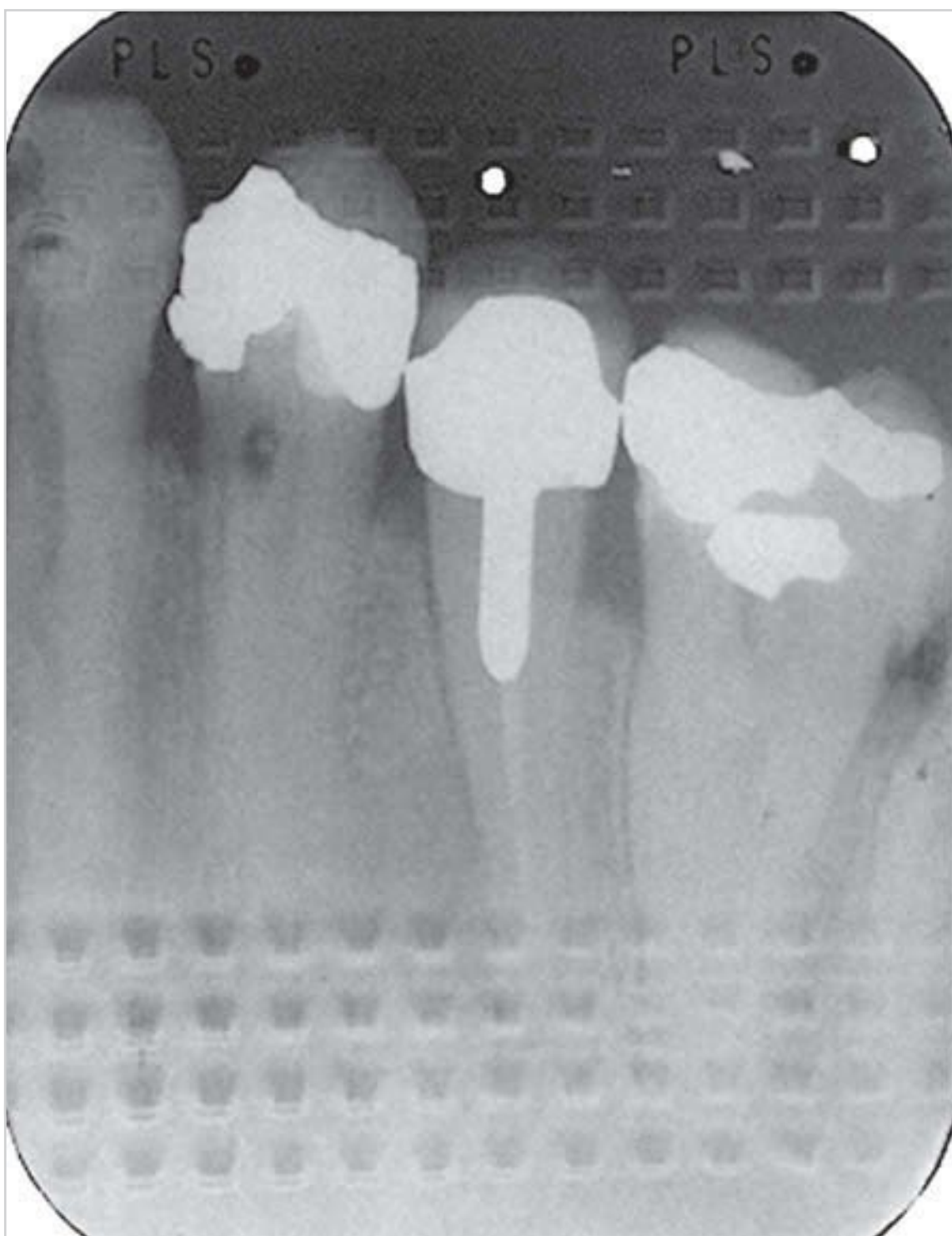


Fig. 6.11 If X-ray film is exposed on the wrong side, the pattern embossed on the lead foil can be seen.

Construction of Radiographic Film

To obtain the maximum yield of X-rays and light from the intensifying screen, the emulsion layer of radiographic film must contain as many silver bromide crystals as is technically feasible. Since each emulsion layer can contain only a limited number of silver bromide crystals, most radiographic films have two layers of emulsion, one on the front and one on the back (□ Fig. 6.9). The central film base separating the two layers is a thin polyester sheet ~0.2 mm thick. Polyester is a transparent and flame-retardant material.

A thin layer of adhesive is applied to each side of the film base. The adhesive layers serve to firmly attach the emulsion containing the silver bromide crystals to the film base. Each emulsion layer is embedded in gelatin. The gelatin not only serves as a binder for the emulsion layer, but also affects the speed (sensitivity) and contrast of the film. Finally, the film is enclosed in a protective layer designed to prevent mechanical damage, safeguard the emulsion, and improve gliding of the film through the film processors.

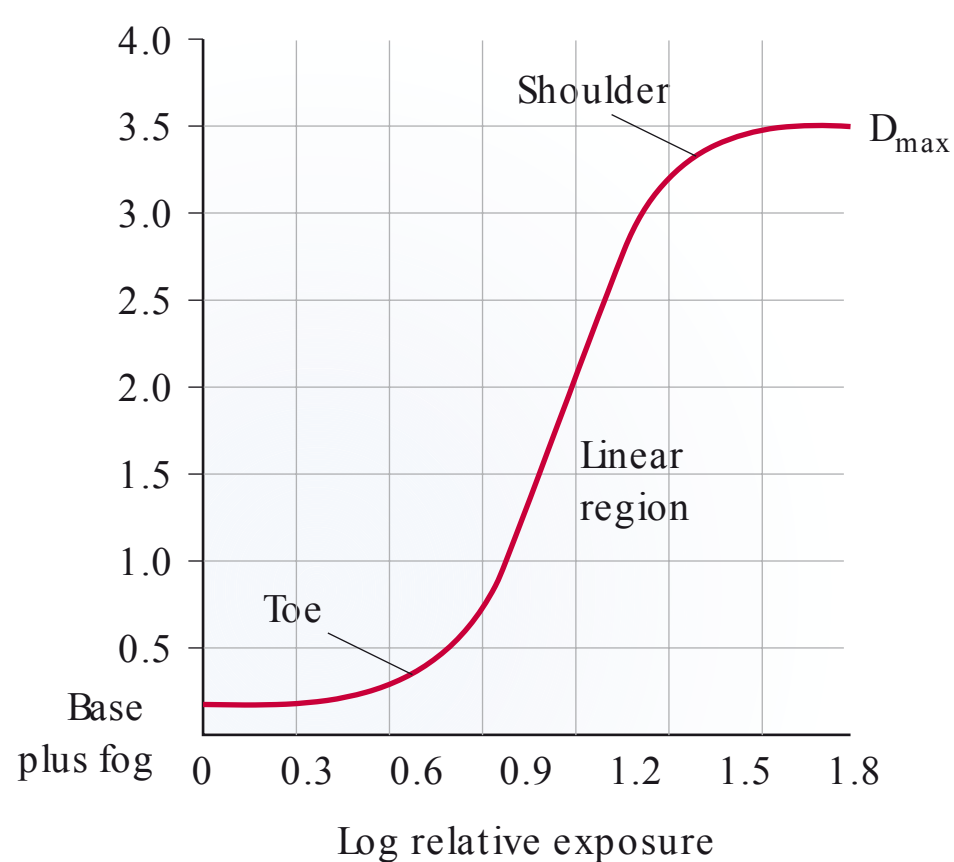
Only a few incident X-rays strike intraoral films without an intensifying screen. Therefore, in addition to the two-sided coatings described above, the films have another layer that contains as much silver as is technically feasible. Modern non-screen dental films contain ~200 g of silver per square meter, whereas radiographic films with an intensifying screen only have ~40 g of silver per square meter. The main reason for this difference is probably the price of silver, in addition to the use of an intensifying screen.

The film packaging must be light and waterproof and must provide sufficient stability. The covers are made of plastic. To provide stability, the film is also encased in cardboard (□ Fig. 6.10).

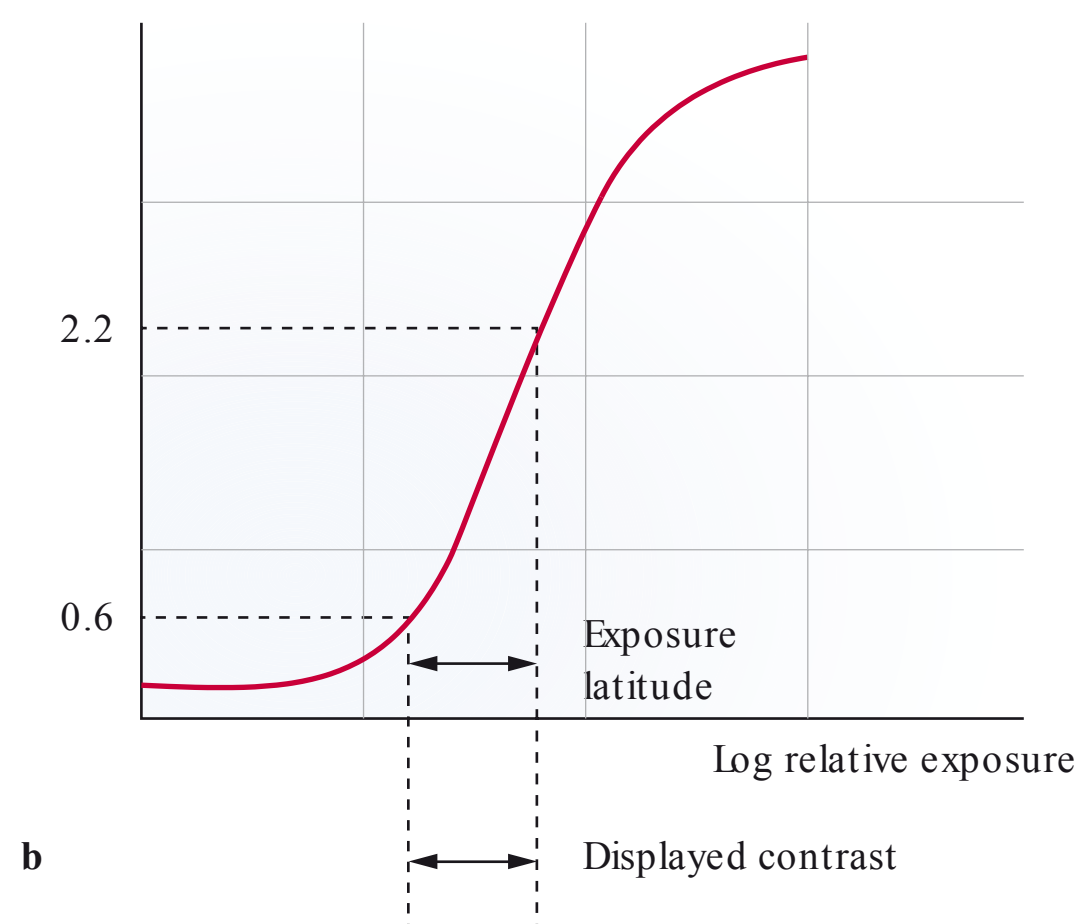


Fig. 6.12a–c Over-exposure, normal exposure, and under-exposure.

- a** Too light.
- b** “Normal.”
- c** Too dark.



a



b

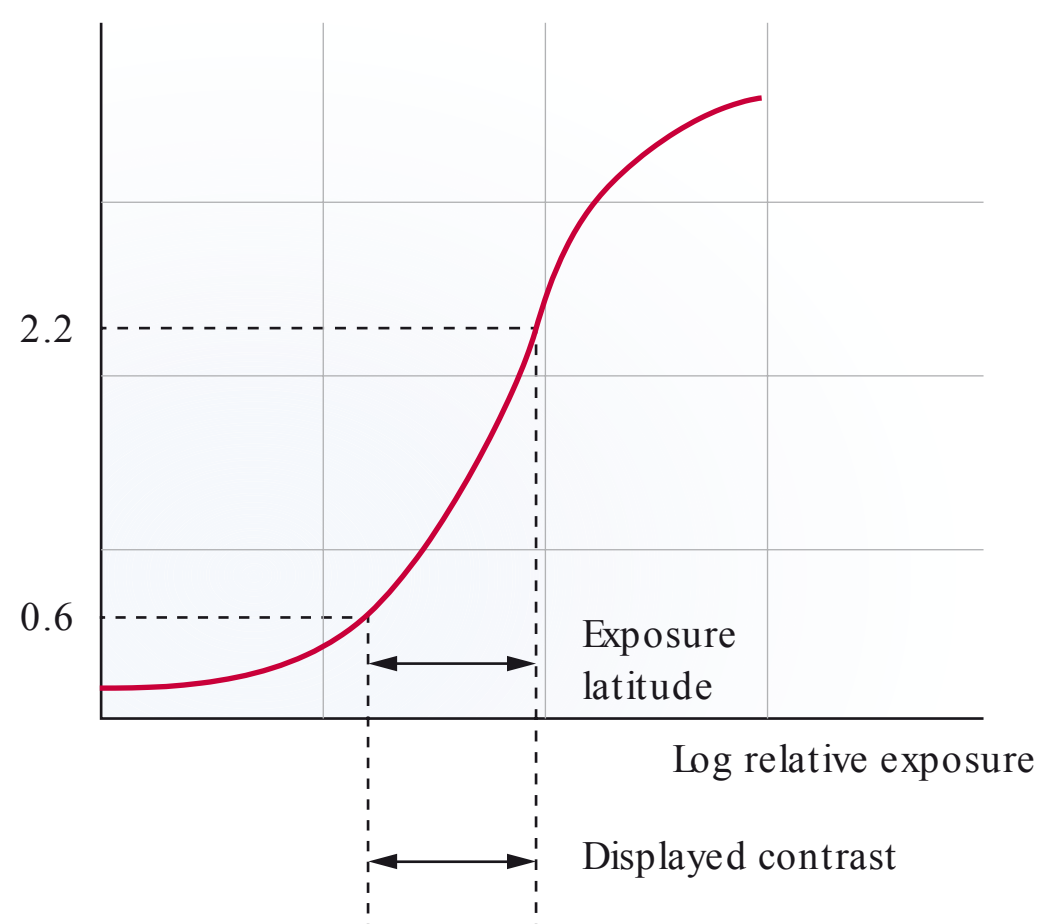


Fig. 6.13a, b Characteristic curves. (From: Ewen K, ed. *Moderne Bildgebung*. Stuttgart: Thieme; 1998.)

- a** Characteristic curve of radiographic film showing log relative exposure and the resulting optical density. D_{\max} : maximum optical density.
- b** Characteristic curves of films with different contrast characteristics. The film on the **right**, which has a steeper linear region or slope, has higher contrast but low exposure latitude. The film on the **left**, which has lower contrast, has wider exposure latitude and is especially well suited for radiographs of areas that require high-contrast imaging, such as the facial skeleton.

On the back side of the film cassette, there is a thin sheet of lead foil that absorbs both the radiation that passes through the film as well as the scattered radiation that reaches the film from the tissues. The lead foil serves to provide radiation protection and to improve image quality. A pattern embossed on the lead foil indicates when radiographic film is mistakenly exposed from the back. If the film is exposed on the wrong side, the X-ray appears too light and the pattern can be seen (□ Fig. 6.11).

Graphical Representation of Film Characteristics: Characteristic Curve

The characteristic curve describes the relationship between film exposure—including development—and the resulting optical density.

When exposing and developing radiographic film, the goal is to ensure that the optical density of the film is always in a range that is suitable for diagnostic interpretation (□ Fig. 6.12). The characteristic curve, or density curve, is a graph used to show how the characteristics of the radiographic film affect the X-ray image (□ Fig. 6.13).

The characteristic curve is composed of different regions. The middle linear region of the curve (slope) reveals the most important information about the contrast of the film. The steeper the linear region or slope, the higher the contrast of the film.

The two curved portions at the beginning and end of the curve are referred to as the toe and shoulder of the curve. They mark the regions that are not suitable for diagnostic radiology.

The characteristic curve does not start at zero. Instead, it starts at a level called background fog. Background fog is the inherent level of background blackening that may occur on radiographic film, but the fog density must not exceed a level of 0.25. Background fog is caused by the base and the emulsion of radiographic film. Film storage conditions, as well as environmental conditions in the darkroom, are factors that can result in an increase in background fog levels.

6.3.2 Radiographic Film with Intensifying Screens

Intensifying screens are used in combination with radiographic films for all extraoral images. Intensifying screens are typically mounted on the inside of film cassettes, on both the front and back of the cassette. Like radiographic films, intensifying screens consist of a plastic base layer to which an emulsion layer is attached. The emulsion contains fluorescent crystals. The main purpose of intensifying screens is to reduce the amount of radiation needed for the production of radiographic images, by reinforcing the action of X-rays. This occurs as a result of luminescence of the incident X-rays that strike the intensifying screen; the luminescence is in the range of the visible light spectrum.

Fluorescence has a long history, and it was the glow from such a layer of fluorescent material that led to the discovery of X-rays. Intensifying screens have been used since the beginning of radiography. Calcium tungstate phosphors were used for decades. Since 1978, calcium tungstate screens have been replaced with rare-earth screens using green-glowing gadolinium phosphors.

Calcium tungstate and gadolinium crystals have individual light-emission characteristics, which must be precisely matched, to correspond to the characteristics of the film (□ Fig. 6.14 and □ Fig. 6.15).

The sensitivity of a screen/film system is determined by the dose that induces a specified degree of blackening of the film. The sensitivity class is mainly determined by screen thickness.

The speed of intensifying screens is divided into dimensionless speed classes. Only class 200 to 250 and 400 fast screens with high intensifying power are used in dental radiography.

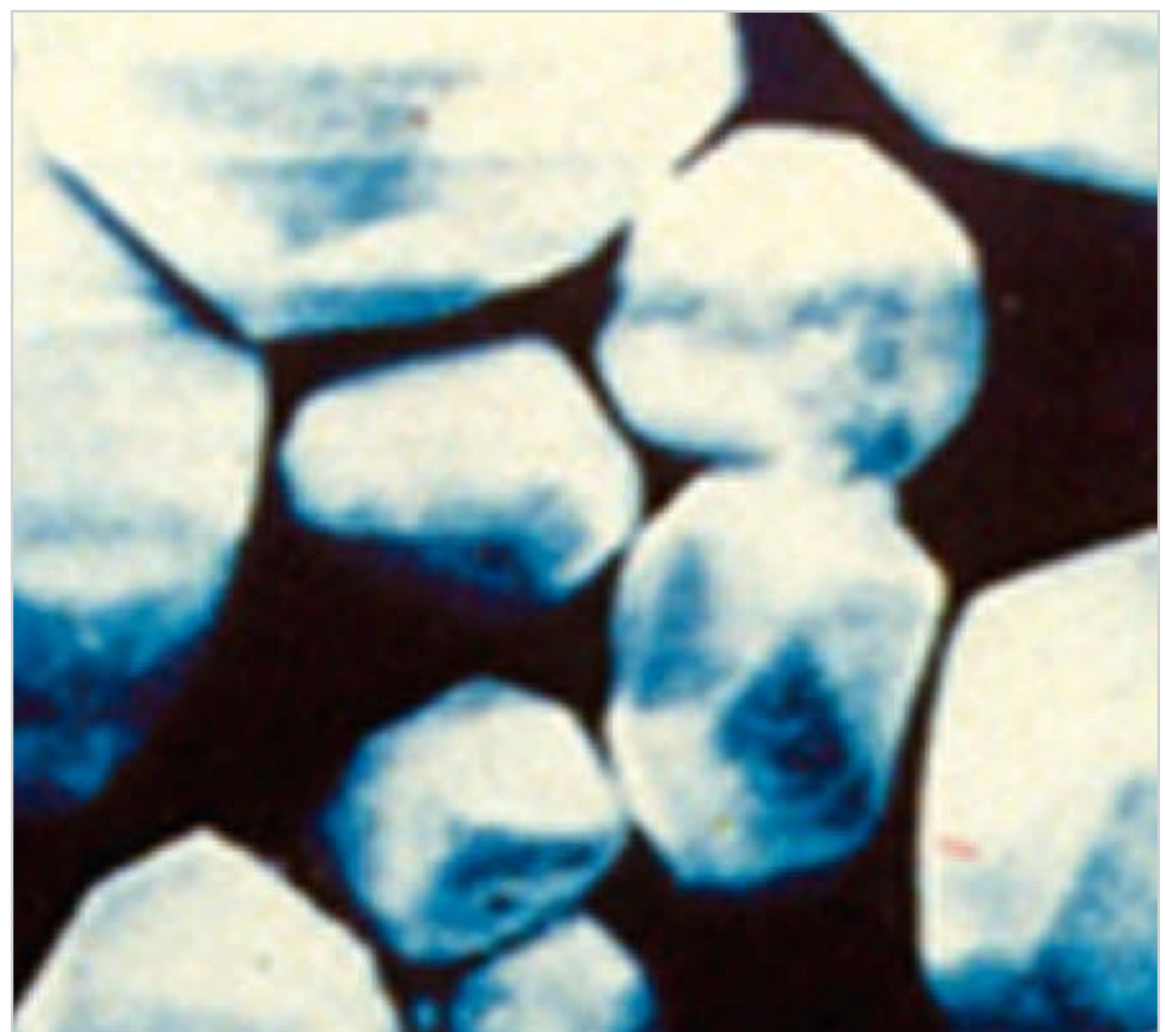


Fig. 6.14 Calcium tungstate crystals.

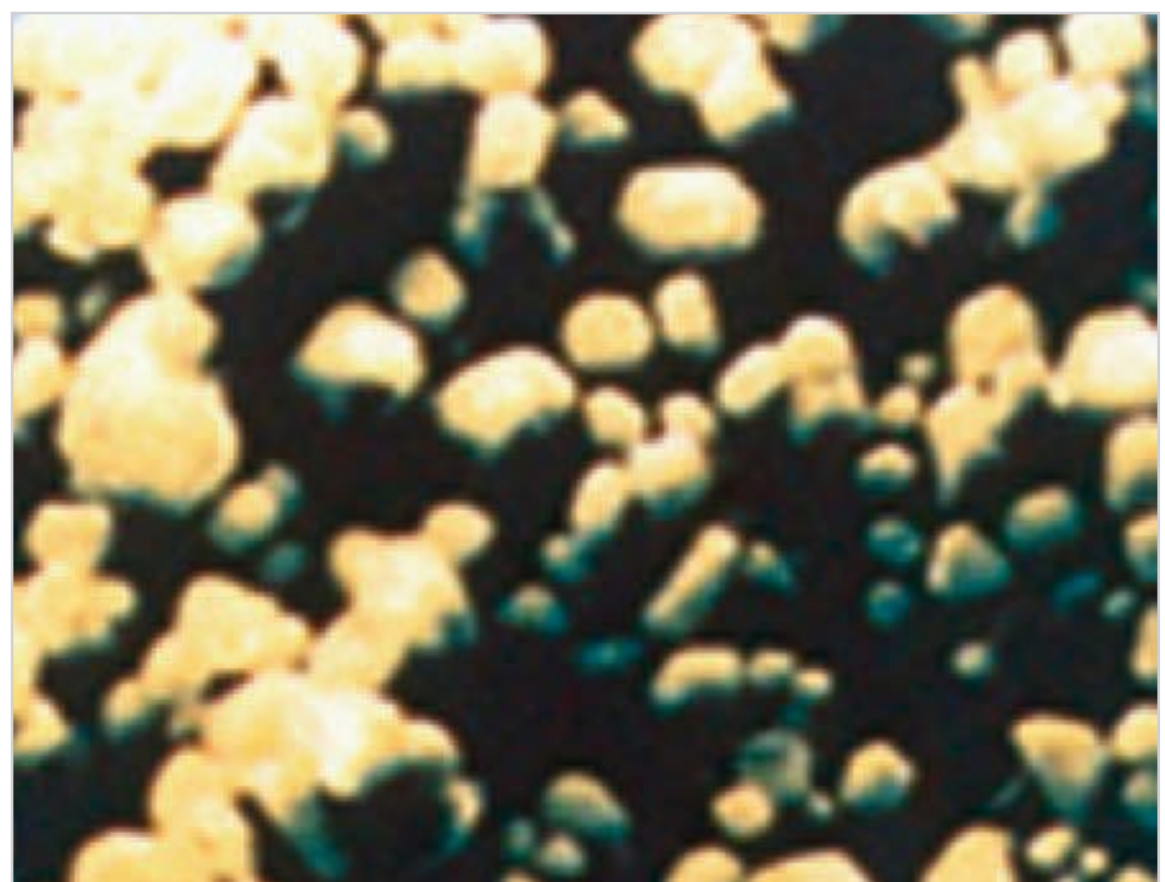


Fig. 6.15 Gadolinium crystals (rare earths).

Note

High-speed (400) intensifying screens must be used for the acquisition of cephalometric radiographs in children. All other extraoral radiographs can be taken using intensifying screens with a speed of 200 to 250 (□ Fig. 6.16).

Disadvantages of Intensifying Screens

Intensifying screens achieve dose reduction for the patient, at the expense of image quality.

One of the main factors responsible for the blurring associated with intensifying screens is the size of the crystals: screen crystals are not as small as silver bromide crystals. The thickness of the screen is another important factor. The thicker the screen, the longer the distance the light must travel and thus the greater the degree of scattering. This effect increases if light does not strike any silver bromide crystals in the first emulsion (striking only those in the second emulsion), or if the emulsion

is exposed from the rear by light reflected from the back wall of the cassette. This effect is referred to as crossover. Crossover can also have an adverse effect on image quality (□ Fig. 6.17).

6.4 Processing of Radiographic Films

Radiographic film can be developed by manual, semi-automatic, or fully automatic processing methods. The introduction of modern quality assurance standards have made manual and semi-automatic processing practically obsolete.

One of the many advantages of automatic processing at higher temperatures is that higher temperature results in an increase in film speed and contrast. Thus, two practical benefits of fully automatic development are reduction of the patient dose and additional improvement of image quality.

The roller transport system of automatic processors meets the quality assurance requirements for radiographic film development in accordance with international standards (□ Fig. 6.18).

If no darkroom is available, the automatic processor can be fitted with a daylight loader that allows safe film development (□ Fig. 6.19).



Fig. 6.16 Cassette and film.

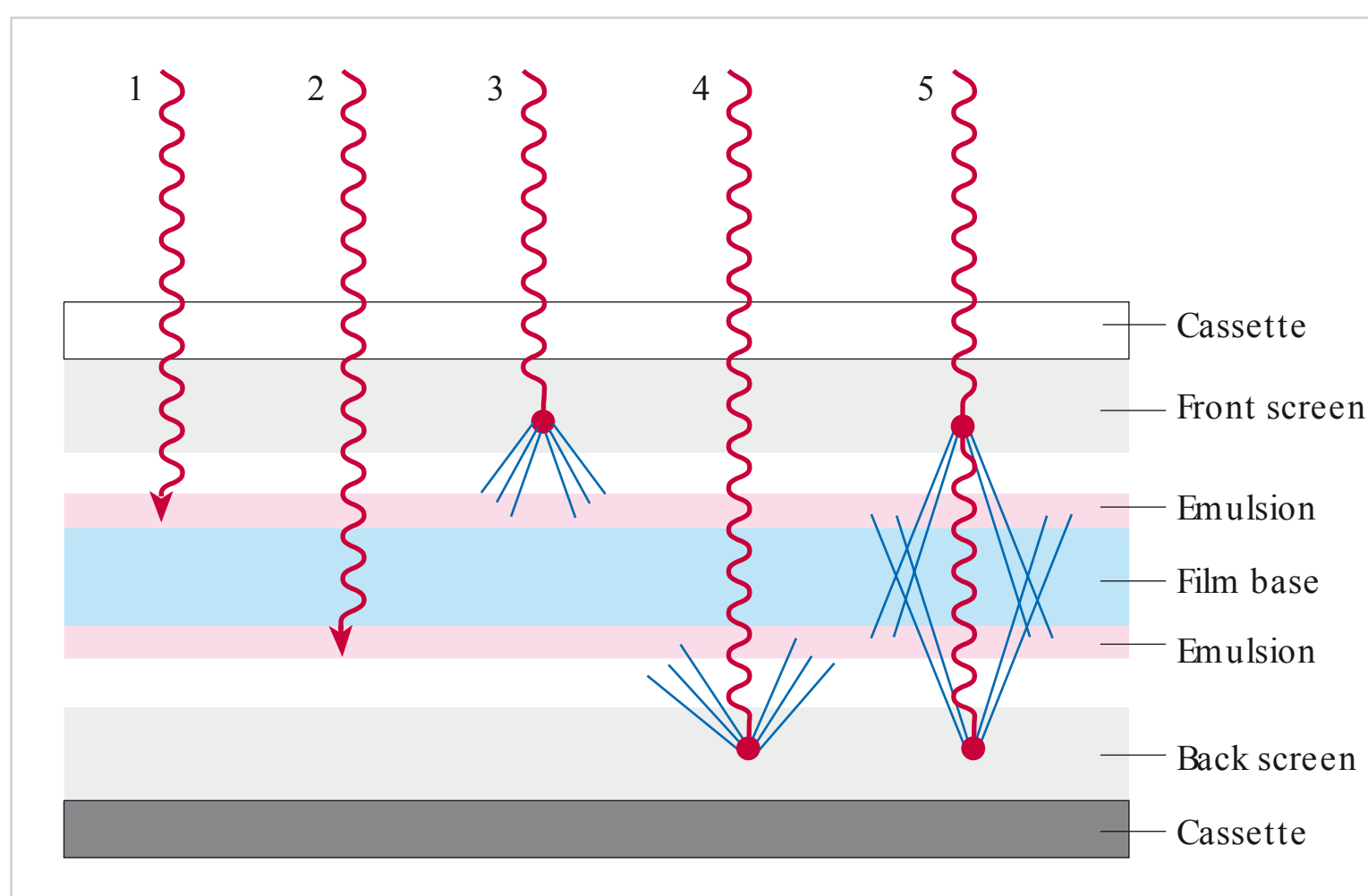


Fig. 6.17 Screen unsharpness (schematic diagram). (From: Pasler FA, Visser H. Zahnmedizinische Radiologie. 2nd ed. Stuttgart: Thieme; 2000. Farbatlanten der Zahnmedizin; Band 5.)

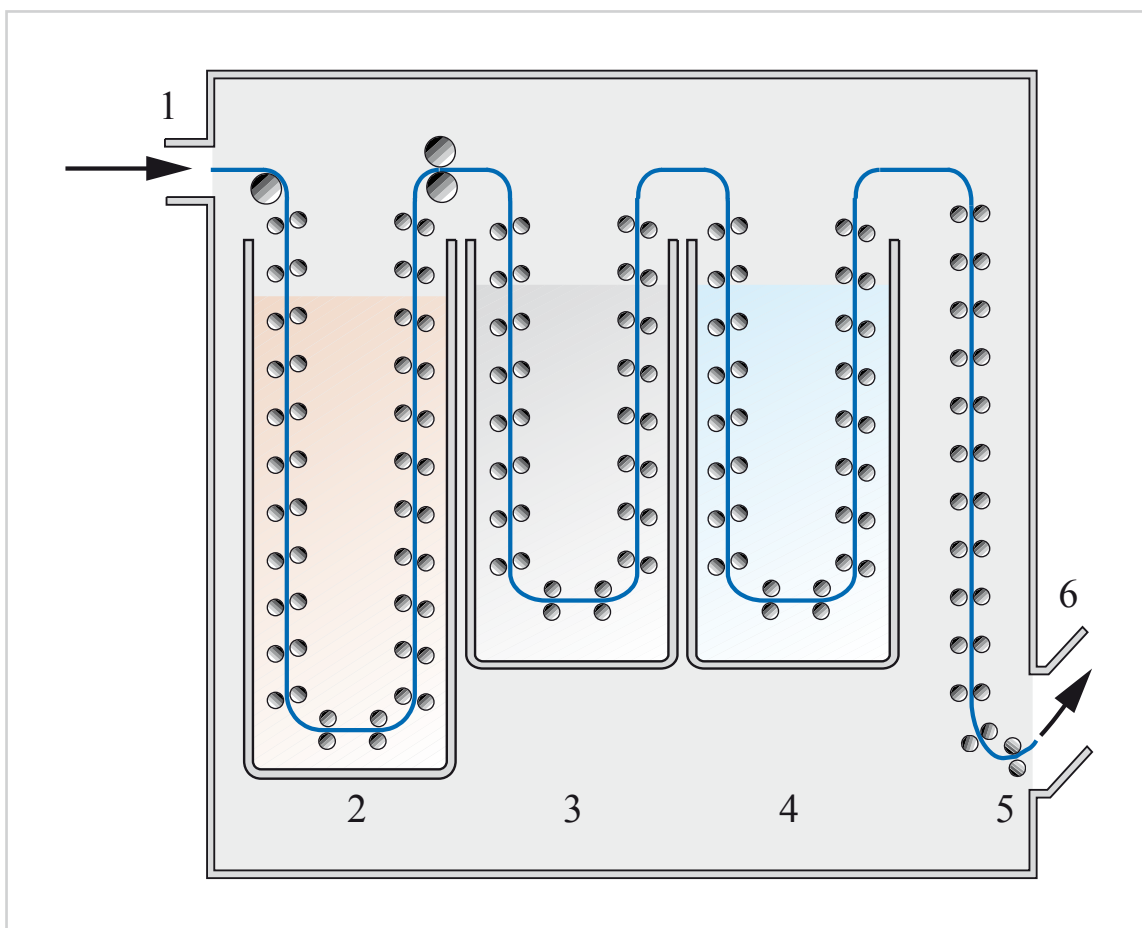


Fig. 6.18 Automatic processor with rollers: 1 Film feed, 2 Developer, 3 Fixer, 4 Wash water, 5 Dryer, 6 Outlet. (From: Pasler FA, Visser H. Zahnmedizinische Radiologie. 2nd ed. Stuttgart: Thieme; 2000. Farbatlant der Zahnmedizin; Band 5.)



Fig. 6.19 Automatic processor with daylight loading apparatus.

Chapter 7

Digital Dental Radiography

7.1	Sensors	47
7.2	Storage Phosphor Imaging Plates	48
7.3	Advantages of Digital Radiography	50



7 Digital Dental Radiography

The use of digital image receptors in dental radiography began with the launch of the first commercial system in 1986. This technology, called the RadioVisioGraphy system, used a charge-coupled device (CCD) for digital intraoral X-ray imaging. Digital imaging plate scanner systems were introduced as the second digital X-ray imaging technology in the mid-1990s.

Meanwhile, the technology used in intraoral and extraoral digital imaging systems has become so good that the diagnostic image quality of digital X-rays is now equal, if not superior, to that of conventional X-rays.



Fig. 7.1 Digital radiography sensor and cable.



Fig. 7.2 Digital imaging plate with protective cover.

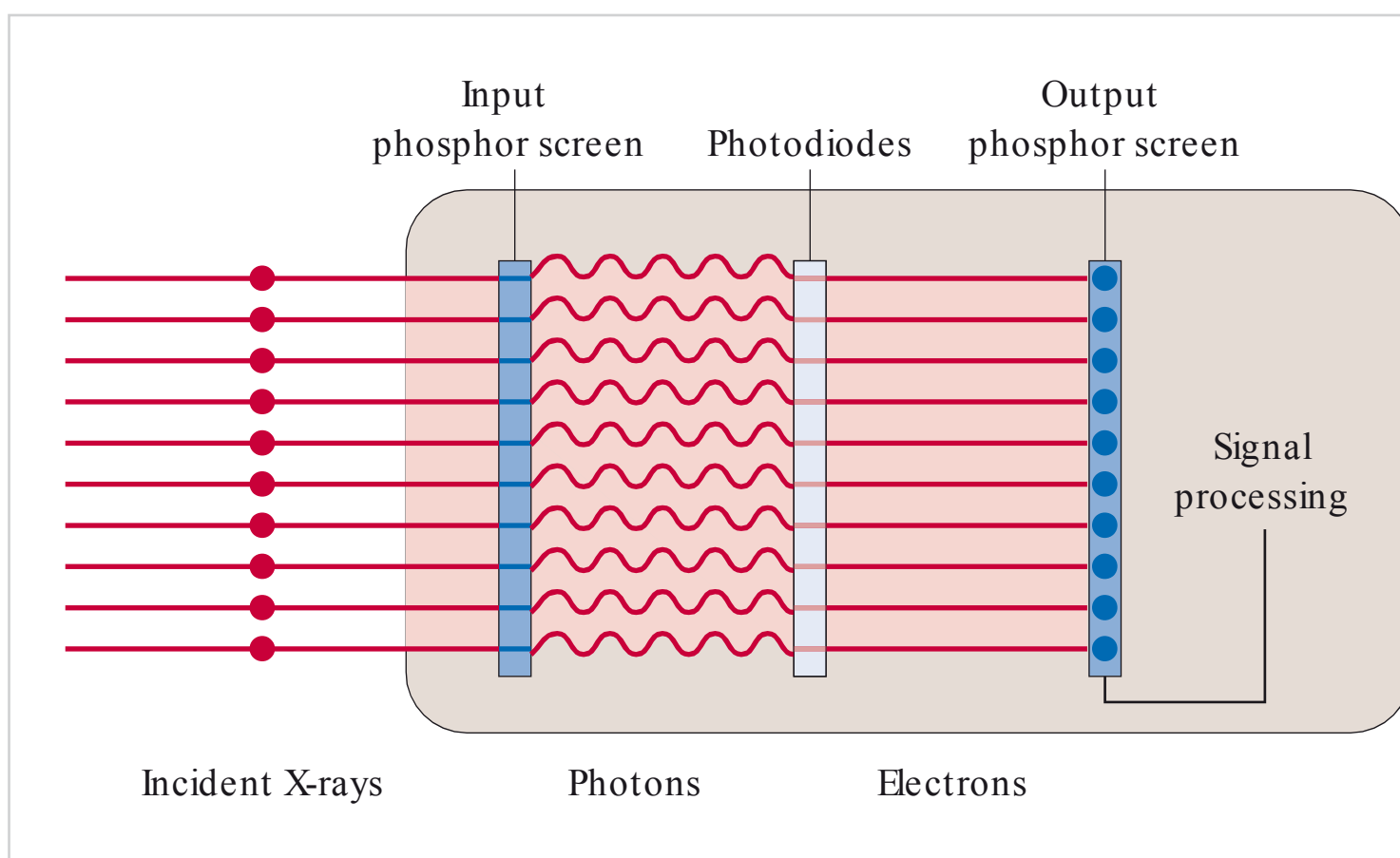


Fig. 7.3 Flat panel detector (schematic diagram).

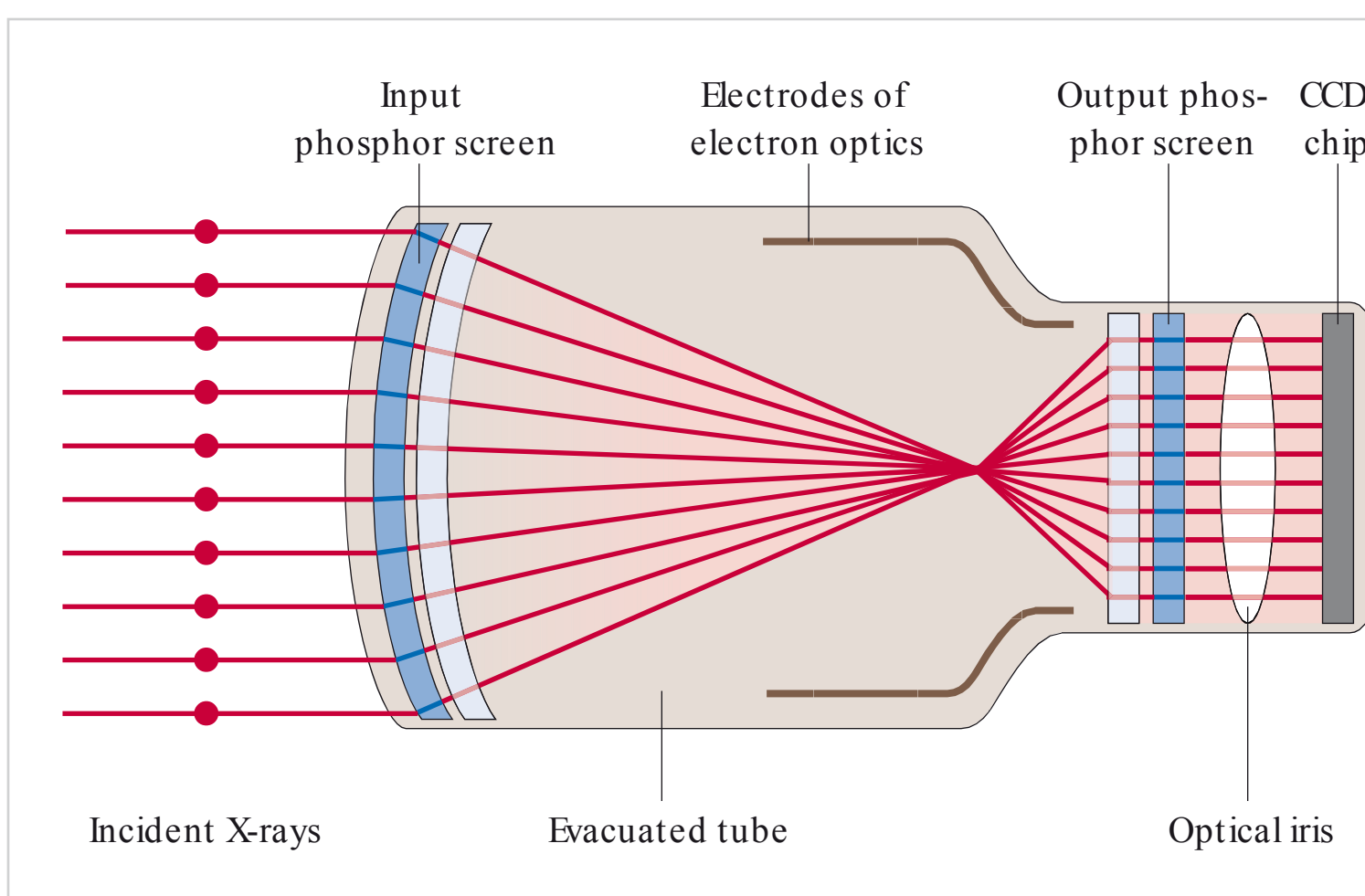


Fig. 7.4 Image intensifier (schematic diagram). CCD: charge-coupled device.

The term digital radiography, or digital X-ray imaging, refers to the technique of acquisition and display of radiographic images by means of electronic data-processing technology. Conventional X-ray images are acquired using a radiographic film or film–screen combination. Digital X-rays, on the other hand, are acquired and processed using digital sensor systems and imaging plates. A computer with appropriate software is needed to process and display the digital image data on a high-performance monitor.

All digital imaging systems need a system for the conversion of analog signals into digital image signals, and a detector that converts X-ray photons into electric charges.

Several different devices are used for this purpose in dental digital X-ray imaging:

- Sensors (□ Fig. 7.1) and imaging plates (□ Fig. 7.2) are used in digital intraoral and panoramic radiography systems.
- Flat panel detectors (□ Fig. 7.3) and, in some cases, image intensifiers (□ Fig. 7.4) are used in cone beam computed tomography (digital volume tomography).

7.1 Sensors

Sensors are image-capturing devices that consist of quadratic light-sensitive photodiodes. Each photodiode acts as a picture element, which is abbreviated as pixel.

The energy of the incident photons is transferred to the electrons of a semiconductor that acts as a capacitor (e.g., a CCD chip). The charges generated in the process flow into a “potential pot,” where they are collected and then read out (□ Fig. 7.5).

The image sensors used in dental digital radiography differ, in some cases significantly, in their structure and mode of operation. There are three types available:

- CCD sensors
- CMOS sensors (complementary metal oxide semiconductors)
- CdTe sensors (cadmium telluride sensors).

□ CCD sensors: CCD sensors read out charges as follows: the electrons are transported across the chip row by row, in the vertical and the horizontal direction, from one pixel to the next, as in a bucket brigade. The electrical analog signals are then amplified and converted into digital signals by an analog-to-digital converter. The main disadvantage of CCD sensors is that if there are very large amounts of charge (that is, over-exposure), the small potential pots overflow. This is reflected as ink-blot-type zones of radiolucency on the images. This problem, known as blooming, is one of the reasons why CCD sensors are being increasingly replaced by CMOS sensors. Other disadvantages of CCD sensors are their narrow exposure latitude (owing to blooming) and relatively long readout time.

□ CMOS sensors: CMOS sensors use a different readout technique, in which each pixel can be read out individually. Furthermore, each pixel has its own amplifier for analog signal processing and its own analog-to-digital converter. Since CMOS sensors can perform these and many other functions, they are called active pixel sensors (APS). This technology will replace the old CCD-based technology because it enables CMOS sensors to achieve faster readout times and less noise than CCD sensors.

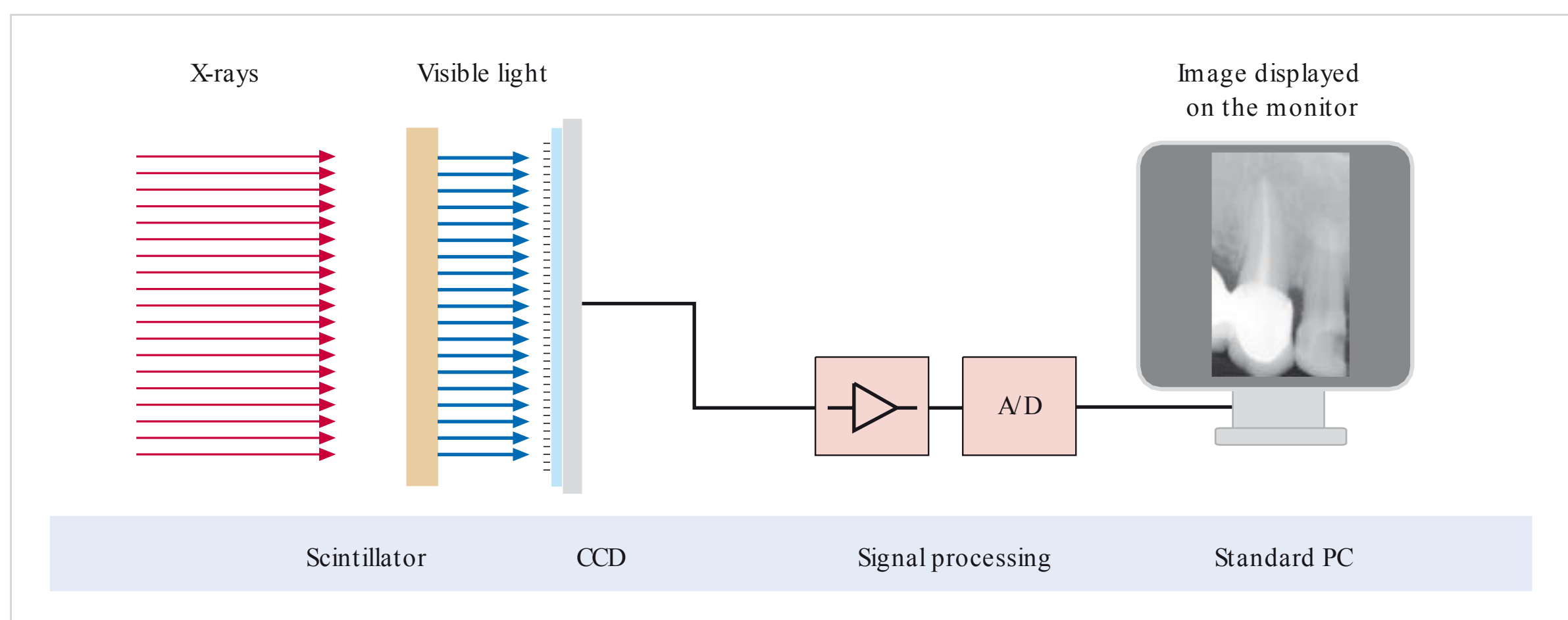


Fig. 7.5 Signal processing with a digital sensor (schematic diagram). CCD: charge-coupled device. (From: Pasler FA, Visser H. Zahnmedizinische Radiologie. 2nd ed. Stuttgart: Thieme; 2000. Farbatlant der Zahnmedizin; Band 5.)

□ CdTe sensors: CdTe sensors have a thin layer of cadmium telluride rather than a light-emitting layer. Almost all sensors today work with a luminescent layer that is firmly vapor-deposited on the sensor, similar to an intensifying screen. Whereas the first generation of sensors had layers doped with rare-earth ions, cesium iodide (CsI) is used today. Cesium iodide crystals are characterized by their small size and narrow, tapered needle structure. This technology reduces light scatter nearly completely. The light protects the sensor from X-rays, which have extremely short wavelengths.

CdTe sensors were developed in an attempt to digitize X-rays without light and to obtain radiographic images with even better resolution.

7.1.1 Spatial Resolution

The spatial resolution of a sensor is dependent on the physical pixel size. Modern sensors have a pixel size of $15 \times 15 \mu\text{m}$. Spatial resolution is generally expressed in units of line pairs per millimeter (lp/mm). Sensors with a pixel size of $15 \times 15 \mu\text{m}$ have a theoretical spatial resolution of 33 lp/mm. However, this theoretical mathematical physical value is never achieved in practice, owing to several interfering factors, such as image noise and geometrical unsharpness.

Image noise is produced by the random manner in which photons are distributed in a defined area of the image receptor. The noise component is solely dependent on the number of photons incident on the detector. Therefore, the downside of increasing the dose (to improve image quality) is a larger noise component.

Geometric unsharpness is the loss of detail caused by increasing the size of the focal spot (non-point source), which, together with other unfavorable imaging parameters, can decrease image quality to a variable degree.

Pixel binning is another procedure used in digital image processing. In binning, the charge from four adjacent pixels is generally combined to shorten processing times

and to reduce storage requirements. Another important benefit of pixel binning is that it can reduce the dose to the patient. In any case, it must be noted that pixel binning offers several advantages but reduces spatial resolution.

7.2 Storage Phosphor Imaging Plates

In contrast to the intensifying screens, storage phosphor imaging plates do not convert X-rays into visible light immediately; instead, excited electrons are “trapped” in the crystal lattice of the storage phosphor layer of the plate. Storage phosphor imaging plates are semiconductor plates with a storage phosphor layer, which generally consists of a europium-doped barium fluorohalide phosphor. The storage phosphor layer contains so-called electron traps, or chemical traps (□ Fig. 7.6). A laser is used to scan the storage phosphor imaging plate and convert the latent image into a digital image, by the process of photo-stimulated luminescence (PSL) (□ Fig. 7.7).

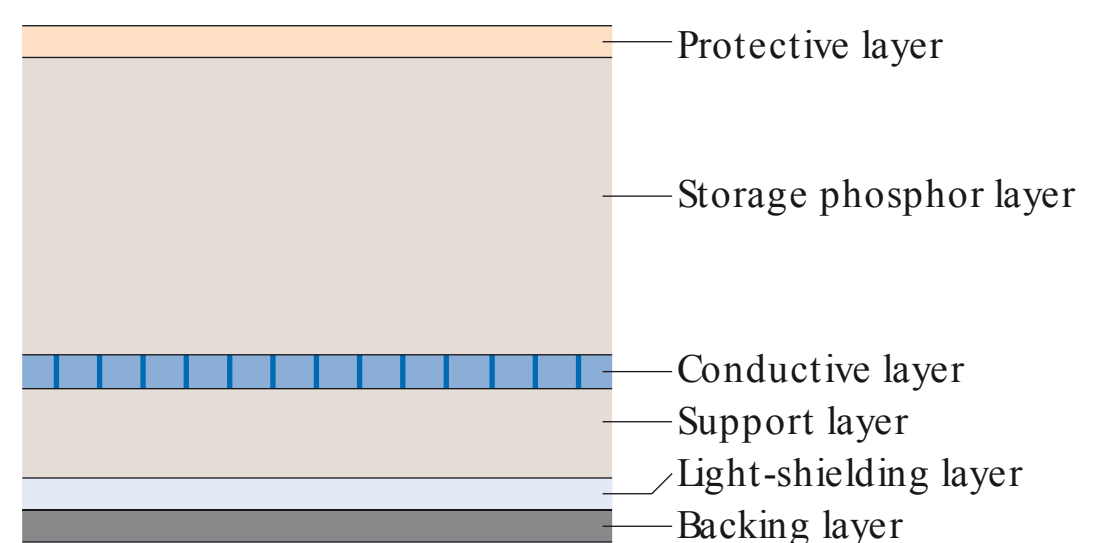


Fig. 7.6 Structure of an imaging plate. The imaging plate consists of a layer of X-ray sensitive crystals (storage phosphor layer), usually europium-doped barium fluorohalide phosphor (BaFBr:Eu^{2+}) on a polyester base (support layer).

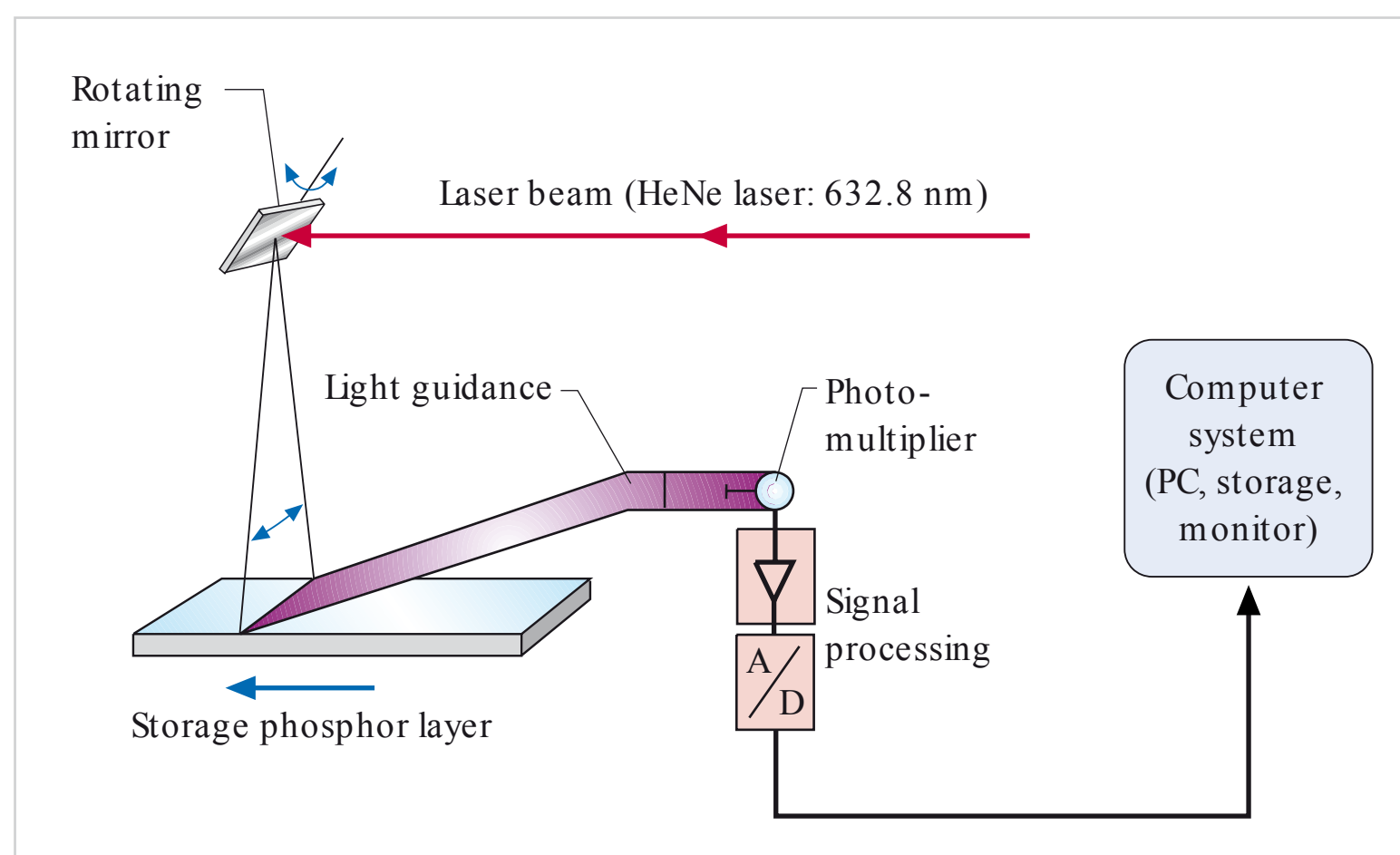


Fig. 7.7 Imaging plate readout. HeNe: helium–neon. (From: Pasler FA, Visser H. Zahnmedizinische Radiologie. 2nd ed. Stuttgart: Thieme; 2000. Farbatlant der Zahnmedizin; Band 5.)



Fig. 7.8 Imaging plates of different formats.



Fig. 7.9 Imaging plate scanner.

Dental digital intraoral and panoramic imaging systems come equipped with various digital intraoral or panoramic storage phosphor imaging plates (□ Fig. 7.8) and the appropriate scanners to read them (□ Fig. 7.9 and □ Fig. 7.10).

As in luminescence, X-ray exposure causes the europium electrons to rise to a higher energy level, referred to



Fig. 7.10 Imaging plate scanner for small formats.

as the excited state. They do not fall back to their ground state immediately, but are first stored in electron traps in the storage phosphor layer, where they remain as the unprocessed latent image for up to 7 hours (□ Fig. 7.11).

Subsequently, the storage phosphor screen is scanned and stimulated by laser light, inducing the release of electrons. As a result, the electrons fall back to their original energy level (ground state), emitting energy as photons of visible light in the process. These photons of emitted light (luminescence) are counted by a photomultiplier. The data are then forwarded to the analog-to-digital converter and digitized by the computer (□ Fig. 7.12).

One of the main advantages of storage phosphor imaging plates is their wide dynamic range, which is now paralleled by that of some CMOS sensors.

However, unlike digital sensor technology, storage phosphor imaging plates require higher doses of radiation for noise-free imaging.

In practice, the handling of storage phosphor imaging plates is very similar to that of dental X-ray film. Storage

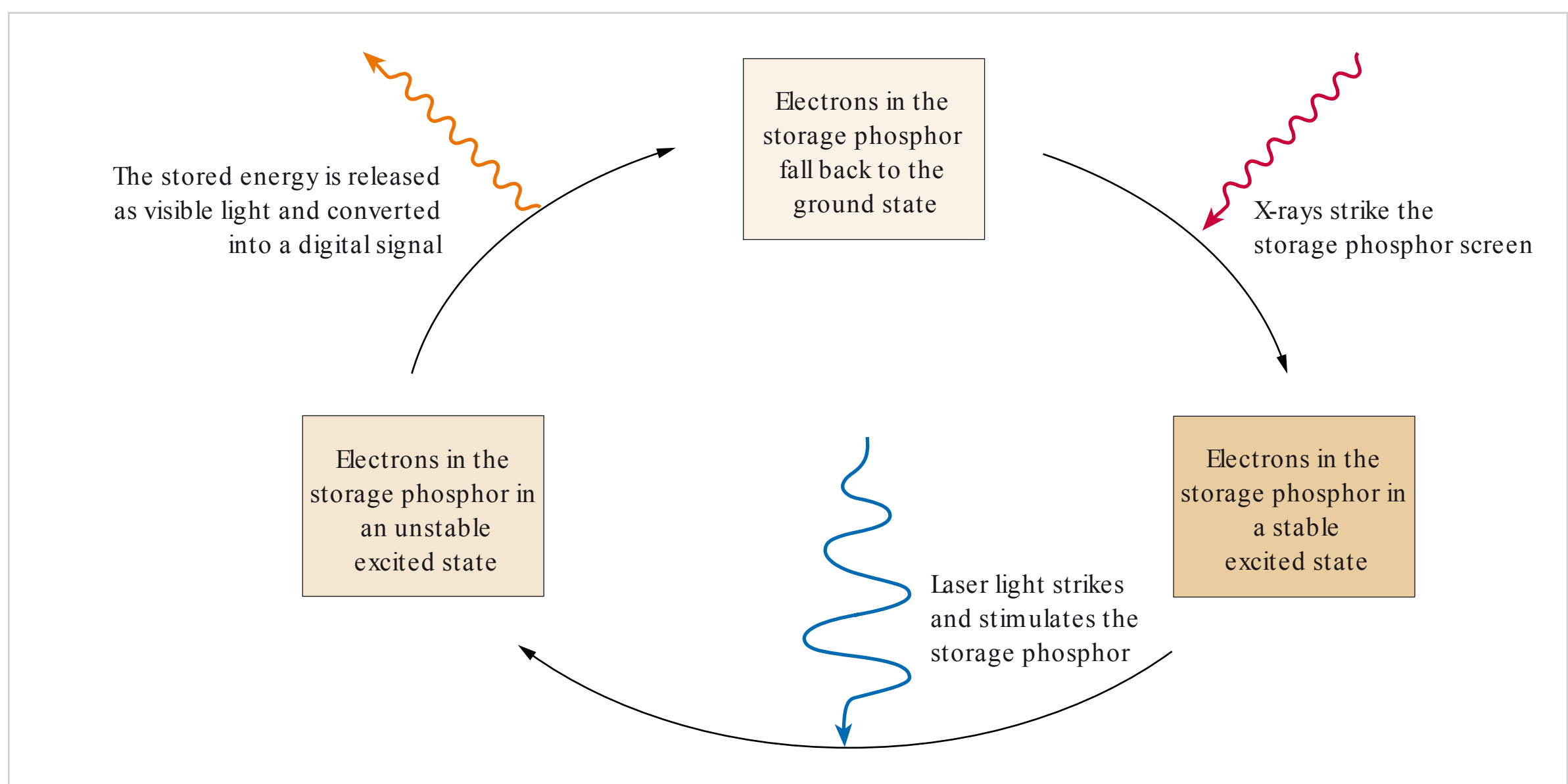


Fig. 7.11 Process of photostimulated luminescence.

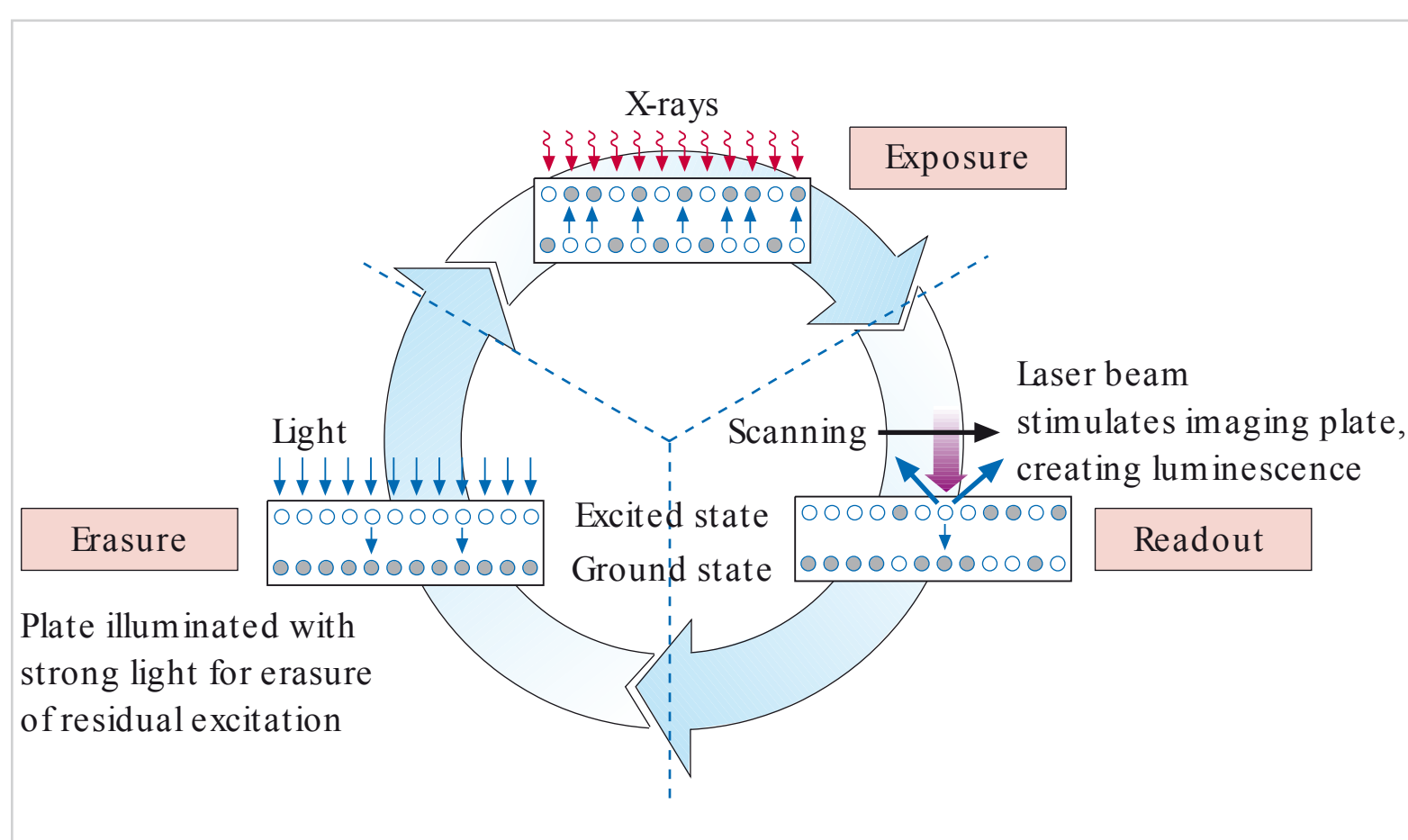


Fig. 7.12 Process of reading a phosphor storage imaging plate. (From: Pasler FA, Visser H. Zahnmedizinische Radiologie. 2nd ed. Stuttgart: Thieme; 2000. Farbatlanten der Zahnmedizin; Band 5.)

phosphor imaging plate systems may at first seem easier to use than digital sensor systems, but this assessment is relative because the practical execution of digital intra-oral imaging depends on several other factors besides the image receptor.

Even if storage phosphor imaging plates are very similar to conventional film, it is important to remember that they are very delicate and can be easily damaged by improper handling. When mechanically induced damage occurs, every scratch produces a visible bright line on the image (□ Fig. 7.13 and □ Fig. 7.14). These damage-related marks increase the risk of misdiagnosis.

7.3 Advantages of Digital Radiography

□ **Wide dynamic range:** The image quality of digital X-ray images is determined by the number of photons converted into electric signals and used to produce the image. Detective quantum efficiency (DQE) is a measure used to describe how many (percentage fraction) incident quanta are converted into imaging signals. Therefore, the DQE value describes the sensitivity of a detector.

The dose range that the digital image receptor can convert into actionable data is referred to as the dynamic range. Digital radiography systems achieve a much higher yield than conventional X-ray systems. The characteristic curve describes the contrast characteristics of the

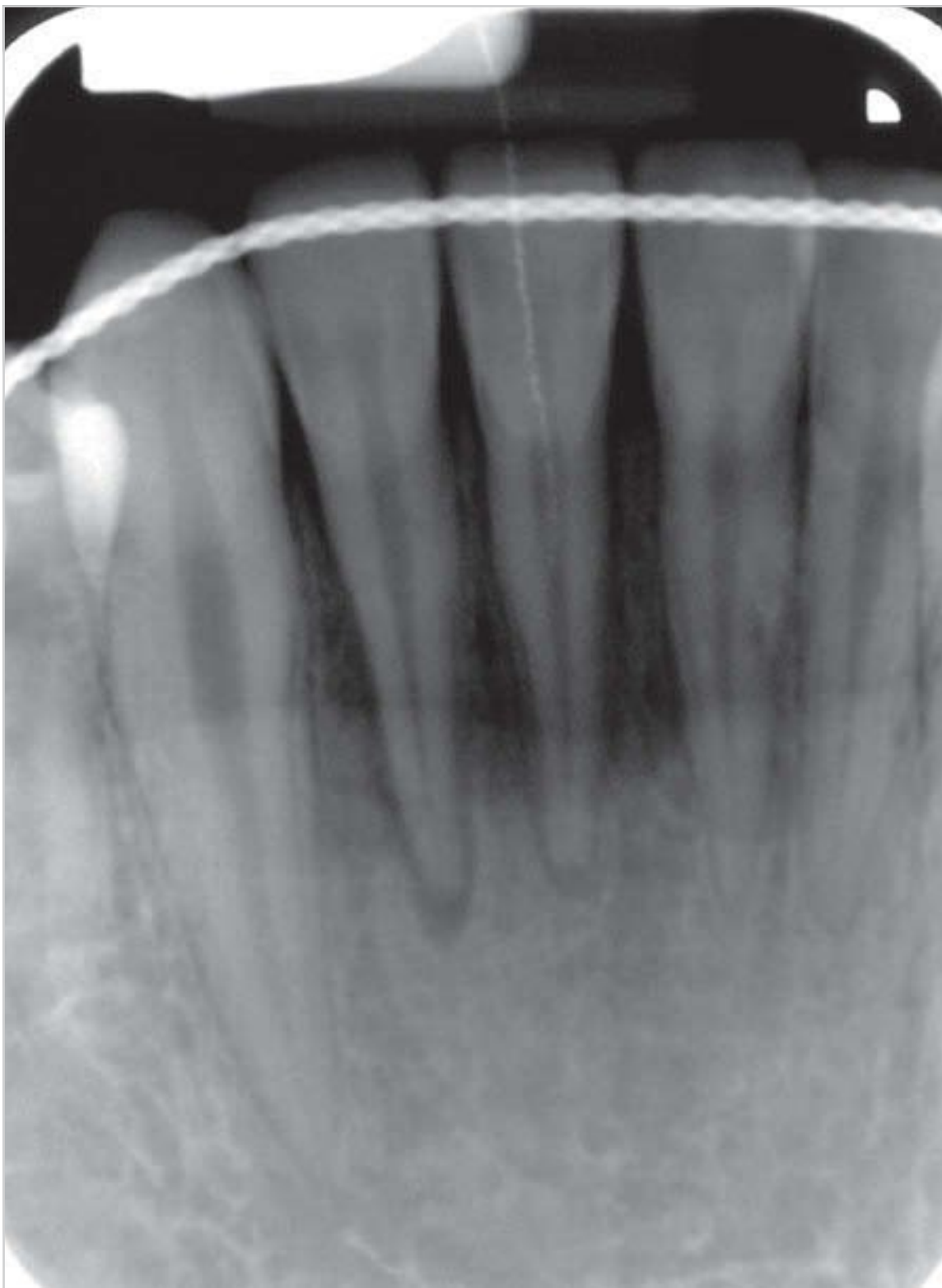


Fig. 7.13 Scratches on an imaging plate.



Fig. 7.14 Heavily scratched imaging plate.

film. Conventional film has an S-shaped characteristic curve, and only a small portion of the curve, the linear part, is relevant for imaging. In contrast, the characteristic curve for digital radiography is continuously linear. Because only the middle part of the characteristic curve

for conventional film is linear, the useful range is very small (□ Fig. 7.15). Comparison of characteristic curves shows that film has a dynamic range of around 1:30, whereas imaging plates have dynamic ranges approaching 1:10,000.

□ Elimination of developing and fixing solutions: The use of processing chemicals for film development is very problematic. It is very time consuming because processing machines must be cleaned regularly. In most cases, the processing chemicals must be replaced once a month. Disposal of the used chemicals takes time and money, and ultimately places an extra burden on the environment.

□ Digital images can be edited and enhanced: The film development process is unalterable. The work steps and procedures involved in radiographic film processing are covered in detail by standard operating procedures, which must be followed to the letter. This also means that correct exposure and film processing procedures are key determinants of the quality of an X-ray image. The radiograph leaving the processing machine is the final image. If not developed properly, it may appear too light or dark, or may not have enough contrast (□ Fig. 6.12). In any case, post-processing of developed radiographic film generally is not possible and, if it is, then it is very costly and reduces image quality. Digital images can be edited in many ways to compensate for exposure errors. However, it must not be forgotten that sufficient darkening by an adequate number of photons is needed to produce radiographs of diagnostic quality. It is wrong to think that editing underexposed digital images can make up for insufficient optical density and image quality. Every image receptor requires the radiation dose specified in its system requirements to achieve the necessary image quality.

□ More rapid availability: Digital radiographs are more rapidly available than film radiographs. Film development in automatic processors takes almost eight minutes. Digital sensors display images on the monitor immediately after exposure. Imaging plates take a bit longer, owing to their longer readout times. The imaging plate workflow resembles that of film development, except that a scanner is used instead of a processing machine.

□ Data storage and transfer: Digital images can be easily stored and quickly retrieved from memory. Therefore, they cannot be lost (conventional dental radiographs were often lost or misplaced). Electronic data storage saves space and can be carried out simultaneously at multiple sites.

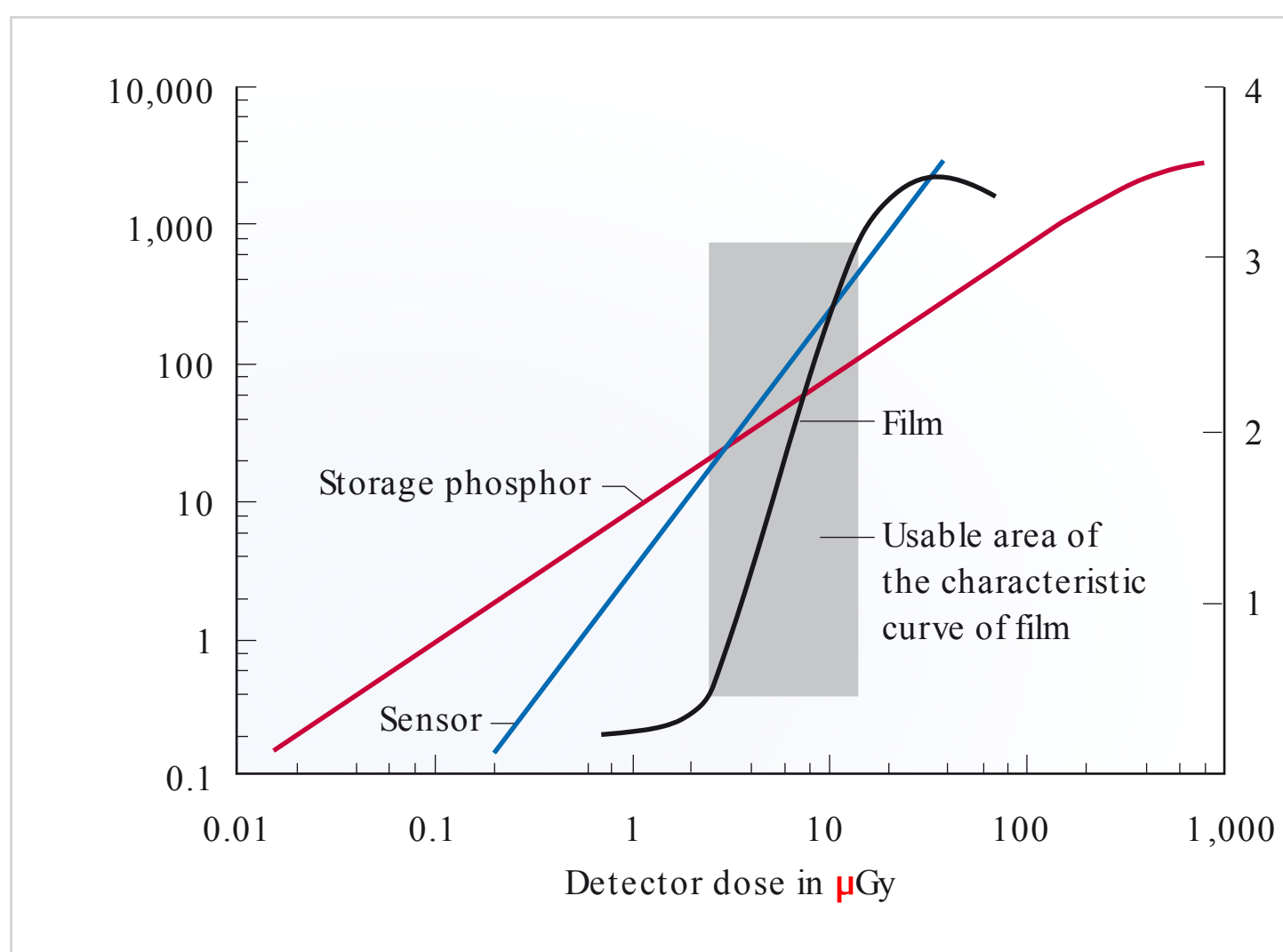


Fig. 7.15 Characteristic curves of conventional film, digital sensors, and storage phosphor imaging plates. (From: Pasler FA, Visser H. Zahnmedizinische Radiologie. 2nd ed. Stuttgart: Thieme; 2000. Farbatlanten der Zahnmedizin; Band 5.)

Chapter 8

Radiation Protection and Quality Assurance in Dental Radiology

8.1	History of Radiation Protection	54
8.2	Responsibility for Radiation Protection	55
8.3	Need and Justification	55
8.4	Optimization of Radiation Protection	55
8.5	Implementation of Recommendations by the International Commission on Radiological Protection	55
8.6	Quality Assurance in Dental Radiology	56
8.7	Procedures to Ensure Compliance with Basic Principles of Radiation Protection	56

8 Radiation Protection and Quality Assurance in Dental Radiology

The two pillars of dental radiology are radiation protection and image quality. In X-ray imaging, the goal of any exposure is to obtain the required image quality at the lowest possible dose.

8.1 History of Radiation Protection

The fact that X-rays can also cause damage was recognized even at the beginning of the history of the use of Roentgen rays for diagnostic and therapeutic purposes.

The first reports of radiation dermatitis, a side effect of radiation characterized by sunburn-like skin reactions, were published in 1896. The development of skin cancer secondary to radiation dermatitis was first described in 1902, in the German journal entitled *Advances in the Field of X-rays and Nuclear Medicine*. In 1911, 94 cases of skin cancer developing on healthy skin after prolonged radiation exposure were classified as radiation cancer.

Radiation damage and changes to germ cells were detected soon thereafter. Scientific proof of the mutagenic effects of radiation, however, was not established until 1927, when H. J. Muller published the results of his fruit fly (*Drosophila*) experiments.

In response to these findings, the International Commission on Radiological Protection (ICRP) was founded at the Second International Congress of Radiology in Stockholm in 1928.

The goal of the ICRP is to find ways and means to continuously reduce radiation exposure, in order to provide workers, the population in general, and patients in particular better protection from ionizing radiation.

8.1.1 Structure of the International Commission on Radiological Protection

The ICRP consists of the main commission and five standing committees devoted to the following subject areas:

- Radiation effects
- Doses from radiation exposure
- Radiation protection in medicine
- Application of the commission's recommendations
- Protection of the environment.

A scientific secretariat in Sweden oversees the ICRP and its committees. In addition to the permanent committees, the ICRP also has temporary task groups that deal with specific tasks and problems of radiation protection.

The ICRP is an independent organization that collaborates closely with many other international organizations. It has more than 200 volunteer members from over 30 countries around the world. Leading scientists and policy-makers in the field of radiation protection are included in its ranks.

Some of the most important organizations that collaborate closely with the ICRP are:

- European ALARA Network (EAN)
- European Commission (EC)
- European Nuclear Installations Safety Standards Initiative (ENISS)
- European Platform on Preparedness for Nuclear and Radiological Emergency Response and Recovery (NERIS)
- Heads of the European Radiological Protection Competent Authorities (HERCA)
- Ibero-American Forum of Radiological and Nuclear Regulatory Agencies (FORO)
- International Atomic Energy Agency (IAEA)
- International Commission on Radiological Units and Measurements (ICRU)
- International Radiation Protection Association (IRPA)
- United Nations Scientific Committee on the Effects of Atomic Radiation (UNSCEAR)
- World Health Organization (WHO).

8.1.2 Tasks and Content of the Various Activities of the International Commission on Radiological Protection

Initially (in 1928), limitation of the hours of work involving medical radiation sources was the only recommendation for radiation protection in medicine, and the first threshold was defined in 1934.

Scientifically based evidence of increased cancer incidence among American radiologists, and the known cases of leukemia after the atomic bombings in Japan, changed opinions regarding the threshold above which damage from ionizing radiation might occur.

Consequently, monthly and annual limits for workers and for the population were recommended in 1956.

The realization that it is not possible to set a threshold led to the recommendation to limit the radiation dose to the lowest level possible. This wording was later improved and refined to include phrases such as:

- "To the lowest level" (1955)
- "As low as practicable" (1959)
- "As low as reasonably achievable" (ALARA) (1966)
- "As low as reasonably achievable, economic and social factors taken into account" (1973).

The main objective is to reduce the dose to acceptable levels. When doing so, deterministic effects must be avoided and stochastic effects reduced to an acceptable level. The term “acceptable level” is defined relative to other risks of daily life.

Together with the IAEA, the ICRP compiled several *Fundamental Safety Principles*, which were published in 2006.

8.2 Responsibility for Radiation Protection

The sole person bearing the responsibility for protection against ionizing radiation is the doctor or dentist responsible for the radiology equipment with which the radiographs are taken.

8.2.1 Supervisory Duty of the Government

It must be ensured that each state has an effective legal and regulatory framework for radiation protection. Independent and competent regulatory authorities must ensure that national laws and regulations are followed.

8.2.2 Administration and Management of Safety

Effective administration and quality-assured management of protection from the risks of ionizing radiation must be practiced by organizations that are affected by radiation risks, or that operate facilities and engage in activities that give rise to radiation risks.

8.3 Need and Justification

No radiation risk can be justified unless it has a net positive benefit. Every radiograph requires justification, and any medical radiation exposure in dentistry must have a sufficient net positive benefit.

8.4 Optimization of Radiation Protection

The ALARA principle must be applied to all X-ray examinations. In other words, radiation exposure must always be kept as low as reasonably achievable.

8.4.1 Limitation and Monitoring of Individual Dose Limits

Limits must be introduced and it must be ensured that radiation doses to individuals do not exceed the limits specified for the respective conditions.

8.4.2 Prevention of Accidents and Protection against Existing or Unregulated Radiation Risks

Avoidable damage from ionizing radiation must be prevented by all reasonable means. The protection and reduction of existing or unregulated (natural) radiation risks must be responsible and optimized.

8.5 Implementation of Recommendations by the International Commission on Radiological Protection

The recommendations formulated by the ICRP are adopted by the responsible committees and published in the form of guidelines that serve as the prescribed legal basis for practical implementation of the commission’s recommendations in the different countries.

The most important radiation protection organization in Europe is the European Atomic Energy Community (EURATOM), which was founded in 1959. This international organization, established by the Treaties of Rome, regulates the use of radioactive materials and serves as the international basis for all national regulations.

The EC is working on specific radiation protection guidelines. After hearings by the European Parliament and adoption by the Council of Ministers, these guidelines will be binding for all Member States and must be implemented in national law. EURATOM thus declared the *Fundamental Safety Principles* of the ICRP binding for all EU Member States, in Directive 2009/71/EURATOM. The individual Member States are encouraged to implement the enacted guidelines in national law.

The United States has a well-developed system of organizations responsible for radiation protection. These include the following organizations, among others:

- Biological Effects of Ionizing Radiation Committee (BEIR)
- Environmental Protection Agency (EPA)
- National Center on Devices and Radiological Health (NCDHR)
- National Council on Radiation Protection and Measurements (NCRP)
- Nuclear Regulatory Commission (NRC)

- Occupational Safety and Health Administration (OSHA)
- U.S. Department of Health and Human Services
- U.S. Food and Drug Administration (FDA).

In addition, the use of X-ray equipment is regulated by the individual states, in cooperation with the FDA. They manage the registration and control of X-ray equipment used in the medical, dental, and veterinary applications.

The NCRP publishes recommendations for radiation protection in dentistry. It also issues reports on topics such as “Radiation Protection in Dentistry” and “Implementation of the Principle of As Low As Reasonably Achievable (ALARA) for Medical and Dental Personnel.”

In summary, it can be stated that increasing numbers of countries around the world have established national guidelines on radiation protection in dental X-ray facilities. In many cases, these are type tests. For example, the devices are tested for conformity to national requirements when first installed. These tests include dose measurements, determination of half-value layer, filtration tests, and voltage checks. The technician who evaluates these values sends the results to the competent authority. This procedure serves to ensure the successful monitoring of dental radiographic equipment in the respective country.

8.6 Quality Assurance in Dental Radiology

Quality assurance is a broad term that includes all planned and systematic actions by the dentist to provide confidence that:

- The X-ray examination is necessary and appropriate for diagnosis of the clinical problem at hand
- The radiograph provides adequate diagnostic information to address the clinical questions being asked
- The contents of the radiograph can be interpreted correctly and made available in a timely manner
- The X-ray examination can be performed with minimum radiation exposure and with minimum discomfort to the patient.

8.6.1 Standards

Regarding technical concerns in radiology, there are standards governing quality assurance in particular, as well as standards that play a major role in regulating the technology used in X-ray equipment. International Basic Safety Standards (BSS) were introduced for international standardization purposes. These globally valid standards apply to all manufacturers of dental X-ray equipment.

Uniform international acceptance tests for X-ray equipment still do not exist, despite various attempts to introduce such standards. In most cases, only type tests and regular quality inspections are performed. However, it is important to have international standards that are recognized and observed across all borders.

The International Organization for Standardization’s (ISO’s) Technical Committee 106 Dentistry is responsible for the development and implementation of all ISO standards related to dentistry.

In Europe, the European Committee for Standardization is responsible for the development of generally applicable standards. EN 60601 is the standard that covers safety requirements for medical electrical equipment and systems. There is a special series of standards for dental radiology, for example, EN 60601-2-63 for dental extraoral X-ray equipment, and EN 60601-2-65 for dental intraoral X-ray equipment.

In the USA, the American Dental Association (ADA) Standards Committee on Dental Products is the responsible body for standards for dental X-ray equipment. The ADA represents the interests of American dentists around the world, by collaborating with organizations such as the ISO.

8.7 Procedures to Ensure Compliance with Basic Principles of Radiation Protection

Generally speaking, it can be said that the following procedures, as described in the current guidelines of the EC, ensure that the goals of radiation protection and quality assurance can be met:

- Risk/benefit assessment for justification of the use of ionizing radiation
- Valid clinical indication for any radiological examination after the general medical/dental examination
- Optimization procedures:
 - Adequacy and quality of premises and equipment
 - Quality assurance
 - Quality control program
 - Patient dose measurement and assessment
- Designation of responsibilities, including lines of authority and radiation safety responsibilities
- Adequate training in the radiological procedures to be performed and the corresponding radiation protection requirements
- Continuing education and training, which is necessary as a result of the rapid developments in medical science and technology.

Chapter 9
Practical Dental
Radiography

9.1	Intraoral Radiography	58
9.2	Conventional Tomography	77
9.3	Panoramic Tomography	79
9.4	Cone Beam Computed Tomography	109



9 Practical Dental Radiography

9.1 Intraoral Radiography

Intraoral radiography was the most important dental imaging technique for decades but lost some of its importance after the introduction of panoramic radiography and digital cone beam computed tomography (CBCT). In many cases, intraoral radiography is still of great diagnostic value in dental radiography, when used as a supplementary examination for optimal visualization of the teeth and adjacent structures.

Because intraoral single-tooth radiographs vary greatly depending on the findings and are primarily used to show fine detail, they must meet very high diagnostic image quality standards.

The diagnostic image quality of intraoral radiographs depends mainly on the type and quality of performance of the intraoral radiography technique. Also, as the development of intraoral radiographic techniques has shown, the use of technical aids such as an appropriate film-holding device has proved to be another important factor.

Intraoral radiography is performed according to certain basic principles that serve to ensure that all diagnostically important image features, details, and clinically relevant structures are visualized according to the current standards of dentistry and technology.

According to these standards, all intraoral radiographs must provide complete, superimposition-free, and distortion-free orthogonal images of the teeth. The image quality of the radiograph must be good enough to ensure unequivocal diagnosis of the crown, pulp, root canal, periodontal ligament, apical region, cancellous bone, and neighboring structures.

The radiographer must employ a radiographic technique that meets these requirements. When the general rules of central ray projection are considered in this context, it quickly becomes evident that there are qualitative differences in the available techniques for intraoral radiology and that not every technique produces results of the desired quality.

9.1.1 Quality Criteria for Intraoral Radiography

To enable comprehensive and optimal diagnostics, intraoral radiographs must meet the following image quality criteria:

- Completeness of visualization:
 - The entire crown, root, and periapical region must be shown on the intraoral radiograph.
 - Radiographs lacking crowns or root tips no longer meet modern dental radiography standards (□ Fig. 9.1).

- Superimposition-free orthogonal imaging:
 - Intraoral radiography plays a major role in diagnosis of caries. Therefore, periapical and (in particular) bitewing radiographs must be acquired in such a way that the interproximal surfaces are shown without superimposition (□ Fig. 9.2).
 - Regardless of which radiographic technique is used, the successful production of superimposition-free images is solely dependent on the quality of execution.
 - Every intraoral radiograph must provide a superimposition-free view of the interproximal areas. The only person responsible for ensuring that this is accomplished is the person who takes the radiographs. Regardless of which adjustment system is used, beam angulation must be individually adjusted for each patient, to achieve orthogonal projection geometry. When positioned orthogonally, the central ray is directed perpendicular to the interproximal surfaces of the teeth. Orthogonal projection geometry

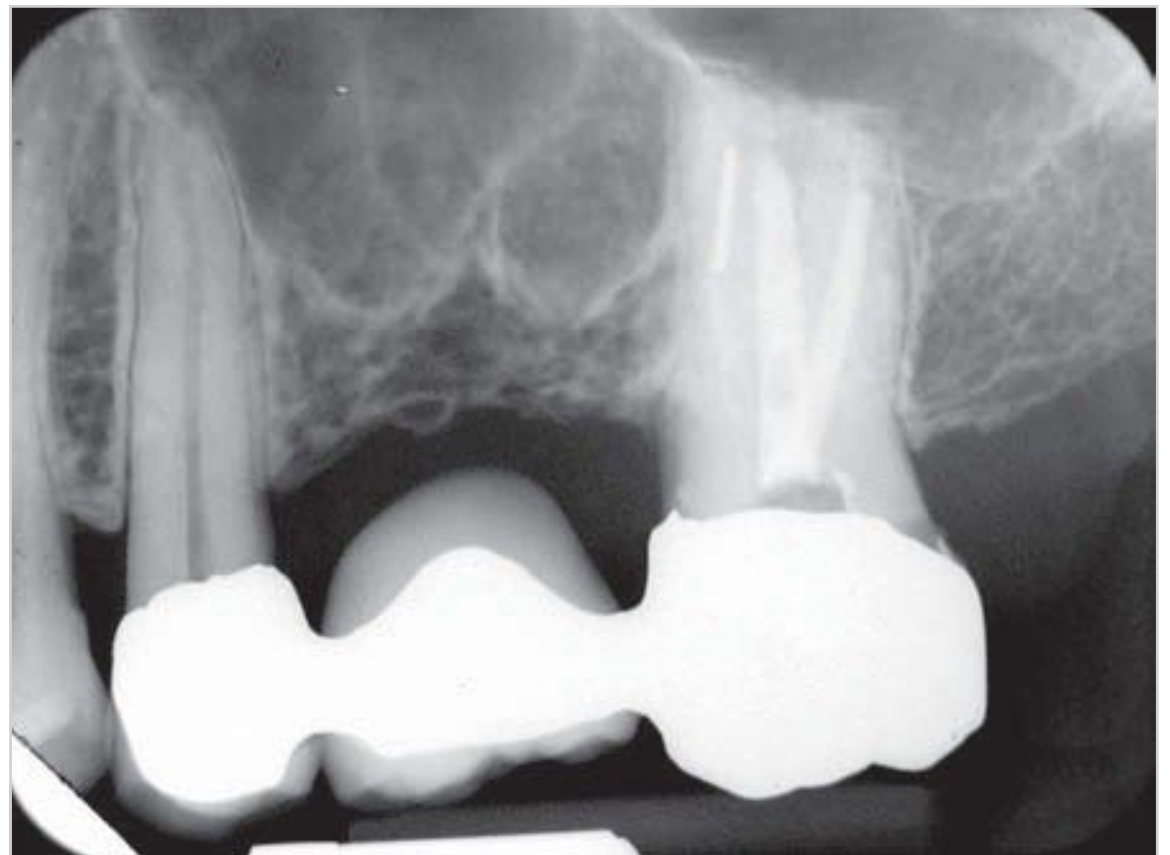


Fig. 9.1 Correct maxillary periapical radiograph of the entire tooth.

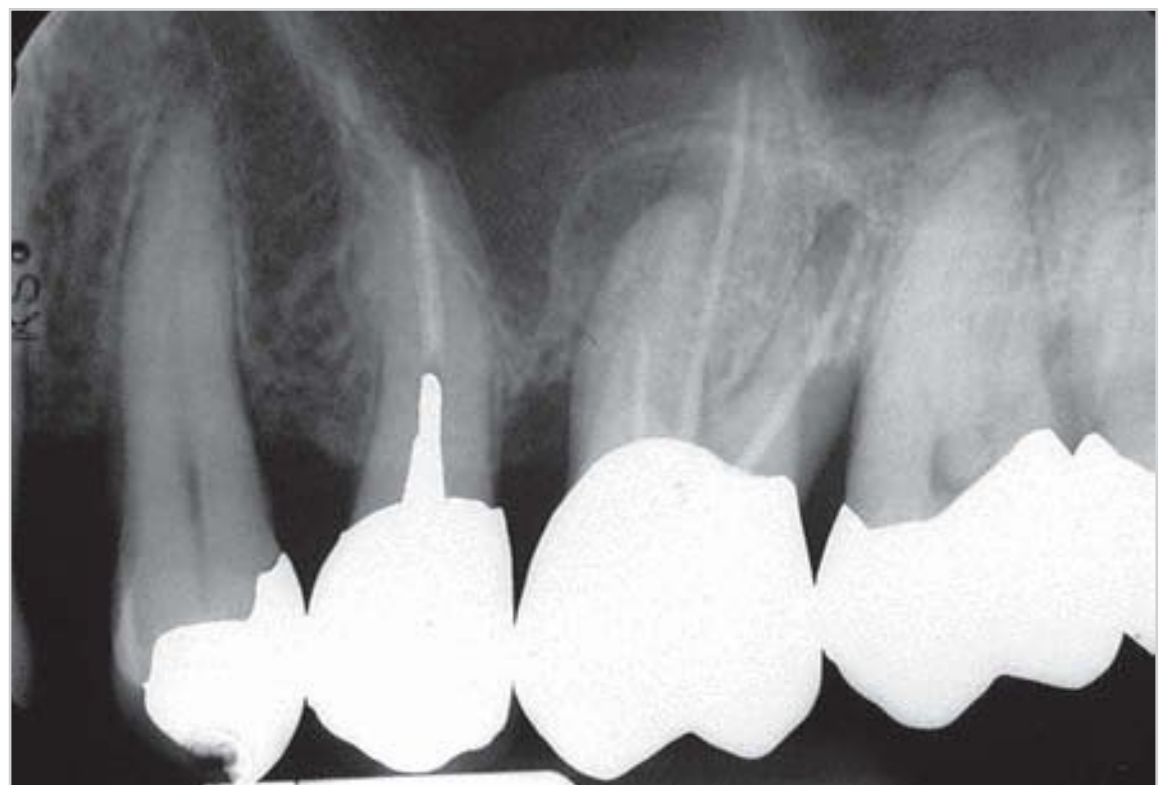


Fig. 9.2 Orthogonal imaging of teeth 17 to 15.

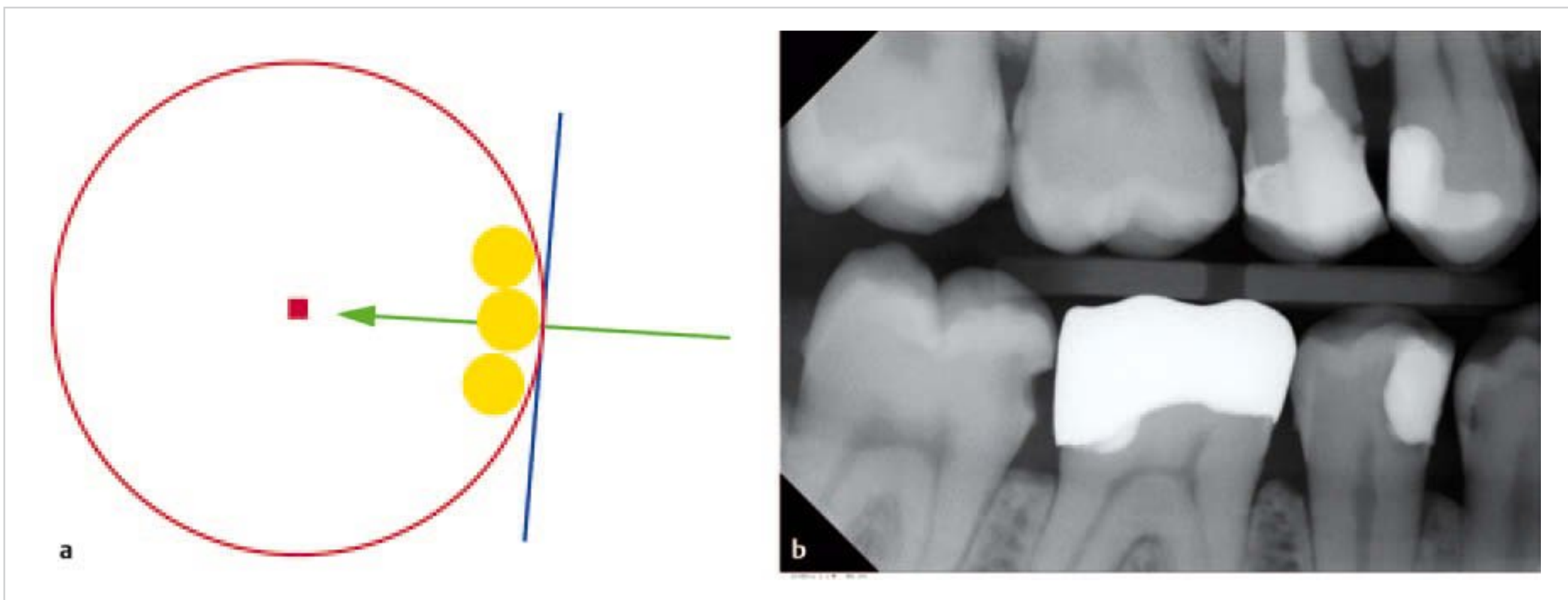


Fig. 9.3a, b Orthogonal projection geometry.

- a** Schematic: in orthogonal imaging, the central ray projects toward the projection radius from a given position.
b Radiograph acquired with orthogonal projection geometry.

is best achieved by aiming the central ray perpendicular to the imaginary line of the buccal surfaces of the teeth, and by placing the film parallel to this line. Based on the film position, it is easy to check whether the beam is correctly aimed perpendicular to the tooth (□ Fig. 9.3).

- **Reproducibility:**
 - Intraoral radiographs must be reproducible. When interpreting radiographs, dentists basically compare them to the images stored in their memory. This is the key to optimal interpretation of new X-rays. Moreover, it is sometimes necessary to compare previous X-rays of a given case to follow-up X-rays over time.
 - The use of standardized radiographic procedures is crucial for diagnostic reliability. When taking intraoral radiographs, the tooth axis must always be perpendicular to the lower edge of the film or bite block. If this rule is followed when positioning the X-ray film, a high degree of reproducibility can be achieved.
 - The reproducibility of radiographic images is a very important element of diagnostics. To be comparable, intraoral radiographs must be taken in the same manner and must show the target anatomical structures in the same manner. Reproducibility facilitates the identification of differences, regardless of whether these are normal variants or pathologic changes (□ Fig. 9.4).
- **Distortion-free imaging:** the successful production of distortion-free images of the teeth is highly technique sensitive. Distortion practically never occurs:
 - if a long cone (30 cm) is used
 - if the central ray of the X-ray beam is perpendicular to the image receptor and (ideally) to the long axis of the tooth (□ Fig. 9.5 and □ Fig. 9.6).

9.1.2 Principles of Projection Geometry

The basic principles of projection geometry can be summarized as follows:

- The X-ray beam must be directed perpendicular to the image receptor and the object (□ Fig. 9.7).
- Beam divergence must not occur.

A long cone is required for the production of parallel rays in intraoral radiography. Moreover, a suitable film-holding device is crucial to ensure that the X-rays are directed perpendicular to the film or other type of image receptor.

However, true parallelism between the tooth and the image receptor cannot always be achieved, owing to the anatomical constraints within the oral cavity.

Implementation and Application of the Rules of Projection Geometry

The requirements for ideal imaging vary, depending on the individual radiographic technique. At the same time, the extent to which the rules of projection geometry can be applied vary and must be known. The greater the extent of conformity with the rules of projection geometry, the higher the quality of the image from the radiographic technique will be.

Regardless of which radiographic technique is used, there is always a compromise between the achievable and the ideal projection geometry for intraoral radiography (□ Fig. 9.8). This applies regardless of whether radiographic film, sensors, or phosphor storage plates are used. Although it is not possible to meet all the requirements for ideal projection geometry, it is crucial to use an intraoral radiology technique that comes as close to the ideal as possible.

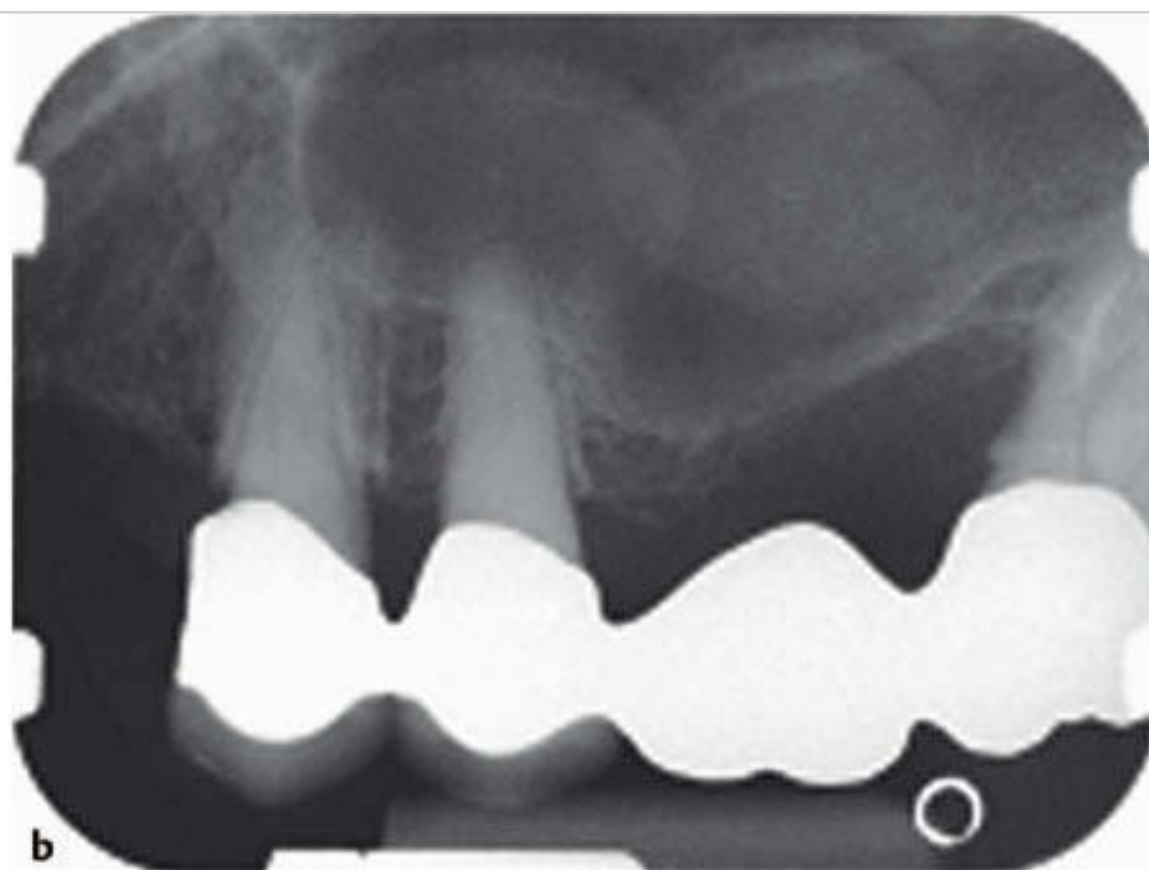


Fig. 9.4a, b Reproducible and correct tooth positioning.

a Reproducibility: the long axis of the tooth (arrow) must be perpendicular to the bite block.

b Radiograph acquired with correct tooth positioning.



Fig. 9.5 Maxillary radiograph with distortion characteristic of the bisecting-angle technique.

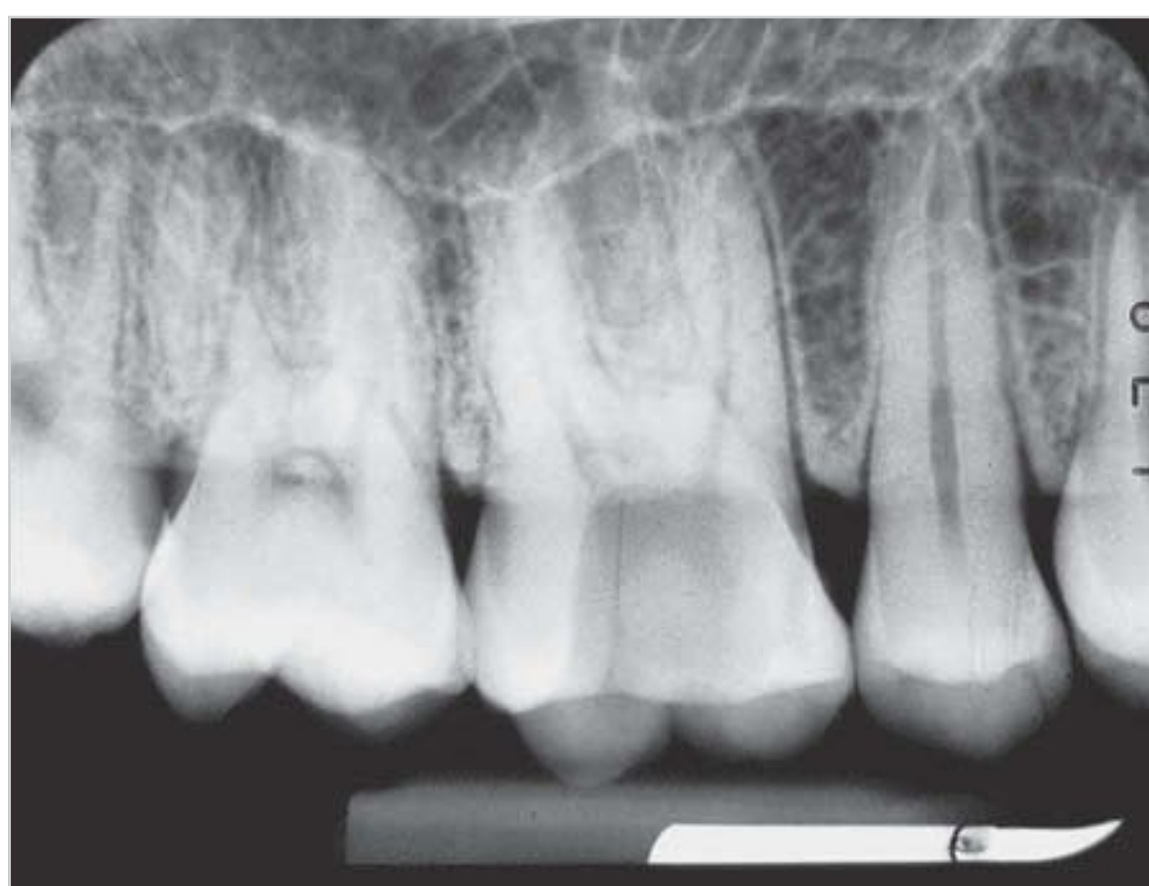


Fig. 9.6 The comparison radiograph obtained with the paralleling technique has no distortion.

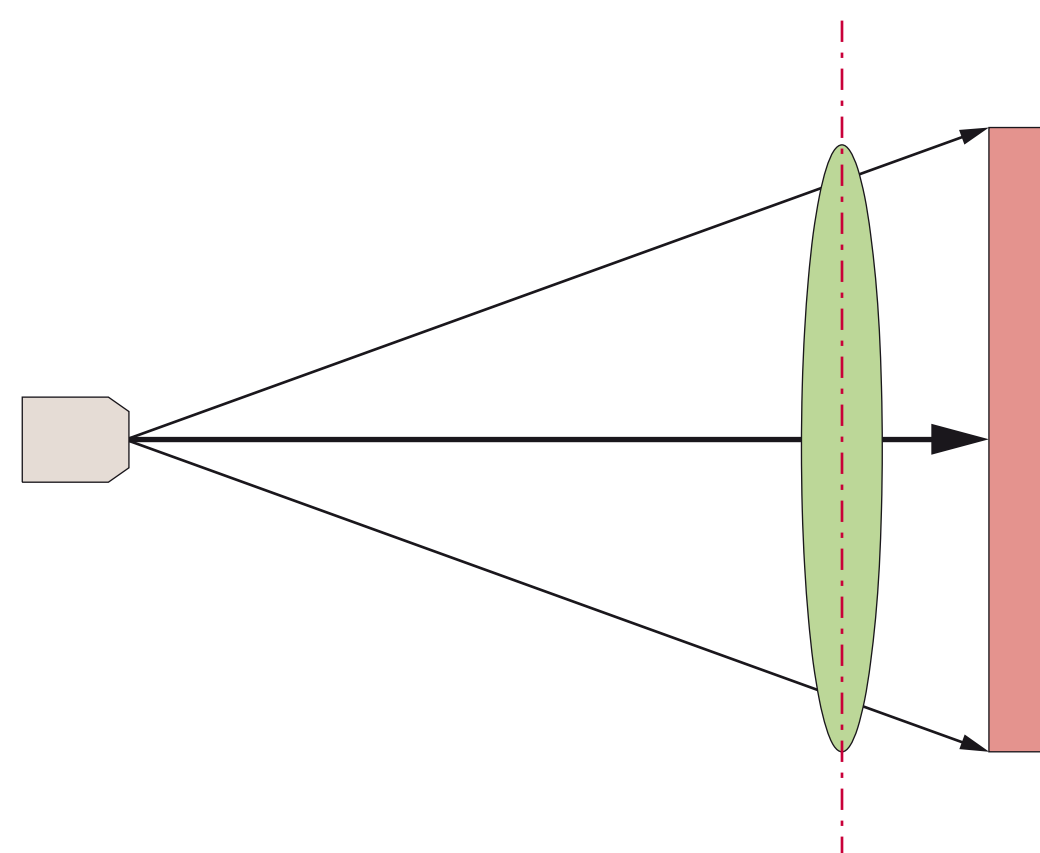


Fig. 9.7 Schematic of the X-ray source and beam path relative to the object of interest and the image receptor (film, sensor, or phosphor storage plate).

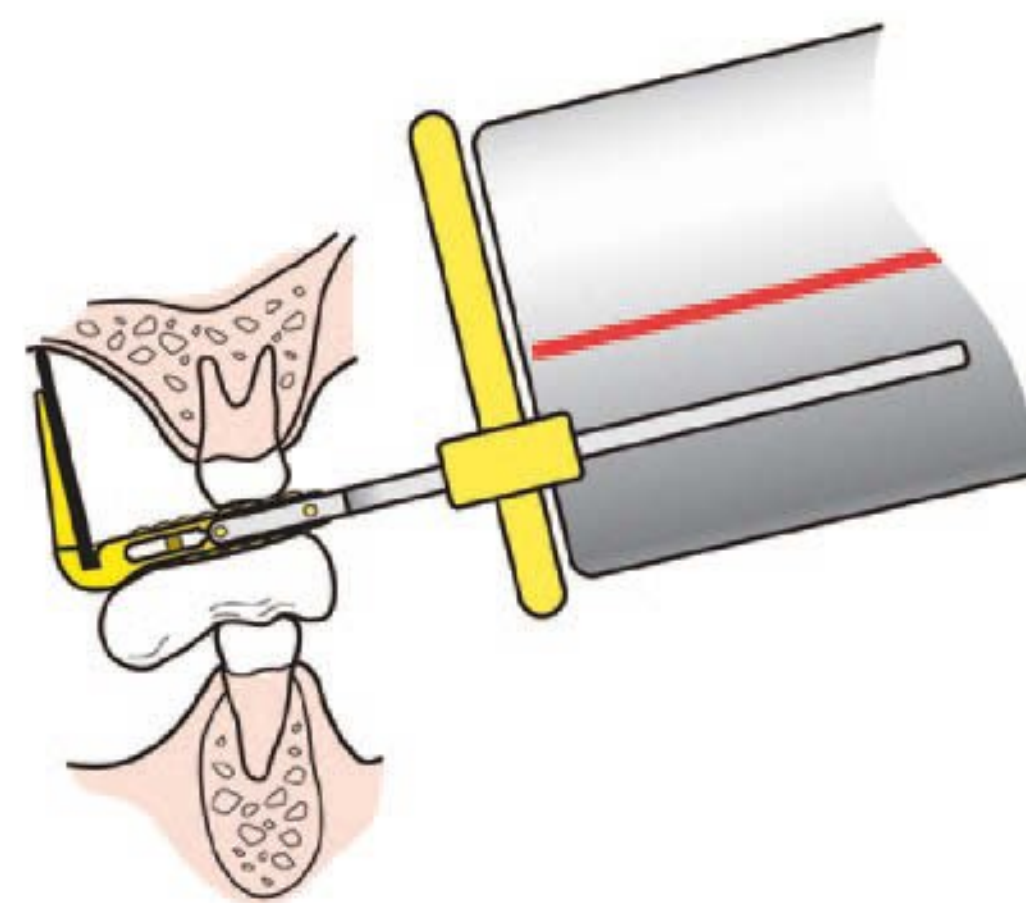


Fig. 9.8 Ideal positioning for intraoral radiography (schematic). (With the kind permission of Dentsply Rinn.)

Periapical Radiography

The conventional periapical radiograph is used to obtain a view of the entire tooth and its surrounding structures. Two film sizes are employed for periapical radiography: 3×4 cm and 2×3 cm.

Periapical radiographs of the premolars and molars are usually taken with the film packet (normally 3×4 cm) inserted horizontally. Horizontally positioned film can record up to three teeth.

If smaller film sizes are used, the film packet must be positioned upright, to capture the entire length of the tooth.

Both 3×4 cm and 2×3 cm film sizes may be used for periapical anterior radiographs. The film packet should always be inserted upright for canine and anterior periapicals (□ Fig. 9.9 and □ Fig. 9.10).



Fig. 9.9 Typical anterior radiograph.



Fig. 9.10 Typical posterior radiograph.

9.1.3 Paralleling Technique

Principles of the Paralleling Technique

Two radiographic techniques are used in periapical radiography: the paralleling technique and the bisecting-angle technique. The goal of the paralleling technique is to achieve the ideal positioning requirements for intraoral radiography. One of the main requirements, recognized by even the early pioneers of dental radiology, is that the film should be positioned parallel to the long axis of the tooth under investigation. Other requirements are that the film must be flat and that the central ray of the X-ray beam must be oriented perpendicular to the tooth and the film.

C. E. Kells is considered to be the founder of the paralleling technique. The use of a suitable film-holding device is necessary because the patients themselves cannot hold the film in the correct position. The first film-holder for the paralleling technique was introduced by Kells in 1896, but proved unsatisfactory in practice. Several different film-holding devices for the paralleling technique were developed in subsequent years, but decades passed before one was introduced that proved effective in everyday practice.

Consequently, the bisecting-angle technique remained the standard technique of periapical radiography for decades. Later research work by F. G. Fitzgerald (1947) and D. T. Waggener (1947), translated into practice by W. J. Updegrave (1951), ultimately made it possible to gain the scientific basis needed to establish the paralleling technique as a better alternative to the bisecting-angle technique. A typical film-holder designed for the paralleling technique is shown in □ Fig. 9.11.

- A long cone (30 cm) should be used for the paralleling technique.
 - Instead of a short cone (see □ Fig. 2.5), a long cone (see □ Fig. 2.6), or position-indicating device, is employed for the paralleling technique, to ensure that only parallel rays contribute to image formation. This serves to minimize image magnification.
 - From orthodontic radiography, it is known that a very long focus-to-object distance (FOD) produces radiographs with very low distortion. Because orthodontic radiography captures images of almost the entire skull, a distance of at least 1.5 m is required to ensure



Fig. 9.11 Film-holder for the paralleling technique. (With the kind permission of Dentsply Rinn.)

that the skull is only struck by parallel rays. Because the field size used in periapical radiography is much smaller (6 cm), a distance of only 30 cm is sufficient to ensure that the part of the beam used for X-ray image formation only consists of parallel rays.

- Previously, a longer exposure time was said to be the main disadvantage of a large FOD, because this is associated with a higher risk of unsharpness. However, modern high-performance dental X-ray systems that use ultrasensitive image receptors (film as well as phosphor storage plates and sensors) have extremely short exposure times. Consequently, the use of a long-cone technique should not result in impairment of image quality due to motion blur. The minimum length requirement for long cones is 20 cm.
- Parallel rays must be directed perpendicular to the image receptor. The film, sensor or phosphor storage plate must always be positioned in the bite block of the holder, such that the parallel rays are directed perpendicular to the image receptor and the long axis of the tooth (see □ Fig. 9.8).

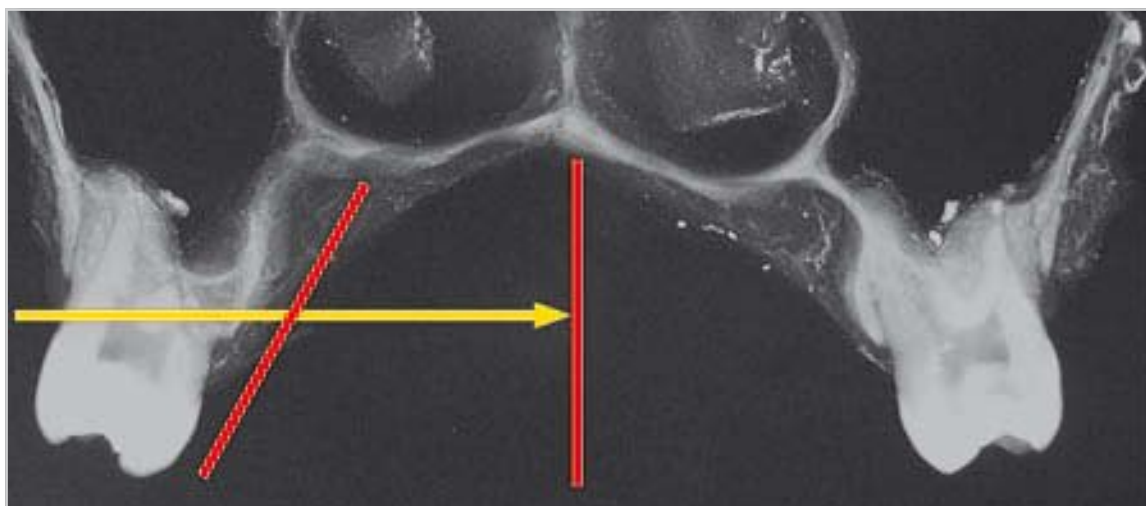


Fig. 9.12 The film packet is positioned in the middle of the oral cavity such that the central ray (arrow) is perpendicular to the film.

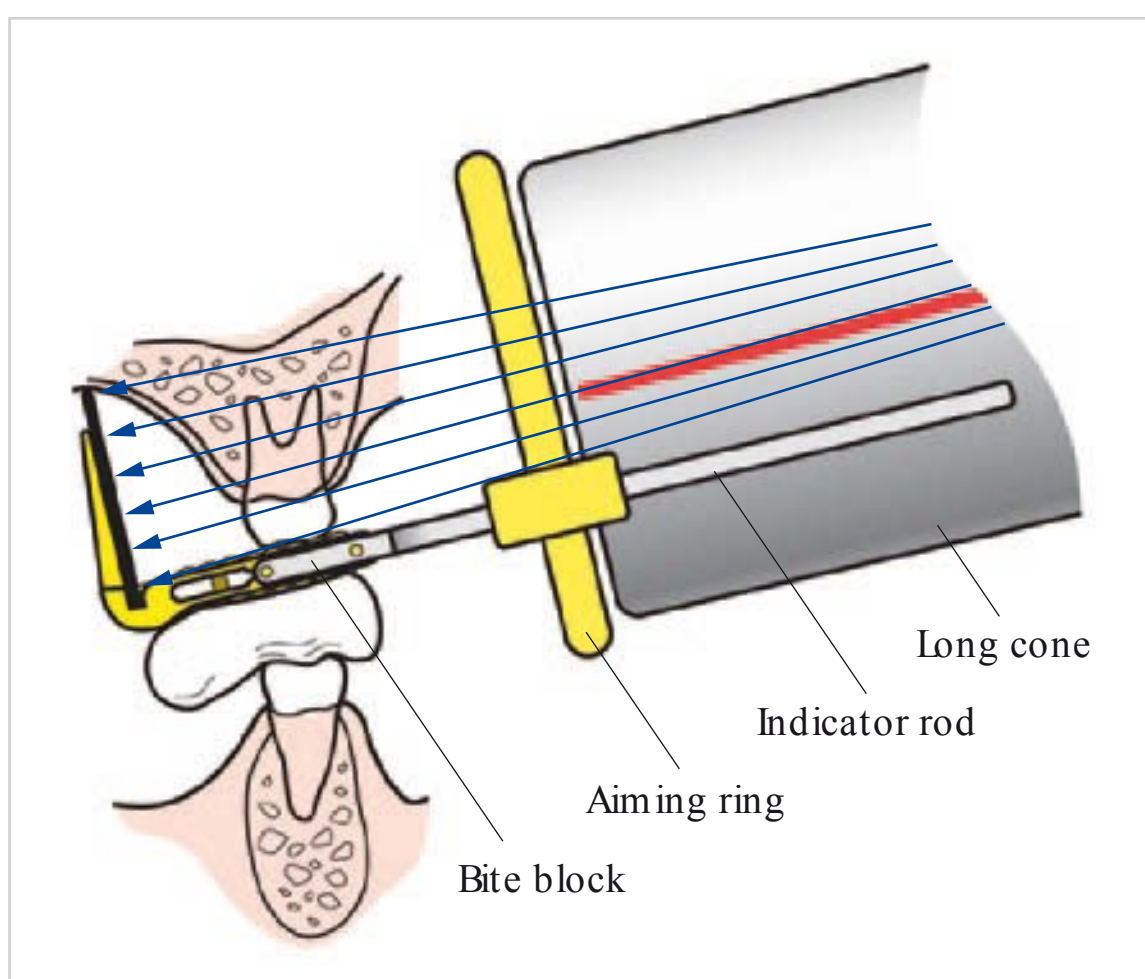


Fig. 9.13 Correct positioning of the film-holder in contact with the tooth crown and hard palate. The central ray of the X-ray beam consists of mostly parallel rays. It is perpendicular to the image receptor and (ideally) to the long axis of the tooth. (With the kind permission of Dentsply Rinn.)

- The image receptor may be placed in the middle of the oral cavity.
 - The middle of the oral cavity is the site where the greatest degree of parallelism can be achieved between the image receptor and the tooth to be radiographed. Only the height of the hard palate can restrict or prevent their parallel positioning.
 - However, it should be remembered that because posterior teeth often have bifurcated roots that are not parallel to each other, absolute parallelism can never be achieved, even if the height of the palate is sufficient (□ Fig. 9.12).

Effects of Increasing the Object-to-Film Distance

Because the large FOD of 20 to 30 cm results in parallel rays, increasing the object-to-film distance by up to 2 cm will not have a negative effect on image quality or sharpness. The theoretical increase in geometric unsharpness is negligible.

Function and Importance of the Bite Block

A bite block is an essential component of film-holders used for the paralleling technique. It serves to ensure good and stable fixation of the film-holder (□ Fig. 9.13).

The film is always in contact with the hard palate on the maxillary side, and with the floor of the mouth or the dorsum of the tongue on the mandibular side. These contact points provide very stable and secure positioning of the film packet in the oral cavity.

Likewise, this constellation ensures that the entire tooth is shown on the radiograph if the X-ray beam is correctly aligned. Moreover, if the patient has a shallow palate, foreshortening of the teeth will be minimal and the long object-to-film distance partially compensates for this.

The bite block eliminates the need for adjustment of the vertical angle, as is necessary with the bisecting-angle technique. Consequently, the use of a bite block enhances the reproducibility of periapical radiographs by eliminating arbitrary adjustment of the vertical angle. With the paralleling technique, the vertical angle is solely determined by the anatomical space conditions and is the same for each radiograph.

Because the crown is in contact with the platform of the bite block, and the image receptor is in contact with the hard palate, the respective position of the image receptor is fixed and defined. In most cases, there is a high degree of parallelism between the tooth and the image receptor. There is never a significantly large angle between the tooth and the image receptor, except in a few patients with an extremely shallow palate. These cases underline the advantages of the paralleling technique, in which parallel rays are always oriented perpendicular to the image receptor, independent of the anatomical situation.

Importance of Film-holders for Orthogonal Projection Geometry

Orthogonal projection geometry can be achieved more reliably with film-holding devices than without film-holders or bite blocks (□ Fig. 9.14 and □ Fig. 9.15; see also □ Fig. 9.3).

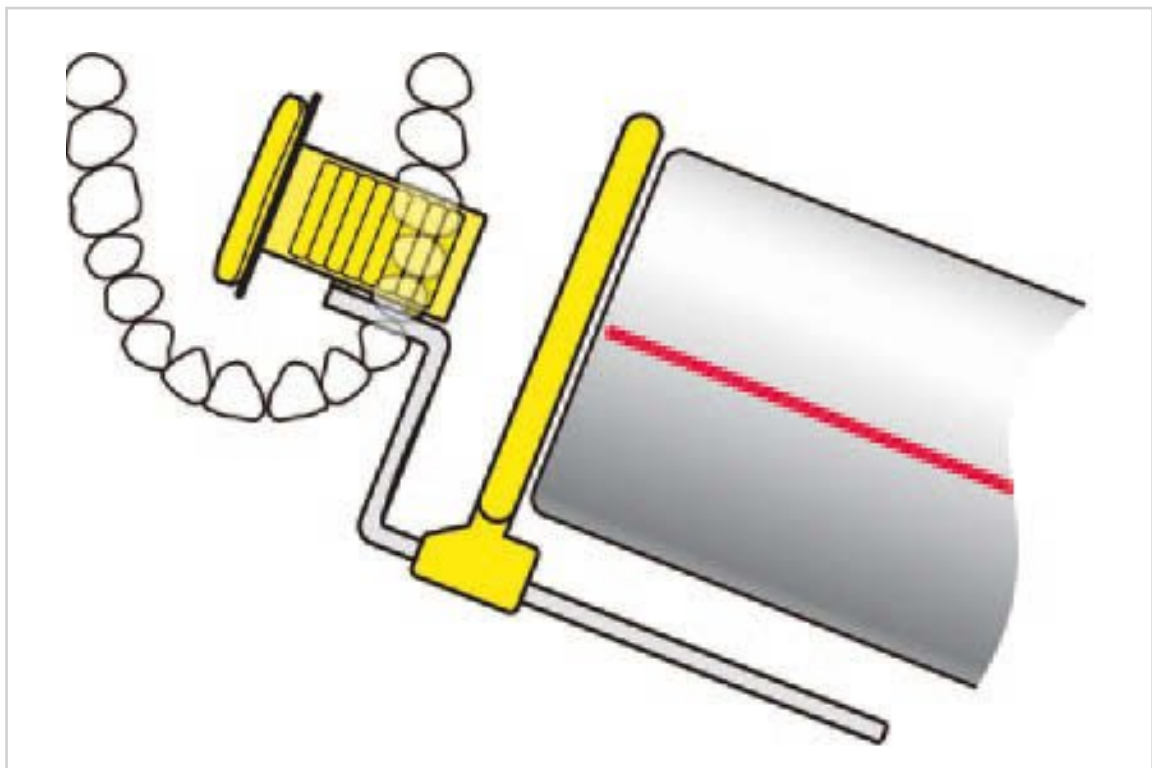


Fig. 9.14 Orthogonal projection geometry for the premolars. (With the kind permission of Dentsply Rinn.)

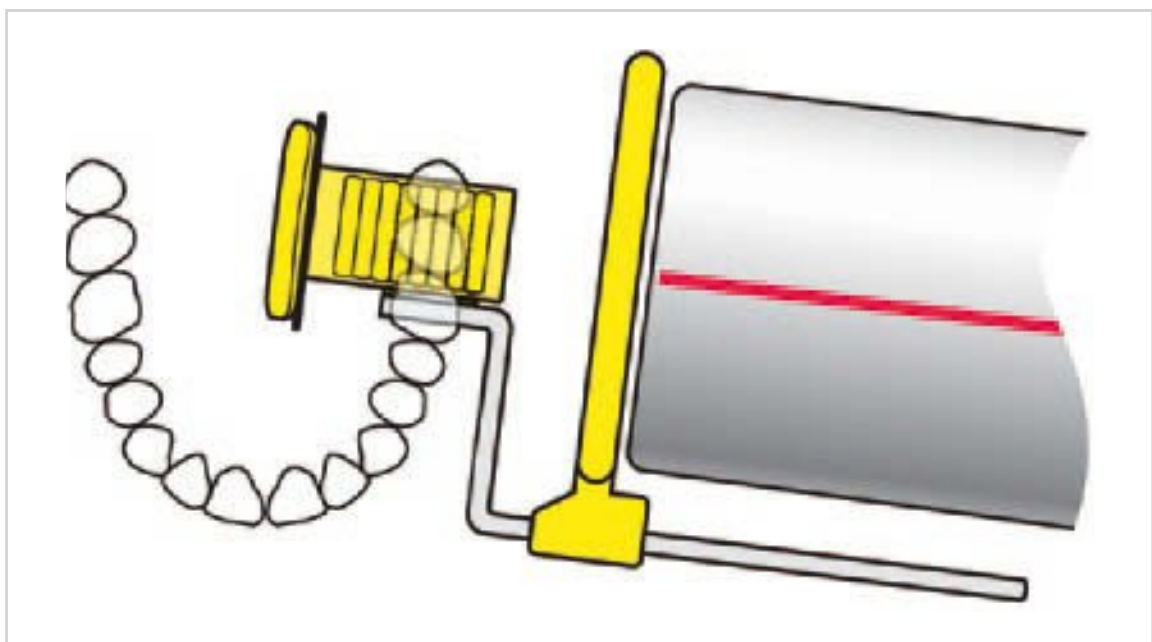


Fig. 9.15 Orthogonal projection geometry for the molars. (With the kind permission of Dentsply Rinn.)

Importance of Film-holders for Reproducibility

If a film-holding device is used, the patient cannot influence the position of the film. Therefore, the use of a film-holder makes it possible to obtain a standard film position in which the long axis of the teeth is always oriented perpendicular to the bite block. This enhances the reproducibility of the radiographs (cf. □ Fig. 9.4, which shows reproducible projection geometry with correct root alignment).

Note

The paralleling technique is easier to use than the bisecting-angle technique: if the film-holder is positioned correctly, orthogonal beam angulation is the only adjustment needed.

An intraoral radiograph is used for the visualization of individual teeth. A conventional full-mouth series consists of 14 intraoral radiographs (□ Fig. 9.16). In modern dental radiography, a full-mouth series generally is not justified because a panoramic radiograph can visualize the majority of the teeth with the same diagnostic quality. In special cases, the panoramic radiograph may be supplemented by individual intraoral radiographs as needed.

Bitewing radiography has a special status in dental radiography: it is the best radiographic technique for the detection of interproximal caries.

Paralleling Technique: Methodology

In the paralleling technique, the crowns of the teeth must be firmly positioned on the bite block and the film packet must be positioned in the mouth as follows:

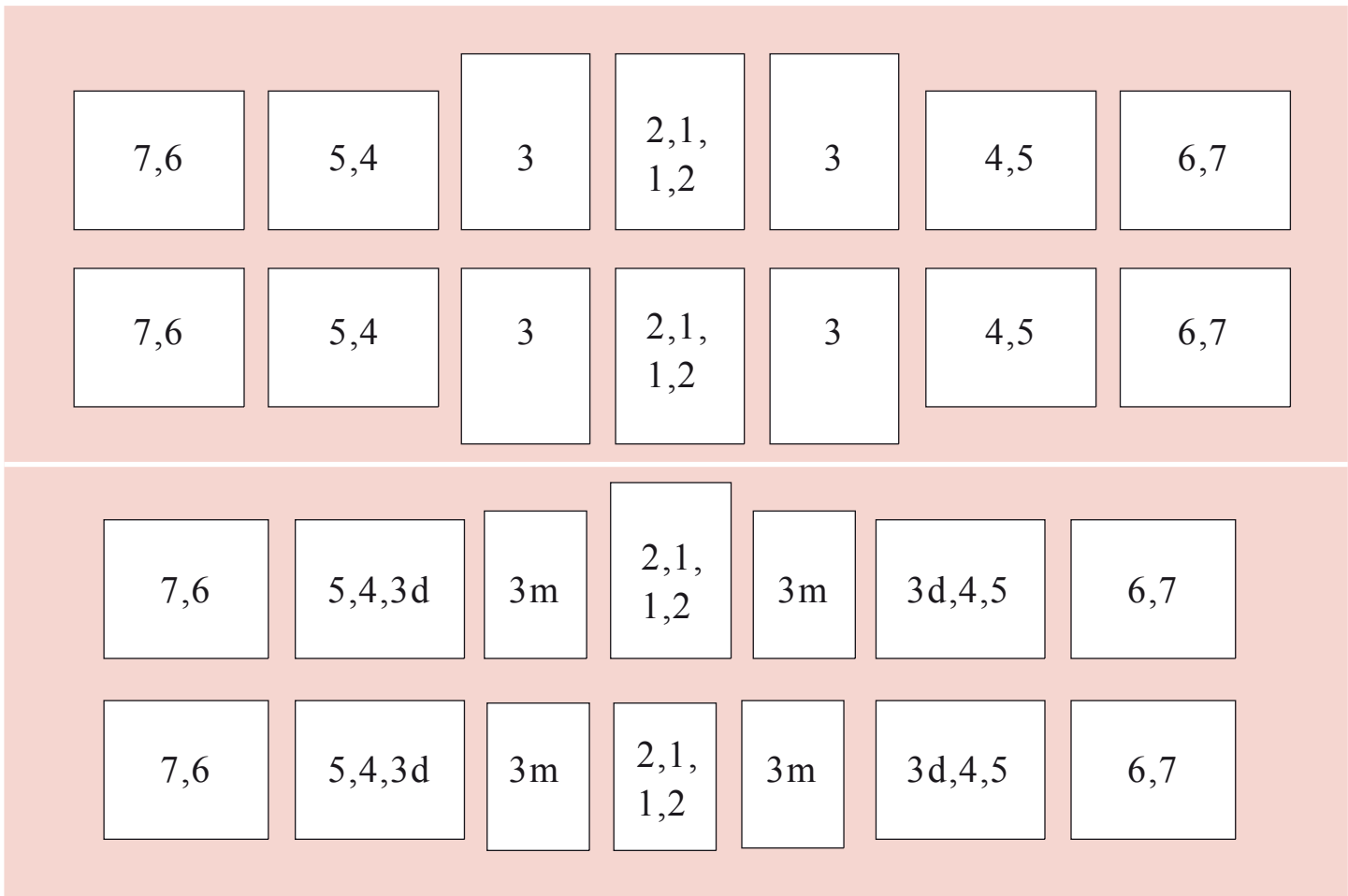


Fig. 9.16 Full-mouth series of 14 radiographs. The upper panel shows the usual full-mouth series for adults, and the lower panel shows that used for evaluation of the periodontal status. The numbers reflect the tooth numbers. M: mesial; d: distal. (From: Pasler FA, Visser H. Zahnmedizinische Radiologie. 2nd ed. Stuttgart: Thieme; 2000. Farbatlant der Zahnmedizin; Band 5.)



Fig. 9.17a–c Diagonal position of the film-holder during insertion.

- a** Diagonal position outside the mouth.
- b** Diagonal position inside the mouth.
- c** Incorrect position inside the mouth.

- Maxilla: in contact with the hard palate and floor of the nose (see □ Fig. 9.8)
- Mandible: in contact with the floor of the mouth or dorsum of the tongue (see □ Fig. 9.25).

This positioning geometry provides a high degree of stability and decisively contributes to obtaining a correctly adjusted exposure with good image quality.

It also ensures that the entire tooth will be shown on the radiograph. This requires proper alignment of the spacer cone, aiming ring, and indicator rod.

If this is ensured, parallelism of the tooth and image receptor is only dependent on the height of the hard palate. The use of a long cone can overcome anatomical limitations associated with a shallow palate because the parallel rays and increased object-to-film distance associated with a long cone prevent radiographic distortion and minimize foreshortening.



Fig. 9.18 Correct position inside the mouth.

The bite block is inserted in such a way that it first comes in contact with the crown before the film touches the palate, floor of the mouth, or dorsum of the tongue.

Next, the holder must be aligned orthogonally. It is pivoted more distally for molars and more mesially for premolars. The position of the image receptor is crucial: the plane of the film packet must be tangential to the tooth under investigation (see, e.g., □ Fig. 9.15).

In addition to ensuring orthogonal projection geometry, it is also important to ensure that the holder is not tilted forward or backward and that there is no space or angle between the crowns and the bite block.

Once the holder is correctly positioned, the patient is instructed to close the teeth slowly on the bite block and hold it firmly between the teeth without excessive pressure (□ Fig. 9.19).

Next, the operator must slide the aiming ring down the indicator rod to the patient's cheek; this serves to ensure that the maximum limits of field size are not exceeded. The operator then checks to make sure that the holder is stably in place.

Finally, the spacer cone is aligned so that its longitudinal axis is parallel to the indicator rod and the collimator is parallel to the indicator ring.

Inserting the Film-holder in the Mouth

The film-holder must be inserted and positioned in the oral cavity, while ensuring that the crowns are in contact with the bite block. The film-holder is inserted into the mouth in a gentle, twisting motion without jerky movements. The techniques for insertion in different parts of the maxillary and mandibular arch are described below.

Maxillary Premolars and Molars

The film-holder is held diagonally and inserted into the mouth in an upward motion (□ Fig. 9.17); the bite block and the front part of the indicator rod should lie completely within the oral cavity (□ Fig. 9.18).

The film packet is positioned in the middle of the oral cavity, to ensure that the film is parallel to the tooth, while accommodating its height as the space in the oral cavity allows. Since premolars and molars usually have bifurcated roots, it is impossible to position the film in the oral cavity so that it is absolutely parallel to the roots.

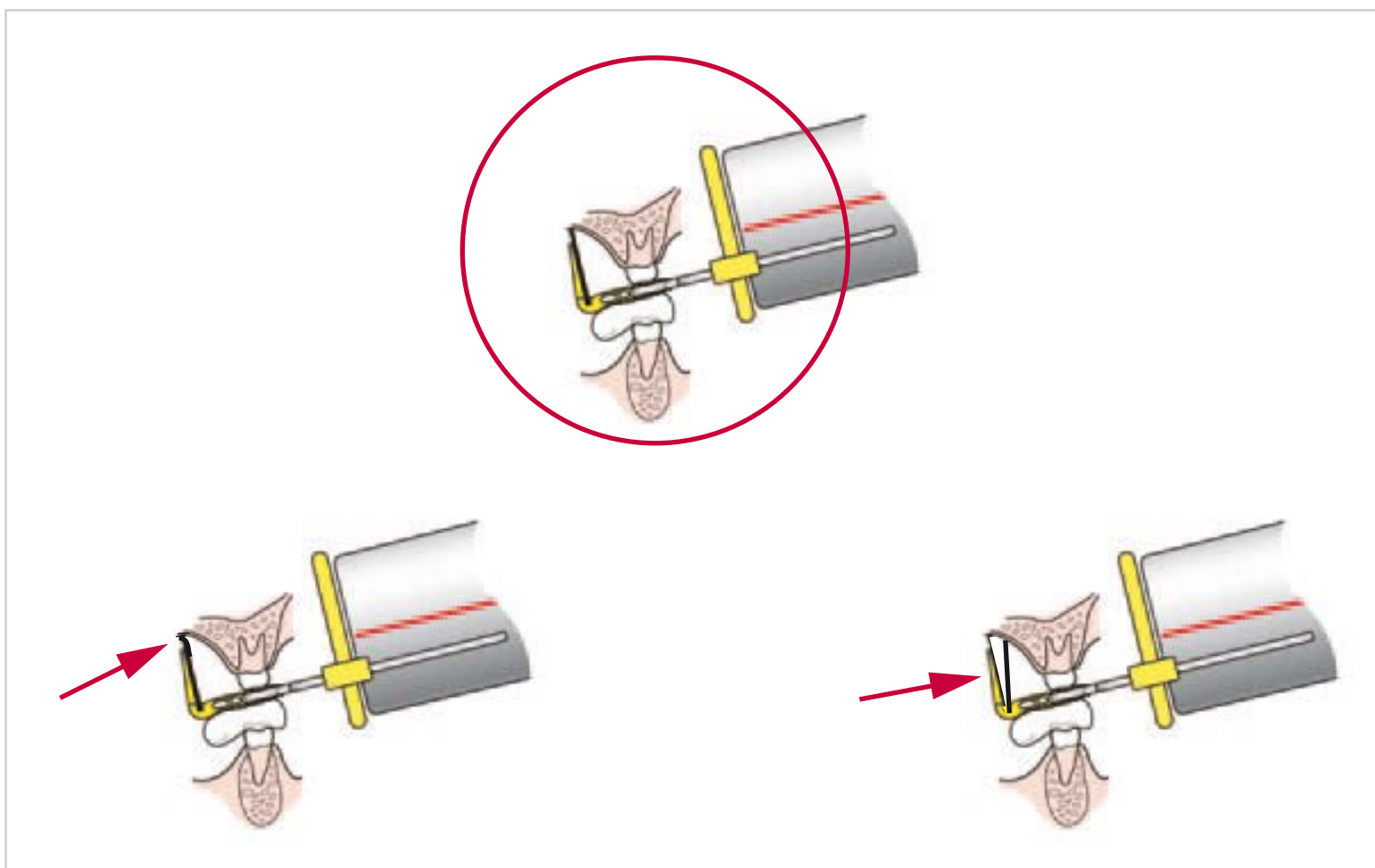


Fig. 9.19 Errors caused by bending of film: correct position (**top**); bend in film (arrow, **bottom left**); bent edge (arrow, **bottom right**). (With the kind permission of Dentsply Rinn.)



Fig. 9.20 Anterior holder for the paralleling technique. (With the kind permission of Dentsply Rinn.)

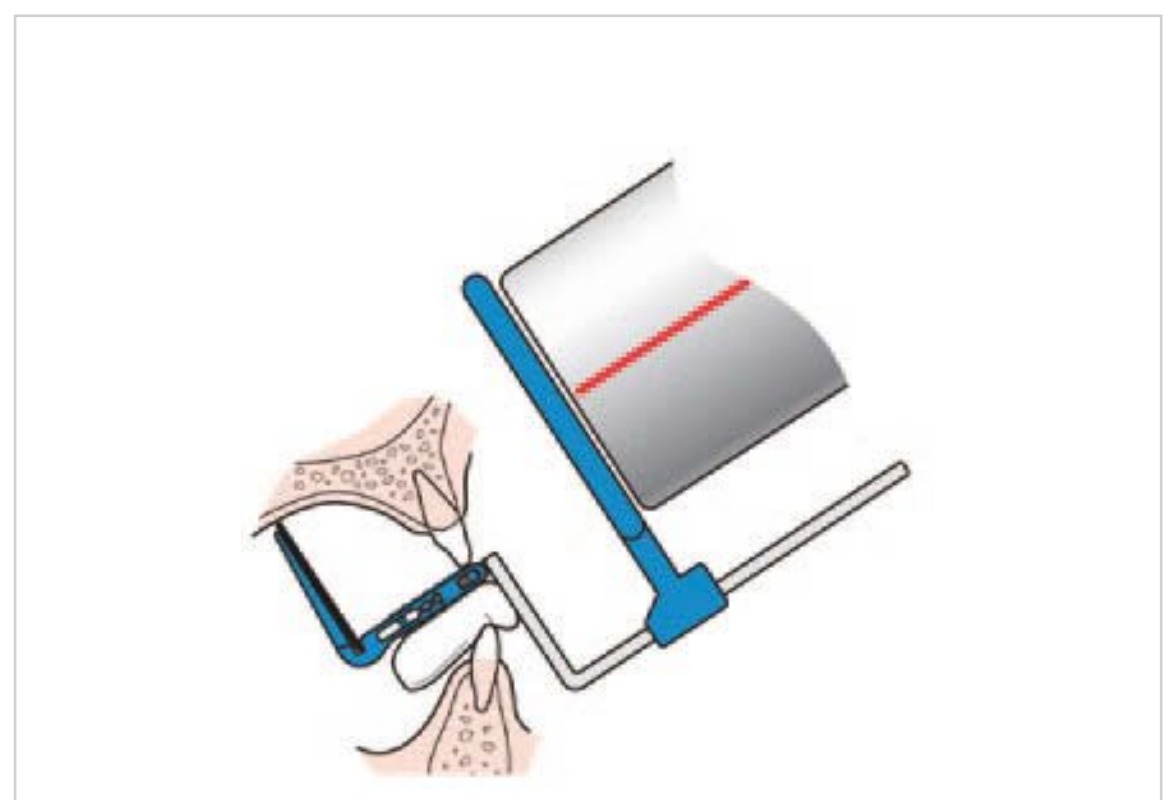


Fig. 9.21 Anterior holder placement inside the mouth. (With the kind permission of Dentsply Rinn.)



Fig. 9.22 Anterior holder placement for anterior and canine periapicals. (With the kind permission of Dentsply Rinn.)

Maxillary Incisors and Canines

An anterior holder is positioned upright in the anterior region (□ Fig. 9.20). The holder is inserted into the oral cavity at the best angle permitted by the bite block (□ Fig. 9.21). The patient is instructed to close the teeth slowly on the bite block and hold it firmly between the teeth without excessive pressure.

For canine periapicals, the holder is rotated slightly to the right or left (□ Fig. 9.22).

The axis of the canines must be aligned in the center of the image receptor. Especially when taking canine periapicals, it is crucial to ensure that the tooth axis is perpendicular to the bite block and not tilted toward the roots (□ Fig. 9.23).

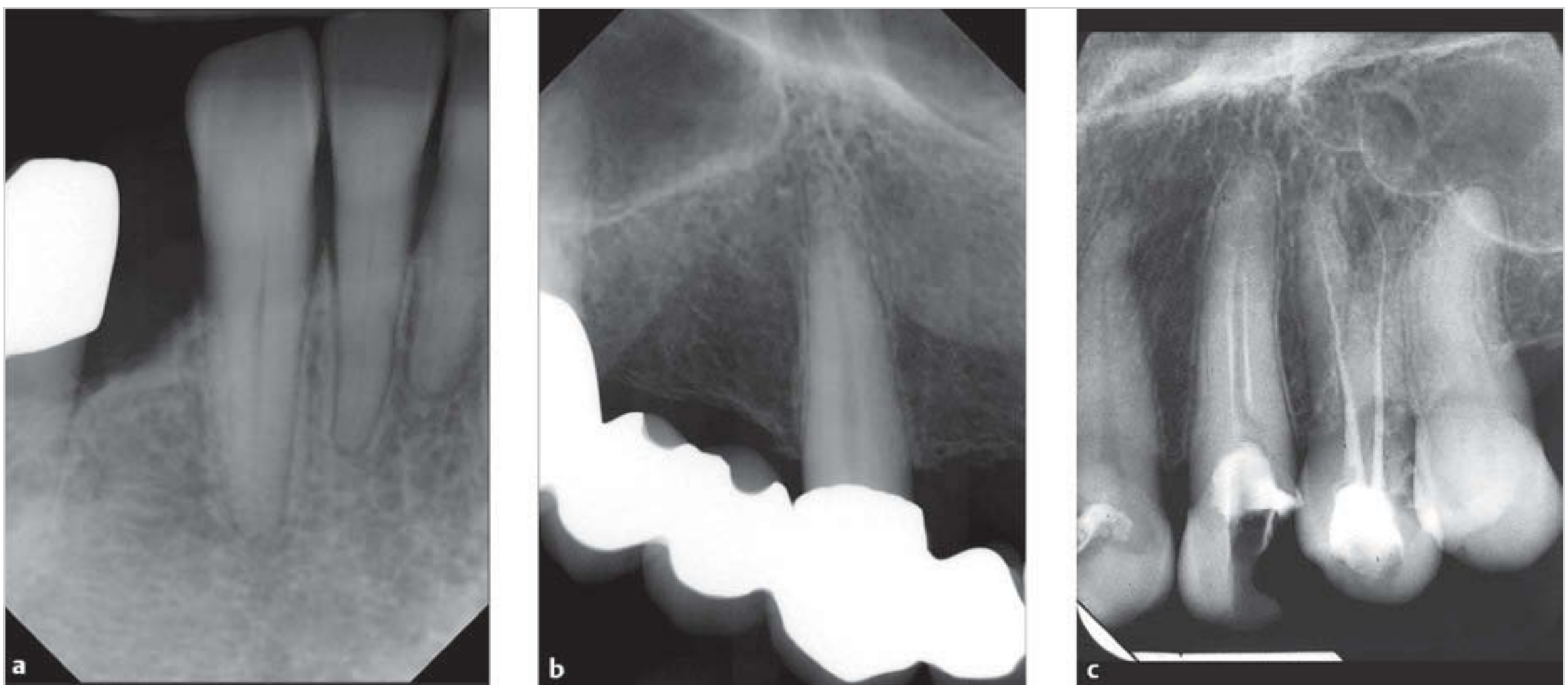


Fig. 9.23 a–c Canine periapical radiographs.

- a** Periapical radiograph showing bone loss in tooth 43.
- b** Periapical radiograph of bridge abutment tooth 13.
- c** Periapical radiograph of endodontically treated tooth 23.

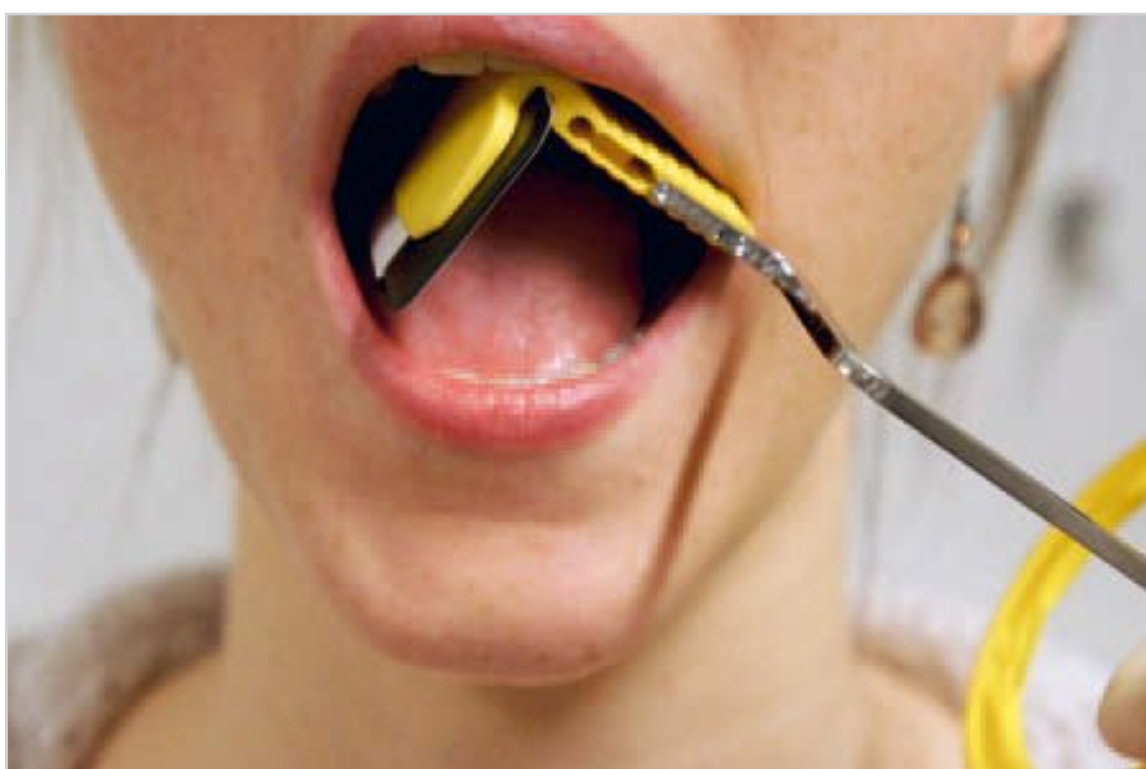


Fig. 9.24 Film insertion angle for mandibular radiographs.



Fig. 9.25 Film placed along the midline of the tongue.

Mandibular Premolars and Molars

Although the mandible may seem to offer ideal anatomical conditions for parallel tooth and film alignment, experience has shown that many patients find the film packet pressing against the floor of the mouth too painful. Consequently, they tend to push film packets and phosphor storage plates with sharp edges out of position, which may result in the root tips being cut off the radiograph. An alternative method is to position the film packet on the dorsum of the tongue. Because the tongue is less sensitive than the floor of the mouth, the film packet is usually better tolerated on the tongue.

Difficult anatomical conditions that prevent the use of a film-holder are encountered in the mandibular arch more often than in the maxillary arch. In these cases, the operator must decide whether intraoral radiography is possible and, if so, with which technique a radiograph could be obtained.



Fig. 9.26 Film placed on the dorsum of the tongue.

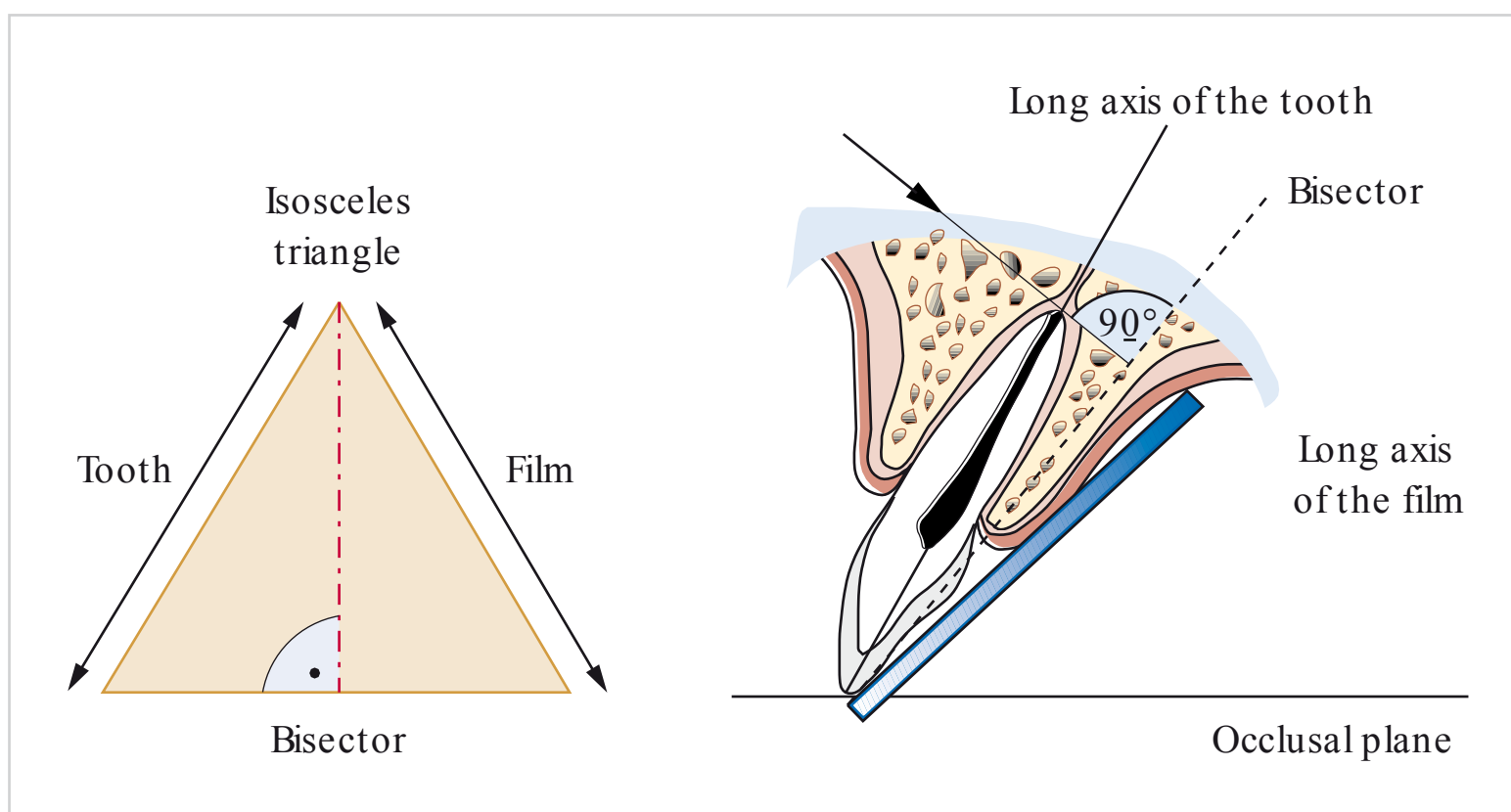


Fig. 9.27 Schematic of the bisecting-angle technique. (From: Schwenzer N, Ehrenfeldt M, eds. *Chirurgische Grundlagen*. 4th ed. Stuttgart: Thieme; 2008.)

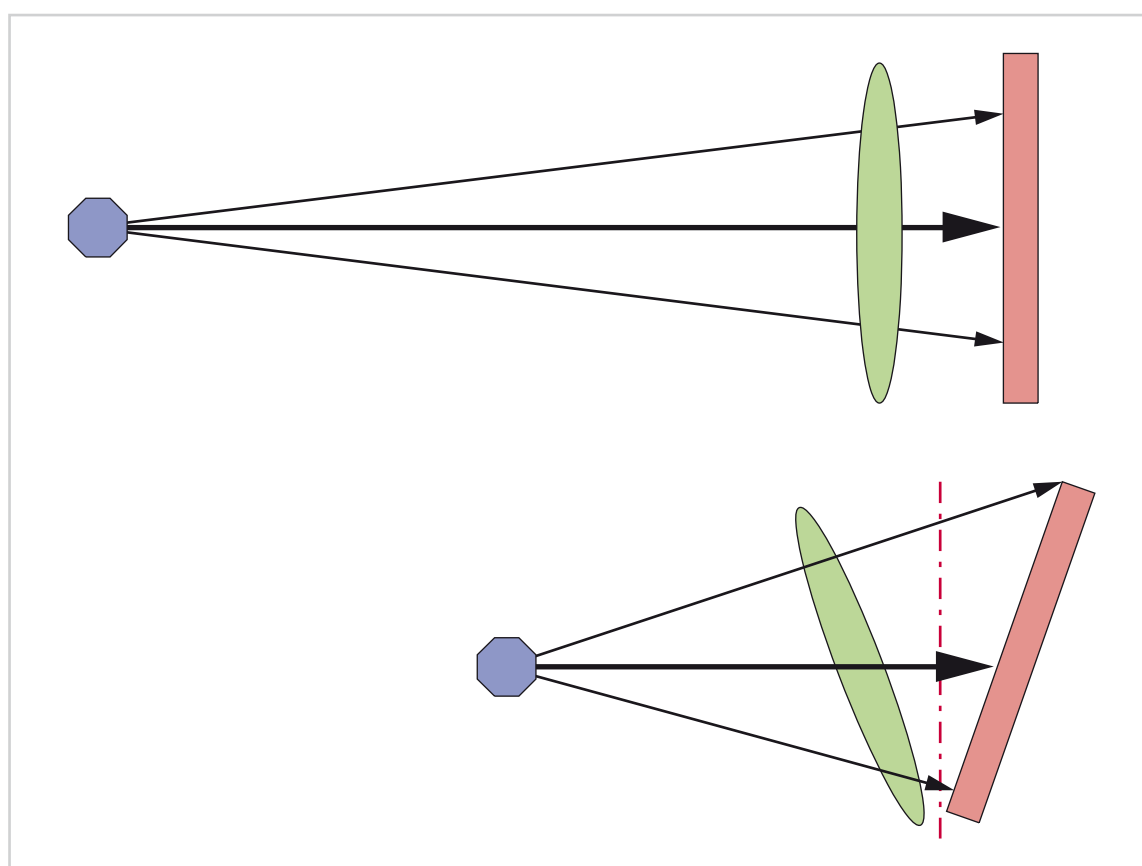


Fig. 9.28 Bisecting-angle technique (bottom) versus parallelizing technique (top).

The film-holder is held diagonally and inserted downward into the mouth. The bite block and the front part of the indicator rod lie completely within the oral cavity (□ Fig. 9.24).

If the patient finds the film next to the tooth too uncomfortable on the floor of the mouth, then the film packet should be positioned on the tongue in the middle of the oral cavity (□ Fig. 9.25). Afterwards, the operator checks to make sure that the image receptor is completely cushioned by the tongue and that no hard or sharp edges are causing pain and discomfort.

The holder is then aligned orthogonally. It is pivoted more distally for molars and more mesially for premolars. With mandibular periapicals, pressure can be exerted when the tongue is used. The position of the image receptor is crucial: the plane of the film packet must be tangential to the tooth under investigation.

Mandibular Incisors and Canines

Placement of the film packet on the tongue is also recommended for mandibular incisors and canine periapicals. This creates more space to accommodate the width of the film packet and to achieve parallelism (□ Fig. 9.26).

9.1.4 Bisecting-angle Technique

The bisecting-angle technique of periapical radiography was designed for use in cases where it is not possible to achieve parallelism between the film and the teeth, owing to either anatomical constraints or the lack of a suitable film-holder. It is an alternative method of obtaining anatomically correct intraoral radiographic images of the teeth.

In principle, the film packet is firmly placed against the tooth under investigation, without bending. This forms an angle between the long axis of the tooth and the film. The central ray is aimed perpendicular to the imaginary bisector (the plane that bisects the film and the tooth). The bisecting-angle technique provides anatomically correct images of the teeth, based on simple rules of geometry. This geometric configuration corresponds to an isosceles triangle (□ Fig. 9.27 and □ Fig. 9.28).

The patient's thumb or index finger can be used to stabilize the film packet in the mouth, by gently pressing it against the palatal or lingual side of the upper or lower arch.

Especially in the maxillary arch, there are anatomical structures that can increase the angle between the tooth and the film to as much as 45 degrees. In the mandibular arch, the film can theoretically be pressed far enough into the floor of the mouth that the tooth and the film are nearly parallel (□ Fig. 9.29).

Geometrically accurate images of single-rooted teeth can easily be achieved by correct vertical angulation of the X-ray beam. Multi-rooted teeth are more problematic. In many cases, correct vertical angulation is not possible because the roots of the tooth are not parallel to each other. The larger volume of the premolars and molars also has an unfavorable effect on the projections.

The bisecting-angle technique may result in more or less image distortion, owing to technique-related factors. Especially when using a short cone (10 cm), image distortion is particularly problematic because of increased beam divergence. Distortion may be readily apparent; for example, there may be conspicuous elongation of palatal roots in the maxillary posterior region, or crowns may be cut off at an angle (□ Fig. 9.30 and □ Fig. 9.31).

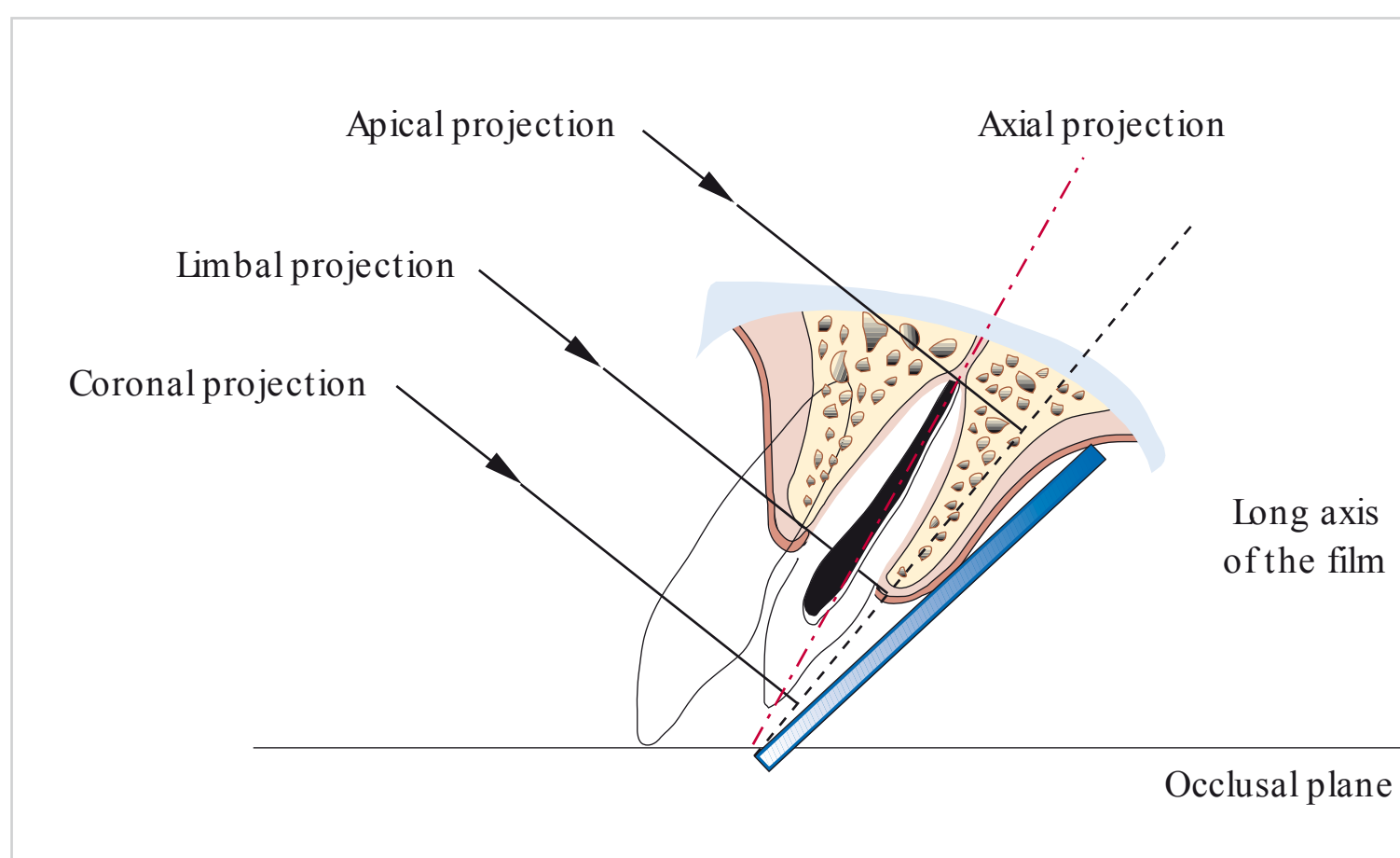


Fig. 9.29 Bisecting-angle technique: projection geometry for maxillary anterior radiographs. (From: Schwenzer N, Ehrenfeldt M, eds. Chirurgische Grundlagen. 4th ed. Stuttgart: Thieme; 2008.)



Fig. 9.30 Bisecting-angle technique: radiograph of the right maxillary teeth of a phantom head.

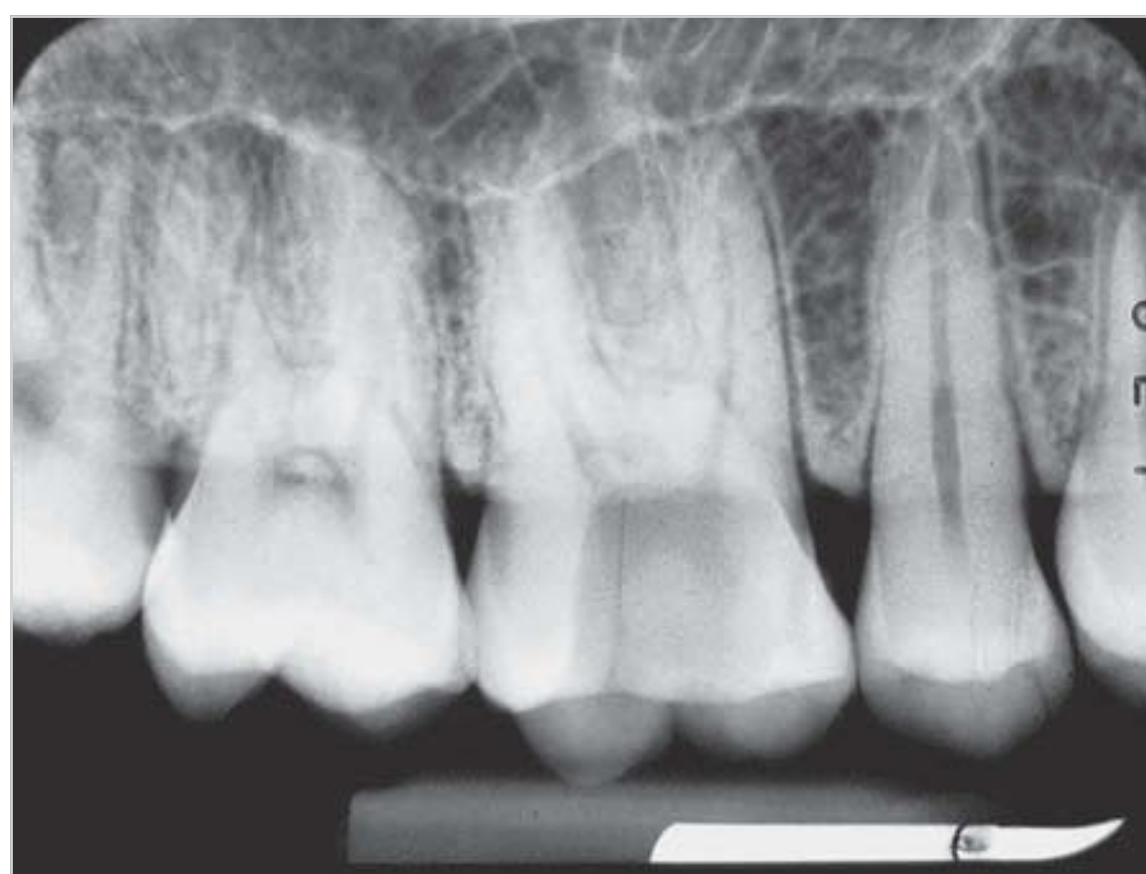


Fig. 9.31 Paralleling technique: radiograph of the right maxillary teeth (same as in Fig. 9.30).

Because of technique-related factors and the general lack of positioning devices, the bisecting-angle technique has many disadvantages.

It generally requires larger vertical angulation, which makes it harder to achieve orthogonal projection geometry (Fig. 9.32). The zygomatic bone often projects onto the apices of the molar roots, owing to excessive vertical angulation (Fig. 9.33).

Moreover, it is not always easy to hit the bisector correctly. Incorrect vertical angulation results in elongation (Fig. 9.34) or foreshortening of the image (Fig. 9.35).



Fig. 9.32 Radiograph acquired with nonorthogonal projection geometry (angle too steep).



Fig. 9.33a, b Projection of the zygomatic bone.

a Zygomatic bone.

b Projection in the molar apical region.

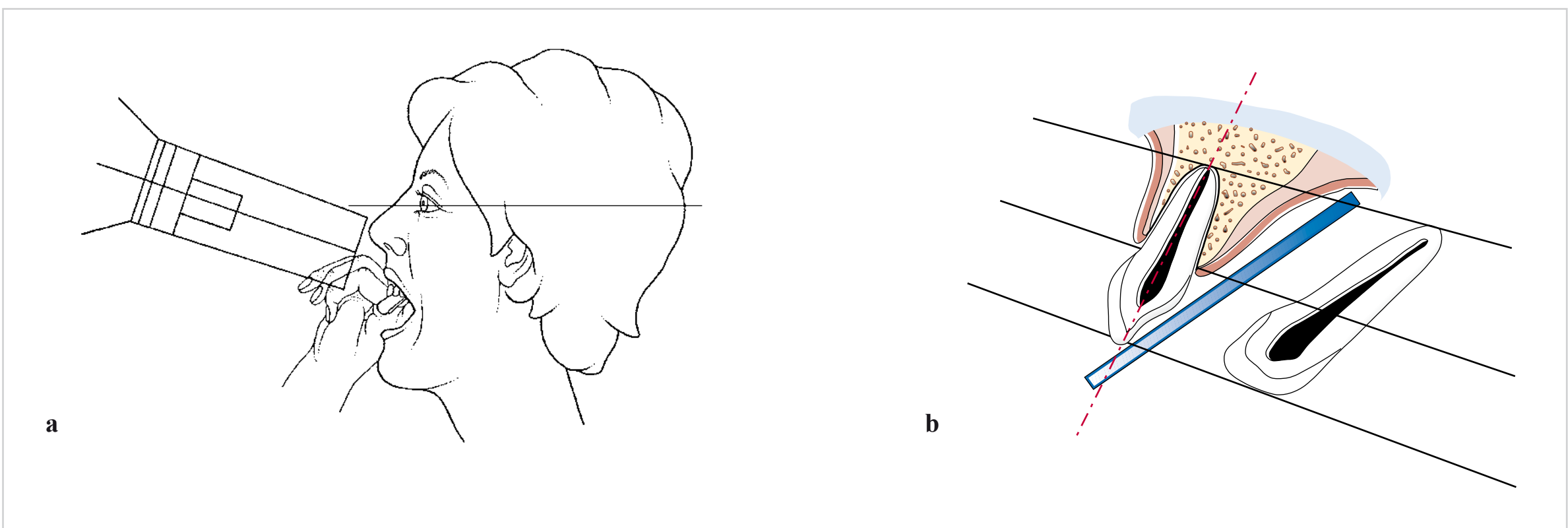


Fig. 9.34a, b Bisecting-angle technique: too shallow an angle results in elongation of the teeth. (**a** from: Pasler FA. Zahnärztliche Radiologie. 5th ed. Stuttgart: Thieme; 2008; **b** from: Schwenzer N, Ehrenfeldt M, eds. Chirurgische Grundlagen. 4th ed. Stuttgart: Thieme; 2008.)

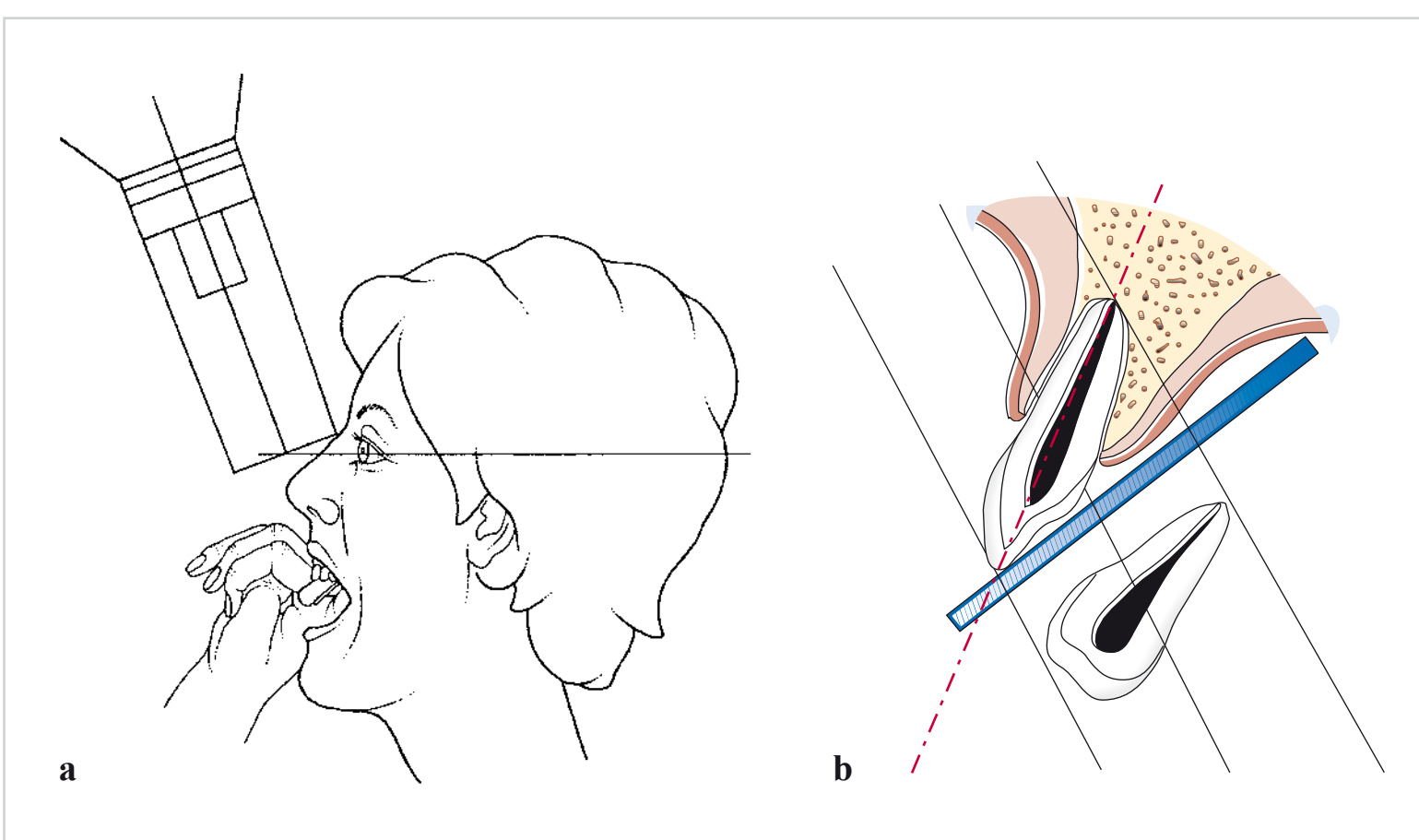


Fig. 9.35a, b Bisecting-angle technique: too steep an angle results in foreshortening of the teeth. (**a** from: Pasler FA. Zahnärztliche Radiologie. 5th ed. Stuttgart: Thieme; 2008; **b** from: Schwenzer N, Ehrenfeldt M, eds. Chirurgische Grundlagen. 4th ed. Stuttgart: Thieme; 2008.)

Film or plate bending can also result in image distortion. This occurs due to excessive pressure during handling or from the film being pressed against the palate or floor of the mouth.

Radiographs acquired using the bisecting-angle technique have geometrically correct size equality but are not true to scale (□ Fig. 9.36).

Excessive vertical angulation is also not recommended for reasons of radiation protection, because a larger portion of the beam would irradiate the trunk of the body. There is a risk of exposing other parts of the patient's body to primary radiation, even if a radiation-protection apron is correctly placed.

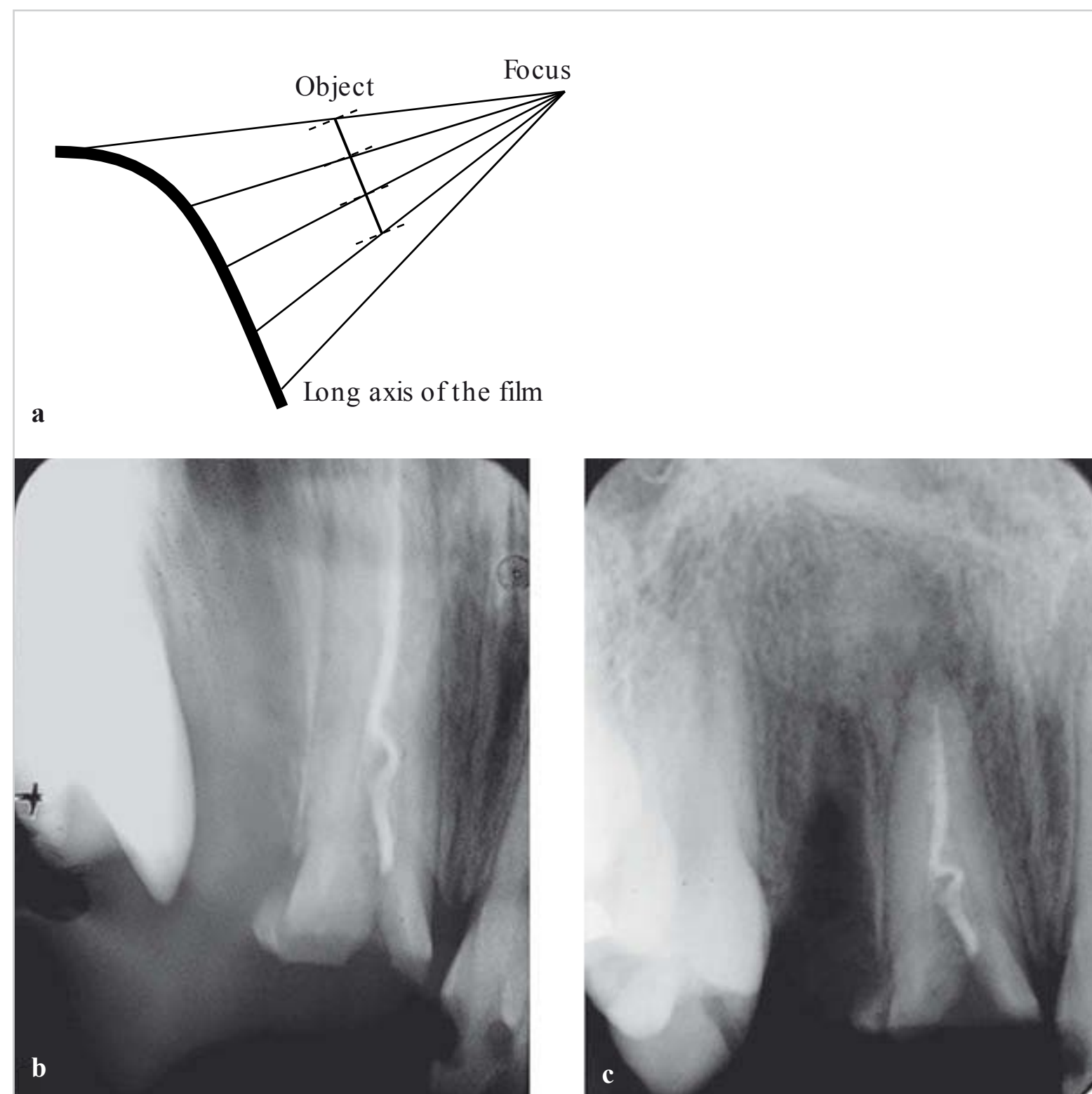


Fig. 9.36a–c Radiographic distortion caused by bends in the film.

a Bisecting-angle technique (schematic diagram): there is great divergence of the beam and bending of the flexible image receptor (film and image plate) in the apical region, near the palate. (From: Pasler FA. Zahnärztliche Radiologie. 5th ed. Stuttgart: Thieme; 2008.)

b Note the elongation of the root-filled tooth. The apex is not visualized on the image. This problem occurred because the angle of incidence is too shallow and the film is bent in the apical region.

c The paralleling technique was used for this radiograph. All important areas are visualized without distortion.

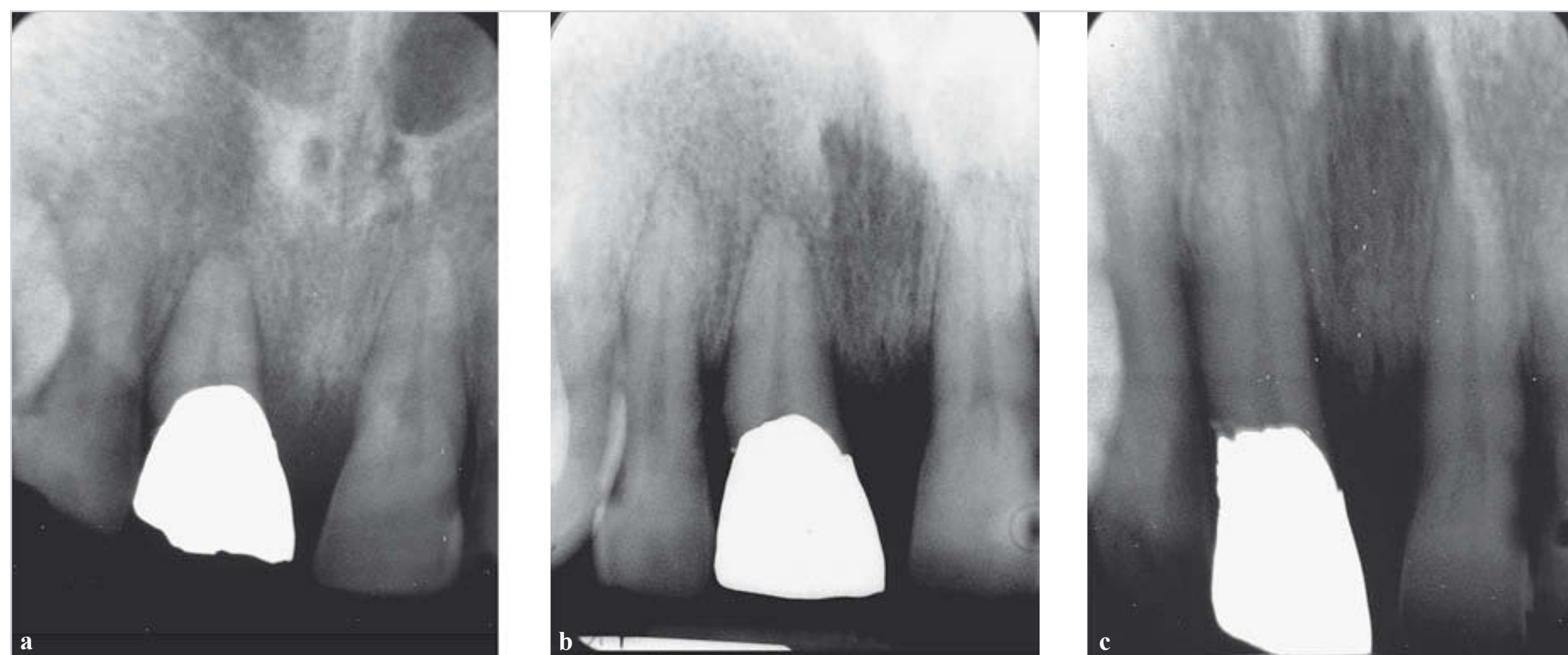


Fig. 9.37a–c Comparison of three periapical radiographs.

a Bisecting-angle technique: too steep an angle results in foreshortening of the teeth.

b Paralleling technique: geometrically correct image of the teeth.

c Bisecting-angle technique: too shallow an angle results in elongation of the teeth.

Moreover, use of the bisecting-angle technique decreases radiographic reproducibility. The reproducibility of radiographs is a very important element of radiographic diagnosis. To be comparable, radiographs must show the target anatomical structures in the same manner. Reproducibility facilitates the identification of differences, regardless of whether these are normal variants or pathologic changes (□ Fig. 9.37).

Note

The bisecting-angle technique does not conform to the rules of projection geometry because the X-ray beam, including the central ray, is not oriented perpendicular to the film and the long axis of the tooth. Moreover, the use of a short cone results in considerable beam divergence and image distortion. Only those X-rays near the central ray are likely to form images without major geometric unsharpness.

This problem resulted in the development of so-called apical, coronal, and marginal projections, in which the central ray was aimed at the center of the apex, the crown, or the alveolar ridge, depending on the clinical question, in an attempt to image these regions without distortion. However, these methods were never able to produce intraoral radiographs of the entire tooth in a single exposure without distortion.

The bisecting-angle technique is only recommended for use in certain exceptional cases. Furthermore, the use of a short cone is no longer permitted today: an FOD of at least 20 cm is required for reasons of radiation protection. Otherwise, the X-rays responsible for image formation would not be perpendicular to the image receptor, resulting in image distortion.

On first glance, the bisecting-angle technique might seem to be easy to use, but it is not easy to learn. Even experienced radiographers sometimes have problems correctly calculating the imaginary line that bisects the image receptor and the long axis of the tooth and aiming the central ray perpendicular to the bisector (□ Fig. 9.38).

Bisecting-angle Technique: Methodology

The bisecting-angle technique is usually performed without a film-holder or aiming device (e.g., aiming ring and indicator rod). Therefore, there are many more factors to consider than with the paralleling technique.

For example, the head positioning is more important for the bisecting-angle technique than for the paralleling technique. The occlusal plane must be aligned strictly horizontal and parallel to the floor. This means that the head must be tilted slightly forward for maxillary radiographs, and slightly backward for mandibular radiographs. Correct head position can be checked against the position of the tooth axes, which should be perpendicular to the floor.

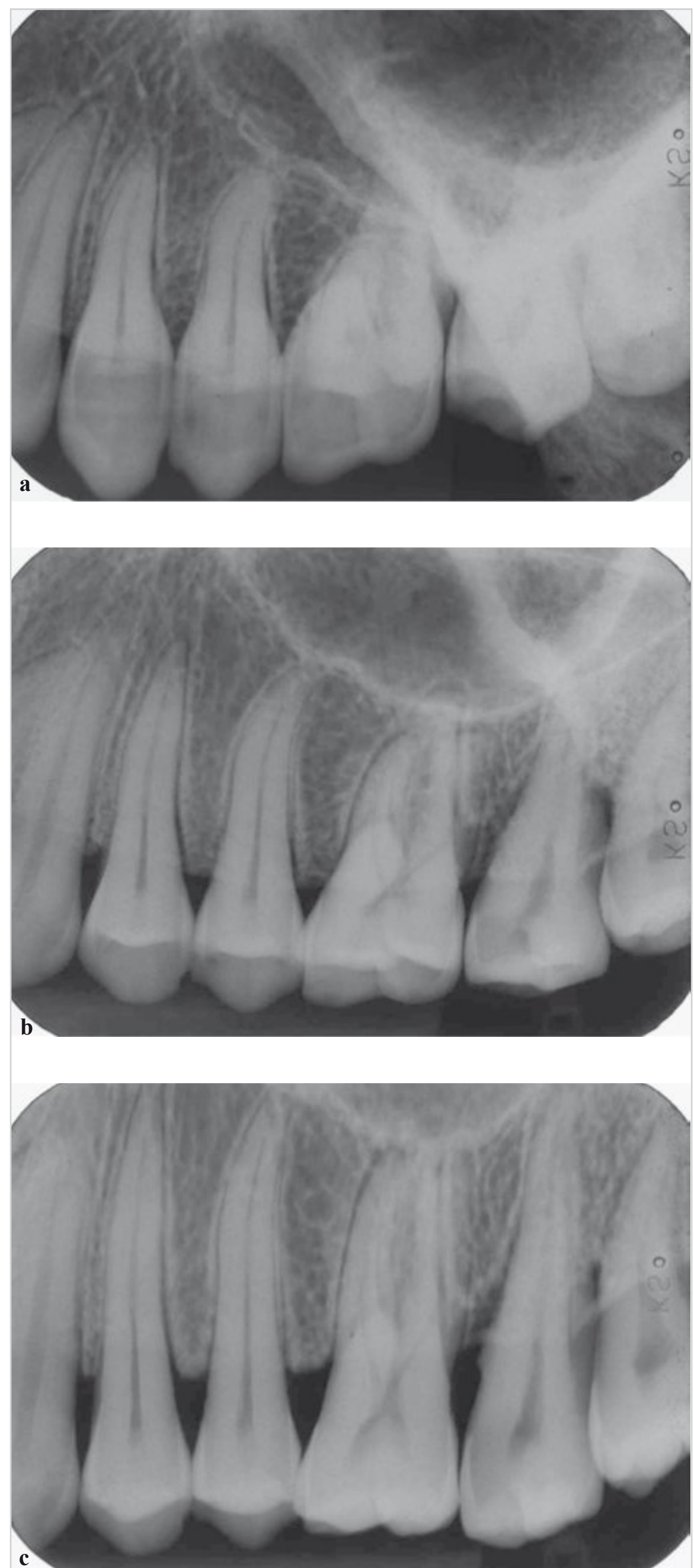


Fig. 9.38a–c Bisecting-angle technique: both vertical angulation of the beam and orthogonal projection geometry must be considered. **Vertical** angulation adjustments can result in three possible outcomes:

- a** Too steep an angle (perpendicular to the film).
- b** Correct angle (perpendicular to the bisector).
- c** Too shallow an angle (perpendicular to the tooth).

For anatomical reasons, the **film** is placed in the oral cavity at an angle, pressed against the tooth. This configuration makes it hard to check the position of the **film** for correctness. When the patient holds the **film** with a **finger**, it is usually not possible to determine whether the position of the **film** changed until after **film** development.

The position of the bisector is different for each patient because of the individual nature of each person's anatomy and the resulting **film** position. In practice, it is usually easy to mentally bisect the angle formed by the **film** and the long axis of the tooth and aim the central ray perpendicular to the imaginary bisector. If this is done correctly, the vertical angle is usually correct.

When centering, the edge of the cone should be as parallel as possible to the visible edge of the **film**. When the **film** is positioned correctly (□ Fig. 9.39), the central ray should be perpendicular to the imaginary plane that bisects the angle formed by the **film** and the long axis of the tooth.

9.1.5 Right-angle Technique

The right-angle technique is usually considered to be the same as the paralleling technique. However, the only thing the two techniques have in common is that a film-holding device is used to direct the central ray of the beam perpendicular to the film. As in the paralleling technique, the image receptor is positioned in the middle of the oral cavity, in order to obtain parallelism between the image receptor and the long axis of the tooth. The difference is that the right-angle technique is performed without a bite block (□ Fig. 9.40). Instead, the holder is mounted on a spacer cone.

Owing to the lack of a bite block, the right-angle technique is a combination of the paralleling technique and the bisecting-angle technique. In the paralleling technique, the vertical angle is determined by the bite block, whereas in the right-angle technique, the vertical angle is determined and set according to the laws of the bisecting-angle technique (□ Fig. 9.41).

The main disadvantage of the right-angle technique, which was introduced by Hielscher and modified by Pasler, is that it is not always reliable for visualizing the apical region (□ Fig. 9.42). Parallelism between the long axis of the tooth and the image receptor should be achieved in the right-angle technique, but if the patient has a shallow palate, the upper edge of the **film** may fall below the apical region. This results in the apical region being cut off the **film**. The bisecting-angle technique must be used in this situation.

Other disadvantages of the right-angle technique include the following:

- The **film**-holder must be mounted on the spacer cone: this makes the right-angle technique more difficult to perform and results in low acceptance by patients.



Fig. 9.39 Correct position of the **film** packet in the lower arch. (From: Pasler FA, Visser H. Zahnmedizinische Radiologie. 2nd ed. Stuttgart: Thieme; 2000. Farbatlant der Zahnmedizin; Band 5.)



Fig. 9.40 Right-angle technique: **film**-holder without a bite block is mounted on the cone. (Adapted from: Pasler FA, Visser H. Zahnmedizinische Radiologie. 2nd ed. Stuttgart: Thieme; 2000. Farbatlant der Zahnmedizin; Band 5.)

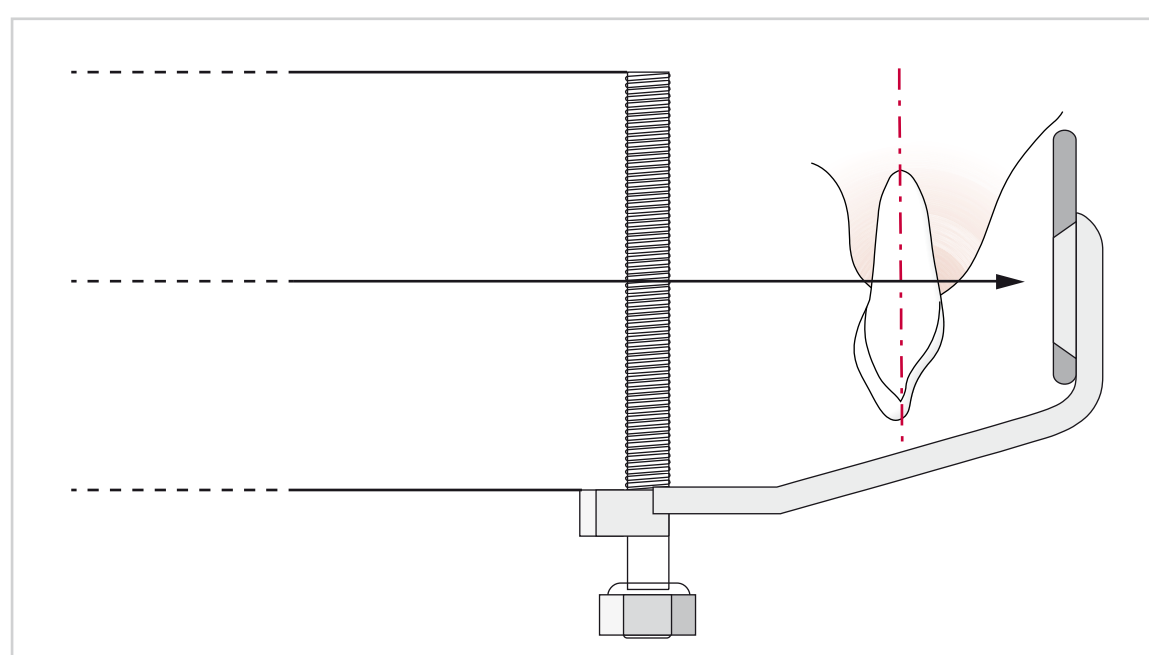


Fig. 9.41 Ideal parallelism between the **film** and the tooth (in the upper arch).

- The holder positioning is not reproducible: when taking follow-up radiographs (e.g., after implant surgery), the holder position in the mouth changes, owing to the lack of a bite block.

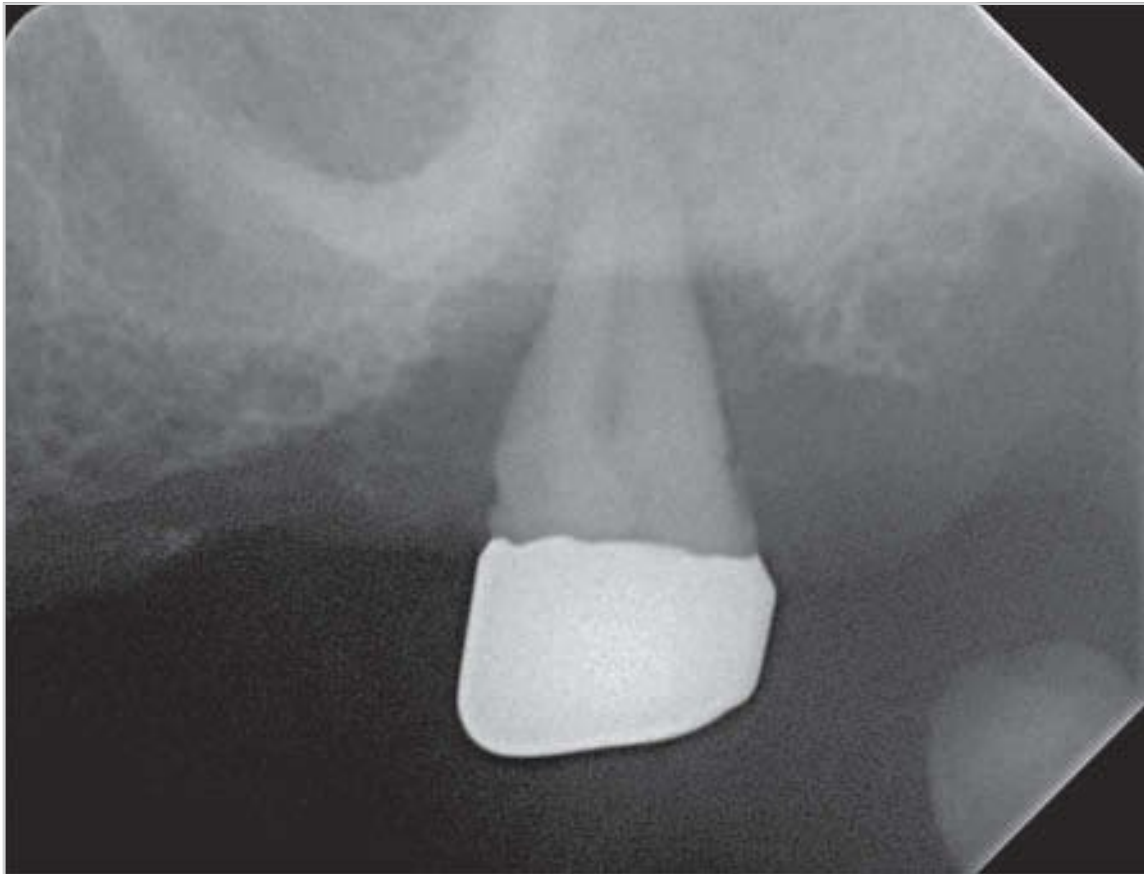


Fig. 9.42 Right-angle technique: radiograph of the maxilla.

- Parallel positioning of the film is arbitrary: consequently, the root tips may be cut off the radiograph.
- Superimposition due to film positioning errors may occur: if the film is placed in a slanted mesial or distal position, the tooth axes will be radiographed at an angle, and interproximal superimposition artifacts may occur.

9.1.6 Bitewing Radiography

Bitewing radiography was introduced by Raper in 1925. It is the most important radiographic technique for diagnosis of caries. Bitewing radiographs show the alveolar ridge without distortion. They demonstrate salivary stones well and are useful for evaluating the marginal integrity of crowns and fillings (□ Fig. 9.43).

Bitewings should always be obtained supplementary to the clinical examination in cases where the mesial and distal contact areas cannot be evaluated by visual inspection. Approximal caries is usually overlooked when bitewing radiographs are not made supplementary to the clinical examination. This is especially true in cases where

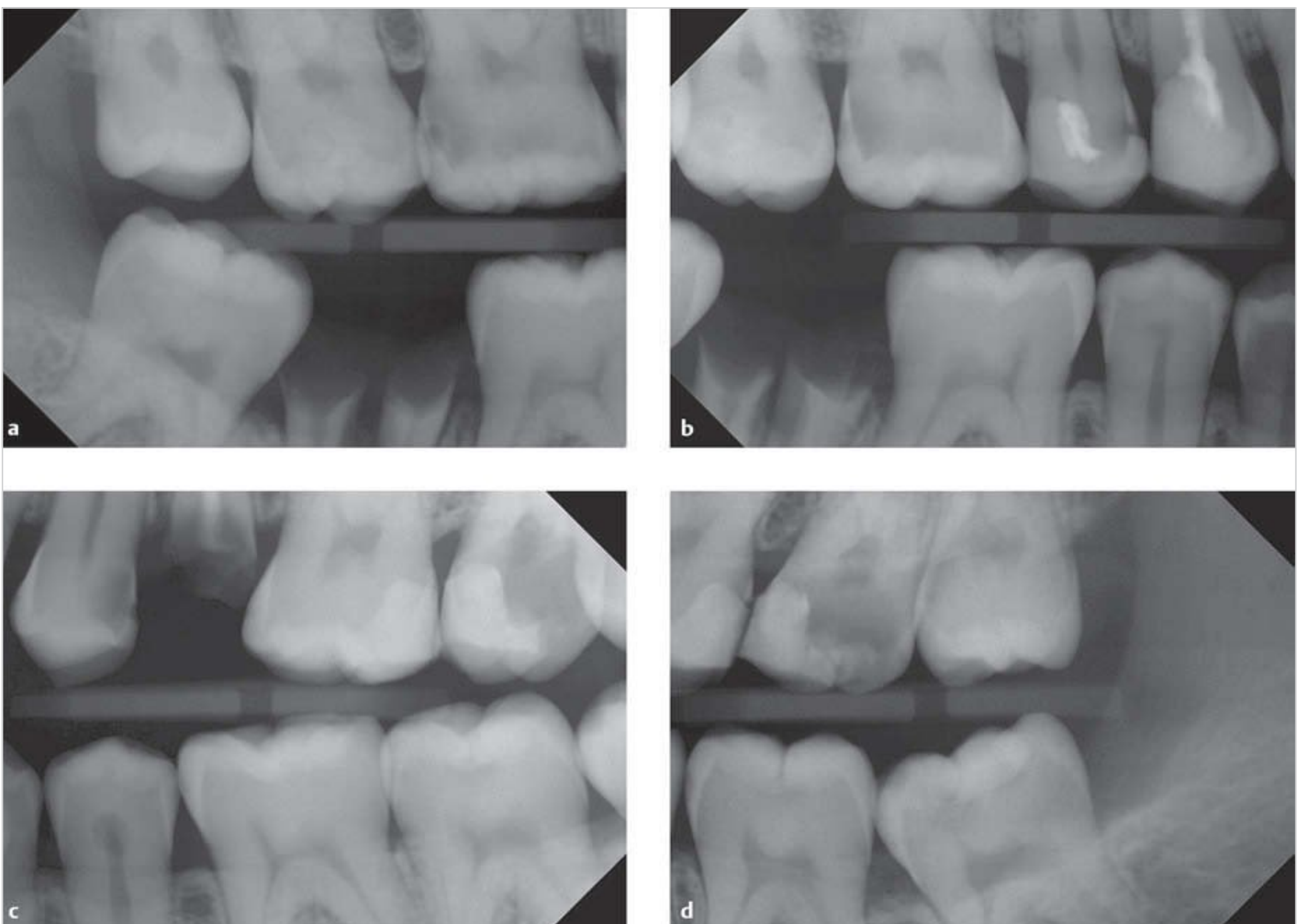


Fig. 9.43a–d Bitewing radiographs.

- a** Right molars.
- b** Right premolars.
- c** Left premolars.
- d** Left molars.

invasive caries tunnels through the interproximal enamel to the dentin and undermines the enamel. In diagnostic radiography, early detection of dental caries is still one of the main strategies for promoting dental health in broad segments of the population.

Size 3×4 cm film is generally used for bitewing radiography. Long and narrow film (2.7×5.4 cm) is no longer recommended, for two reasons: first, it is not always possible to achieve orthogonal imaging of all molars and premolars in a single projection and, second, the film is too short to capture the alveolar crest.

Bitewing Radiography: Methodology

Because bitewings are used for evaluation of interproximal areas, a film-holder and aiming ring should always be used in bitewing radiography (□ Fig. 9.44).

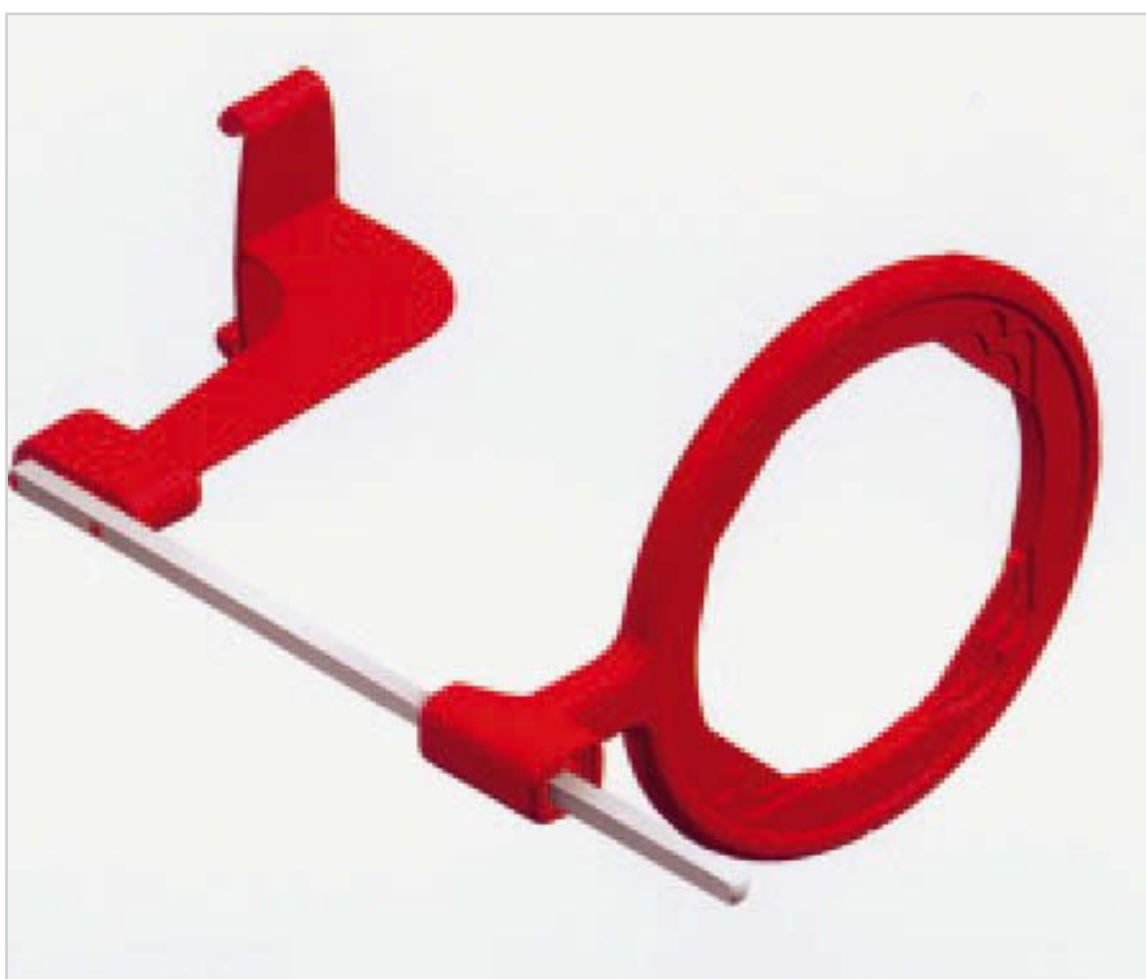


Fig. 9.44 Bitewing film-holder. (With the kind permission of Dentsply Rinn.)

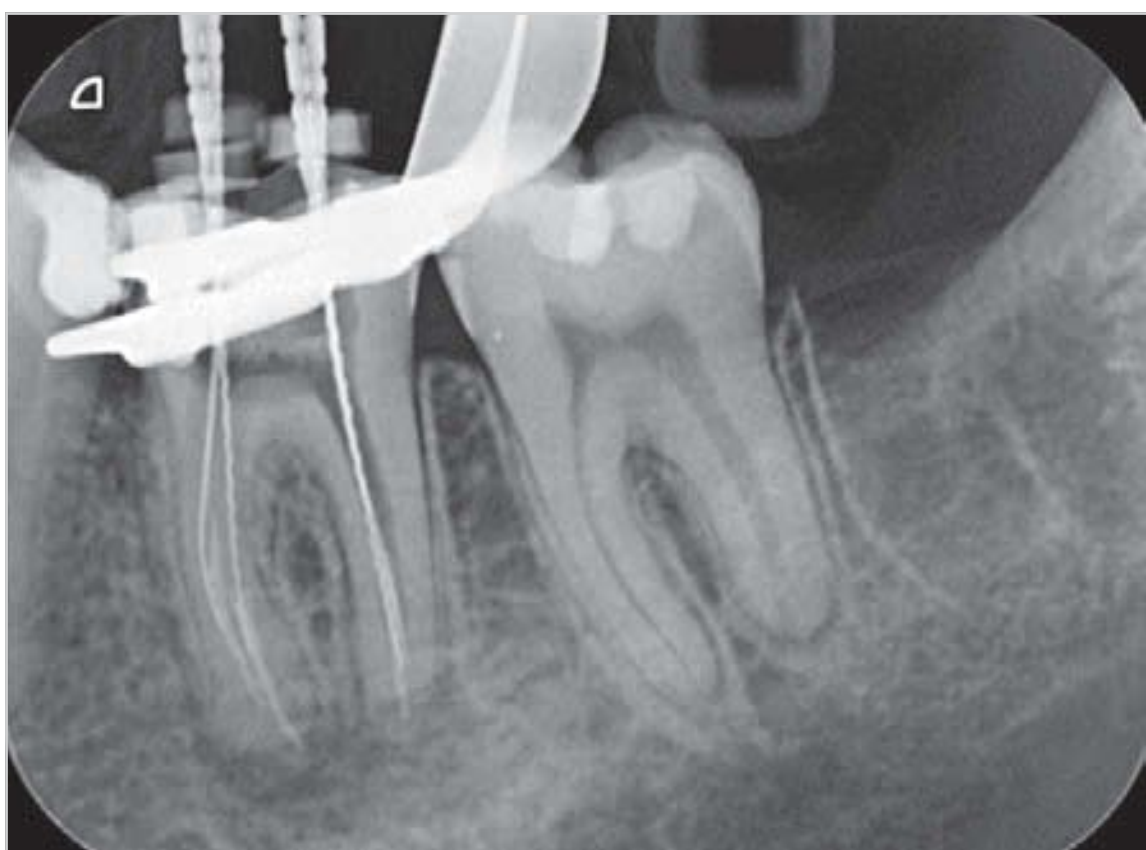


Fig. 9.45 Radiographic measurement of the working length of a root canal.

9.1.7 Radiographic Measurement Techniques

Radiographic measurement techniques are used to determine the working length of root canals (□ Fig. 9.45). Since these radiographs must be taken with root-canal instruments and a rubber dam in place, technical difficulties may occur. Ideally, they should be obtained using the paralleling technique, but this is not possible with conventional film-holders.

The Endo-Holder was designed to simplify the radiographic measurement of root-canal working length (□ Fig. 9.46). Its raised basket-like bite block makes it possible to take the X-rays with root-canal instruments and a rubber dam in place. As in the parallel technique, the Endo-Holder has an aiming ring and indicator rod, and the X-rays are directed perpendicular to the image receptor. This makes it possible to obtain reproducible working length measurements in endodontic applications.

9.1.8 Occlusal Radiography

Occlusal film is screenless film. Compared with bitewing film, the only difference is that occlusal film is larger; the standard size is 7.5×5.5 cm (□ Fig. 9.47). Its size makes occlusal film very versatile. Occlusal radiographs can supplement or replace other intraoral radiographic examinations.

Phosphor storage plates are the only types of digital image receptors available for occlusal radiography. Occlusal radiography is not limited to the use of large film: the 3×4 cm size can also be used.

The film packet is placed in the mouth parallel to the occlusal surfaces of the teeth. There should be an angle of 90 degrees between the film and occlusal plane.

The two main techniques used for occlusal radiography are:

- Bisecting-angle technique
- Axial projection technique.

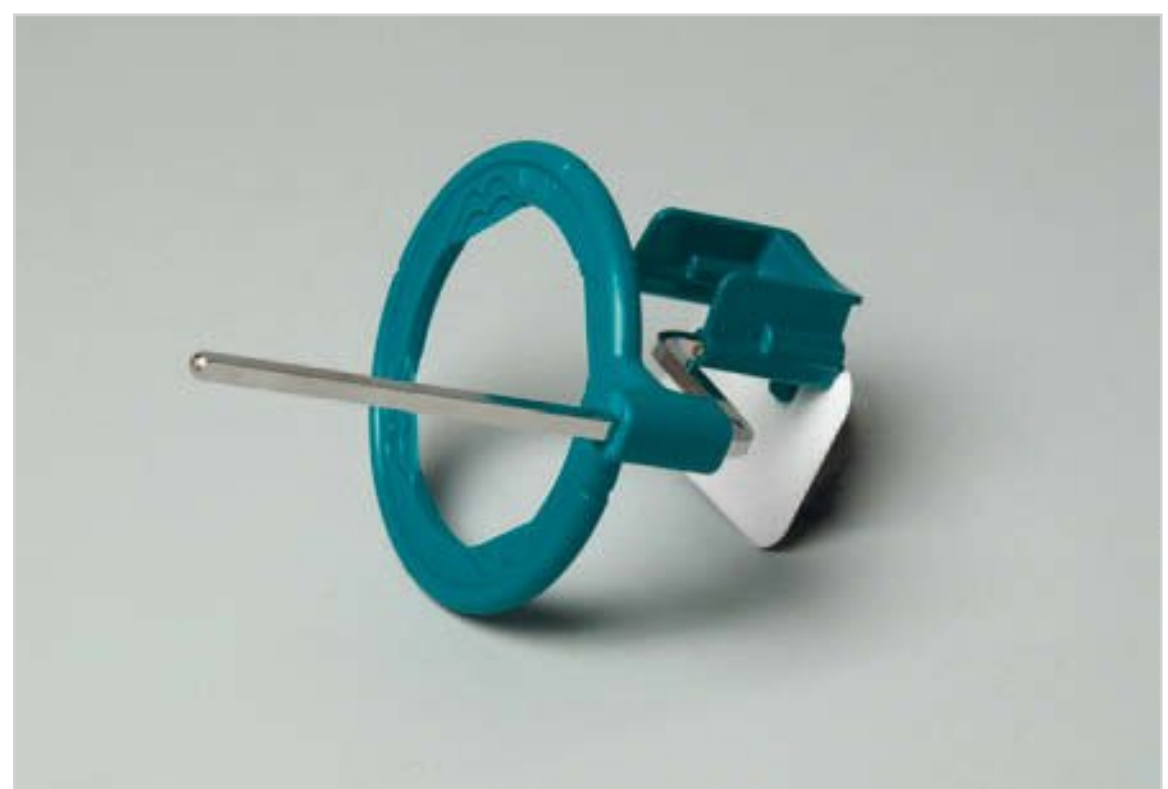


Fig. 9.46 Dentsply Rinn Endo-Holder for radiographic measurement.

Occlusal Radiography: Bisecting-angle Technique

The bisecting-angle technique must be used in occlusal radiography.

As many as **five** teeth can be depicted on a single posterior occlusal radiograph when large **film** is used. Anterior and canine occlusal radiographs show the teeth and large segments of the bone. Mandibular occlusal radiographs show the entire mandibular arch, including the cortical bone. Dental radiographs taken using larger **film** formats generally provide more information by virtue of their larger size (□ Fig. 9.48). Occlusal radiography is



Fig. 9.47 Occlusal **film** (left) versus bitewing **film** (right).



Fig. 9.48 This maxillary anterior occlusal radiograph obtained using the bisecting-angle technique shows a large area of osteolysis.

sometimes possible in cases where other intraoral radiographic techniques cannot be performed, for example, in situations where panoramic radiography or other techniques of intraoral radiography cannot be performed successfully because of physical constraints.

Because of the ease of **film** placement, occlusal radiography is especially useful for the assessment of anterior tooth trauma in children.

Bisecting-angle Technique: Methodology

The film packet must be positioned in the patient's mouth on the occlusal surfaces of the teeth, such that the outer edge of the film packet is parallel to the crowns of the teeth of interest. This edge forms the tangent line that the central ray must intersect at right angles for proper orthogonal imaging (□ Fig. 9.49 and □ Fig. 9.50).

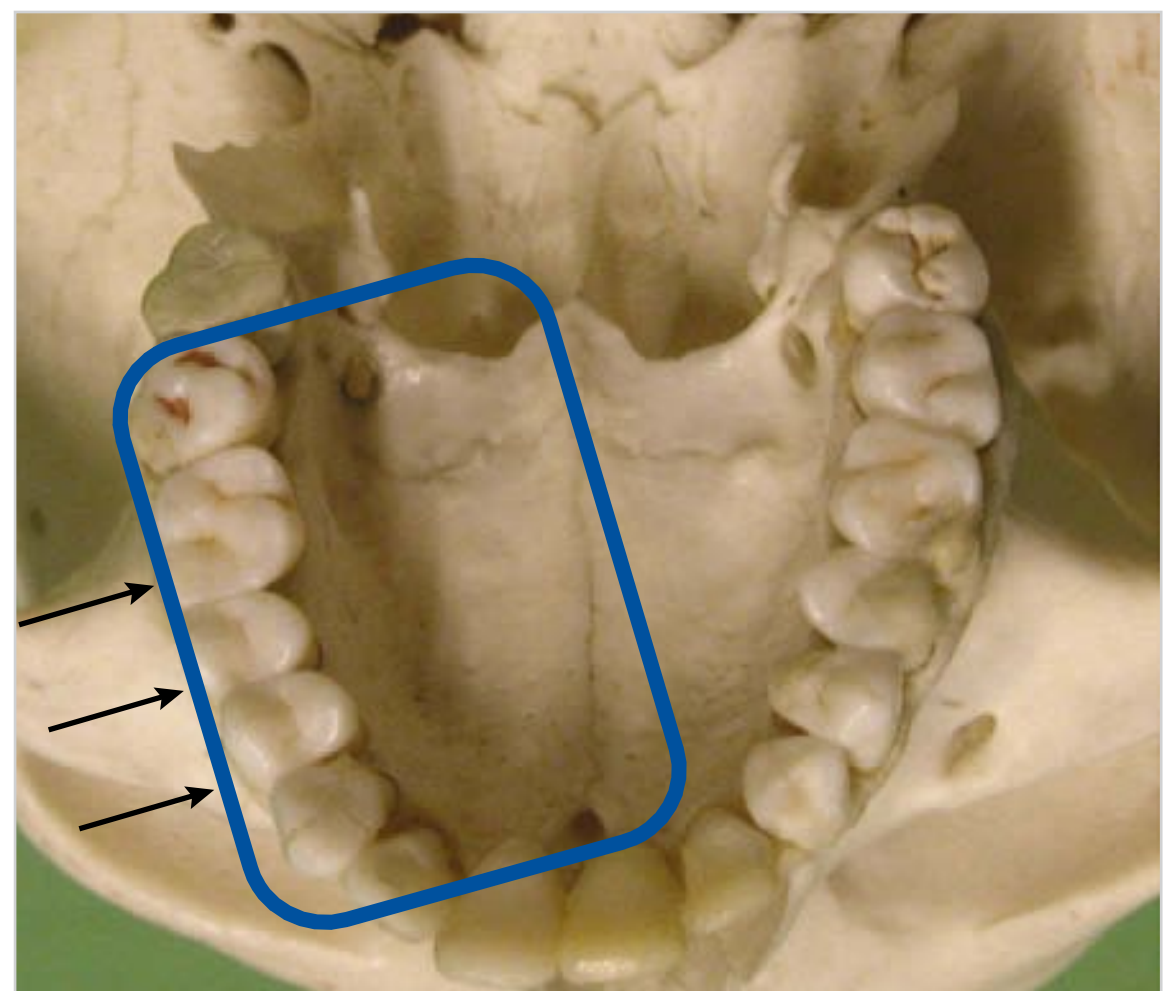


Fig. 9.49 Correct **film** positioning for maxillary posterior occlusal radiographs.



Fig. 9.50 Occlusal radiograph of the maxillary posterior teeth.

Occlusal Radiography: Axial Projection Technique

In the axial projection technique of occlusal radiography, the axial projection of the beam results in a second plane that can provide a spatial image impression when combined with other radiographs. Film positioning is different from that of the bisecting-angle technique. Because this projection is used to identify pathological changes in the buccolingual dimension, the mandible must always be positioned in the center of the film, as parallel to the edges of the film packet as possible (□ Fig. 9.51).

The course or dislocation of mandibular fractures can then be viewed in a second plane in supplement to panoramic radiographs (□ Fig. 9.52 and □ Fig. 9.53). The axial projection technique can also be used to visualize impacted teeth or space-occupying lesions.

Because of radiation-protection and image-quality standards, the axial projection technique of occlusal radiography should be used for evaluation of the mandible only.

Moreover, CBCT now provides images in multiple planes and with better diagnostic quality than can be achieved with the axial projection technique of occlusal radiography.

Visualization of sialolithiasis in the ducts of the submandibular gland is a special indication for the axial projection technique of occlusal radiography. The exposure time must be reduced significantly to detect radiopaque objects such as sialoliths (□ Fig. 9.54).

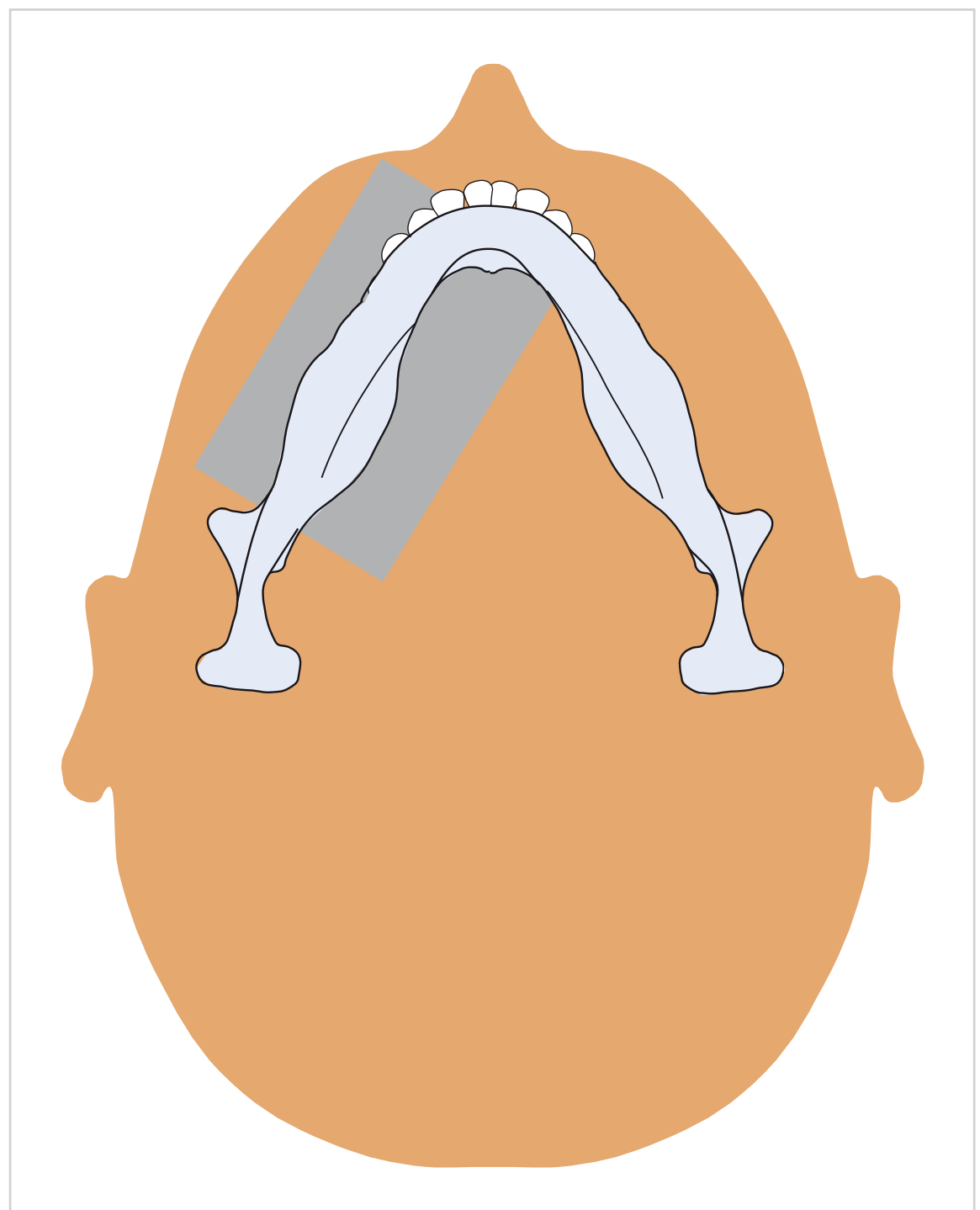


Fig. 9.51 Correct positioning for occlusal radiography of the mandibular posterior teeth using the axial projection technique.



Fig. 9.52 Axial projection technique of occlusal radiography used to show a second dimension, to identify the spatial position of fractures.



Fig. 9.53 Axial projection technique of occlusal radiography used to show a second dimension revealed a cyst.

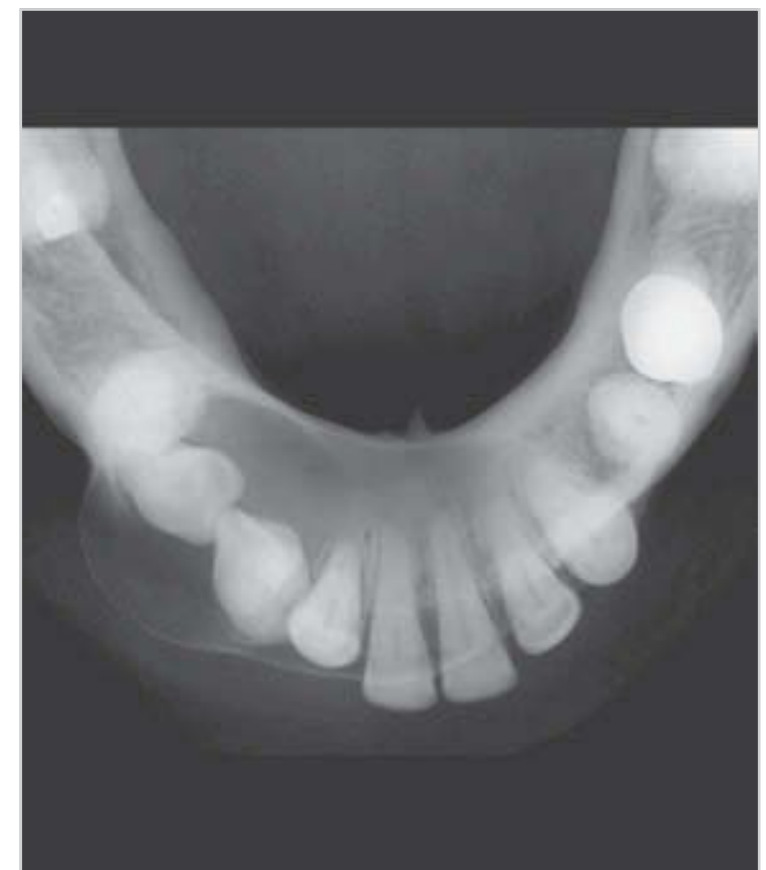


Fig. 9.54 Occlusal radiograph of the floor of the mouth revealed a sialolith in the duct of the submandibular gland.

9.2 Conventional Tomography

A conventional radiographic image is the sum of an infinite number of anatomical slices. It contains countless details, all of which arise from a single focus of projection. A single projection that visualizes every detail without superimposition does not exist. Therefore, a summation

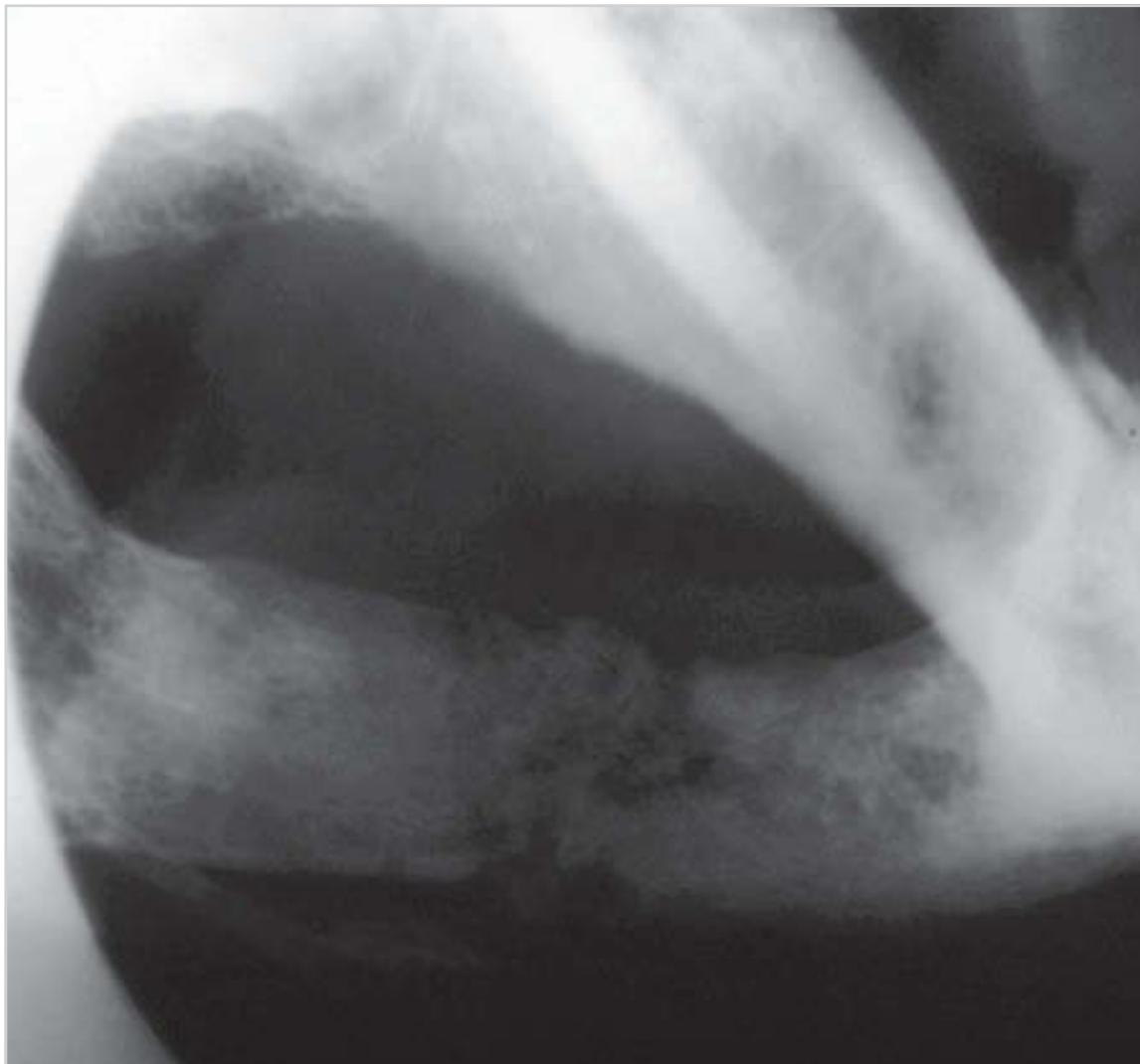


Fig. 9.55 Partial-arch projection showing osteolysis in the horizontal ramus of the mandible.

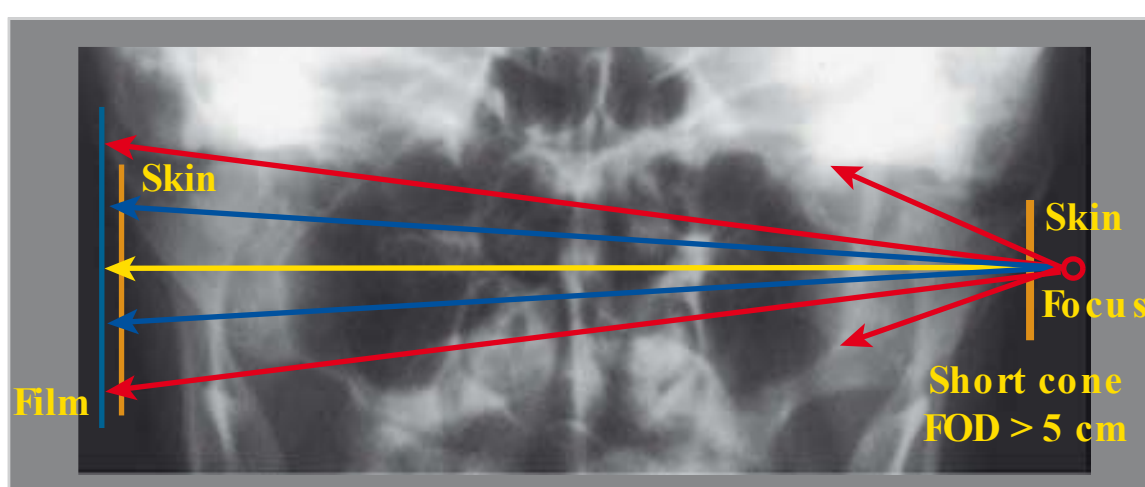


Fig. 9.56 Close-up view of the temporomandibular joint (Parma projection). FOD: focus-to-object distance.



Fig. 9.57 Close-up view of the temporomandibular joint.

radiograph is only capable of depicting a few structures optimally.

In many cases, the characteristic image features cannot be adequately visualized on radiographic images that only show a single plane. Even if intraoral radiographs could reproduce the finest anatomical structures, it would not be possible to display a tooth in its entirety. Supplementary special intraoral radiographic projections (e.g., mesial and distal eccentric projections) can sometimes reveal previously unrecognizable structures without superimposition, but the diagnostic quality is not satisfactory.

The easiest way to display certain areas without superimposition is to blur out structures above and below the plane of interest. This is done by changing the angle of head position as needed, to visualize an isolated aspect of the mandible or midface, for example, by blurring out the temporal bones from the maxillary sinus (□ Fig. 9.55).

Close-up imaging is another way to image regions without superimposition. In X-ray imaging, this is done using a short cone and is based on the principle of geometric unsharpness (□ Fig. 9.56 and □ Fig. 9.57).

The introduction of tomography by Bocage in 1922 provided a new and better method.

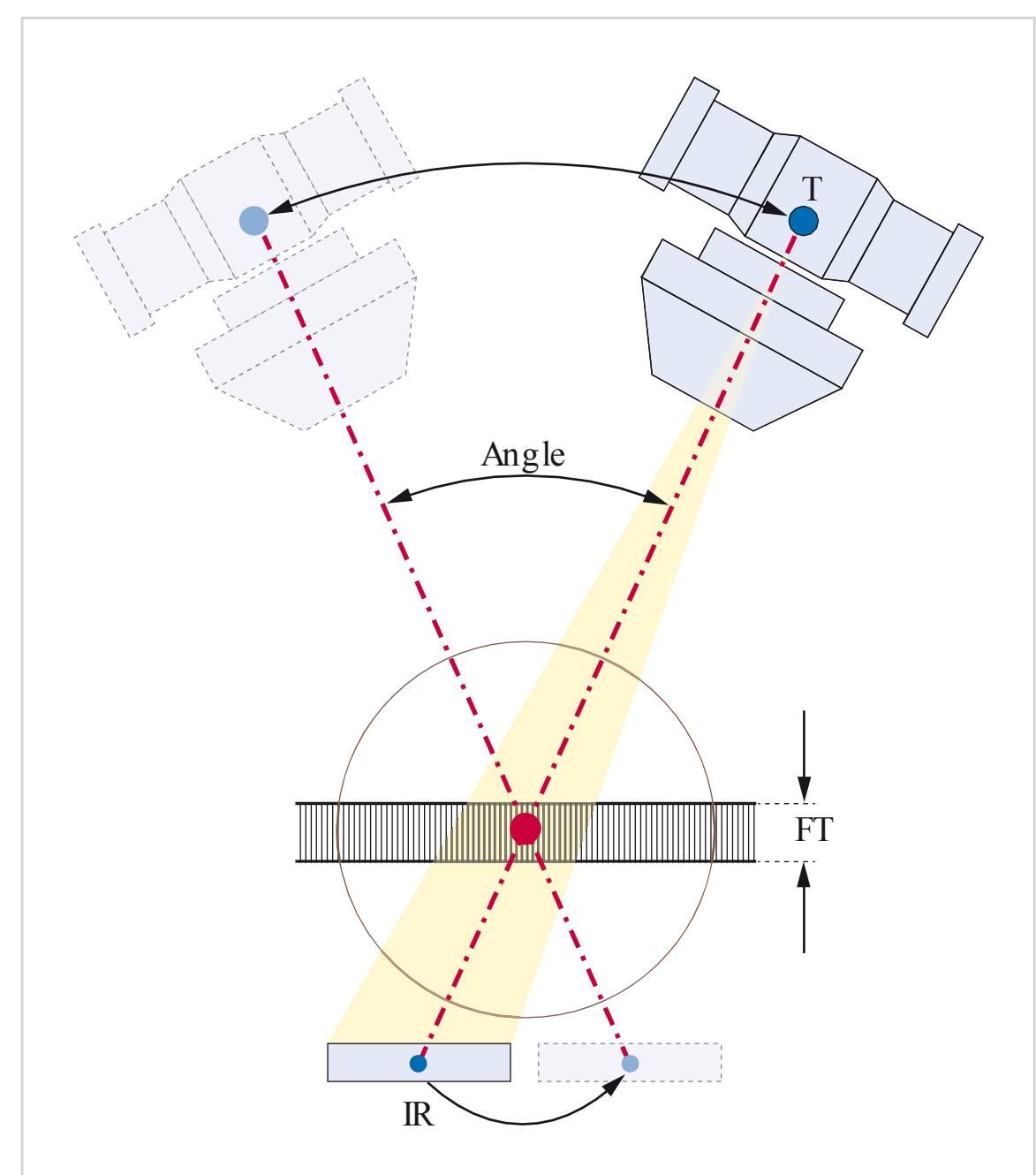


Fig. 9.58 Basic principle of tomography (schematic): structures in the selected slice, or focal trough (FT), of the object appear in sharp focus while those outside the focal trough appear blurred. The rotational movements of the tubehead (T) and image receptor (IR) are synchronized. Blurring is lowest at the rotation center (red dot). The plane of the rotation center is the in-focus slice. The larger the angle of rotation, the thinner the slice.

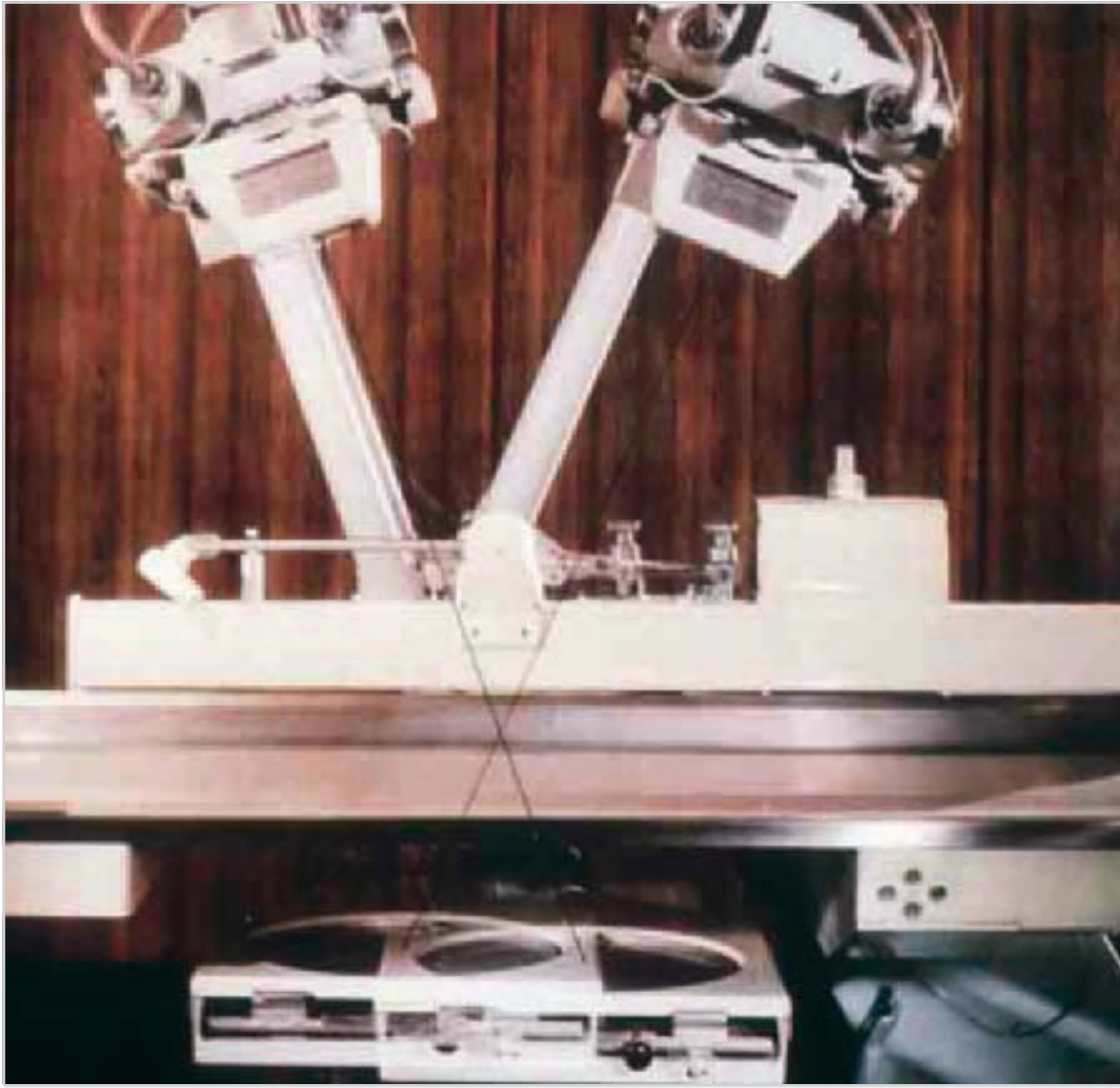


Fig. 9.59 Polytomes in movement.

In principle, conventional tomography consists of three components—the X-ray tubehead (T), image receptor (IR), and object (O), two of which are mobile. In most cases, the tubehead and image receptor are in motion, while the object remains stationary and motionless (□ Fig. 9.58).

Because the movement of the tubehead and image receptor around the rotation center is synchronized (□ Fig. 9.59), only those structures located within the plane of the center of rotation—that is, the image layer/focal trough—appear in sharp focus, while structures outside the focal trough are blurred. During and because of tubehead rotation, structures outside the focal trough are not projected on the same spot, but on different points across the film, and thus appear blurred on the image.

Conversely, all objects located within the focal trough are projected on exactly the same spot during the entire exposure cycle, and thus appear in sharp focus on the image (□ Fig. 9.58).

Tomographic systems may be classified according to the extent and type of blurring.

The extent of blurring is dependent on the angle of rotation (ϕ), which is determined as the points where tubehead movement begins and ends (□ Fig. 9.58). As the angle of rotation increases, the degree of blurring increases and the thickness of the image layer (focal trough) decreases.

The type of blurring is determined by the geometry of the movement of the X-ray source. The goal of tubehead movement and the resultant blurring is to make structures that lie outside the image layer (focal trough) so indistinct that they are no longer recognizable as structures, but only as homogeneous film blackening. This ensures that structures that are blurred out do not lead to radiographic misinterpretation.

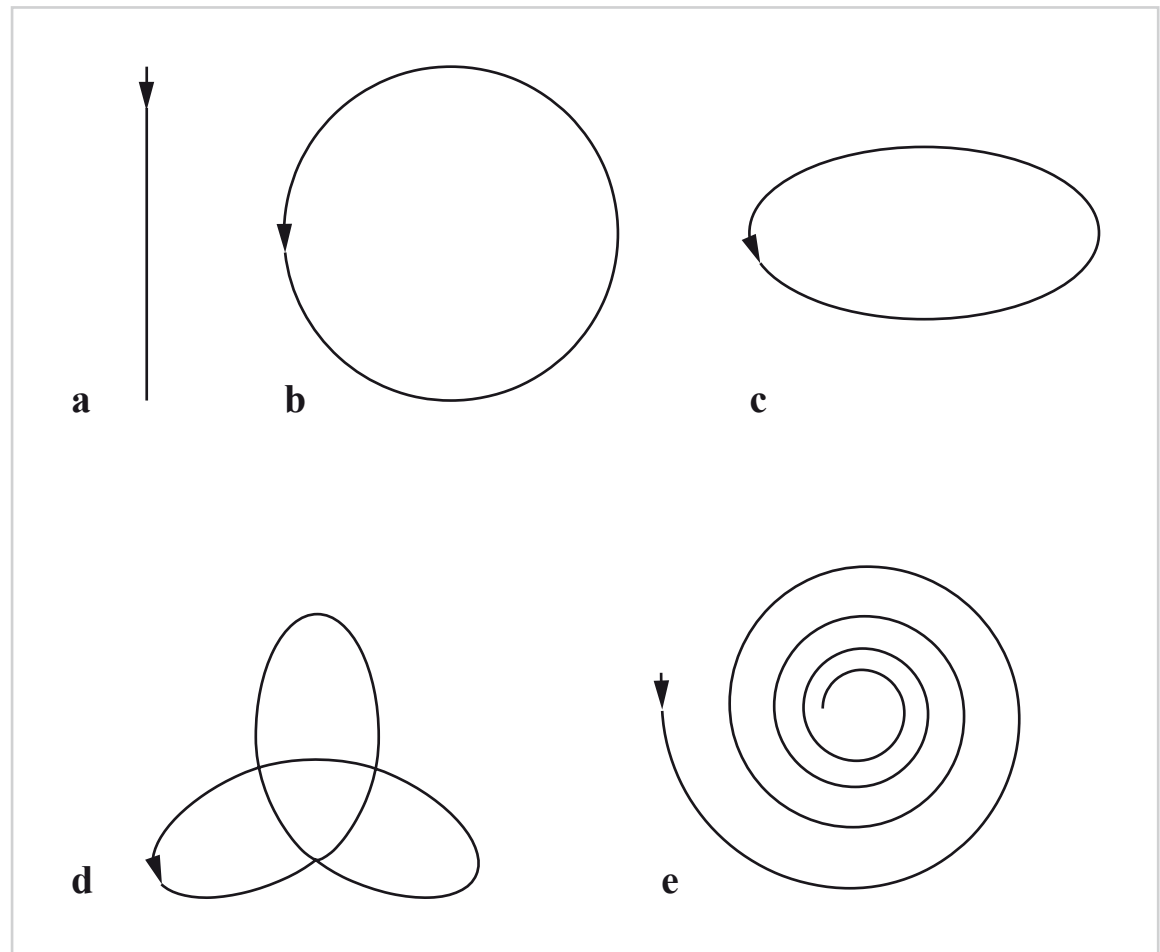


Fig. 9.60a–e Blurring patterns in conventional tomography.

- a** Linear.
- b** Circular.
- c** Elliptical.
- d** Hypocycloidal.
- e** Spiral.



Fig. 9.61 Tomographic image of the maxillary sinuses.

One-dimensional (linear) and multi-dimensional or planar (circular, spiral, and hypocycloidal) blurring movements are well known (□ Fig. 9.60). Generally speaking, one can say that the multi-dimensional movements blur better and thus are also better for the diagnostic evaluation of bony structures of the facial skeleton (□ Fig. 9.61). Linear blurring usually causes blurring shadows that frequently cannot be distinguished from pathological processes.

The large traditional tomographic imaging systems had a blurring angle of almost 50 degrees and a spiral or hypocycloidal blurring motion, resulting in the generation of images with slice thicknesses of ~1 mm without interference shadows. The only disadvantage of these images was their relatively low contrast.

9.3 Panoramic Tomography

The origins and course of development of panoramic tomography are completely different from those of the conventional tomography technique as conceived by Bocage.

Because of the complex anatomy of the dental arches and facial skeleton, it is difficult to depict these structures in their entirety on a single radiograph. Most of these structures are circular, oval, or arcuate, and hardly any of their bony margins are situated at right angles to each other. To obtain diagnostically useful radiographs of the dentition, the teeth have to be visualized on individual intraoral radiographs. Diagnostic assessment of the entire facial skeleton by conventional radiography (e.g., by using radiographs of the maxillary region) is also difficult, owing to the round shape and close proximity of several relatively small and often duplicate structures (□ Fig. 9.62).

9.3.1 Panoramic Radiography with a Slit Collimator

These problems prompted several independent dental researchers to investigate the question of how to generate panoramic radiographs that provided scout images of the entire dentition or, better yet, of the entire facial skeleton. The basic idea was to develop a method of producing panoramic scout images that takes the round to oval structures of the facial skeleton into account while enabling simultaneous and complete reproduction of the teeth, jaws, temporomandibular joints, and basal maxillary sinuses.

The principles of panoramic radiography for dental applications were first described in a U.S. patent filed by A.F. Zulauf in 1922. Panoramic images were generated using long film which, similar to bitewing film, was placed in the patient's mouth to obtain separate exposures of the maxillary and mandibular arch. The key to success was the use of a very narrow vertical slit collimator (□ Fig. 9.63). This device made it possible to produce images of the maxillary and mandibular teeth in two separate exposure cycles.

Zulauf merely filed a patent for the principle of dental panoramic radiography in 1922, whereas Numata (1933) and Paatero (1946) were the first to actually build a machine capable of producing panoramic images using a slit collimator (see □ Fig. 1.6).

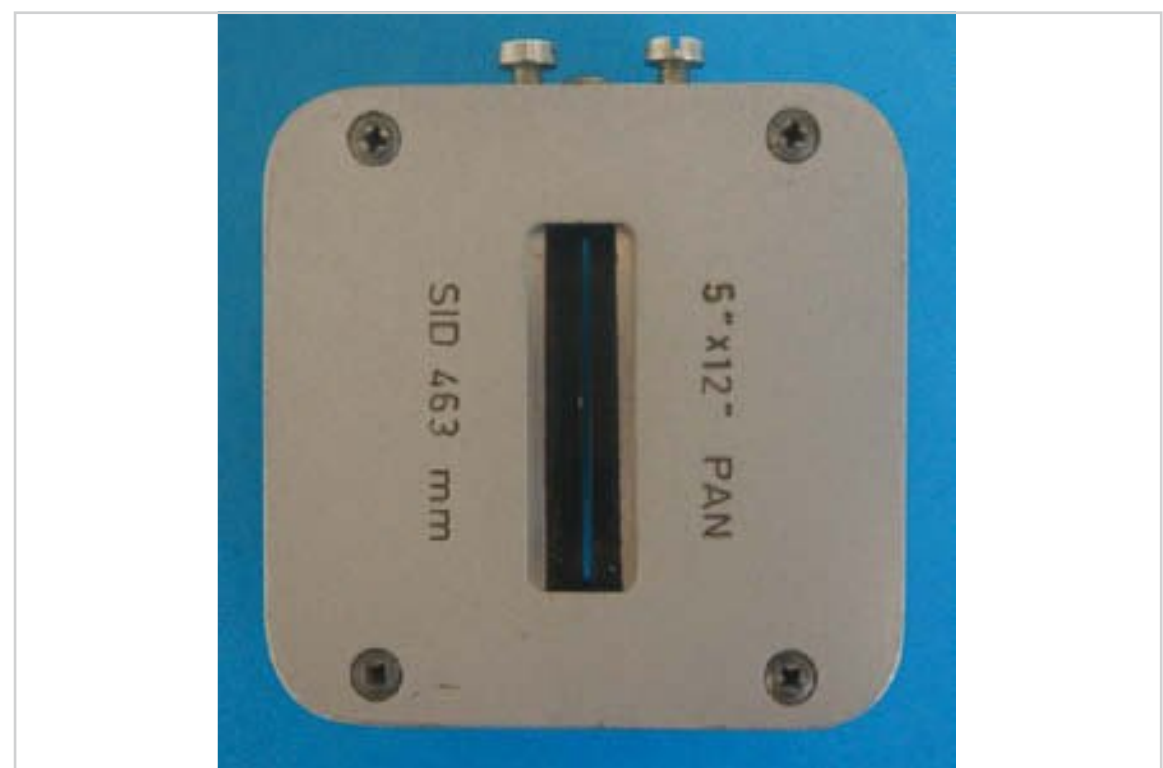


Fig. 9.63 Slit collimator.



Fig. 9.62 Panoramic photomontage according to Pasler.

While Zulauf, Paatero, and Numata focused on panoramic imaging of the teeth, the radiologist Heckmann developed a method for the production of panorama-like radiographs of superficial structures of the entire facial skeleton using extraoral film, which he introduced in 1939.

9.3.2 Panoramic Radiography with an Intraoral Source

Panoramic radiography with an internal source was conceived as a concept in which the anode is placed intraorally, in order to direct the beams of X-rays from inside to outside the mouth, to produce panoramic images of the teeth. This radiographic technique, which is now obsolete, employed a special rod-shaped X-ray tube that was placed in the patient's mouth (□ Fig. 9.64; see also □ Fig. 1.8).

The film was contained in a flexible cassette, which was positioned on the upper or lower arch, to allow separate exposures of the maxilla or mandible, depending on the direction of the anode.

The Frenchman Bouchacourt was the first to propose the concept of panoramic radiography of the jaw using a specially designed intraoral X-ray tube, in 1898. Patents filed by Koch and Sterzel in Germany in 1943 and by Ott in Switzerland in 1951 launched the development of this technology.

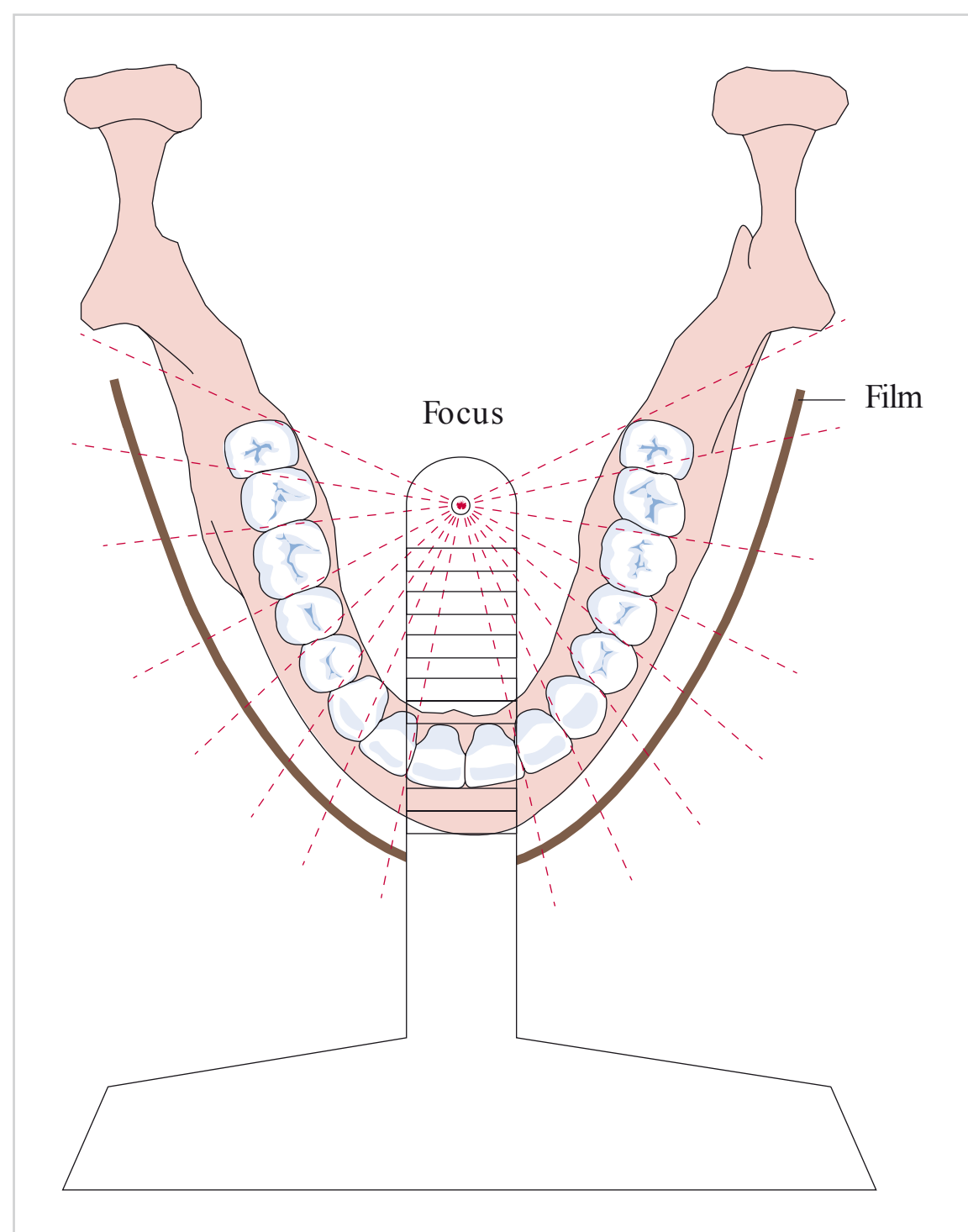


Fig. 9.64 Placement of the X-ray tube in panoramic radiography with an intraoral source.

In 1961, the first system for panoramic radiography with an intraoral source was introduced in practice. If used correctly, the machine produced satisfactory panoramic images of the maxillary and mandibular teeth, respectively. The best diagnostic quality was achieved in the anterior region because image magnification occurred toward the posterior region (see □ Fig. 1.9).

Panoramic radiography with an intraoral source has not been used for decades. Because this technology uses a very small FOD, it emits ionizing radiation above the level prescribed by regulation. Consequently, it is now classified as a prohibited radiation source.

9.3.3 Rotational Panoramic Radiography

The concept of panoramic imaging was a crucial step forward in dental radiology considering that, without this technology, only intraoral radiographs of the teeth and extraoral radiographs of parts of the mandible were available. It was not possible to produce diagnostic quality radiographs of the maxillary and mandibular arches and their associated structures until the advent of panoramic radiography with a rotating extraoral source of radiation.

Paatero introduced the basic concept of intraoral panoramic radiography in 1948. As long intraoral film proved to be very impractical, he experimented with extraoral film. This allowed him to produce panoramic images of the superficial layers of the midface that were very similar to those produced by Heckmann (□ Fig. 9.65).

Paatero made the next decisive step toward achieving tomographic images, by devising a system in which the patient and the film simultaneously moved on synchronized paths around a center of rotation, while the X-ray beam, which was narrowed to a blade by a vertical slit collimator, remained stationary (□ Fig. 9.63).

The narrow beam passed through the rotational axis and center of both the object and the film, which was attached to a round film-holder. If two points on the same radius move at the same velocity, they will always be at rest rela-

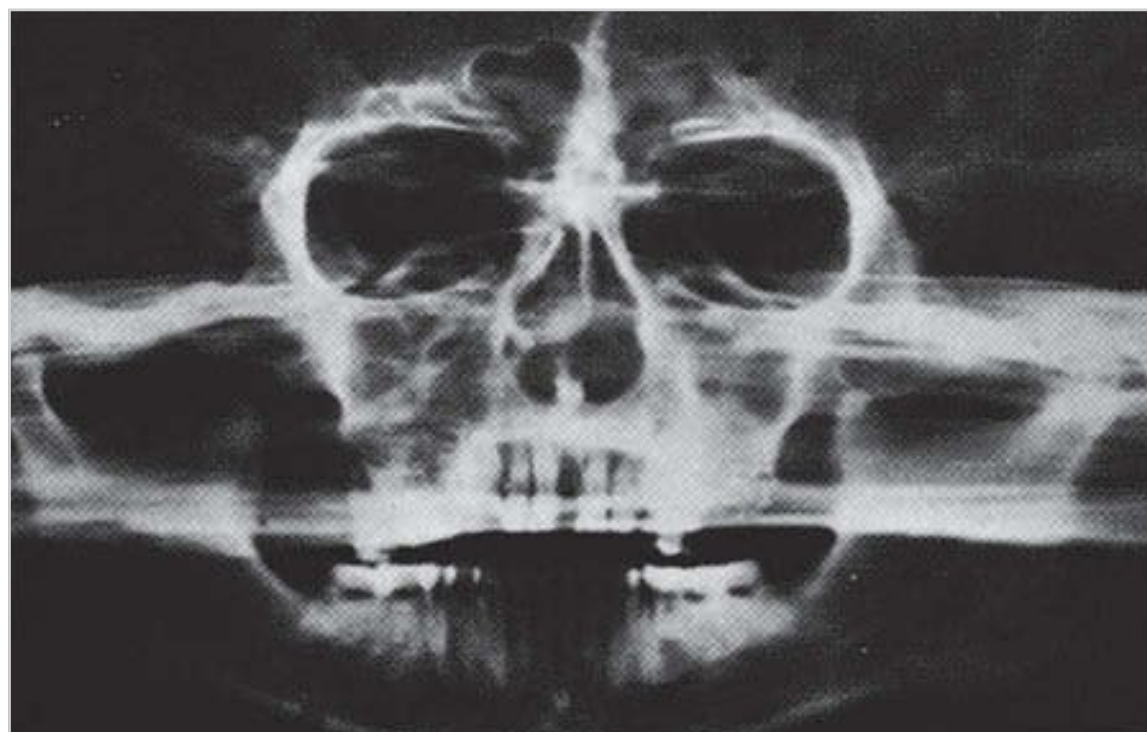


Fig. 9.65 Panoramic radiograph of the image without the tomographic effect.

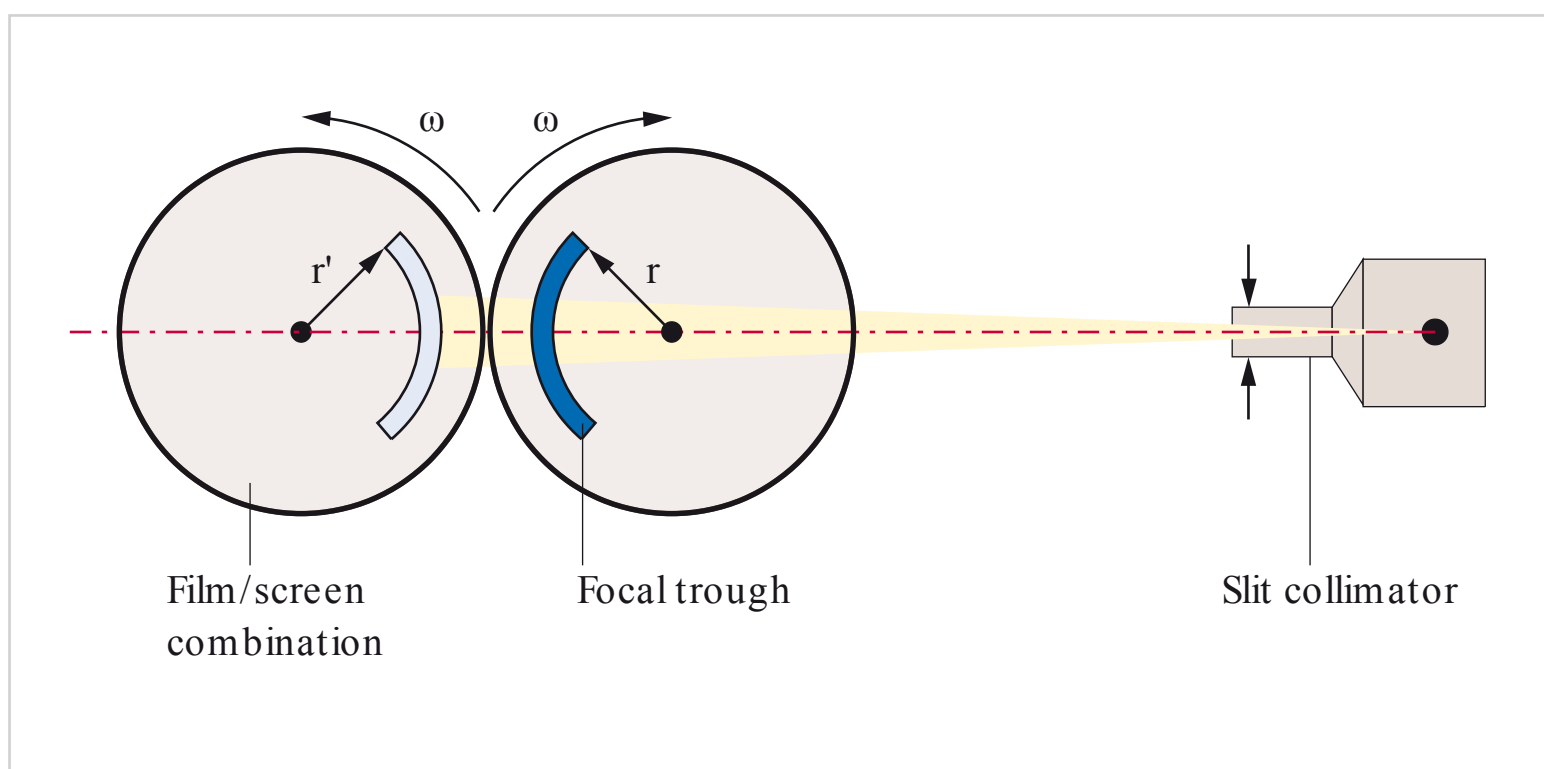


Fig. 9.66 Principle of rotational panoramic radiography (see text for explanation). ω : angular velocity; r : radius.

tive to each other. If one of the points is part of the object of interest and the other is part of the film, then that part of the object will always appear in sharp focus on the film.

This technique was further refined and, in 1955, a pantomograph built in Helsinki was put into operation in London.

Principle of Rotational Panoramic Radiography

The principle of rotational panoramic radiography can be explained as follows: two adjacent rotating disks with the same radius (r) are rotating in opposite directions at the same angular velocity (ω) as the X-ray beam passes through their centers of rotation (□ Fig. 9.66). The object of interest (in this case, the tooth) moves on radius r of the first disk, while the film moves on radius r' of the second disk. Because the radii are equal ($r'=r$), the object and the film move at the same velocity on their respective disks. If the central ray is limited to a very narrow (1 mm) vertical beam by a narrow slit collimator, and the object and the film rotate past the slit at the same time and are thus irradiated simultaneously, then the object will be displayed sharply on the film. This is possible because the radii of the two disks are equal and because the two disks rotate at the same velocity; consequently, the object and the film are at rest relative to each other.

If it is possible to keep the radius of the object and the film equal throughout the entire exposure cycle, it is also possible to display arbitrarily shaped objects (such as the dental arches) in sharp focus on dental film, or any other type of image receiver.

Adapting the Focal Trough to the Dental Arch

If the dental arch were circular, then it would be no major problem to obtain sharp images of the teeth in the focal trough (image layer). However, since the two dental arches are horseshoe shaped, the radius of the target structures changes during the exposure cycle. Circular movement of the film is not appropriate for producing sharp

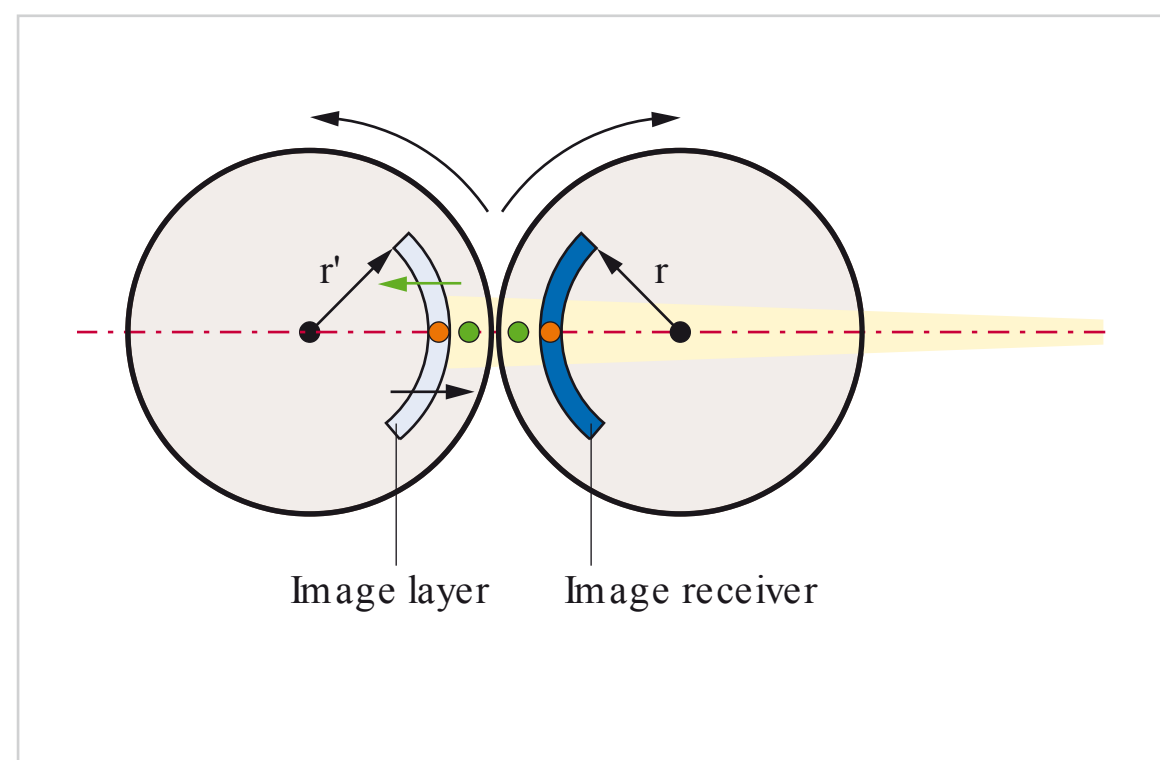


Fig. 9.67 Adjusting the focal trough to accommodate the dental arch (schematic). r : radius.

images of the maxillary and mandibular arches in a circular image layer (focal trough).

Consequently, the position of the film must be adapted to the shape of the dental arch.

Because it is difficult to change the film radius by mechanical means, the panoramic film velocity is continuously increased and decreased during the exposure cycle, to accordingly increase or decrease the width of the image layer (focal trough) to accommodate the shape of the dental arch. Any arch can be centered within the focal trough by this method (□ Fig. 9.67 and □ Fig. 9.68).

The source–patient–film configuration of modern equipment has been modified, such that the patient remains stationary while the tubehead and film move on synchronized paths around the patient's head.

Orthopantomography: Orthogonal Imaging of the Teeth

The first step toward a panoramic imaging technique that provided diagnostically relevant information was the development of a means of positioning the teeth precisely in the focal trough. The original panoramic system could not achieve orthogonal imaging of all teeth because it only had one rotating disk. Only the anterior crown region was shown without superimposition.

The next task was therefore to work out how to project the beam in such a way as to irradiate both the anterior and posterior region as orthogonally as possible. The solution was to add more rotating disks to the panoramic machine.

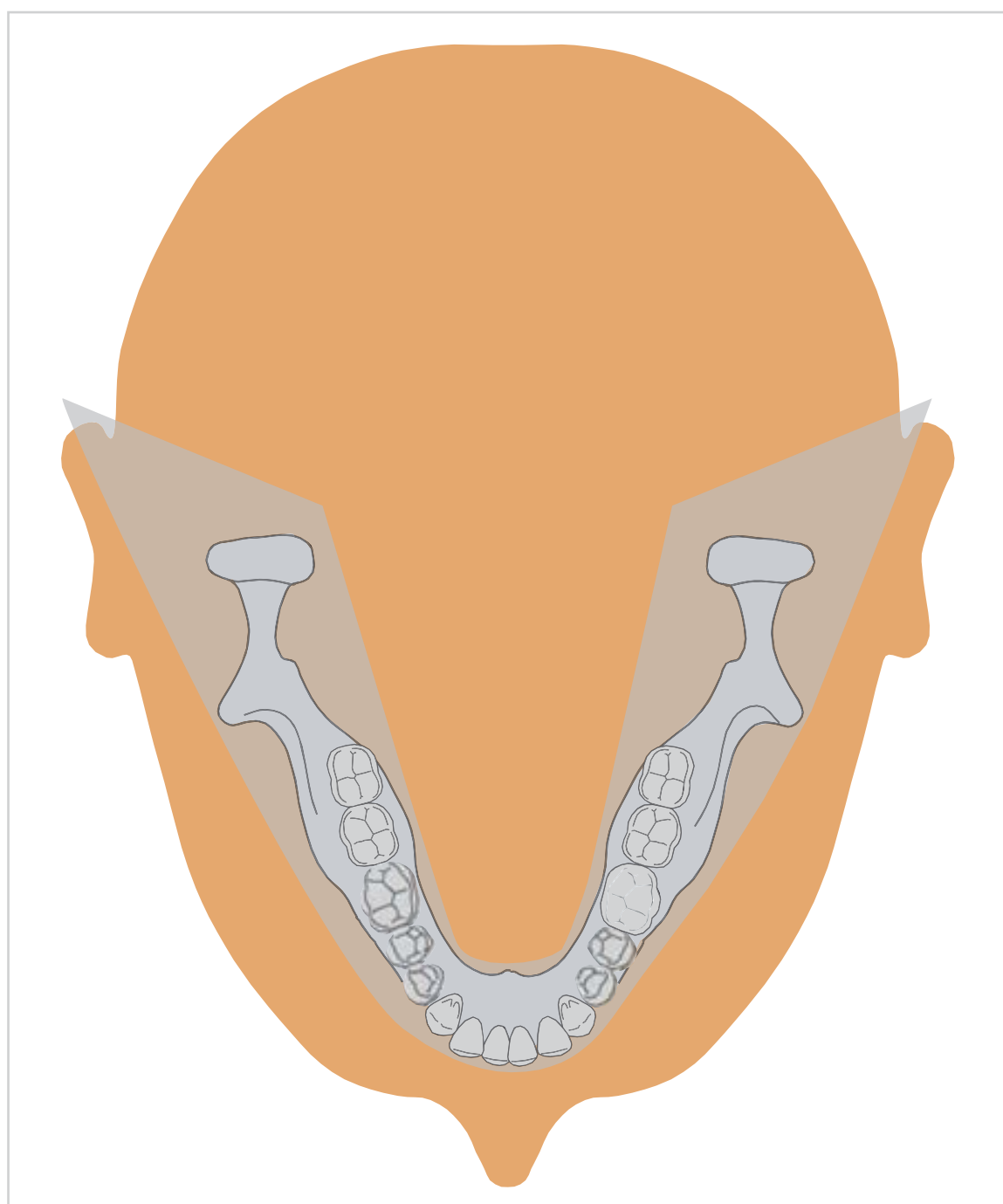


Fig. 9.68 Focal trough adjusted to accommodate the dental arch.

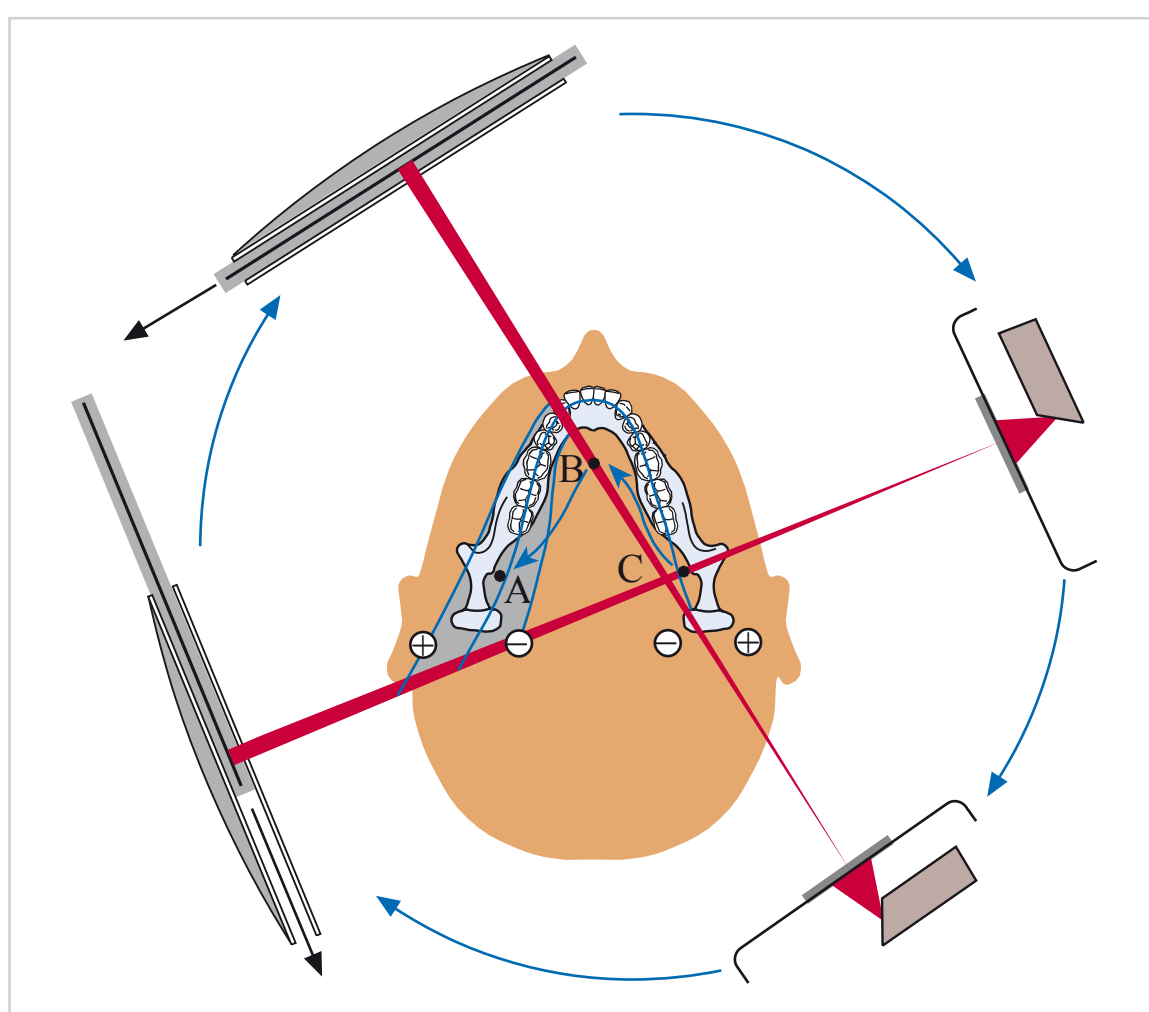


Fig. 9.69 Direction of incidence during the rotation cycle of rotational panoramic radiography. The X-ray tube and film rotate clockwise around rotation centers A, B, and C, around the patient's head. Because orthogonal projection geometry must be ensured, a separate rotation center (effective focus of projection of the narrow beam) is needed for each segment of the arch. (From: Pasler FA, Visser H. Zahnmedizinische Radiologie. 2nd ed. Stuttgart: Thieme; 2000. Farbatlant der Zahnmedizin; Band 5.)

As in intraoral radiography, the correct angle of incidence for each region of interest must be ensured for the production of superimposition-free images in rotational panoramic radiography (□ Fig. 9.69).

Since orthogonal imaging of the molars cannot be achieved from the anterior aspect, additional rotation centers were needed for rotational panoramic radiography. These centers of rotation must be positioned such that parallel rays strike the posterior teeth orthogonally as the tubehead revolves around the patient's head. Once a system with two additional rotation centers for the posterior region was built, it finally became possible to achieve orthogonal panoramic imaging of the molars and premolars. This feat was accomplished by Paatero, who presented a small prototype of a panoramic machine called the orthopantomograph, in 1957.

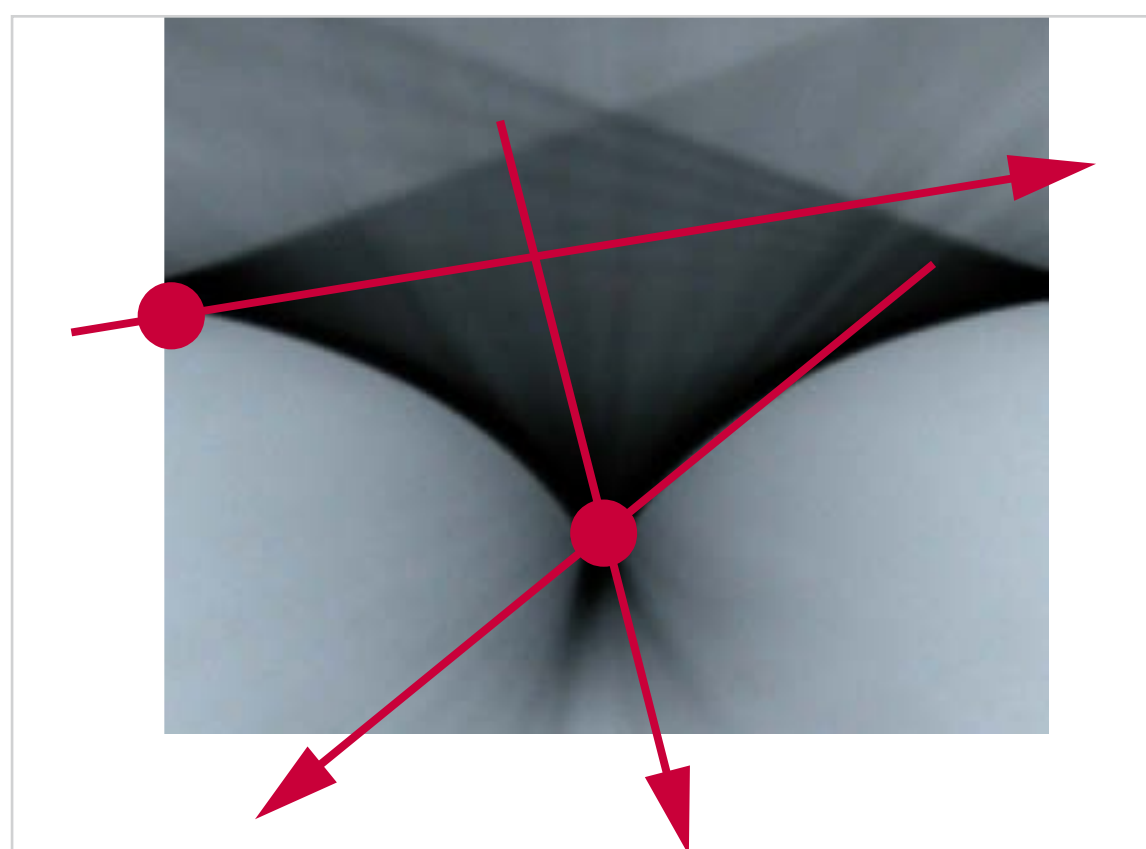


Fig. 9.70 If there are at least three rotation centers (ideally, “flying” rotation centers that continuously change positions during the rotation cycle), the narrow beam will strike the image receptor and all teeth in the entire arch orthogonally.

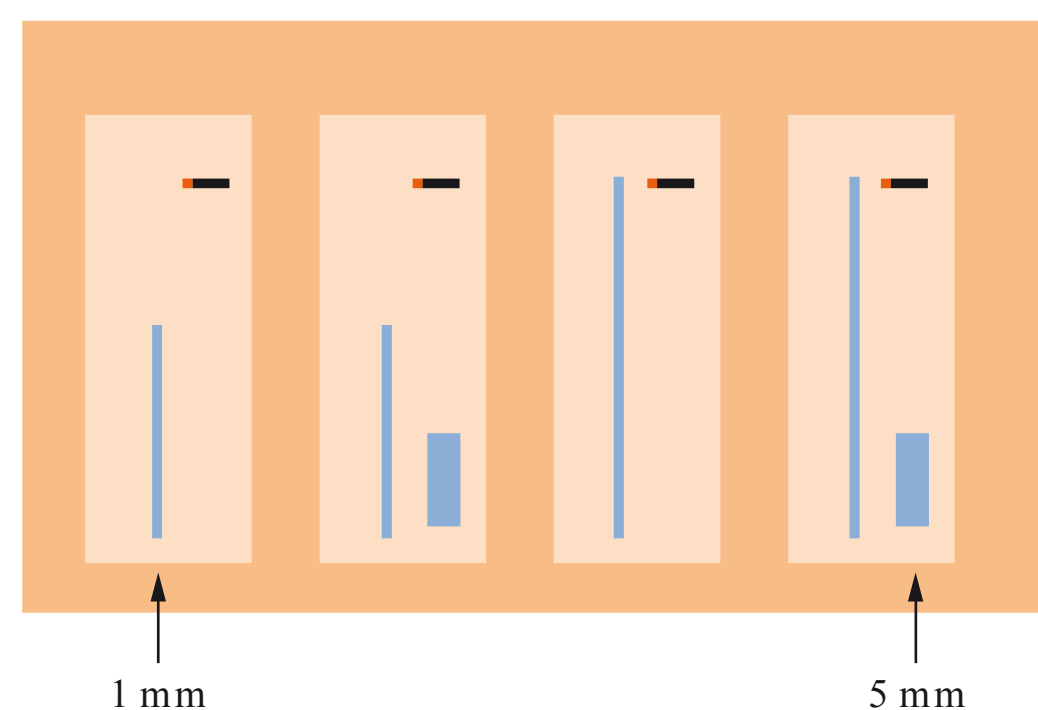


Fig. 9.71 Slit collimator widths available for various view options (schematic representation). Currently, only a slit width of 1 mm tends to be used. A wide slit width of 5 mm is needed for thin layers. CEPH: cephalometric; CS: cross-sectional; PAN: panoramic.

To accomplish the goal of orthogonal imaging of all of the teeth, the original single-disk pantomograph was modified to accommodate three rotating disks (□ Fig. 9.70).

The development was completed in 1959 and the first Orthopantomograph became commercially available for use in dental practice in 1961.

Image Layer Thickness and Blurring Mechanism

In contrast to conventional tomography, there is no tomographic angle in rotational panoramic radiography. The slit collimator assumes the role of the tomographic angle. Most slit collimators used in panoramic imaging are 1 mm in width. Slit collimators with a wider aperture (5 mm) can be used for special programs.

As beam width is proportional to the tomographic angle, the use of a narrow-slit collimator is associated with a small tomographic angle and thus with low blurring. Therefore, the image layers used in rotational panoramic radiography are also relatively thick (10–25 mm). A slit collimator width of 1 mm corresponds to a tomographic angle of ~10 degrees.

Zonography is a tomographic technique using a narrow exposure angle of less than 10 degrees.

Under favorable anatomical conditions, a collimator width of 5 mm has an effect similar to that of a tomographic angle of 15 to 20 degrees and an image layer thickness of 1 to 2 mm (□ Fig. 9.71).

The projection radius, defined as the distance between the rotation center and the center of the image layer, is the second factor that influences the thickness of the image layer. The rotation center constantly changes position during the exposure cycle, because the projection direction constantly changes to maintain orthogonal projection geometry. As the moving rotation center travels a predetermined path from the posterior to the anterior region and back, the projection radius, and thus the image layer thickness, also changes constantly. The image layer is narrower in the anterior region and wider in the posterior region (□ Fig. 9.72):

- 10 mm in the anterior region (because the radius is smaller)
- 20 to 30 mm in the posterior region (because the radius is larger).

Characteristics of Imaging Geometry

Two different types of projections are used in rotational panoramic radiography: projection in the vertical plane and projection in the horizontal plane.

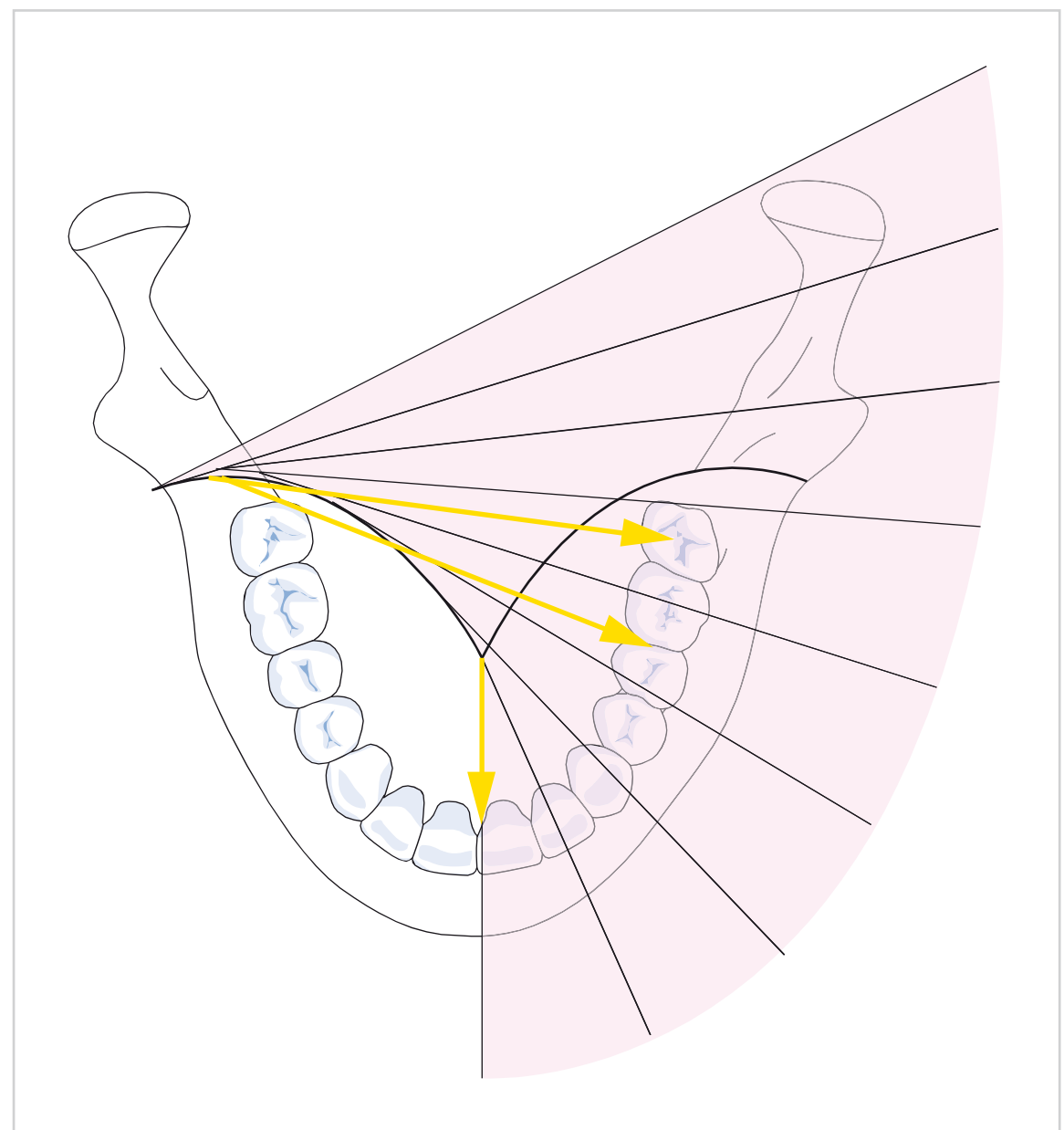


Fig. 9.72 Unlike conventional tomography, the slice thickness of rotational panoramic radiography is not determined by the tomographic angle, but rather by the radius and the width of the slit collimator (see □ Fig. 9.71). The radius (arrow) is the distance from the rotation center (effective focus of projection) to the image layer (focal trough).

Projection in the Vertical Plane

As the tubehead with the vertical narrow X-ray beam revolves in linear motion around an imaginary rotation center located within the mouth, the position of the rotation center changes constantly during the rotation cycle.

The narrow beam acts like the central projection in intraoral radiography. The beam path is not purely horizontal, but moves inferior to superior at a projection angle of –4 to –7 degrees (□ Fig. 9.73).

Projection in the Horizontal Plane

All of the X-rays pass through the respective centers of rotation throughout the exposure cycle (see □ Fig. 9.70). The X-rays appear to diverge from the rotation centers. Therefore, the rotation centers function as the effective focus of projection (□ Fig. 9.74).

As the tubehead rotates around the patient's head, the X-rays diverging from the rotation centers have effects on the horizontal dimension. Each rotation center serves as an effective focus of projection for the horizontal dimension of the image. The rotation center has a very large and usually negative influence on panoramic image formation. Incorrect positioning may result in geometric unsharpness and distortion in the horizontal dimension of all parts of the jaws, if the distance between the rotation center and the jaw is too small.

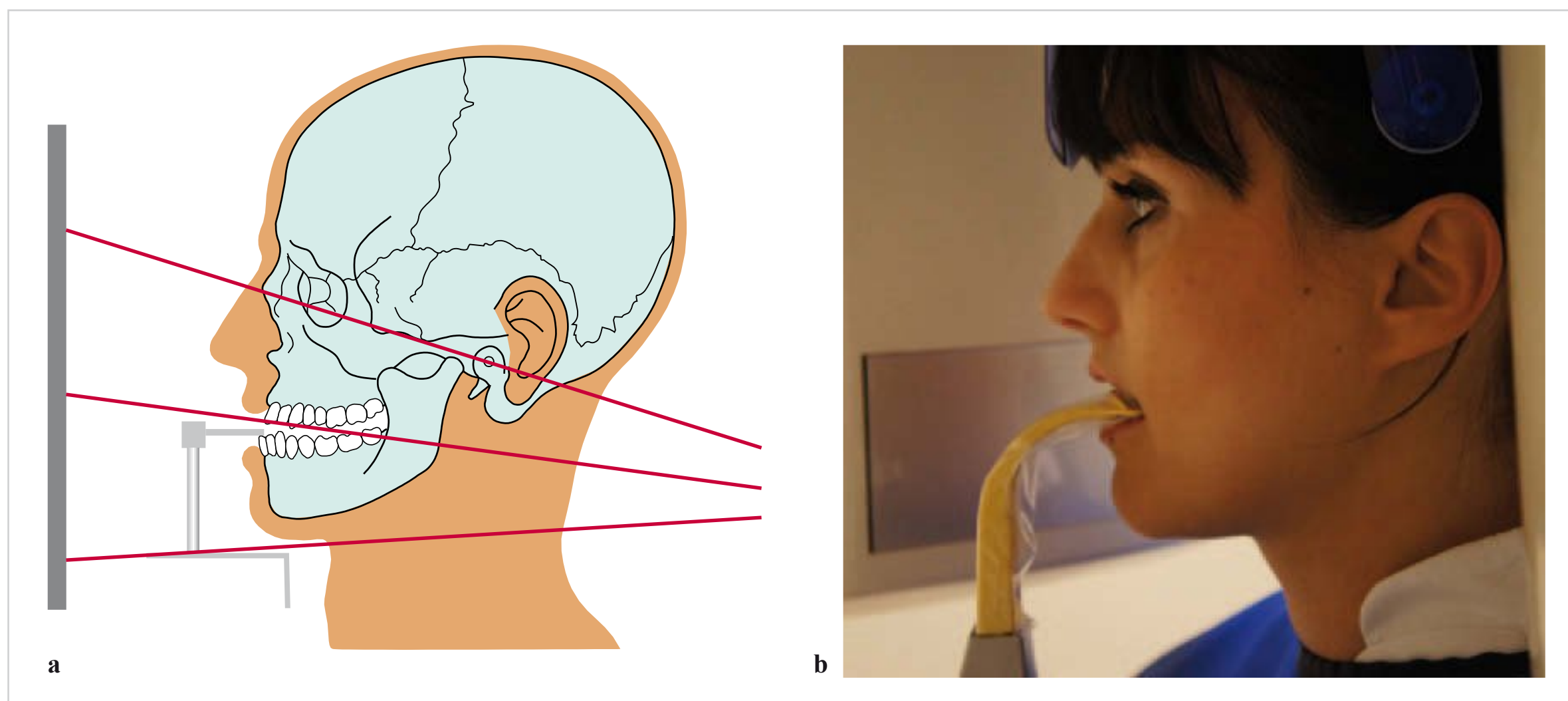


Fig. 9.73 a, b Projection geometry and head positioning in panoramic radiography.

a Oblique angle of incidence.

b Correct head position.

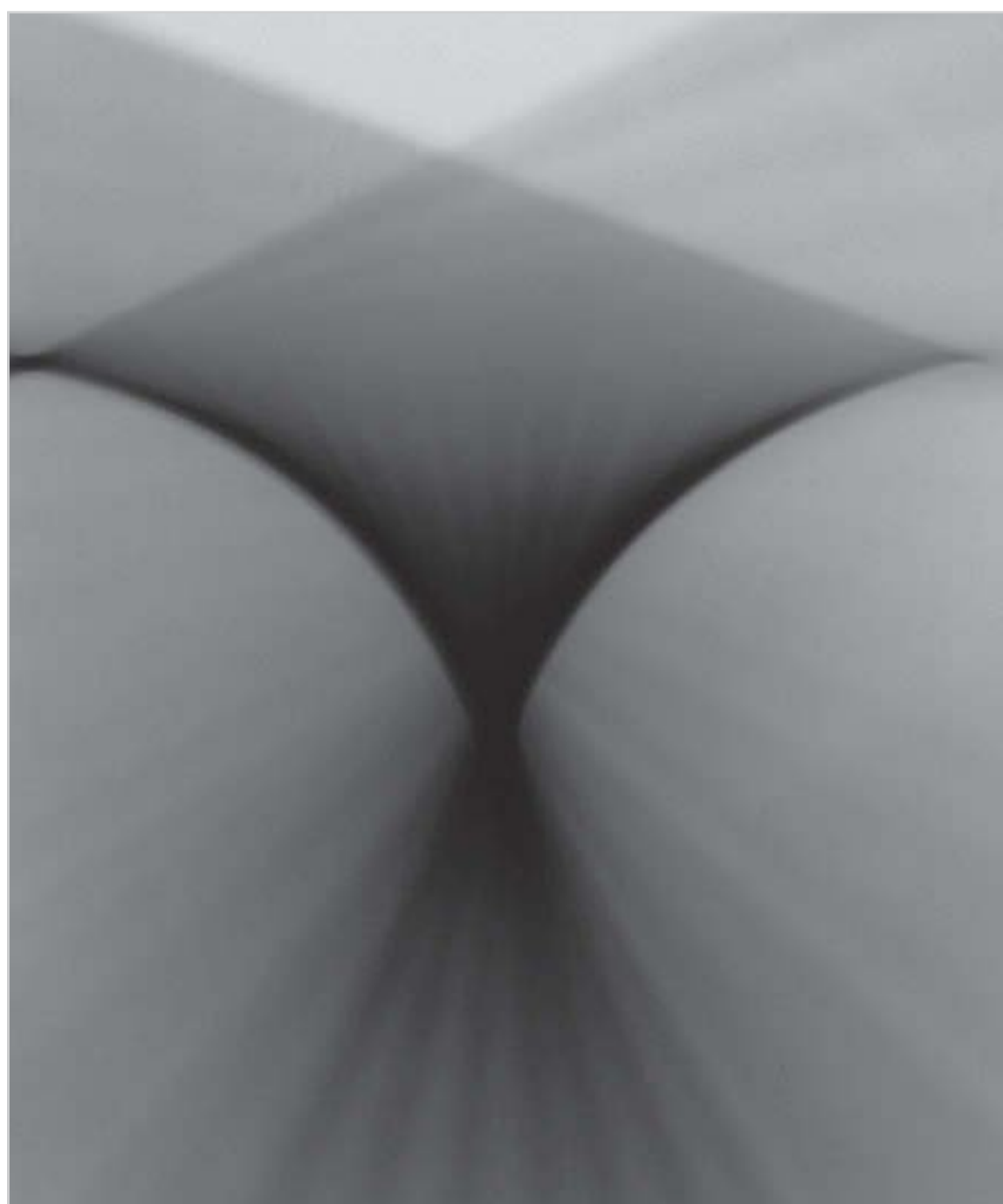


Fig. 9.74 The rotation centers serve as effective foci of projection.

The principle of rotational panoramic radiography will only work if:

- The shape of the focal trough is optimally adjusted to that of the dental arch
- The rotation centers are adjusted as individually as possible
- The patient is optimally positioned in the system (□ Fig. 9.75).



Fig. 9.75 Each panoramic unit has positioning guides for correct patient positioning.

Advances in Rotational Panoramic Radiography

With the advent of orthopantomography, an imaging system was introduced that, by virtue of its panoramic function, has become the most important radiographic technique in dental, oral, and maxillofacial radiology.

An orthopantomogram can serve as the basis of further examinations, such as individual intraoral radiographs for simple clinical questions, or CBCT for complex questions.

After recognizing the potential of rotational panoramic radiography, researchers started to develop additional programs for these machines in 1975. In the course of these developments, panoramic machines that could image not only

the maxillary and mandibular arches and their supporting structures, but also many other parts of the facial skeleton, were placed on the market (□ Fig. 9.76; see also □ Fig. 1.10).

The Scanora system, for example, can also produce very impressive panoramic images. This multimodal tomographic system offers a combination of panoramic radiography, conventional tomography, and spiral tomography.

The Scanora was the first system capable of generating cross-sectional tomographic images (□ Fig. 9.77). This

was a crucial step toward three-dimensional imaging, as is now possible with CBCT, the successor to the conventional tomography in dental radiography.

Modern panoramic machines with the corresponding technical capabilities offer a wide range of special programs with different functions.

Special Programs

In partial-arch projections using special programs with one rotating disk or with the standard panoramic program, the following structures are of particular practical interest:

- Partial-arch segments
- Anterior tooth region
- Alveolar crest and interproximal margins
- Midface
- Temporomandibular joints.

Viewing Partial-arch Segments

When investigating specific questions, it would seem logical to investigate not always the full arch, but only the current region of interest. Partial-arch panoramic radi-

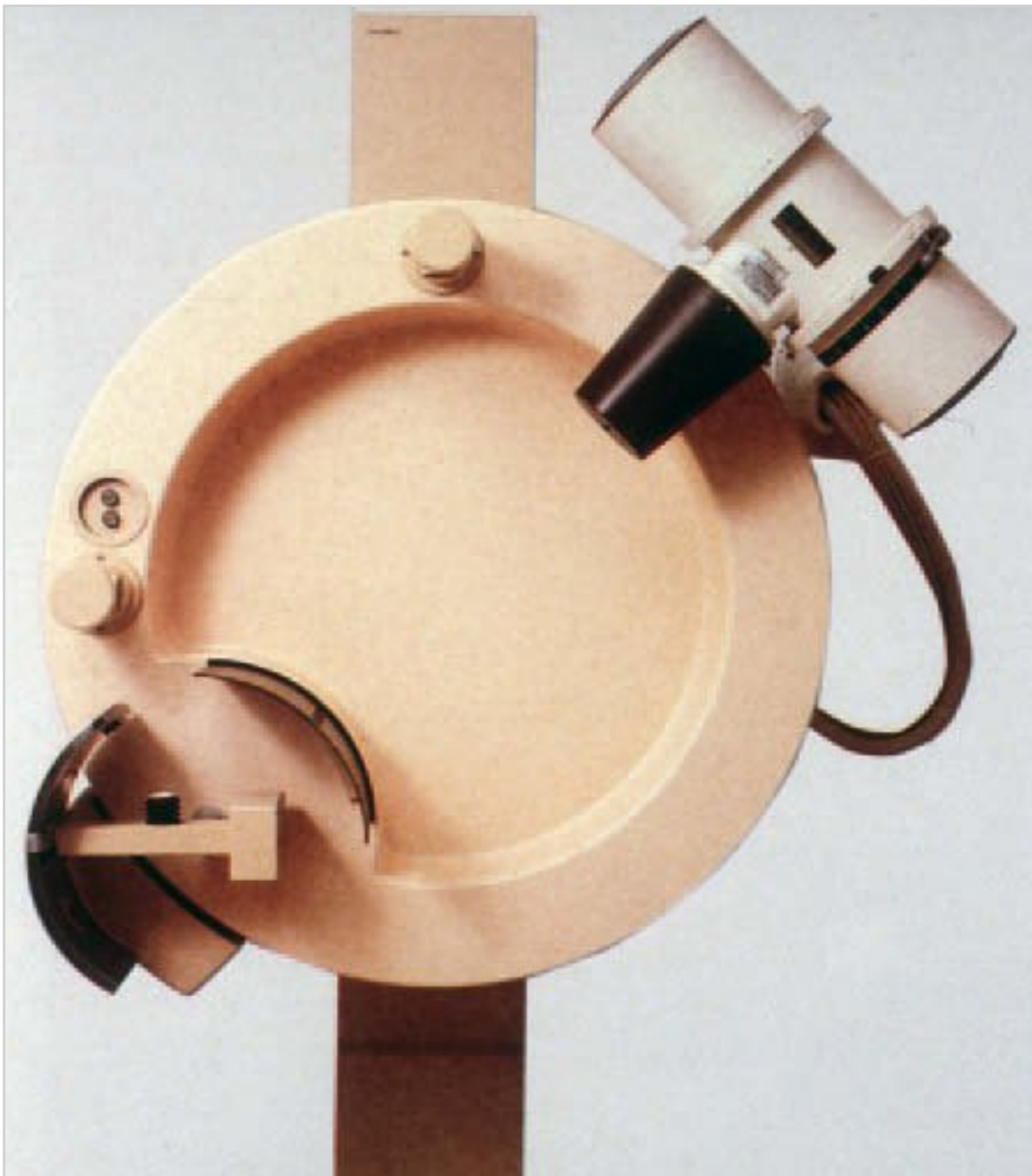


Fig. 9.76 The Zonarc rotational panoramic radiography machine for recumbent patients has several special programs.



Fig. 9.77 This implant on this cross-sectional tomographic image is sharply defined.



Fig. 9.78 Partial-arch view of the left maxilla.

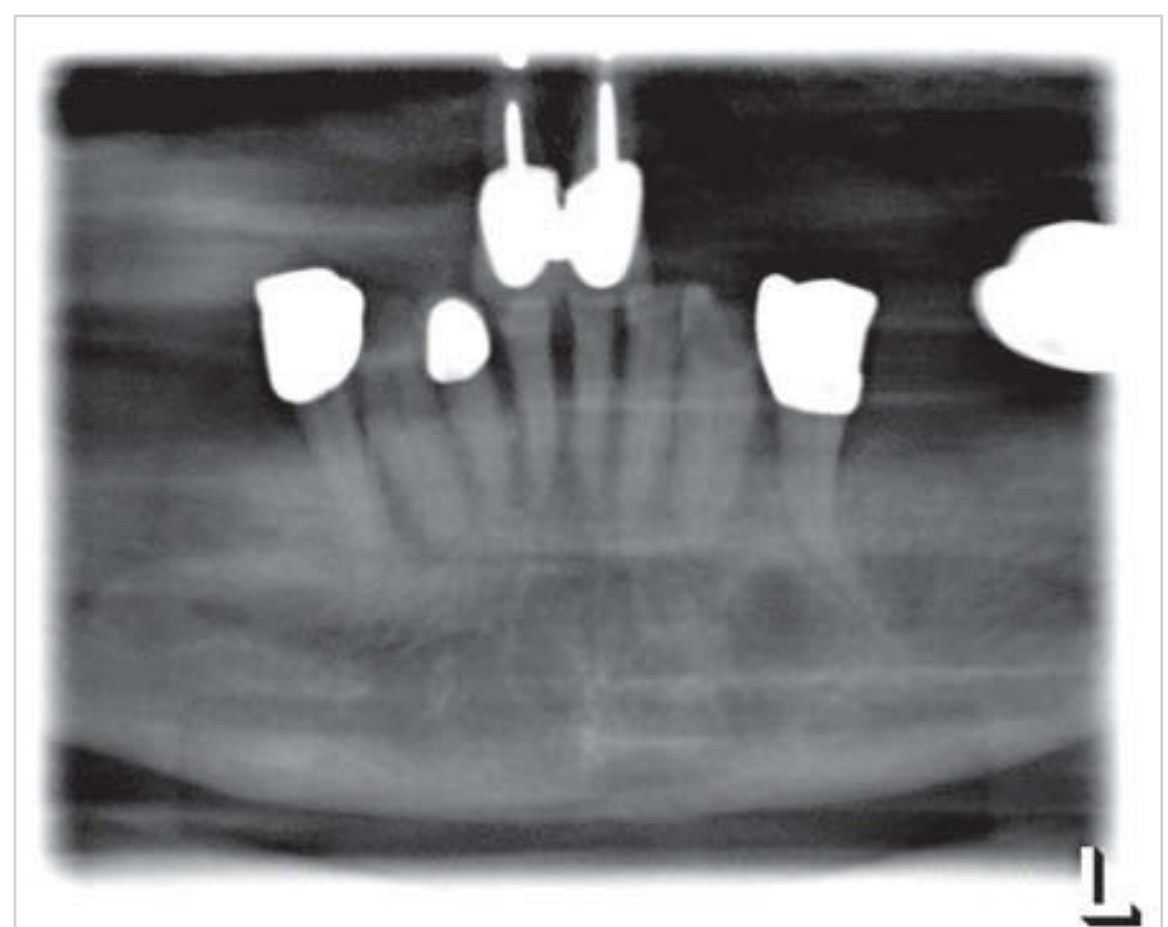


Fig. 9.79 Partial-arch view of the mandible.

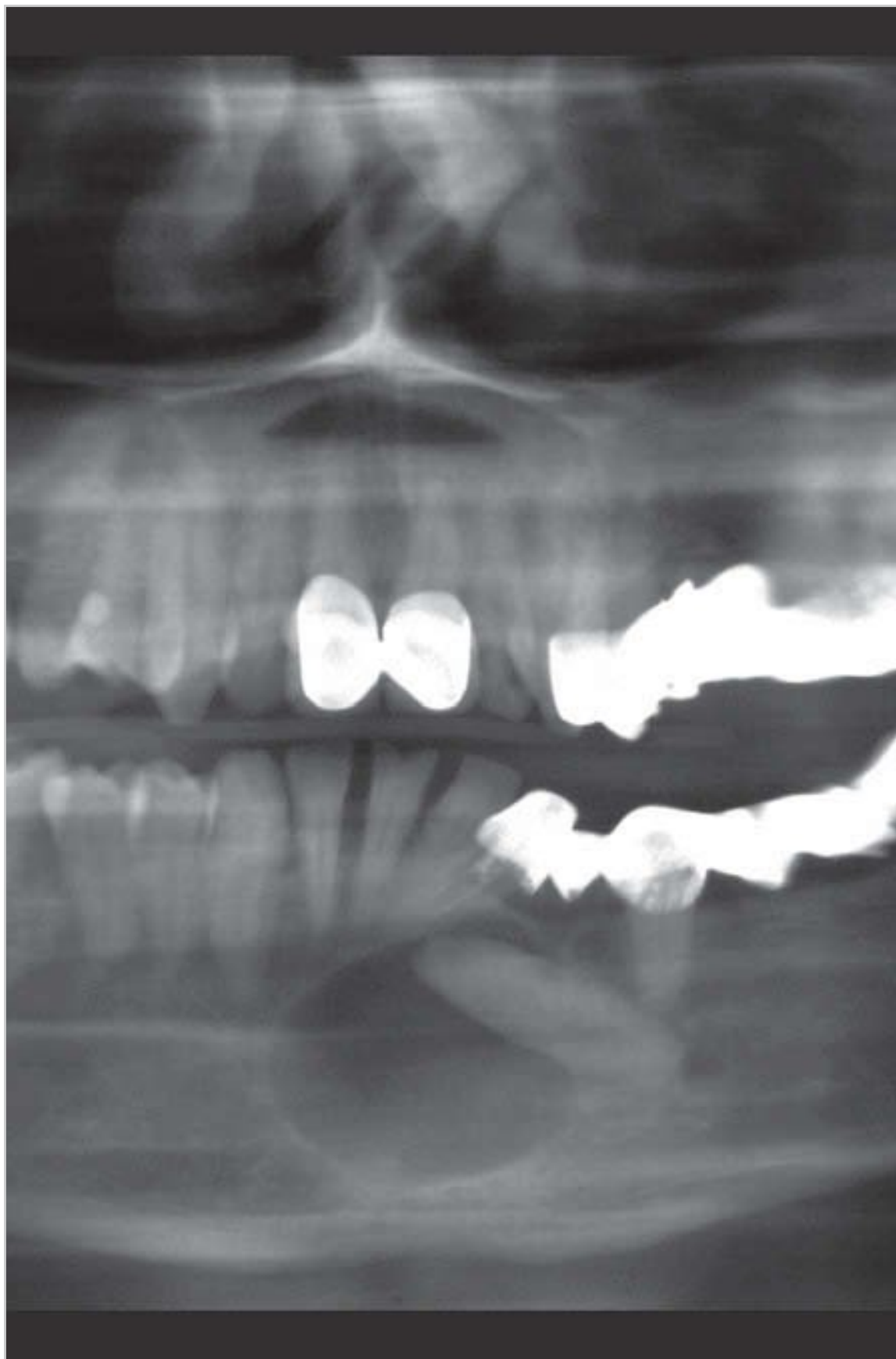


Fig. 9.80 Owing to the larger radius and adjusted movement path, the anterior program depicts the anterior region with much less geometric unsharpness.

ography allows dose reduction relative to full-arch panoramic radiography, but visualizes a larger area than an intraoral radiograph (□ Fig. 9.78 and □ Fig. 9.79).

Viewing the Anterior Tooth Region

Special rules apply to anterior panoramic radiography. The image quality of anterior panoramic radiographs can be enhanced by using a special anterior program with a thicker image layer. Anterior programs greatly reduce spinal shadows and geometric unsharpness on anterior panoramic radiographs (□ Fig. 9.80).

Alveolar Crest and Interproximal (Bitewing) Views

Through advances in digital technology, modern panoramic machines now have special programs for areas previously reserved for intraoral bitewing radiographs.

Because the projection angle remains constant, modern panoramic machines can generate uniform and anatomically correct panoramic views of the alveolar crest.

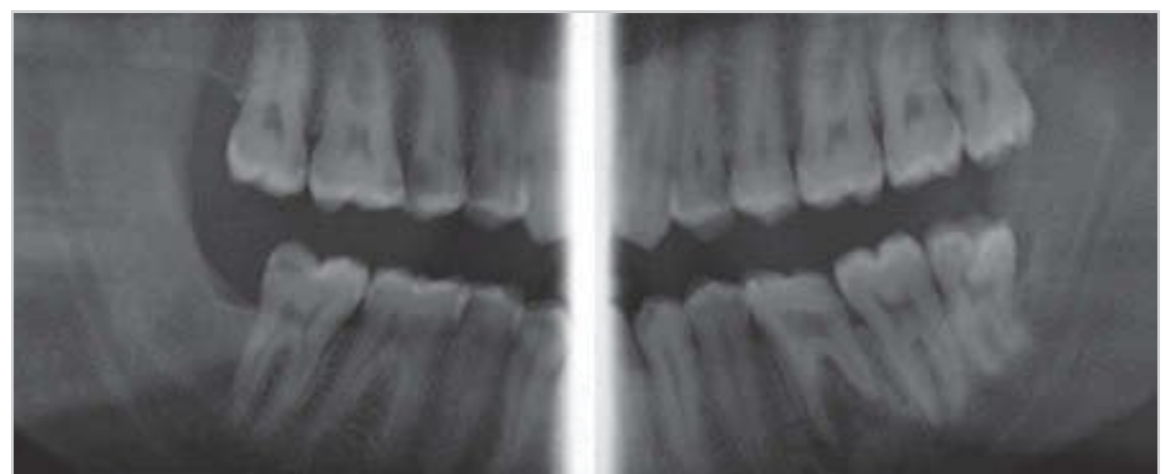


Fig. 9.81 Panoramic radiography: bitewing program.

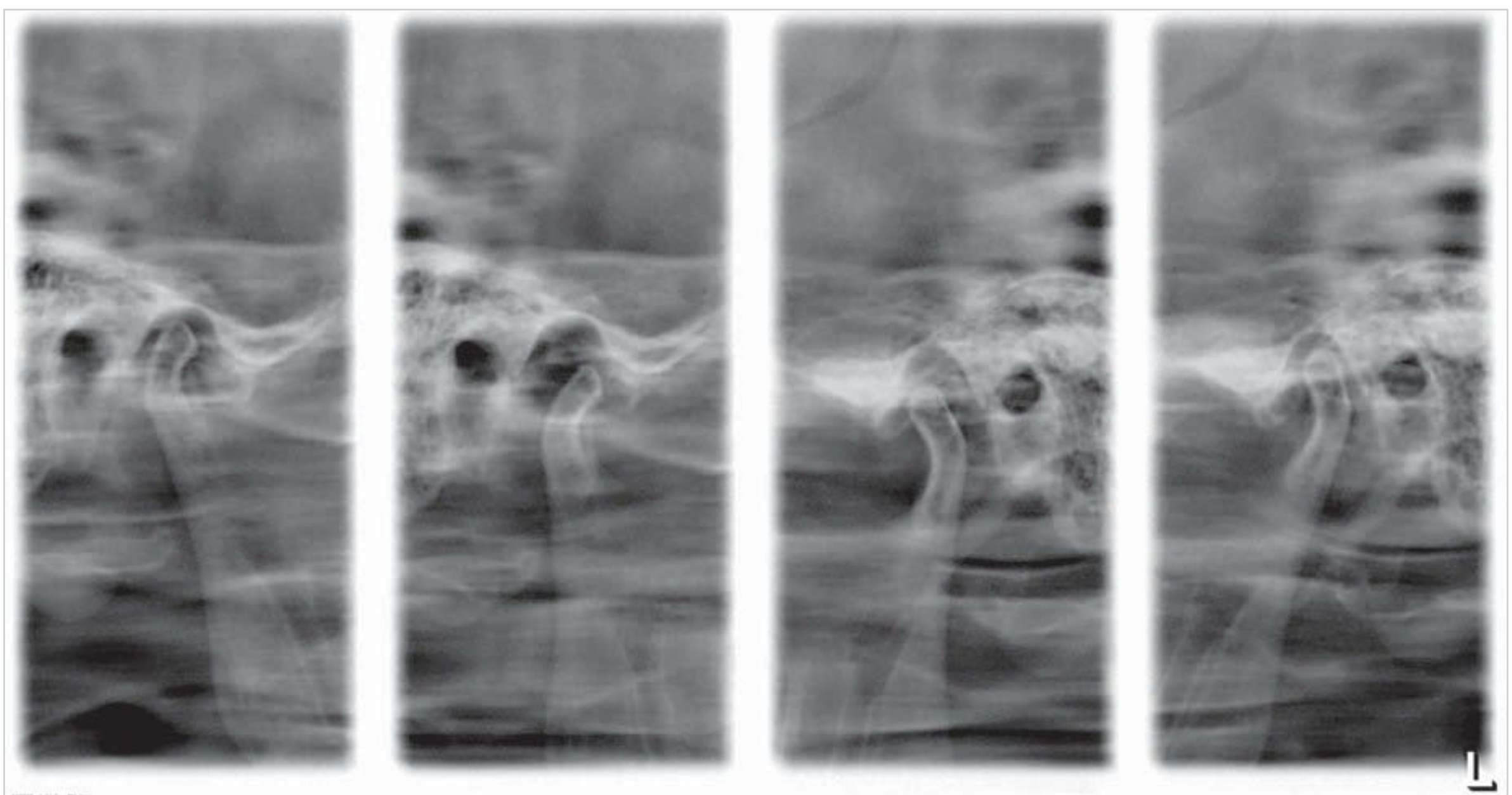


Fig. 9.82 Orthophos XG program, showing the temporomandibular joint with the mouth open (**outer images**) and closed (**inner images**).

Likewise, bitewing programs provide increasingly better superimposition-free interproximal views of coronal aspects of the dentition (□ Fig. 9.81).

Viewing the Temporomandibular Joints

Temporomandibular joint disorders are usually of a functional nature. The first question is how the head of the condyle is positioned within the fossa and how much mouth opening is possible. Magnetic resonance imaging is usually performed for further functional diagnosis. In practice, however, the status of the temporomandibular joint with the mouth closed and during maximal opening can be assessed in a simple manner, using the temporomandibular joint program of a panoramic machine (□ Fig. 9.82 and □ Fig. 9.83).

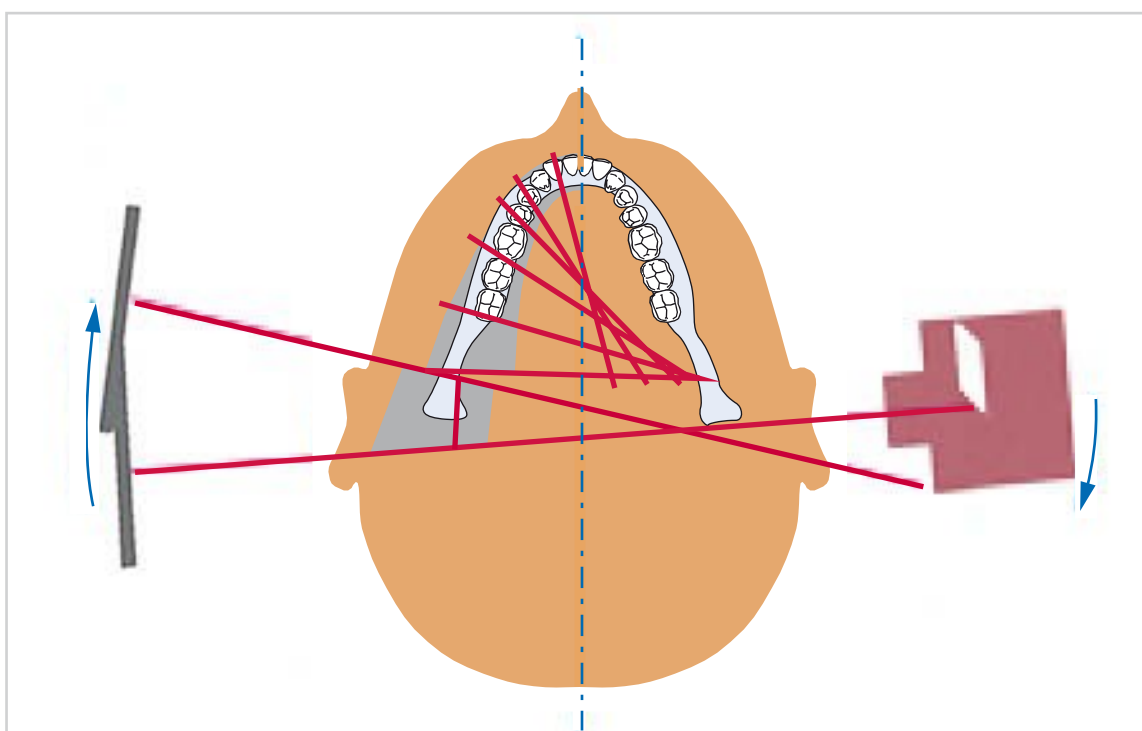


Fig. 9.83 Rotational movement path for panoramic imaging of the temporomandibular joint. (From: Pasler FA, Visser H. Zahnmedizinische Radiologie. 2nd ed. Stuttgart: Thieme; 2000. Farbatlant der Zahnmedizin; Band 5.)

There are other special programs for assessment of changes in the bony structures of the temporomandibular joint by panoramic radiography. Digital volume tomography (CBCT) is, however, the preferred technique for investigating special questions regarding the bone.

Viewing the Midface

Before the advent of CBCT, orthopantomography was used for radiographic visualization of the midface region. It provided a simple and useful way of obtaining diagnostically useful information about structures above the maxilla (□ Fig. 9.84).

This radiographic technique has also been replaced by CBCT because thin-slice images in multiple planes are needed for successful diagnostic imaging of the midfacial region.



Fig. 9.84 Panoramic radiograph of the midfacial region.

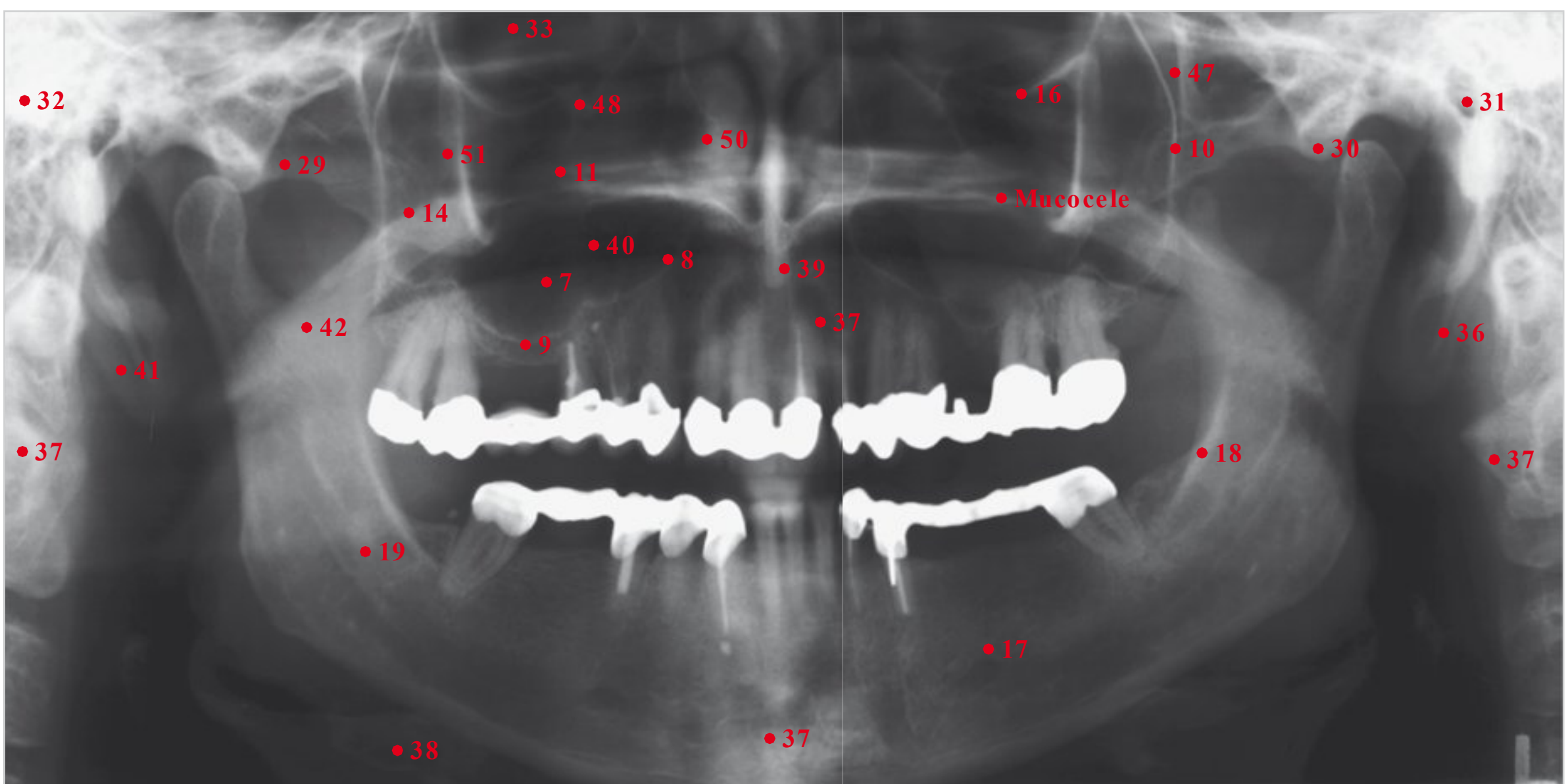


Fig. 9.85 Panoramic radiographic anatomy of the mandibular and maxillary region. See □ Table 9.1 for key to numbers.

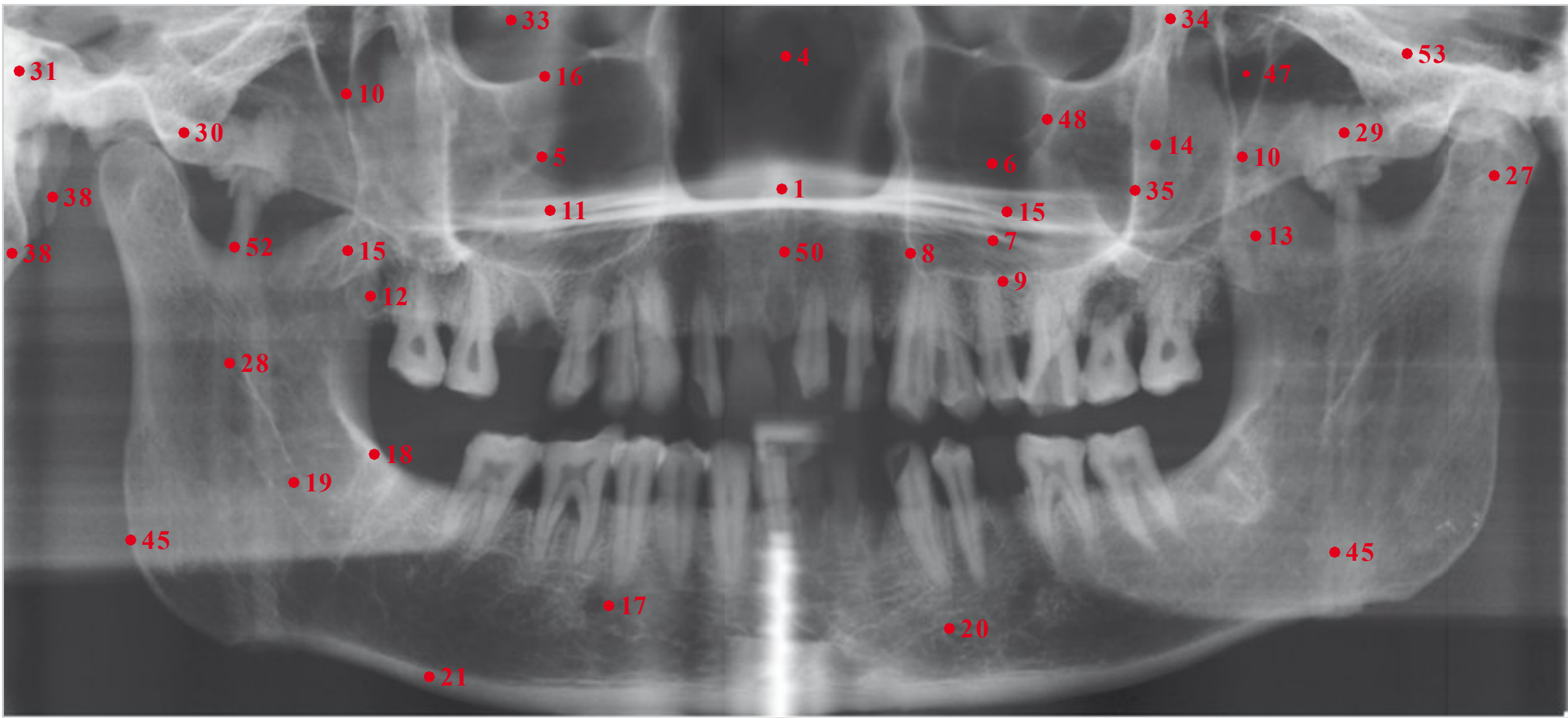


Fig. 9.86 Panoramic radiographic anatomy, demonstrated using a head phantom. See □ Table 9.1 for key to numbers.

Table 9.1 Panoramic radiographic anatomy

Number	Structure
1	Anterior nasal spine
2	Incisive foramen
3	Piriform aperture
4	Nasal septum
5	Nasal cavity
6	Maxillary sinus
7	Alveolar recess of the maxillary sinus
8	Medio-anterior wall of the maxillary sinus
9	Inferior wall of maxillary sinus
10	Posterior wall of the maxillary sinus
11	Hard palate
12	Maxillary tuberosity
13	Pterygoid process
14	Zygomatic bone
15	Coronoid process
16	Infraorbital margin
17	Mental foramen
18	External oblique line
19	Mandibular canal
20	Trabecular bone
21	Cortical bone
22	Dentin
23	Root canal
24	Periodontal ligament space
25	Lamina dura
26	Condylar process
27	Head of the condyle

Table 9.1 (Continuation)

Number	Structure
28	Mandibular foramen
29	Zygomatic arch
30	Articular tubercle
31	External acoustic opening
32	Petrous bone
33	Orbit
34	Lateral wall of the orbit
35	Posterior wall of zygomatic bone
36	Hyoid bone
37	Image of the cervical spine
38	Styloid process
39	Shadow of the nose
40	Air between the tongue and hard palate
41	Ear lobe
42	Soft palate and uvula
43	Pharynx
44	Nasal floor
45	Mandible, opposite side
46	Mastoid process
47	Pterygopalatine fossa
48	Infraorbital foramen
49	Sphenoid sinus
50	Median palatine suture (intermaxillary suture)
51	Nasal conchae
52	Semilunar notch
53	Skull base

Radiographic Anatomy of Panoramic Radiography with Special Consideration of Orthopantomography

Knowledge of the relevant anatomical structures is the crucial basis for interpretation of any radiographic image. It is not possible to detect pathological changes if one does not know what the normal anatomy of the region of interest looks like in its healthy state. There are countless normal anatomical variants of the facial skeleton, and even these pose a high risk of misinterpretation of radiographic findings.

As described in Section 6.1, central projection (and its special image-formation characteristics) is the main reason why it is often difficult to detect pathological changes. Because the panoramic view is curved, the interpretation of the individual structures is more difficult and the view itself is new and unfamiliar. A photomontage by Pasler shows a very impressive panoramic view of the maxilla, mandible, and basal maxillary sinus (□ Fig. 9.85). For comparison, an orthopantomogram of a skull phantom is shown, with the key anatomical structures labeled (□ Fig. 9.86).

Panoramic Radiology: Methodology and Avoidance of Errors

The facial skeleton is made up of many different anatomical structures. Most of them are bony in nature, but some are soft-tissue structures that are visible on radiographs. The oral cavity and nasopharyngeal region contain many air-filled spaces that are also evident on dental panoramic tomographs. The sum of all of these structures makes the panoramic radiograph an X-ray image that is not easy to interpret or understand. Correct patient positioning is extremely important, as this helps to ensure that the many different types of structures in the facial skeleton can be interpreted correctly.

Positioning and Positioning Errors

Each panoramic X-ray machine has a focal trough that is individually adjusted to accommodate the patient's dental arch. Standard focal trough shapes can be programmed, based on standard arch form data. Digital systems allow for optimal individual focal trough adjustment based on patient-specific data collected during the exposure. Furthermore, panoramic machines have a head positioner and other measurement tools that can be utilized to generate custom focal-trough profiles for patient-specific arch forms (□ Fig. 9.75).

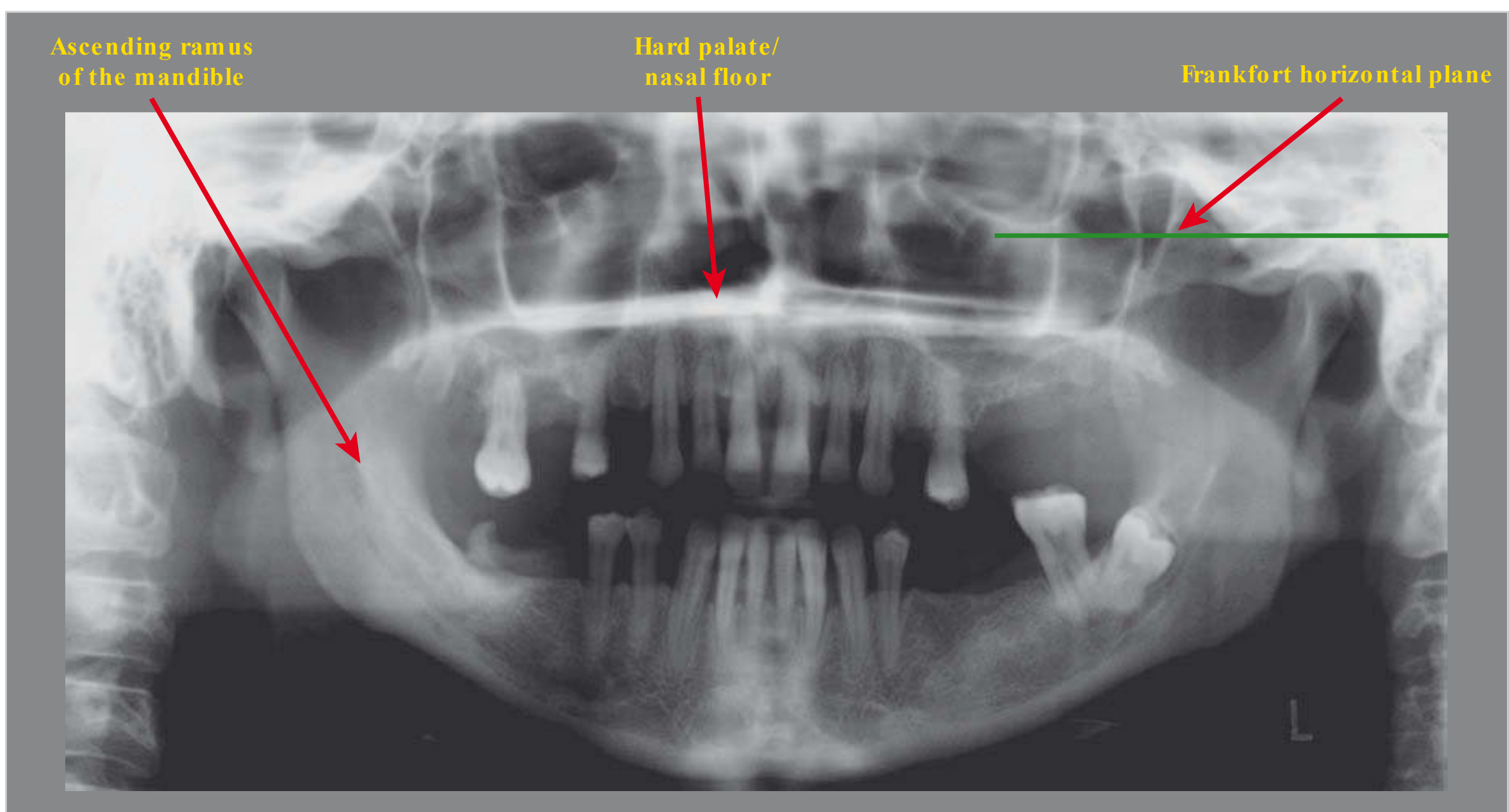


Fig. 9.87 Correct head position, as evidenced by the horizontal line of the hard palate, which should normally be parallel to the Frankfort horizontal plane.

Regardless of the method of focal trough adaptation, the patient must be correctly centered in the adapted focal trough. This ensures that the central ray strikes each tooth as orthogonally as possible and prevents the reduction of image quality due to distortion and geometric unsharpness.

Errors in the positioning of the head have two main causes:

- Tilting of the head
- Displacement and rotation of the head.

Any change in head position means that the head is no longer exactly in the focal trough. This results in unwanted superimposition and distortion in the horizontal dimension. Superimposition is caused by tilting of the head, distortion by displacement of the teeth out of the focal trough, and geometric distortion by the location of objects in the rotation center (effective focus of projection).

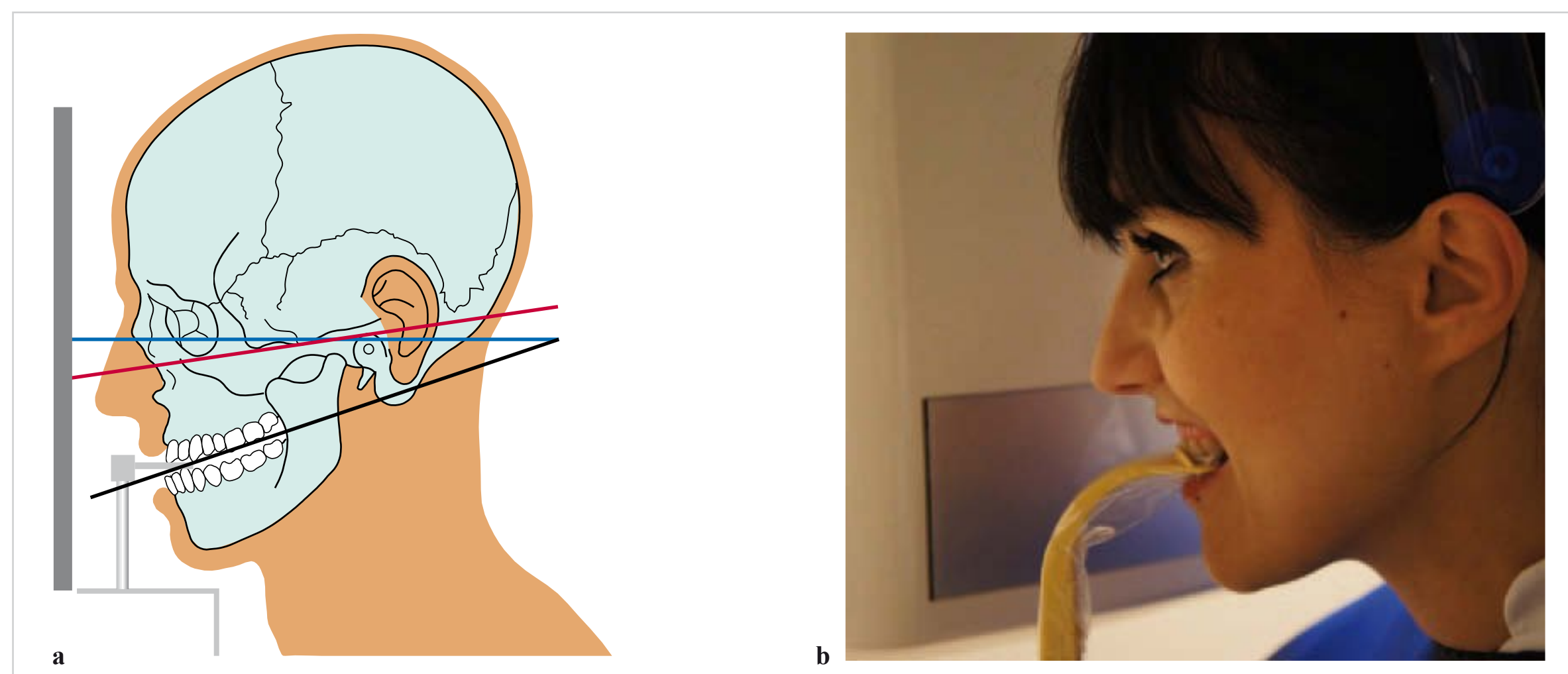


Fig. 9.88a, b Head tilted too far forward.

a Head tilted too far forward (schematic diagram). **Red line:** Frankfort horizontal plane with head tilted too far forward. **Blue line:** Frankfort horizontal plane with head positioned correctly. **Black line:** occlusal plane. (From: Pasler FA, Visser H. Zahnmedizinische Radiologie. 2nd ed. Stuttgart: Thieme; 2000. Farbatlant der Zahnmedizin; Band 5.)

b Patient with head tilted too far forward.

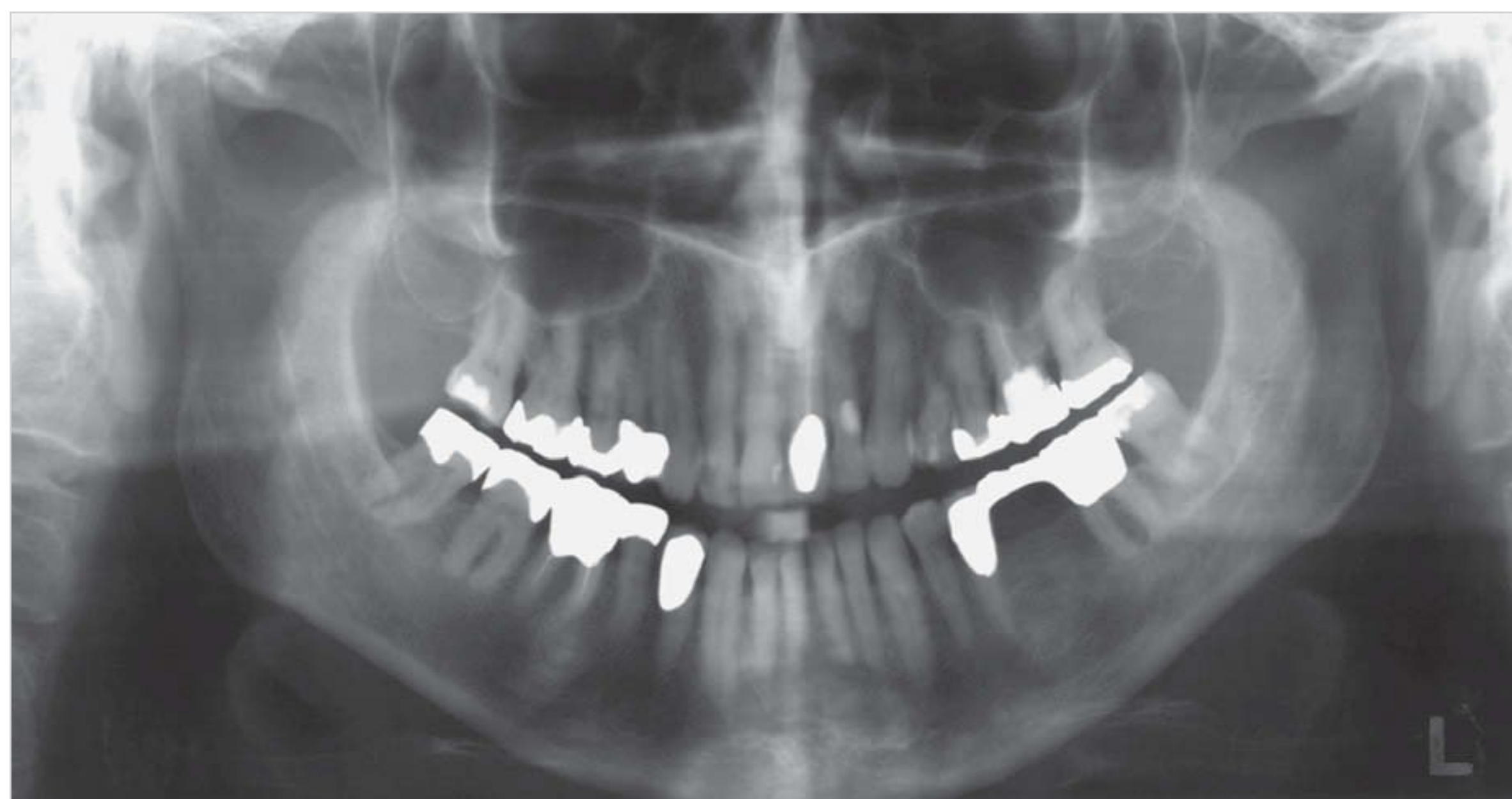


Fig. 9.89 Panoramic radiograph taken with the head tilted forward.

Tilting of the Head

It is possible to determine whether the patient's head is tilted forward or backward, based on the following structures:

- If positioned correctly, the hard palate and nasal floor should be depicted as a straight horizontal line parallel to the lower border of the radiograph.
- It is possible to check for correct head position with respect to the Frankfort horizontal plane: this reference plane is an imaginary line joining the external auditory meatus to the infraorbital margin (□ Fig. 9.87).

If the head is tilted too far forward, the two posterior ends of the hard palate may open superiorly, forming a blunt or pointed “V” (□ Fig. 9.88 and □ Fig. 9.89).

If the head is tilted too far backward, the hard palate will appear as an inverted “V.” There is a risk that the floor of the nose and the hard palate may be superimposed on the apices of the maxillary teeth. The visual effect is widening of the entire image, which may result in the heads of the condyles being cut off (□ Fig. 9.90 and □ Fig. 9.91).

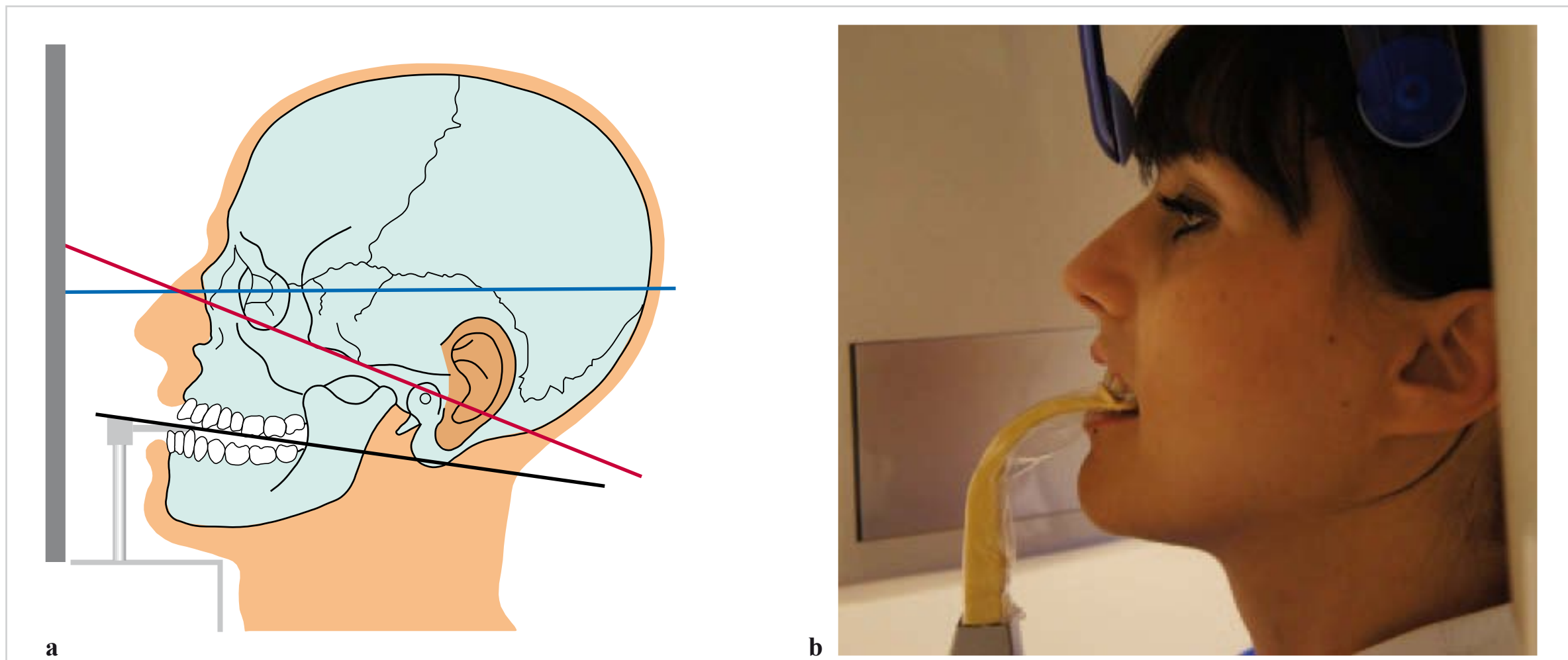


Fig. 9.90a, b Head tilted too far backward.

a Head tilted too far backward (schematic diagram). **Red line:** Frankfort horizontal plane with head tilted too far backward. **Blue line:** Frankfort horizontal plane with head positioned correctly. **Black line:** occlusal plane. (From: Pasler FA, Visser H. Zahnmedizinische Radiologie. 2nd ed. Stuttgart: Thieme; 2000. Farbatlant der Zahnmedizin; Band 5.)

b Patient with head tilted too far backward.



Fig. 9.91 Panoramic radiograph taken with the head tilted backward.

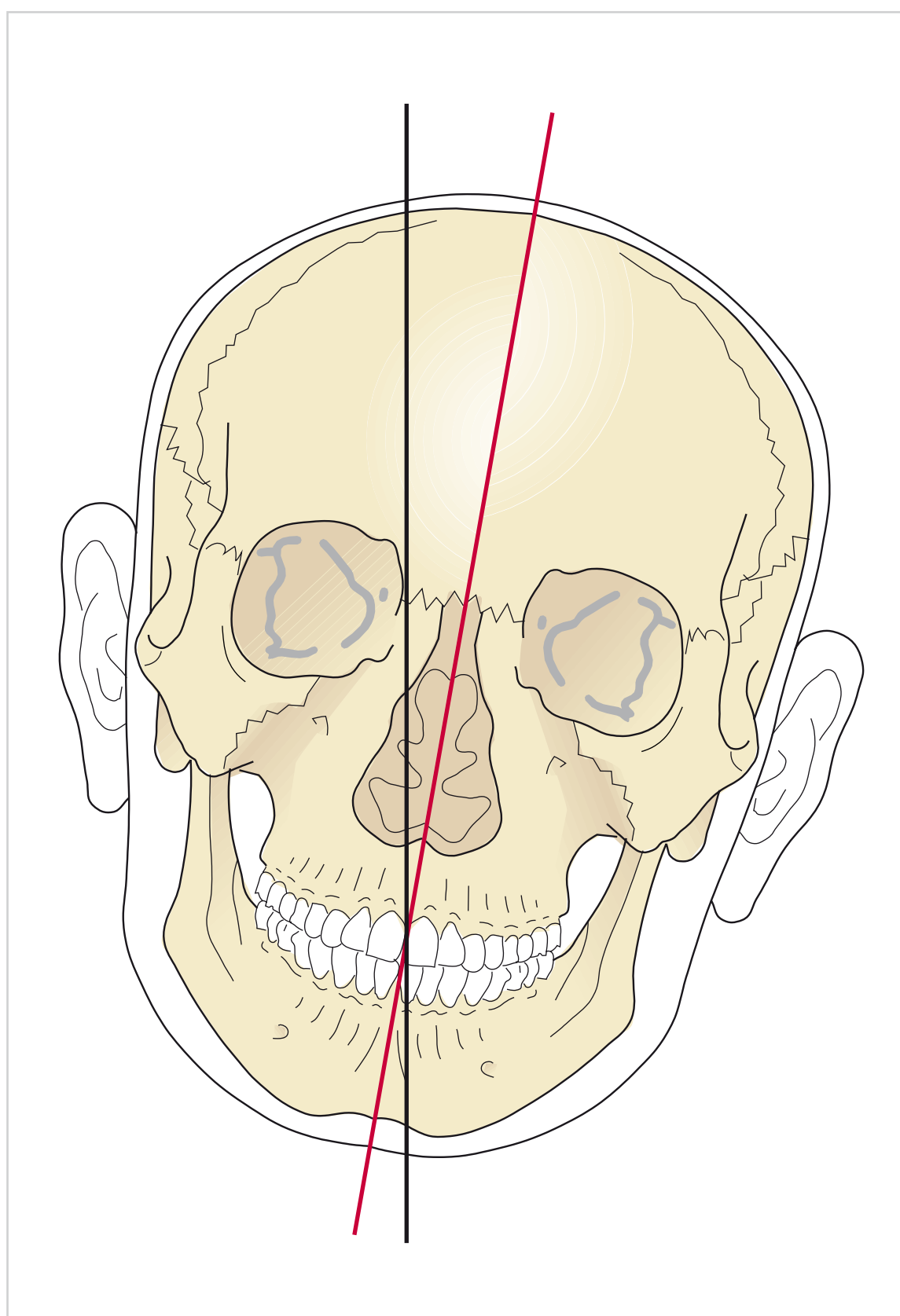


Fig. 9.92 Head slanted to the side. (From: Pasler FA, Visser H. Taschenatlas der zahnärztlichen Radiologie. Stuttgart: Thieme; 2003.)

Lateral tilting does not affect image quality as much as anterior and posterior tilting. Nevertheless, this hampers comparison with previous radiographs, making it more difficult to interpret the affected radiograph (□ Fig. 9.92 and □ Fig. 9.93).

Displacement and Rotation of the Head out of the Focal Trough

If the patient's head tilts in the vertical plane, the maxilla and mandible still remain largely in the focal trough. Only excessive tilting has an effect on the image, namely, widening in the anterior region. If head displacement or rotation occurs, the distance to the rotation center changes, resulting in geometric unsharpness and widening or narrowing of the jaws on the image.

Because of a rotation center located in the anterior floor of the mouth, anterior or posterior displacement of the anterior teeth out of the focal trough results in geometric unsharpness. The further backward the teeth are positioned relative to the central plane of the focal trough, the wider they appear on the image. The further forward the teeth are positioned, the narrower they appear on the image.

□ Posterior displacement of the anterior teeth: If the patient's head is tilted too far back, the anterior teeth are displaced posterior of the focal trough, and the distance to the rotation center decreases. Consequently, the anterior teeth are irradiated in the zone of increasing beam divergence, and visible widening of the anterior teeth occurs on the image (□ Fig. 9.94 and □ Fig. 9.95).

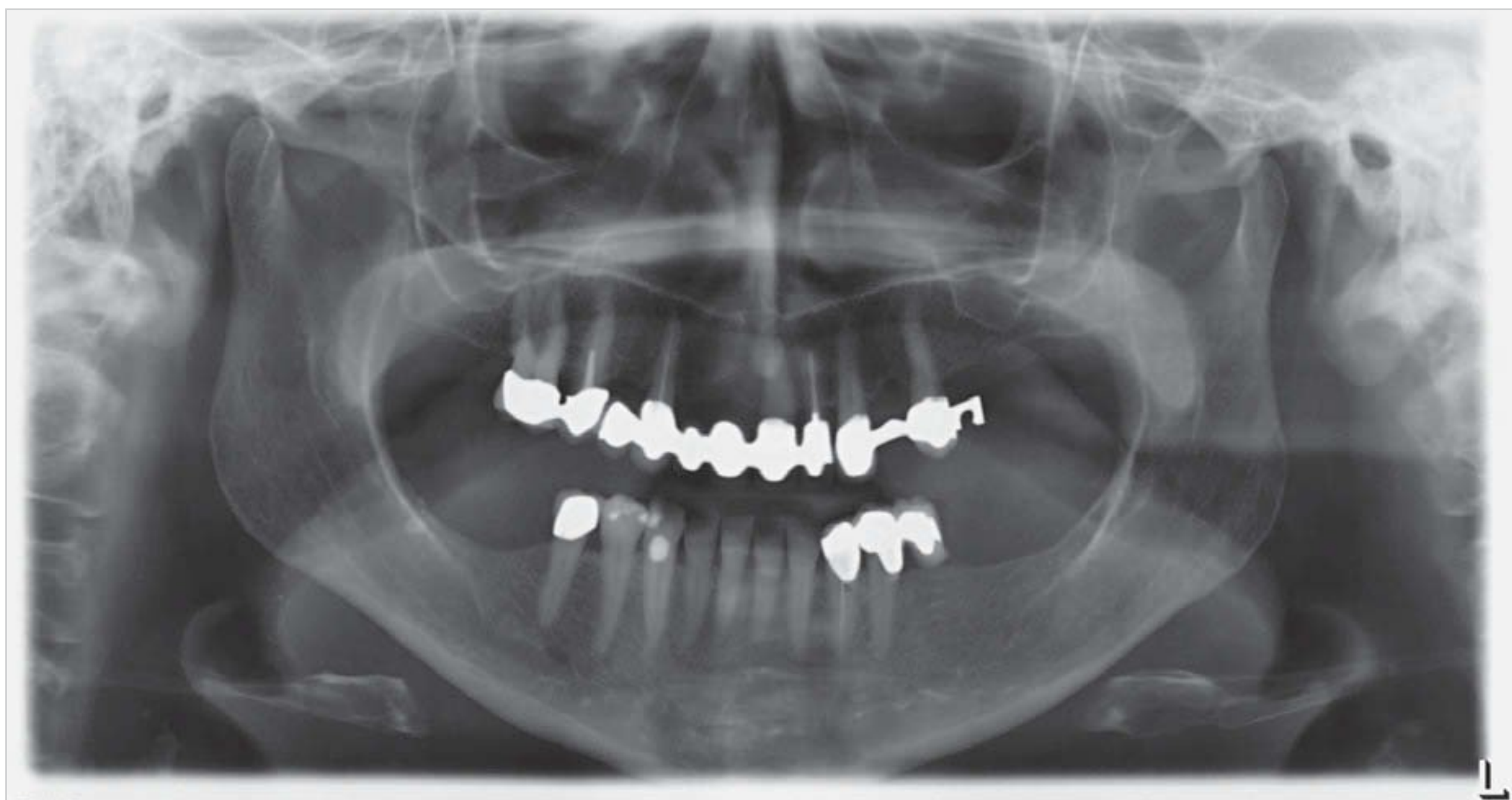


Fig. 9.93 Panoramic radiograph taken with the head slanted to the side.

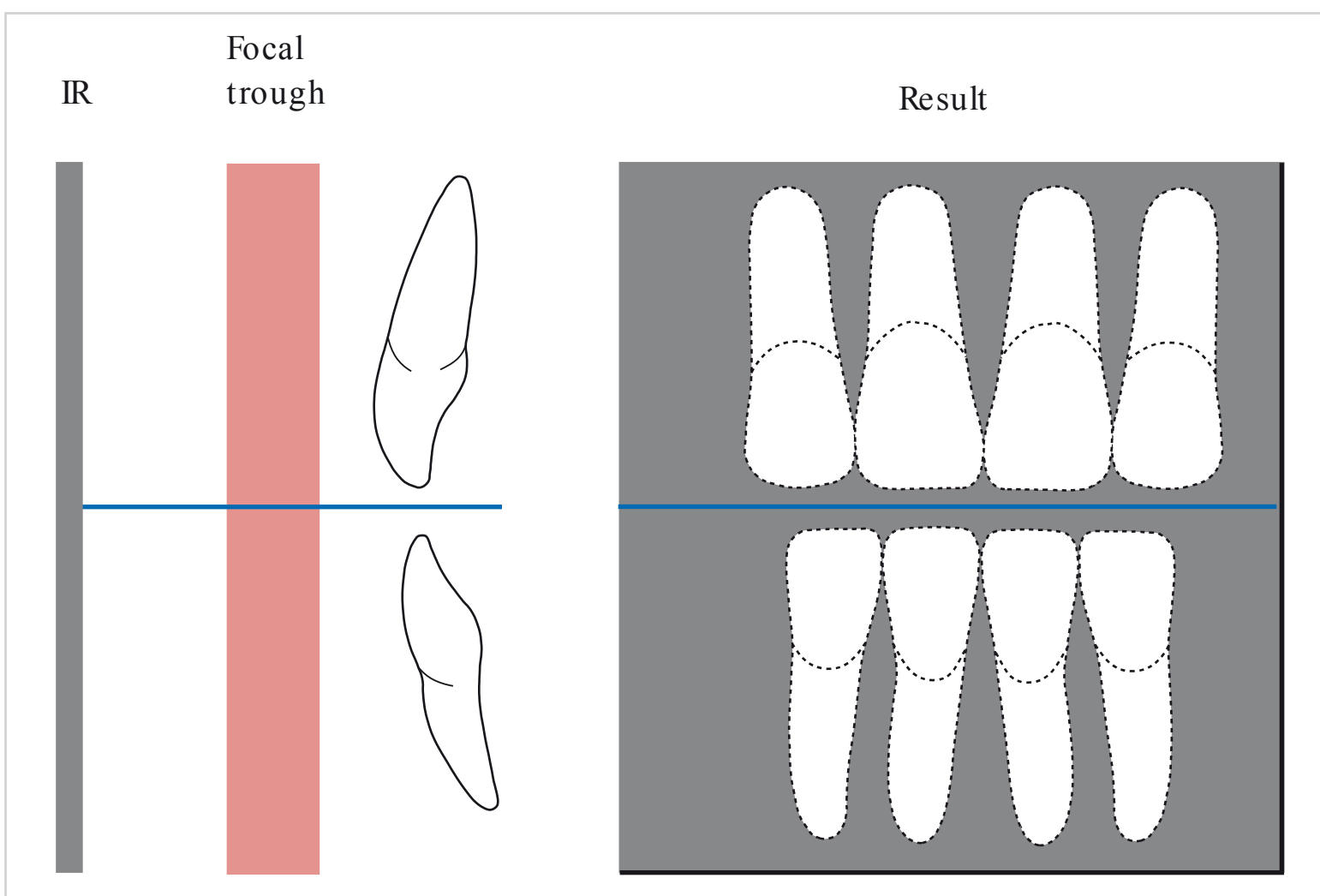


Fig. 9.94 Schematic of posterior displacement. If the teeth are located posterior to the focal trough, they appear wider on the radiograph. IR: image receptor. (From: Pasler FA, Visser H. Zahnmedizinische Radiologie. 2nd ed. Stuttgart: Thieme; 2000. Farbatlant der Zahnmedizin; Band 5.)

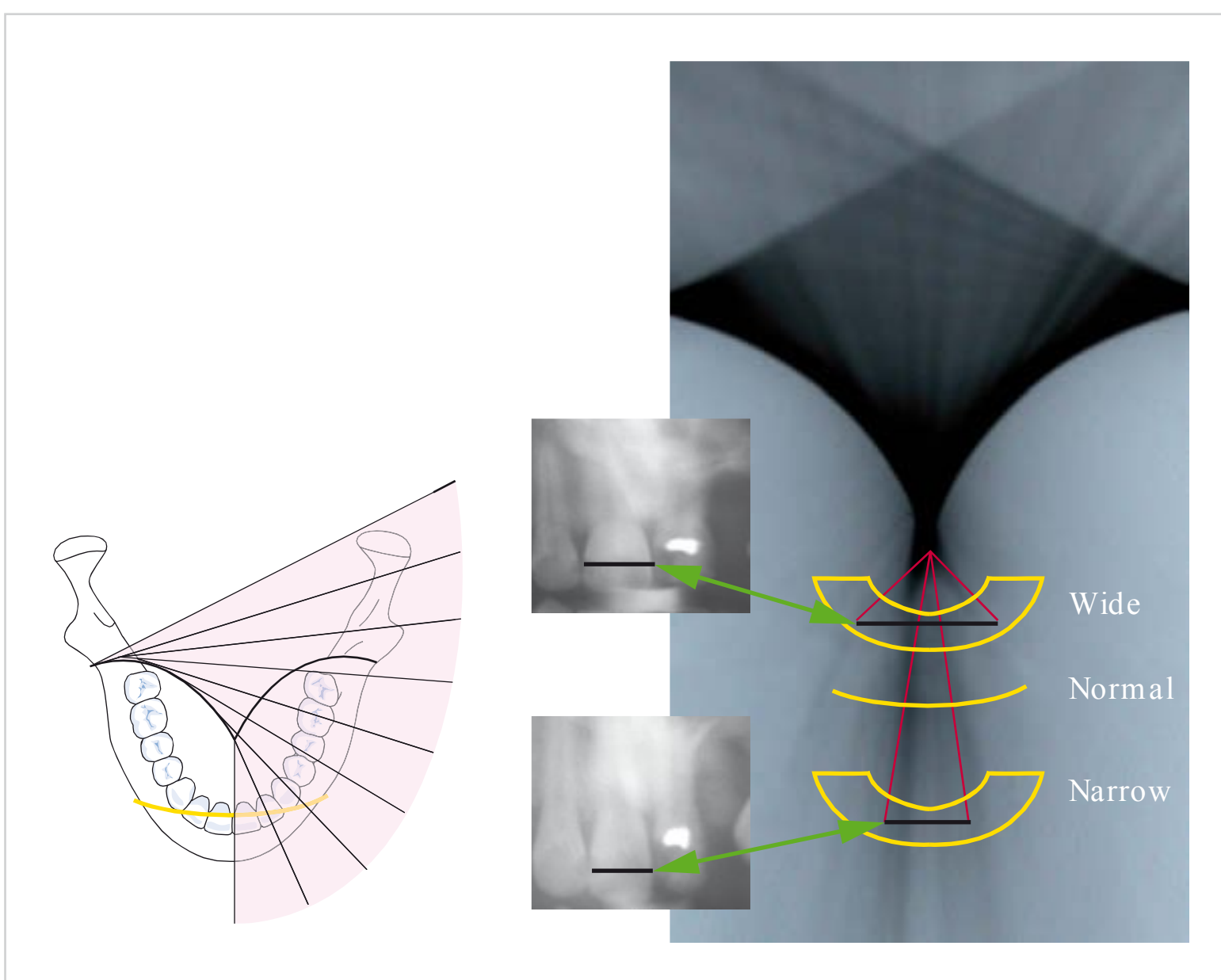


Fig. 9.95 The further the anterior teeth are located posterior to the focal trough, the wider they appear on the radiograph.

Practice

To avoid such positioning errors, it is crucial to ensure that the anterior teeth are properly aligned in the middle of the focal trough.

- A bite-rod positioning device must be used in **dentate** patients. Modern panoramic machines also have correction options that should be used for these cases.
- In **edentulous** patients, close attention to proper positioning is especially important. In the case presented in □ Fig. 9.96, a bite rod was not used because tooth 21

was missing. This resulted in improper alignment of the anterior teeth and marked widening of the maxillary and mandibular anteriors. Consequently, there was a significant decrease in anterior image quality. It is also evident that no bite rod was used in this case. In the repeat exposure, correct anterior alignment was achieved (□ Fig. 9.97), that is, the anterior teeth were correctly positioned within the focal trough. As is clearly visible on the repeat radiograph, this resulted in significant improvement of diagnostic image quality.



Fig. 9.96 Posterior displacement: because the patient was positioned posterior to the focal trough, the images of the anterior teeth appear wider.



Fig. 9.97 In the repeat radiograph (same patient as in □ Fig. 9.96), the patient was positioned correctly and the teeth are depicted correctly.

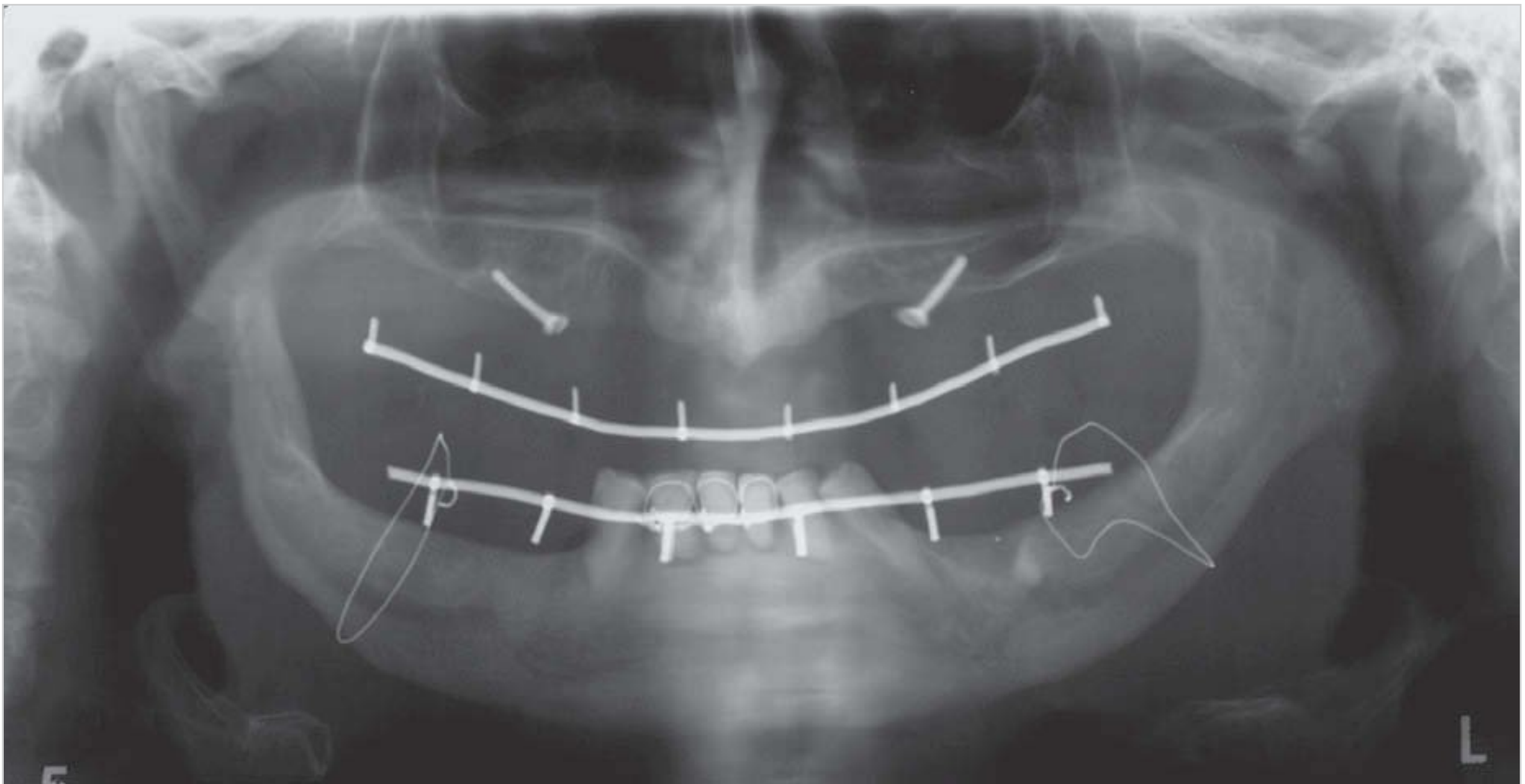


Fig. 9.98 In this panoramic radiograph of a patient with an edentulous anterior maxillary and mandibular arch, the anterior region appears extremely widened.

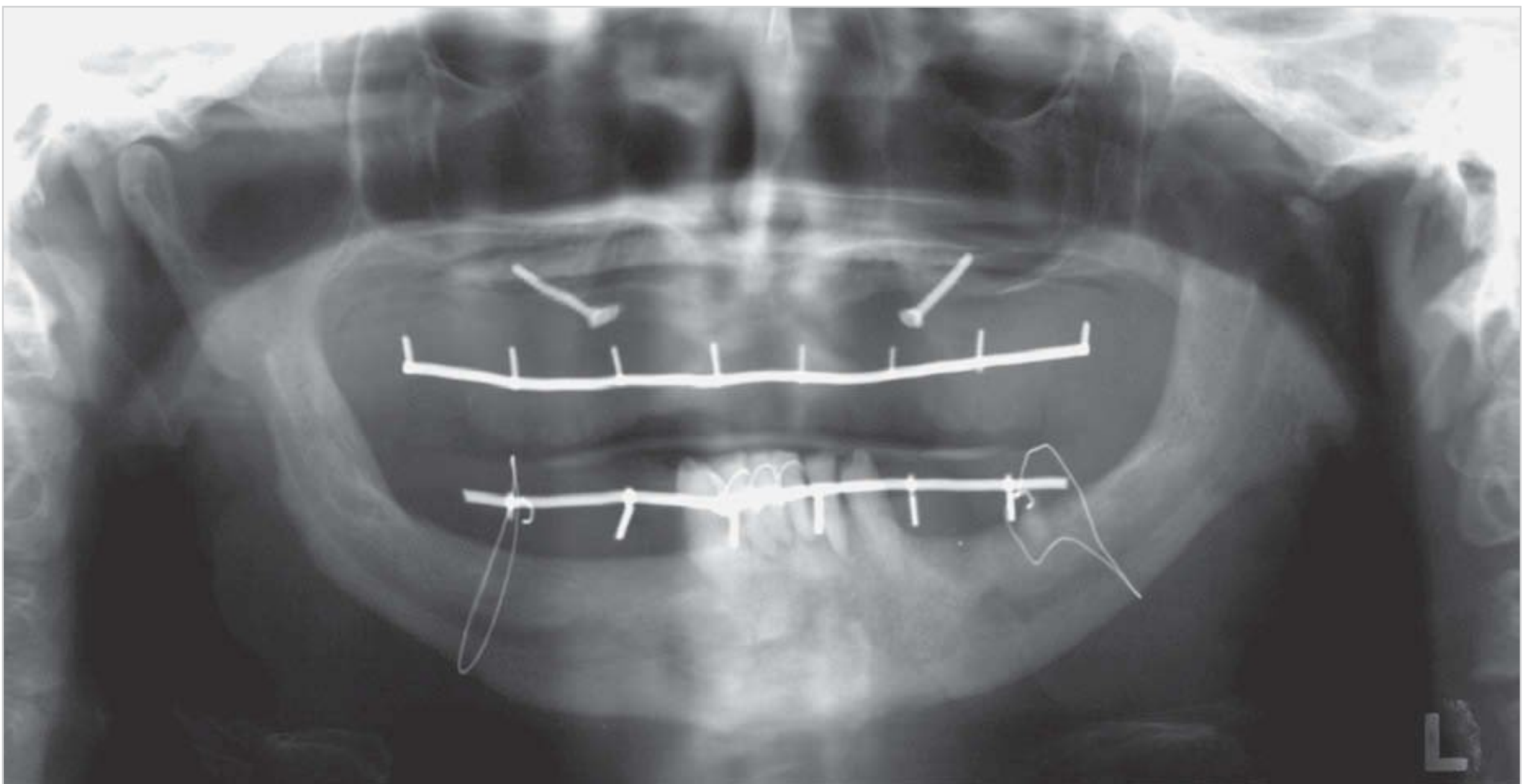


Fig. 9.99 On a later radiograph of the same patient, there was much less anterior widening.

In partially and fully edentulous patients, there is a higher chance that the anterior teeth will not be correctly positioned in the focal trough. The reason is that these patients are suboptimally immobilized in the focal trough, owing to the lack of appropriate positioning guides (□ Fig. 9.98 and □ Fig. 9.99).

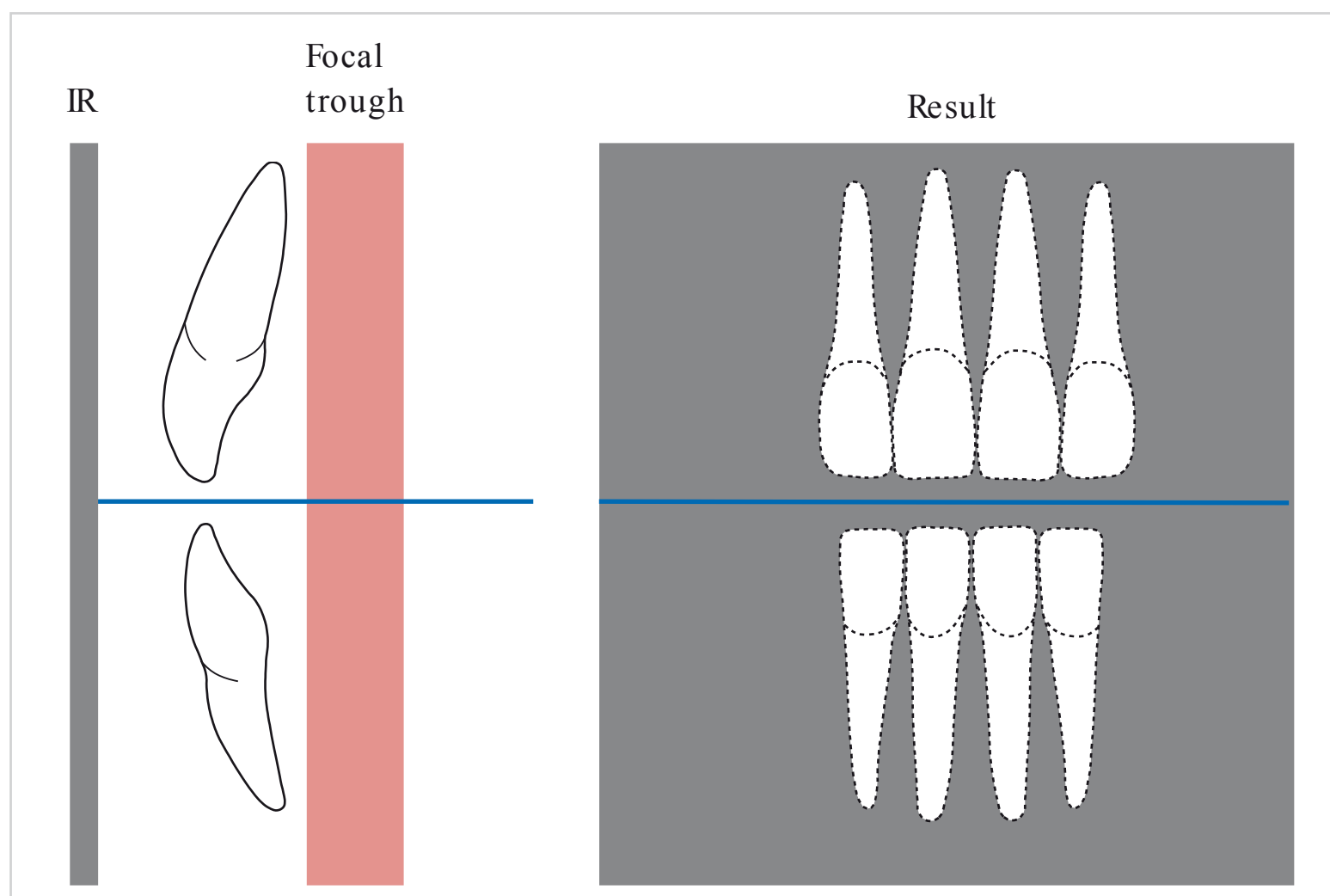


Fig. 9.100 Schematic of anterior displacement of the head. The teeth are positioned anterior to the focal trough. IR: image receptor. (From: Pasler FA, Visser H. Zahnmedizinische Radiologie. 2nd ed. Stuttgart: Thieme; 2000. Farbatlant der Zahnmedizin; Band 5.)



Fig. 9.101 In this panoramic radiograph, taken with the head tilted forward, there is apparent narrowing of the anterior teeth.

□ Anterior displacement of the anterior teeth: According to the general principle of tomographic blurring, if the anterior teeth are displaced too far forward and lie outside the focal trough, they appear blurred and narrow and are not shown completely on the image (□ Fig. 9.100 and □ Fig. 9.101).

□ Rotation of the head out of the median plane: If the head is rotated slightly to the side, structures appear distorted and wider on one side than on the other, because a rotation center is located in the posterior region. This is more or less apparent on the panoramic radiograph, depending on the degree of head rotation (□ Fig. 9.102 and □ Fig. 9.103).

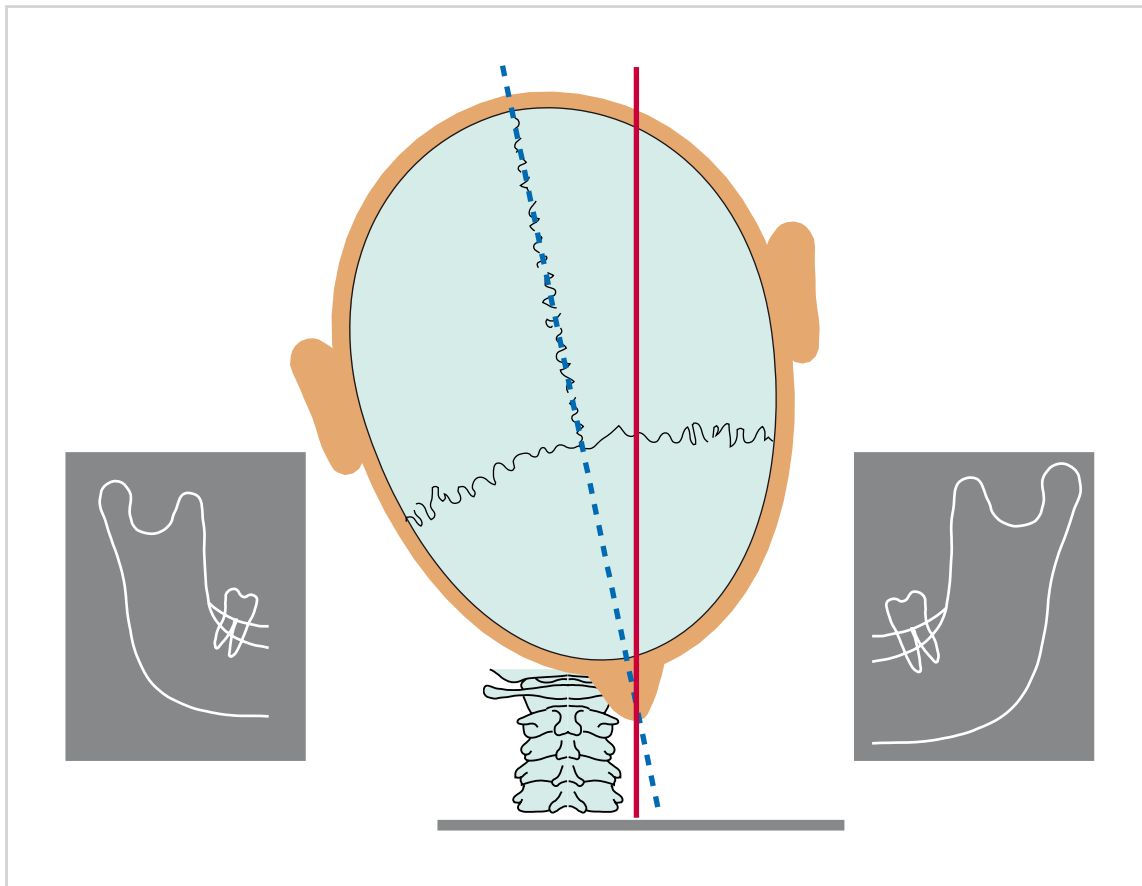


Fig. 9.102 Schematic demonstrating rotation of the head out of the median plane. (From: Pasler FA, Visser H. Zahnmedizinische Radiologie. 2nd ed. Stuttgart: Thieme; 2000. Farb-
atlanten der Zahnmedizin; Band 5.)

Other Factors Influencing Image Quality and Diagnostic Quality

In addition to positioning errors, other factors that affect the quality of dental panoramic images, sometimes very strongly, must be taken into consideration during radiographic interpretation and diagnosis. These include superimpositions, soft-tissue shadows, and ghost images (radiographic artifacts that appear on panoramic film when a radiodense object is penetrated multiple times by the X-ray beam).

Common ghost images and soft-tissue shadows include:

- Ghost images of the cervical spine
- Ghost images of metallic objects and anatomical structures
- Ghost images of objects located in the rotation center
- Soft-tissue shadows and superimpositions
- Airway shadows from the oral cavity, nasal cavity, and pharyngeal areas.

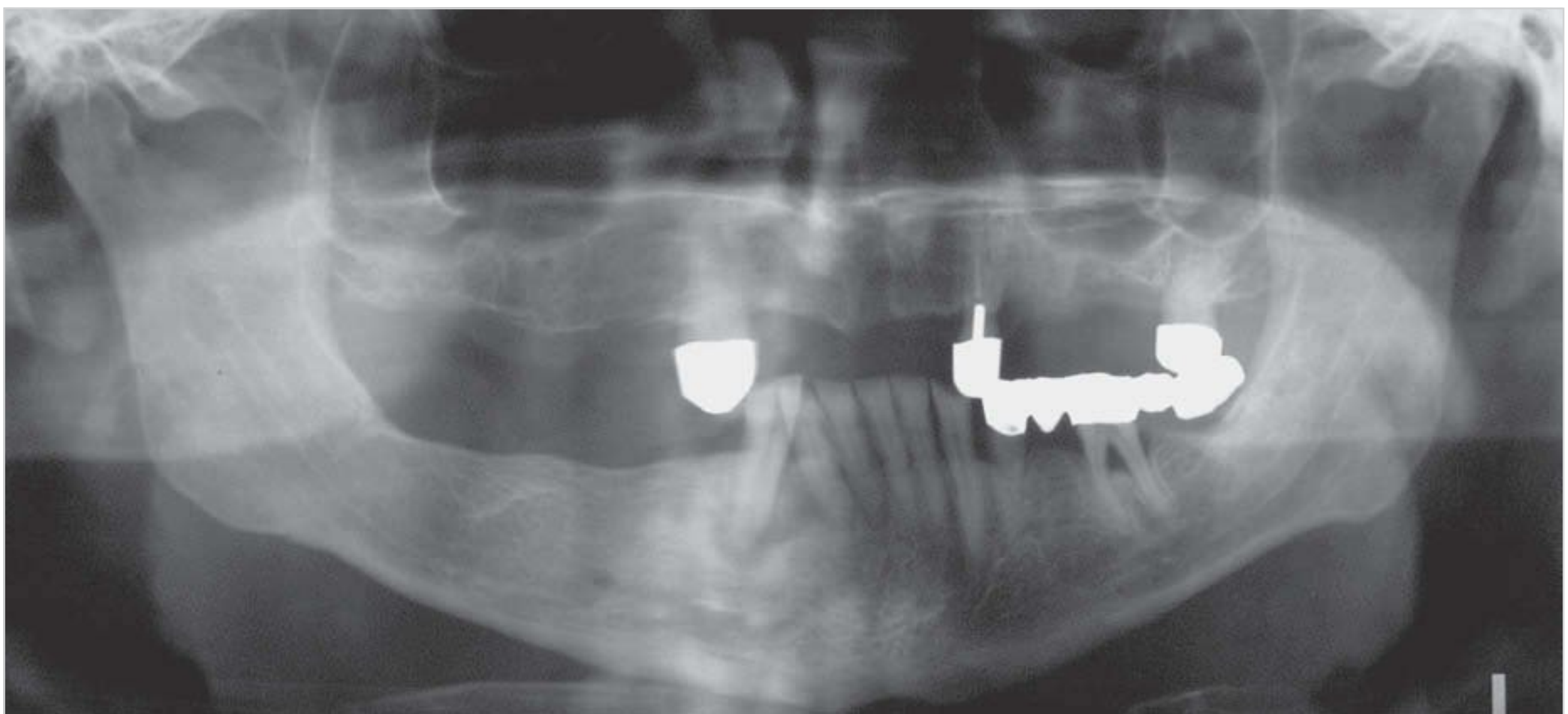


Fig. 9.103 In this panoramic radiograph, taken with the head rotated out of the median plane, the left side appears much wider than the right.

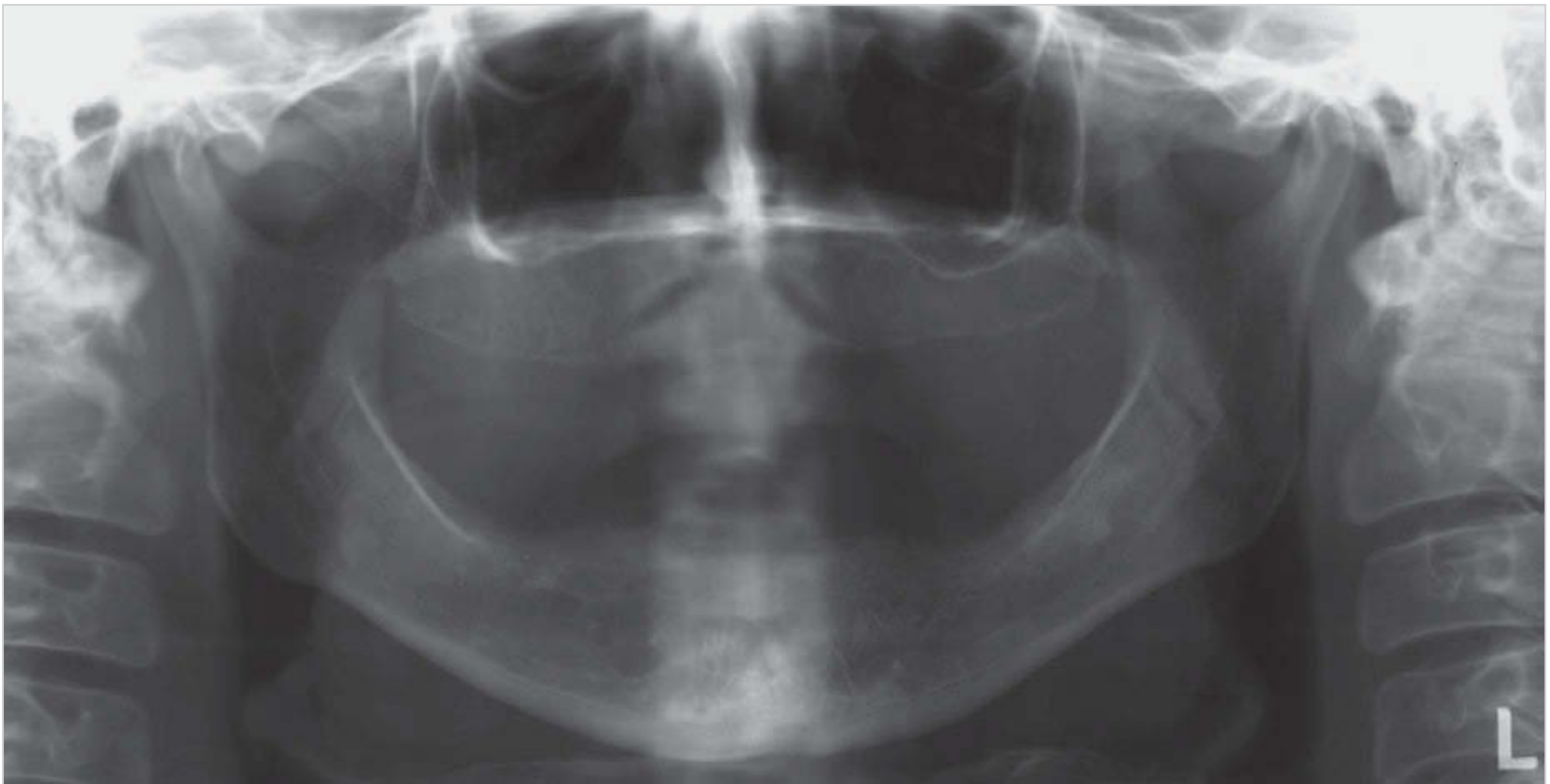


Fig. 9.104 Panoramic radiograph showing ghost images of the cervical spine, projected three times.

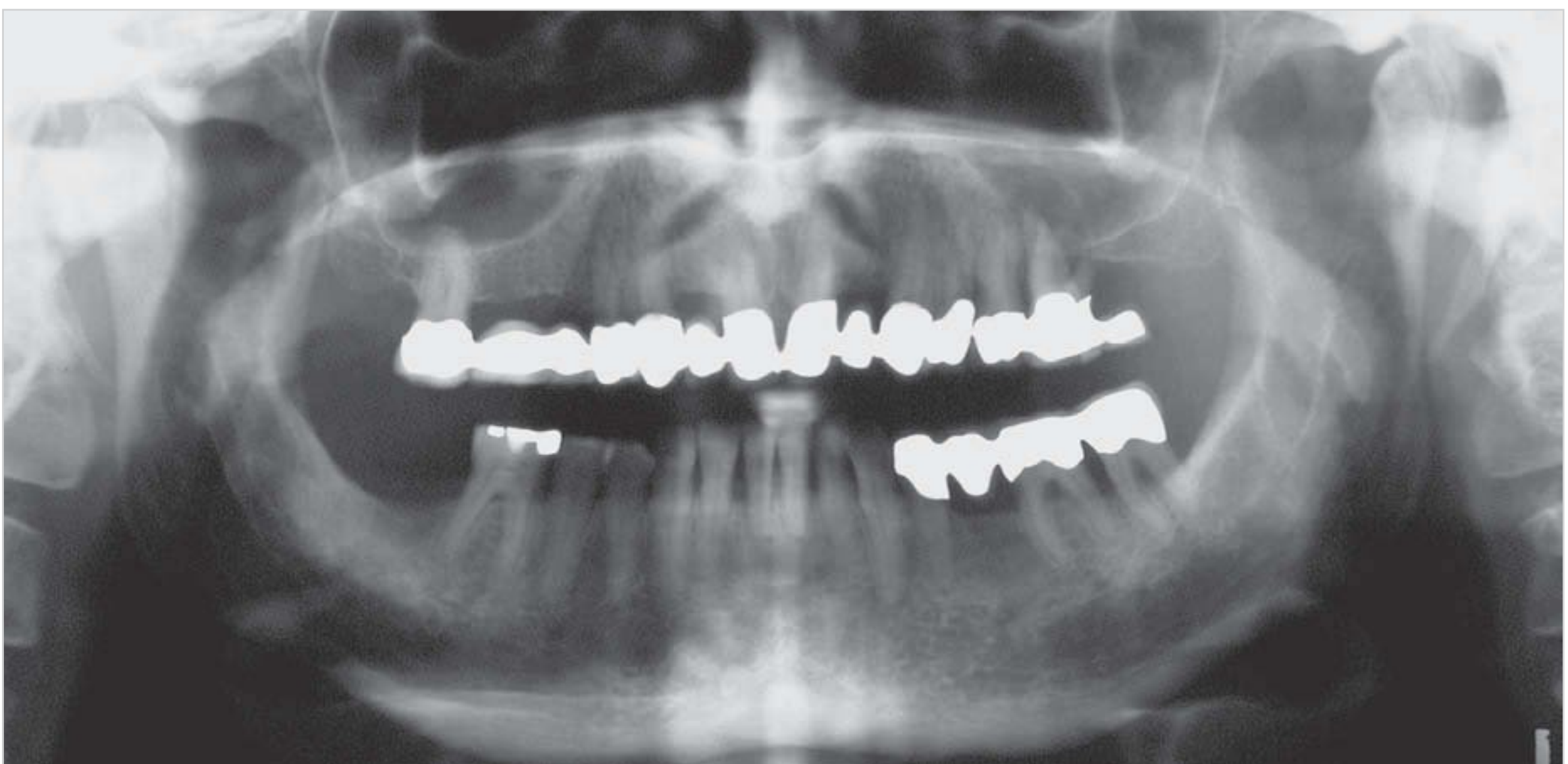


Fig. 9.105 The two diagonal radiolucent lines at the level of the apex of teeth 12 and 22 are projected from the spine.

Ghost Images of the Cervical Spine

Owing to the movement path and projection geometry, the X-ray beam penetrates the cervical spine twice laterally (on the right and left side of the image) and once in the midline (in the center of the image), producing ghost images. The lateral images generally cause no interference, but the central ghost image is a more or less annoying artifact

that can—or rather used to—complicate anterior diagnosis tremendously. Modern panoramic machines have special programs to compensate for ghost images of radiodense structures such as the spinal column (□ Fig. 9.104).

The atlas, the **f**irst cervical vertebra, is commonly seen on radiographs as a conspicuously symmetrical structure associated with the spinal column (□ Fig. 9.105).

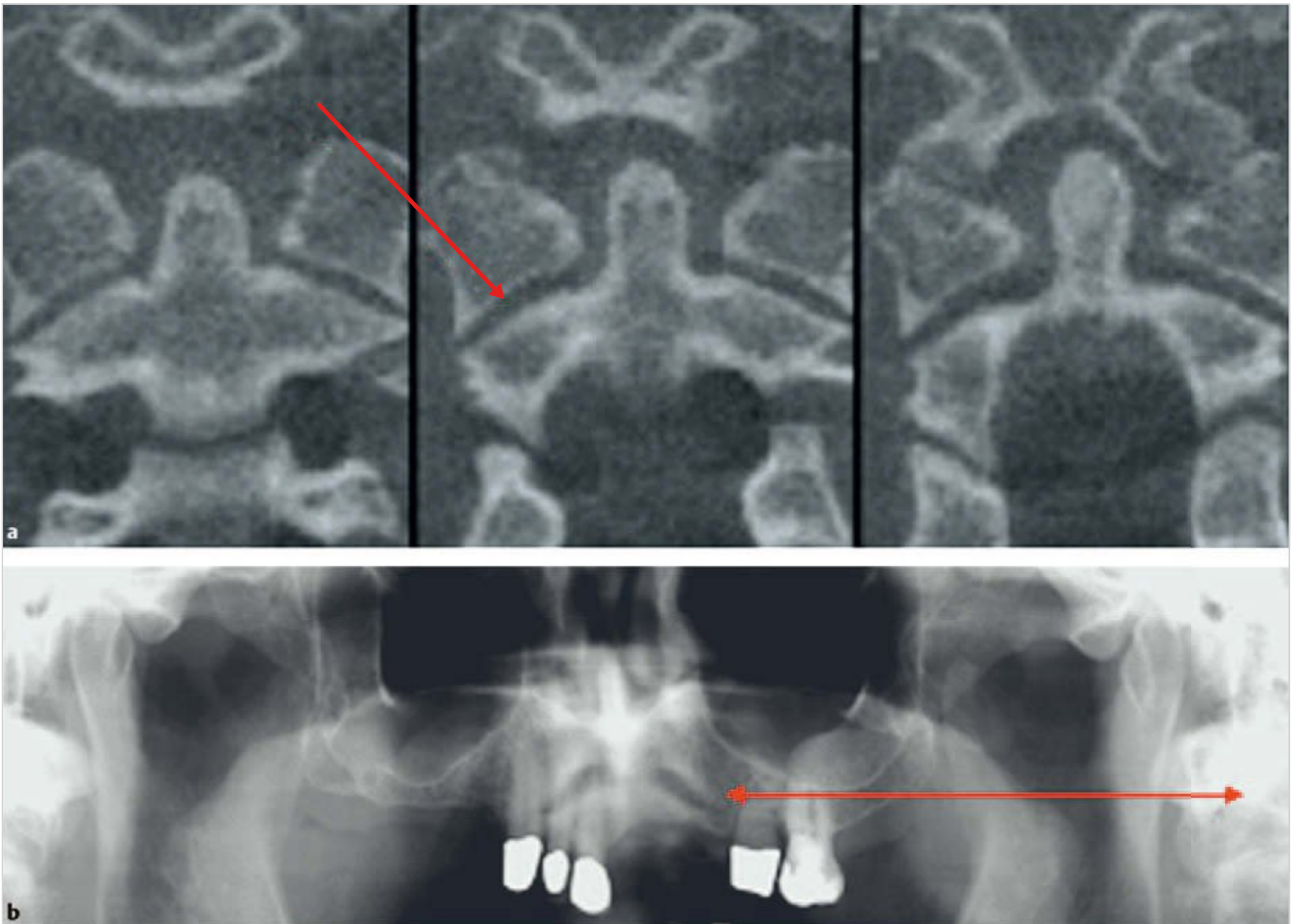


Fig. 9.106a, b The radiolucent lines in the anterior apical region are projected from the atlas.

a Joint space of the first cervical vertebra (arrow).

b Panoramic appearance of the radiolucent lines (arrow).

It appears as a symmetrical, short oblique bright line in the apical areas of the anterior teeth. Although often misinterpreted as an anterior periapical radiolucency, its symmetry is more suggestive of an anatomical structure. Two radiolucent lines arise from the joint space between the first and second cervical vertebrae, as shown on the CBCT image of the atlas (□ Fig. 9.106).

Ghost Images of Metallic Objects in the Head and Neck Region

All metallic objects in the neck region must be removed prior to exposure of the panoramic radiograph because they are located in the path of the beam. Metal artifacts are most commonly caused by lead aprons (if placed too high) and necklaces.

If placed too high at the back of the neck, lead aprons cause metal artifacts that often obscure large areas of the anterior mandible and cause unnecessary radiation exposure by making it necessary to repeat the radiographic examination (□ Fig. 9.107).

Parts of a necklace located at the back of the neck produce ghost images in the mandibular anterior region (□ Fig. 9.108).

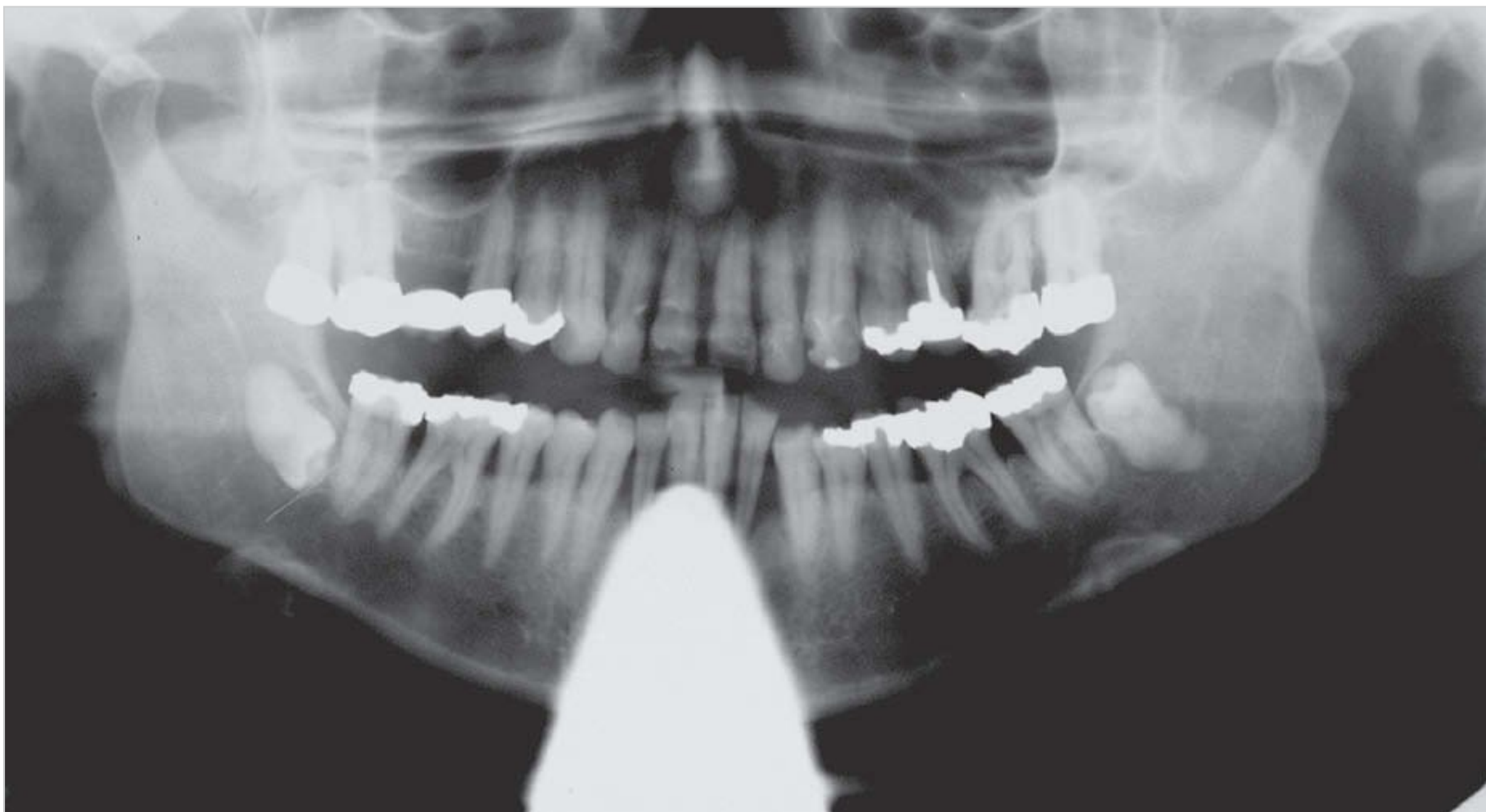


Fig. 9.107 Lead apron artifact projected on the anterior region of a panoramic radiograph.

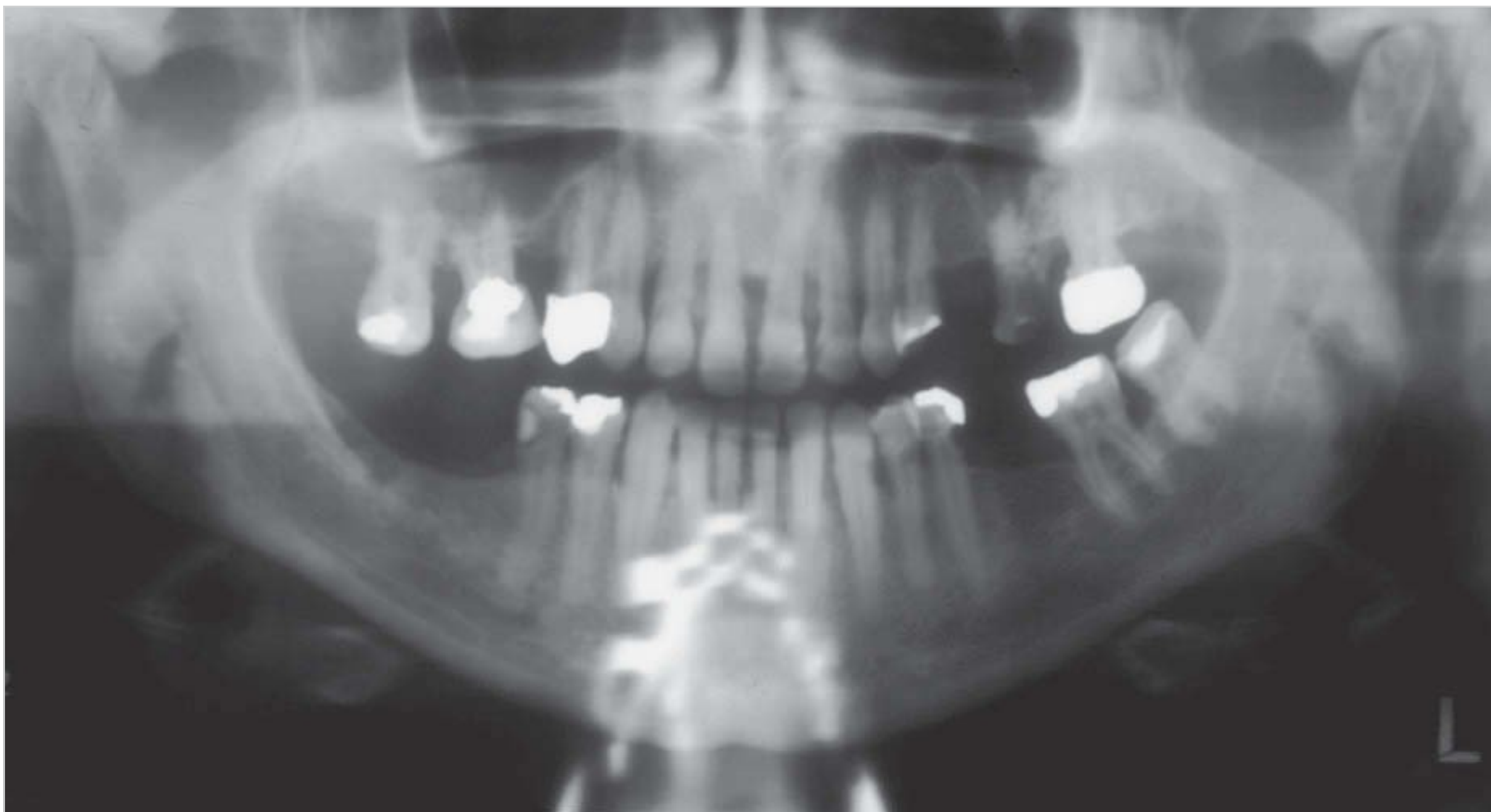


Fig. 9.108 Ghost image of a necklace appearing in the anterior region of a panoramic radiograph.

Mandibular and Maxillary Dentures

All metal objects in the oral cavity, particularly maxillary and mandibular dentures, appear on the film. Before starting the panoramic exposure, the patient should be instructed to remove all dentures from both the maxillary and the mandibular arch, even if only one arch is being investigated (□ Fig. 9.109).

Complete dentures with no metal components can be left in the mouth to better position the patient in the machine. However, it cannot be recommended to leave complete dentures in the mouth during a panoramic exposure because this method is not reliable (□ Fig. 9.110).

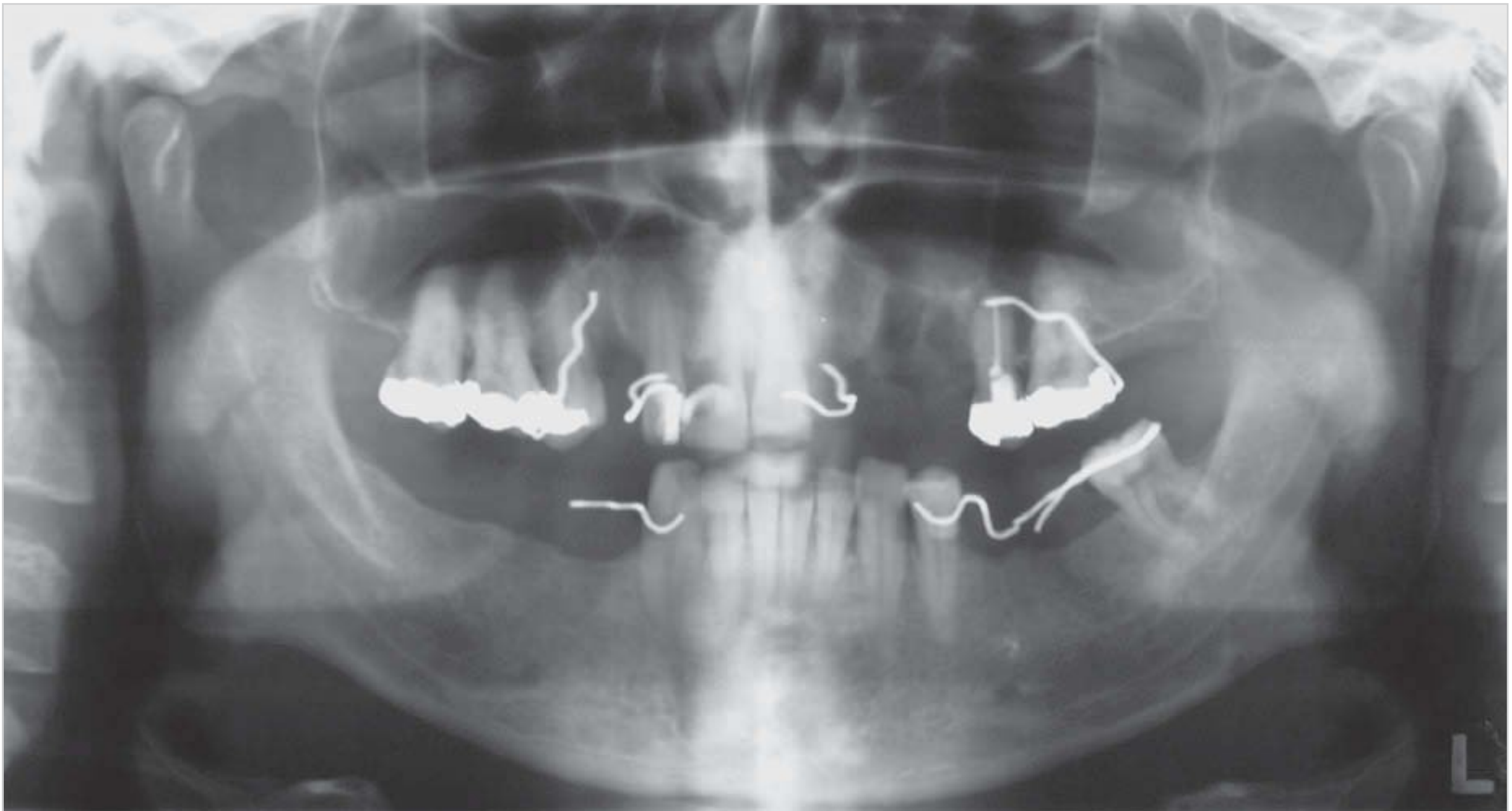


Fig. 9.109 Metal clasps of maxillary and mandibular partial dentures.

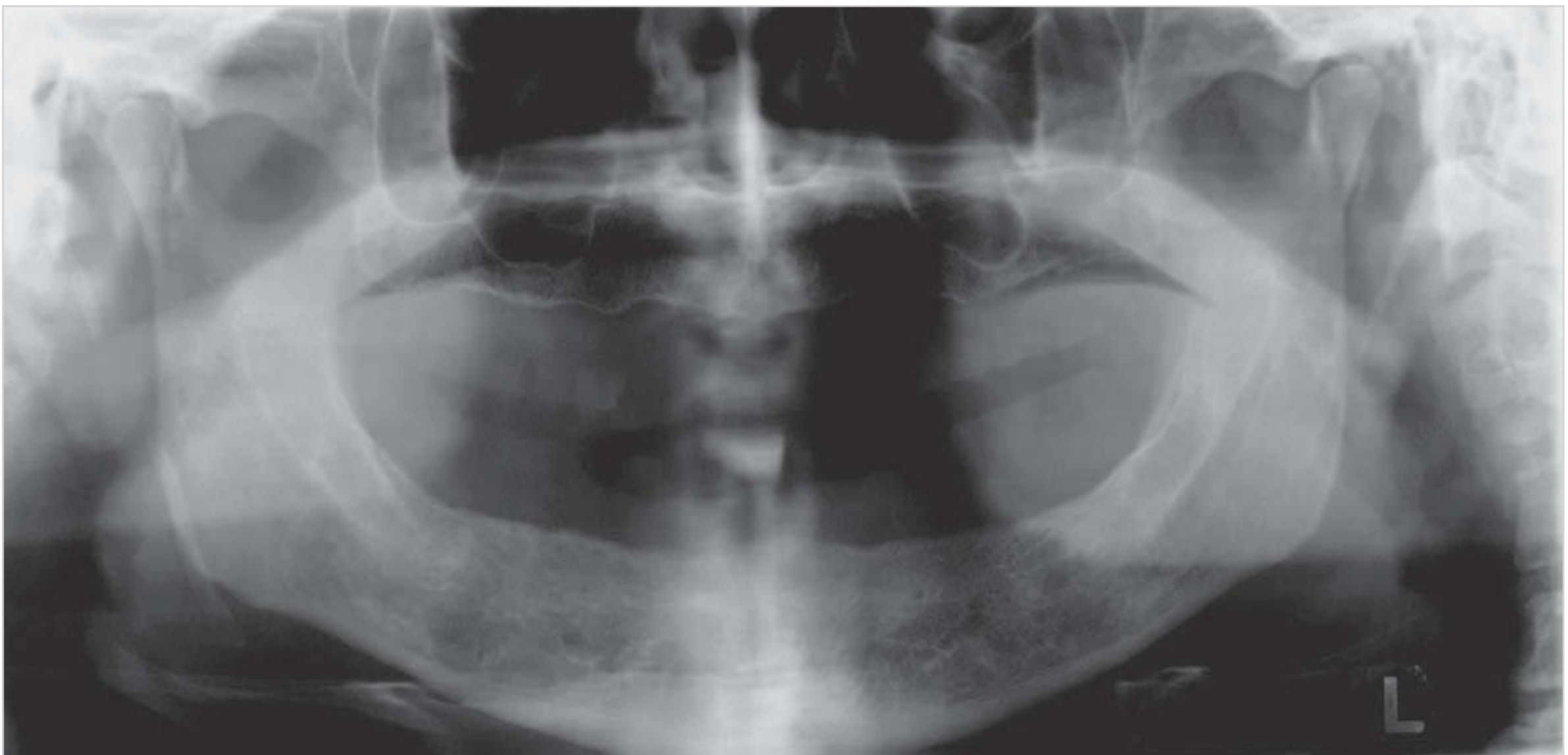


Fig. 9.110 Maxillary and mandibular complete dentures.

Ghost Images of Anatomical Structures

Ghost images of structures in the region of the angle of the mandible may appear on the opposite side of the film, owing to low blurring.

Depending on the degree of head tilting, ghost images of the horizontal posterior ramus of the mandible and parts of the ascending ramus may appear as anatomical structures on the opposite side of the film. The inferior cortical bone frequently appears as a well-defined radiopaque line (□ Fig. 9.111).

In the figure, a horizontal radiopaque line that turns slightly upward in the region of tooth 45 appears at the level of the hyoid bone on the right side. On the left side, the line is located slightly higher because the head is tilted slightly to the left. This phenomenon can be demonstrated by positioning three lead spheres along the posterior border of the ascending ramus of the mandible (□ Fig. 9.112).



Fig. 9.111 The posterior mandible and angle of the mandible project onto the opposite side.

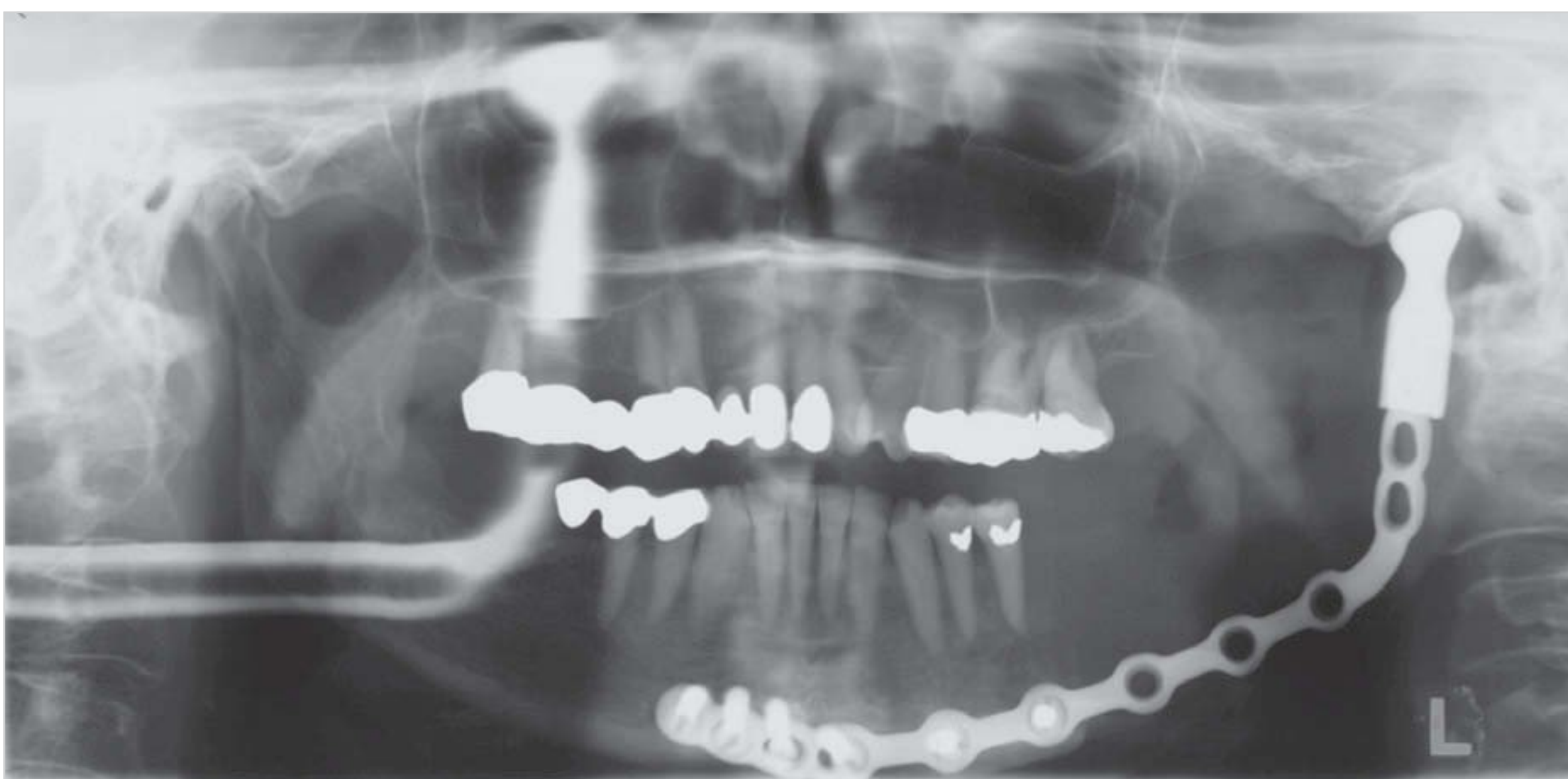


Fig. 9.112 Lead spheres were placed along the left angle of the mandible to demonstrate the projection of the left mandible and right half of the jaw.

Ghost Images of Earrings and other Ear Jewelry

Earrings and other metallic ear jewelry are the best known and most common cause of ghost images in panoramic radiography (□ Fig. 9.113). The inferior–superior beam path and projection-related magnification can be readily identified.

Ghost Images and Blurring of Objects Located in the Rotation Center

Objects located directly in a rotation center (effective focus of projection) produce ghost images that contribute to image formation as long as they remain in the rotation center.

In the case example, a barbell-type tongue piercing with spherical beads was attached on the top and bottom of the tongue (□ Fig. 9.114). On the panoramic radiograph, the beads do not appear as circles but as elongated ovals. This indicates that they are located in the oral cavity, posterior to the focal trough. The upper bead produces not only an oval artifact, but also a bright stripe that extends horizontally across the **film**. The only explanation for this phenomenon is that the bead was located in the rotation center and was thus imaged throughout the entire exposure cycle as it remained in the **effective** focus of projection. In the subsequent exposure, the tongue was pressed far enough against the roof of the mouth that the



Fig. 9.113 Ghost images of earrings appear on the respective opposite side.

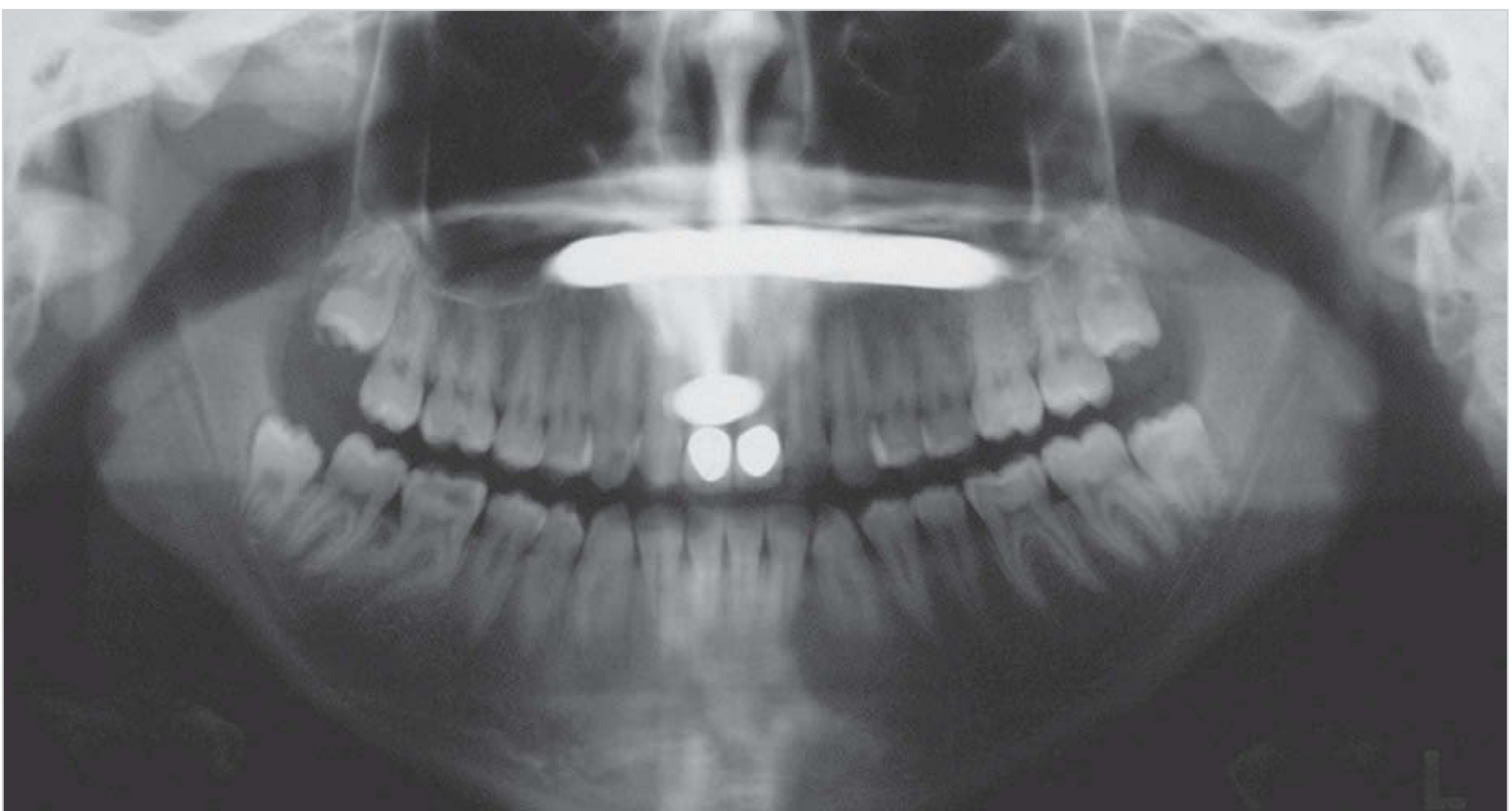


Fig. 9.114 Ghost images: barbell-shaped tongue piercing located in the rotation center for the anterior teeth.

upper bead of the tongue piercing projected just below the nasal floor and hard palate; as it was located in the rotation center, it appears as a long shadow stripe extending from tooth 15 to tooth 25.

The diagram in the right panel of Fig. 9.115 shows and explains why the upper bead located in the rotation center (effective focus of projection) appeared as a bright stripe on the film.

Practice

Jewelry, piercings, and dentures should be removed before a panoramic examination.

If the head is incorrectly positioned posterior to the focal trough (as evidenced by widening of the anterior teeth), the crowns of the molars and premolars may shift their rotation center and produce ghost images that appear in the apical region on the opposite side of the film (Fig. 9.116).

Soft-tissue Shadows and Superimpositions

Many soft-tissue structures in the facial region produce shadows on panoramic radiographs that may lead to uncertainty and misinterpretation.

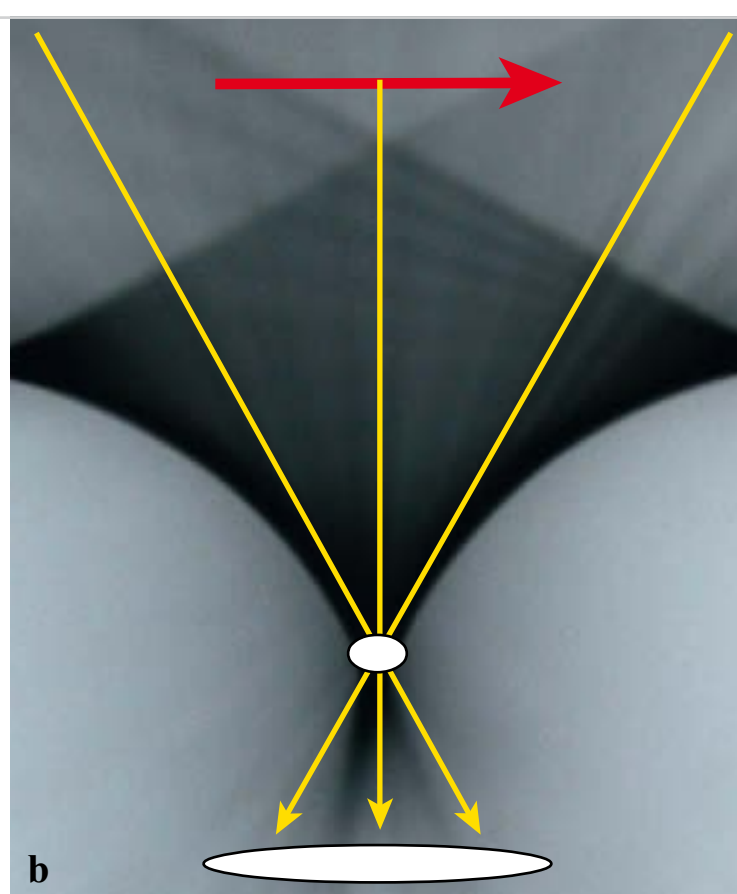
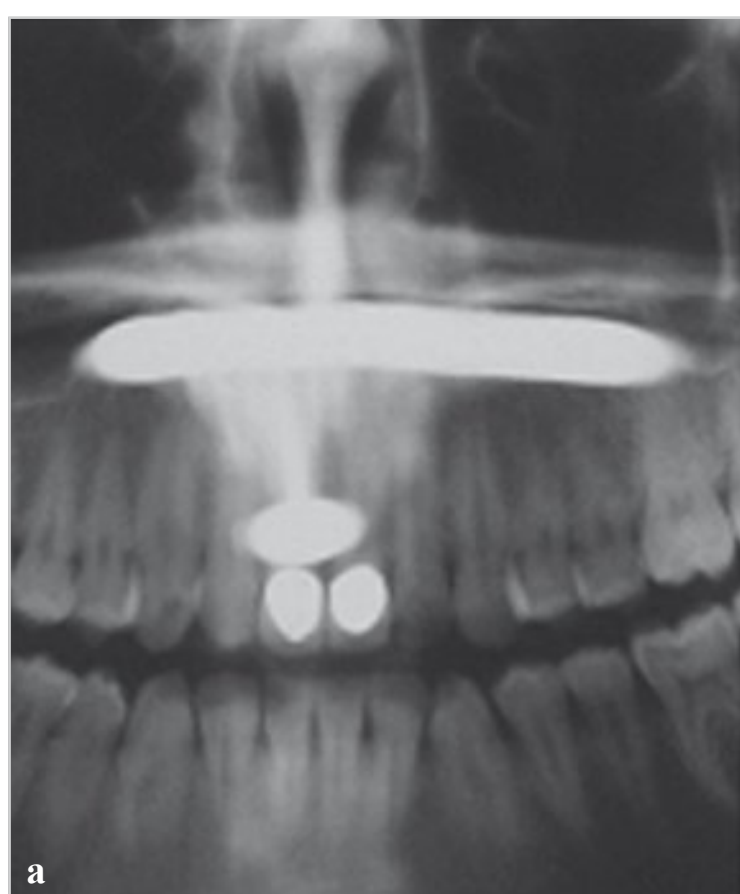


Fig. 9.115a, b Effect of tongue piercing located in the rotation center of panoramic radiography.

- a** Ghost images of tongue piercing on panoramic radiograph (cf. Fig. 9.114).
- b** Schematic explaining the phenomenon (with rotation center).

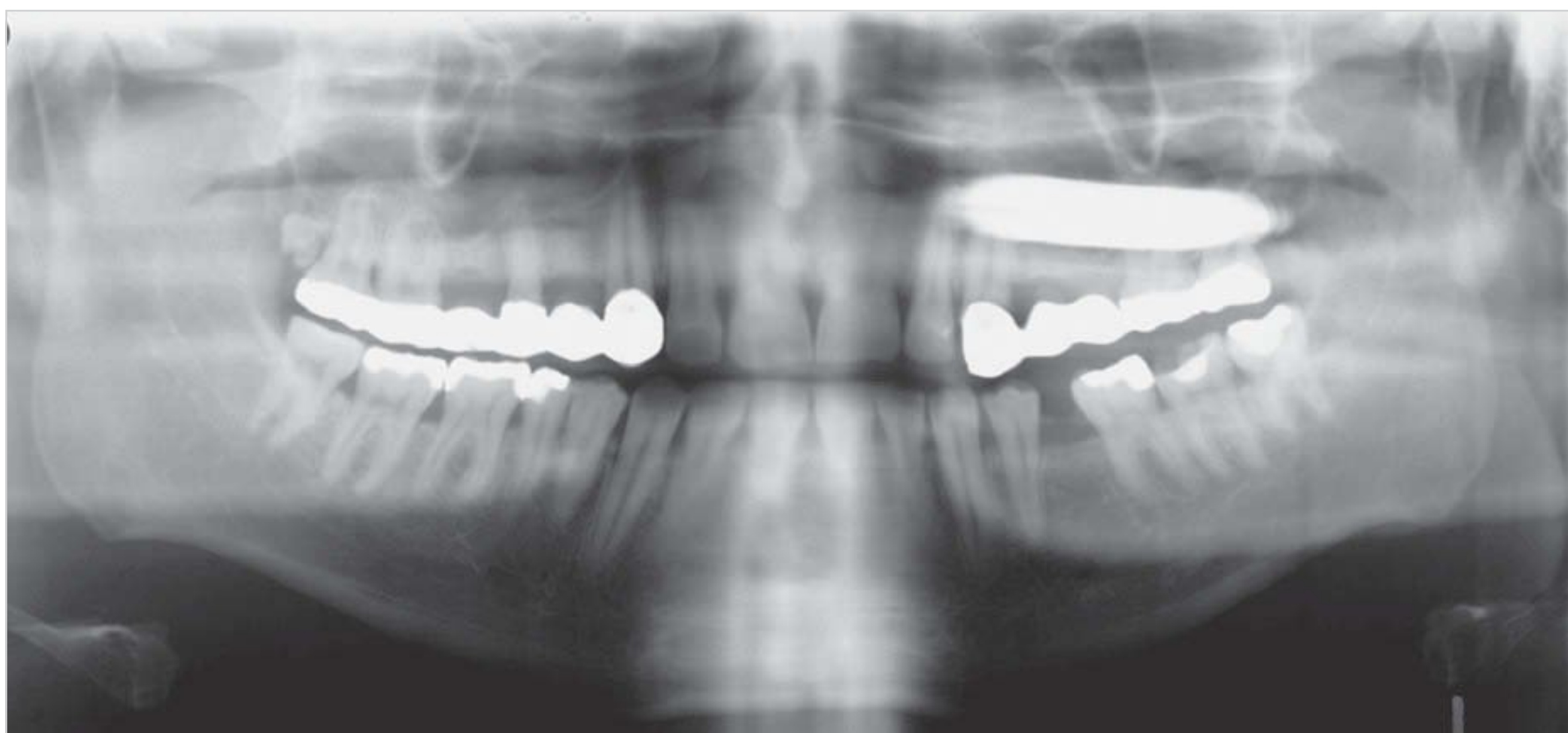


Fig. 9.116 Ghost images of right maxillary crowns located in the rotation center.

While earlobe shadows are usually easy to identify and generally cause no radiographic problems, owing to their lateral position, soft-tissue shadows of the nose, nasal conchae, and soft palate may sometimes lead to confusion (□ Fig. 9.117).

□ Nasal conchae: The panoramic radiograph is a tomographic image with a relatively large slice thickness (in the order of 10–25 mm). Therefore, this X-ray technique is chiefly indicated for imaging areas with no structures that are situated close together. This mainly applies to the mandibular arch, but also applies to the maxilla.

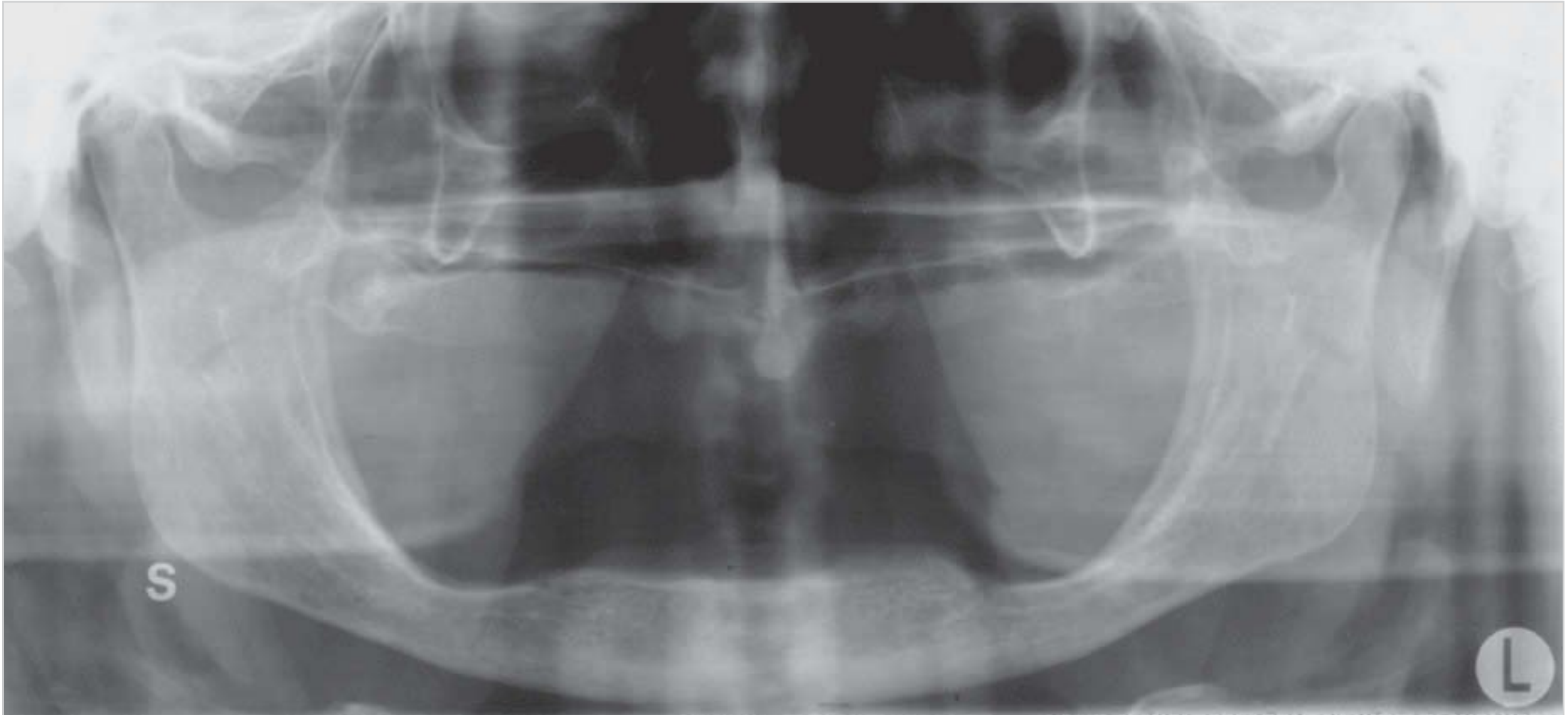


Fig. 9.117 Soft-tissue shadows of the nose and ear lobe on a panoramic radiograph.

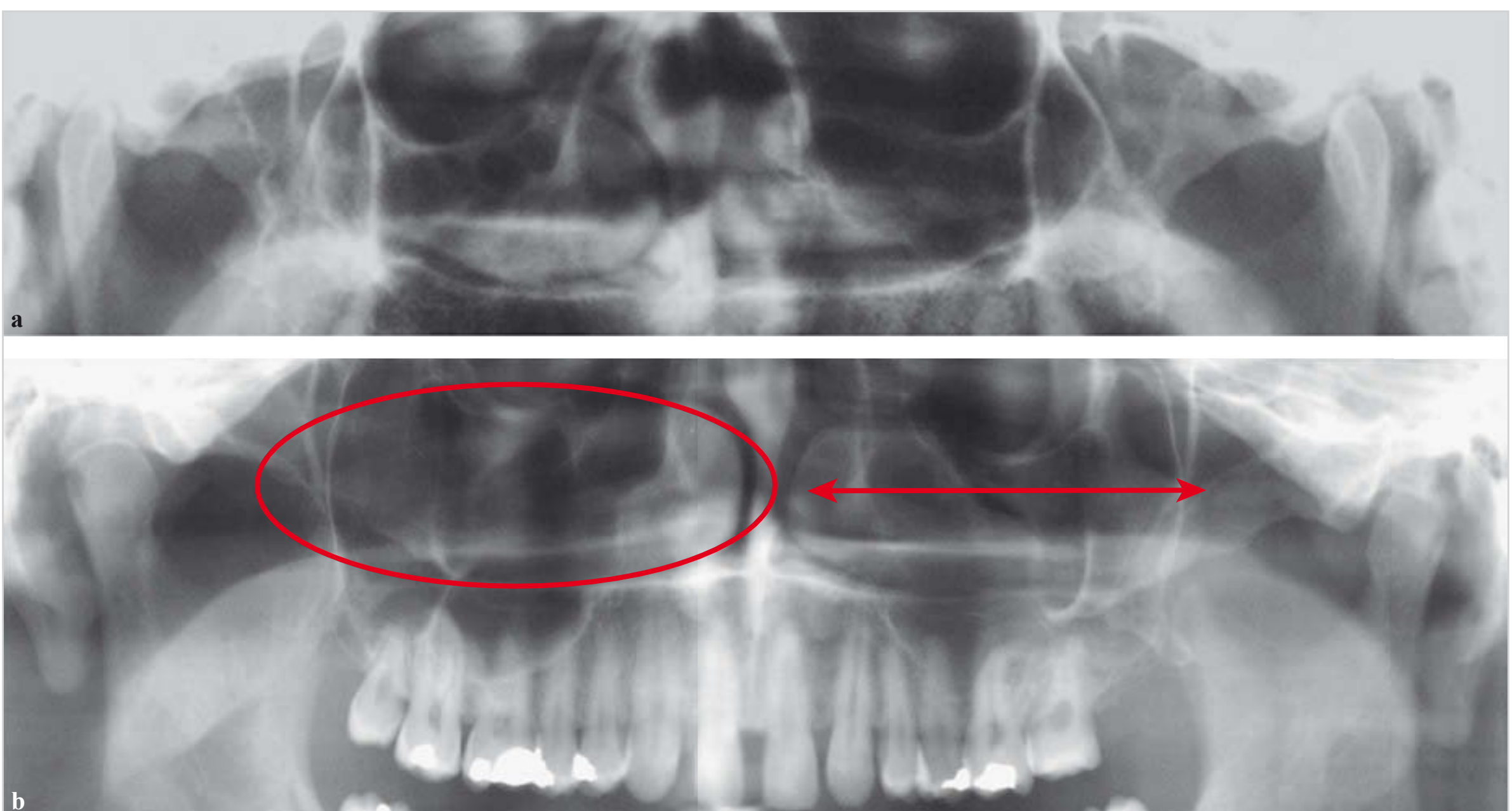


Fig. 9.118a, b Shadows caused by the nasal conchae.

a Marked right nasal concha.

b Extension of the nasal conchae. The oval marks the right nasal concha. The double-ended arrow shows the shadow of the left nasal concha extending in the frontal and anteroposterior direction.

Panoramic image quality becomes critical in parts of the maxilla superior to the hard palate and nasal floor, where the nasal cavity lies in close proximity to the maxillary sinus. Neither area can be displayed separately on panoramic radiographs because the image layer is not thin enough. This is why comprehensive panoramic radiographic diagnosis of the sinus cavity is not possible (and may even be dangerous).

Basal maxillary sinus shadows with a clearly identifiable, characteristic shape (e.g., a mucocele or odontogenic cyst) and location on the floor of the maxillary sinus can be diagnosed with a high degree of confidence. More superi-

orly located lesions or changes cannot be reliably detected or interpreted by panoramic radiography (□ Fig. 9.118).

Overlapping structures on thick-layer panoramic images can be interpreted well by magnetic resonance imaging, which can be used for separate assessment of the nasal cavity and maxillary sinus (□ Fig. 9.119).

□ Soft-tissue shadow of the nose: If the focal trough is too far anterior, or for anatomical reasons, the nose may appear as a soft-tissue shadow in the maxillary anterior region that cannot immediately be interpreted with certainty (□ Fig. 9.120).

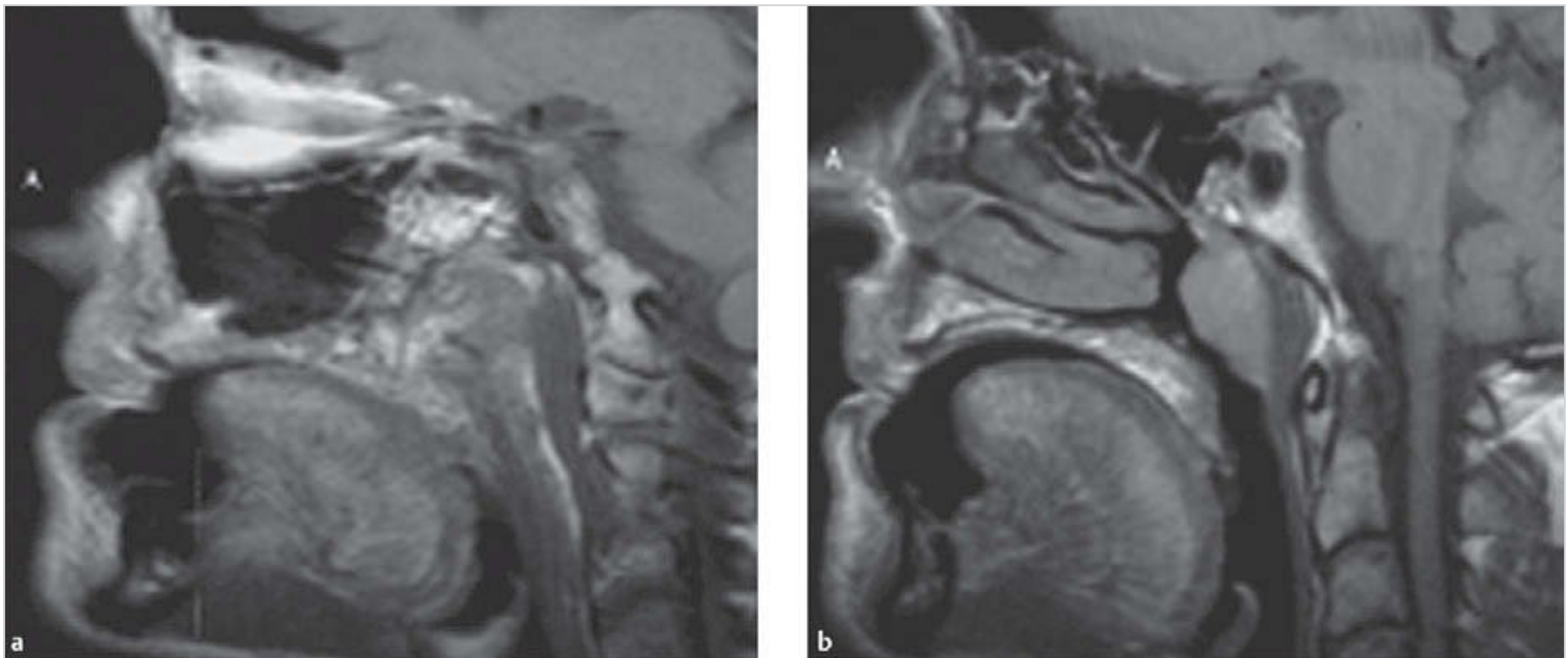


Fig. 9.119a, b Nasal conchae and maxillary sinuses.

a Maxillary sinus.

b Nasal conchae.

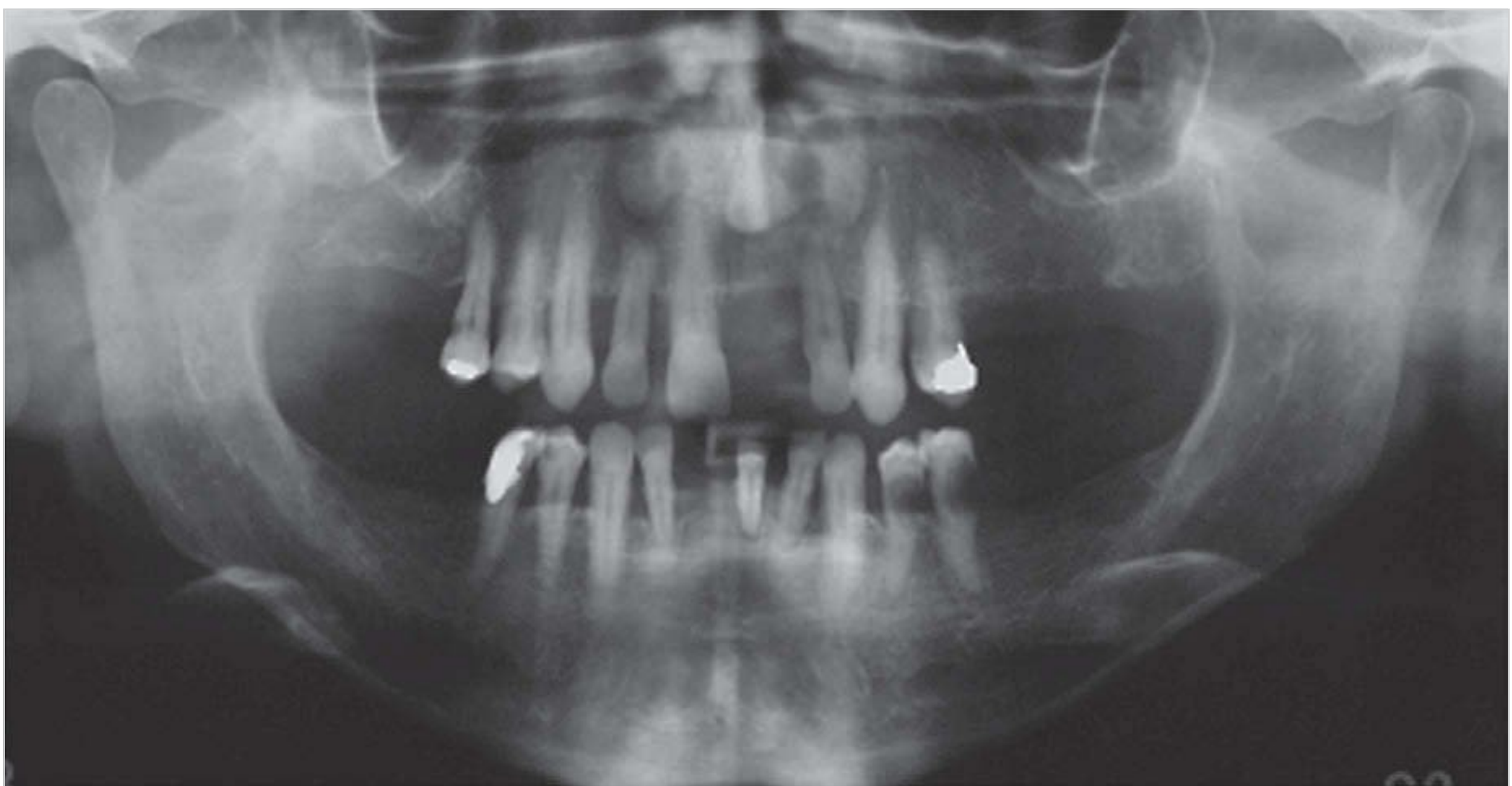


Fig. 9.120 Soft-tissue shadow of the nose in the upper anterior region of a panoramic radiograph.

□ Soft palate: The panoramic appearance of the soft palate is variable. The only way it can be identified is by the presence of air from the nasopharynx and oral cavity along its borders. It can usually be identified as an elongated soft-tissue structure that extends slightly downward. Owing to tongue and swallowing movements, the shape of the soft palate may vary or it may not be visible at all (□ Fig. 9.121).

□ Tongue shadow: Because the tongue is positioned in the lower part of the oral cavity, there is an air-filled space between the dorsum of the tongue and the hard palate. This air-filled space may appear as a black field of interference on panoramic radiographs, extending from the soft palate from the right side to the left.

This may completely obscure the roots of the maxillary teeth. If obscured by the tongue “shadow,” the roots can no longer be made visible, especially when digital systems are used.

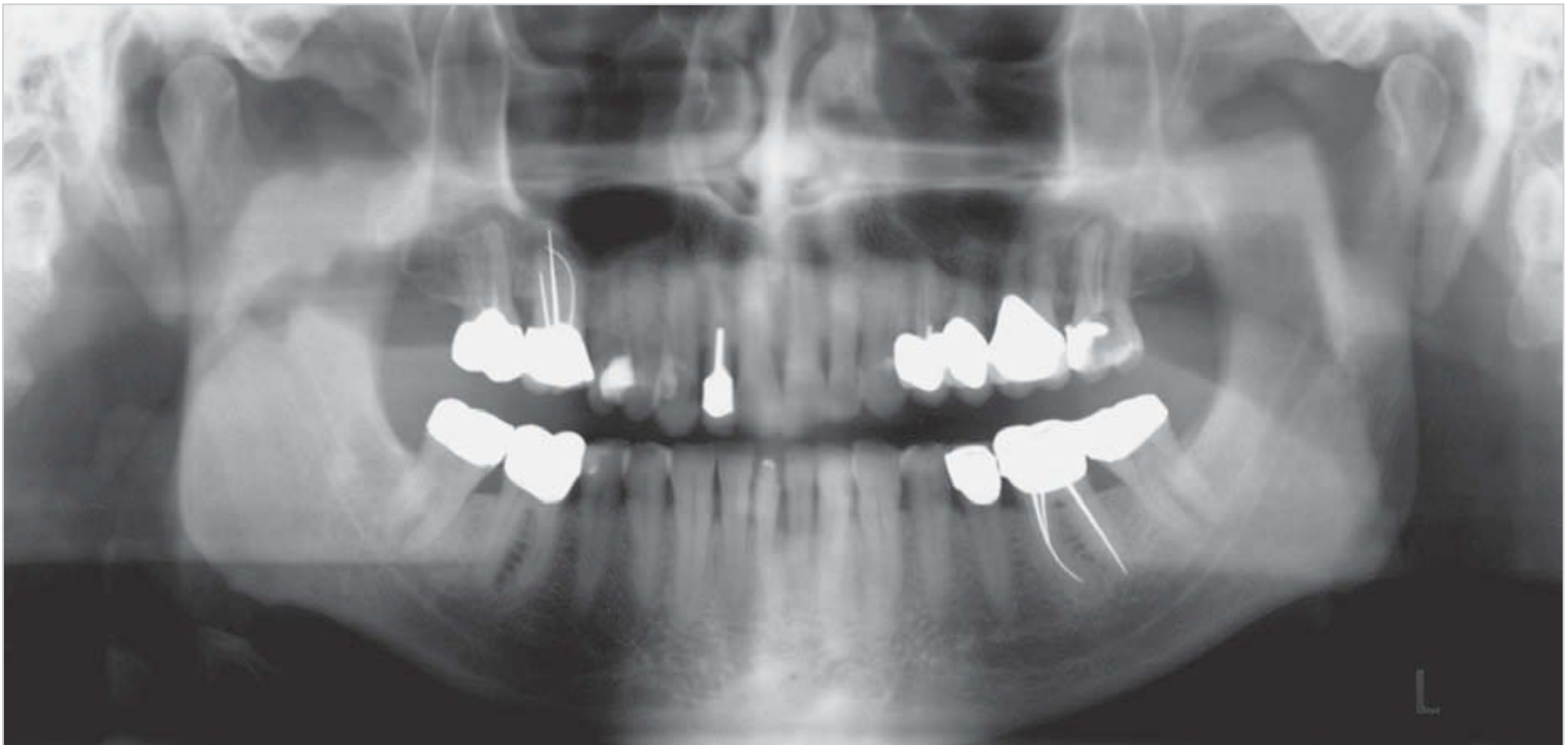


Fig. 9.121 Panoramic appearance of the soft palate as rectangular shadow on the left, and as a sausage-shaped shadow on the right.

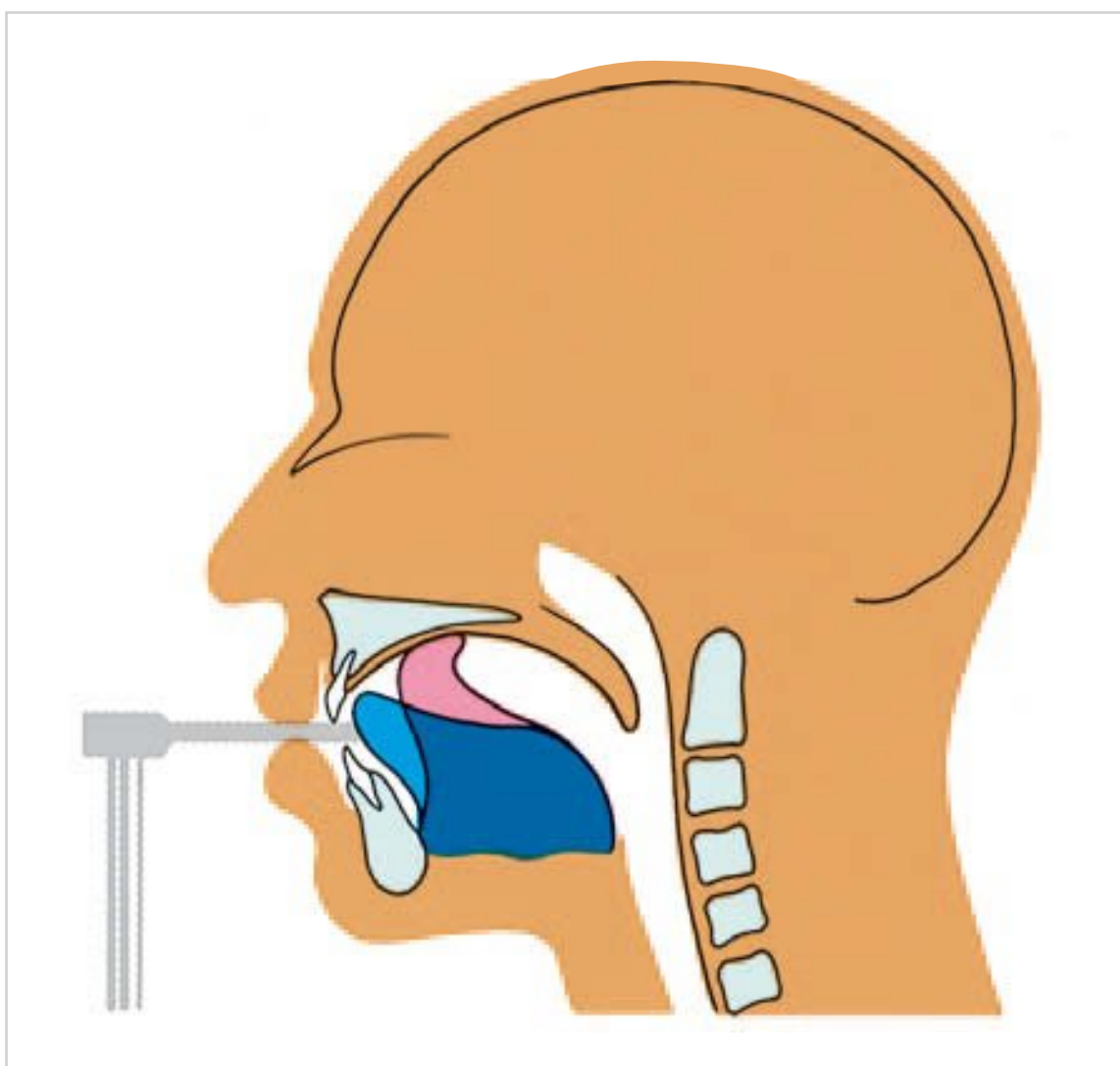


Fig. 9.122 Correct tongue position for panoramic radiography (schematic). The tongue should be pressed against the roof of the mouth during the exposure. (From: Pasler FA, Visser H. Zahnmedizinische Radiologie. 2nd ed. Stuttgart: Thieme; 2000. Farbatlant der Zahnmedizin; Band 5.)



Fig. 9.123 The tongue is clearly seen on this lateral cephalogram.

Practice

It is therefore of utmost importance to ensure that the patient's tongue is pressed well against the nasal floor and hard palate during the exposure cycle. Because of its muscle mass, the tongue acts as a filter, and more radiation is absorbed (□ Fig. 9.122 and □ Fig. 9.123).

If the tongue is not positioned against the roof of the mouth, a radiolucent zone will appear that may partial-

ly or completely obscure diagnostic information (□ Fig. 9.124).

On the repeat radiograph, successful imaging of the maxilla was achieved because the tongue was firmly pressed against the roof of the mouth (□ Fig. 9.125).

Because the patient forgot to press the tongue against the palate at the beginning of the exposure, a conspicuous black air artifact appeared in the left maxillary region. Later, as the right side was being exposed, the patient pressed the tongue against the roof of the mouth (□ Fig. 9.126).



Fig. 9.124 Tongue shadow due to improper tongue positioning is clearly seen on this panoramic radiograph.



Fig. 9.125 There is no tongue shown on this panoramic radiograph because the tongue was properly positioned against the roof of the mouth during the exposure.

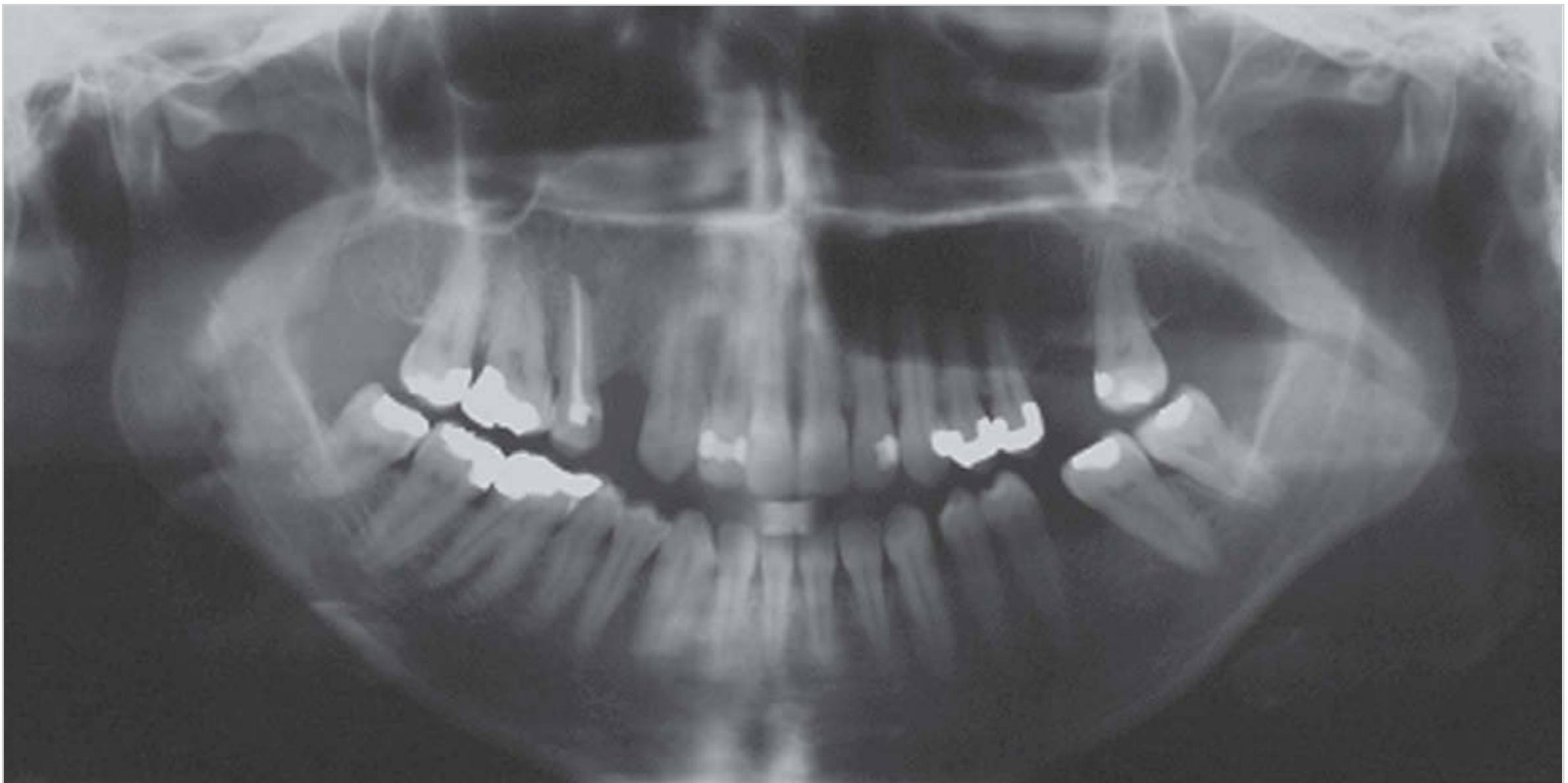


Fig. 9.126 Because the tongue was not positioned against the roof of the mouth at the beginning of the exposure, a black stripe appeared in the left maxillary region of the panoramic radiograph. Later, when the beam scanned the right maxillary region, the tongue was properly positioned against the hard palate.

Practice

To be able to press the tongue against the palate correctly, the patient must be told how to do so just before each exposure. To avoid faulty radiographs and unnecessary radiation exposure, the correct tongue position should be practiced before the patient is positioned in the machine. This takes a little more time but certainly helps to improve diagnostic image quality.

9.4 Cone Beam Computed Tomography

CBCT, also known as digital volume tomography, is the first fully fledged tomographic technique designed specifically for the field of dental, oral, and maxillofacial radiology that was capable of providing optimal tomographic images of osseous structures of the facial skeleton. CBCT can be considered the direct successor to conventional tomography based on the blurring principle. Unlike conventional tomography, CBCT is readily available for dental, oral, and maxillofacial radiology. Because of its cutting-edge technology, CBCT has a much larger imaging spectrum than tomography based on the blurring principle.

In the late 1990s, the NewTom became the first CBCT system available for in-office use. The NewTom CBCT unit may look very similar to a conventional computed tomography (CT) machine on the outside but, on closer

inspection, fundamental differences in the internal technology of the two systems become evident.

9.4.1 Technique and Image Formation in Cone Beam Computed Tomography

Technical Developments from Computed Tomography to Cone Beam Computed Tomography

CT was independently introduced by Godfrey N. Hounsfield and Allan McCormack in 1972, as a technique capable of producing tomographic images by a method that was completely different from conventional tomography based on the blurring principle.

In CT, the X-ray tube and the digital detector array revolve around the patient in a circular movement (to generate cross-sectional [slice] images using a finely collimated, fan-shaped X-ray beam). Modern third- and fourth-generation CT scanners use a significantly enlarged fan-beam. This aperture enlargement serves to ensure more efficient utilization of X-rays. However, because only a small area of skin is exposed, multiple rotations of the tubehead around the patient are needed to expose a given volume of tissue. By using a larger collimator aperture, the X-ray tube can be moved continuously without linear displacement. This results in a substantial reduction of rotation time.

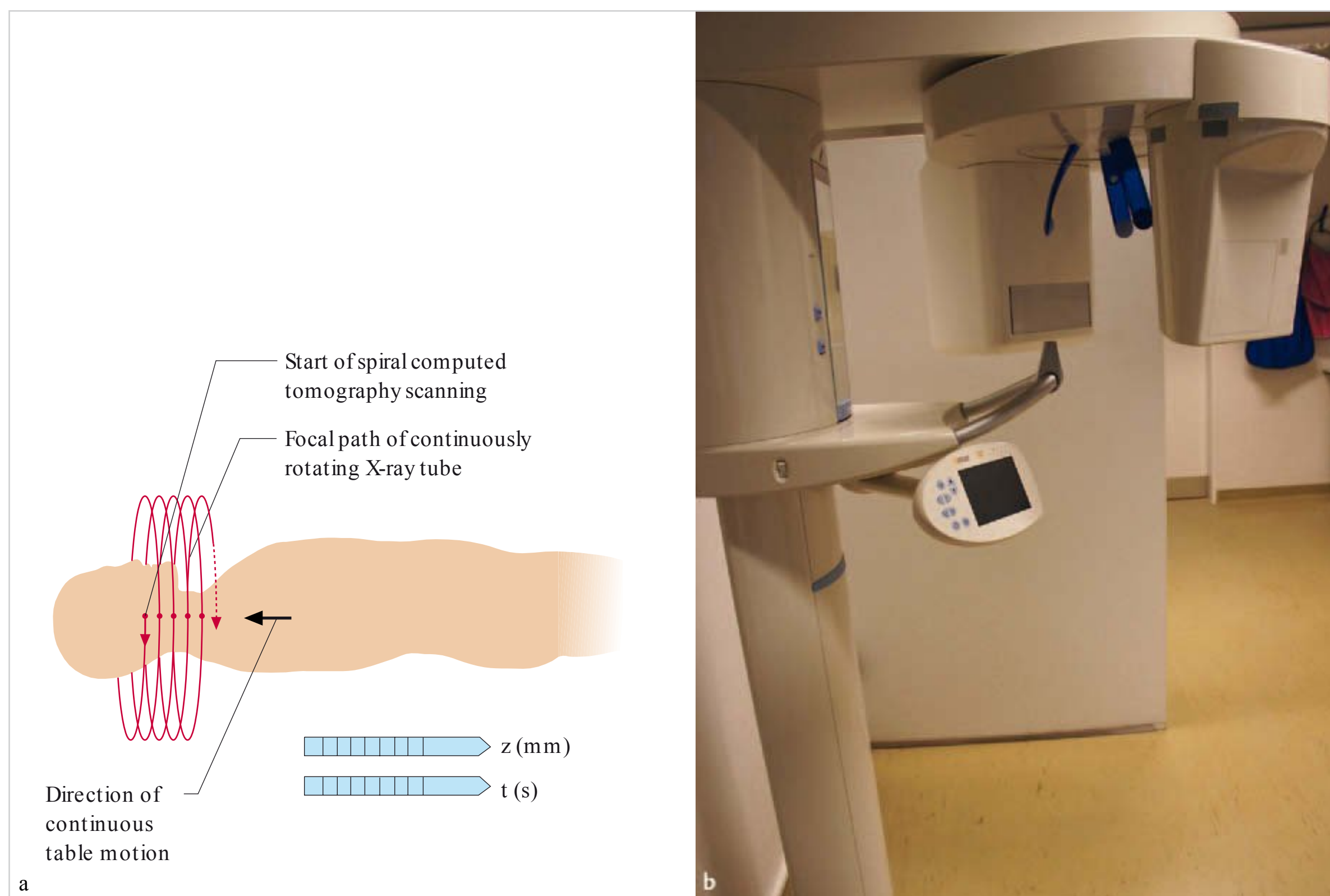


Fig. 9.127a, b Spiral computed tomography.

a Schematic. z : slice thickness; t : time. (From: Pasler FA, Visser H. Zahnmedizinische Radiologie. 2nd ed. Stuttgart: Thieme; 2000. Farbatlanten der Zahnmedizin; Band 5.)

b Orthophos XG 3D cone beam machine with combined digital CBCT and panoramic imaging capabilities.

Spiral CT, introduced by Willi Kalender in 1989, was a significant advance in CT technology. In spiral CT, the patient lies on a motorized table, which is continuously advanced through the gantry while the X-ray tube and detectors revolve around the patient. Although multiple rotations of the X-ray tube are still required to image the area of the body being investigated, this technique produces a continuous image without gaps between slices (□ Fig. 9.127a).

The next advance in CT technology was the integration of an additional collimator aperture and utilization of the full beam for the acquisition of a complete dataset. These machines, which have a cone-shaped beam and fan-shaped detector array, basically represent another new generation of CT scanners. Because of the large volume of the X-ray beam, they can image the entire volume of an organ in only one rotation.

Currently, this technique can only be used to image small anatomical structures, owing to equipment size constraints and the very complex imaging geometries. This special CT imaging procedure is particularly well suited for imaging the facial skeleton—the focus of dental, oral, and maxillofacial radiographic diagnostics.

A new digital volumetric CBCT system developed specifically for dental applications was introduced by Mozzo and colleagues in 1998. This marked the start of the development of digital volumetric CBCT and its use in dental, oral, and maxillofacial radiology (□ Fig. 9.127b).

Data Reconstruction and Image Formation

When an X-ray beam travels through tissues, all structures in the path of the beam attenuate the beam to different degrees, resulting in a greater or lesser degree of blackening of the film or image receptor. The degree of blackness is the sum (of radiographic densities) of all irradiated structures. A single exposure does not provide enough data to determine the exact location where a given amount of absorption took place. To determine the spatial distribution, a sufficiently large number of exposures must be taken from many different angles. Therefore, scanners take at least 200 exposures per rotation around the patient's head. Pulsed radiation is generally used, but continuous radiation may be used for small-volume scanning, to improve image quality and to achieve shorter rotation times.

Absorption values for each projection can be mathematically back-calculated to precise spatial positions of a given slice. Each absorption value can thus be mapped back to the exact spatial position where the absorption took place within the irradiated tissue.

In CT, a two-dimensional dataset is generated as an axial tomographic image. The computer software transforms the two-dimensional axial slice images into a three-dimensional image, which ideally should not contain any gaps between slices. In spiral CT, the individual slices are combined without gaps, so that three-dimensional volumetric datasets can be acquired.

CBCT systems can directly generate three-dimensional volumetric datasets, owing to the cone-beam geometry. Most CBCT systems use flat panel detectors, but some use image intensifiers. The detectors consist of charge-coupled device (CCD) or complementary metal oxide semiconductors (CMOS) image sensors. Image intensifiers use phosphors such as cesium iodide.

Image formation is by primary and secondary reconstruction.

Primary Reconstruction

Several steps are involved in transforming raw data into a reconstructed image by mapping the attenuation coefficients (absorption characteristics, gray-scale values) of the individual volumes of irradiated tissue. Mapping of the precise spatial distribution of the attenuation coefficients is of critical importance for diagnostic image quality.

The mathematical foundation for the reconstruction of CT images was laid by the Bohemian mathematician Johann Radon, who, in 1917, proposed a CT reconstruction algorithm using the attenuation coefficients as the basis of calculation. His mathematical method of filtered back projection and different modifications of it are still used for CT image reconstruction today.

Filtered back projection is also used in CBCT image reconstruction. Because of its cone-beam geometry, CBCT is a mathematically more challenging back-projection problem than conventional fan-beam CT, which involves less volumetric data. Radon's filtered back projection alone is not sufficient for CBCT image reconstruction. Therefore, the Feldkamp algorithm, proposed in 1984, is also commonly used for CBCT image reconstruction today.

The volumetric dataset consists of a grid of cubic volume elements, or *voxels*, in three-dimensional space. The voxel is the three-dimensional variant of the pixel. Each voxel is assigned a gray-scale number (representing the degree of attenuation of the X-ray beam by the material within the voxel). Each position of the object is assigned an exact gray-scale number in three-dimensional space

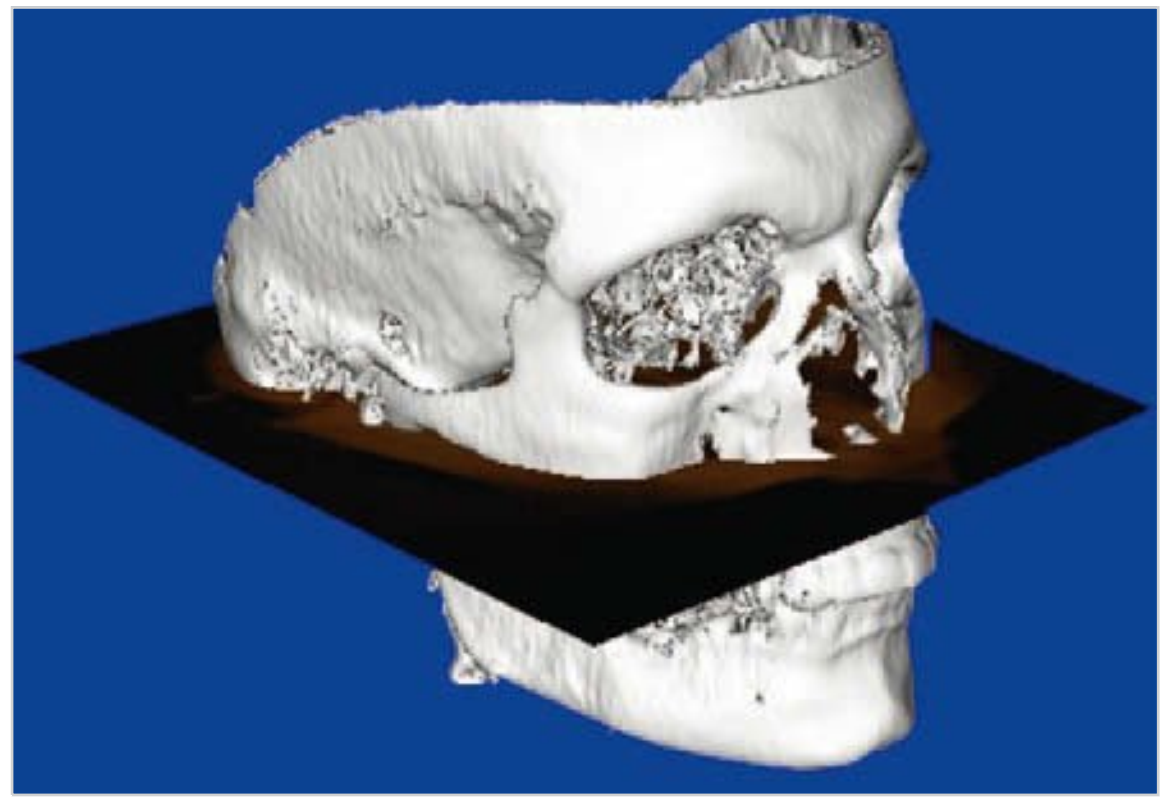


Fig. 9.128 Result of a CBCT reconstruction. After primary reconstruction, various secondary reconstructions (e. g., axial, sagittal, and coronal views) can be performed.

by means of back projection. From the sum of voxels in the irradiated region, secondary reconstruction is performed to create a reconstructed CBCT image that, to a great degree, reflects the anatomical and pathological conditions within the region (□ Fig. 9.128).

Secondary Reconstruction

The processed volumetric dataset can be used to generate images of any desired cross-sectional slice of the scanned object. In addition to the typical sagittal, coronal, and axial views used in cranial diagnostics, it is also possible to reconstruct cross-sectional views adapted to the specific questions addressed in dental, oral, and maxillofacial radiology (□ Fig. 9.129, □ Fig. 9.130, □ Fig. 9.131).

The diverse possibilities to reconstruct basically any slice plane from the volumetric dataset makes CBCT so especially interesting for dental, oral, and maxillofacial radiology.

The anatomy of the facial skeleton is very complex. This applies not only to bony structures of the face, but also, and equally, to the teeth and the adjacent bony structures of the maxilla and mandible. Preformed standardized slices have proved unsatisfactory for visualization of the small individual anatomical structures in the dental field. CBCT must provide the opportunity to create a custom slice for each region.

The intraoral or panoramic radiograph is a finished radiograph whose projection geometry cannot be changed. In CBCT, on the other hand, the practitioner must individually select the slice that is most appropriate for the clinical question. This is precisely the area where the problems and the diverse diagnostic possibilities of CBCT lie close together (□ Fig. 9.132 and □ Fig. 9.133).



Fig. 9.129 Orthopantomogram showing radiolucencies of unclear etiology in the lateral mandible.

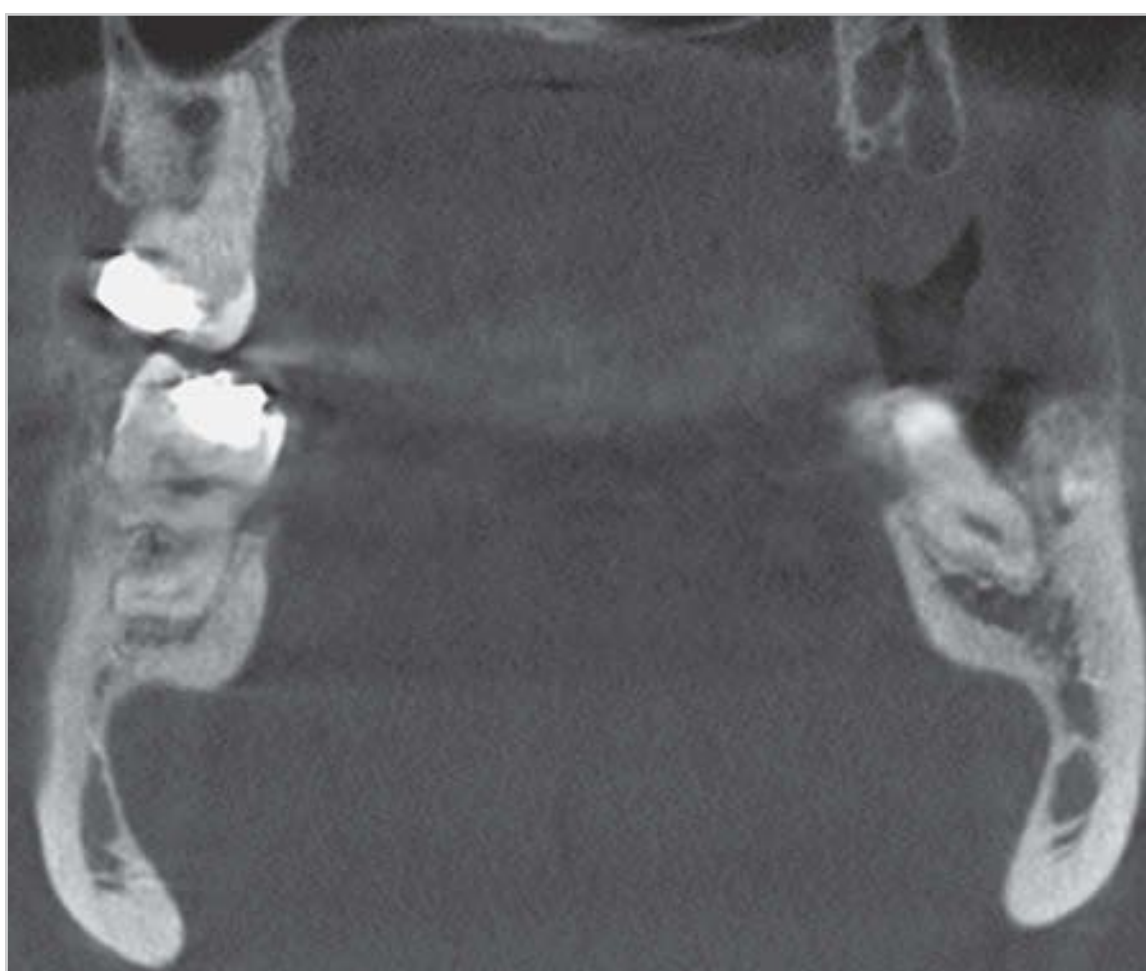


Fig. 9.130 This secondary coronal reconstruction shows a normal anatomical variant of the mandible. Because of the low thickness, hypodense areas appear in the lateral view.

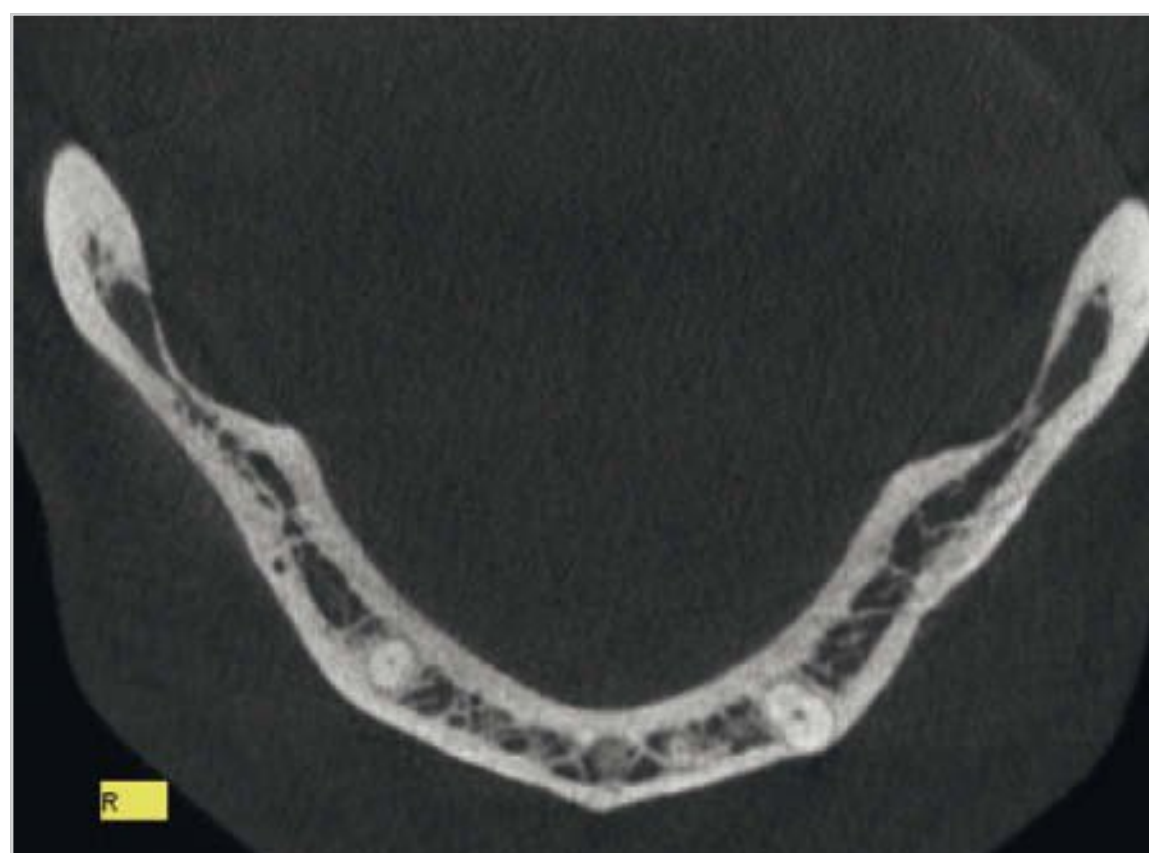


Fig. 9.131 The normal variant is clearly identifiable in the axial view (cf. □ Fig. 9.130).

with CT are artifacts caused by filtered back projection, and relatively high radiation exposure.

9.4.2 Limitations of Computed Tomography and Cone Beam Computed Tomography

CT is the standard imaging modality used to answer most clinical questions across the entire field of medicine. It is capable of producing three-dimensional images with very good image quality. Two disadvantages associated

Artifacts

Metal artifacts are among the easiest artifacts to spot on CT images. They occur when an object produces such strong absorption of radiation that it cannot be compensated by back projection. Partial volume artifacts are another major type of artifact to look out for. They manifest as extinction effects in reconstructions with large contrast differences between the target object and its



Fig. 9.132 Secondary reconstruction corresponding to an orthopantomogram.

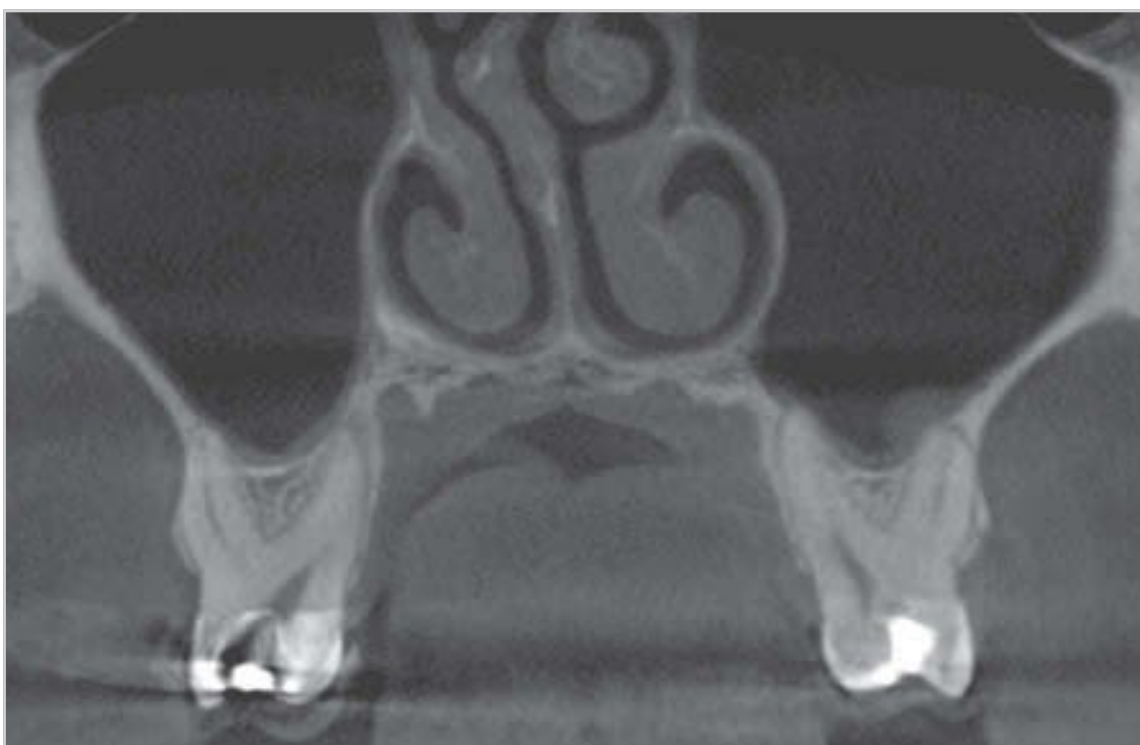


Fig. 9.133 In contrast to the classical orthopantomogram, views of the maxillary sinus can also be reconstructed from the dataset.



Fig. 9.134 Motion blur on a CBCT scan.

surroundings. Motion artifacts play a minor role in CT, but may become significant as the irradiated volume increases.

CBCT is also subject to metal artifacts, but to a much lesser extent. Volume artifacts may also occur. Motion artifacts can be considered a major disadvantage of CBCT (□ Fig. 9.134).

Radiation Exposure

A major advantage of CBCT is that radiation exposure is significantly lower than that with conventional CT. The main reason is that the three-dimensional volumetric dataset is acquired in a single rotation of the beam and scanner. In addition, much lower milliamperere levels are needed for CBCT scans.

According to the guidelines for CBCT, the effective dose is significantly lower than for conventional CT.

According to literature sources, effective doses for conventional CT range from 180 to 2,100 μSv , while those for most CBCT systems range from 11 to 674 μSv . In practice, however, effective doses of only 11 to 96.2 μSv are used, especially for dental implant planning.

The ICRP 2007 recommendations provide the following effective doses for routine dental procedures:

- Cephalometric radiograph: 5.6 μSv
- Panoramic radiograph, digital: 2.7 to 24.5 μSv
- Intraoral radiograph: 34.9 to 388 μSv
- CBCT: 11 to 674 μSv
- CT: 180 to 2,100 μSv .

Actually, the only “price” for the lower radiation dose is that CBCT is unsuitable for soft-tissue imaging. However, this is not needed for most of the clinical questions posed in dental, oral, and maxillofacial radiology.

9.4.3 Volume Size

Since all data for CBCT are collected in a single rotation, the volume size for a given clinical question must always be selected before starting the scan.

The first digital CBCT machines had large volume sizes (field of view: 15–18 cm) that could provide a complete picture of the whole facial skeleton in its entirety. Over time, CBCT systems were developed that had smaller volumes of around 5 × 5 cm to 8 × 8 cm. Large volumes continue to be used parallel to the smaller volumes. Considering the size of the jaw region, a volume size of ~8 × 8 cm should be quite sufficient for most indications.

Two main advantages of using smaller volumes are lower radiation doses and shorter reconstruction times. Because sensor size also determines the price of a CT system, CBCT systems also cost less than conventional CT systems. Furthermore, much higher image quality can be achieved by using smaller volumes. Among other things, this has led to an expansion of clinical indications for CBCT because modern CBCT systems can depict even very small anatomical structures in excellent detail (□ Fig. 9.135 and □ Fig. 9.136).

9.4.4 Clinical Indications for Cone Beam Computed Tomography

Three-dimensional imaging is necessary when conventional two-dimensional images fail to provide sufficient information to answer the clinical question. Supplementary three-dimensional radiographic imaging should contribute to supporting therapeutic decision-making. The purpose is to provide a better overview for surgical and other treatment planning.

The need for supplementary diagnostic procedures is strongly dependent on the experience of the clinician. Ultimately, the justifying indication determines whether CBCT is necessary.

Basic Rules for the Generation of Individual Reconstructions

Diagnosis based on cross-sectional CBCT images requires proper application of the known rules of intraoral and extraoral panoramic radiography. The production of anatomically correct views of the upper and lower jaw and teeth is of central importance.

The most basic rule is that the beam must be perpendicular to the long axis of the teeth for orthogonal imaging. Proper application and use of the tools supplied with each respective CBCT system is the prerequisite for achieving this goal.

Similar to panoramic radiography, the slice thickness and position of CBCT reconstructions can be varied. These two parameters must always be considered when taking cross-sectional images. The choice of slice position is of major importance. The slice plane should always be positioned at right angles to the anatomically relevant axes of the maxilla and mandible and to the axes of the diagnostically relevant teeth.

Correct adjustment of these parameters requires an exact knowledge of the anatomy and a good spatial imagination.

If these basic rules are ignored or followed incorrectly, then there is a risk that the anatomical situation and/or any pathological changes that might be present will be misinterpreted. Arbitrary plane selection results in a lack of comparability and increases the risk that important details will be overlooked.

It is important to ensure that the center of the slice is exactly parallel to the object it passes through (□ Fig. 9.137). All other slices must be at a right angle to the object. If the slice axis deviates by several degrees, then the image of the scanned structures will not be anatomically correct (□ Fig. 9.138).

Indications for Cone Beam Computed Tomography

Clinical indications for CBCT have developed in all areas of dental, oral, and maxillofacial radiology over the years. In the beginning, CBCT was mainly used for planning dental implants, which is still the main indication for the examination. Over time, however, indications for CBCT have developed over the entire field of dentistry.

CBCT should only be used if the three-dimensional images will provide important new information that is needed to answer the clinical question. The implications for treatment should always be taken into account when considering a referral for CBCT.

If a panoramic or intraoral radiograph alone does not provide sufficient diagnostic information, a CBCT examination is generally justified.



Fig. 9.135 Panoramic reconstruction with a spherical volume of 16 cm.

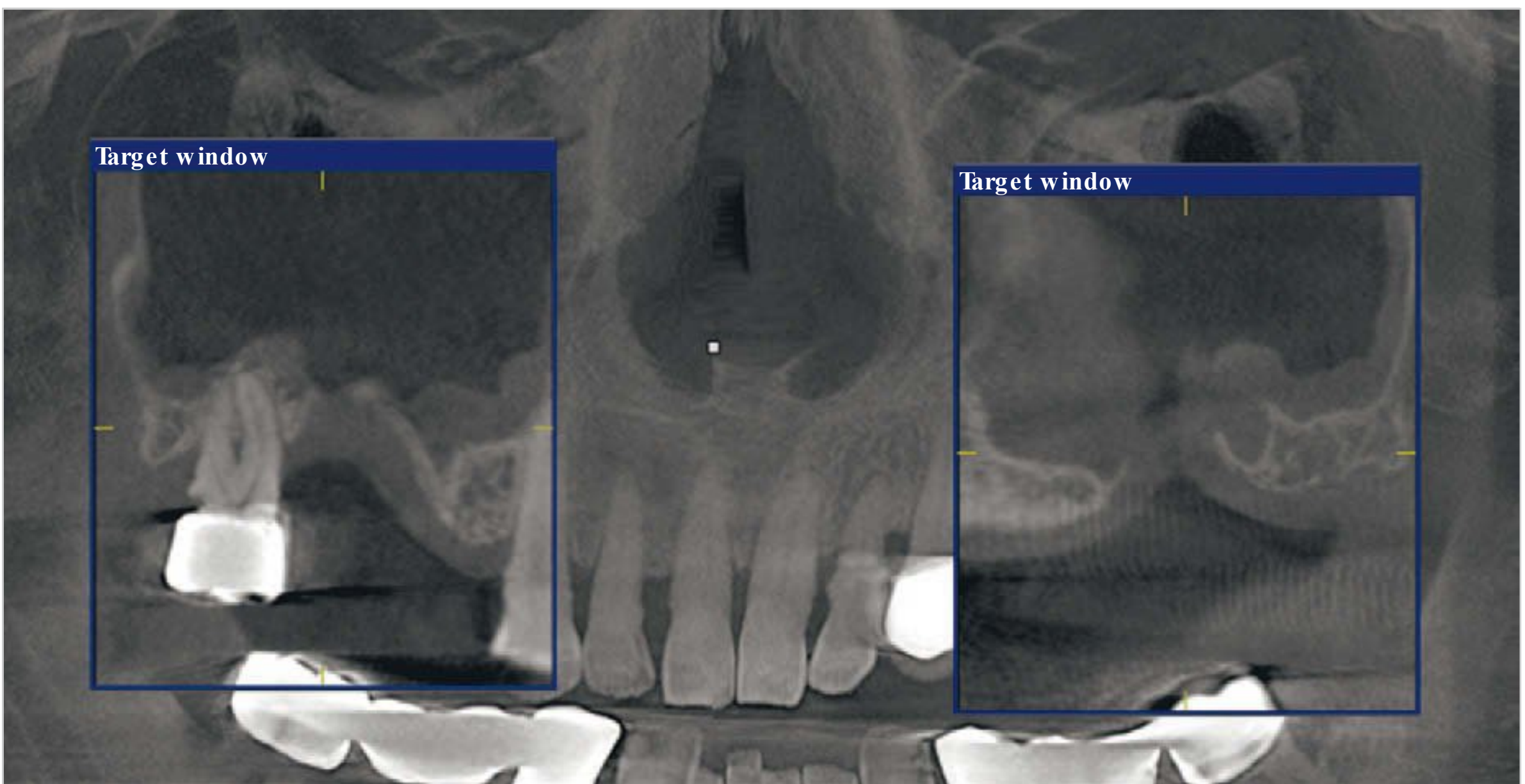


Fig. 9.136 Bilateral arteriovenous malformation visualized by panoramic image reconstruction.

In one case example, plain film radiography and clinical examination did not provide sufficient information to determine whether osteolysis and root fracture were present in an endodontically treated tooth 26 (□ Fig. 9.139). High-resolution multiplanar reconstruction images obtained by CBCT were needed to reveal the true extent of inflammation (□ Fig. 9.140 and □ Fig. 9.141).



Fig. 9.139 Intraoral radiograph of endodontically treated tooth 26.

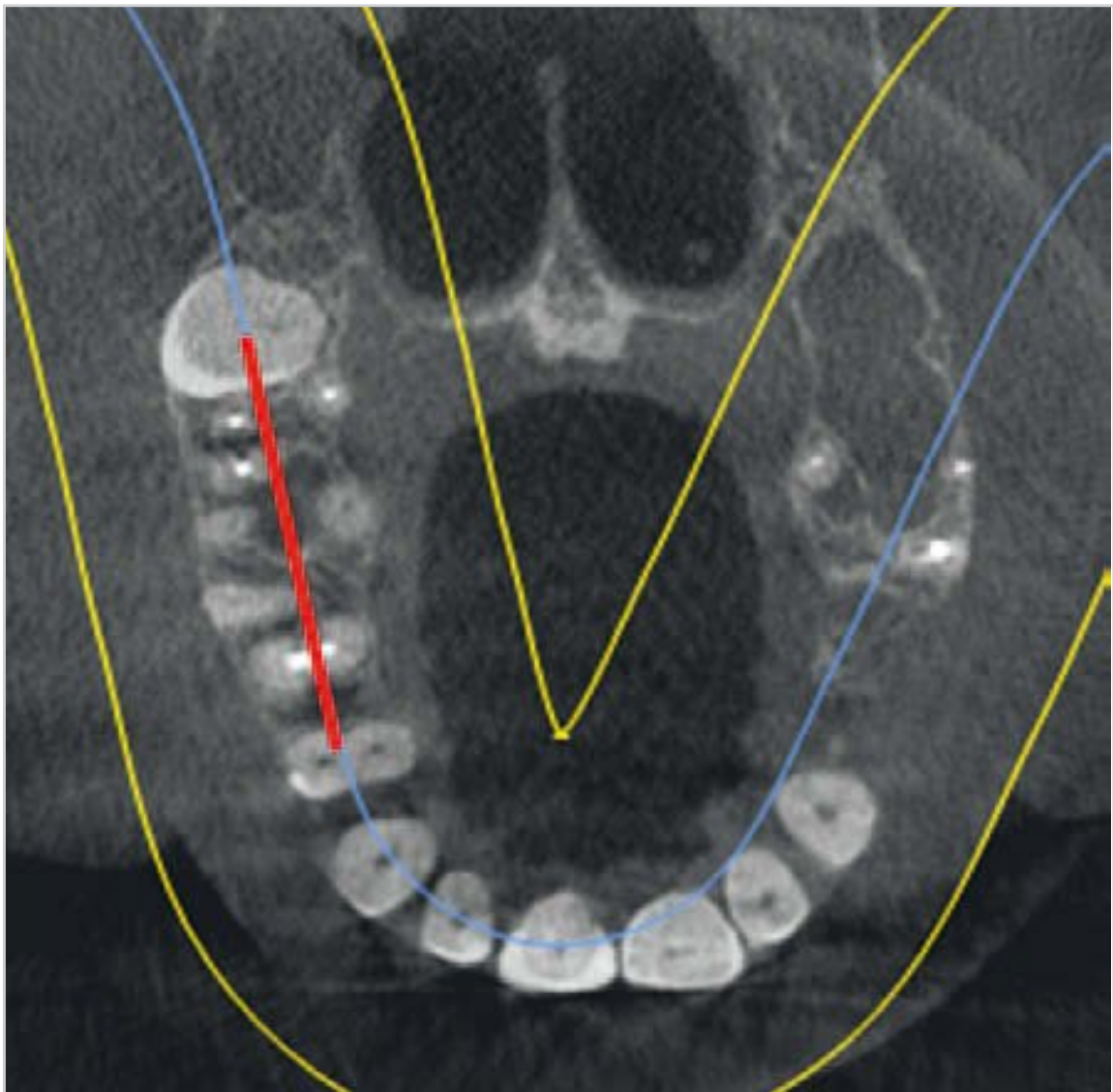


Fig. 9.137 Correct position of the image layer in the upper arch (red and blue lines). The layer thickness is marked by the yellow line.

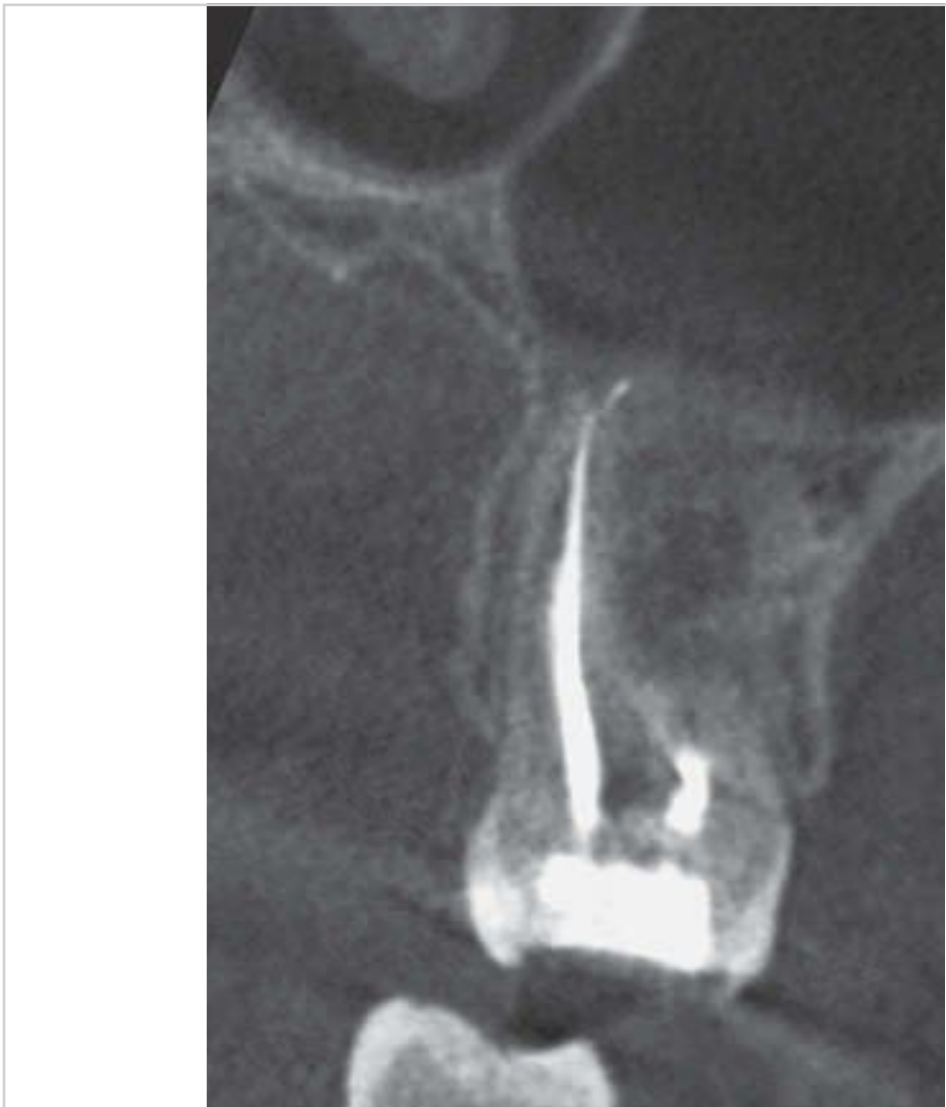


Fig. 9.140 CBCT coronal view of tooth 26.

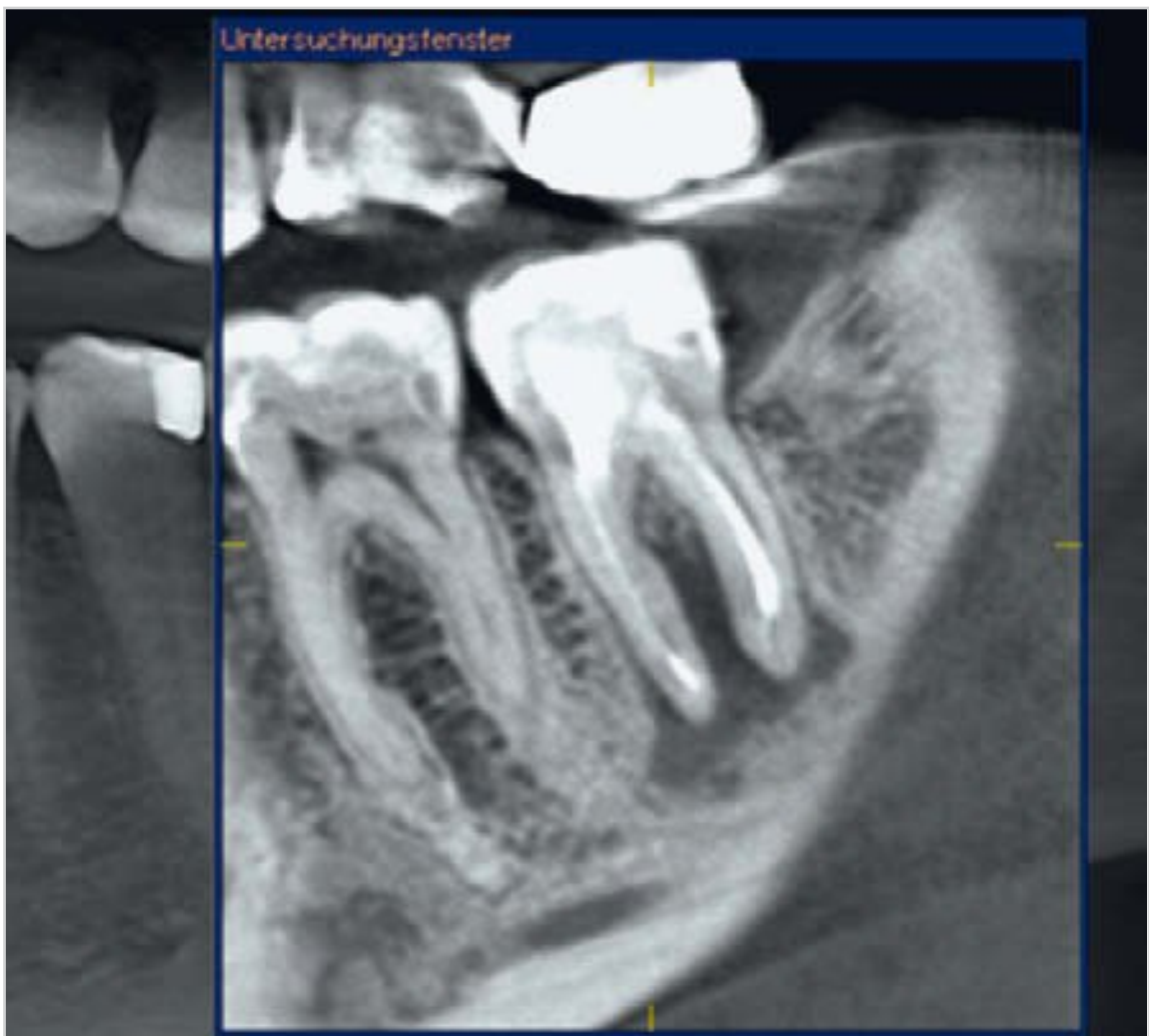


Fig. 9.138 Incorrect position of the image layer in the lower arch.



Fig. 9.141 CBCT axial view of tooth 26.

In a second case example, plain film radiographic findings were equivocal for oro-antral communication (□ Fig. 9.142). The oro-antral communication could be seen unequivocally on the adjunct CBCT images of the right and left mandible (□ Fig. 9.143 and □ Fig. 9.144).



Fig. 9.142 Conventional panoramic radiography was equivocal for oro-antral communication.



Fig. 9.143 Oro-antral communication was unequivocally shown by CBCT (left mandible).



Fig. 9.144 Oro-antral communication was unequivocally shown by CBCT (right mandible).

1

Chapter 10

Anatomy and Topography of the Facial Skeleton

10.1 The Teeth and Tooth-supporting Structures	121
10.2 The Mandible	123
10.3 The Maxilla	124
10.4 Panoramic Radiographic Anatomy	125

10 Anatomy and Topography of the Facial Skeleton

A precise knowledge of radiographic anatomy is essential for the correct interpretation of radiographs. Comprehension of their arrangement in three-dimensional space is also of fundamental importance.

In contrast to photography, the diagnostic interpretation of radiographs depends not only on the visible image, but also on the beam path (projection) underlying the process of image formation (□ Fig. 10.1).

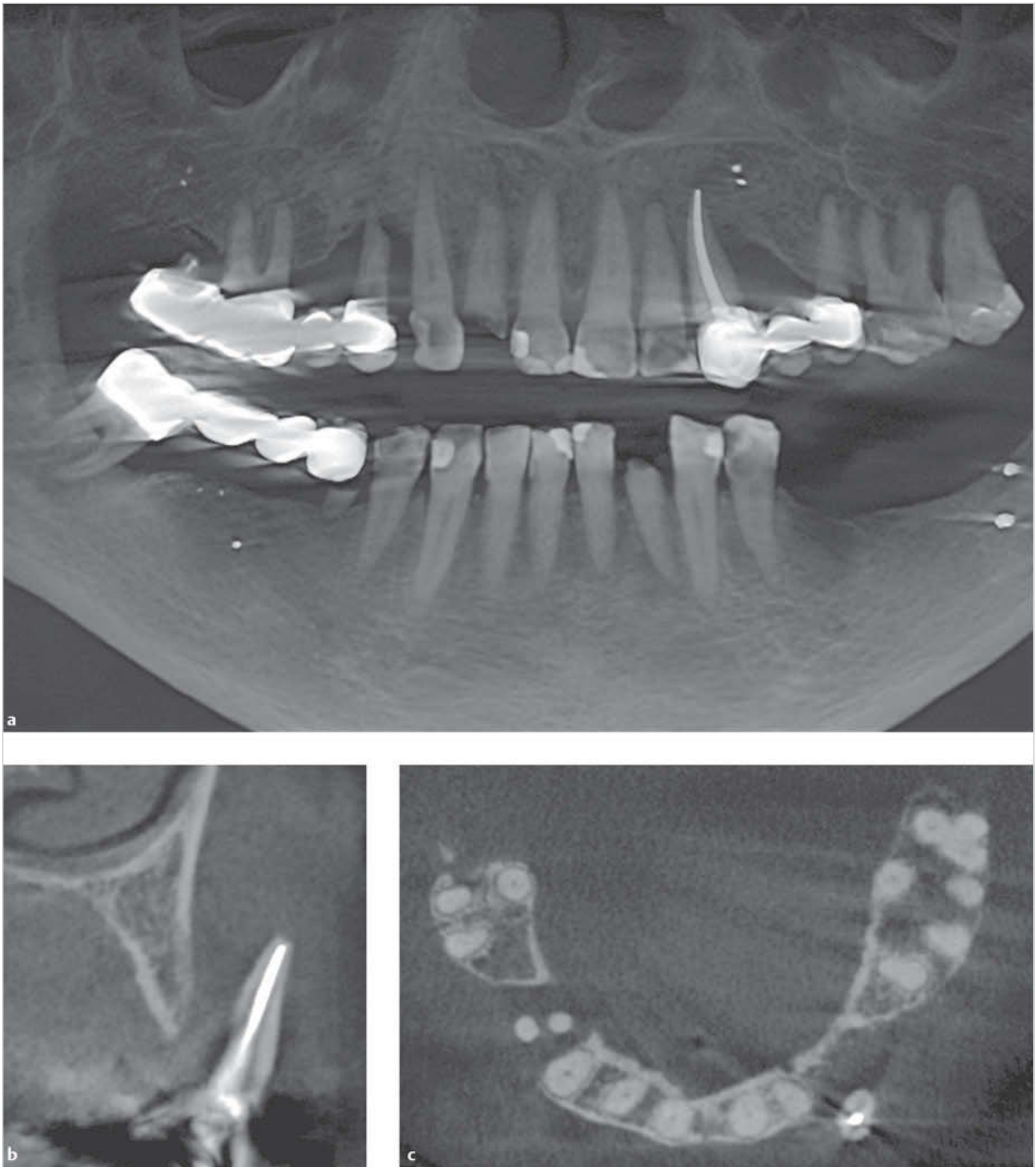


Fig. 10.1a–c This panoramic radiograph (a) revealed deep vertical bone loss on the distal surface of tooth 22. Periapical radiographs did not show any abnormalities. Transverse (b) and axial (c) views were needed to demonstrate that a cyst was causing vestibular displacement of the endodontically treated tooth.

Because of central projection, all structures of the target object are struck by X-rays and projected on the image. Many anatomical structures contribute to image formation through summation. Summation can be tricky because bony structures located outside the target region can contribute to image formation and, if they do, there is always a risk of misinterpretation.

Therefore, the configurations seen on radiographic images do not always accurately reflect true underlying anatomical conditions. In intraoral radiography, for example, even the presence of multi-rooted teeth can cause diagnostic difficulties. Superimposition of the zygomatic bone (cheekbone) over the maxillary region can also lead to misinterpretation.

10.1 The Teeth and Tooth-supporting Structures

The teeth and tooth-supporting structures are among the smallest and finest anatomical structures that can be visualized radiographically.



Fig. 10.2 The lamina dura appears as a thin, solid, radiopaque line surrounding each tooth socket.

The lamina dura is of great importance for the identification of pathological changes in the alveolar area. The lamina dura is the thin layer of compact alveolar bone that lines the tooth socket (alveolus). Its thickness varies from 0.1 to 0.4 mm. Because it looks like a sieve containing many small holes, the lamina dura is also referred to as the “cribriform plate.” It is attached to the trabeculae of the cancellous bone. The cribriform plate appears as a radiopaque line called the lamina dura on radiographs in the vestibulo-oral projection, for example, on bitewing radiographs (□ Fig. 10.2 and □ Fig. 10.3).

Naturally, the interradicular bone septum must be included to evaluate the bifurcation and the rich variety of forms of the pulp chamber and root canals. This pushes intraoral radiography to the limits, and additional three-dimensional imaging studies such as cone beam computed tomography (CBCT) may be needed to address diagnostic questions in this complex area (□ Fig. 10.4).

Correct visualization of the alveolar ridge and interdental bone septum on intraoral radiographs is highly dependent on the radiographic technique and the X-ray projection angle. If the beam is not directed at right angles to the alveolar ridge, there is a risk of misrepresentation of the height of the alveolar ridge on the radiograph. In this case, the alveolar ridge seen on the radiograph usually seems higher than it really is.

Bitewings, panoramic radiographs (orthopantomograms), or special settings for the alveolar crest in panoramic radiography may then be needed for proper visualization of the alveolar ridge (□ Fig. 10.5).

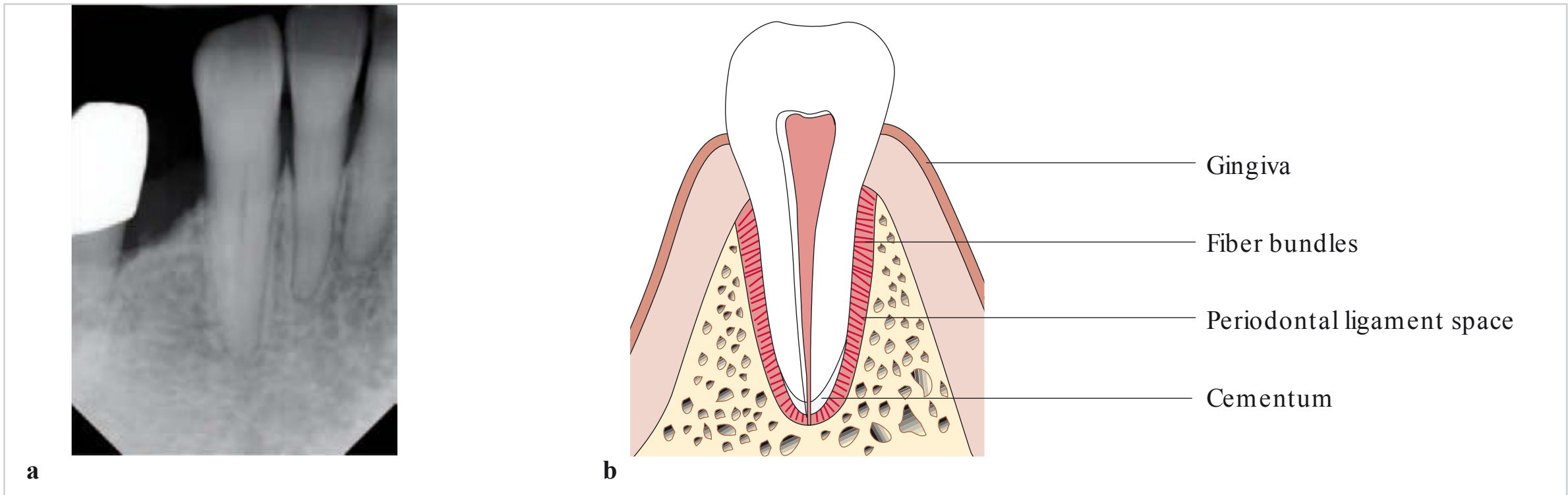


Fig. 10.3a, b Tooth and tooth-supporting structures.
a The anatomical alveolus appears as a thin radiopaque line called the lamina dura.
b Longitudinal cross-sectional view of the tooth and supporting structures.

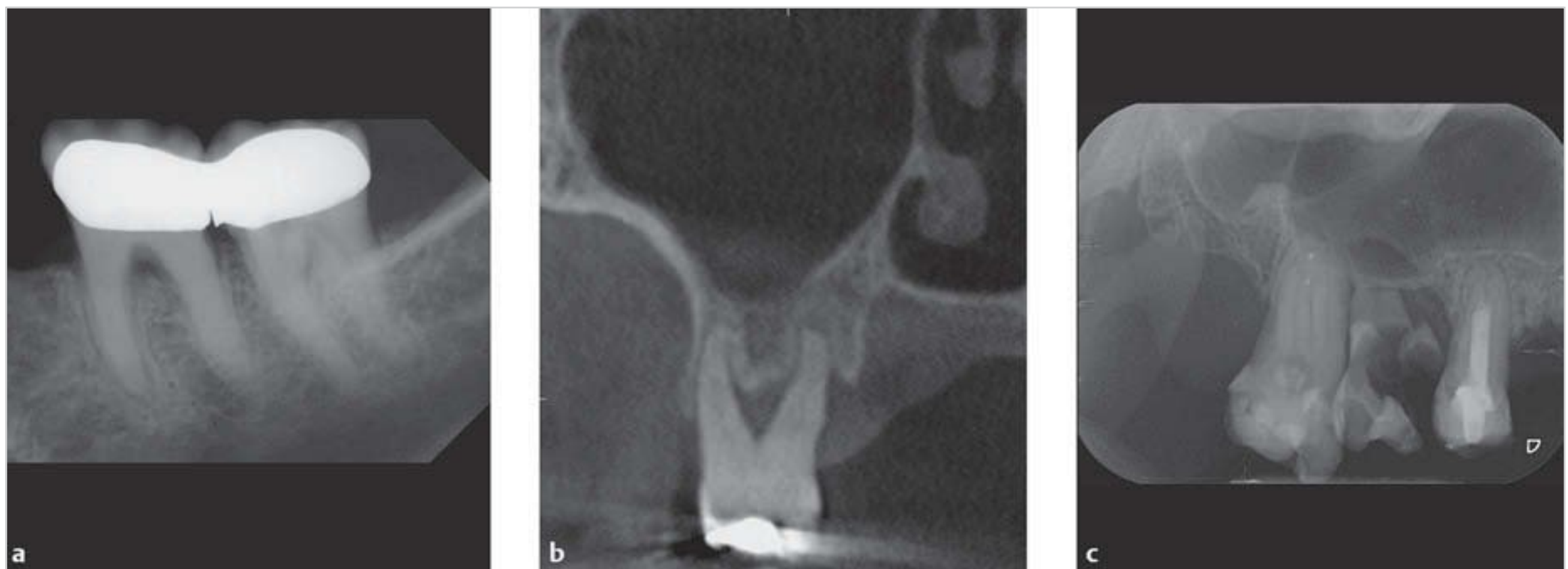


Fig. 10.4a–c Interradicular bone septum, bifurcation, pulp chamber, and root canals.

- a** The exposed bifurcation of tooth 36 is clearly visible. In tooth 37, the oblique line appears at the level of the alveolar ridge as a broad, radiopaque line that projects onto the distal root.
- b** This transverse CBCT image shows the full extent of bone loss in a second plane.
- c** Fractures in the root region of tooth 16 complicate the diagnosis, but significant widening of the periodontal ligament space can be seen. Tooth 15 has an incomplete root filling. The fillings of tooth 17 show irregularities and the pulp cannot be diagnosed with certainty. The coronoid process shows anatomical irregularities in the vicinity of the maxillary tuberosity. The pterygoid process appears distal to the maxillary tuberosity. The posterior part of the zygomatic bone appears in the upper part of the X-ray image. The border of the maxillary sinus appears as a thin radiopaque line.



Fig. 10.5a, b Anatomically correct representation of the alveolar ridge can only be achieved when a parallel beam of incident radiation is highly perpendicular to the mandible and image receiver. These conditions are best achieved in panoramic radiography and vertical bitewing radiography.

- a** Bitewing radiograph acquired using a panoramic radiography machine (Orthophos XG).
- b** Vertical bitewing radiograph (intraoral).



Fig. 10.6 The dark areas appearing at the necks of teeth 16 and 15 could be mistaken for cervical caries, but their shape and structure is indicative of cervical burnout. The enamel damage seen on the distal surface of tooth 35, on the other hand, is indicative of caries.

□ **Cervical burnout:** Another radiological phenomenon is cervical burnout, which appears as a radiolucent area in the cervical region of a tooth. This diffuse brightening is caused by anatomical factors. Because the enamel tapers toward the root, there is decreased X-ray absorption at the cemento-enamel junction, making the area appear darker.

Note

Cervical burnout is similar in appearance to root caries. Therefore, care must be taken to avoid misinterpretation of cervical burnout as caries (□ Fig. 10.6).

10.2 The Mandible

Only a few anatomical structures in the mandibular region are of particular interest in dental radiography.

In the posterior mandibular region, the oblique line (oblique ridge) generally projects to the root region of the wisdom teeth and second molars. The oblique line of the mandible (linea obliqua) appears as a slightly curved,

thin radiopaque line with a width of 1 to 2 mm. It may cause diagnostic problems if it extends to the apical region (□ Fig. 10.7).

The mental foramen is usually visible only on panoramic radiographs. The mandibular nerve canal appears as a radiolucent band between two parallel radiopaque lines. In most cases, it can be easily identified on radiographs.



Fig. 10.7a–c Depending on its shape and on the radiographic projection, the oblique line appears at the level of the alveolar crest and projects to the root area of the wisdom tooth and second molars.

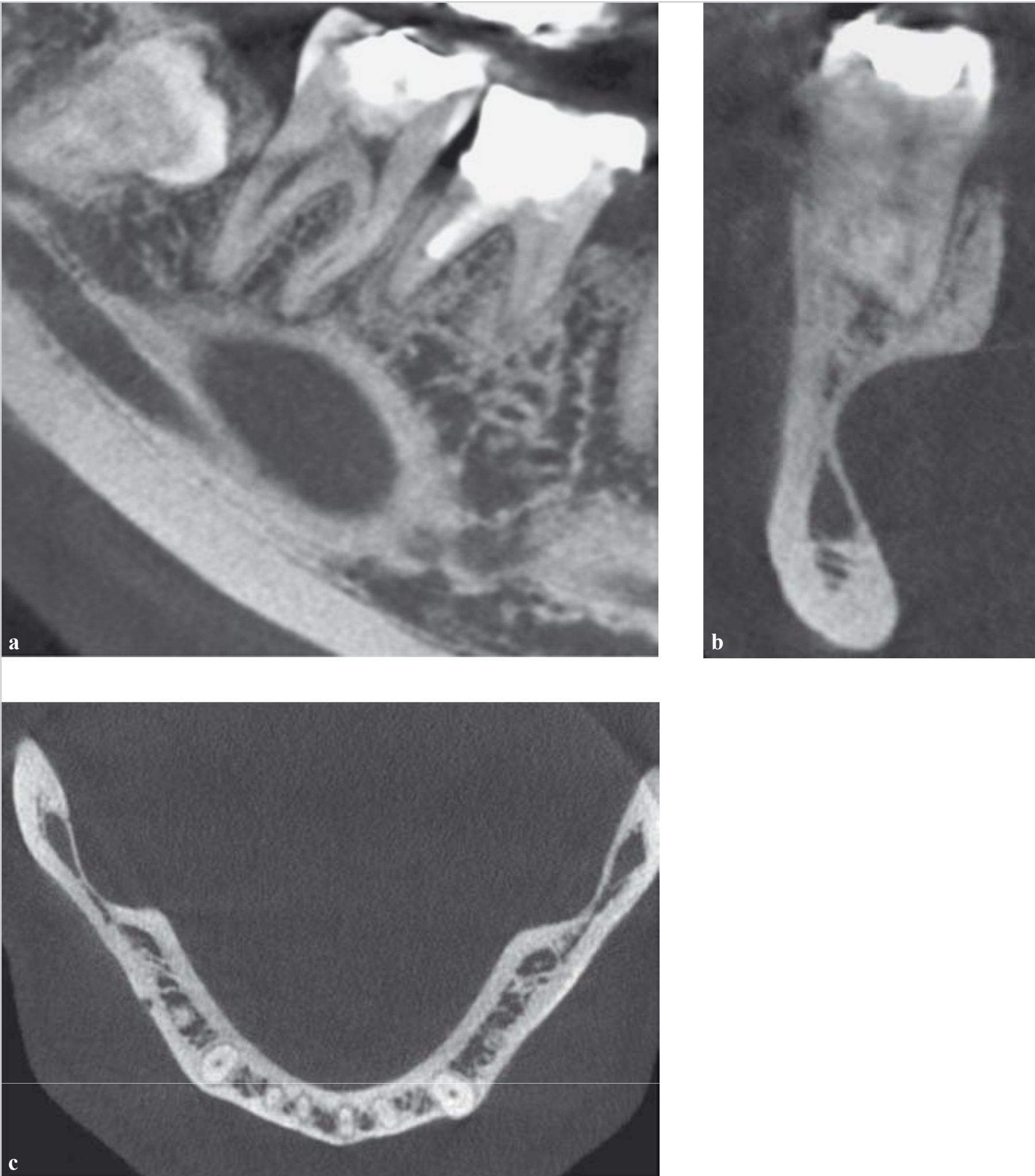


Fig. 10.8a–c Pathologic process or normal anatomical variation?
a This lateral view shows a sharply defined, hypodense, oval area resembling a cystic lesion.
b Marked thinning of the mandibular cortex is seen on this radiograph.
c The symmetrical pattern of thinning of the mandibular cortex can be seen in this plane. This thinning is the cause of the questionable hypodense oval area observed in (a).

Caution

In some cases, the nerve canal cannot be visualized on either conventional or panoramic images. If this is the case, even greater caution is needed when performing surgical procedures in this region.

□ **Anatomical variations:** There are many variations of the normal anatomy of the mandible. The cross-sectional anatomy of the mandible can lead to misinterpretation of radiographic images. If, for example, there is radiolucency of unclear origin, side-to-side comparison is always necessary to differentiate between normal variations of the mandibular anatomy and pathological processes. If in doubt, additional CBCT studies can help determine whether a questionable area of radiolucency is due to a pathological process or a normal anatomical variant (□ Fig. 10.8).

10.3 The Maxilla

The maxillary region contains significantly more structures of interest (besides the teeth and the alveolar ridge) than the mandible.

The incisive canal, which varies in anatomical width and size, appears on maxillary anterior radiographs as a radiolucent band between two parallel radiopaque lines that extend vertically.

Caution

In the presence of a nasopalatine cyst, the incisive canal may be widened and rounded. However, this sign alone is not reliably indicative of a cystic lesion.

The median palatine suture and, in many cases, the anterior nasal spine, also appear on maxillary anterior radiographs. The soft-tissue shadow of the nose superimposes on the maxillary anterior region. In intraoral radiography, this often makes the root region seem denser than it actually is. However, the soft-tissue shadow of the nose can be easily identified on most intraoral radiographs as the curved line corresponding to the curvature of the nostrils (□ Fig. 10.9).

Above the maxillary canines, the radiopaque lines formed by the medioventral border of the maxillary sinus and by the nasal floor intersect, forming an “inverted Y.” A brighter, denser area can be seen mesial to the canines; as in the maxillary anterior region, this is caused by the soft-tissue shadow of the nose (□ Fig. 10.10).

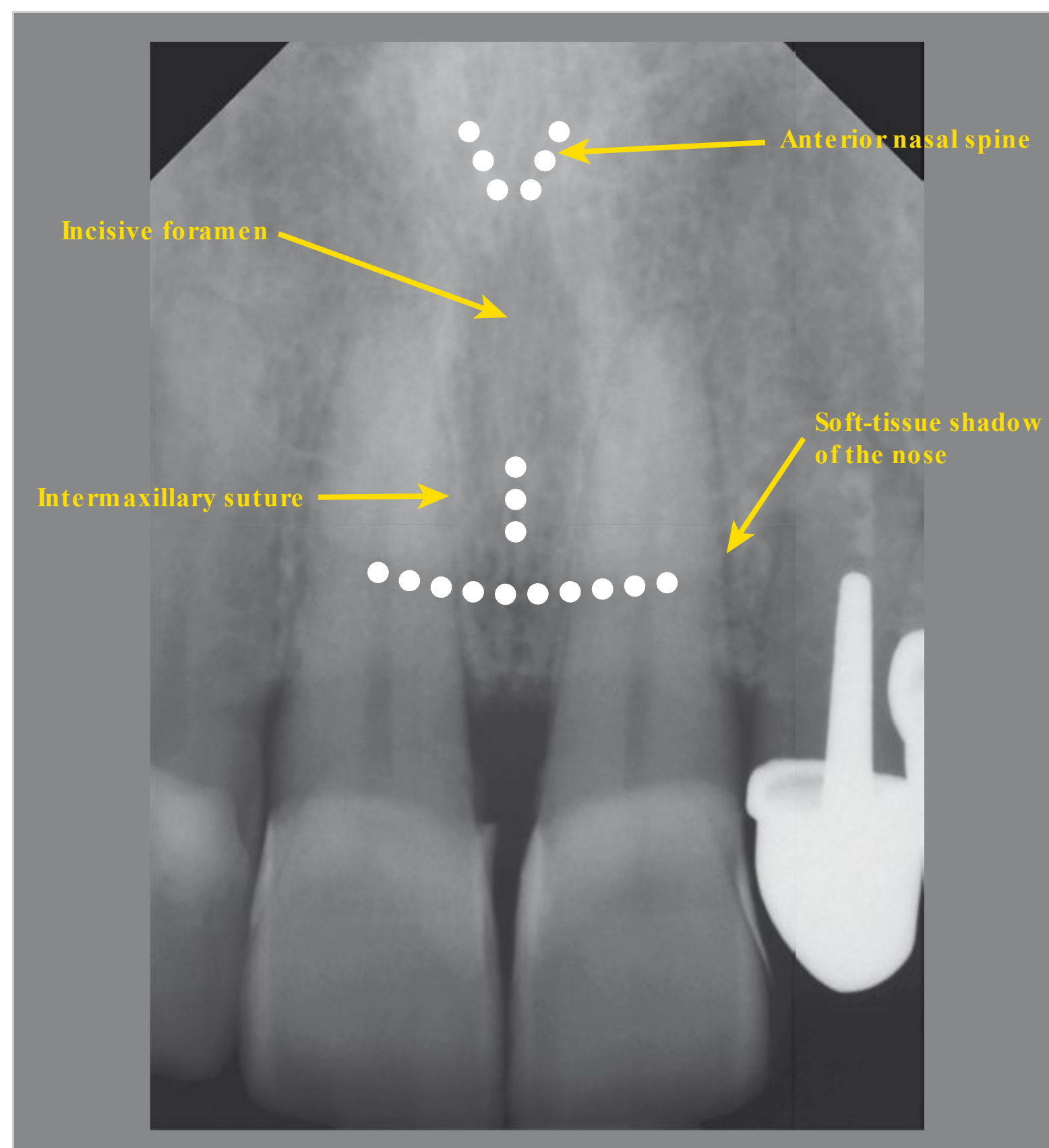


Fig. 10.9 Maxillary anterior region and radiographically relevant (generally identifiable) anatomical structures.

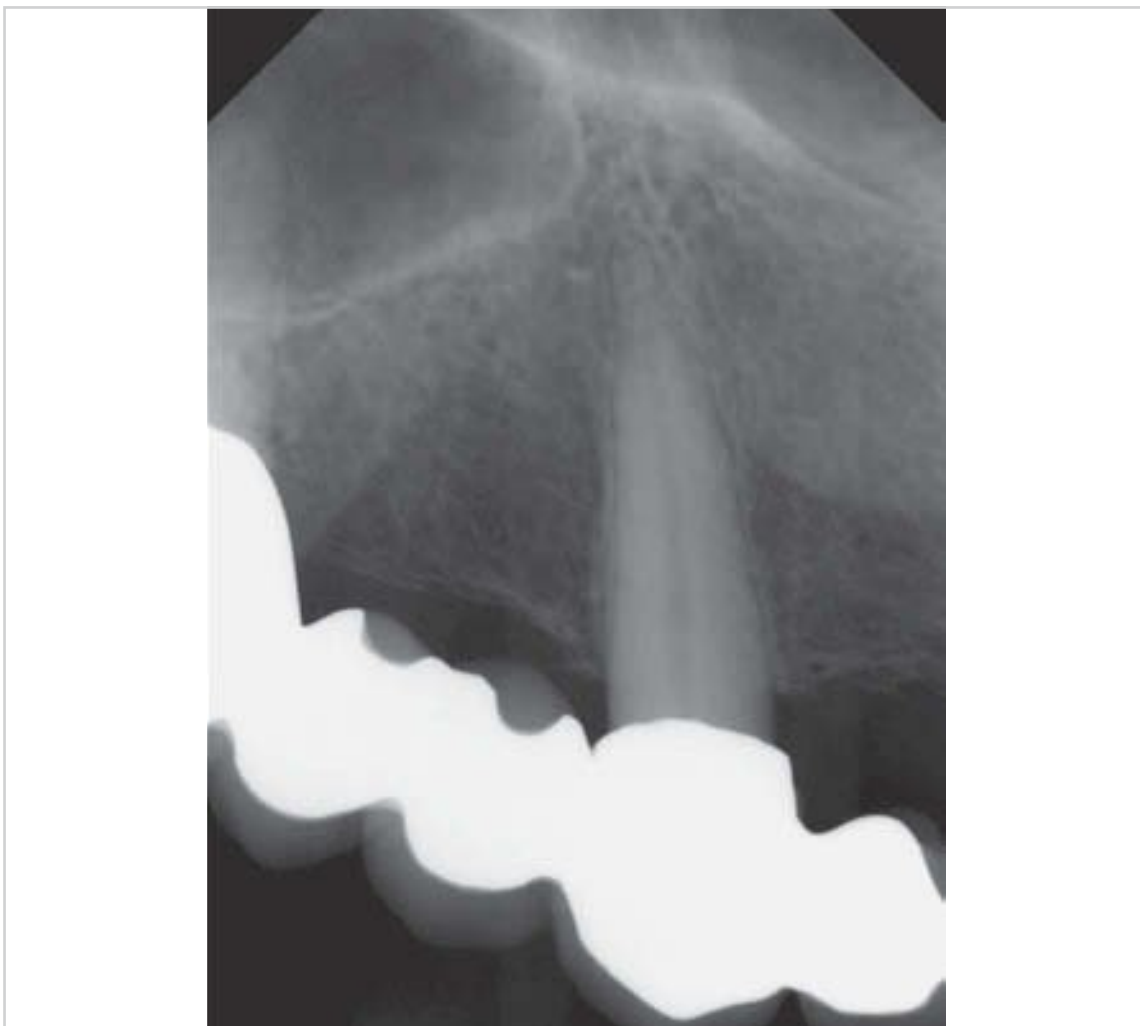


Fig. 10.10 X-ray image of tooth 13 (canine), showing the border of the maxillary sinus (distal), floor of the nasal cavity (cranial), and soft-tissue shadow of the nose (mesial).



Fig. 10.11 High palate: only a small portion of the floor of the nasal cavity appears as a radiopaque line above the maxillary molars.



Fig. 10.12 Molar region with small root fragments at the level of the alveolar ridge. The posterior margin of the alveolar process appears as a thin radiopaque line. The posterior part of the zygomatic bone appears in the upper part of the X-ray image.



Fig. 10.13a, b In both radiographs, the zygomatic bone is very low.
a The zygomatic bone covers the apex.
b The zygomatic bone projects to the root region.

Medioventrally, the border of the maxillary sinus appears as a faint, thin radiopaque line that typically extends across the hard palate/nasal floor. The hard palate/nasal floor appears as a straight horizontal radiopaque line that, unlike the radiopaque line of the border of the maxillary sinus, is always readily identifiable (□ Fig. 10.11).

The alveolar recess is a part of the maxillary sinus that appears posterior to the hard palate/nasal floor. It may cause diagnostic problems if it appears as a radiolucent area resembling a cyst.

In the posterior maxillary region, the bony border of the maxillary sinus always appears as a very thin, curved (concave) radiopaque line in the area of the molar and premolar roots (□ Fig. 10.12).

In subjects with a flat hard palate, the radiopaque line of the zygomatic bone can “migrate” posteriorly (e.g., when using the bisecting-angle technique) and superimpose on the molar apices (□ Fig. 10.13).

The coronoid process of the mandible can sometimes be seen on very distal views (□ Fig. 10.14).

10.4 Panoramic Radiographic Anatomy

Because it covers a larger area, panoramic radiography, or orthopantomography, naturally shows more anatomical structures than intraoral radiography. While the anatomical structures in the mandibular region are usually clearly visualized and identified, those in the maxillary and bifacial region frequently present diagnostic challenges.

Two main reasons for this are the thickness of the image layer (up to 25 mm) and superimposition of a variety of different anatomical structures in the image layer (□ Fig. 10.15).

10.4.1 The Mandible

The mandibular canal is usually well visualized on radiographs, as are the mental foramen and the mandibular foramen. The mandibular canal is extremely variable in location and shape and should always be assessed by left-right comparison.

The anatomy of the so-called ascending branch of the mandible, including the mandibular angle, is characterized by the nerve canal that opens superiorly into the

fossa of the mandible. The coronoid process, the mandibular notch, and the caput and collum of the mandible are usually clearly visualized on radiographs. However, diagnostic problems may arise in the area, owing to soft-tissue structures, which cause anatomically induced problems such as those normally seen only on panoramic radiographs. Because these soft-tissue shadows (and air shadows) differ greatly from one individual to another, radiographic diagnosis in this region is particularly more challenging than in other areas.

Radiographic shadows of the opposite jaw, the soft palate, and the tube of air from the mouth and the nasal cavity generally project on the ascending branch of the mandible. The two shadows meet at the pharynx, forming different shapes that project on the ascending branch of the mandible. These radiographic shadows can easily be misinterpreted.

The maxillary tuberosity is located at the posterior end of the maxilla. It is clinically relevant when tuberosity fractures occur during tooth extraction. The poste-

rior border of the maxillary sinus extends cranially as a thin radiopaque line. A second, thin, vertical radiopaque line extends posteriorly. Both lines mark the borders of the pterygopalatine fossa. The pterygoid process or plate is not always visible radiographically, and the pterygoid hamulus is rarely visible. The styloid process can be more clearly identified as a more or less thin radiopaque line that extends posteriorly and can be very long in the presence of calcification.

Panoramic radiography shows the soft-tissue shadow of the auricle (pinna) of the ear, in addition to that of the nose. The characteristic shape of the ear flaps generally leaves no room for misinterpretation. The soft palate, which extends as a relatively thick, dense soft-tissue structure from the end of the hard palate to the pharynx, is more problematic. The soft palate is identified by the air that surrounds it. This air comes from the nasal cavity and from the posterior oral cavity, which unite in the pharynx. Problems in assessment of the soft palate may arise, owing to the fact that the soft palate can assume many different shapes as a result of technique-related imaging factors.

The tongue is another important soft-tissue shadow to be considered in dental radiography in general, but in panoramic radiography in particular.

The most important anatomical structures in dental radiography are shown in □ Fig. 10.16 (I), □ Fig. 10.17 (II), □ Fig. 10.18 (III), □ Fig. 10.19 (IV).



Fig. 10.14 Tooth 17, with a view of the coronoid process of the mandible.



Fig. 10.15 Panoramic radiograph obtained with an X-ray sensor, showing a complete view of the upper and lower jaw, the basal maxillary sinus, and the bony joint surfaces.

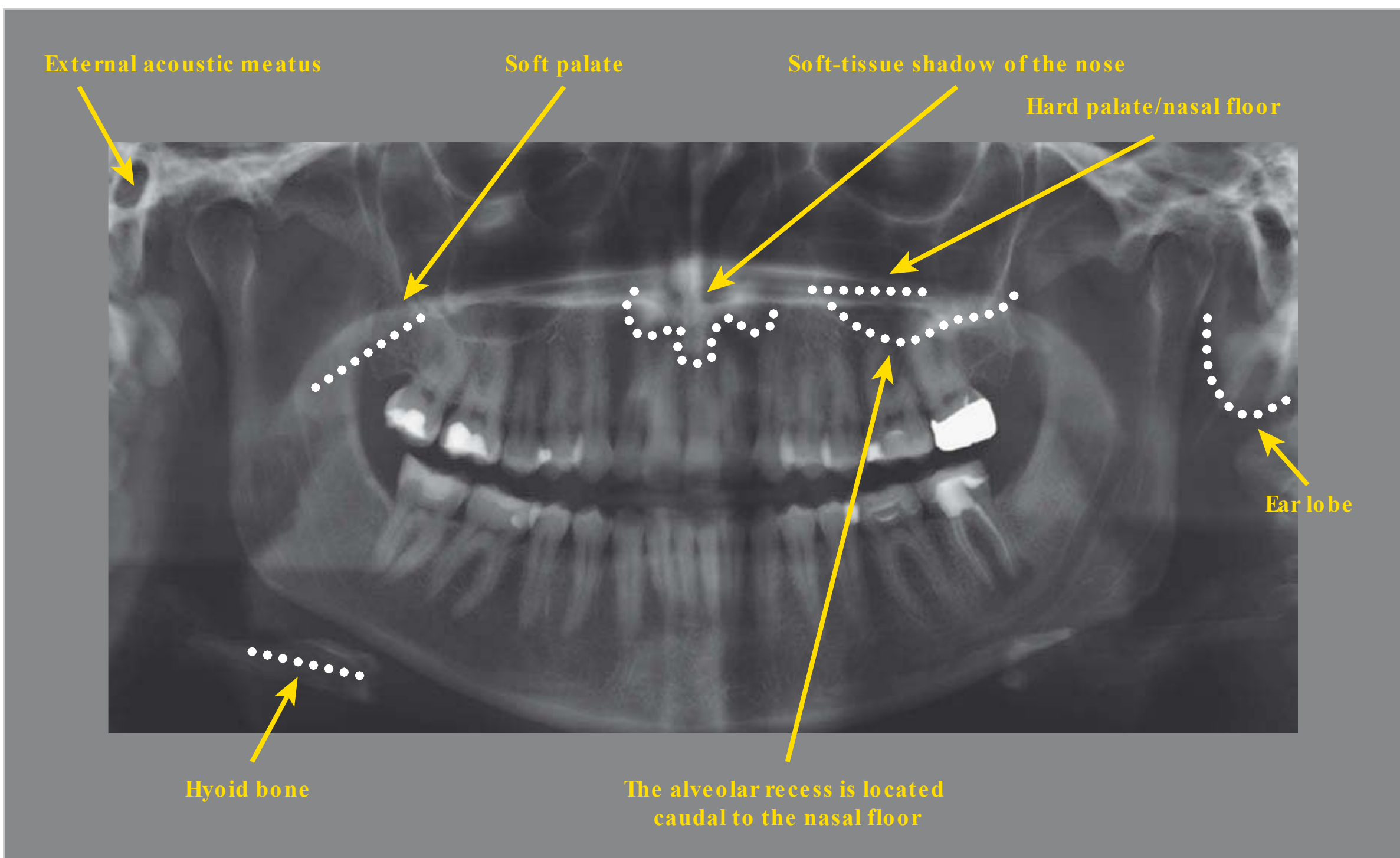


Fig. 10.16 Panoramic radiography: anatomical structures I.

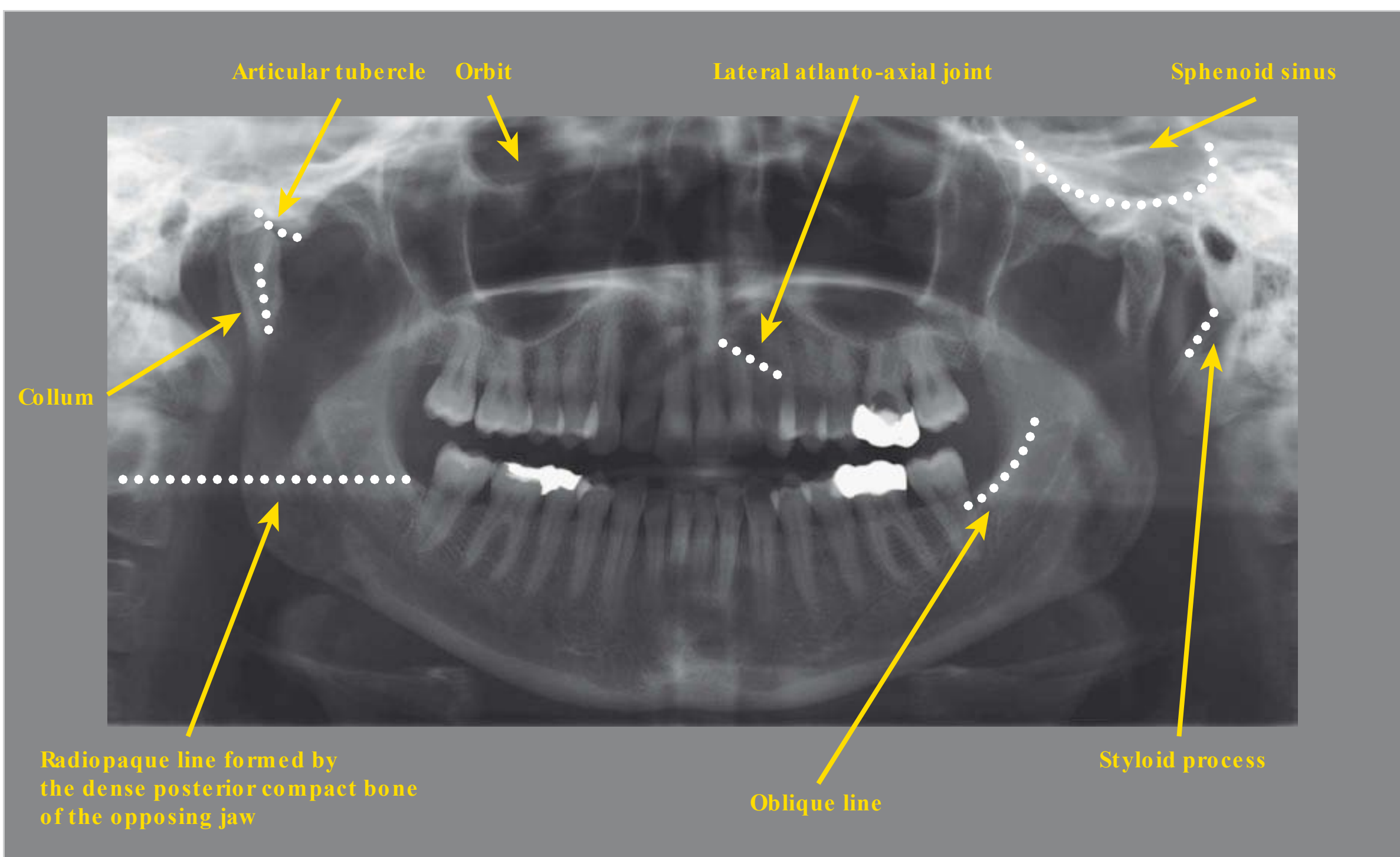


Fig. 10.17 Panoramic radiography: anatomical structures II.

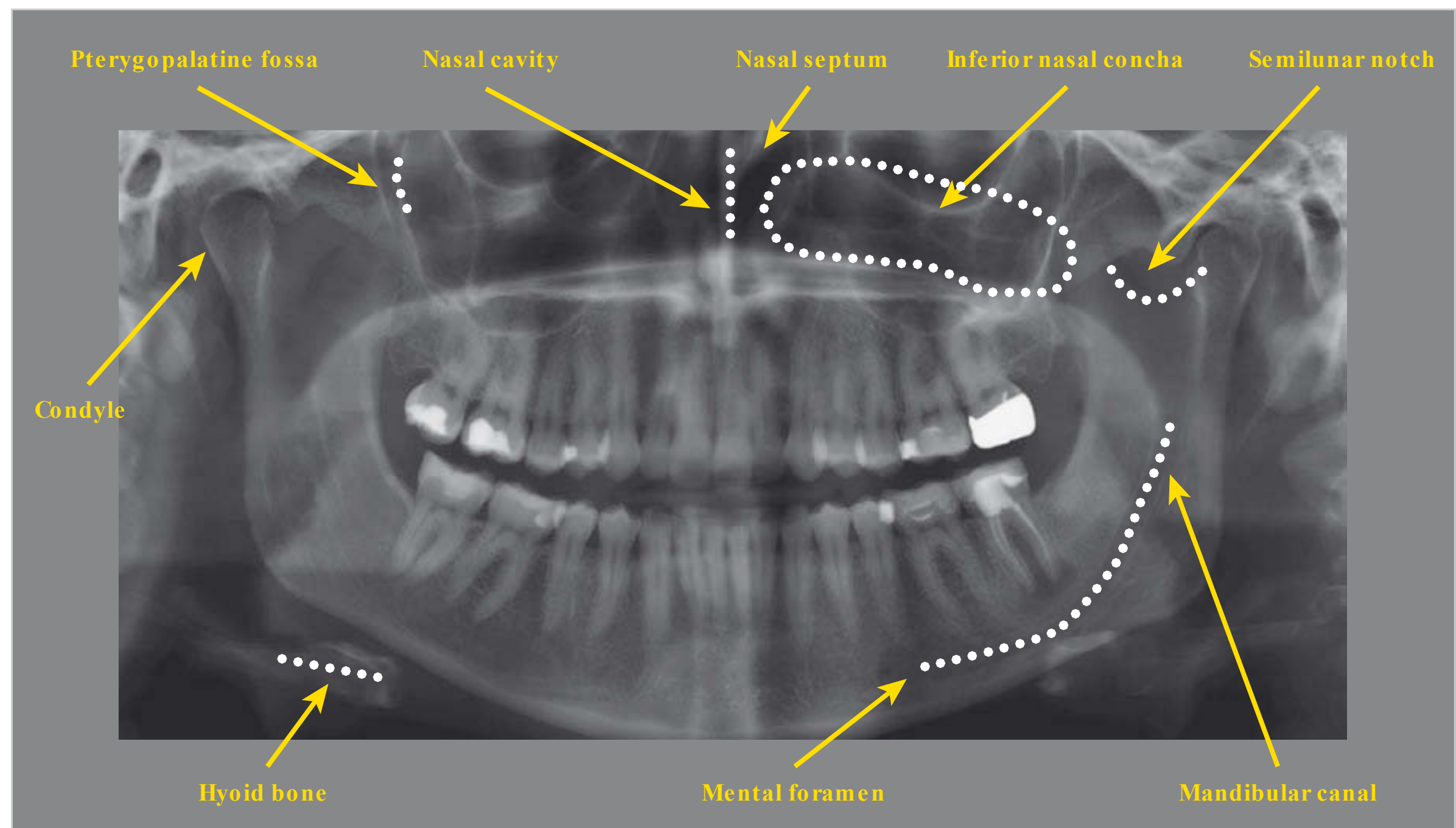


Fig. 10.18 Panoramic radiography: anatomical structures III.

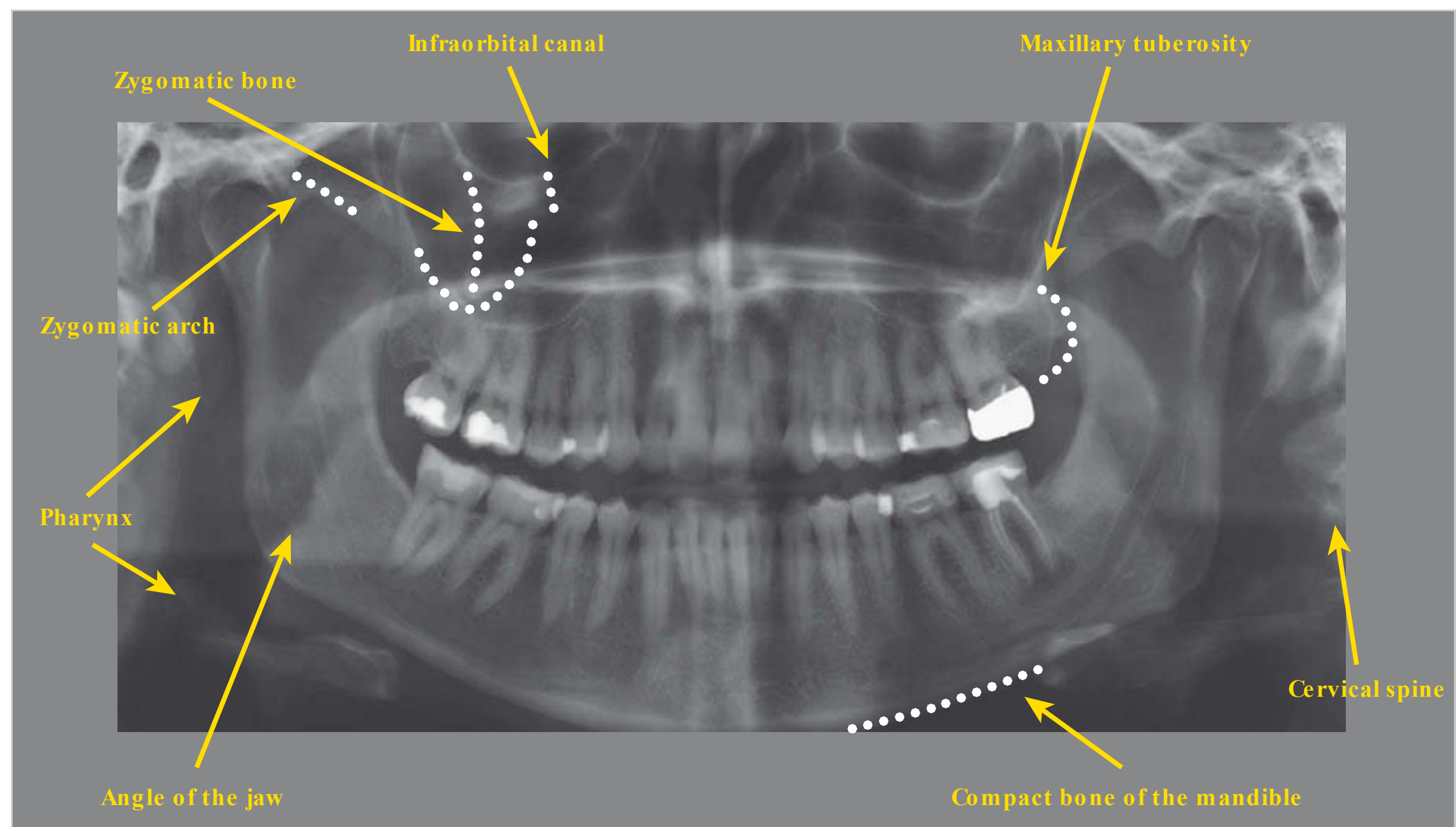


Fig. 10.19 Panoramic radiography: anatomical structures IV.

10.4.2 The Maxilla and Midface

The midface is connected to the maxilla. The zygomatic bones are the most commonly imaged midfacial structures in radiography. Depending on the angle of incidence

of the beam, the zygomatic bones may appear as dense, V-shaped, radiopaque lines. The shape and extent of the remaining parts of the zygomatic bones are sometimes clearly identified on radiographs.

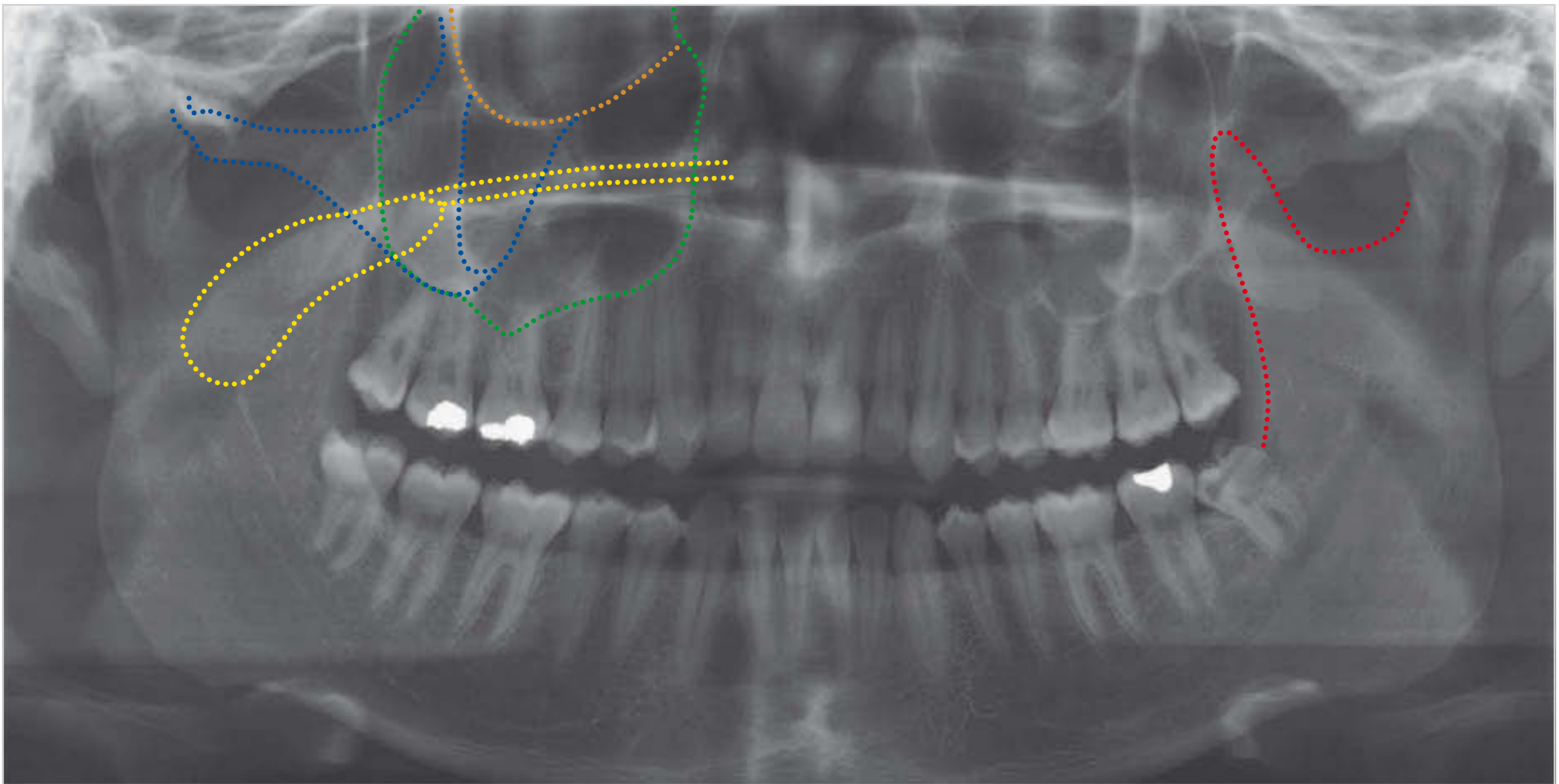


Fig. 10.20 The zygomatic bone, coronoid process, maxillary sinus, and nasal cavity superimpose on each other in the lateral maxillary and midfacial region. This makes radiographic diagnosis difficult, if not impossible. **Blue:** zygomatic bone; **yellow:** hard and soft palate; **green:** maxillary sinus; **brown:** orbit; **red:** coronoid process.

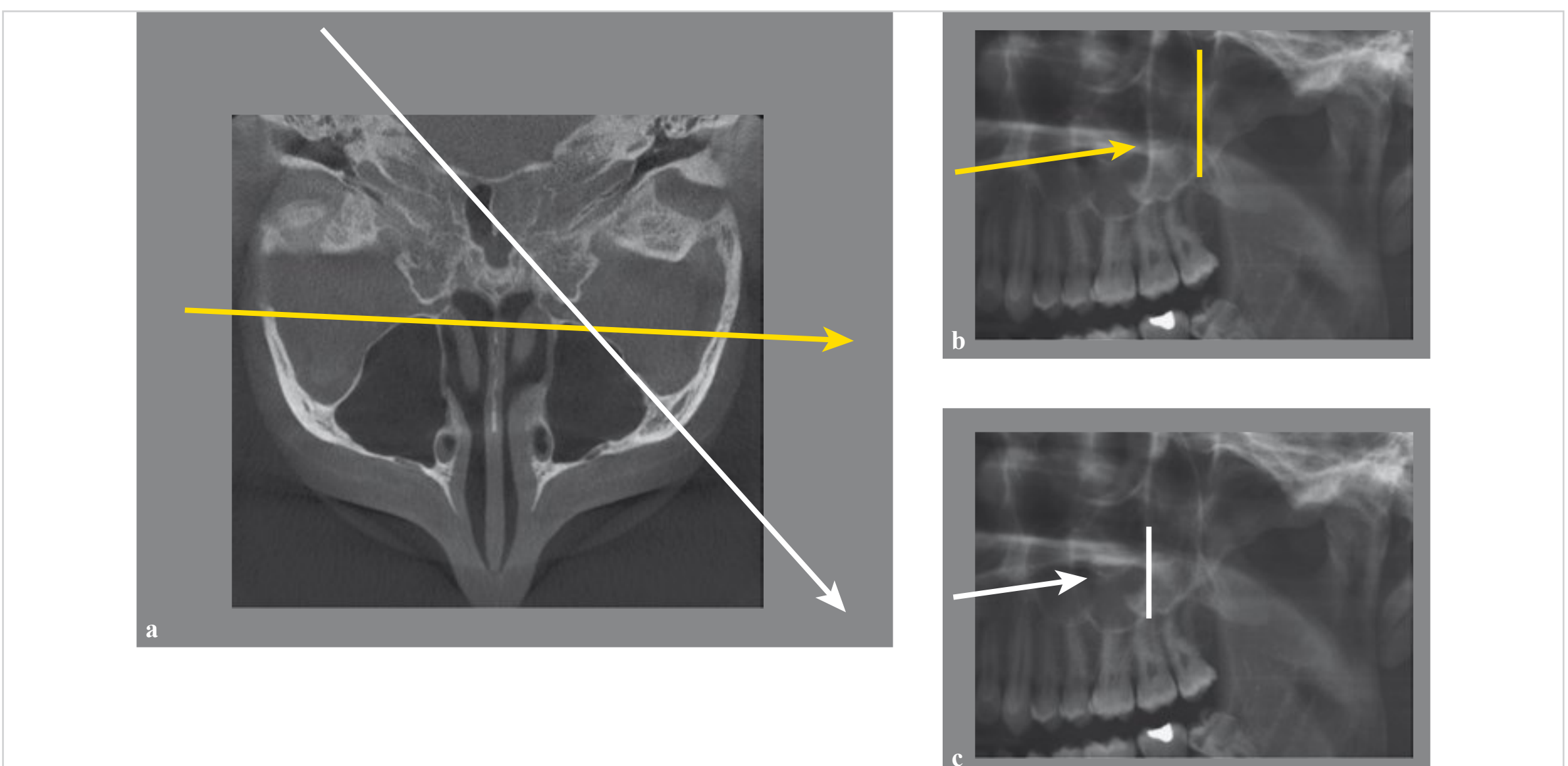


Fig. 10.21a–c Visualization of the posterior and lateral walls of the maxillary sinuses by panoramic radiography. First, the posterior wall of the maxillary sinus (**yellow**) was visualized as a summation effect. Then, a tangential projection along the lateral wall of the maxillary sinus showed a second vertical line (**white**).

a Beam path.

b Owing to rotation of the tube, the posterior wall is depicted as the first vertical line (**yellow**).

c The second vertical line (**white**) appears, owing to summation of the lateral wall of the antrum.

The mandible, maxilla, and midface are generally visualized in panoramic radiography. Because the image layer thickness in the maxillary region is in the centimeter range, the maxillary sinus and nasal cavity cannot be visualized separately. Only the alveolar recess is seen

without superimposition. The inferior turbinates project from the hard palate/nasal floor to the maxillary sinus. They can be identified as relatively homogeneous, elongated soft-tissue shadows that extend from the anterior to posterior wall of the maxillary sinus.

For technical reasons, structures whose anatomically correct position is posterior are positioned laterally on panoramic radiographs. Panoramic imaging provides a very good overview, but makes correct anatomical identification and diagnosis more difficult.

Proceeding toward the eye socket (orbit), the thin radiopaque line of the maxillary sinus often projects onto the orbit. Owing to the funnel shape of the eye socket, cranial areas of the maxillary sinus superimpose on parts of the orbit.

The infraorbital canal often appears on radiographs as a pair of parallel radiopaque lines at the level of the infraorbital ridge. The infraorbital foramen, if visible, appears in the vicinity of the maxillary sinus.

The posterior–lateral part of the maxillary sinus is a radiographically challenging anatomical region. The highlighted lines in □ Fig. 10.20 show how many different structures superimpose on each other and their unusual appearance resulting from the panoramic effect.

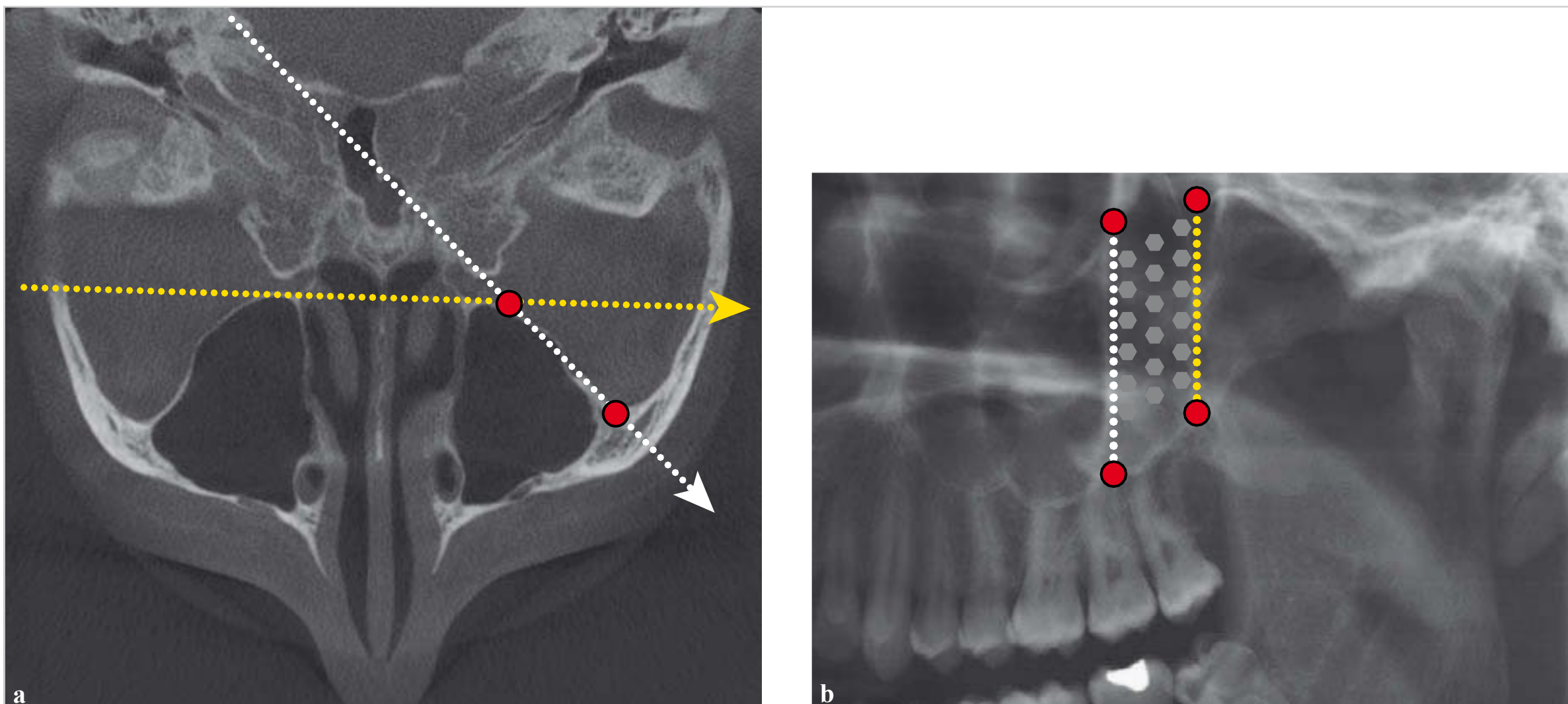


Fig. 10.22a, b Visualization of the lateral walls of the maxillary sinuses by panoramic radiography.

a Beam path.

b The lateral wall of the maxillary sinus is bounded dorsally by the **yellow line** at the posterior boundary and ventrally by the **white line**.

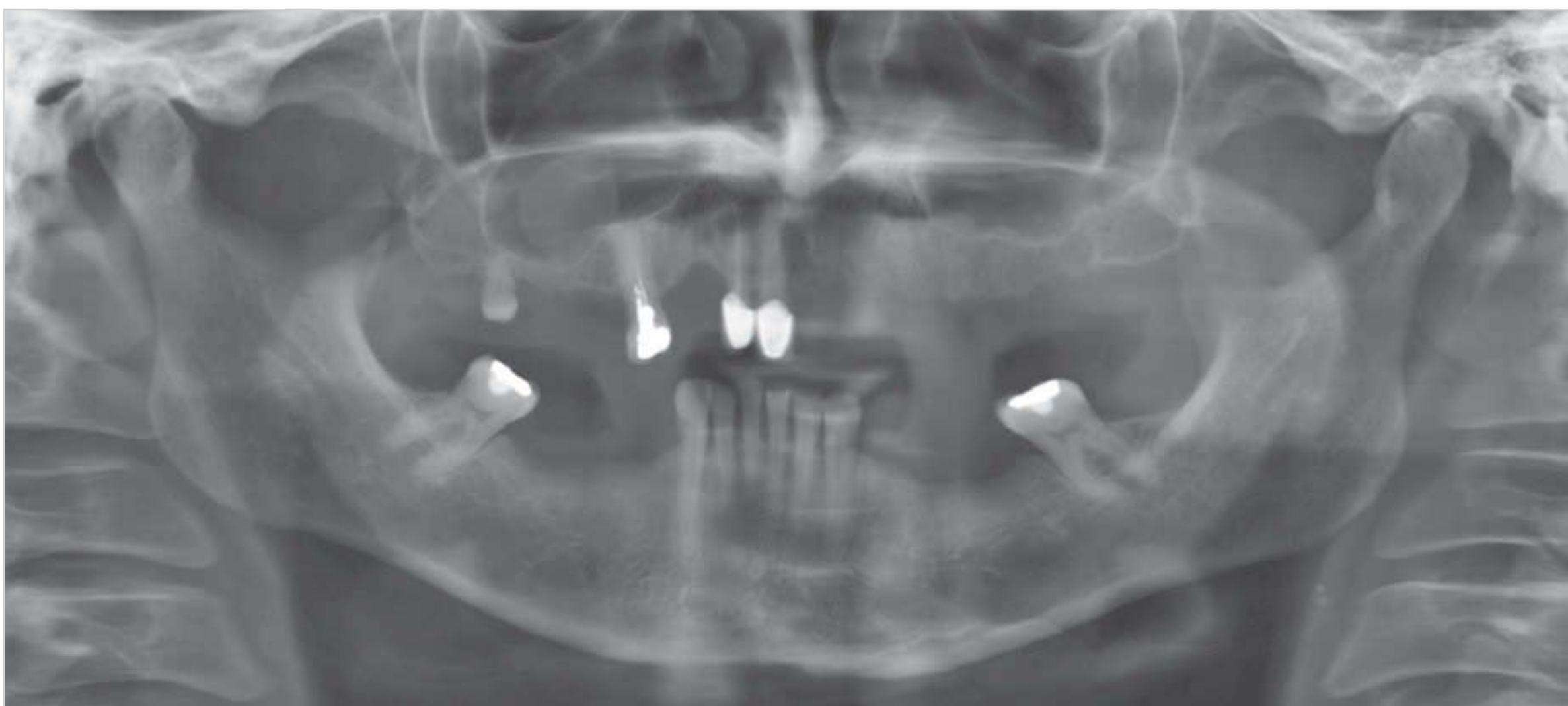


Fig. 10.23 Around, convex soft-tissue mass consistent with a mucocoele appears in the region of the floor of the right maxillary sinus. The area superior to the nasal floor cannot be assessed.

To understand how panoramic images of the posterior and lateral walls of the maxillary sinuses are formed, it is always necessary to consider the beam path and the fact that the X-ray tube moves around the patient in a circular fashion (□ Fig. 10.21).

The area between the two lines in □ Fig. 10.21 represents the lateral wall of the maxillary sinus, as shown in □ Fig. 10.22.

Owing to anatomical and technical limitations, panoramic radiography is not a reliable procedure for diagnostic evaluation of the maxillary sinus. The only structures that can be reliably assessed by panoramic radiography are the alveolar recess and the posterior wall of the maxillary sinus (□ Fig. 10.23).

Note

Anatomical relationships superior to the hard palate/nasal floor prohibit the use of panoramic radiography for diagnostic evaluation of the maxillary sinus. Panoramic radiography can only detect such abnormalities if the alveolar process is the site of origin of the lesion. The posterior wall of the maxillary sinus can also be assessed.

Chapter 11

Radiographic Findings and Diagnosis

- 11.1 Systematic Image Analysis and Interpretation 134
- 11.2 Assessment and Diagnosis of the Most Common Pathological Changes 136

11 Radiographic Findings and Diagnosis

11.1 Systematic Image Analysis and Interpretation

Many requirements must be met for optimal interpretation of dental radiographs:

- The target structures must be completely visible and clearly identifiable on the radiograph.
- Standard radiographic techniques and projections must be used to ensure comparability and reproducibility. This is the only way to produce radiographs that can be compared with previous radiographs. The comparison of current radiographs with previous radiographs obtained from the same patient enables the clinician to better recognize deviations associated with pathological processes.
- To achieve these objectives, it is crucial to follow a systematic radiographic procedure. This is the only way to ensure the comparability of radiographs taken by a specific individual with those taken by another person.

Note

Two basic rules to remember:

- Always take only as many X-rays as absolutely necessary, keeping all exposures as low as reasonably achievable (ALARA principle).
- Always ensure that the system provides the specified image quality (established in acceptance testing) with the lowest dose possible.

11.1.1 Film and Monitor Viewing Conditions

A suitable light source is required for proper film viewing. A monitor that can correctly display very fine anatomical structures is needed to view digital X-ray images. The monitors used in dental radiography must meet very high quality standards.

A darkened room is needed for both film viewing and monitor viewing. Proper diagnostic evaluation is not possible in a brightly lit treatment room. Light boxes or monitors in a well lit room are for guidance only, but not suitable for diagnostic assessment.

The clinician should assess the quality of the radiographic image before starting the process of image analysis and interpretation. First, the radiograph should be evaluated for proper optical density. This also applies, albeit to a lesser extent, to digital X-rays. Although digital radiography systems have wide exposure latitude, it is not possible to compensate for gross under-exposure. The next step is to evaluate the visualized target region for completeness, taking care to ensure that a margin ex-

tending around the entire useful radiation field is seen on large-format films. Finally, the quality of the radiographic settings and positioning of the patient, film, and X-ray tubehead is checked.

After this quality control check, a methodical examination of all regions of the radiograph for the presence of lesions or changes can begin. A thorough and systematic approach is required, particularly when viewing panoramic radiographs and cone beam computed tomography (CBCT) images.

The viewing of panoramic radiographs proceeds from one quadrant to the next, starting with the teeth and proceeding to the alveolar process and maxillary region, including the floor of the maxillary sinus. The next step is to inspect the entire mandible, including the condylar heads.

The size and clinical relevance of lesions or changes determine the length and scope of the written report. The written report must provide a clear and complete description of the radiographic findings.

11.1.2 Steps from Findings to Diagnosis

The path to a possible diagnosis is a multi-step process. The first task is to ensure that all findings (lesions, changes) have been detected.

Identification of Pathological Changes

The examiner must detect any change or deviation from the normal or healthy condition on first viewing a radiograph. All parts of the radiograph that deviate from the normal must be identified.

A preliminary assessment of radiographic quality is crucial to ensure that nothing is overlooked. In addition to correct exposure, other factors that play an important role—particularly in panoramic and intraoral radiography—include patient positioning (in panoramic tomography) and positioning of the image receptor (in intraoral radiography).

Caution

Experience shows that even minor errors in radiographic settings can lead to major differences in radiographs, owing to the complex nature of the dental/facial anatomy and the types of radiographic techniques used. This is equally true for both intraoral and panoramic radiographs.

Radiographic Findings Suggestive of Lesions or Changes

In principle, pathological lesions or changes can appear as an increase or decrease in bone substance. This applies to inflammations, cysts, and tumors, but not to fractures, which still can usually be diagnosed reliably and without difficulty. The presence of a break in continuity of the bone is highly indicative of a fracture.

Description of Radiographic Findings

All lesions or changes discovered must be carefully described. A proper description is essential for evaluating whether a radiographic finding is indicative of a pathological or a normal variant.

Radiographic features that should be described include the following:

- Location/site: left mandibular, tooth 18, periapical, radicular, coronal, lateral, medial, posterior, etc.
- Shape: round, oval, elliptical, cloudy, multicystic, etc.
- Margins: well-defined, poorly defined, irregular, etc.
- Size: size relative to that of adjacent structures and exact extent (from ... to ...), in metric units such as millimeters, if possible
- Internal structure: homogeneous, inhomogeneous, septate, bowl-shaped, etc.
- Density: comparative descriptions, such as bone-, soft-tissue-, tooth-, metal- or filling-dense, are often helpful
- Relationship to adjacent structures: adjacent teeth, maxillary sinus, mandibular nerve canal, floor of the nose, etc.
- Effect on adjacent structures: infiltration, displacement, thinning, etc.

Evaluation of Radiographic Findings

Once all potential lesions or changes identified have been documented in writing, the evaluation process can begin.

If, on further evaluation, the radiographic finding appears clearly deviant, the probability that the identified structure is a pathological process increases. However, the possibility that the finding may also be a normal variant must always be taken into consideration. It is often difficult to differentiate between the range of normal appearances and pathological processes. This takes practice and requires comparison of the current findings with previous findings seen in the course of one's radiological experience.

Diagnosis

The probability of correlation between radiographic findings and diagnoses varies. A definitive diagnosis cannot be made unless the agreement between the radiographic finding and the diagnosis is unequivocal, for example, in the case of a fracture. In most other cases, only a tentative diagnosis can be established.

Written Report of Radiographic Findings

The written report of radiographic findings forces the person writing the report to focus on the essentials. It has considerable impact and relevance in clinical and forensic practice.

Radiological Report

The radiological report contains a description of the examination procedure, the clinical questions posed, and the responses to these questions. The structure and content of radiological reports should comply with local standards. A radiological report should always include the patient details and information regarding the radiographic technique.

Challenging Radiographic Findings in Routine Dental Practice

In dental practice, some radiographic findings are very common and recurrent, while others are uncommon and continually challenging.

In dental radiography, attention is focused on the teeth and adjacent structures. While the diagnosis of pathological changes in the teeth themselves should be routine, diagnostic uncertainty starts when the focus shifts to the periapical area and adjacent bone structures of the mandible. Parts of the floor of the maxillary sinus are also difficult to assess, particularly if an area superior to the nasal floor is to be evaluated.

The most common clinical questions posed include caries diagnosis, apical and marginal periodontal diseases, and the range of different dense and usually benign shadows, mainly in the mandibular region. Cystic lesions; displaced, supernumerary, and impacted teeth; and osseous lesions in the temporomandibular joint are less common but generally do not cause diagnostic difficulties. Conversely, radiolucencies of unclear etiology cause diagnostic problems. They are frequently interpreted as osteolysis because they have poorly defined margins and could be indicative of a malignant process.

When viewing radiographs, it is crucial to not overlook any pathological change, but to ensure that all have been detected and identified.

Any irregularity could be due to an error in radiographic technique. In panoramic radiography, in particular, many shadows and radiolucencies occur as a result of technique-related factors and positioning errors alone.

Note

There are many variations of the normal anatomy of the facial skeleton. Side-to-side comparison helps to exclude pathological processes.

If suspicious findings cannot be attributed to technique-related factors and normal variants, then a detailed description of the change is needed for diagnostic evaluation.

The other steps are less difficult but require a certain level of experience. A thorough and systematic approach to the description of findings is the prerequisite for correct radiographic diagnosis.

In case of doubt, the radiographs should be submitted to an experienced dental radiologist for interpretation. This can help to prevent misinterpretation. The patient should not be referred to a specialist before this is done, to rule out the possibility that there is no pathological finding.

11.2 Assessment and Diagnosis of the Most Common Pathological Changes

11.2.1 Carious Lesions

Caries is the most common disease of the dental hard tissues. Failure to detect and treat dental caries early can result in a loss of vitality of the affected tooth and lead to inflammation (usually periapical inflammation).

Bitewing radiography, introduced by Raper (1925), is the radiographic technique of choice for the diagnosis of approximal caries. Although it has some shortcomings, bitewing radiography is still superior to all other methods available for the diagnosis of initial caries (primary caries). The extent and location of caries and the selected technique are crucial factors. Approximal caries can be diagnosed at an earlier stage than fissure caries and caries of vestibular and oral tooth surfaces, owing to the direction of the beam in intraoral radiography. Early detection of interproximal caries is possible because of the beam direction and tangential effect. Conversely, summation effects associated with the superimposition of intact tooth substance on tooth surfaces impede the early diagnosis of fissure caries.

Practice

Holders with a position-indicating device and the paralleling technique should always be used.

The radiographic conditions for bitewing radiography are much more favorable than those for periapical radiography. The image receptor can usually be placed parallel to the crown of the teeth being radiographed.

As in all dental radiographic techniques, errors in the execution of bitewing radiography are a major weak point. Ideally, one radiograph per side should be sufficient for unequivocal diagnosis of the various stages of caries. However, a more reliable diagnosis is obtained by taking two radiographs per side: one of the premolars and one of the molars. This corresponds to the procedure for evaluation of periodontal status.

With the current state of technology, conventional and digital bitewing radiography systems provide images of equal quality. However, the use of a sensor or storage phosphor plate results in relatively large diagnostic gain, owing to image-processing capabilities. Therefore, preference should be given to digital bitewing radiographs. Moreover, the use of sensors cuts the patient's dose in half compared with the exposure rates associated with the use of imaging plates and E- and F-speed film.

There are predilection sites for caries occurrence. Children and adolescents often have a bilateral and symmetrical pattern of caries occurrence. The maxillary arch is more commonly affected than the mandibular arch. Caries of the maxillary canines is less common than caries of the incisors, while the reverse usually applies to the mandibular canines and incisors. The maxillary and mandibular six-year molars are always more commonly affected by caries than the other molars and premolars. Other predilection sites include interproximal niches, which can be made inaccessible and hard to clean by anomalies of tooth position, and the cemento-enamel junction of the second molars in patients with mesially tilted, half-impacted wisdom teeth. The accumulation of plaque below the contact points can quickly lead to approximal caries. Periodontal pockets can result in cementum caries at the cemento-enamel junction. If cavities are not carefully prepared, residual caries can develop below fillings. If there is poor marginal seal, secondary caries can occur in the interdental spaces, as a result of poor dental hygiene.

After reaching a certain size, caries appears on radiographs as a clearly identifiable, roundish, wedge-shaped lesion with variably well-defined margins. Large carious lesions appear as irregularly shaped defects.

Radiographically, primary caries is divided into four types, based on tissue involvement. Radiographic classification types C1 to C4 correspond to clinical types D1 to D4 (□ Fig. 11.1):

- D1: superficial caries (limited to the enamel)
- D2: moderate caries
- D3: deep caries
- D4: deep complicated caries.

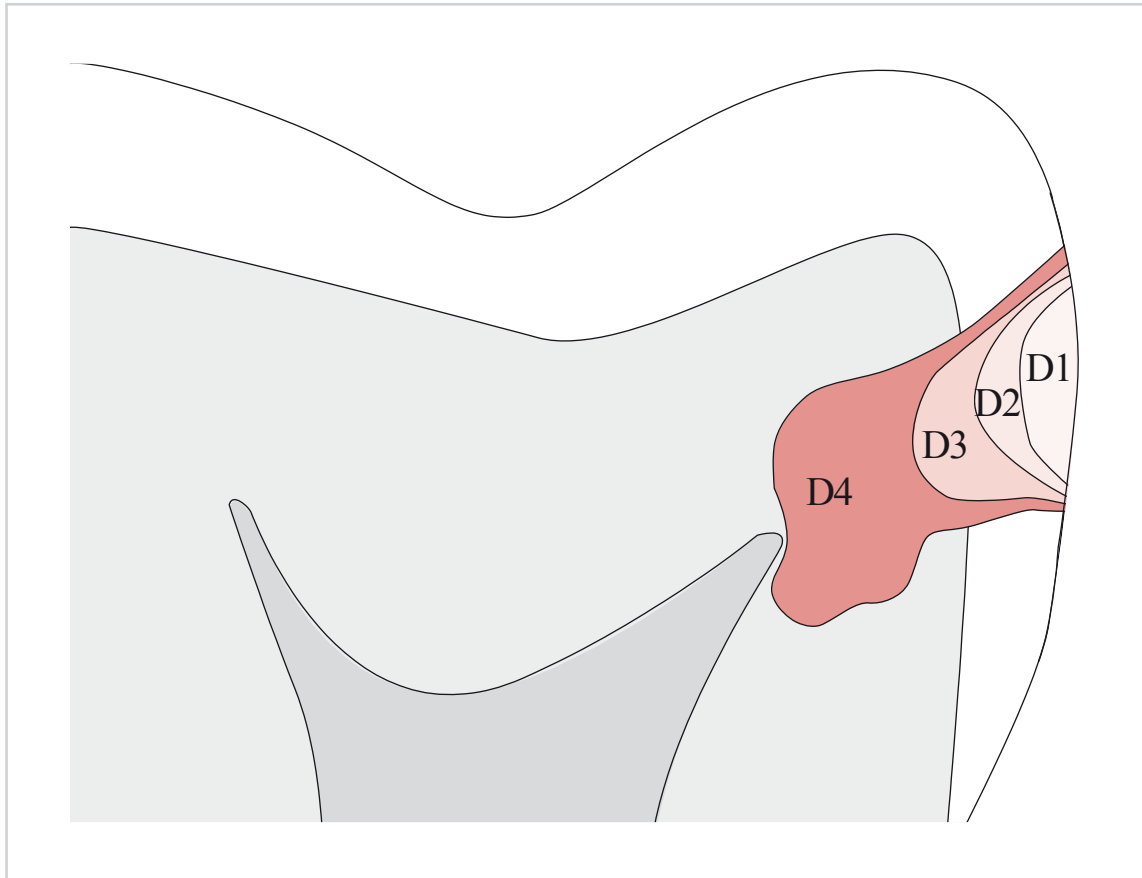


Fig. 11.1 Stages of caries progression (approximal caries). **D1**: lesion in the outer half of the enamel; **D2**: lesion in the inner half of the enamel; **D3**: lesion in the outer half of the dentin; **D4**: lesion in the inner half of the dentin. (From: Weber T. Memorix Zahnmedizin. 3rd ed. Stuttgart: Thieme; 2010.)

Examples of Carious Lesions

Superimposition-free visualization of the approximal surfaces is required for optimal caries diagnosis (□ Fig. 11.2).

□ C1: Superficial caries: Superficial caries (enamel caries) appears as a wedge-shaped defect that involves the enamel layer but has not yet penetrated the dentin (□ Fig. 11.3).

□ C2: Moderate caries: The carious lesion has spread to the inner enamel region and has penetrated up to the dentin and spread two-dimensionally (□ Fig. 11.4).

□ C3: Deep caries: Deep structural defect that involves the entire dentin thickness up to the dentin layers close to the pulp (□ Fig. 11.5).

□ C4: Deep complicated caries: Caries has led to opening of the pulp (□ Fig. 11.6).

Radiographically, caries lesions on occlusal surfaces are more difficult to diagnose than those on approximal surfaces. Unequivocal radiographic diagnosis of occlusal caries is not possible until caries has spread to the inner half of the dentin (□ Fig. 11.7). Radiographic diagnosis of stage C3 is possible only if there is extensive spread.

Radiographic diagnosis of recurrent or secondary caries is not always possible.



Fig. 11.2a–c Regardless of whether acute or chronic, initial caries generally is not detectable radiographically or, if so, only in conjunction with the findings of clinical examination.



Fig. 11.3a–c Superficial caries: note the defects in the enamel.

- a Distal part of tooth 35.
- b Distal part of tooth 35.
- c Distal part of tooth 13.



Fig. 11.4a–c Moderate caries.

a On the distal part of tooth 46, caries has progressed to the dentin.

b There is greater dentin involvement on the mesial aspect of tooth 15.

c A carious radiolucency is readily identifiable in the deeper layers of dentin on the distal part of tooth 16.



Fig. 11.5a–c Deep caries: in all three cases, caries has spread to the dentin layers very close to the pulp.



Fig. 11.6a–c Deep complicated caries: in all three cases, there is extensive caries involvement in all segments of the crown.

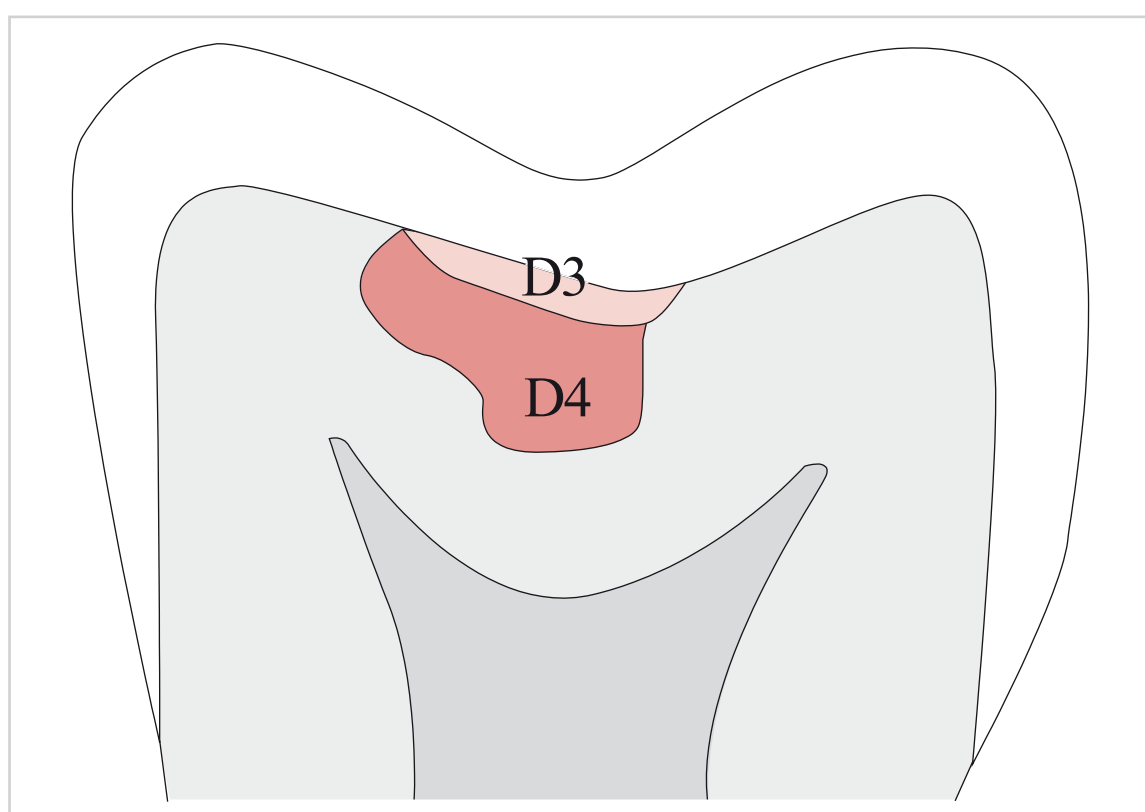


Fig. 11.7 Occlusal caries stages: radiographic diagnosis of **D1** to **D2** occlusal caries in the enamel is not possible. **D3**: carious lesion in the outer half of the dentin; **D4**: carious lesion in the inner half of the dentin. (From: Weber T. *Memorix Zahnmedizin*. 3rd ed. Stuttgart: Thieme; 2010.)

Intraoral radiographs are the product of the two-dimensional superimposition or summation of shadows from three-dimensional anatomical structures. Addition and subtraction effects can lead to artificially increased radiopacity and radiolucency. Depending on the intensity of the superimposed structures, defects may appear smaller and indistinct on radiographs, owing to the addition effect, or they may be brighter and extinguished, owing to the subtraction effect.

Caution

In the case of caries, the addition effect means that the extent of the initial caries lesion is underestimated on the radiograph, owing to the superimposition of intact enamel and dentin on the carious area.

Cariou lesions that have infiltrated the dentin generally have poorly defined margins; in the case of deep caries, they are often separated by a dense reactive zone of endangered and retracted pulp.

Owing to the tangential effect of the X-ray beam, radiographic detection of developmental defects, such as pits and irregularities on the enamel surface of the crown, is not possible unless they are located on the approximal surfaces of the teeth. If they appear as a radiolucent area with well-defined margins, they can sometimes be differentiated from initial caries. Such radiolucencies must be monitored at least once a year because it is impossible to radiographically distinguish initial caries from developmental defects in the enamel surface, or from demineralization disorders beginning at this stage.



Fig. 11.8 Note the approximal caries on tooth 74 and the discrete radiolucency on the mesial surface of tooth 75.

Recurrent caries beneath radiopaque crowns and fillings can be impossible to visualize properly. Difficulties also arise in digital radiography if these lesions are too strongly processed by filters. The metallic margins of dental crowns and fillings often appear as thin radiolucent bands, causing artifacts that make radiographic diagnosis of caries difficult to impossible in these regions.

Early childhood caries is a special form of caries that affects the primary dentition. Destruction of the remaining teeth can occur in the advanced stage associated with apical inflammation. To keep radiation exposure as low as reasonably achievable, sensor systems should always be used in pediatric patients. Small sensors produce radiographs of good diagnostic quality in children (□ Fig. 11.8 and □ Fig. 11.9).

11.2.2 Horizontal Bone Loss with Vertical Bone Defects

The height of the alveolar crest decreases over time, and the rate of decrease varies from one individual to another. Generalized horizontal bone loss is often accompanied by vertical bone defects and, in the advanced stages, by exposed bifurcations.

As a baseline examination, panoramic radiography is suitable for visualization of the alveolar crest. Owing to significant improvements in image quality in recent years, and the constant angles of incidence of the X-ray beam,



Fig. 11.9a–c Large carious lesions in the primary dentition.

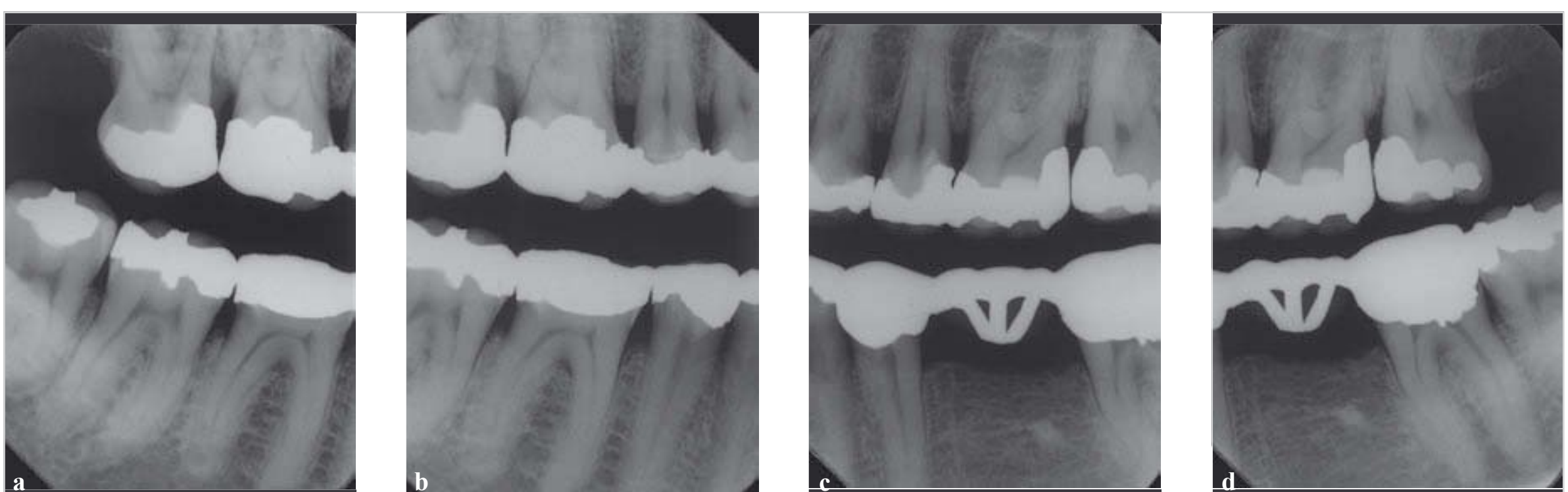


Fig. 11.10a–d Vertical bitewings provide a view of the crowns and alveolar bone.

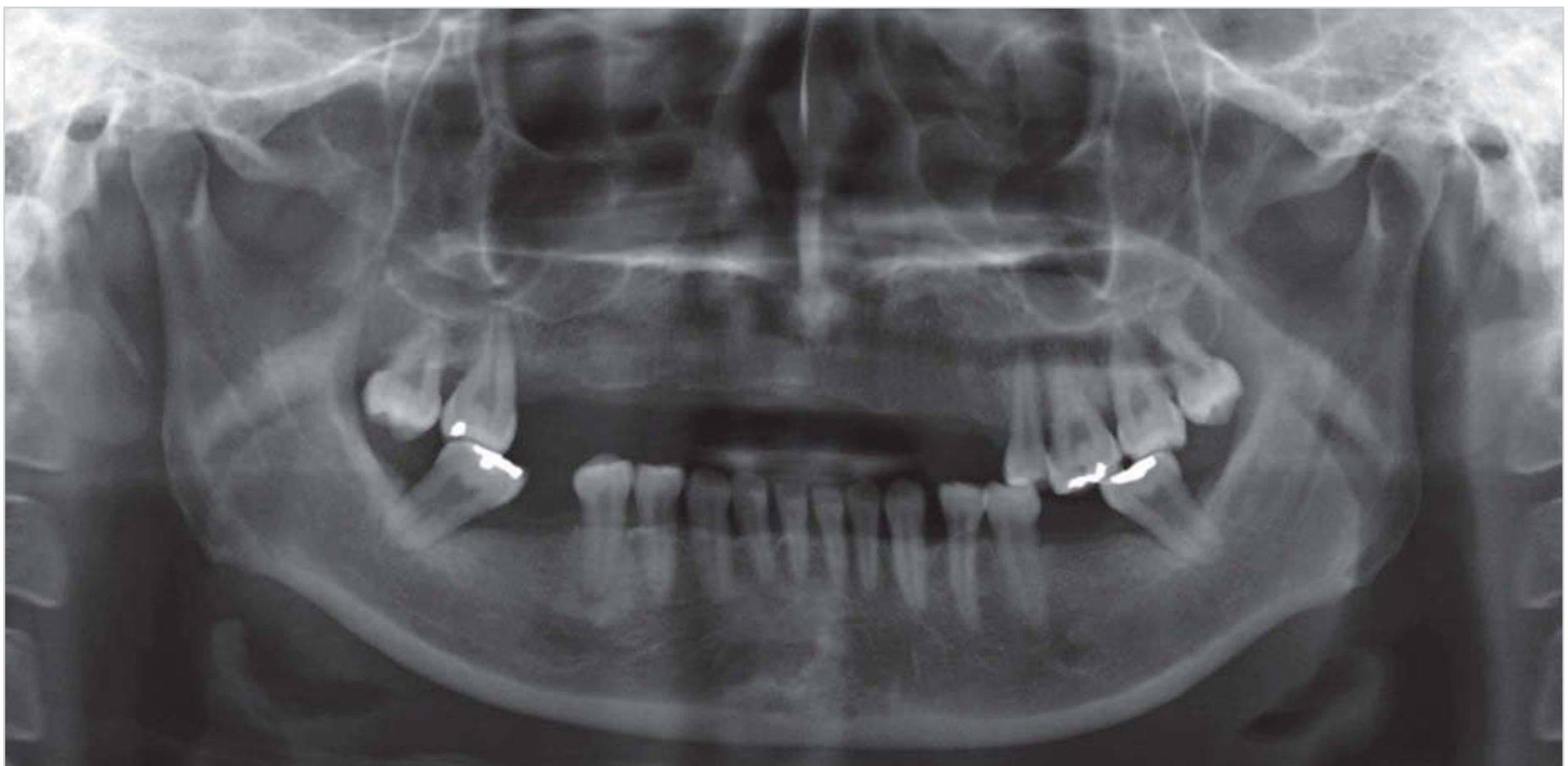


Fig. 11.11 Generalized horizontal bone loss and small vertical bone defects in the remaining maxillary and mandibular dentition.

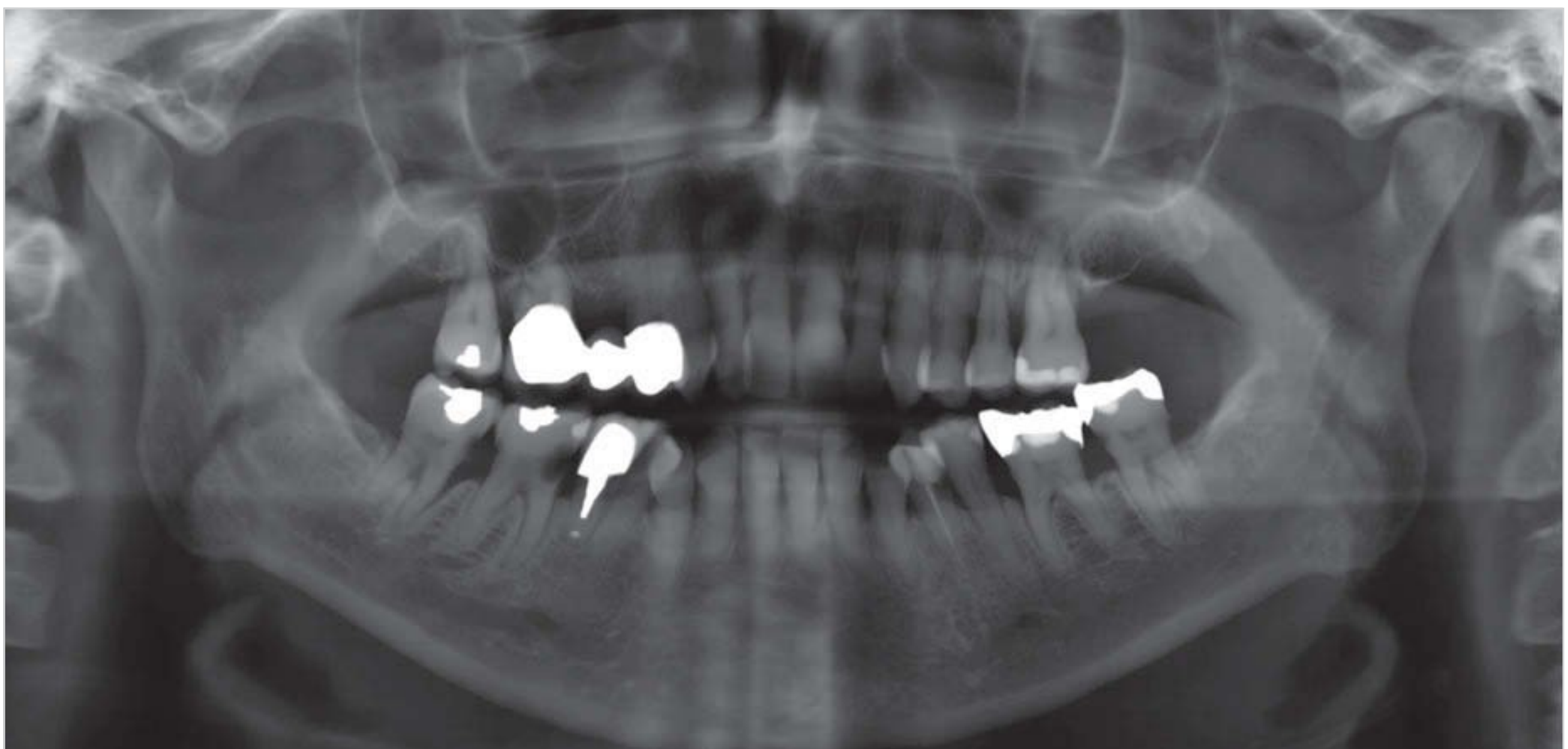


Fig. 11.12 Advanced generalized horizontal bone loss and marked vertical bone defects. Periapical widening of the periodontal ligament space of tooth 26 and a large carious lesion on the mesial surface of tooth 46.

panoramic radiography allows highly correct visualization of the mandible and maxilla. Panoramic radiographs should be supplemented with intraoral radiographs only in isolated cases. However, reliable assessment of all teeth in the crown region is not possible in most cases, owing to the superimposition of structures. Bitewing radiographs are more suitable for this than X-rays of the whole tooth. Vertical bitewing radiographs provide another option to visualize not only the crown region but also the alveolar ridge, with high resolution and without distortion (□ Fig. 11.10).

Panoramic radiographs usually enable a comprehensive and good assessment of bone conditions in the maxilla and mandible (□ Fig. 11.11 and □ Fig. 11.12).

Intraoral radiographs can provide more precise images, which are needed for clarification of particularly unusual findings (□ Fig. 11.13). Tomographic imaging techniques provide a broader overview. In recent years, CBCT, also known as digital volume tomography, has proved very useful for this. Transverse and axial views are needed for a complete analysis of bony periodontal defects.



Fig. 11.13a–c These intraoral radiographs clearly show the extent of vertical bone defects.

- a** Vertical bone defect on tooth 15.
- b** Vertical bone defect on tooth 15.
- c** Difficult situation on fractured tooth 16.

11.2.3 Apical Periodontitis

Pulpitis, pulp necrosis, failed root-canal treatment, and traumatic dental injuries can lead to apical periodontitis and advanced forms of marginal periodontitis.

Acute and chronic forms of apical periodontitis are generally distinguished. The severity of the disease is determined by the virulence of the causative pathogen and the status of the host's immune system.

Acute and Chronic Apical Periodontitis

Even if acute clinical symptoms are present, radiographs cannot demonstrate inflammatory responses if no changes have occurred that affect the integrity of the periapical structure. There is a latency period before acute intraosseous inflammation can be radiographically detected. Precise visualization of the apical region is needed to detect any changes in the lamina dura as early as possible. Radiographically, acute inflammation that infiltrates beyond the apical foramen is characterized by widening of the periodontal ligament space and diffuse periapical radiolucency. Any loss of continuity of the lamina dura around the apex of the affected tooth indicates the presence of a periapical inflammatory process. Chronic apical periodontitis is characterized by loss of the periodontal ligament space, which ends as a periapical radiolucency. A granuloma is a chronic mass of granulation tissue that forms in response to inflammation. It is characterized by fusion of the lamina dura with the dense margins of the granuloma, causing marginal discontinuity and radiolucency at the apex of the involved tooth.



Fig. 11.14 Widening of the periodontal ligament space suggestive of acute apical periodontitis.

Radiographic Features of Apical Periodontitis

- Acute apical periodontitis usually has a radiographically normal appearance but sometimes produces discrete apical widening of the periodontal ligament space (□ Fig. 11.14).
- Chronic apical periodontitis appears as widening of the periodontal ligament space and variable, diffuse, periapical radiolucencies (□ Fig. 11.15).
- If the inflammation persists, the apical tissue transforms into granulation tissue, the radiolucency becomes surrounded by a dense sclerotic margin, and chronic granulomatous apical periodontitis develops (□ Fig. 11.16).

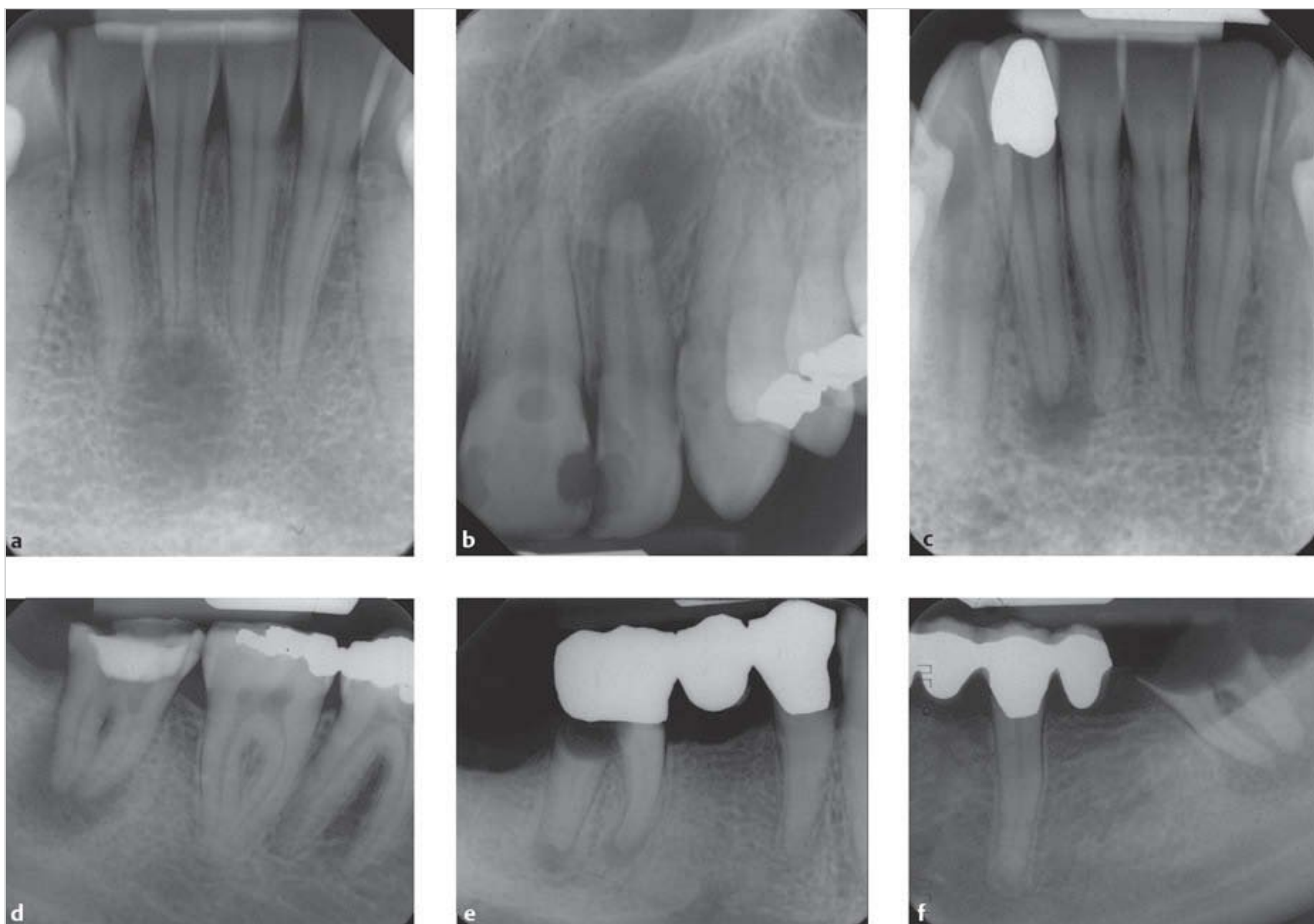


Fig. 11.15a–f Diffuse periapical radiolucencies.

- a** Tooth 31.
- b** Tooth 22.
- c** Tooth 42.
- d** Tooth 48.
- e** Tooth 47.
- f** Tooth 37.



Fig. 11.16a–c Endodontically treated tooth (**a**), carious tooth (**b**), and residual root (**c**) with periapical radiolucencies demarcated by a thin radiopaque margin; the findings are suggestive of a chronic process.

- a** Endodontically treated tooth 45.
- b** Carious tooth 47.
- c** Residual root of tooth 12.

11.2.4 Cystic Lesions

Cysts are defined as pathological cavities that are lined by epithelium and filled with fluid, semi-fluid or gaseous contents. Cysts are still classified according to the World Health Organization (WHO) classification of 1992; two types of epithelial cysts are distinguished:

- Odontogenic epithelial cysts of developmental origin
- Nonodontogenic epithelial cysts.

Keratocysts are another type of odontogenic cysts. According to the WHO classification of 2005, they are no longer considered to be developmental cysts but are now classified as odontogenic tumors.

Radiologically, the most important odontogenic cyst of developmental origin is the follicular cyst (dentigerous cyst). By definition, a follicular cyst is a cyst that surrounds the crown of an unerupted tooth and attaches at the cemento-enamel junction. It develops due to the accumulation of fluid between the enamel epithelium and the tooth crown, or in the layers of the enamel epithelium itself, and slowly increases in size, owing to osmotic internal pressure. Follicular cysts usually occur in association with impacted mandibular third molars and maxillary canines, but infrequently involve the maxillary third molars and the mandibular premolars. After the radicular cyst, the follicular cyst is the second most common cyst of the jaw.

Radiographically, it appears as a round to oval radiolucency surrounded by a thin radiopaque line. The clinician should always check to determine whether this radiopaque line ends at the cemento-enamel junction. If this is not the case, then there is a strong suspicion of a keratocystic odontogenic tumor.

Like all cysts, follicular cysts displace the surrounding structures. In the mandibular region, the teeth, as well as the mandibular nerve canal on the affected side, are displaced and no longer show symmetry with the opposite side (□ Fig. 11.17 and □ Fig. 11.18).

The nasopalatine duct cyst, although not very common, is a nonodontogenic epithelial cyst that must be considered when the incisive canal is pathologically enlarged. On radiographs, it appears as a cystic mass that is positioned exactly midline and completely enclosed within the incisive canal.

Practice

Panoramic radiographs do not provide adequate visualization of nasopalatine duct cysts, especially not to distinguish whether a suspicious findings is actually a cyst or not. CBCT is the imaging technique of choice in cases where there is clinical and radiographic suspicion of a nasopalatine duct cyst. Tomographic images in multiple planes are needed for proper visualization of this difficult part of the maxillary anterior region (□ Fig. 11.19).

The second group of cysts consists of those that develop from the epithelial cell rests of Malassez because of inflammation. Because their growth is triggered by pulp necrosis, a nonvital tooth is the prerequisite for the development of radicular cysts.

The radicular cyst (also termed periapical cyst) is the most common cystic lesion of the jaw, comprising 90% of all jaw cysts. It involves the maxilla more frequently than the mandible. Radiographically, this odontogenic cyst, like all cysts, appears as a round or ovoid radiolucent area

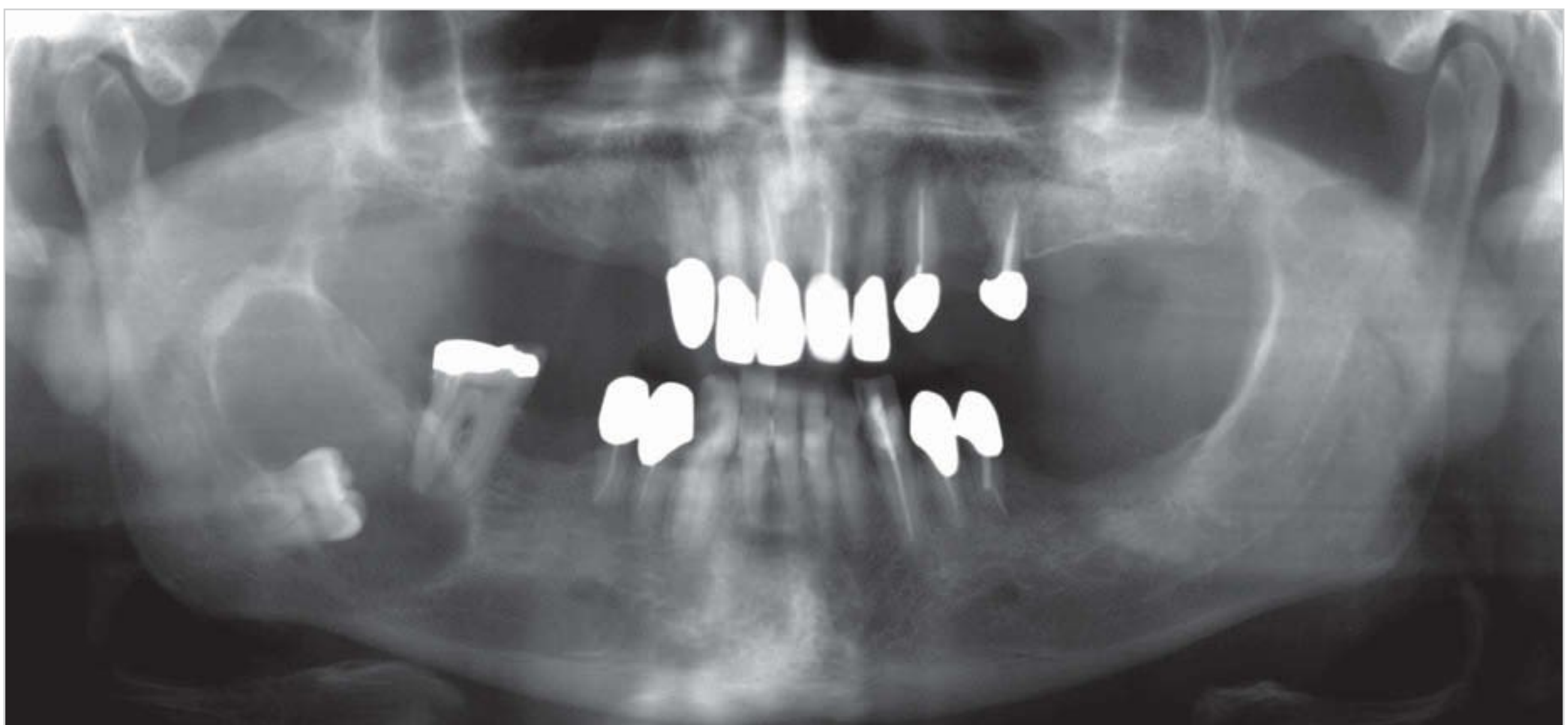


Fig. 11.17 Note the follicular cyst arising from an impacted and dislocated wisdom tooth 48; the cyst margin is attached to the cemento-enamel junction. Tooth 37 shows no signs of root resorption.

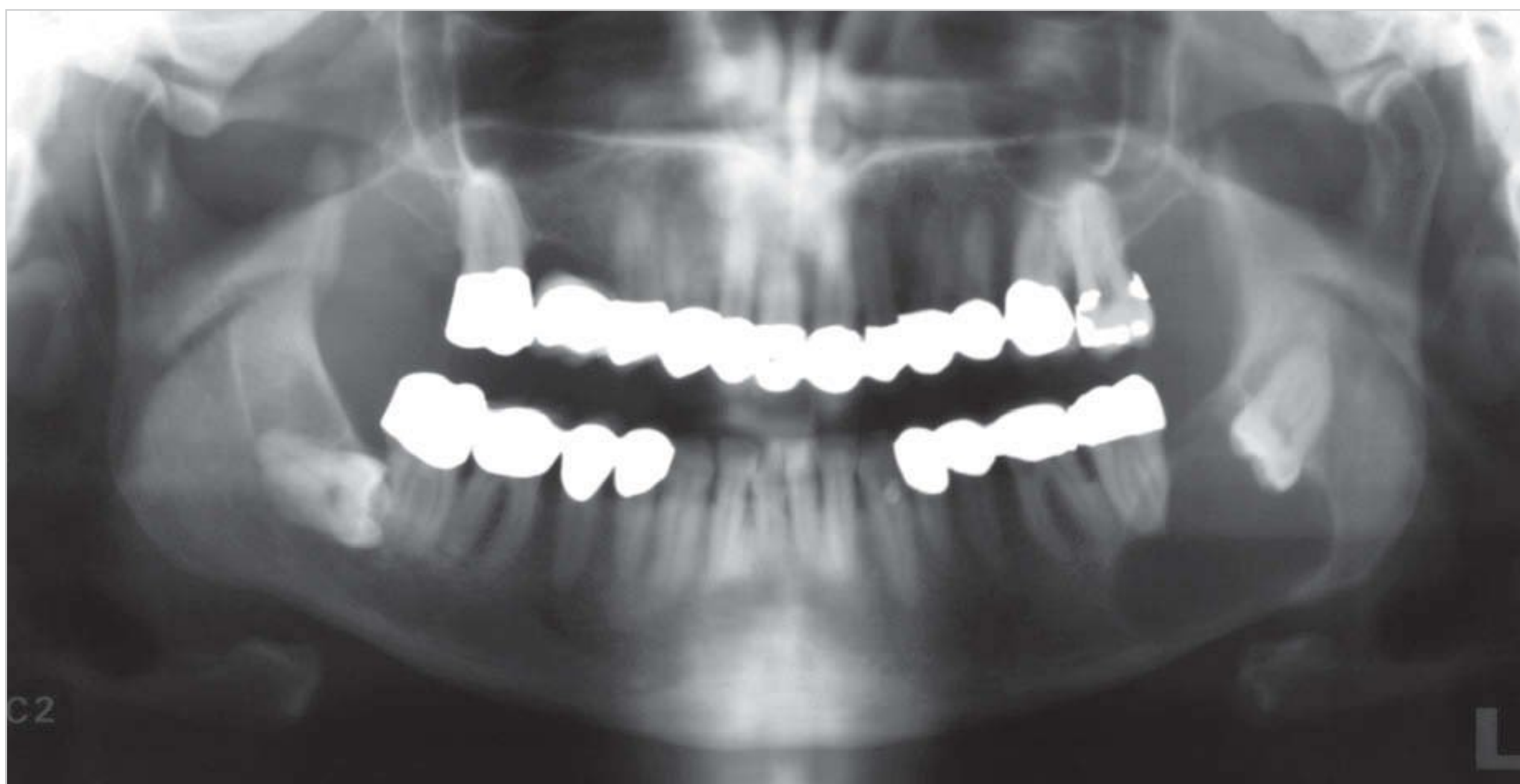


Fig. 11.18 Follicular cyst arising from impacted and dislocated wisdom tooth 38; the cyst margin is also attached to the cemento-enamel junction. Tooth 37 also shows no signs of root resorption.

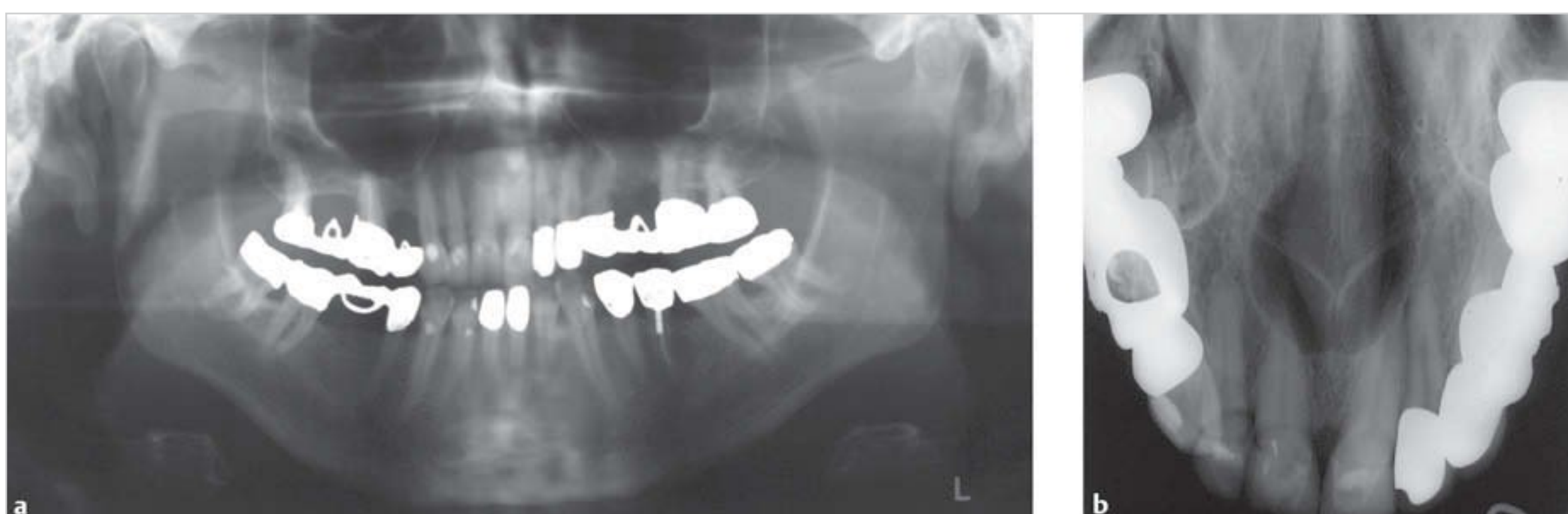


Fig. 11.19a, b The findings are suggestive of a nasopalatine duct cyst.

a An indistinct circular radiopaque line in the maxillary anterior region is the only finding on the panoramic radiograph.

b This additional occlusal radiograph shows a very large cystic process suggestive of a nasopalatine duct cyst in the vicinity of the incisive canal.

surrounded by a thin radiopaque margin. If infected, the radicular cyst may have an interrupted radiopaque margin and resemble a tumor-like mass, depending on the severity of infection. Radicular cysts are unilocular cystic lesions that can become very large, depending on the duration of the phase of cyst enlargement (□ Fig. 11.20 and □ Fig. 11.21). If such expansion has occurred, they lose their spherical shape and can take on a variety of irregular shapes.

Practice

Dental panoramic radiography is used for primary diagnosis, but multi-dimensional tomographic imaging is recommended once the cysts reach a certain size.

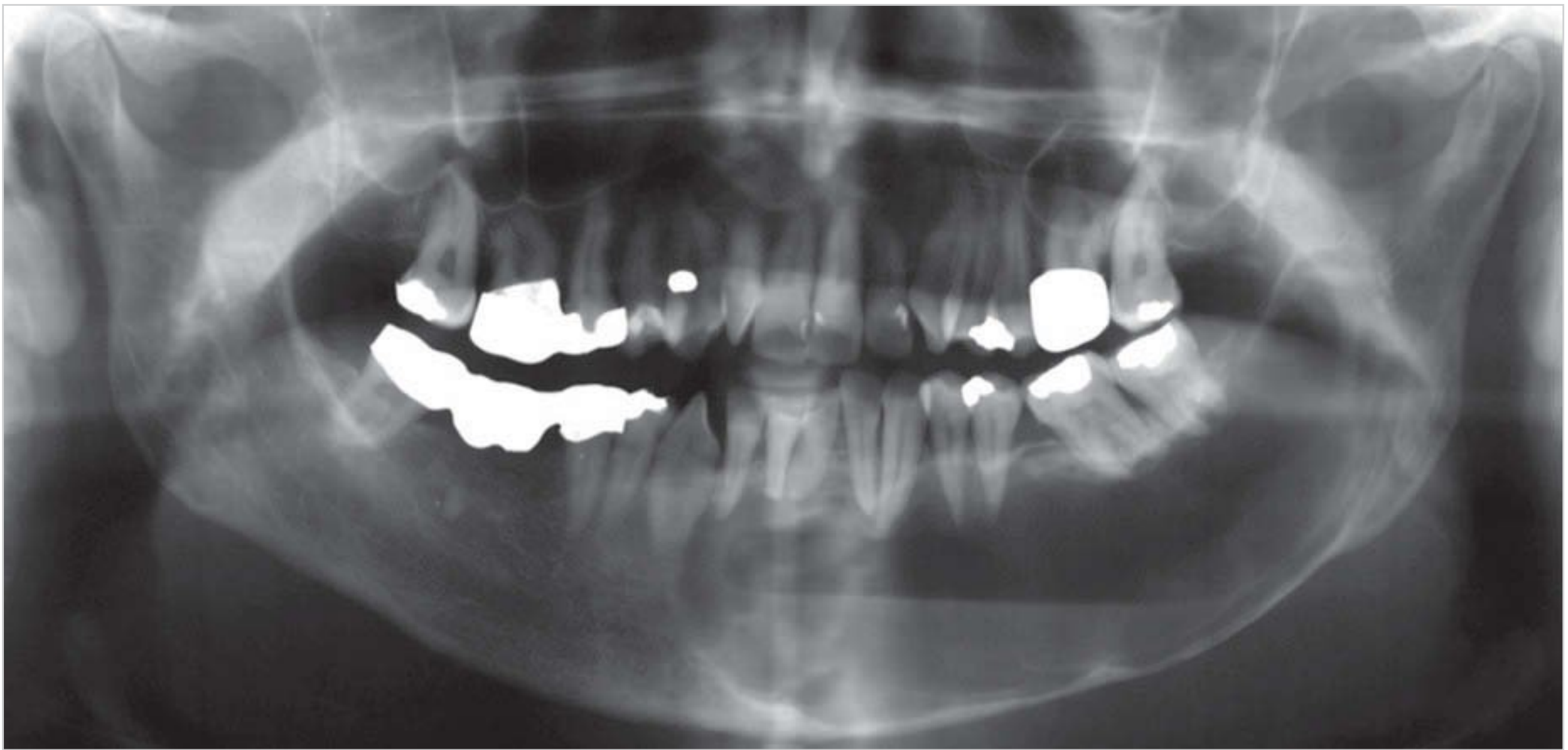


Fig. 11.20 Very large radicular cyst in the left mandible, arising from tooth 35.



Fig. 11.21 Around cystic radiolucency arising from the residual root of tooth 17 can be seen in the right mandible and maxillary sinus. It is a radicular cyst whose origin is the residual root of tooth 17, which projects into the cyst. The radiopaque line that surrounds the radiolucency is also suggestive of a cyst.

11.2.5 Malignant Lesions

Cancer of the Floor of the Mouth

Carcinoma of the oral mucosa is the most common type of cancer of the oral cavity. Squamous cell carcinoma of the floor of the mouth involves the lingual cortical bone of the mandible; it can infiltrate and destroy the alveolar process and even the entire mandible in the advanced

stages. A panoramic dental X-ray should be performed to carefully evaluate the alveolar ridge for signs of osteolysis, especially in elderly and edentulous patients. If there is generalized horizontal bone loss, cases where the margins of the alveolar ridge are no longer smooth but have breaks in continuity indicative of infiltration by a carcinoma of the floor of the mouth are sometimes overlooked (□ Fig. 11.22 and □ Fig. 11.23).



Fig. 11.22 On side-to-side comparison, a discrete, tub-like osseous depression in the alveolar ridge can be detected on the right side. There is a risk of misinterpretation of this radiographic finding as normal inflammatory bone loss. On closer inspection one can see that the margin of the alveolar ridge is irregular, which is indicative of a destructive process.

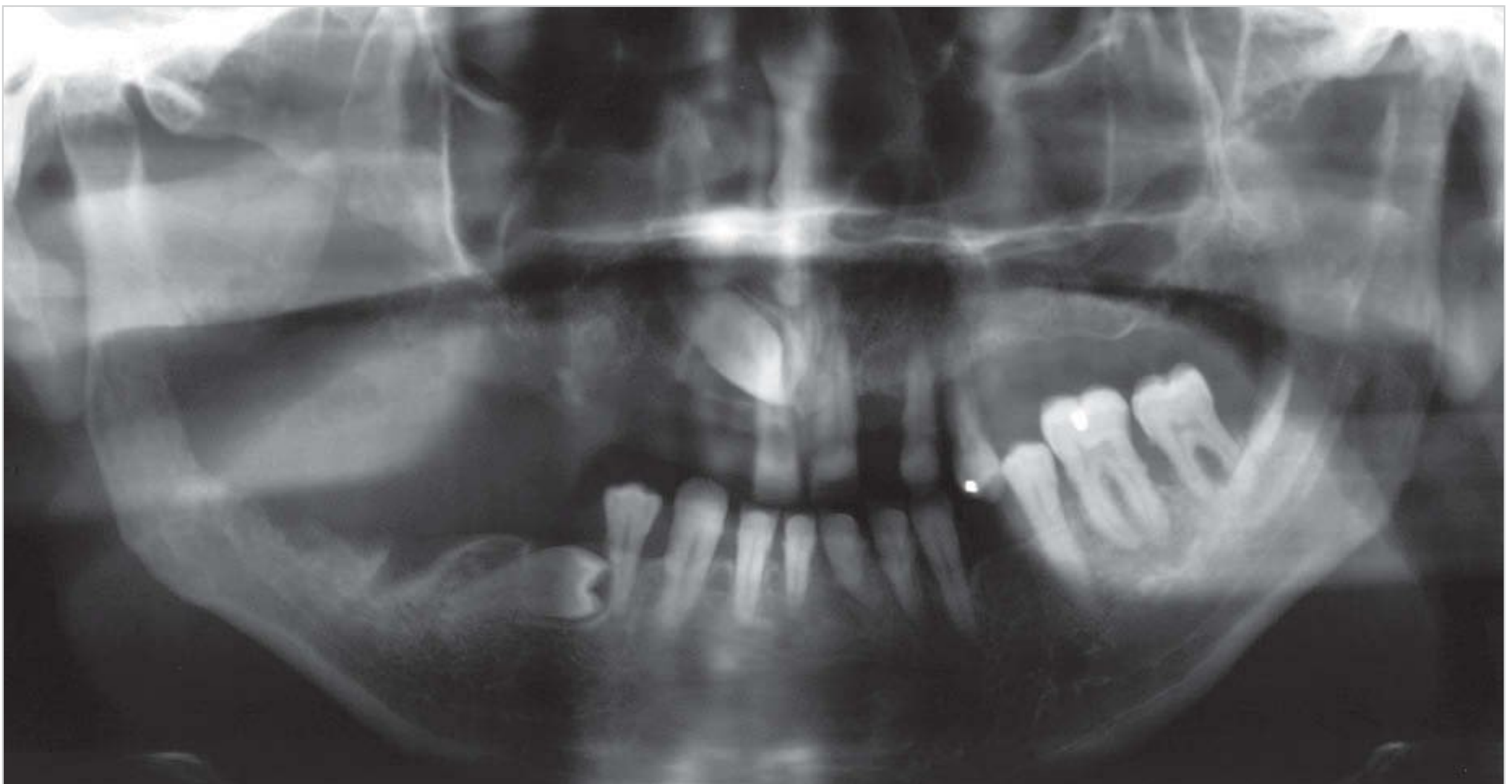


Fig. 11.23 In this case, marked osteolysis was visible not only in the right mandible, but also in the right maxilla. In the maxillary arch, destruction of the alveolar ridge extends into the right maxillary sinus.

Osteolysis of the lingual cortical bone cannot be detected by panoramic radiography. Tomographic images in multiple planes are needed for visualization of this region. However, CBCT is not satisfactory for detection of

soft-tissue involvement or, in particular, lymph node involvement from carcinoma. Computed tomography and magnetic resonance imaging are the imaging techniques of choice in these cases.

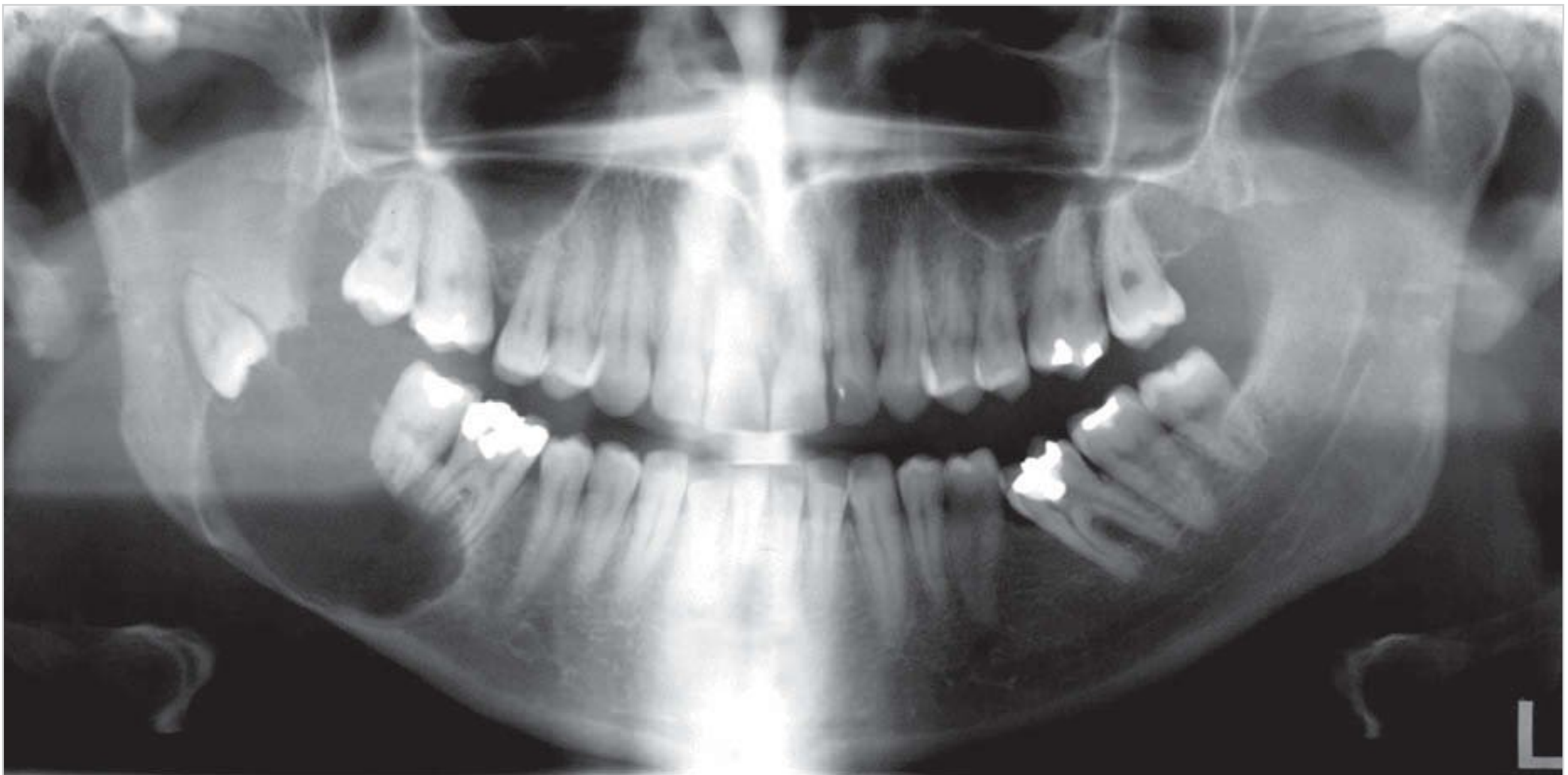


Fig. 11.24 Ameloblastoma of the right mandible with resorption of the roots of teeth 46 and 47.

Odontogenic Tumors

Odontogenic tumors or tumor-like lesions that arise from the tooth-forming structures are rare. Their radiographic appearance can be more or less typical. Therefore, whenever a tumor-like lesion is detected on a radiograph, regardless of whether it is presumed to be benign or malignant, a histological examination is always necessary to confirm the diagnosis.

Note

Radiographic images only provide information and clues of variable accuracy. Ultimately, a reliable diagnosis cannot be established based on radiographic images alone. The choice of radiographic images can increase the reliability of the diagnosis, but radiographs alone can never provide a completely reliable diagnosis of tumors and tumor-like lesions.

WHO revised and refined its classification of odontogenic tumors in recent years. Radiographically, they are still divided into two main groups:

- Pathological changes that appear as cystic lesions
- Pathological changes that arise from mesenchymal tissues and bone.

Solid and Multicystic Ameloblastomas

The conventional ameloblastoma can occur in all parts of the maxilla and mandible. The ameloblastoma is the second most common type of odontogenic tumor after the keratocystic odontogenic tumor, which was previously referred to as the odontogenic keratocyst.

Note

Whenever a cystic lesion does not clearly originate from the apex of a tooth, follicular cyst, keratocyst (keratocystic odontogenic tumor), and ameloblastoma must be considered in the differential diagnosis.

The most common site of occurrence (in 80% of cases) is the mandibular molar region, followed by the mandibular premolar region and, less commonly, the mandibular anterior region and maxillary molar region. The features of ameloblastoma vary—they may appear as unilocular or multilocular cystic lesions. Ameloblastoma is often associated with an impacted tooth. Therefore, if a follicular cyst is detected, the exact site of origin must be determined.

Ameloblastomas, like cysts, tend to displace surrounding structures, resulting in thinning and expansion of the cortical bone. Displacement of the mandibular nerve canal is a sign of ameloblastoma expansion. Resorption of roots of the involved teeth is an important and reliable sign of ameloblastoma (□ Fig. 11.24, □ Fig. 11.25, □ Fig. 11.26).

Ameloblastic fibroma, fibrodentinoma, and ameloblastic fibro-odontoma are rare variants of ameloblastoma that are classified as benign mixed odontogenic tumors. These mixed tumors have both epithelial and ectomesenchymal components and often involve the dental hard tissues. Unlike the pure ameloblastoma, mixed odontogenic tumors are usually multilocular cystic lesions that are not uniformly structured.



Fig. 11.25 Multicystic ameloblastoma of the left mandible with resorption of the roots of teeth 35, 36, and 38; the third molar (tooth 38) is displaced and tooth 37 is missing.



Fig. 11.26 Multicystic ameloblastoma of the right mandible.

Ameloblastic **f**ibroma and **f**ibro-odontoma are very rare tumors composed of both odontogenic epithelium and odontogenic ectomesenchyme, with or without involvement of dental hard tissue (□ Fig. 11.27 and □ Fig. 11.28).

Keratocystic Odontogenic Tumor

The keratocystic odontogenic tumor is a benign tumor of odontogenic origin, which, like the ameloblastoma, may appear as a unilocular or multilocular radiolucent lesion. As the name implies, the special features of the keratocystic odontogenic tumor are:

- Parakeratosis of the epithelium
- Aggressive and **i**nfiltrating behavior.

These tumors have a high recurrence rate and a tendency to form daughter cysts. They can be identified based on the budding of daughter cysts, which are initially roundish but later converge to form masses, giving keratocystic odontogenic tumors their characteristic scalloped margins and distinct appearance. Radiographs often underestimate the extent of keratocystic odontogenic tumors because of the density and superimposition of intact adjacent bony structures on the daughter cysts. These summation effects make early and complete detection of keratocystic odontogenic tumors by intraoral and panoramic radiography extremely difficult (□ Fig. 11.29, □ Fig. 11.30, □ Fig. 11.31).



Fig. 11.27 Histologically, this ameloblastic fibro-odontoma was classified as benign, but its radiographic appearance is suggestive of a malignant tumor.

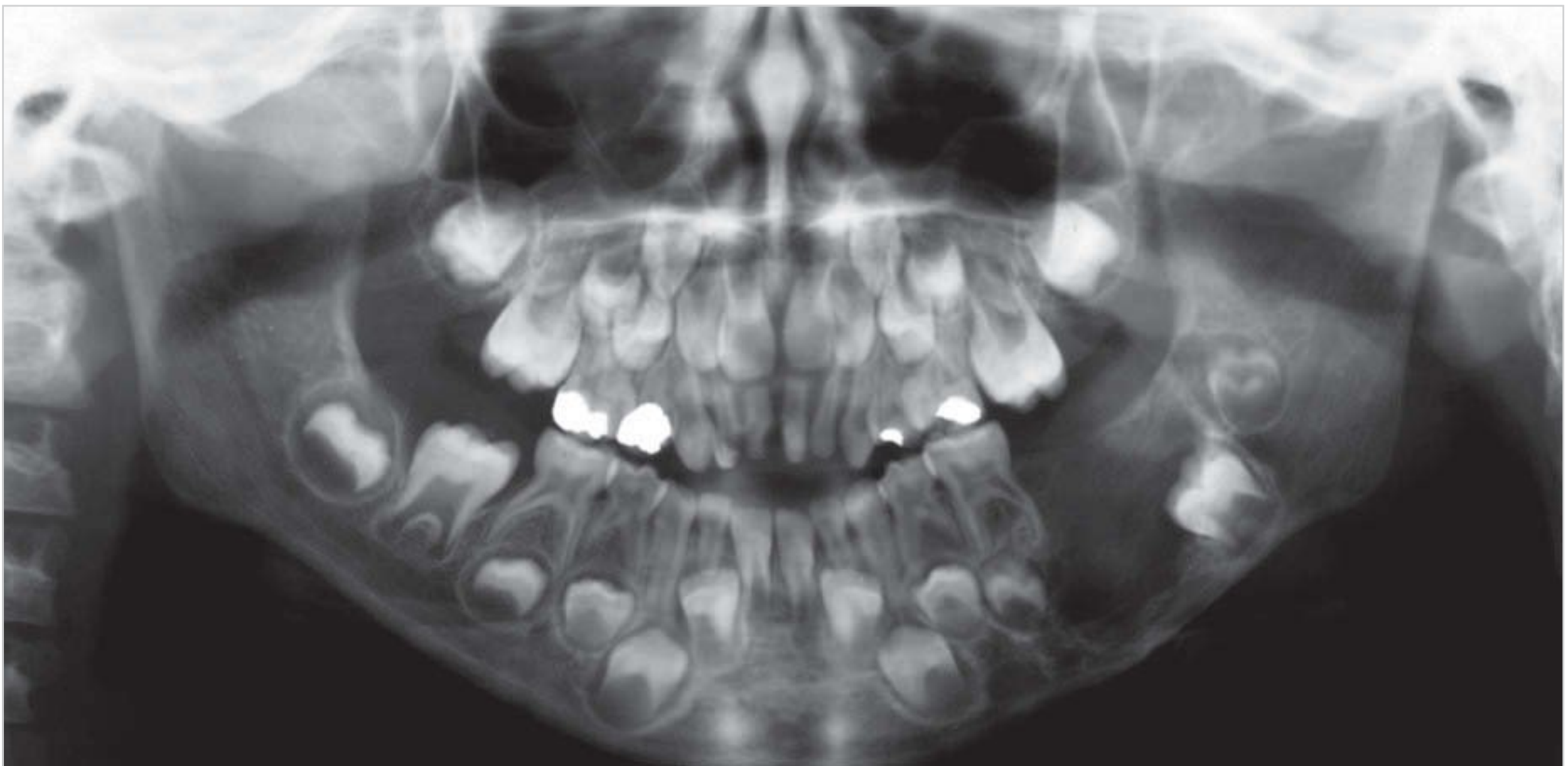


Fig. 11.28 Ameloblastic fibroma.

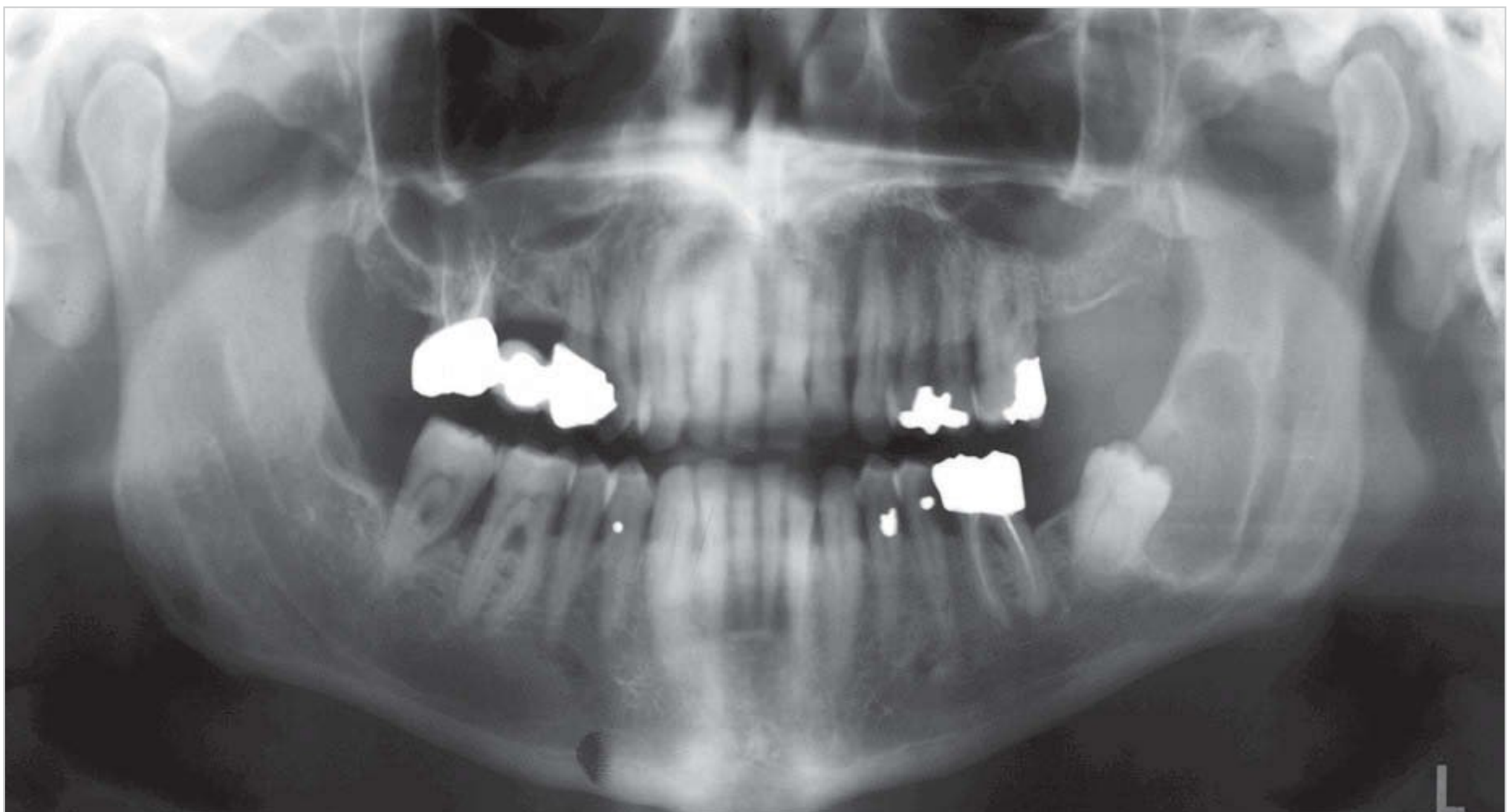


Fig. 11.29 Typical keratocystic odontogenic tumor with an adjacent tooth. The tumor displaces the tooth but is not attached to it. This type of radiographic constellation can easily be misinterpreted as a follicular cyst.

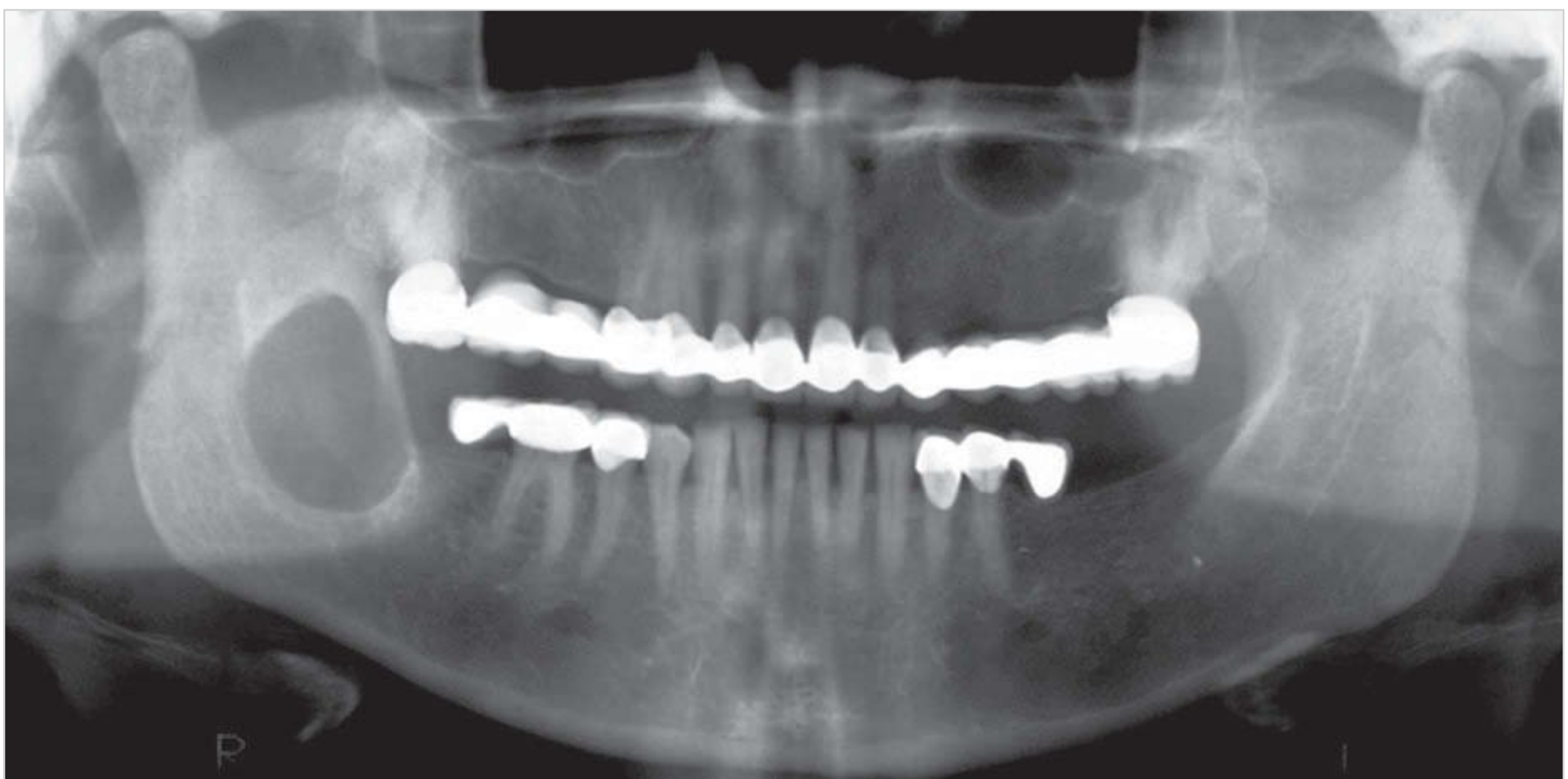


Fig. 11.30 This unilocular, oval cystic lesion in the right angle of the jaw is a variant of a keratocystic odontogenic tumor.

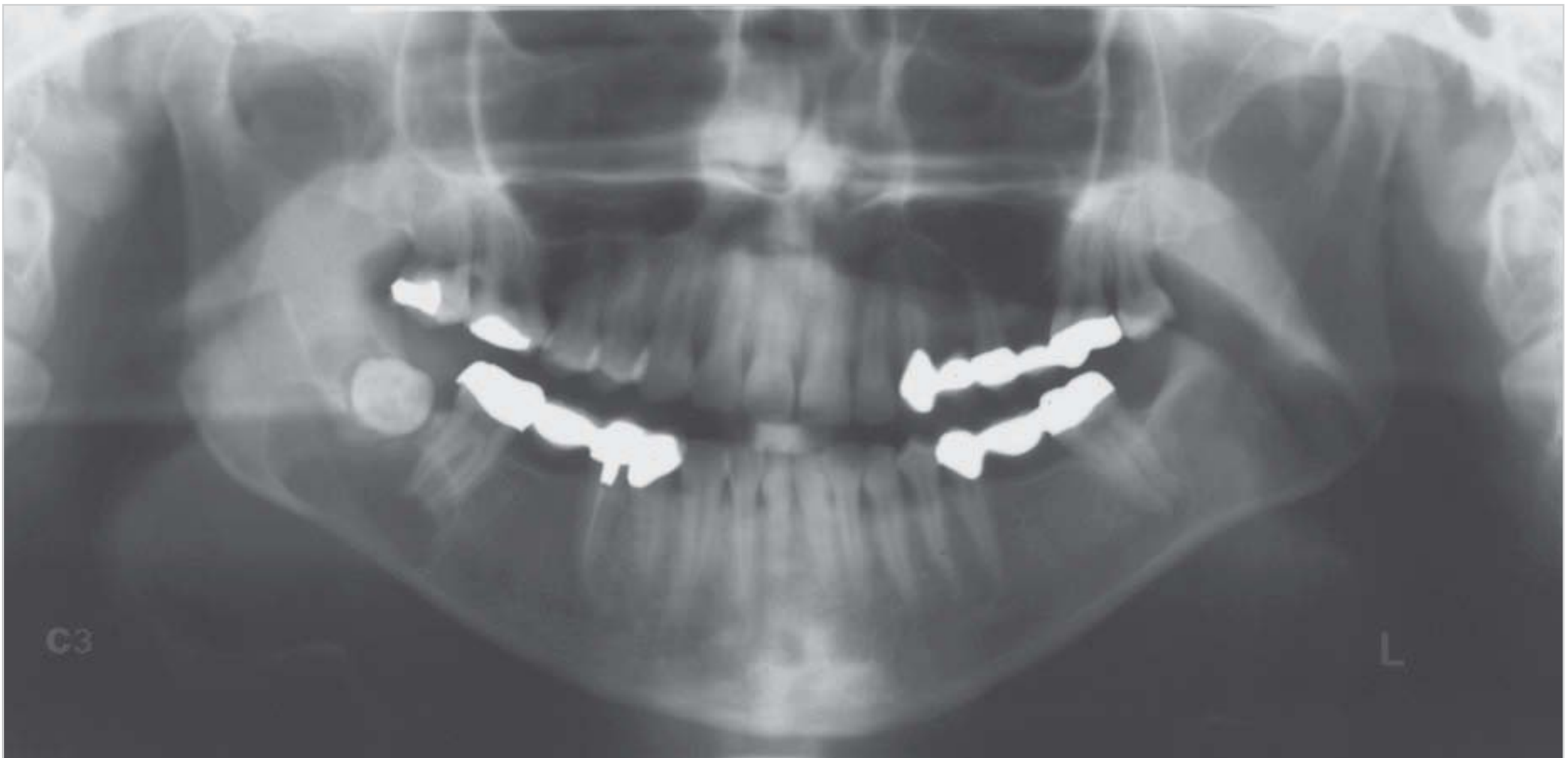


Fig. 11.31 Unilocular keratocystic odontogenic tumor in the right angle of the mandible. The radiolucent lesion is not clearly attached to teeth 47 and 48.

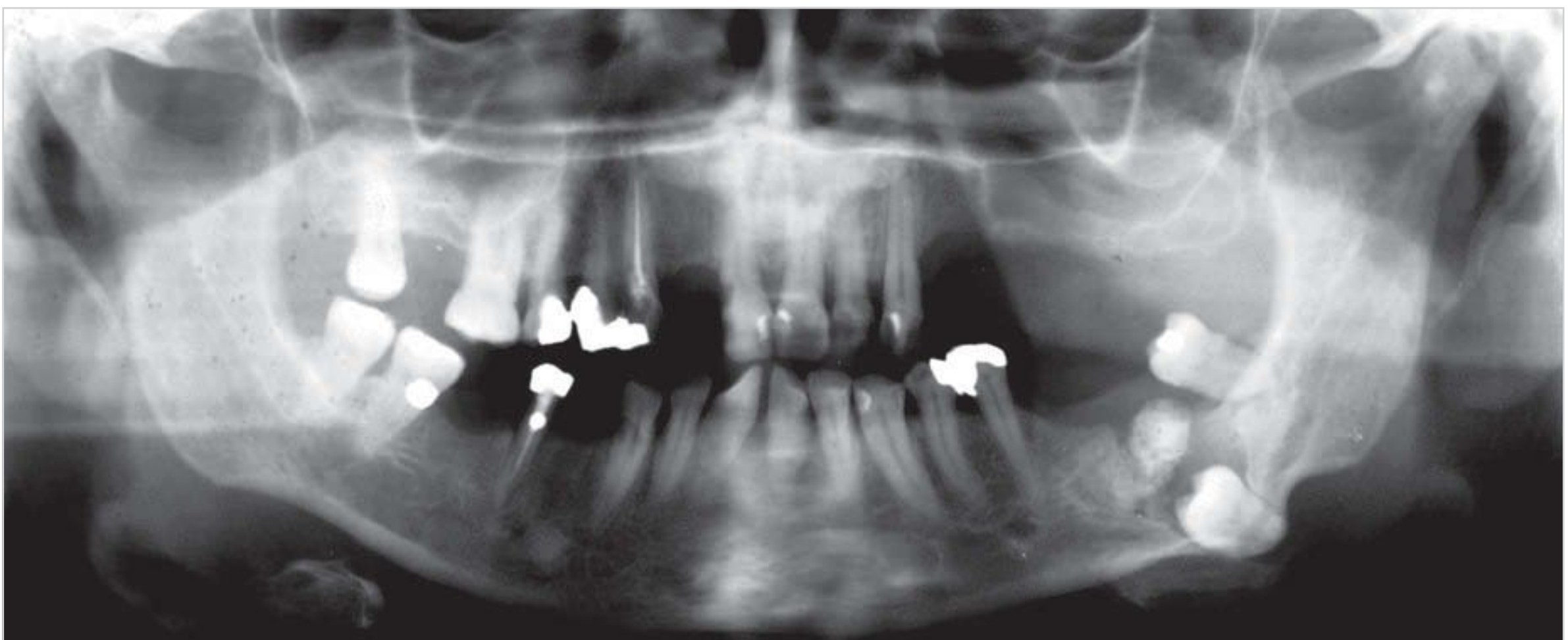


Fig. 11.32 This complex odontoma appears as a homogeneous, sharply demarcated pericoronal radiolucency on tooth 37, which is deeply impacted. The odontoma is preventing the tooth from erupting.

Odontoma

The odontoma is a developmental anomaly that resembles a tumor but is a hamartoma of odontogenic origin. It consists of several large and small tooth-like structures or a conglomerate of different dental tissues. Two types of odontoma are distinguished: compound and complex.

- The complex odontoma is a tumor-like malformation (hamartoma) characterized by the formation of an amorphous mass of enamel, dentin, and cementum (□ Fig. 11.32). It is frequently located on an impacted molar, which itself may be hardly visible, owing to the superimposition of shadows from the lesion.

- The compound odontoma is a developmental anomaly (hamartoma) that resembles a tumor and consists of several fully developed small teeth or tooth-like denticles. Its radiographic appearance varies, depending on the stage of development. It appears as a well-demarcated area of osteolysis in the early stages. In later stages, slowly developing tooth elements may be surrounded by a wide radiolucent margin indicative of a growth zone (□ Fig. 11.33). In the final stage, the denticles are surrounded by a thin radiolucent margin.

Compound odontomas are usually diagnosed before the age of 20 years. They most commonly occur in the anterior teeth, followed by the premolar region.



Fig. 11.33a–d Compound odontoma: the CBCT images (**b**, **c**, and **d**) clearly visualize the tooth buds.
a Around, very dense area surrounded by a thin radiolucent margin can be seen in the mandibular anterior region on this panoramic radiograph.
b Lateral view CBCT image.
c Lateral view CBCT image.
d Axial CBCT image.

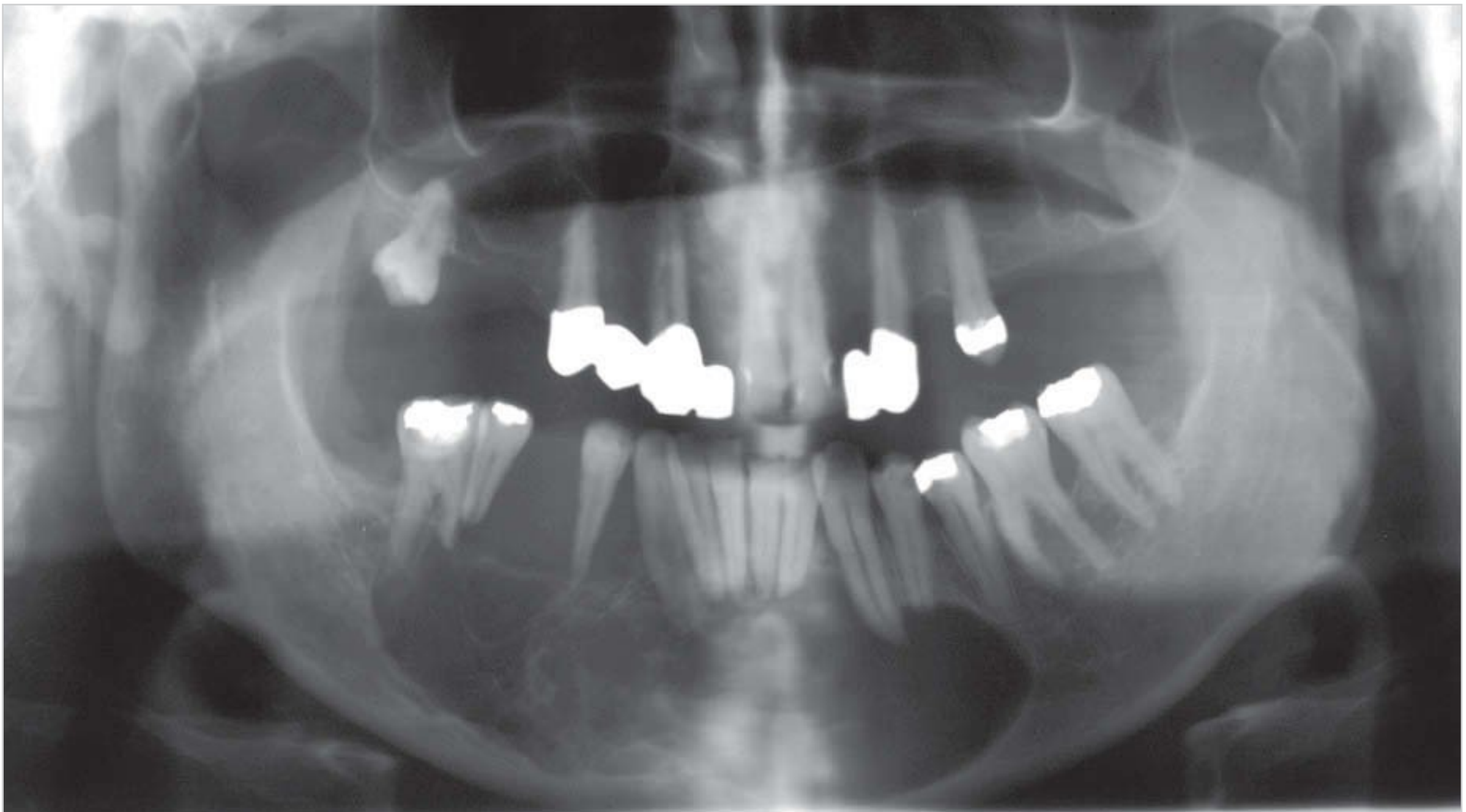


Fig. 11.34 Odontogenic myxoma (myxofibroma): The radiograph reveals a large radiolucency that extends from tooth 35 to tooth 46 and contains trabeculae. The teeth appear to be slightly tilted. Resorption of the roots of teeth 34 and 32 cannot be excluded.

Odontogenic Myxofibroma (Odontogenic Myxoma)

The odontogenic myxofibroma (odontogenic myxoma) is an intraosseous neoplasm. Odontogenic myxofibromas are benign but locally invasive tumors of the jaw. They have a relatively high recurrence rate of up to 25%. On the panoramic radiograph, they appear as a multilocular radiolucency associated with destruction of the mandible. They often contain delicate trabeculae, giving the lesion an irregular multilocular appearance (□ Fig. 11.34).

Cementoma (Cementoblastoma)

Benign cementoma (synonym: cementoblastoma) is characterized by the production of a bulbous mass of cementum-like tissue that is attached to the roots of the tooth. Its radiographic appearance is variable. Cementomas usually arise in association with the apices of the mandibular first molars and mandibular second premolars, and they usually occur during the second and third decades of life. The cementoma grows slowly in layers around the root of the involved tooth. Because it is attached to the tooth root, extraction may be difficult.

With progressive development and cementum deposition, the cementoma appears as a radiopaque mass with either a mottled, floccular, mosaic-like appearance or a uniformly radiopaque appearance. It is often, but not always, surrounded by a thin radiolucent border. The presence of a radiolucent border may be a sign of a growth zone or sequestration (□ Fig. 11.35).

Cemento-osseous Dysplasia

The two main types of cemento-osseous dysplasia are:

- Periapical cemental dysplasia
- Florid cemento-osseous dysplasia.

Periapical cemental dysplasia most commonly involves the mandibular anterior teeth. Radiographically, the initial stage of development is characterized by osteolysis and fibrosis. The second stage is characterized by the start of the deposition of cementum, as reflected by the appearance of dense cementum-like radiopacities. Pulp vitality testing indicates that neither apical periodontitis nor radicular cysts are the cause of the radiolucencies.

Radiographically, florid cemento-osseous dysplasia appears as a large radiolucency surrounded by a radiopaque margin characterized by the deposition of cementicles in dense connective tissue stroma (□ Fig. 11.36).

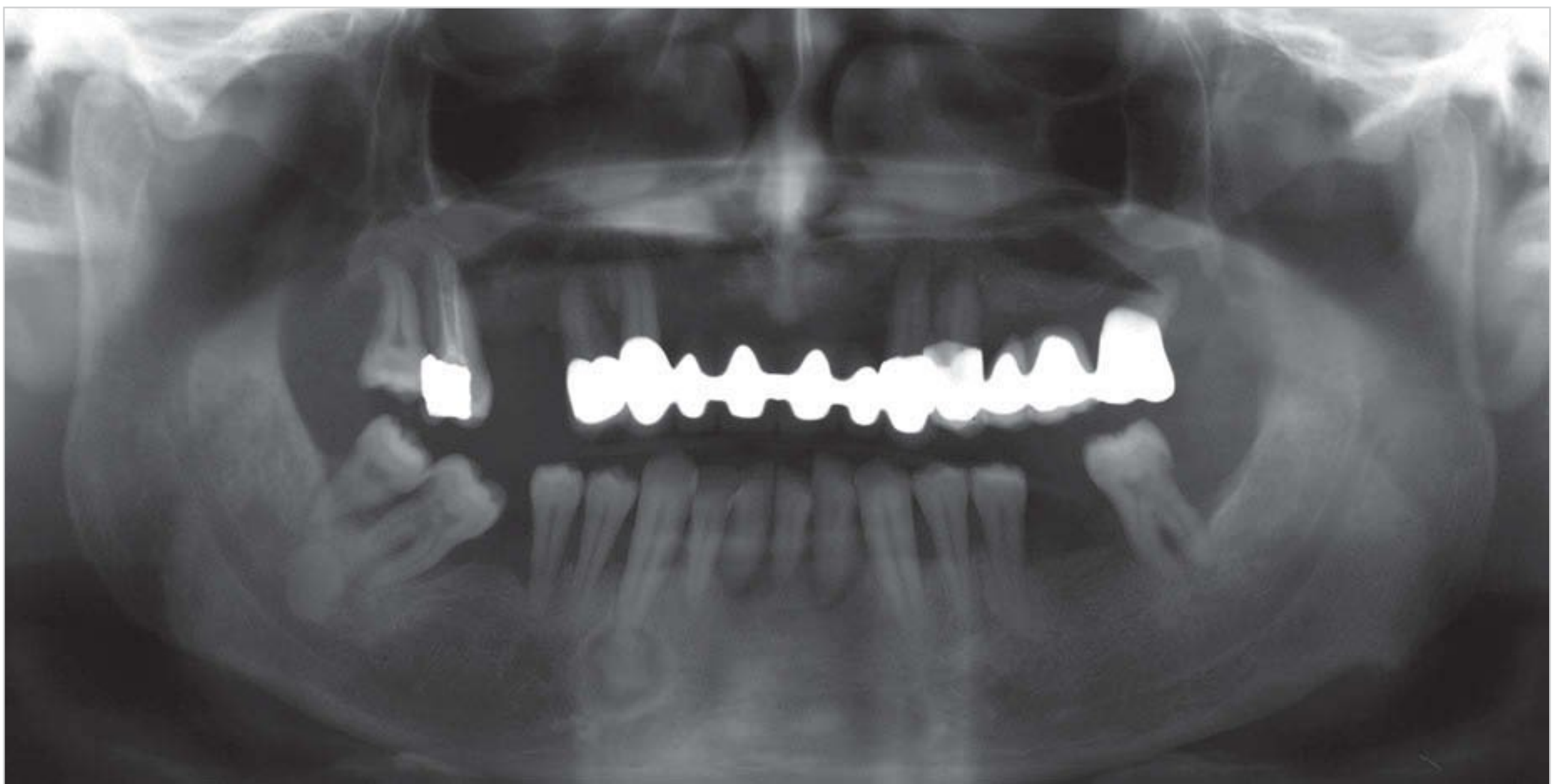


Fig. 11.35 Cementoma (cementoblastoma): The radiograph reveals a radiopaque mass that is closely connected to the apex of tooth 43 and surrounded by a radiolucent margin.



Fig. 11.36 Cemento-osseous dysplasia: edentulous spaces 37 and 46 show the typical radiographic features of cemento-osseous dysplasia; cementicles are deposited in the connective tissue stroma.

11.2.6 Bone Diseases of the Jaw

In addition to inflammations, cysts, and tumors of the jaw, bone diseases of the jaws are other typical pathologies that do not fit into the above categories.



Fig. 11.37 Osteomyelitis with the formation of sequestrum (dead bone) as a complication of open fracture.

Many are not detected in routine X-ray examinations. Important bone lesions of the jaws include osteomyelitis, ossifying fibroma, fibrous dysplasia, central giant cell granuloma, aneurysmal bone cyst, and pseudocyst.

Osteoma falls into a special category. Osteoma is defined as a benign neoplasm of mature compact or cancellous bone but is not listed as a tumor in the WHO classification.

Osteomyelitis

Osteomyelitis is an infection of the bone. In patients with a weak immune system, it can occur as a complication of periapical infection, acute necrotizing gingivitis, and untreated open fractures. Radiotherapy of the jaw is also associated with a high risk of osteomyelitis. Acute osteomyelitis is characterized by necrosis and the formation of sequestrum (dead bone) in the area of infection (□ Fig. 11.37).

Ossifying Fibroma

Ossifying fibroma is classified as a benign bone lesion and a true neoplasm. It is most commonly found in the mandibular molar region. Radiographically, the ossifying fibroma appears as mixed radiolucent-radiopaque, containing variably calcium-dense structures with trabeculae (□ Fig. 11.38). It has a typical ground-glass appearance and is well demarcated from the surroundings.

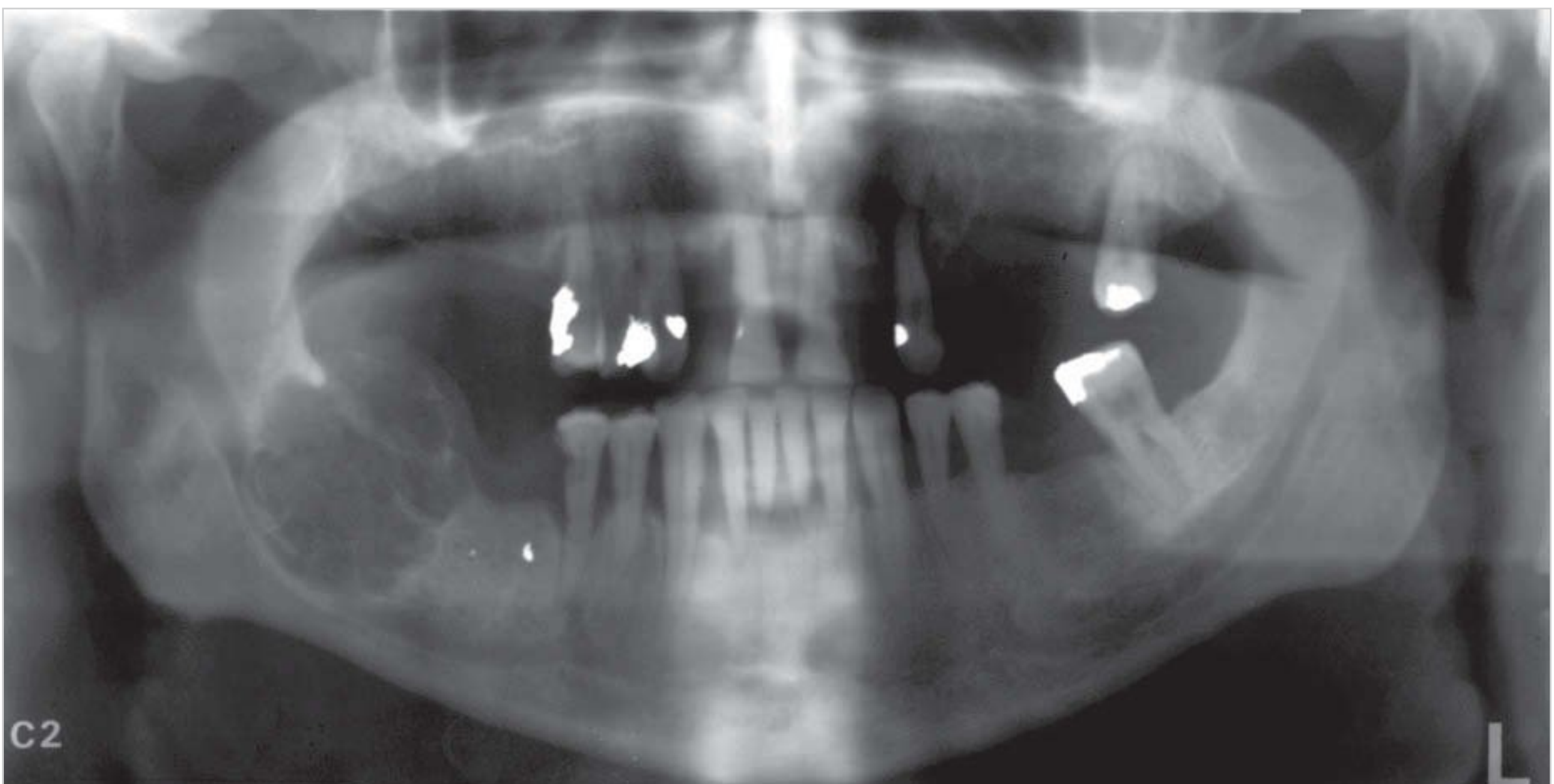


Fig. 11.38 Osteolysis: note the well-defined expansile lytic lesion in the right mandible (edentulous spaces 47–48) containing trabecula-like structures.

Fibrous Dysplasia

Fibrous dysplasia (McCune–Albright syndrome) is a rare, genetically determined bone disease that most commonly involves the maxilla. Fibrous dysplasia is a slowly progressive, episodic disease with symptom-free intervals.

Once the jaw lesion reaches a certain size, it causes facial asymmetry. Adjacent teeth in the maxilla are sometimes displaced. Obliteration of the maxillary sinus may also be observed (□ Fig. 11.39).

Central Giant Cell Granuloma

Central giant cell granuloma is a benign, generally localized but sometimes aggressive proliferating osteolytic lesion (□ Fig. 11.40). Reactive bone formation is a typical radiographic feature.

Central giant cell granuloma is an expansile and often multicystic bone disease. Adjacent teeth are often displaced, and root resorption is possible.



Fig. 11.39 Fibrous dysplasia: the radiograph reveals a homogeneous, hyperdense, sharply demarcated shadow in the left maxillary arch, narrowing of the maxillary sinus, and caudal displacement of molar teeth 26 and 28.

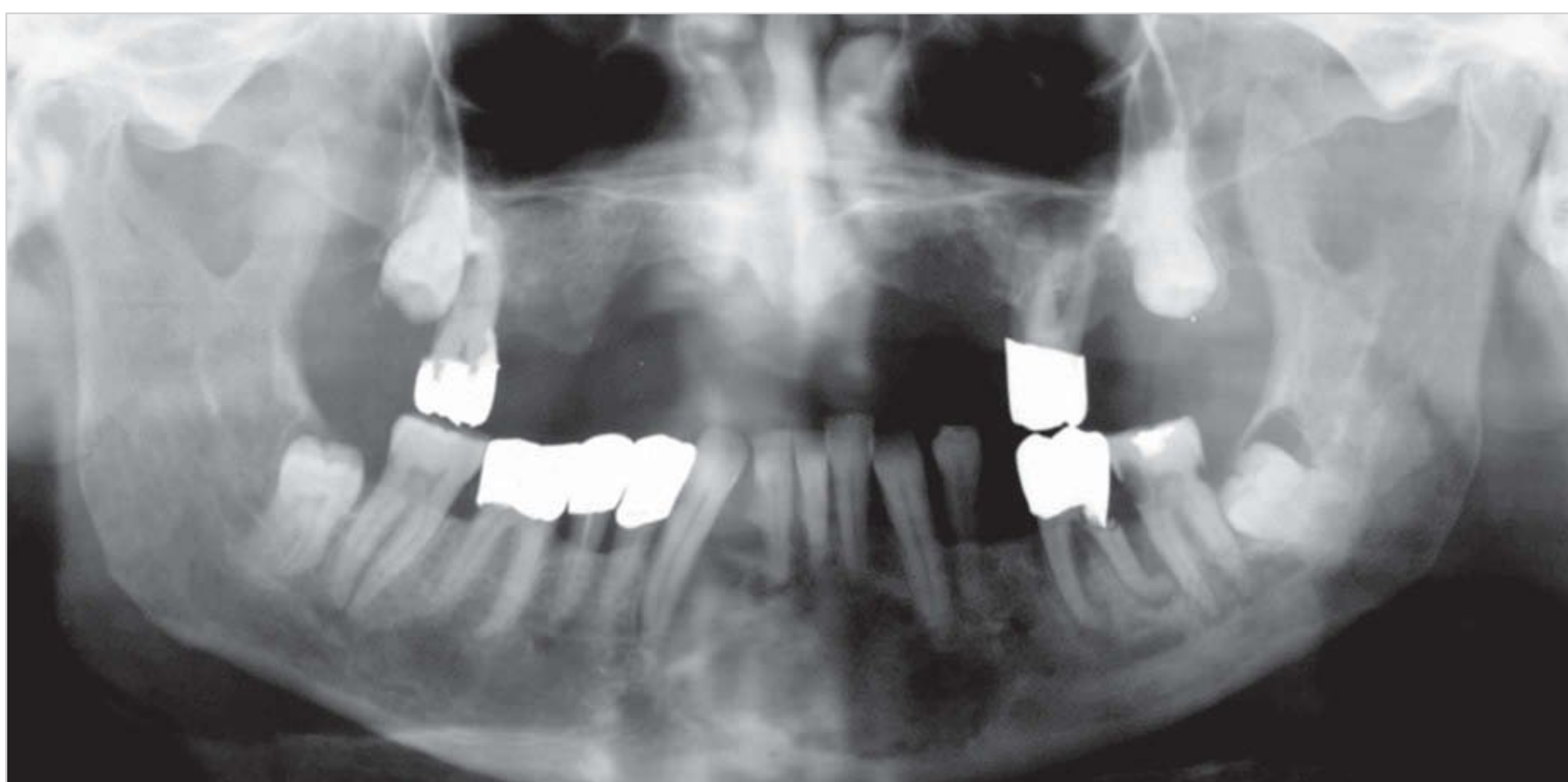


Fig. 11.40 Central giant cell granuloma: note the discernible but not sharply demarcated round radiolucency in the anterior mandibular region, which appears oval as a result of distortion related to the radiographic technique.

11.2.7 Sialolithiasis

Functional integrity of the salivary glands and proper saliva secretion are crucial for a wide range of different physiological processes occurring in the oral cavity. Abnormally reduced or increased saliva flow can result in dehydration of the oral mucosa, which can lead to infections and other painful conditions.

Diagnostic imaging of the salivary glands does not actually fall into the **f**ield of dentistry. However, sialoliths (salivary stones) are frequently detected as incidental or

secondary **f**indings on dental panoramic radiographs in the dental practice (□ Fig. 11.41).

Shadows from salivary stones often project onto the mandible. Therefore, if a radiopaque white zone is detected in the lower jaw, the examiner must **f**irst decide if it is located within the bone or on the **f**loor of the mouth. A second radiograph is then needed for localization. Previously, a survey of the **f**loor of the mouth was used as the second plane to image the **f**loor of the mouth. However, CBCT is now able to provide high-quality images and exact localization of salivary stones (□ Fig. 11.42 and □ Fig. 11.43).



Fig. 11.41 Sialolithiasis: a salivary stone in the right duct appears as a large, inhomogeneously radiopaque lesion on the right side of the mandible.



Fig. 11.42 This panoramic CBCT image shows a large sialolith in the bend of the right submandibular gland.

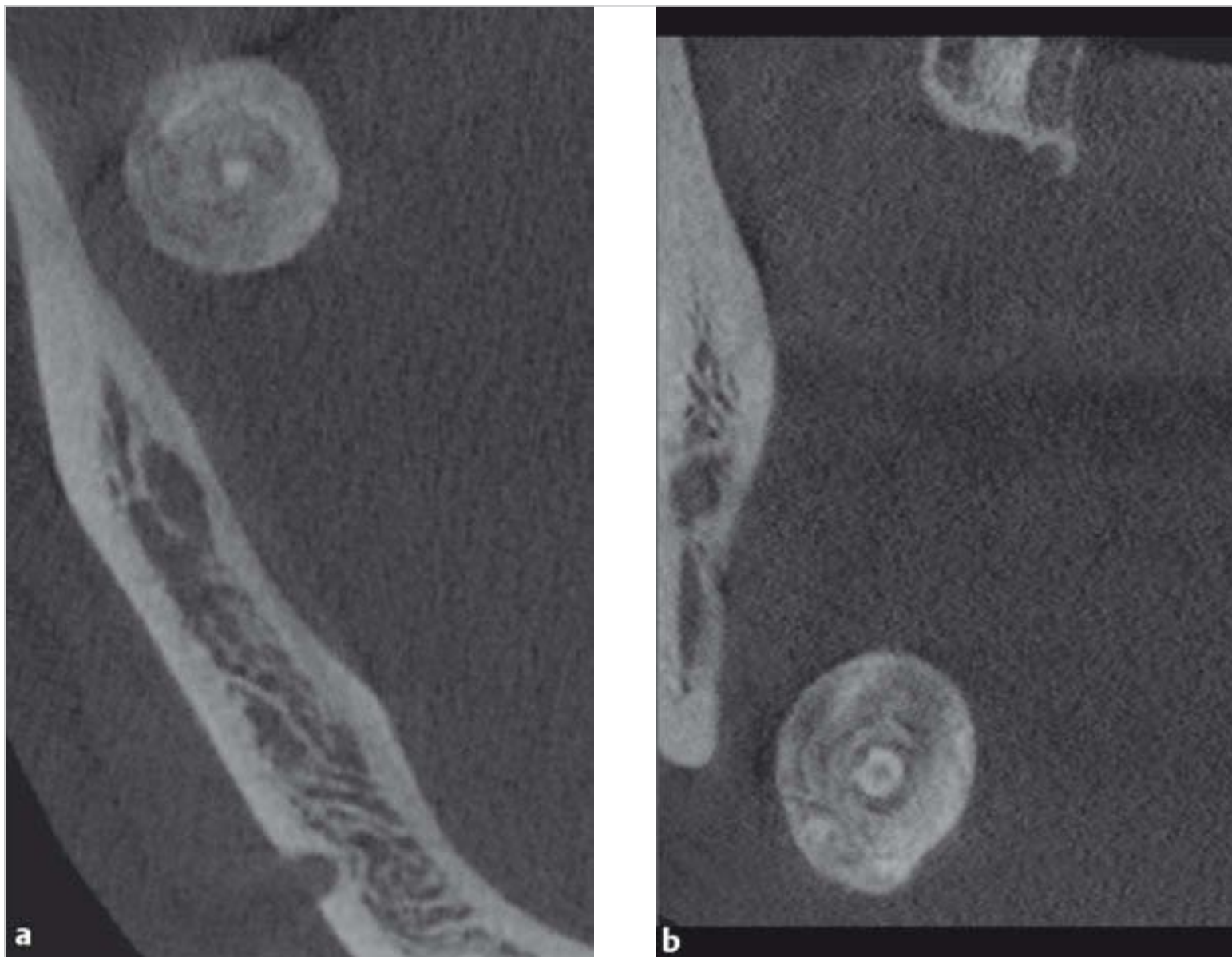


Fig. 11.43a, b Salivary stones in the sub-mandibular gland.

a Axial view.

b Coronal view.

11.2.8 Tooth Fractures

Radiographic examination of the mandible, maxilla, and midface for fractures is not normally performed in a dental practice. If such studies are necessary, CBCT can provide comprehensive images of difficult-to-detect mandibular fractures in multiple planes (□ Fig. 11.44). Most of the fractures diagnosed in normal dental practice are associated with traumatic dental injuries—in most cases, anterior tooth trauma, which must be adequately visualized and diagnosed. Three main types of traumatic dental injuries are tooth luxation, intrusion, and fracture.

The radiographic examination procedure for each type is the same. Intraoral radiographic techniques are usually recommended for optimal visualization of traumatic dental injuries.

Note

In patients presenting with tooth luxation, careful examination of the alveolar sockets is recommended, to rule out the possible presence of a fracture in this region.

Fracture diagnosis is generally straightforward in single-rooted anterior teeth. Conversely, fractures in the molar region can cause diagnostic difficulties, regardless of whether they are of traumatic or idiopathic origin. Again, CBCT can provide precise answers to these clinical questions (□ Fig. 11.45).

Root fractures can involve all segments of the root. Different radiographic techniques and projections are recommended, depending on the type of fracture and the angle of the exposure. If the patient's condition allows, the paralleling technique should always be used for radiographic examination and diagnosis of tooth fractures. This is the only way to ensure the reproducibility of radiographic examinations, which is especially important for fracture follow-up (□ Fig. 11.46).

Tooth fractures can occur in association with fractures of the mandible. Dental fractures (usually longitudinal) can also occur as a complication of dental interventions. Root resorption often occurs as a complication of tooth fractures (□ Fig. 11.47, □ Fig. 11.48, □ Fig. 11.49).

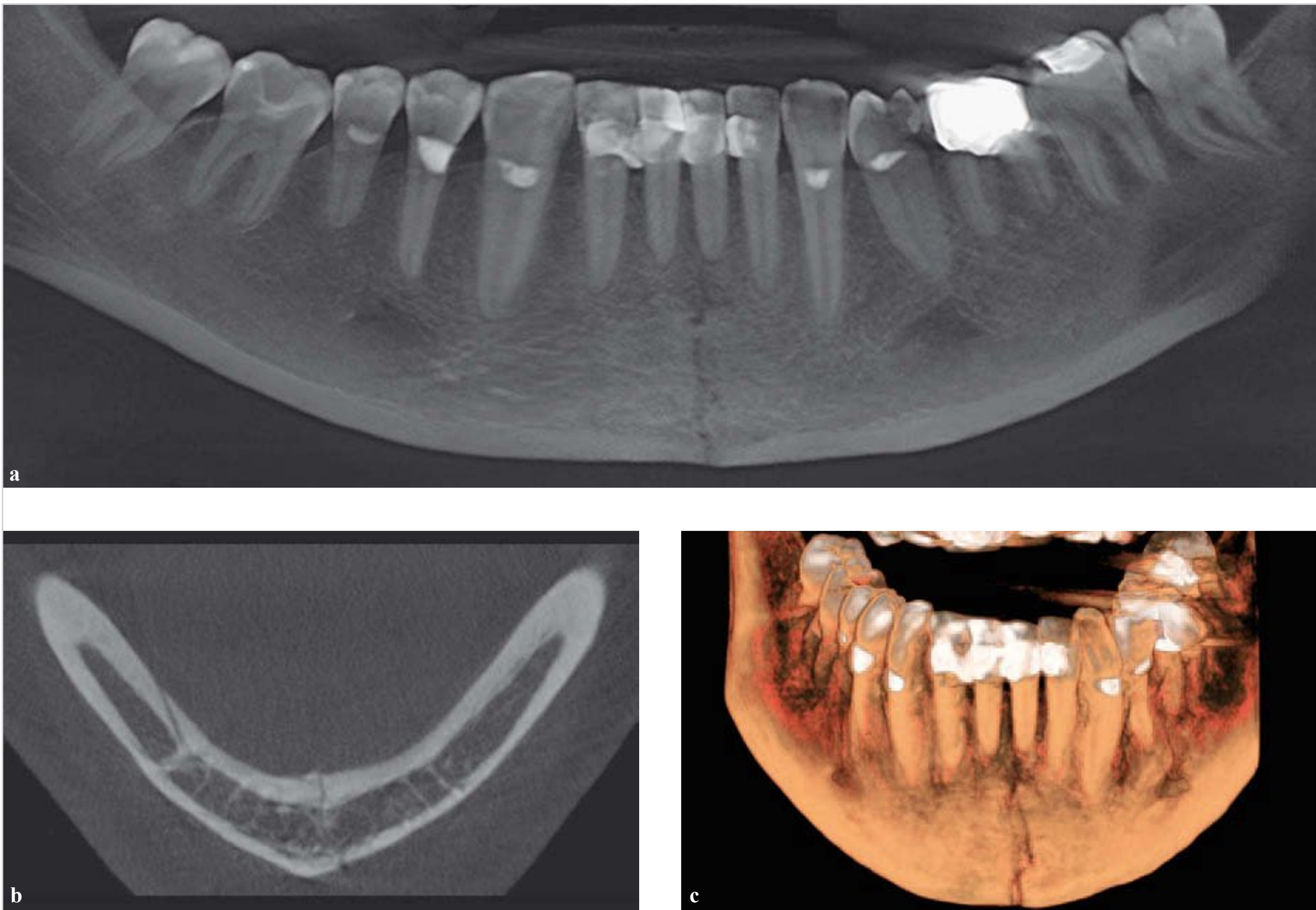


Fig. 11.44a–c Median mandibular fracture.
a This CBCT panoramic reconstruction shows a thin vertical fracture line on tooth 31, with no signs of dislocation.
b The axial view confirms the diagnosis of mandibular fracture without dislocation at edentulous space 32, as well as a second fracture without dislocation on the right side of the mandible. The second fracture line extends diagonally.
c This three-dimensional view obtained by volume rendering also shows only the fracture in the anterior region.

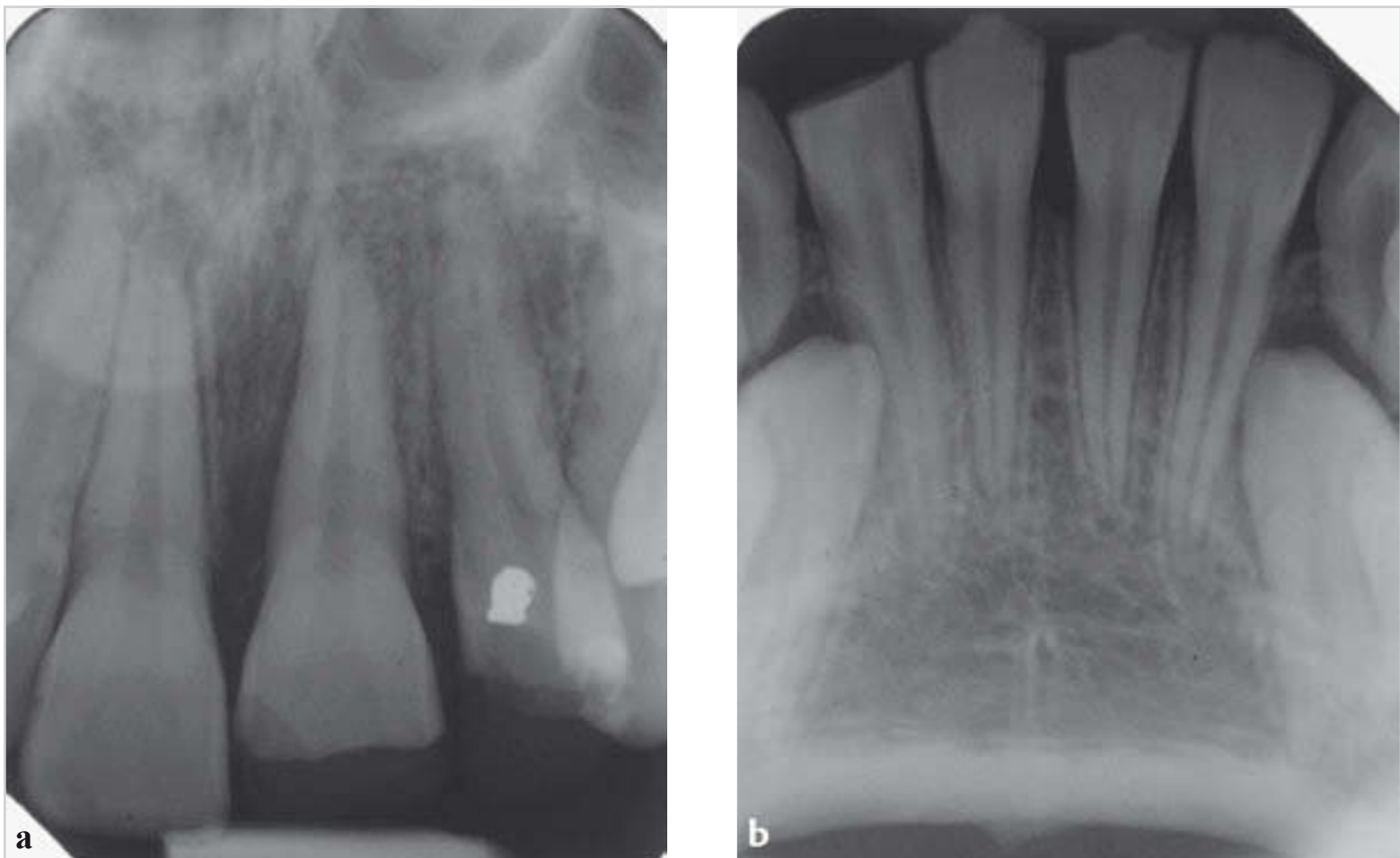


Fig. 11.45a, b Crown fractures.
a Crown fracture of tooth 21.
b Crown fracture of tooth 42.

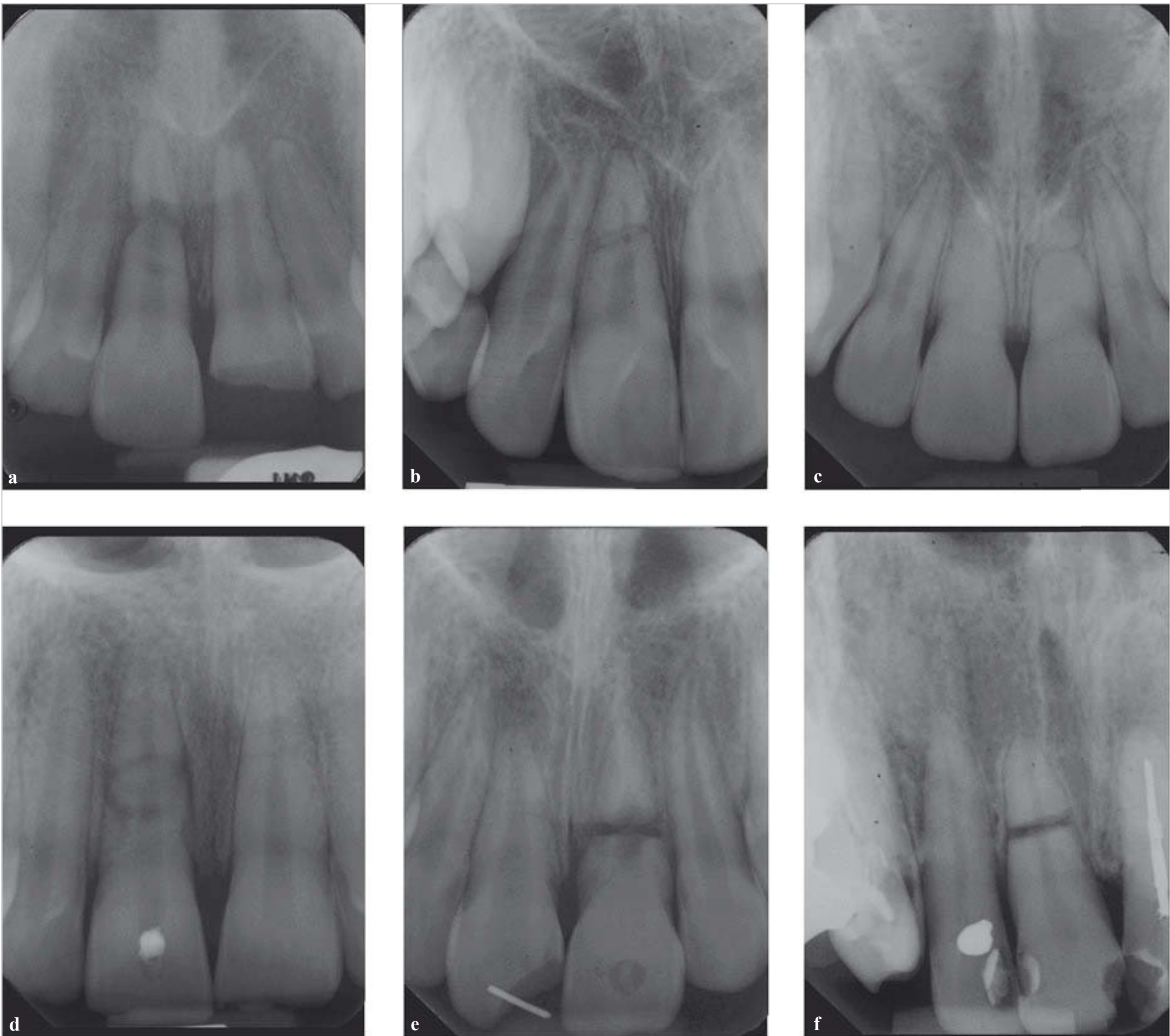


Fig. 11.46a–f Multiple transverse root fractures in the maxillary anterior teeth.



Fig. 11.47 Mandibular fracture with tooth involvement.

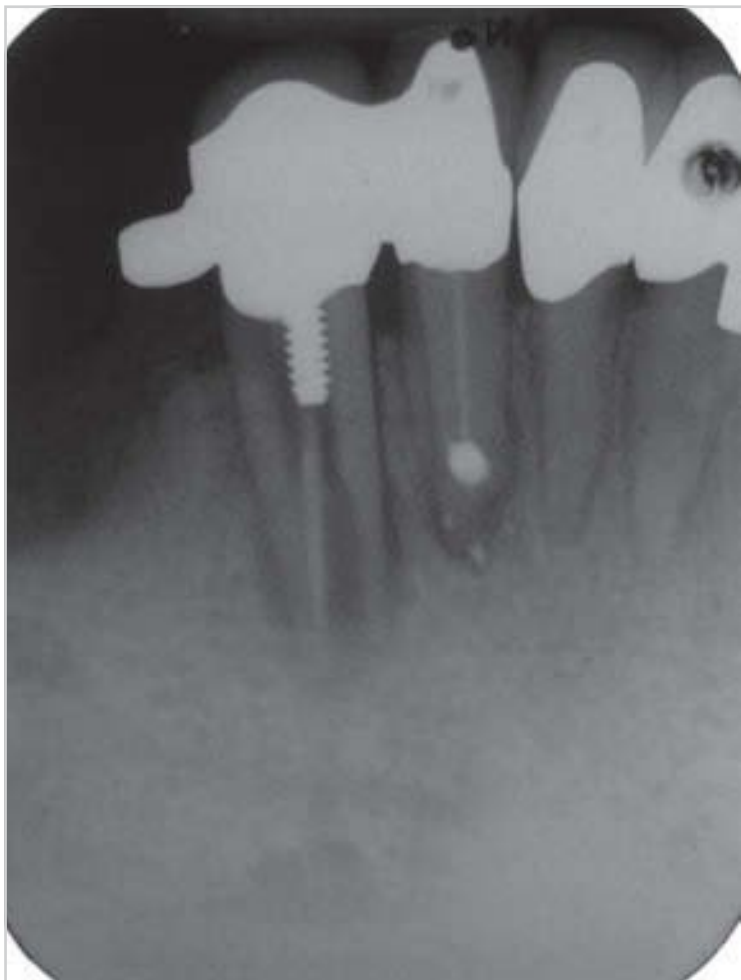


Fig. 11.48 Longitudinal fracture caused by a screw root.



Fig. 11.49 Root resorption in teeth 21 and 22, induced by anterior tooth trauma.

References

- Arai Y, Tammisalo E, Iwai K, Hashimoto K, Shinoda K. Development of a compact computed tomographic apparatus for dental use. *Dentomaxillofac Radiol* 1999;28(4):245–248
- Barr JH, Grøn P. Palate contour as a limiting factor in intraoral x-ray technique. *Oral Surg Oral Med Oral Pathol* 1959;12(4):459–472
- Buchmann F. Die Prinzipien des Dental-Tomographen. *Röntgenstrahlen* 1974;31:24–29
- Cawson RA, Odell EW. *Essentials of Oral Pathology and Oral Medicine*. 7th ed. Edinburgh: Churchill Livingstone; 2002
- Chomenko AG. *Atlas for Maxillofacial Pantomographic Interpretation*. Chicago: Quintessenz; 1985
- Cieszyński A. Beiträge zur Technik bei Zahnaufnahmen mittels Röntgenstrahlen: Neue Filmhalter. *Correspondenz-Blatt* 1907;36:289–305
- Cieszyński A. *Die Röntgenuntersuchung der Zähne und der Kiefer*. Leipzig: JA Barth; 1913
- Delbalso AM, ed. *Maxillofacial Imaging*. Philadelphia: Saunders; 1990
- Döhring W, Prokop M, Bergh B, et al. Prinzip und Anwendung der digitalen Lumineszenzradiographie. *Röntgenstrahlen* 1986;56:16–23
- Düker J. *Röntgendiagnostik mit der Panoramaschichtaufnahme*. 2nd ed. Heidelberg: Hüthig; 2000
- Düker J. *Praxisleitfaden Zahnärztliche Radiologie*. Munich: Urban & Fischer; 2006
- Duhamel J. Les procédés de radiographie en coupe non rigoureux: Une forme nouvelle de phototomographie. *Sc Ind Photogr* 1954;25(2):353–355
- Eckerman K, Endo A. ICRP Publication 107. Nuclear decay data for dosimetric calculations. *Ann ICRP* 2008;38(3):7–96
- Eversole LR. *Clinical Outline of Oral Pathology*. 2nd ed. Philadelphia: Lea & Febiger; 1984
- Ewen K, ed. *Moderne Bildgebung: Physik, Gerätetechnik, Bildbearbeitung und -kommunikation, Strahlenschutz, Qualitätskontrolle*. Stuttgart: Thieme; 1998
- Farman AG, Farman TT. RVG-ui: a sensor to rival direct-exposure intra-oral x-ray film. *Int J Comput Dent* 1999;2(3):183–196
- Farman TT, Farman AG. Evaluation of a new F speed dental X-ray film. The effect of processing solutions and a comparison with D and E speed films. *Dentomaxillofac Radiol* 2000;29(1):41–45
- Farman AG, Farman TT. A status report on digital imaging for dentistry. *Oral Radiol* 2004;20:9–14
- Farman AG, Scarfe WC. Development of imaging selection criteria and procedures should precede cephalometric assessment with cone-beam computed tomography. *Am J Orthod Dentofacial Orthop* 2006;130(2):257–265
- Feldkamp LA, Davis LC, Kress JW. Practical cone-beam algorithm. *J Opt Soc Am A Opt Image Sci Vis* 1984;1:612–619
- Fitzgerald GM. Dental roentgenography: an investigation in adumbration, or the factors that control geometric unsharpness. *J Am Dent Assoc* 1947;34(1):1–20
- Friedrich RE, Fuhrmann A, Scheuer HA, Zustin J. Small peripheral developing odontoma of the maxilla in a 3-year-old patient depicted on cone-beam tomograms. *In Vivo* 2010;24(6):895–898
- Friedrich RE, Scheuer HA, Fuhrmann A, Zustin J, Assaf AT. Radiographic findings of odontogenic myxomas on conventional radiographs. *Anticancer Res* 2012;32(5):2173–2177
- Friedrich RE, Scheuer HA, Fuhrmann A, Hagel C, Zustin J. Osteochondroma of the mandibular condyle. Report of a case with 5-year follow-up. *Anticancer Res* 2012;32(10):4553–4556
- Fuhrmann A, Albers HK. Die Anwendung der Paralleltechnik für Messaufnahmen in der Endodontie. *Quintessenz* 1986;37(9):1565–1568
- Fuhrmann A. Probleme und Fortschritte der Nativdiagnostik im dento-maxillo-fazialen Bereich. In: Schwenzer N, Pfeifer G, eds. *Fortschritte der Kiefer- und Gesichts-Chirurgie*. Vol 32. Stuttgart: Thieme; 1987:11–14
- Fuhrmann A, Rother U. Improved cross-sectional images with rotational panoramic radiography. Abstract presented at: 5th European Congress on Dental and Maxillofacial Radiology; November 8–11, 1995; Cologne, Germany
- Fuhrmann A, Schulze D, Rother U, Vesper M. Digital transversal slice imaging in dental-maxillofacial radiology: from pantomography to digital volume tomography. *Int J Comput Dent* 2003;6(2):129–140
- Fuhrmann A. Der Stellenwert der transversalen Panoramaschichtaufnahme im Vergleich zur digitalen Volumentomographie. *Quintessenz* 2009;60:741–745
- Garretson JL. A new system of dental radiography. *Dental Cosmos* 1919;61:862–865
- Grauer P. Über den Wert der axialen Unterkieferaufnahme. *Fortschr Röntgenstr* 1928;37:503–505
- Gundlach KKH, Fuhrmann A, Beckmann-Van der Ven G. The double-headed mandibular condyle. *Oral Surg Oral Med Oral Pathol* 1987;64(2):249–253
- Hallikainen D, Gröndahl HG, Kanerva H, Tammisalo E. Optimized Sequential Dentomaxillofacial Radiography. The Scanora Concept. Helsinki: Yliopistopaino; 1992
- Hallikainen D. History of panoramic radiography. *Acta Radiol* 1996;37(3 Pt 2):441–445
- Hassan B, van der Stelt P, Sanderink G. Accuracy of three-dimensional measurements obtained from cone beam computed tomography surface-rendered images for cephalometric analysis: influence of patient scanning position. *Eur J Orthod* 2009;31(2):129–134
- Heckmann K. Die Röntgenperspektive und ihre Umwandlung durch eine neue Aufnahmetechnik. *Fortschr Röntgenstr* 1939;60:144–157
- Heckmann K. Die Entwicklung der Schlitzaufnahmen. *Röntgen-Bl* 1984;37:29–39
- Heilmann HP. Der Röntgenbefund: Stiefkind der Radiologie. *Fortschr Röntgenstr* 1981;135:220–224
- Hielscher W. Parallel plate technic in enoral tooth radiography [in German]. *Dtsch Zahnärztl Z* 1955;10(8):601–616
- Holzknicht G. Projektionsrichtung, Projektionsdistanz. Eine allgemeine röntgenologische Bemerkung. *Fortschr Röntgenstr* 1931;44:400–406
- Hounsfield GN. Computerized transverse axial scanning (tomography). 1. Description of system. *Br J Radiol* 1973;46(552):1016–1022
- ICRP-International Commission on Radiological Protection. The 2007 Recommendations of the International Commission on Radiological Protection. ICRP publication 103. *Ann ICRP* 2007;37(2-4):1–332
- Jung T, eds. *Panorama Röntgenographie*. Symposium, Hannover, 29.-30. Oktober 1982. Heidelberg: Hüthig; 1984
- Kalender WA. *Computertomographie*. Munich: Publicis MCD; 2000
- Katzberg RW, Westesson PL, eds. *Diagnosis of the Temporomandibular Joint*. Philadelphia: Saunders; 1993
- Kells CE. Roentgen rays. *Dental Cosmos* 1899;16:1014–1029
- Langland OE, Sippy FH. A study of radiographic longitudinal distortion of anterior teeth using the paralleling technique. *Oral Surg Oral Med Oral Pathol* 1966;22(6):737–749
- Langland OE, Sippy FH, Langlais RP. *Textbook of Dental Radiology*. 2nd ed. Springfield: Thomas; 1984
- Langlais RP, Langlang OE, Nortje CJ. *Diagnostic Imaging of the Jaws*. Baltimore: Williams & Wilkins; 1995
- Langland OE, Langlais RP, Preece JW. *Principles of Dental Imaging*. Baltimore: Lippincott Williams & Wilkins; 2002
- Langland OE, Langlais RP, McDavid WD, Delbalso AM. *Panoramic Radiology*. 2nd ed. Philadelphia: Lea & Febiger; 1989
- Langland OE, Langlais RP, Morris CR. *Principles and Practice of Panoramic Radiology: Including Intraoral Radiographic Interpretation*. Philadelphia: Saunders; 1982
- Laubenberger T, Laubenberger J. *Technik der medizinischen Radiologie*. 7th ed. Cologne: Deutscher Ärzte-Verlag; 1999
- Ludlow JB, Abreu M Jr. Performance of film, desktop monitor and laptop displays in caries detection. *Dentomaxillofac Radiol* 1999;28(1):26–30
- Ludlow JB, Ivanovic M. Comparative dosimetry of dental CBCT devices and 64-slice CT for oral and maxillofacial radiology. *Oral Surg Oral Med Oral Pathol Oral Radiol Endod* 2008;106(1):106–114
- Ludlow JB, Davies-Ludlow LE, White SC. Patient risk related to common dental radiographic examinations: the impact of 2007 International

- Commission on Radiological Protection recommendations regarding dose calculation. *J Am Dent Assoc* 2008;139(9):1237–1243
- Manson-Hing LR. *Fundamentals of Dental Radiography*. Philadelphia: Lea & Febiger; 1979
- Mason RA, Bourne S. *A Guide to Dental Radiography*. 4th ed. Oxford: Oxford University Press; 1998
- McDavid WD, Langlais RP, Welander U, Morris CR. Real, double, and ghost images in rotational panoramic radiography. *Dentomaxillofac Radiol* 1983;12(2):122–128
- McGowan DA, Baxter PW, James J. *The Maxillary Sinus and Its Dental Implications*. Oxford: Butterworth-Heinemann; 1993
- Molander B, Ahlqwist M, Gröndahl HG, Hollender L. Agreement between panoramic and intra-oral radiography in the assessment of marginal bone height. *Dentomaxillofac Radiol* 1991;20(3):155–160
- Mourshed F, McKinney AL. A comparison of paralleling and bisecting radiographic techniques as experienced by dental students. *Oral Surg Oral Med Oral Pathol* 1972;33(2):284–296
- Mouyen F, Benz C, Son nabend E, Lodter JP. Presentation and physical evaluation of RadioVisioGraphy. *Oral Surg Oral Med Oral Pathol* 1989;68(2):238–242
- Mozzo P, Procacci C, Tacconi A, Martini PT, Andreis IA. A new volumetric CT machine for dental imaging based on the cone-beam technique: preliminary results. *Eur Radiol* 1998;8(9):1558–1564
- Nelsen RJ, Kumpula JW. Panographic radiography. *J Dent Res* 1952;31(2):158–165
- Numata H. Considerations of the parabolic radiography of the dental arch. *J Shimazu Stud* 1933;10:13
- Paatero YV. A new radiographic method in dentistry. *Suom Hammaslaak Toim* 1946;87:37–42
- Paatero YV. A new tomographical method for radiographing curved outer surfaces. *Acta Radiol* 1949;32(2-3):177–184
- Paatero YV. Pantomography in theory and use. *Acta Radiol* 1954;41(4):321–335
- Paatero YV. Orthoradial jaw pantomography. *Ann Med Intern Fenn Suppl* 1959;48(Suppl 28):222–227
- Paatero YV. Pantomography and orthopantomography. *Oral Surg Oral Med Oral Pathol* 1961;14:947–953
- Parma Č. Der Canalis incisivus im Röntgenbilde. *Z Stomatol* 1927;25:776–788
- Parrott LA, Ng SY. A comparison between bitewing radiographs taken with rectangular and circular collimators in UK military dental practices: a retrospective study. *Dentomaxillofac Radiol* 2011;40(2):102–109
- Pasche O. Ueber eine neue Blendenvorrichtung in der Röntgentechnik. *Dtsch Med Wochenschr* 1903;29(15):266–267
- Pasler FA, Visser H. *Pocket Atlas of Dental Radiology*. Stuttgart: Thieme; 2007
- Pasler FA. *Zahnärztliche Radiologie*. 5th ed. Stuttgart: Thieme; 2008
- Pasler FA, Visser H. *Zahnmedizinische Radiologie: Bildgebende Verfahren*. 2nd ed. Stuttgart: Thieme; 2000. *Farbatlanten der Zahnmedizin*; vol 5
- Pindborg JJ, Hjørting-Hansen E. *Atlas of Diseases of the Jaws*. Copenhagen: Munksgaard; 1974
- Praeger W. Grundlagen der zahnärztlichen Röntgentechnik. *Dtsch Zahn-ärztl Wochenschr* 1938;37:865–869
- Ponce AZ, McDavid WD, Underhill TE, Morris CR. Use of E-speed film with added filtration. *Oral Surg Oral Med Oral Pathol* 1986;61(3):297–299
- Raper HR. Practical clinical preventive dentistry based upon periodic roentgen ray examinations. *J Am Dent Assoc* 1925;12:1084–1100
- Richards AG, Colquitt WN. Reduction in dental X-ray exposures during the past 60 years. *J Am Dent Assoc* 1981;103(5):713–718
- Von Reckow JF. Die Untersuchungstechnik in der Zahnrontgenologie. *Rontgenpraxis* 1937;9:668–683
- Rottke B. Die Bedeutung der Röntgenschnittuntersuchung für die Zahn-, Mund- und Kieferheilkunde. *Dtsch Zahnärztekalendar* 1971;30:101–115
- Rottke B, Fuhrmann A. Fortschritte und Probleme in der Röntgendiagnostik des Kiefergelenks. In: Schwenzer N, Pfeifer G, eds. *Fortschritte der Kiefer- und Gesichtschirurgie*; vol 25. Stuttgart: Thieme; 1980:21–23
- Rushton VE, Horner K. The use of panoramic radiology in dental practice. *J Dent* 1996;24(3):185–201
- Rushton VE, Rout J. *Panoramic Radiology*. London: Quintessenz; 2006
- Sanderink GC, Huiskens R, van der Stelt PF, Welander US, Stheeman SE. Image quality of direct digital intraoral x-ray sensors in assessing root canal length. The RadioVisioGraphy, Visualix/VIXA, Sens-A-Ray, and Flash Dent systems compared with Ektaspeed films. *Oral Surg Oral Med Oral Pathol* 1994;78(1):125–132
- Scarfe WC, Farman AG, Sukovic P. Clinical applications of cone-beam computed tomography in dental practice. *J Can Dent Assoc* 2006;72(1):75–80
- Schröder HE. *Orale Strukturbilogie*. 4th ed. Stuttgart: Thieme; 1992
- Schulze D, Heiland M, Thurmman H, Adam G. Radiation exposure during midfacial imaging using 4- and 16-slice computed tomography, cone beam computed tomography systems and conventional radiography. *Dentomaxillofac Radiol* 2004;33(2):83–86
- Schulze R, Heil U, Gross D, et al. Artefacts in CBCT: a review. *Dentomaxillofac Radiol* 2011;40(5):265–273
- Schulze RK, Berndt D, d'Hoedt B. On cone-beam computed tomography artifacts induced by titanium implants. *Clin Oral Implants Res* 2010;21(1):100–107
- Sitzmann F, ed. *Radiologieatlas der Zahn-, Mund- und Kiefererkrankungen*. 2nd ed. Munich: Urban & Fischer; 2003
- Son nabend E, Benz C. *Das Röntgenbild in der zahnärztlichen Praxis*. 3rd ed. Heidelberg: Hüthig; 1998
- Stender HS, Stieve FE, eds. *Bildqualität in der Röntgendiagnostik*. Cologne: Deutscher Ärzte-Verlag; 1990
- Stephens RG, Barr JH. Anatomic limitations in intraoral roentgenography of the upper molar region. *Oral Surg Oral Med Oral Pathol* 1955;8(12):1272–1277
- Stieve F. Bevorzugte Darstellung einzelner Körperschichten. In: Diethelm L, Olsson O, Strnad F, Vieten H, Zuppinger A, eds. *Allgemeine röntgendiagnostische Methodik. Handbuch der medizinischen Radiologie*, vol 3. Berlin: Springer; 1967:716–1041
- Tyndall DA, Brooks SL. Selection criteria for dental implant site imaging: a position paper of the American Academy of Oral and Maxillofacial radiology. *Oral Surg Oral Med Oral Pathol Oral Radiol Endod* 2000;89(5):630–637
- Updegrave WJ. The paralleling extension-cone technique in intraoral dental radiography. *Oral Surg Oral Med Oral Pathol* 1951;4(10):1250–1261
- Updegrave WJ. Simplifying and improving intraoral dental roentgenography. *Oral Surg Oral Med Oral Pathol* 1959;12(6):704–716
- Updegrave WJ. Higher fidelity in intraoral roentgenography. *J Am Dent Assoc* 1961;62:1–8
- van Aken J. Limitations in clinical diagnosis of dental caries of approximal surfaces. *Adv Fluorine Res* 1966;4:89–92
- van Aken J. Optimum conditions for intraoral roentgenograms. *Oral Surg* 1969;27:475–481
- van Aken J, Verhoeven JW. Factors influencing the design of aiming devices for intraoral radiography and their practical application. *Oral Surg Oral Med Oral Pathol* 1979;47(4):378–388
- van Straaten FJ, van Aken J. The optimum circular field size for dental radiography with intraoral films. *Oral Surg Oral Med Oral Pathol* 1982;54(3):347–359
- Visser H, Hermann KP, Bredemeier S, Köhler B. Dose measurements comparing conventional and digital panoramic radiography [in German]. *Mund Kiefer Gesichtschir* 2000;4(4):213–216
- Waggener DT. The right-angle technique using the extension cone. *Dent Clin North Am* 1960;11:783–788
- Wall BF, Kendall GM. Collective doses and risks from dental radiology in Great Britain. *Br J Radiol* 1983;56(668):511–516
- Wenzel A, Møystad A. Work flow with digital intraoral radiography: a systematic review. *Acta Odontol Scand* 2010;68(2):106–114
- Whaites E. *Essentials of Dental Radiography and Radiology*. 4th ed. Philadelphia: Elsevier; 2007
- White SC. Assessment of radiation risk from dental radiography. *Dentomaxillofac Radiol* 1992;21(3):118–126
- White SC, Pharoah MJ. *Oral Radiology*. 5th ed. St. Louis: Mosby; 2004
- Zabel H. *Kurzlehrbuch Physik*. Stuttgart: Thieme; 2011
- Zulauf AF. Panoramic X-Ray apparatus. US patent 1408. March 7, 1922

Index

Note: Page numbers followed by *f* and *t* indicate figures and tables, respectively.

A

Acceptable level [term], 55
 Acceptance tests, 56
 Accident(s), prevention of, 55
 Active pixel sensors (APS), 47
 Addition, 35–36, 138
 Age (patient), and X-ray image formation, 36
 Alpha particles, 8, 11
 – ionization density of, 22
 – radiation weighting factor for, 22
 Alveolar crest, age-related changes in, 139
 Alveolar recess, radiographic appearance of, 125, 127*f*, 129, 131
 Alveolar ridge, 121, 122*f*
 Alveolus, 121, 121*f*
 Ameloblastoma(s), 147, 147*f*
 – multicystic, 147
 – variants of, 147–148, 148*f*
 American Dental Association (ADA), Standards Committee on Dental Products, 56
 Angle of jaw, 128*f*
 Angle of rotation (ϕ), in tomography, 78
 Anode(s)
 – angulation of, 14, 14*f*
 – rotating, 13, 14*f*
 – stationary, 13, 13*f*
 – of X-ray tube, 12, 13–14, 13*f*, 14*f*
 — interactions of electrons with, 15
 Anterior nasal spine, 124, 124*f*
 Anti-scatter grids, 36–37, 37*f*
 Apoptosis, 27–28
 Articular tubercle, 127*f*
 As low as reasonably achievable (ALARA) principle, 134
 Atlanto-axial joint, lateral, 127*f*
 Atom(s), 9
 – electron shells, 9, 10
 Atomic number, 9, 34
 Attenuation, 10, 16, 34
 Auger effects, 26*f*
 Automatic film processor(s), 42, 43*f*
 – with daylight loader, 42, 43*f*
 Axial projection technique, for occlusal radiography, 76, 76*f*

B

Background fog, 41
 Beam-indicating device (BID), 17–18
 Beta particles, 8, 11
 Beta rays, radiation weighting factor for, 22
 Bisecting-angle technique, 2, 3*f*, 61, 63, 67–72, 67*f*, 68*f*
 – disadvantages of, 68–71, 68*f*–70*f*

– image distortion in, 67–71, 68*f*, 69*f*, 70*f*
 – methodology, 71–72, 72*f*
 – for occlusal radiography, 75, 75*f*
 – and paralleling technique, comparison of, 67, 67*f*, 70*f*
 – and radiation protection, 70
 – and reproducibility, 71
 – vertical angulation and, 71, 71*f*
 Bite block, and paralleling technique, 62, 62*f*
 Bitewing radiography, 73–74, 73*f*, 121, 122*f*
 – of caries, 136
 – methodology, 74, 74*f*, 136
 – vertical, 139*f*, 140
 Blackman, Sydney, 3
 Blooming, 47
 Blurring, in tomography, 78
 – extent of, 78
 – patterns of, 78, 78*f*
 – type of, 78
 Blurring out, 77, 77*f*
 Bocage, André, 2, 77
 Bohr, Niels, 9
 Bone, X-ray appearance of, 34
 Bone defects, vertical, 139–140, 140*f*, 141*f*
 Bone diseases, of jaw, 155–156
 Bone loss, horizontal, 139–140, 140*f*, 145, 146*f*
 Bouchacourt, Léon, 80
 Braking radiation. *See* Bremsstrahlung
 Bremsstrahlung, 15–16, 16*f*, 26*f*
 Broadbent, B. Holly, 3

C

Calcium tungstate crystals, 41, 41*f*
 Cancer, radiation-induced, 31, 32*f*
 Caries
 – approximal, 136
 – assessment and diagnosis of, 136–139
 – C1 (superficial), 137, 137*f*
 – C2 (moderate), 137, 138*f*
 – C3 (deep), 137, 138*f*, 139
 – C4 (deep complicated), 137, 138*f*
 – cementum, 136
 – and cervical burnout, differentiation of, 122, 122*f*
 – and developmental defects, differentiation of, 139
 – differential diagnosis, 139
 – early childhood, 139, 139*f*
 – enamel, 137, 137*f*
 – fissure, 136
 – interproximal, 136
 – occlusal, 137, 138*f*
 – predilection sites for, 136
 – primary (initial), 136, 137*f*
 — types of, 137, 137*f*

– progression, stages of, 137, 137*f*
 – radiographic appearance of, 136
 – recurrent, 137, 139
 – secondary, 136, 137
 Cathode, of X-ray tube, 12–13, 13*f*
 CCD sensors, 47
 CdTe sensors, 48
 Cell death, programmed, 27–28
 Cell function, impairment of, 27
 Cementoblastoma, 153, 154*f*
 Cementoma, 153, 154*f*
 Cemento-osseous dysplasia, 153, 154*f*
 – florid, 153
 Central giant cell granuloma, 156, 156*f*
 Central projection, 34, 121
 Cephalometric radiograph, effective dose for, 114
 Cervical burnout, 122, 122*f*
 Cervical spine, 128*f*
 Cesium iodide crystals, 48
 Characteristic curve(s)
 – for digital radiography, 51, 52*f*
 – of radiographic film, 40*f*, 41, 50–51
 — shoulder of, 40*f*, 41
 — toe of, 40*f*, 41
 – for storage phosphor imaging plates, 51, 52*f*
 Chemical trap(s), 48
 Cieszynski, A., 2
 Clinical indications, for radiological examination, 56
 Close-up imaging, 77, 77*f*
 CMOS sensors, 47
 Collimator(s), 17–18, 18*f*, 19*f*, 37
 – geometry of, and radiographic technique, 18, 19*f*
 Collimator holder, 18
 Comparability, of radiographs, 134
 Compton effect (Compton scattering), 11, 11*f*, 26, 26*f*
 Computed tomography (CT)
 – artifacts, 112–113
 – effective dose for, 113–114
 – historical perspective on, 109–110
 – limitations of, 112–114
 – principles of, 109
 – radiation exposure in, 113–114
 – spiral, 110, 110*f*
 Cone beam computed tomography (CBCT), 5, 5*f*, 47, 85, 87, 109–117
 – artifacts, 113
 – basic rules for, 114
 – of bone conditions, 140
 – clinical applications of, 114–117, 115*f*–117*f*, 121, 122*f*
 – data reconstruction, 110–111
 – development of, 109–110
 – effective dose for, 113–114
 – flat panel detectors for, 111

– image formation, 110–111
 – image intensifiers for, 111
 – of nasopalatine duct cyst, 143
 – primary reconstruction, 111, 111*f*
 – radiation exposure in, 113–114
 – secondary reconstruction, 111, 111*f*, 112*f*, 113*f*
 – of sialolithiasis, 157, 157*f*, 158*f*
 – slice position, 114, 116*f*
 – slice thickness, 114, 116*f*
 – systems, cost of, 114
 – of tooth fractures, 158, 159*f*, 160*f*
 – volume size for, 114, 115*f*
 Continuing education, and radiation protection, 56
 Contrast. *See* Film, contrast; Object contrast
 Coolidge, William, 13
 Corpuscular radiation, 8
 Cosmic rays, 30
 Coulomb per kilogram (C/kg), 22
 Cribriform plate, 121, 121*f*
 Crossover, 42, 42*f*
 Current intensity, and image formation, 36
 Cyst(s), 120, 120*f*
 – definition of, 143
 – follicular (dentigerous), 143, 143*f*, 144*f*, 147
 – nasopalatine duct, 124, 143, 144*f*
 – nonodontogenic epithelial, 143
 – odontogenic epithelial, 143
 – radicular (periapical), 143–144, 145*f*
 – radiographic appearance of, 135
 – WHO classification of, 143

D

Dental radiography, historical perspective on, 2–5
 Dental X-ray head, 3, 3*f*
 Dental X-ray tube, 12, 12*f*
 – design of, 12, 12*f*, 13*f*
 – kilovoltage and, 11, 15
 Dentures, and panoramic radiography, 101, 101*f*
 Dermatitis, radiation-induced, 54
 Detective quantum efficiency (DQE), 50
 Deterministic effects, 28, 31, 32*f*
 Diagnosis, radiographic findings and, 135
 Diagnostic radiology, physics of, 10–11, 11*f*
 Digital dental radiography
 – advantages of, 50–51
 – data storage in, 51
 – definition of, 47
 – editing of, 51

- enhancement of, 51
- equipment for, 46*f*, 47
- flat panel detectors for, 46*f*, 47
- historical perspective on, 46
- image acquisition in, 47
- image intensifier for, 46*f*, 47
- imaging plate for, 46*f*, 47, 48–50
- rapid availability of image in, 51
- sensors for, 46*f*, 47–48, 47*f*
- spatial resolution in, 48
- Digital radiography, historical perspective on, 5
- Digital volume tomography. *See* Cone beam computed tomography (CBCT)
- Distortion, imaging free of, in intra-oral radiography, 59, 60*f*
- DNA (deoxyribonucleic acid)
 - base damage, 27, 27*f*
 - double-strand breaks, 27, 27*f*
 - radiation damage to, 27, 27*f*, 31
- biological effects of, 27–28
- repair mechanisms, 27
- single-strand breaks, 27, 27*f*
- Dose–area product, 23, 23*f*
- Dose limit(s), 55
 - monitoring of, 55
- Dose limitation, 17–18
- Dose units, 22
- Dosimetry, units and terms for, 22–23
- Dynamic range, 50–51

E

- Ear lobe, shadow, on panoramic radiography, 105, 126, 127*f*
- Edison, Thomas, 2
- Effective dose, 23
 - for CBCT, 113–114
 - for cephalometric radiograph, 114
 - for CT, 113–114
 - for digital panoramic radiograph, 114
 - for intraoral radiograph, 114
- Effects of radiation. *See* Radiation effects
- Electric field strength, 8*f*, 9
- Electromagnetic spectrum, 9, 9*f*
- Electromagnetic waves, 8–9, 8*f*
- Electron(s), 9
 - interactions with anode material, 15
 - release of, 26, 26*f*
 - shell-to-shell transitions, 10
- Electron beam(s), radiation weighting factor for, 22
- Electron shell(s), 9, 10
- Electron trap(s), 48, 49
- Endo-Holder, 74, 74*f*
- Epithelial cell rests of Malassez, 143
- Equipment (dental X-ray), radiation-proof housing, 12, 12*f*
- Equivalent dose, 22
- Erythema, radiation-induced, 31

- European Atomic Energy Community (EURATOM), 55
- European Committee for Standardization, 56
- Excitation, 10
- Exposure. *See* Radiation exposure
- Exposure time, and image formation, 36
- External acoustic meatus, 127*f*

F

- Feldkamp algorithm, 111
- Fibrodentinoma, 147
- Fibroma
 - ameloblastic, 147–148, 149*f*
 - ossifying, 155, 155*f*
- Fibro-odontoma, ameloblastic, 147–148, 149*f*
- Fibrous dysplasia, 156, 156*f*
- Film
 - bending of, errors caused by, 65*f*, 70, 70*f*
 - characteristic curves, 40*f*, 41, 50–51, 52*f*
 - contrast, 37, 50–51
 - and characteristic curve, 40*f*
 - cross-sectional structure of, 39, 39*f*
 - for dental X-ray, characteristics of, 37–38, 37*f*
 - development of, disadvantages of, 51
 - D-speed, 38
 - emulsion layer, 39, 39*f*
 - E-speed, 38
 - F-speed, 38
 - with intensifying screens, 41–42, 41*f*
 - disadvantages of, 42
 - sensitivity of, 41
 - normal exposure of, 40*f*
 - for occlusal radiography, 74, 75*f*
 - over-exposure of, 40*f*
 - packaging of, 39, 39*f*
 - processing of, 42, 43*f*
 - screenless, 37–38
 - for occlusal radiography, 74
 - sharpness (resolution), 37–38, 37*f*
 - silver content of, 39
 - speed (sensitivity), 37–38
 - under-exposure of, 40*f*
 - viewing, conditions for, 134
 - wrong-side exposure of, 39*f*, 41
- Film holder
 - anterior, for paralleling technique, 65, 65*f*
 - for bitewing radiography, 74, 74*f*
 - insertion into mouth, 64–67, 64*f*–66*f*
 - and orthogonal projection geometry, 63, 63*f*
 - for paralleling technique, 61, 61*f*
 - with position-indicating device, 136
- Filter(s), aluminum, 17
- Filtered back projection, 111

- Filtration
 - by aluminum filters, 17
 - inherent, 17
 - total tube, 17
 - of X-rays, 17
- Findings (radiographic)
 - challenging and/or uncommon, 135–136
 - density of, 135
 - description of, 135
 - and diagnosis, 135
 - effect on adjacent structures, 135
 - evaluation of, 135
 - internal structure of, 135
 - location/site of, 135
 - margins of, 135
 - and normal variants, 135–136
 - relationship to adjacent structures, 135
 - shape of, 135
 - suggestive of lesions/pathological changes, 135
 - written report of, 135
- Fitzgerald, F. G., 61
- Fluorescence, 41
- Focal spot, 13–14, 14*f*
 - actual, 14, 14*f*
 - apparent (effective), 14, 14*f*
 - size of, 13–14
- Focus-to-object distance (FOD), for orthodontic radiography, 61–62
- Food and Drug Administration (FDA), and radiation protection, 56
- Fracture(s). *See also* Tooth fractures
 - mandibular, 158, 159*f*, 160*f*
 - radiographic appearance of, 135
- Frankfort horizontal plane, 89*f*, 91, 91*f*
- Free radicals, 27

G

- Gadolinium crystals, 41, 41*f*
- Galileos digital cone beam computed tomography system, 5, 5*f*
- Gamma rays, 8, 9, 9*f*, 11
 - radiation weighting factor for, 22
- Garretson, J. L., 2
- Gehler intensifying screen, 2
- Generator(s), multi-pulse, 14, 15*f*
- Genetic defects, radiation-induced, 31, 32*f*. *See also* Mutation(s)
- Geometric unsharpness, 48
- Ghost images, in panoramic radiography
 - of anatomical structures, 102, 102*f*
 - of cervical spine, 98–99, 98*f*, 99*f*
 - definition of, 97
 - of earrings and other ear jewelry, 103, 103*f*
 - of metallic objects, 100, 100*f*
 - of molar/premolar crowns, 104, 104*f*
- of objects in rotation center, 103–104, 103*f*, 104*f*
- types of, 97
- Granuloma, 141. *See also* Central giant cell granuloma
- Gray (Gy), 22
- Gray-scale range, 34, 35–36

H

- Hard palate, radiographic appearance of, 125, 125*f*, 127*f*, 129*f*
- Heckmann, K., 80
- Hofrath, H., 3
- Holzkecht, Guido, 35
- Hounsfield, Godfrey N., 109
- Hyoid bone, 127*f*, 128*f*

I

- Image analysis, systematic, 134
- Image formation, 34
 - factors affecting
 - film-related, 37–42
 - image receptor-independent, 35–37
- Image interpretation, systematic, 134
- Image noise, 48
- Image quality, 17–18
 - assessment of, 134
- Imaging plate(s). *See also* Storage phosphor imaging plates
 - for digital radiography, 46*f*, 47
 - dynamic range of, 51, 52*f*
- Incisive canal, 124
- Incisive foramen, 124*f*
- Inflammation. *See also* Periodontitis
 - of endodontically treated tooth, CBCT of, 116, 116*f*
 - radiographic appearance of, 135
- Infraorbital canal, 128*f*, 130
- Infraorbital foramen, 130
- Intensifying screen(s), 2, 41–42, 41*f*
 - disadvantages of, 42
 - speed classes of, 41–42
- Interdental bone septum, 121
- Intermaxillary suture, 124*f*
- International Atomic Energy Agency (IAEA), 54, 55
- International Basic Safety Standards (BSS), 56
- International Commission on Radiological Protection (ICRP)
 - activities of, 54–55
 - collaborators with, 54
 - goals of, 54
 - historical perspective on, 54
 - recommendations formulated by, implementation of, 55–56
 - standing committees of, 54
 - structure of, 54
- International Organization for Standardization (ISO), Technical Committee 106 Dentistry, 56

Interradicular bone septum, 121, 122*f*
 Intraoral radiography
 – of bone conditions, 140, 141*f*
 – clinical applications of, 58
 – completeness of visualization in, 58, 58*f*
 – diagnostic image quality of, 58, 138
 – distortion-free imaging, 59, 60*f*
 – **e**ffective dose for, 114
 – full-mouth series, 63, 63*f*
 – image receptor positioning for, 134
 – orthogonal imaging
 — projection geometry for, 58–59, 59*f*
 — superimposition-free, 58–59, 58*f*
 – periapical, 61, 61*f*
 – principles of, 58
 – quality criteria for, 58–59
 – reproducibility, 59, 60*f*
 – standards for, 58
 – superimpositions in, 138
 Inverse square law, 36, 36*f*
 Ion dose, 22
 Ionization, 9–10, 10, 16
 – de**f**inition of, 8
 – direct, 8
 – indirect, 8
 Ionizing radiation, 8
 – **e**ffects of. *See also* Radiation **e**ffects (biological **e**ffects/**e**ffects in tissue)
 — direct, 27
 — on DNA, 27–28, 27*f*
 — indirect, 27
 Isotope(s), radioactive, 11

J

Jaws. *See also* Mandible; Maxilla
 – bone diseases of, 155–156

K

Kalender, Willi, 110
 Kells, C. Edmund, 2, 61
 Keratocysts, 143. *See also* Tumor(s), odontogenic
 Kilovoltage, of dental X-ray machines, 11, 15
 Koch and Sterzel, 80
 König, Walter, 2

L

Lamina dura, 121, 121*f*
 Latent period, 31
 Lead line grid, 36–37, 37*f*, 38
 Le Master, Collins, 2
 Leukemia(s), radiation-induced, 32*f*
 Light
 – ultraviolet. *See* Radiation, ultraviolet
 – visible, 9*f*, 10

Linea obliqua. *See* Oblique line
 Linear energy transfer (LET), 22, 22*f*
 Line pairs per millimeter (lp/mm), 48
 Luminescence, 16, 17*f*
 – photo-stimulated, for imaging plate readout, 48, 48*f*, 49, 50*f*

M

Magnetic **f**lux density, 8*f*, 9
 Malignant lesions, 145–154
 Malignant transformation, 31
 Mandible
 – anatomical variations, 123*f*, 124
 – bone conditions in, assessment of, 140, 140*f*
 – collum, 126, 127*f*
 – compact bone of, 128*f*
 – condyle, 128*f*
 – coronoid process, radiographic appearance, 125, 126*f*, 129*f*
 – radiographic anatomy of, 123–124, 123*f*
 — panoramic, 125–126, 126*f*, 127*f*, 128*f*
 Mandibular (nerve) canal, 123, 124, 125, 128*f*, 143
 Mandibular foramen, 125
 Mandibular fracture(s), 76, 76*f*
 Maxilla
 – bone conditions in, assessment of, 140, 140*f*
 – radiographic anatomy of, 124–125, 124*f*, 128–131, 129*f*–130*f*
 Maxillary sinus
 – diagnostic evaluation of, 131
 – lateral wall, on panoramic radiography, 129*f*, 130*f*, 131
 – mucocoele in, 130*f*
 – posterior wall, on panoramic radiography, 129*f*, 131
 – radiographic appearance of, 124–125, 125*f*, 126, 129*f*, 130
 – residual root in, 4*f*
 – shadow, on panoramic radiography, 106, 106*f*
 Maxillary tuberosity, radiographic appearance of, 126, 128*f*
 McCormack, Allan, 109
 McCune-Albright syndrome, 156
 Median palatine suture, 124
 Mental foramen, 123, 125, 128*f*
 Metal artifacts
 – on CBCT, 113
 – on CT, 112
 – in panoramic radiography, 100, 100*f*
 Midface
 – panoramic radiography of, 87, 87*f*
 – radiographic anatomy of, 128–131, 129*f*–130*f*
 Monitor viewing, conditions for, 134
 Motion artifacts
 – on CBCT, 113, 113*f*
 – on CT, 113

Mouth, **f**loor of, cancer of, 145–146, 146*f*
 Mozzo, P., 110
 Mucocoele, in maxillary sinus, 130*f*
 Muller, H. J., 54
 Mutation(s), 28, 31, 32*f*, 54
 Myxo**f**ibroma, odontogenic, 153, 153*f*
 Myxoma, odontogenic, 153, 153*f*

N

Nasal cavity, 128*f*, 129*f*
 Nasal conchae, shadows, on panoramic radiography, 105–106, 105*f*, 106*f*, 128*f*
 Nasal **f**loor, radiographic appearance of, 125, 125*f*, 127*f*
 Nasal septum, 128*f*
 National Council on Radiation Protection and Measurements (NCRP), 55, 56
 Neutron(s), 11
 – ionization density of, 22
 NewTom cone beam computed tomography system, 5*f*, 109
 Nose, shadow
 – on intraoral radiograph, 124, 124*f*
 – on panoramic radiography, 106, 106*f*, 126, 127*f*
 – on radiograph, 124, 124*f*, 125*f*
 Nuclei
 – stable, 8, 11
 – unstable, 8, 11
 Nuclide(s), radioactive, 11. *See also* Radionuclides
 Numata, H., 3, 4*f*, 79–80

O

Object contrast, 36
 Object-to-**f**ilm distance, and paralleling technique, 62
 Oblique line, of mandible, 123, 123*f*, 127*f*
 Occlusal radiography, 74–76
 – axial projection technique for, 76, 76*f*
 – bisecting-angle technique for, 75, 75*f*
 – **f**ilm for, 74, 75*f*
 Odontoma, 151
 – complex, 151, 151*f*
 – compound, 151, 152*f*
 Optimization procedures, 56
 Oral cavity, cancer of, 145–146
 Orbit, 127*f*, 129*f*, 130
 Oro-antral communication, CBCT of, 117, 117*f*
 Orthodontic radiography, 61–62
 Orthogonal imaging, 81–83
 Orthogonal projection geometry, 58–59, 59*f*
 – **f**ilm holders and, 63, 63*f*
 – for molars, 63, 63*f*
 – for premolars, 63, 63*f*
 Orthopantomography, 3, 81–83, 84–85, 88*f*, 89, 112*f*

Orthophos XG 3D cone beam machine, 110*f*
 Osteoma, 155
 Osteomyelitis, 155, 155*f*
 Ott, Walter, 3, 80

P

Paatero, Y. V., 3, 4*f*, 79–80, 82
 Pair production, 11
 Panoramic radiography, 79–108, 121, 122*f*, 139–140
 – air shadows in, 126
 – of alveolar crest, 86
 – anatomy, 87*f*, 88*f*, 88*t*, 89, 125–131
 – of anterior tooth region, 86, 86*f*
 – bitewing views, 86*f*, 87
 – of bone conditions, 139–140, 140*f*
 – of cysts, 120, 120*f*, 143, 143*f*–145*f*, 144
 – in dentate patients, bite-rod positioning device for, 93
 – dentures and, 101, 101*f*
 – in edentulous patients, positioning for, 93–95, 94*f*, 95*f*
 – **e**ffective dose for, 114
 – errors in
 — anterior displacement of anterior teeth, 96, 96*f*
 — head displacement or rotation, 92–97
 — head positioning, 90–97
 — head rotation out of median plane, 97, 97*f*
 — head tilt, 90–92, 90*f*–92*f*
 — posterior displacement of anterior teeth, 92, 93*f*
 – with extraoral **f**ilm, 80
 – focal trough adjustment to dental arch in, 81, 81*f*, 82*f*
 – ghost images in, 97
 — of anatomical structures, 102, 102*f*
 — of cervical spine, 98–99, 98*f*, 99*f*
 — of earrings and other ear jewelry, 103, 103*f*
 — of metallic objects, 100, 100*f*
 — of molar/premolar crowns, 104, 104*f*
 — of objects in rotation center, 103–104, 103*f*, 104*f*
 – head positioning for, 89–90, 89*f*
 — errors in, 90–97
 – historical perspective on, 3–5, 4*f*, 5*f*, 79–80
 – with intraoral source, 80, 80*f*
 – methodology, 89–108
 – of midface, 87, 87*f*
 – of partial-arch segments, 85–86, 85*f*
 – patient positioning for, 84, 84*f*, 134
 – rotational, 80–81, 80*f*
 — advances in, 84–85
 — angle of incidence in, 82, 82*f*

- head positioning in, 83, 84*f*
 - image layer thickness in, 83, 83*f*
 - and orthogonal imaging, 81–83
 - patient positioning in, 84, 84*f*
 - principle of, 81, 81*f*
 - projection geometry, 83–84, 84*f*
 - projection in horizontal plane, 83, 84*f*
 - projection in vertical plane, 83, 84*f*
 - projection radius in, 83, 83*f*
 - rotation centers in, 82–83, 82*f*, 83–84, 84*f*
 - slit collimator widths in, 82*f*, 83, 83*f*
 - with slit collimator, 79–80, 79*f*
 - soft-tissue shadows in, 97, 104–109, 126
 - special programs, 85–88
 - superimpositions in, 97, 104–109
 - of temporomandibular joint, 86*f*, 87, 87*f*
 - Panoramic tomography, 79–108. *See also* Pantomography
 - Panorex X-ray machine, 3
 - Pantomography, 3, 4*f*
 - Paralleling technique, 18, 61–67, 136
 - advantages of, 62, 63
 - and bisecting-angle technique, comparison of, 67, 67*f*, 70*f*
 - bite block and, 62, 62*f*
 - **film** holder for, 61, 61*f*
 - anterior, 65, 65*f*
 - insertion into mouth, 64–67, 64*f*–66*f*
 - **film** positioning in, 63–64, 65*f*
 - image receptor placement in, 62, 62*f*
 - long-cone technique for, 61–62
 - methodology, 63–67
 - for mandibular incisors and canines, 66*f*, 67
 - for mandibular molars and premolars, 66–67, 66*f*
 - for maxillary incisors and canines, 65, 65*f*, 66*f*
 - for maxillary premolars and molars, 64, 64*f*, 65*f*
 - object-to-**film** distance and, 62
 - principles of, 61–62
 - Partial volume artifacts, on CT, 112–113
 - Pathology
 - identification of, on radiographs, 134–135
 - versus normal variants, 135–136
 - and X-ray image formation, 36
 - Periapical cemental dysplasia, 153
 - Periapical radiography, 61, 61*f*. *See also* Bisecting-angle technique; Paralleling technique
 - Periodontitis, apical
 - acute, 141
 - radiographic features of, 141, 141*f*
 - chronic, 141
 - radiographic features of, 141, 142*f*
 - chronic granulomatous, radiographic features of, 141, 142*f*
 - radiographic features of, 141, 141*f*, 142*f*
 - Pharynx, 128*f*
 - Photoelectric **effect**, 10–11, 11*f*, 16, 17*f*, 26, 26*f*
 - Photon(s), scattering of, 11, 11*f*, 26, 26*f*
 - Photon energy, transfer to matter, 10, 26, 26*f*. *See also* Excitation; Ionization
 - Photon radiation, 8–9
 - Photo-stimulated luminescence (PSL), for imaging plate readout, 48, 48*f*, 49, 50*f*
 - Pixel binning, 48
 - Potassium, 30
 - Price, W. A., 2
 - Projection geometry
 - implementation of, 59–61, 60*f*
 - principles of, 59–61, 60*f*
 - Proton(s), 8, 9, 11
 - ionization density of, 22
 - Pterygopalatine fossa, 126, 128*f*
- ## Q
- Quality assurance, 56
 - standards for, 56
- ## R
- Radiation. *See also* Ionizing radiation
 - absorption of, 10, 22. *See also* X-ray(s), absorption of
 - alpha, 8
 - **artificial**, 12
 - beta, 8
 - cosmic, 12, 30, 31*f*
 - **definition** of, 8
 - electromagnetic, 8–9, 8*f*
 - infrared, 8, 9*f*
 - and matter, interactions between, 9–10, 26, 26*f*
 - naturally occurring (background), 8, 30
 - scattered, 37, 37*f*. *See also* Scattering
 - secondary, 37, 37*f*
 - solar, 30
 - terrestrial, 12, 30, 31*f*
 - types of, 8
 - ultraviolet, 8, 9*f*
 - Radiation absorbed dose, 22
 - Radiation **effects** (biological effects/**effects** in tissue), 26, 26*f*
 - biological phase, 26–28, 26*f*, 27*f*
 - chemical phase, 26, 26*f*
 - deterministic, 28, 31, 32*f*
 - indirect, 27
 - physical phase, 26, 26*f*
 - stochastic, 31, 32*f*
 - Radiation exposure
 - **artificial**, 30, 31*f*
 - natural, 30, 30*f*, 31*f*
 - occupational, 30, 31*f*
 - Radiation protection, 17–18
 - administration of, 55
 - bisecting-angle technique and, 70
 - historical perspective on, 54
 - legal and regulatory framework for, 55
 - management of, 55
 - and need/**justification**, 55
 - optimization of, 55
 - procedures for, 56
 - responsibility for, 55
 - Radiation quality, 22
 - Radiation risk(s)
 - and need/**justification**, 55
 - reduction of, 55
 - Radiation sickness, acute, 31
 - Radiation weighting factor (W_R), 22
 - Radioactivity, 8, 11–12
 - Radiographic measurement, 74, 74*f*
 - Radioisotopes, 11
 - Radionuclides, 11
 - terrestrial, 30
 - Radiosensitivity, 23
 - RadioVisioGraphy system, 46
 - Radon, Johann, 111
 - Radon gas, 30, 30*f*, 31*f*
 - Raper, Howard R., 2, 73, 136
 - Rare-earth screens, 41, 41*f*
 - Report, radiological, 135
 - Reproducibility
 - of images in intraoral radiography, 59, 60*f*, 71
 - of radiographs, 134
 - Right-angle technique, 72–73, 72*f*, 73*f*
 - Risk/**benefit** assessment, 56
 - Roentgenogram, **first**, 2
 - Roentgen rays, 2
 - Roller transport system, of automatic **film** processor, 42, 43*f*
 - Röntgen, Wilhelm Conrad, discovery of X-rays, 2
 - Root canal, working length of, radiographic measurement of, 74, 74*f*
 - Root resorption
 - with ameloblastoma, 147, 147*f*, 148*f*
 - trauma-induced, 158, 160*f*
 - Rutherford, Ernest, 9
- ## S
- Scanora, 5, 85
 - Scattering, 11, 11*f*, 26, 26*f*, 37, 37*f*
 - intensifying screens and, 42
 - Semiconductor **effect**, 16
 - Semilunar notch, 128*f*
 - Sensor(s), for digital radiography, 46*f*, 47–48, 47*f*
 - active pixel, 47
 - CCD, 47
 - CdTe, 48
 - CMOS, 47
 - signal processing with, 47, 47*f*
 - spatial resolution of, 48
 - types of, 47
 - Shell capacity, 9
 - Sialolithiasis, 76, 76*f*, 157, 157*f*, 158*f*
 - Siemens X-ray sphere, 3, 3*f*
 - Sievert (Sv), 22, 23
 - Silver bromide crystals, 38–39, 38*f*
 - conventional, 38, 38*f*
 - T-grain (tabular), 38, 38*f*
 - Single-tank design, 12
 - Skin cancer, radiation-induced, 54
 - Slit-beam technique, 3, 4*f*
 - Slit collimator
 - panoramic radiography with, 79–80, 79*f*
 - in rotational panoramic radiography, 82*f*, 83, 83*f*
 - Soft palate, 127*f*
 - radiographic appearance of, 129*f*
 - shadow, on panoramic radiography, 107, 107*f*, 126
 - Soft rays, 11
 - Spacer cone(s), 17–18, 18*f*, 19*f*
 - Sphenoid sinus, 127*f*
 - Standard radiographic projections, 35
 - Standards
 - for intraoral radiography, 58
 - for radiation protection, 56
 - Status-X panoramic X-ray apparatus, 4*f*
 - Stochastic **effects**, 31, 32*f*
 - Storage phosphor imaging plates, 48–50
 - characteristic curve for, 51, 52*f*
 - damage-related marks on, 50, 51*f*
 - formats for, 49, 49*f*
 - latent image on, 49
 - readout, 48, 48*f*, 49, 50*f*
 - scanners for, 49, 49*f*
 - structure of, 48, 48*f*
 - Styloid process, 126, 127*f*
 - Subtraction, 35–36, 138
 - Summation **effect**, 34, 34*f*, 121, 138
- ## T
- Tangential **effect**, 35, 35*f*
 - Teeth. *See also* Tooth
 - radiographic anatomy of, 121–122, 121*f*, 122*f*
 - Temporomandibular joint (TMJ)
 - close-up view of, 77*f*
 - panoramic imaging of, 86*f*, 87, 87*f*
 - Thermionic emission, 13
 - Thorium, 30
 - Threshold dose, 31, 32*f*
 - Tissue(s)
 - **effects** of radiation in. *See* Radiation **effects**

- radiation-induced changes in, 31
- X-ray appearance of, 35
- Tissue weighting factor (W_T), 23, 23*t*
- Tomography
 - blurring in, 78, 78*f*
 - conventional, 77–78, 77*f*, 78*f*
 - principles of, 77*f*, 78, 78*f*
 - digital volume. *See* Cone beam computed tomography (CBCT)
 - panoramic, 79–108. *See also* Pantomography
- Tongue
 - position, for panoramic radiography, 107, 107*f*, 109
 - shadow, on panoramic radiography, 107–108, 108*f*–109*f*, 126
- Tongue piercing, and rotation center of panoramic radiography, 103–104, 103*f*, 104*f*
- Tooth fractures, 158, 159*f*, 160*f*
- Tooth luxation, 158
- Tooth-supporting structures, radiographic anatomy of, 121, 121*f*, 122*f*

- Training, and radiation protection, 56
- Transverse panoramic tomography, 5
- Traumatic dental injuries, 158, 159*f*, 160*f*
- Tumor(s)
 - odontogenic, 147–153
 - benign mixed, 147
 - keratocystic, 143, 147, 148, 150*f*, 151*f*
 - WHO classification of, 147
 - radiographic appearance of, 135
- Turbinates, inferior, radiographic appearance of, 129
- Type tests, 56

U

- Ulcer(s), radiation-induced, 31
- United States, organizations in, responsible for radiation protection, 55–56
- Updegrave, W. J., 61
- Uranium, 30

V

- Vascular system, radiation-induced changes in, 31
- Voltage, and image formation, 36–37
- Volume artifacts, on CBCT, 113
- Voxels, 111

W

- Waggener, D. T., 61
- Walkhoff, Friedrich Otto, 2
- Water, radiolysis of, 27
- Wehnelt cylinder, 13, 13*f*, 14

X

- X-ray(s), 8, 9*f*
 - absorption of, 10, 22, 34
 - factors affecting, 35–36
 - characteristic, 10, 15, 16*f*
 - discovery of, 2
 - filtration of, 17
 - ionization density of, 22

- and matter, interactions between, 9–10, 26, 26*f*
- production of, 10
- in dental X-ray equipment, 12–16
- properties of, 16
- radiation weighting factor for, 22
- of teeth, first, 2
- X-ray beam(s), attenuation of, 10, 16, 34
- X-ray machine, dental, first, 2

Z

- Zonarc panoramic X-ray machine, 3, 5*f*
- Zonarc rotational panoramic radiography machine, 85*f*
- Zonography, 83
- Zulauf, A. F., 79–80
- Zygomatic arch, 128*f*
- Zygomatic bone, radiographic appearance of, 125, 125*f*, 128, 128*f*, 129*f*

